

EAST PILBARA CRATON:
A RECORD OF ONE BILLION YEARS
IN THE GROWTH OF ARCHEAN
CONTINENTAL CRUST

by
AH Hickman





Government of **Western Australia**
Department of **Mines, Industry Regulation
and Safety**

REPORT 143

EAST PILBARA CRATON: A RECORD OF ONE BILLION YEARS IN THE GROWTH OF ARCHEAN CONTINENTAL CRUST

by
AH Hickman

PERTH 2021



**Geological Survey of
Western Australia**

MINISTER FOR MINES AND PETROLEUM
Hon Bill Johnston MLA

DIRECTOR GENERAL, DEPARTMENT OF MINES, INDUSTRY REGULATION AND SAFETY
David Smith

EXECUTIVE DIRECTOR, GEOLOGICAL SURVEY AND RESOURCE STRATEGY
Jeff Haworth

REFERENCE

The recommended reference for this publication is:

Hickman, AH 2021, East Pilbara Craton: a record of one billion years in the growth of Archean continental crust: Geological Survey of Western Australia, Report 143, 187p.

ISBN 978-1-74168-899-3

ISSN 1834-2280



A catalogue record for this
book is available from the
National Library of Australia

Grid references in this publication refer to the Geocentric Datum of Australia 1994 (GDA94). Locations mentioned in the text are referenced using Map Grid Australia (MGA) coordinates, Zone 50. All locations are quoted to at least the nearest 100 m.

Disclaimer

This product uses information from various sources. The Department of Mines, Industry Regulation and Safety (DMIRS) and the State cannot guarantee the accuracy, currency or completeness of the information. Neither the department nor the State of Western Australia nor any employee or agent of the department shall be responsible or liable for any loss, damage or injury arising from the use of or reliance on any information, data or advice (including incomplete, out of date, incorrect, inaccurate or misleading information, data or advice) expressed or implied in, or coming from, this publication or incorporated into it by reference, by any person whatsoever.

Published 2021 by the Geological Survey of Western Australia

This Report is published in digital format (PDF) and is available online at <www.dmirs.wa.gov.au/GSWApublications>.



© State of Western Australia (Department of Mines, Industry Regulation and Safety) 2021

With the exception of the Western Australian Coat of Arms and other logos, and where otherwise noted, these data are provided under a Creative Commons Attribution 4.0 International Licence. (<http://creativecommons.org/licenses/by/4.0/legalcode>)

Further details of geoscience publications are available from:

Information Centre
Department of Mines, Industry Regulation and Safety
100 Plain Street
EAST PERTH WESTERN AUSTRALIA 6004
Telephone: +61 8 9222 3459 Email: publications@dmirs.wa.gov.au
www.dmirs.wa.gov.au/GSWApublications

Cover photograph: Radiometric ternary image (KTU) of the east Pilbara Craton (from Brett, 2018), showing the ovoid granitic cores (orange–yellow–white) of nine domes separated by greenstones belts (dark colours), and in places by the unconformably overlying Fortescue Group

Contents

Abstract	1
Introduction	2
Examples of issues discussed in the Report	2
Report content	3
Pilbara nomenclature.....	3
Tectonic unit terminology.....	5
Composition and extent of the Pilbara Craton.....	6
Greenstone belts and granitic complexes	6
Tectonic divisions of the northern Pilbara Craton.....	6
Concealed Pilbara Craton	6
Fragment of a Neoproterozoic supercontinent	8
Paleo–Mesoproterozoic breakup	8
Vaalbara ancestry.....	9
Evidence used in this Report	9
Pilbara Craton Mapping Project	9
Geochronology and isotope data	9
Sm–Nd and Lu–Hf model ages.....	12
Pilbara Craton overview.....	15
Tectonic units of the northern Pilbara Craton	15
Eoarchean to early Proterozoic evolution	16
Remnants of pre-3530 Ma crust	21
Warrawagine Dome.....	21
Shaw Dome.....	21
Muccan Dome	21
Other evidence of pre-3530 Ma crust	22
Isotopic evidence of pre-3530 Ma crust.....	22
Xenocrystic zircons older than 3530 Ma in igneous rocks.....	22
Evidence from detrital zircon ages.....	23
Whole-rock Sm–Nd isotope data	39
Zircon Lu–Hf data	41
Current data	42
Summary	47
East Pilbara Terrane.....	49
Pilbara Supergroup	49
Volcanic cycles.....	50
Geochemistry	51
Warrawoona Group	51
Strelley Pool Formation.....	72
Kelly Group.....	80
Sulphur Springs Group	83
Large igneous provinces of the EPT	89
Warrawoona LIP	89
Kelly LIP	89
Granitic supersuites of the EPT	89
Mulgundoon Supersuite (3530–3490 Ma)	90
Callina Supersuite (3484–3462 Ma)	91
Tambina Supersuite (3451–3416 Ma)	91
Emu Pool Supersuite (3324–3290 Ma)	91
Cleland Supersuite (3270–3223 Ma)	92
Granitic intrusion and felsic volcanism.....	92
Tectonic processes in the EPT	93
Doming and sagduction	94
Tectonic setting of the EPT	97
Tectonic events in the EPT	98
D ₁ , 3530–3477 Ma.....	98
D ₂ , 3477–3459 Ma.....	99
D ₃ , 3455–3420 Ma.....	99
D ₄ , 3360–3350 Ma.....	100
D ₅ , 3335–3325 Ma.....	101
D ₆ , 3325–3290 Ma	102
Metamorphism in the EPT	103
Kurrana Terrane	105
Northern KUT stratigraphy.....	105
EPT ancestry of the KUT?.....	105
Kurrana Shear Zone.....	106

The beginning of plate tectonics in the Pilbara Craton	106
East Pilbara Terrane Rifting Event, 3280–3165 Ma	107
D ₇ , 3280–3220 Ma	108
D ₈ , c. 3220 Ma	108
D ₉ , 3220–3165 Ma	109
Cause of the change in crustal evolution	109
Early Mesoproterozoic basins	109
Soanesville Basin	110
Depositional age	110
Sedimentology	110
Tectonic setting	111
Soanesville Group	111
Budjan Creek Formation	117
Mosquito Creek Basin	117
Coondamar Formation	118
Mosquito Creek Formation	118
Basin evolution	119
Dalton Suite	120
Mount Billroth Supersuite	120
Flat Rocks Tonalite	120
Golden Eagle Orthogneiss	121
Tectonic interpretation	121
Tectonic events in the early Mesoproterozoic basins	121
D ₁₀ Karratha Event, 3160–3140 Ma	121
Prinsep Orogeny	122
Timing of the Prinsep Orogeny	122
D ₁₁ during the Prinsep Orogeny	123
Elizabeth Hill Supersuite	123
Chichester Tectonic Zone	124
De Grey Superbasin	126
Tectonic models	127
East–west extent of the superbasin	127
Gorge Creek Basin	127
Extent of the Mallina Basin	130
Gorge Creek Basin stratigraphy	131
Farrel Quartzite	131
Cleaverville Formation	133
Cundaline Formation	134
Regional continuity of stratigraphic succession	134
Stratigraphic continuity of Gorge Creek Group between greenstone belts	135
Extent of the Gorge Creek Basin	137
Conclusions regarding the Gorge Creek Basin	137
Coonieena Basalt	138
Mallina Basin	139
Croydon Group	139
Sisters Supersuite	142
Cutinduna Supersuite	142
Split Rock Supersuite	143
Tectonic events in the De Grey Superbasin	144
D ₁₂ , c. 3060–3015 Ma	145
D ₁₃ , 3015–2970 Ma	145
D ₁₄ , 2970–2955 Ma	146
D ₁₅ dome reactivation, 3015–2940 Ma	146
North Pilbara Orogeny, 2955–2919 Ma	147
Mosquito Creek Orogeny, D ₁₈ – D ₂₀ between c. 2930 and 2900 Ma	148
Post-orogenic events	149
D ₂₁ , c. 2880 Ma	149
D ₂₂ , 2851–2831 Ma	149
D ₂₃ , 2775–2750 Ma	150
Event history of EPT domes	150
Mineralization	153
Mineralization in the East Pilbara Terrane (3530–3223 Ma)	153
Sediment-hosted, hydrothermal massive sulfates, Dresser Formation	153
Volcanogenic massive sulfides, Duffer Formation	154
Black shale-hosted Cu–Zn, Apex Basalt	154
Vein and hydrothermal base metals, Panorama Formation	155
Copper and molybdenum mineralization at c. 3315 Ma	155
Precious metals, mainly c. 3315 Ma	156
Mineralization during EPTRE rifting (3280–3165 Ma)	157
Sulphur Springs Group	158
Soanesville Group	158
Convergence-related mineralization (3160–3070 Ma)	159
Gold mineralization	159
Mineralization in the De Grey Superbasin (3166–2930 Ma)	159
Gorge Creek Basin	160
Mallina Basin	160
Mosquito Creek Basin	161
Post-orogenic mineralization (2895–2830 Ma)	161
Lithium-bearing pegmatites (c. 2880 Ma)	161
Pegmatite of the 2851–2831 Ma Split Rock Supersuite	162
Gold mineralization (c. 2880 Ma)	162

Summary and conclusions.....	162
Formation of Eoarchean – early Paleoarchean sialic crust between c. 3.80 and 3.53 Ga	162
Summary.....	162
Conclusions	163
Paleoarchean evolution of a volcanic plateau	163
Summary.....	163
Conclusions	164
Mesoarchean crustal evolution.....	164
Summary.....	164
Conclusions	165
Mineralization.....	166
Abbreviations	166
References	167

Figure captions

1. Simplified tectonochronologic divisions of Western Australia, showing concealed extents of the Pilbara and Yilgarn Cratons	4
2. Tectonic units of northwestern Western Australia and setting of the Pilbara Craton	5
3. Major tectonic units of the northern Pilbara Craton	7
4. Stratigraphic comparison of the Pilbara and Kaapvaal successions between 3550 and 2450 Ma	11
5. Simplified geological map of the east Pilbara Craton	17
6. Generalized lithostratigraphy of the Pilbara Supergroup	18
7. Ages and contact relationships of terranes, basins, supersuites and events in the east Pilbara Craton	19
8. Granite–greenstone domes in the east Pilbara Craton	20
9. U–Pb data for zircons from tonalite gneiss samples GSWA 180057 and 142870, Warrawagine Dome	21
10. Relative timing of granitic intrusion and episodes of felsic volcanism in the northern Pilbara Craton	27
11. U–Pb zircon analytical data for sample GSWA 168996, an altered felsic volcanoclastic rock of the c. 3470 Ma Duffer Formation	29
12. Ages of detrital zircons in sedimentary formations of the east Pilbara Craton, excluding the Mosquito Creek and Mallina Formations	30–35
13. Normalized relative probability diagrams and histograms of detrital zircon ages in sedimentary formations of the Croydon, Gorge Creek, Soanesville and Sulphur Springs Groups	37
14. Normalized relative probability diagrams and histograms of detrital zircon ages in the Mallina and Mosquito Creek Basins	38
15. U–Pb analytical data for detrital zircons in a sandstone unit of the Apex Basalt	39
16. Sm–Nd two-stage model ages (T_{DM}^2) for mafic and felsic igneous rocks of the northern Pilbara Craton	40
17. Sm–Nd two-stage model ages (T_{DM}^2) and ϵ_{Nd} vs magmatic ages for the northern Pilbara Craton	43
18. Histograms of zircon crystallization ages and two-stage Lu–Hf model (T_{DM}^2) ages for cognate and xenocrystic zircons from igneous rocks of the EPT	46
19. ϵ_{Hf} evolution diagram for analyses of igneous, xenocrystic and detrital zircons dated between 3550 and 3200 Ma, and whole-rock samples (mainly komatiites), from the east Pilbara Craton	47
20. Histograms of crystallization ages and two-stage Lu–Hf model (T_{DM}^2) ages for igneous and detrital zircons from Paleoarchean and Mesoarchean rocks of the east Pilbara Craton	48
21. Vertical geochemical trends in basaltic rocks of the North Star and Mount Ada Basalts, Marble Bar greenstone belt	52
22. Stromatolites and microbial mats in the c. 3481 Ma Dresser Formation	57
23. Geological map of part of the EPT showing outcrops of the Marble Bar Chert Member	59
24. U–Pb zircon geochronology constraining the depositional age of the Marble Bar Chert Member in the Coongan and Marble Bar greenstone belts	60
25. Geological sketch map of Marble Bar area showing the thickness of the Duffer Formation, and dolerite dykes and sills	62
26. Photomicrograph (plane-polarized light) of ignimbrite in the upper Duffer Formation	63
27. Outcrops of jaspilitic chert of the Marble Bar Chert Member at Marble Bar Pool	65
28. Hydrothermal intrusion and brecciation of the Marble Bar Chert Member and Duffer Formation at Marble Bar Pool	65
29. Stratigraphy of the Marble Bar Chert Member intersected in drillhole ABDP 1	67
30. Tectonostratigraphic units of the Mount Edgar Dome, summarizing domal structure and geochronology	70
31. Geological map of part of the EPT showing outcrops of the Strelley Pool Formation	74
32. Strelley Pool Formation in the central East Strelley greenstone belt, and locations of stratigraphic logs	76
33. Stratigraphic logs of the Strelley Pool Formation in the East Strelley greenstone belt	79
34. Columnar rhyolite in the Wyman Formation	83
35. Geological sketch map of the southern Warralong greenstone belt showing the Wyman Formation bounded by angular unconformities	88
36. Photo of granitic veins intruding metamorphosed pillow structures in the Euro Basalt, Coongan River at Warrery Gap	101
37. Simplified geological map showing distribution of the Emu Pool Supersuite	104
38. Simplified structural geology of the southern Yule Dome showing outcrops of high-Mg diorite and granodiorite	116
39. Geological setting of the Mosquito Creek Basin showing major structures and gold mineralization	118
40. Gneiss and diatextite in the Chichester Tectonic Zone	125
41. Simplified geological map showing distribution of the Mount Billroth and Elizabeth Hill Supersuites	126
42. Simplified geological map showing regional extent and thicknesses of the Gorge Creek Group	132
43. Southeasterly migration of granitic intrusions in the northern Pilbara Craton inferred from trends in geochronology data	140
44. Simplified geological map showing distribution of the Sisters Supersuite	143
45. Simplified geological map showing distribution of the Split Rock Supersuite	144
46. Event history (volcanism, granitic intrusion and sedimentation) of the 11 domes of the EPT	151
47. Mineralization in the east Pilbara Craton	157

Tables

1.	Generalized lithostratigraphy of the east Pilbara Craton	10
2.	Summary of xenocrystic zircon ages >3530 Ma in igneous rocks	13
3.	Summary of geochronology of all granitic intrusions and supersuites	24–26
4.	Sm–Nd model ages (T_{DM}^2) and ϵ_{Nd} values from igneous stratigraphic units of the east Pilbara Craton	44
5.	Members (informal) and facies of the Strelley Pool Formation	78
6.	Outline of the evolution of the Mount Edgar Dome	152

Appendices

Appendices are available with the PDF online as an accompanying digital resource

1.	Obsolete names and revised definitions
2.	Gazetteer of place names
3.	Xenocrystic zircons older than 3490 Ma in igneous rocks in the east Pilbara Craton
4.	Summary of dated samples from igneous suites in the east Pilbara Craton
5.	U–Pb zircon dates from igneous rocks of the east Pilbara Craton
6.	Dated detrital zircons from metasedimentary rocks of the northern Pilbara Craton
7.	Ages of detrital zircons in the Mallina and Mosquito Creek Basins
8.	Sm–Nd data from the east Pilbara Craton
9.	Lu–Hf data from the east Pilbara Craton
10.	References for geochronology data in Figure 43

Plates

Available with the PDF of this Report as an accompanying digital resource

1A.	Interpreted bedrock geology of the east Pilbara Craton – northern sheet
1B.	Interpreted bedrock geology of the east Pilbara Craton – southern sheet
1C.	Reference for interpreted bedrock geology of the east Pilbara Craton

East Pilbara Craton: a record of one billion years in the growth of Archean continental crust

by
AH Hickman

Abstract

The Pilbara Craton provides valuable insights into Paleoproterozoic crustal evolution and how tectonic processes changed at c. 3.22 Ga. This Report discusses available evidence, with particular reference to five key questions: 1) was the 15–20 km-thick volcanic succession of the 3.53 – 3.23 Ga Pilbara Supergroup deposited on older continental crust?; 2) how and when was the dome-and-keel crustal architecture of the east Pilbara Craton formed?; 3) did plate tectonic processes play any part in the Paleoproterozoic crustal evolution of the Pilbara Craton?; 4) to what extent was the Mesoproterozoic evolution of the east Pilbara Craton influenced by plate tectonic events in the northwest Pilbara Craton?; 5) was Paleoproterozoic mineralization of the east Pilbara Craton governed by the style of its tectonic evolution?

U–Pb zircon geochronology, and Sm–Nd and Lu–Hf isotope data, indicate the existence of widespread ‘pre-greenstone’ 3.80 – 3.53 Ga continental crust in the Pilbara Craton during its Paleoproterozoic and Mesoproterozoic evolution. Remnants of this ancient crust have been dated in several areas of the east Pilbara Craton. Additionally, numerous pre-3.60 Ga xenocrystic zircons have been reported from Paleoproterozoic igneous rocks, testifying to underlying Eoarchean crust. Hf two-stage model ages for xenocrystic and detrital zircons from the east Pilbara Craton include early Eoarchean mantle extraction ages. The thickness, lithological composition and lateral extent of the Pilbara Supergroup, combined with geochemical and isotopic evidence, indicate Paleoproterozoic episodic crustal growth on a continental scale. Successive mantle plume events resulted in ultramafic–mafic–felsic volcanic cycles that formed a volcanic plateau between 3.53 and 3.22 Ga. Combined structural, metamorphic and geochronological evidence show that the dome-and-keel structure of the East Pilbara Terrane was formed by periodic diapiric uplift of granitic crust accompanied by sagduction of adjacent greenstones. A new comparison of the 11 domes that make up the East Pilbara Terrane has revealed that between 3.53 and 3.33 Ga the c. 15 km-thick lower and central sections of the Pilbara Supergroup were deposited uniformly across the volcanic plateau. However, between 3.33 and 3.29 Ga there was a disconnect between evolution of the eastern and western halves of the East Pilbara Terrane: whereas doming and sagduction continued in the east until c. 3.22 Ga, the west experienced increasing crustal extension from 3.28 Ga leading to deep rifting of the Paleoproterozoic continental crust.

Deep rifting of the East Pilbara Terrane at 3.22 Ma evolved into the northwest–southeast separation of three microplates (East Pilbara, Kurrana, and Karratha Terranes) separated by two rift basins (Regal and Mosquito Creek Basins) floored by juvenile basaltic crust. The beginning of plate tectonic processes in the Pilbara Craton is exceptionally well defined by the end of Paleoproterozoic vertical deformation and the commencement of Mesoproterozoic horizontal deformation. Paleoproterozoic melts derived from crustal recycling of much older crust were succeeded by Mesoproterozoic juvenile, mantle-derived melts. The northwest–southeast plate separation led to mainly sedimentary deposition of passive-margin successions such as the 3.22 – 3.17 Ma Soanesville Group. A c. 3.16 Ga metamorphic event across the northern Pilbara Craton, coinciding with a change from plate divergence to convergence, is attributed to collision of the Karratha Terrane with an inferred plate to the northwest. Effects of this reversal included intrusion of the granitic Mount Billroth Supersuite and horizontal deformation involving obduction of basaltic crust from the rift basins. At c. 3.07 Ga, the northwestern margin of the East Pilbara Terrane collided with the West Pilbara Superterrane resulting in closure of the Regal Basin, the Prinsep Orogeny, and intrusion of the 3.07 Ga Elizabeth Hill Supersuite.

With amalgamation of the East Pilbara Terrane and the West Pilbara Superterrane, plate interaction shifted to the northwestern margin of the Pilbara Craton. Subduction of the northwestern plate is likely to have commenced shortly after 3.07 Ga, although the oldest magmatic arc exposed on the northwest Pilbara coast is represented by the c. 3.02 Ga Orpheus Supersuite. Southeast of the Orpheus Supersuite arc, the Gorge Creek Group was deposited in a retro-arc basin overlying thick continental crust. The Gorge Creek Basin occupied most of the northern Pilbara Craton. Between c. 3.02 and 2.92 Ga, magmatic arcs related to ongoing subduction along the northwestern margin of the craton migrated progressively southeast, and the East Pilbara Terrane was intruded by granites from c. 2.95 Ga onwards. The North Pilbara Orogeny of the northwest Pilbara Craton was followed by convergence of the East Pilbara and Kurrana Terranes in the southeast Pilbara Craton. This resulted in closure of the intervening Mosquito Creek Basin and the 2.93 – 2.90 Ga Mosquito Creek Orogeny. Post-orogenic granites of the Split Rock Supersuite were intruded between 2.85 and 2.83 Ga, possibly due to movement of the Pilbara Craton across a hot spot.

Mineralization in the east Pilbara Craton is directly related to the different tectonic processes operating in the Paleoproterozoic and Mesoproterozoic. The modest size of the Paleoproterozoic deposits is attributed to vertical crustal reworking which limited the available volumes of potential source regions.

KEYWORDS: Eoarchean crust, diapiric doming, mineralization, plate tectonics, rifting, subduction

Introduction

The 3800–2830 Ma Pilbara Craton is a 500 000 km² segment of Archean granite–greenstone crust underlying the Pilbara region of northwestern Western Australia (Fig. 1). Over 80% of the Pilbara Craton is concealed by unconformably overlying Neoarchean and Proterozoic volcanic and sedimentary successions, although 60 000 km² of the northern part of the craton is exposed in an inlier that extends southeast 500 km inland from the coast of northwest Pilbara (Fig. 2). This Report describes the eastern 40 000 km² of this inlier which exposes the Paleoarchean East Pilbara Terrane (EPT, Fig. 3), several unconformably overlying Mesoarchean basins, and rare outcrops of pre-3530 Ma crust. The EPT is internationally important for many unique insights it provides on Paleoarchean–Mesoarchean crustal evolution, and for an exceptionally well-preserved fossil record of early life on Earth. Only the Barberton Greenstone Belt in the Kaapvaal Craton of southern Africa contains equally well-preserved Paleoarchean geology. Consequently, these two areas have provided most of the direct evidence relating to Paleoarchean and early Mesoarchean crustal evolution.

Examples of issues discussed in the Report

One example of new knowledge obtained from the northern Pilbara Craton relates to the timing and processes of the onset of plate tectonics on Earth. This controversial question was recently reviewed by Cawood et al. (2018). Excluding evidence from the Pilbara Craton, estimates for the timing of the earliest plate tectonic processes have ranged from the Hadean to the Neoproterozoic, although most interpretations have been derived from theoretical modelling rather than direct geological observations and deduction. Some of the previously published Pilbara Craton evidence has been mentioned in the international debate, although until now this has mainly focused on the geochemical evidence for c. 3130 Ma subduction in the northwest Pilbara Craton (Smithies et al., 2005a, 2007a; Furnes et al., 2014; Cawood et al., 2018). Direct evidence for older and additional plate tectonic processes in the Pilbara Craton has been gleaned from combinations of stratigraphic, structural, geochemical and geochronological data. Some of this evidence has already been published (Hickman, 2001a, 2004, 2012, 2016; Van Kranendonk et al., 2002, 2006b, 2007b, 2010; Hickman et al., 2010; Hickman and Van Kranendonk, 2012). This Report re-addresses the issue within the context of the 3280–3165 Ma East Pilbara Terrane Rifting Event (EPTRE); an event which provides the earliest evidence for the commencement of plate tectonic processes in the Pilbara Craton.

A second important question concerns Paleoarchean tectonic processes that formed the dome-and-keel crustal architecture of the EPT (see **Tectonic processes in the EPT**). This type of crustal structure, comprising steep-sided domal granitic complexes separated by relatively narrow but deep synformal greenstone belts (keels), has no Phanerozoic analogues and few close Proterozoic analogues. Stratigraphic, structural and geochronological evidence indicates that development of this structure was integral to the stratigraphic evolution of the EPT (Hickman, 1980e, 1981, 1984, 2004; Hickman and Van Kranendonk,

2004; Pawley et al., 2004; Van Kranendonk et al., 2004a, 2007a,b). From the onset of doming between c. 3477 and 3460 Ma, depositional basins began to be positioned between rising domes of more felsic crust. This control over the stratigraphy increased with time as the amplitude of the granitic domes and the depths of the intervening greenstone basins increased. Although detailed reasons as to why the domes were not produced by horizontal tectonic processes have already been given (Hickman, 1984; Collins et al., 1998; Hickman and Van Kranendonk, 2004; Sandiford et al., 2004; Van Kranendonk et al., 2004a; Thébaud and Rey, 2013; François et al., 2014), some previous researchers have questioned the significance of Paleoarchean vertical tectonic processes (Blewett et al., 2004; De Wit et al., 2011; Nijman et al., 2010, 2017).

A third controversial issue relates to the existence of thick sialic crust prior to deposition of the 3530–3235 Ma Pilbara Supergroup. Some early reviews of Archean granite–greenstone terranes interpreted the greenstones to pre-date the granites, with the implication of an initial oceanic crust (Viljoen and Viljoen, 1971; Glikson, 1972, 1976; Windley, 1973, 1977). Other studies indicated that the granitic rocks of these terranes include remnants of a pre-greenstone basement (Hunter, 1957; Goodwin, 1968; Anhaeusser et al., 1969; Sutton, 1971; Binns et al., 1976; Archibald and Bettenay, 1977). Geological mapping of the northern Pilbara Craton in the 1970s led to an interpretation that the greenstone succession was deposited on sialic crust (Hickman, 1975a, 1981, 1983). Geochemical, geochronological and isotopic lines of evidence have supported the existence of pre-3530 Ma sialic crust (Jahn et al., 1981; Bickle et al., 1989, 1993; Collins, 1993; Green et al., 2000; Van Kranendonk et al., 2002, 2006a, 2007a,b, 2014b; Hickman, 2004, 2012; Smithies et al., 2005b, 2007a, 2009; Kemp et al., 2015a,b; Johnson et al., 2017; Gardiner et al., 2017, 2018; Petersson et al., 2019a–c).

Although some local studies in the North Pole area have interpreted oceanic origins for the Warrawoona Group (Kitajima et al., 2001, 2008; Komiya et al., 2002; Kabashima et al., 2003; Terabayashi et al., 2003), the tectonic models proposed have proved to be inconsistent with regional geological evidence (Van Kranendonk, 2000a; Van Kranendonk et al., 2002, 2006a, 2007a,b; Hickman, 2004, 2012). Features of the Warrawoona Group, and all other sections of the Pilbara Supergroup, that argue against an oceanic origin include:

- the 15–20 km stratigraphic thickness of the Pilbara Supergroup
- the lithological composition of the succession (eight vertically stacked ultramafic–mafic–felsic volcanic cycles)
- the inclusion of five major erosional unconformities overlain by thick conglomerate–sandstone units
- shallow-water stromatolitic carbonates and evaporites at two stratigraphic levels
- the 300 Ma age range of the succession
- intrusion of the greenstones by contemporaneous, genetically-related granitic rocks with a total volume similar to that of the greenstones.

These features support the interpretation that the Pilbara Supergroup was deposited on a volcanic plateau underlain by older crust (Van Kranendonk et al., 2002). However, other criteria are required to indicate if the pre-3530 Ma crust was predominantly mafic or felsic, or if it had a mixed composition as in an older granite–greenstone or gneiss terrane.

Report content

This Report reviews published evidence and interpretations relating to the stratigraphy, structure, geochronology, geochemistry, crustal evolution and mineralization of the eastern half of the northern Pilbara Craton. It draws extensively on information obtained from a major project of detailed systematic geological remapping of the northern Pilbara Craton between 1994 and 2005. This project, referred to as the Pilbara Craton Mapping Project (PCMP), was conducted jointly by the Geological Survey of Western Australia (GSWA) and Geoscience Australia (GA). Apart from providing exploration and mining companies operating in Western Australia with far more detailed geological maps and evidence on controls of mineralization, a key objective of the project was to resolve important differences of geological interpretation concerning the stratigraphy and tectonic subdivisions of the northern Pilbara Craton. The diversity of published interpretations prior to 1994 was mainly a consequence of insufficient detailed regional data.

During the course of the PCMP, and for some years afterwards, GSWA and GA project members published numerous GSWA and GA reports and papers in scientific journals to present new geological data and interpretations on the northern Pilbara Craton. The availability of these references has influenced the presentation of this Report in that previously published evidence for or against certain interpretations might not be repeated. On the other hand, some published interpretations derived from the project, particularly preliminary interpretations prior to project completion, have required revision in this Report; in these instances, reasons for the new interpretations are provided.

GSWA and GA interpretations published prior to the PCMP are also used in this Report, either because they have been confirmed by PCMP evidence or because they provided the foundation for the development of later interpretations. Data and interpretations from external researchers are also widely used and discussed in the Report. For example, 80 of the 225 U–Pb zircon dates referenced in this Report were published by external authors.

Pilbara nomenclature

Literature on the geology of the Pilbara region is now very extensive, with detailed accounts commencing in the 1980s of its stratigraphy, structure, geochemistry, geochronology and tectonic evolution. Changing interpretations during the course of these diverse investigations have been accompanied by revisions of nomenclature, particularly over the last 20 years. Some brief introductory notes regarding past and present nomenclature are therefore provided to assist readers. For example, there are many different applications of the regional name 'Pilbara' in referring to various stratigraphic and tectonic units and events, and to

geographic areas within the Pilbara region. Additionally, other names such as 'Hamersley', 'Gorge Creek', and 'Warrawoona' have been applied to different successions at different times and by different authors (see Appendices 1, 2).

Early investigators used the name 'Pilbara Block' (obsolete name) to refer to the northern 60 000 km² granite–greenstone inlier (Fig. 3; Ryan, 1964; Blockley, 1975; Hickman, 1983). Volcanic and sedimentary units unconformably overlying the 'Pilbara Block', and initially thought to be Proterozoic in age, were assigned to the Fortescue and Hamersley Groups of the Hamersley Basin (Trendall and Blockley, 1970; Trendall, 1975). This division was revised by Trendall (1990a,b, 1995) who combined all these units, plus the overlying c. 2400 Ma Turee Creek Group, under the name 'Pilbara Craton'. This revision was based on an interpretation that lasting crustal stability, marking completion of cratonization, was not attained until c. 2400 Ma. One line of evidence for ongoing instability was that Paleo–Mesoarchean greenstone synclines and associated faults continued to be active during deposition of the Fortescue Group (Kriewaldt, 1964; Hickman, 1983; Blake, 1984b, 1993). Apparently conflicting with the interpretation of continual, uninterrupted crustal evolution of the craton, was the long-established recognition of a major regional unconformity at the base of the Fortescue Group (Noldart and Wyatt, 1962; Blockley, 1975; Hickman, 1983; Blake, 1984a,b). This unconformity separates steeply inclined granite–greenstone units, metamorphosed to greenschist and amphibolite facies, from overlying, almost flat-lying volcanic and sedimentary formations of the Fortescue Group, metamorphosed only to prehnite–pumpellyite facies.

Following the 1994–2005 PCMP, Van Kranendonk et al. (2006a) redefined the Pilbara Craton as the tectonic unit containing the granite–greenstone terranes and excluding all groups within the Hamersley Basin (as then defined). New geochronological data from this project indicated that the unconformity at the base of the Fortescue Group marks a >100 Ma period of relative crustal stability and deep erosion commencing at c. 2900 Ma. Orogenic episodes between c. 2955 and 2900 Ma effectively completed cratonization of the Pilbara Craton.

Other stratigraphic and tectonic units of the Pilbara region incorporating 'Pilbara' in their names include the Pilbara Supergroup, East Pilbara Terrane (EPT), West Pilbara Superterrane (WPS), and Central Pilbara Tectonic Zone (CPTZ). Tectonic events named from the Pilbara region are the East Pilbara Terrane Rifting Event (EPTRE) and the North Pilbara Orogeny. That part of the Pilbara Craton located north of the Fortescue River is referred to as the 'northern Pilbara Craton', referring to its geographic location. Likewise, the terms 'northwest Pilbara Craton' and 'east Pilbara Craton' are occasionally used to refer to geographic areas underlain by the Pilbara Craton. Geographic terms are distinguished from tectonic names by the location qualifiers not being capitalized. The Neoarchean Fortescue Basin, unconformably overlying the Pilbara Craton, is divided into tectonic units named as the Northeast Pilbara Sub-basin, Northwest Pilbara Sub-basin, and South Pilbara Sub-basin. Thorne and Trendall (2001) interpreted these to be sub-basins of the Hamersley Basin, although following subdivision of the Hamersley Basin, these sub-basins are now assigned to the Fortescue Basin.

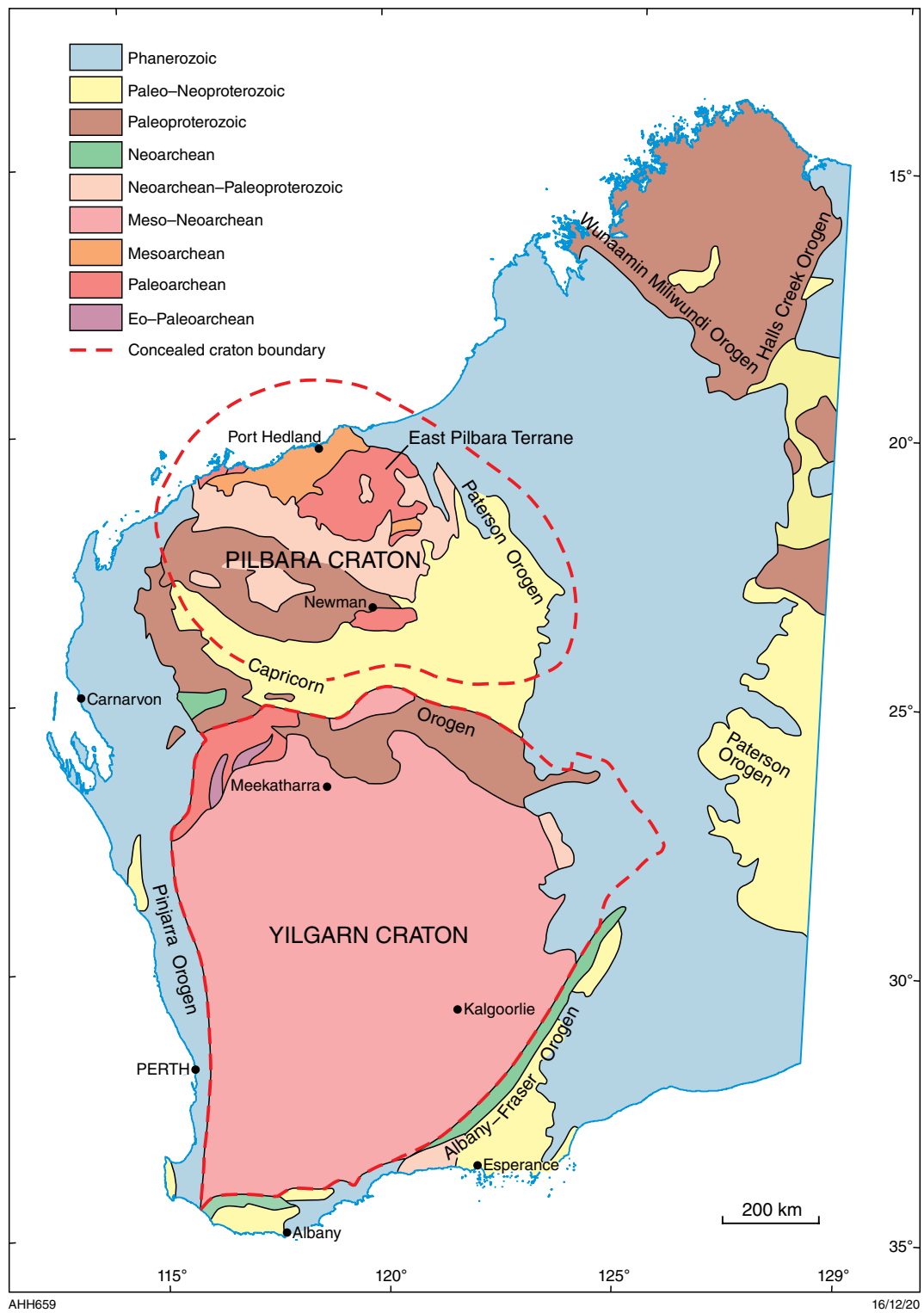


Figure 1. Simplified Archean, Proterozoic and Phanerozoic tectonochronologic divisions of Western Australia, showing an interpretation of the concealed extents of the Pilbara and Yilgarn Cratons

The name 'Pilbara Supergroup' was first used and defined by Hickman (1981, 1983) to refer to the entire greenstone succession of the Pilbara Craton. Subsequently, the term Pilbara Supergroup was redefined to refer only to the Paleoproterozoic greenstone succession of the East Pilbara Terrane (Van Kranendonk et al., 2006a), and comprising the Warrawoona Group, Kelly Group and Sulphur Springs Group (Hickman, 2011). The EPT also includes Paleoproterozoic granitic rocks genetically related to felsic volcanic formations in the Pilbara Supergroup.

At c. 3220 Ma, crustal growth of the EPT was terminated by plate separation during the EPTRE. In the northwest Pilbara Craton, the Paleoproterozoic Roebourne Group was deposited before this rifting event and is correlated with the Sulphur Springs Group (Hickman, 2016). The EPT does not include Mesoproterozoic sedimentary and volcanic basins which unconformably overlie the Pilbara Supergroup and the Paleoproterozoic granitic rocks, or any of the Mesoproterozoic granitic rocks that intrude the terrane. This should be borne in mind when viewing regional tectonic summary maps and figures such as Figure 3.

The WPS comprises three terranes (Karratha, Regal, and Sholl) in the northwest Pilbara Craton that were accreted by plate collision at c. 3070 Ma (Van Kranendonk et al., 2006a).

The CPTZ (Hickman, 1999, 2001a, 2016) is a northeast-trending belt of Mesoproterozoic tectonic and magmatic activity that occupies most of the northwest Pilbara Craton (Fig. 3). Its evolution commenced at c. 3200 Ma during the EPTRE and continued until the end of the North Pilbara Orogeny at c. 2919 Ma. Initially, it formed as a rift basin floored by juvenile, oceanic-like basaltic crust, but subsequent interaction between the independently moving plates of the EPT and Karratha Terrane (KT), and later between the EPT and the WPS, led to obduction, subduction, development of volcanic arcs and back-arc or retro-arc basins, strike-slip basins, and finally deformation and metamorphism during the North Pilbara Orogeny (Hickman, 2016).

Tectonic unit terminology

The east Pilbara Craton is divided into four types of tectonic unit: terranes, basins (including one superbasin), supersuites, and a 'structural corridor'. A terrane is defined as a fault-bounded body of rock of regional extent, characterized by a geological history different from that of contiguous bodies of rock. A basin is an area underlain by a substantial thickness of sedimentary or volcanic rocks, which has unifying characteristics of stratigraphy and structure due

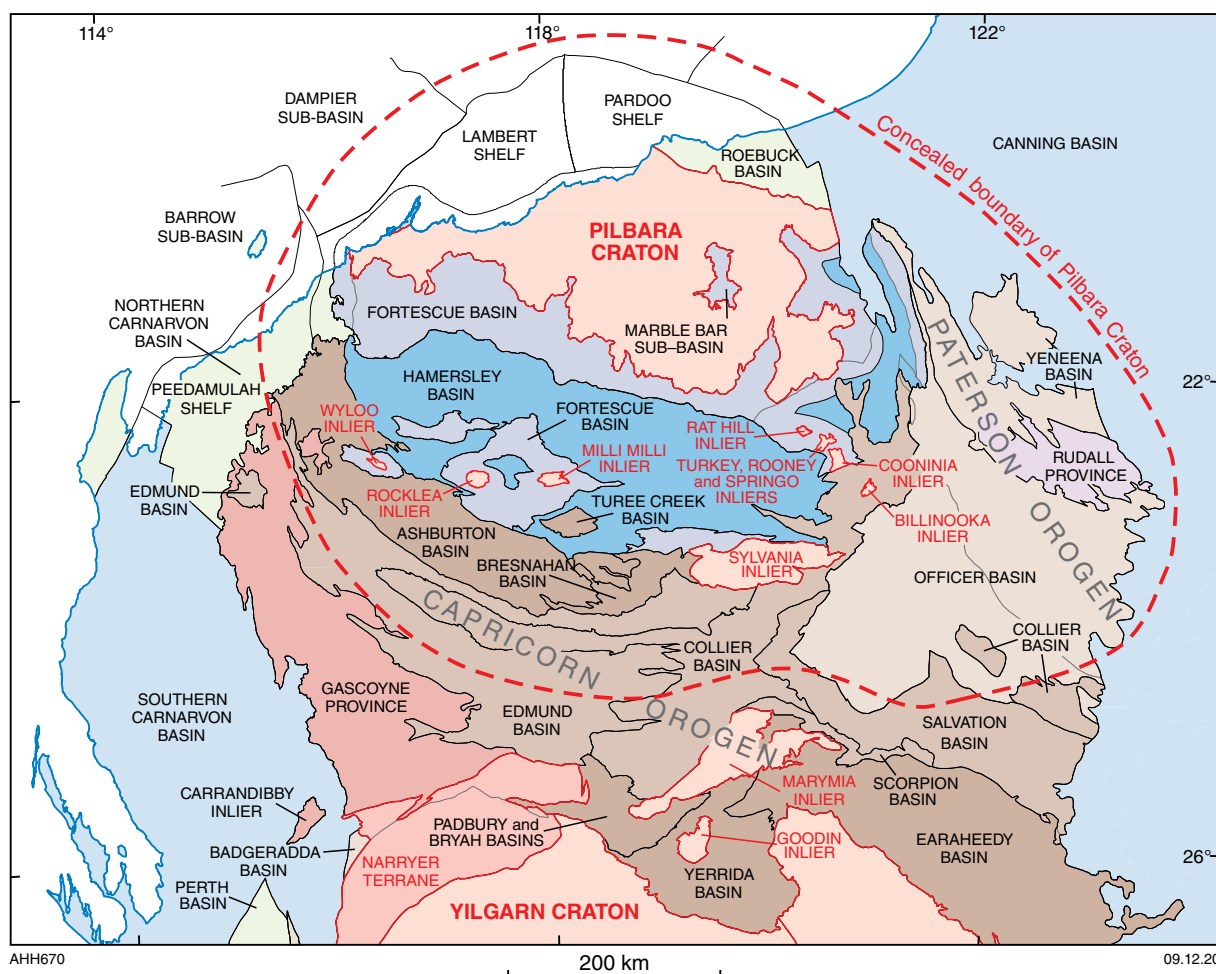


Figure 2. Tectonic units of northwestern Western Australia, showing the setting of the Pilbara Craton (based on Geological Survey of Western Australia, 2017). The southern half of the craton is concealed by Neoproterozoic and Proterozoic rocks except for rare exposures within inliers

to deposition in a regionally restricted area. Basins are bounded by unconformities except where major faults have juxtaposed a basin with another tectonic unit. A superbasin is a connected series of basins. Supersuites, consisting of multiple igneous suites and intrusions, were first established in the Pilbara Craton as lithostratigraphic units by Van Kranendonk et al. (2006a). However, they were emplaced by tectonomagmatic events, which, in some instances (Elizabeth Hill and Split Rock Supersuites), are not known to be represented by any volcanic successions. Accordingly, supersuites are now also used by GSWA as tectonic units. A structural corridor is a broad linear zone of tightly folded and strongly faulted rocks, typically bounded by major faults.

Composition and extent of the Pilbara Craton

Greenstone belts and granitic complexes

As in Archean cratons worldwide, early descriptions of the Pilbara Craton referred to 'greenstone belts' and 'granites' (or 'granite batholiths'). These simple lithological divisions required no prior knowledge of an area's stratigraphy or structure. The term 'greenstone belt' was applied to any tract of country, commonly linear, that was underlain by supracrustal assemblages of metamorphosed volcanic, sedimentary and mafic intrusive rocks, and which contained no large granitic intrusions. Geological investigations suggested that most greenstone belts are broadly synclinal or synformal or, in some instances, volcano-sedimentary packages contained within detached fold limbs. The 'granites', on the other hand, were first interpreted by many workers to be major plutons or batholiths that had intruded the greenstones. Early mapping of the northern Pilbara Craton indicated that the granitic units separating the greenstones were complexes containing granitic intrusions of various ages (Hickman, 1975a, 1983). Increased use of geochronology in the Pilbara Craton confirmed that most of the 'batholiths' are composed of multiple intrusions differing in age by several hundred million years. The term batholith (Hickman, 1980d, 1981, 1983) was eventually replaced by 'Granitoid Complex' (Griffin, 1990), and later by 'Granitic Complex' (Hickman and Van Kranendonk, 2004). However, present Australian stratigraphic nomenclature does not accept 'Granitic Complex' in formal names. Therefore, these large domal granitic units are now informally referred to as 'granitic complexes' (in the northwest Pilbara Craton where granite-greenstone domes are not developed) or 'granitic cores'. The boundaries of the EPT granitic cores, some of which are up to 100 km in diameter, control what has been referred to as the 'dome-and-keel' crustal architecture of the terrane. Successive granitic intrusions, emplaced over hundreds of millions of years, intruded only the pre-existing cores of the domes, thus progressively accentuating the dome-and-keel pattern (Hickman and Van Kranendonk, 2004). Detailed investigation of the east Pilbara Craton dome-and-keel structure has revealed that, rather than being simple greenstone synclines, the 'keels' are composed of two or more fault-bounded greenstone panels overlying adjacent domal granitic cores. Thus, the East Pilbara Terrane can be described as an assemblage of fault-bounded granite-greenstone domes.

Tectonic divisions of the northern Pilbara Craton

The first tectonic subdivision of the northern Pilbara Craton (Hickman, 1980d) was revised based on results of the PCMP (Van Kranendonk et al., 2002, 2006a; Hickman, 2016). The geographic divisions of the northern Pilbara Craton, the east Pilbara Craton and northwest Pilbara Craton, are separated by the northeast-southwesterly trending, linear Tabba Tabba Shear Zone (TTSZ; Hickman, 2016). Within the eastern section of the northern Pilbara Craton, the East Pilbara Terrane (EPT) is separated from the Kurrana Terrane (KUT) by the Mosquito Creek Basin and the Kurrana Shear Zone (KSZ, Fig. 3). The northwest Pilbara Craton exposes the Paleoarchean Karratha Terrane (KT) and several Mesoarchean terranes and basins (Hickman, 2016). The KUT remains to be studied in detail, and large sections of it are concealed by the Fortescue and Hamersley Basins. Available information indicates that the KUT is now mainly composed of Mesoarchean rocks, although isotopic evidence indicates an older Paleoarchean history. As previously interpreted (Van Kranendonk et al., 2002), and explained in more detail in this Report, the EPT overlies a basement of Eoarchean to early Paleoarchean crust. There are very few exposures of this early crust, but its widespread existence in the Archean is revealed by geochemical and isotopic evidence. The southern boundary of the EPT is concealed by the Fortescue and Hamersley Basins. This Report discusses evidence suggesting that the EPT is separated from Archean inliers in the southern half of the Pilbara Craton by an east-southeasterly trending terrane boundary concealed beneath the Chichester Range and Fortescue Valley (major topographic features of the Pilbara region). If this suggestion is correct, the EPT does not extend to the Archean inliers of the south Pilbara Craton (Fig. 2), although these inliers are likely to include crust that was part of the EPT prior to its breakup at c. 3220 Ma.

Concealed Pilbara Craton

A seismic survey (Johnson et al., 2011) between the southern part of the Pilbara Craton and the Gascoyne Province (Fig. 2) indicated that a concealed part of the Pilbara Craton extends up to 200 km beyond the most southerly inliers shown on Figure 2. This concealed southern part of the craton underlies the Proterozoic Ashburton, Edmund and Collier Basins (Johnson et al., 2011, 2013; Korsch et al., 2011; Thorne et al., 2011). Southeast from the Sylvania Inlier (Fig. 2), gravity data suggest an underlying crustal architecture similar to that exposed in the Pilbara Craton.

Geophysical data from the Canning Basin (Frogtech Geoscience, 2017) indicate that the Pilbara Craton extends at least 150 km east of the western boundary of the Paterson Orogen, including the Rudall Province (Fig. 2). These geophysical data support previous structural evidence that the Rudall Province was thrust southwestwards across the eastern margin of the Pilbara Craton (Hickman and Bagas, 1999; Maidment, 2017). Isotope data from the Rudall Province (Kirkland et al., 2013) also support this interpretation. Farther north, Reading et al. (2012) interpreted data from a passive seismic transect to propose a deepening of the Moho across the northeastern margin of the Pilbara Craton.

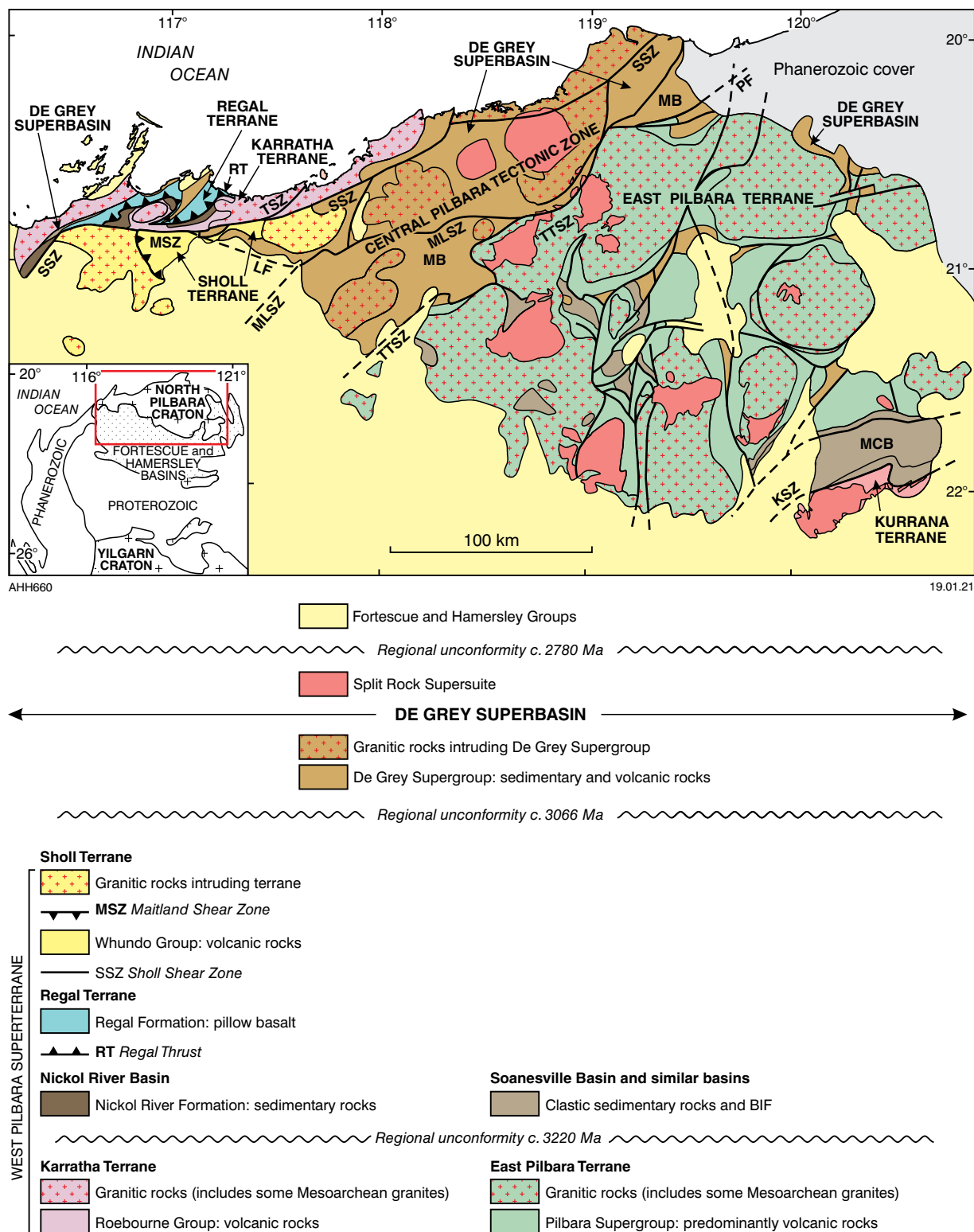


Figure 3. Major tectonic units of the northern Pilbara Craton. The mainly Paleoproterozoic East Pilbara Terrane (EPT) is separated from Mesoproterozoic terranes and basins of the northwest Pilbara by the Tabba Tabba Shear Zone. The Central Pilbara Tectonic Zone is a Mesoproterozoic zone of deformation and magmatic intrusion formed by 3160–2900 Ma plate convergence between the East Pilbara and Karratha Terranes. Abbreviations: KSZ, Kurrana Shear Zone; LF, Loudens Fault; MB, Mallina Basin; MCB, Mosquito Creek Basin; MLSZ, Mallina Shear Zone; PF, Pardoo Fault (part of TTSZ); SSZ, Sholl Shear Zone; TSZ, Terenar Shear Zone; TTSZ, Tabba Tabba Shear Zone

North and northwest from the Pilbara coast, gravity data and numerous seismic lines undertaken during petroleum exploration indicate that the Pilbara Craton extends 150–200 km offshore beneath Phanerozoic sedimentary successions of the Northern Carnarvon Basin. Within 30–150 km of the Pilbara coast, the successions of the Lambert Shelf and Peedamullah Shelf are less than 1 km thick; farther offshore, the Pilbara Craton is covered by thicker Phanerozoic successions in the southeastern section of the Dampier Sub-basin (Fig. 2). Neoarchean and Paleoproterozoic rocks of the Fortescue and Hamersley Basins were thrust onto the western margin of the Pilbara Craton (Hickman and Strong, 1998) during west–east or southwest–northeast crustal shortening of uncertain age.

Fragment of a Neoarchean supercontinent

Several lines of evidence indicate that in the late Mesoarchean and Neoarchean the Pilbara Craton and the overlying Fortescue and Hamersley Basins were joined with Archean crust of the Kaapvaal Craton (Cheney et al., 1988; Cheney 1996; Martin et al., 1998a; Zegers et al., 1998b; Eriksson et al., 2002; Bleeker, 2003; Strik et al., 2003; De Kock et al., 2009, 2012; Huston et al., 2012; Smirnov et al., 2013), and possibly also with Archean parts of Zimbabwe, Tanzania, Madagascar and India (Hickman, 2016). Evidence from the Pilbara indicates that from c. 2775 Ma onwards, this large Archean continental plate, termed ‘Vaalbara’ by Cheney et al. (1988), began to break up (Blake and Barley, 1992; Blake, 1993; Martin et al., 1998a,b; Thorne and Trendall, 2001; Muller et al., 2005; Hickman et al., 2010). Prior to this breakup event, the Pilbara Craton and the overlying Fortescue and Hamersley Basins, would have been part of a much larger area of crust than the ~500 000 km² now preserved (Figs 1, 2; Krapež and Eisenlohr, 1998; Thorne and Trendall, 2001; Barley et al., 2005; Hickman, 2016).

Evidence of the greater pre-breakup size of the Pilbara Craton is provided by lateral thickness continuity in the Neoarchean and Paleoproterozoic successions that unconformably overlie the craton. For example, the 2775–2629 Ma Fortescue Group shows no evidence of lateral stratigraphic thinning towards the present margins of the craton (Blake, 1993; Thorne and Trendall, 2001). Similarly, one of the best exposed and most intensely studied formations of the 2629–2445 Ma Hamersley Group, the Brockman Iron Formation, thins only very gradually from west to east (Morris and Horwitz, 1983). Over a distance of 600 km this formation changes from ~645 m thick on the YARRALOOOLA 1:250 000 map sheet area in the northwest (Williams, 1968) to ~450 m thick on the ROBERTSON 1:250 000 map sheet area in the east (Williams and Tyler, 1991). Therefore, because in all areas of the Pilbara region the Fortescue and Hamersley Groups overlie the Pilbara Craton, these observations establish that between c. 2775 and 2445 Ma the Pilbara Craton extended over a very much larger area than it does today.

Table 1 summarizes the east Pilbara Craton stratigraphy and Figure 4 illustrates the remarkable stratigraphic and geochronological matches between the Pilbara and Kaapvaal successions, with respect to volcanic and sedimentary units, and with regard to episodes of granitic intrusion. The high degree of correlation between: 1) the Pilbara Supergroup (Warrawoona and Kelly Groups) and the Onverwacht Group; and 2) the Fortescue Group – Hamersley Group succession and the Ventersdorp Supergroup – Ghaap Group succession,

leaves no reasonable doubt that the Pilbara and Kaapvaal Cratons evolved in close proximity on the same Archean continent.

Stratigraphic, geochronological, metallogenic and paleomagnetic comparisons (Nelson et al., 1992, 1999; Cheney et al., 1988; Cheney 1996; Wingate, 1998; Martin et al., 1998a; Zegers et al., 1998b; Eriksson et al., 2002; Zhao et al., 2002, 2004; Bleeker, 2003; Pickard, 2003; De Kock et al., 2009, 2012; Huston et al., 2012), and evidence from asteroid impact spherule beds (Lowe and Byerly, 1986; Lowe et al., 1989; Byerly et al., 2002; Simonson and Hassler, 2002; Glikson, 2004, 2005a,b, 2006, 2007b, 2008, 2013, 2014; Rasmussen et al., 2005; Jones-Zimmerlin et al., 2006; Glikson and Vickers, 2006, 2010; Simonson et al., 2009; Hassler et al., 2011; Glass and Simonson, 2012, 2013; Kambhu and Simonson, 2013; Glikson and Pirajno, 2018) support stratigraphic correlation between the two cratons. Additionally, extremely similar microfossils are present in c. 3400 Ma sedimentary units of both cratons (Oelher et al., 2017).

Paleo–Mesoarchean breakup

In this Report, the comparisons and correlations between the Fortescue–Hamersley Group succession in the Pilbara and the Ventersdorp Supergroup – Ghaap Group succession in South Africa (Trendall, 1968; Button, 1976; Blake, 1984b; Cheney et al., 1988; Trendall et al., 1990; Nelson et al., 1992, 1999; Cheney, 1996; Martin et al., 1998a; Pickard, 2003) are interpreted to support the Neoarchean to Paleoproterozoic breakup of Vaalbara. However, in terms of the tectonic evolution of the Pilbara Craton, a far more important earlier event of rifting and continental breakup occurred between 3280 and 3165 Ma – the East Pilbara Terrane Rifting Event (EPTRE).

As discussed in this Report, the EPTRE coincided with a major change in the crustal evolution of the Pilbara Craton in which Paleoproterozoic volcanic activity and granitic intrusion was followed by mainly sedimentary Mesoarchean deposition. The c. 3220 Ma lithological change in the east Pilbara succession was recognized during GSWA mapping in the 1970s (Lipple, 1975; Hickman and Lipple, 1975, 1978b; Hickman, 1980a,b, 1981, 1983) when a simple two-fold division was made between the volcanic Warrawoona Group and the unconformably overlying sedimentary Gorge Creek Group. However, the tectonic significance of this change was not recognized until later (Hickman, 2001a, 2004; Van Kranendonk et al., 2002, 2006a, 2007b, 2010). Notably, a similar lithological change from the Paleoproterozoic to the Mesoarchean was previously documented in the Barberton Greenstone Belt of the eastern Kaapvaal Craton (Anhaeusser et al., 1968, 1969; Anhaeusser, 1971a).

In view of the evidence that the Pilbara Craton was reduced in size by the Neoarchean to Paleoproterozoic continental breakup, and that stratigraphic correlations are possible between Paleoproterozoic successions of the Pilbara and Kaapvaal Cratons (Zegers et al., 1998b; Hickman, 2016), it is concluded that the EPT crust originally extended far outside the present boundaries of this terrane. Between c. 3280 and 3165 Ma this crust rifted and was eventually separated into a number of continental microplates. Within the area of the present-day Pilbara Craton three separate terranes were formed: East Pilbara, Karratha, and Kurrana (Fig. 3). However, plate convergence and collisions from c. 3160 Ma onwards progressively re-assembled these Paleoproterozoic

plates and various intervening Mesoarchean terranes and basins to reconstitute and re-enlarge the Pilbara Craton (Van Kranendonk et al., 2006a, 2007b, 2010; Hickman, 2012; Hickman and Van Kranendonk, 2012).

Deformation and metamorphism at c. 3250 Ma in the Kaapvaal Craton (Moyen et al., 2006; Van Kranendonk, 2011; Van Kranendonk et al., 2014a,b) might mark the same event of continental breakup as recorded in the Pilbara Craton. Van Kranendonk et al. (2014a,b) presented several lines of evidence against an interpretation by Moyen et al. (2006) that the Kaapvaal event was due to subduction.

Vaalbara ancestry

If correct, the interpretation that the Pilbara and Kaapvaal Cratons evolved in close proximity as different parts of Vaalbara implies that evidence on the evolution of one craton is also relevant to the evolution of the other (Van Kranendonk et al., 2014a,b). As first suggested by Zegers et al. (1998b), certain major structures in the Pilbara Craton could be continuous with similar structures identified in the Kaapvaal Craton. Along with the stratigraphic correlations (Fig. 4), this suggests that the scale of the Archean tectonic processes and settings was considerably greater than is evident from within the Pilbara Craton alone. For example, Paleoproterozoic volcanic stratigraphy that is apparently common to the Pilbara and Kaapvaal Cratons suggests that the Vaalbara continent was covered by LIP successions from continental-scale mantle plumes (Arndt et al., 2001; Condie, 2001; Eriksson et al., 2002; Pirajno, 2007; Hickman, 2012). It also seriously questions interpretations in which the EPT, with its present boundaries, has been described as an 'ancient nucleus' on to which younger Pilbara terranes and basins were accreted (Barley, 1997; Van Kranendonk et al., 2002, 2007a,b; Smithies et al., 2005b, 2007c; Petersson et al., 2019c).

The concept of the EPT as an 'ancient nucleus' was originally based on the present boundaries of the EPT, not on its original Archean boundaries, which remain unknown. Also, it takes no account of the greater lateral extent of the Paleoproterozoic volcanic plateau prior to the two breakup events (late Paleoproterozoic and Neoproterozoic). It might be argued that the EPT became a Mesoarchean nucleus for plate tectonic accretion following the EPTRE, but the other Paleoproterozoic microplates produced by the EPTRE also accreted younger terranes and basins, and therefore would constitute additional 'ancient nuclei'. The Regal and Sholl Terranes were accreted onto the Karratha Terrane, whereas the Coondamar and Mosquito Creek Basins were accreted onto the Kurrana Terrane (Fig. 3). Hickman (2004) interpreted Pilbara gravity data to show that the Karratha and Kurrana Terranes are of comparable size to the EPT, and appear to be smaller only because they are now largely concealed. Therefore, the concept that only the EPT acted as a single nucleus onto which all younger terranes and basins of the Pilbara Craton were accreted (Barley, 1997) cannot be sustained. Outside the present area of the Pilbara Craton, the existence of a c. 3220 Ma passive-margin sedimentary basin in South Africa (Moodies Group) suggests similar fragmentation of the Paleoproterozoic continental volcanic plateau in that part of Vaalbara.

A further consideration is that the 3530–3220 Ma EPT is not the most ancient part of the Pilbara Craton. As reviewed in this Report, it is now established from surface geology, geochronology and isotope data that the EPT evolved on top of pre-3530 Ma crust. Evidence is accumulating that the extent of this early crust was considerable, with remnants identified in several granite–greenstone domes of the EPT and in the Sylvania Inlier section of the KUT.

Evidence used in this Report

Pilbara Craton Mapping Project

This Report draws extensively on information obtained from a major project of geological mapping, airborne aeromagnetic and radiometric surveys, U–Pb zircon geochronology, zircon Lu–Hf and whole-rock Sm–Nd isotopes, geochemistry, and investigation of mineral deposits that was conducted jointly by GSWA and GA between 1994 and 2005. Referred to as the Pilbara Craton Mapping Project (PCMP), this collaborative project remapped the northern half of the Pilbara Craton (Fig. 3) and successfully resolved various differences of geological interpretation that had emerged by 1994. Additional sources of information used in this Report include GSWA and GA data obtained prior to this project, and published information from other organizations and researchers.

Early results from the PCMP included new geological maps and stratigraphic revisions in the northwest Pilbara Craton (Smithies, 1996, 1997; Hickman, 1997). A review of later geological revisions in the northwest Pilbara Craton was provided by Hickman (2016). Reinterpretations of east Pilbara Craton geology were made by Van Kranendonk et al. (2002, 2006a), Hickman (2004, 2012), and Hickman and Van Kranendonk (2004, 2008a, 2012).

The PCMP provided a basis for a comprehensive revision of the stratigraphy of the northern Pilbara Craton and reinterpretation of its crustal evolution (Van Kranendonk et al., 2006a). Subsequent publications reviewed and expanded upon various features of the craton's evolution (Champion and Smithies, 2007; Smithies et al., 2007a,b, 2009; Van Kranendonk et al., 2007a,b, 2010; Bagas et al., 2008; Hickman, 2008; Hickman and Van Kranendonk, 2008a). Additional geochronological data (Van Kranendonk et al., 2010) then required several further revisions of the stratigraphy (Hickman, 2011, 2012).

Geochronology and isotope data

Many geological interpretations of the Pilbara Craton published by GSWA since 1996 have relied heavily on geochronology and isotope data obtained during the 1994–2005 PCMP. This Report uses the same data, in combination with geochronology and isotope data obtained outside the project, and also incorporates previously unpublished GSWA Lu–Hf isotope data. This Report also examines U–Pb dates on xenocrystic and detrital zircons obtaining since 1996 to provide insights on crust older than the exposed post-3530 Ma stratigraphy. All data are listed and classified in Appendices 3 to 9, and summaries of the data are presented in Tables 2 to 4.

Table 1. Generalized lithostratigraphy of the east Pilbara Craton

Supergroup	Group (Basin/LIP)	Subgroup	Formation	Age (Ma)*	
De Grey Supergroup	Nullagine Group (Mosquito Creek Basin)	no contact	Mosquito Creek Formation	2980–2930	
			paraconformity		
			Coondamar Formation	3200–3176	
	Croydon Group (Mallina Basin)	disconformity	Lalla Rookh Sandstone	2988–2931	
			Cattle Well Formation	2988–2955	
		erosional unconformity	Coonieena Basalt	3015–2988	
	Gorge Creek Group (Gorge Creek Basin)	unconformity	Cundaline Formation	3015–3015	
			Cleaverville Formation	3022–3015	
			Farrel Quartzite	3066–3022	
(Budjan Creek Basin)	no contact	Budjan Creek Formation	3223–3190		
	Soanesville Group (Soanesville Basin)	unconformity	Empress Formation	3176–3165	
			Hong Kong Chert	3176–3165	
			Pyramid Hill Formation	3185–3165	
			Honeyeater Basalt	3185–3165	
			Paddy Market Formation	3190–3185	
			Corboy Formation	3223–3190	
			Cardinal Formation	3223–3190	
	Pilbara Supergroup	Sulphur Springs Group (Sulphur Springs Basin)	Kangaroo Caves Formation	3253–3235	
			Kunagunarrina Formation	3275–3255	
Leilira Formation			3290–3255		
Kelly Group		erosional unconformity			
			Charteris Basalt		
			Wyman Formation	3325–3315	
Kelly LIP		disconformity	local unconformity		
			Euro Basalt	3350–3335	
Warrawoona Group (Warrawoona LIP)		Salgash Subgroup	Strelley Pool Formation	3426–3350	
			erosional unconformity – paraconformity		
			Panorama Formation	3448–3427	
	Coongan Subgroup	local unconformity			
		Apex Basalt	3459–3440		
		disconformity			
	Talga Talga Subgroup	Duffer Formation	3474–3449		
		Mount Ada Basalt	3470–3469		
		disconformity			
	Coonterunah Subgroup	Dresser/McPhee Formation	3481–3477		
		North Star Basalt	3530–3490		
		no contact			
	inferred unconformity (not exposed)	Double Bar Formation	3515–3490		
		Coucal Formation	3515–3498		
		Table Top Formation	3530–3515		
	Early crust				3800–3530

Note: * Age ranges are inferred from isotopic data and stratigraphic relations

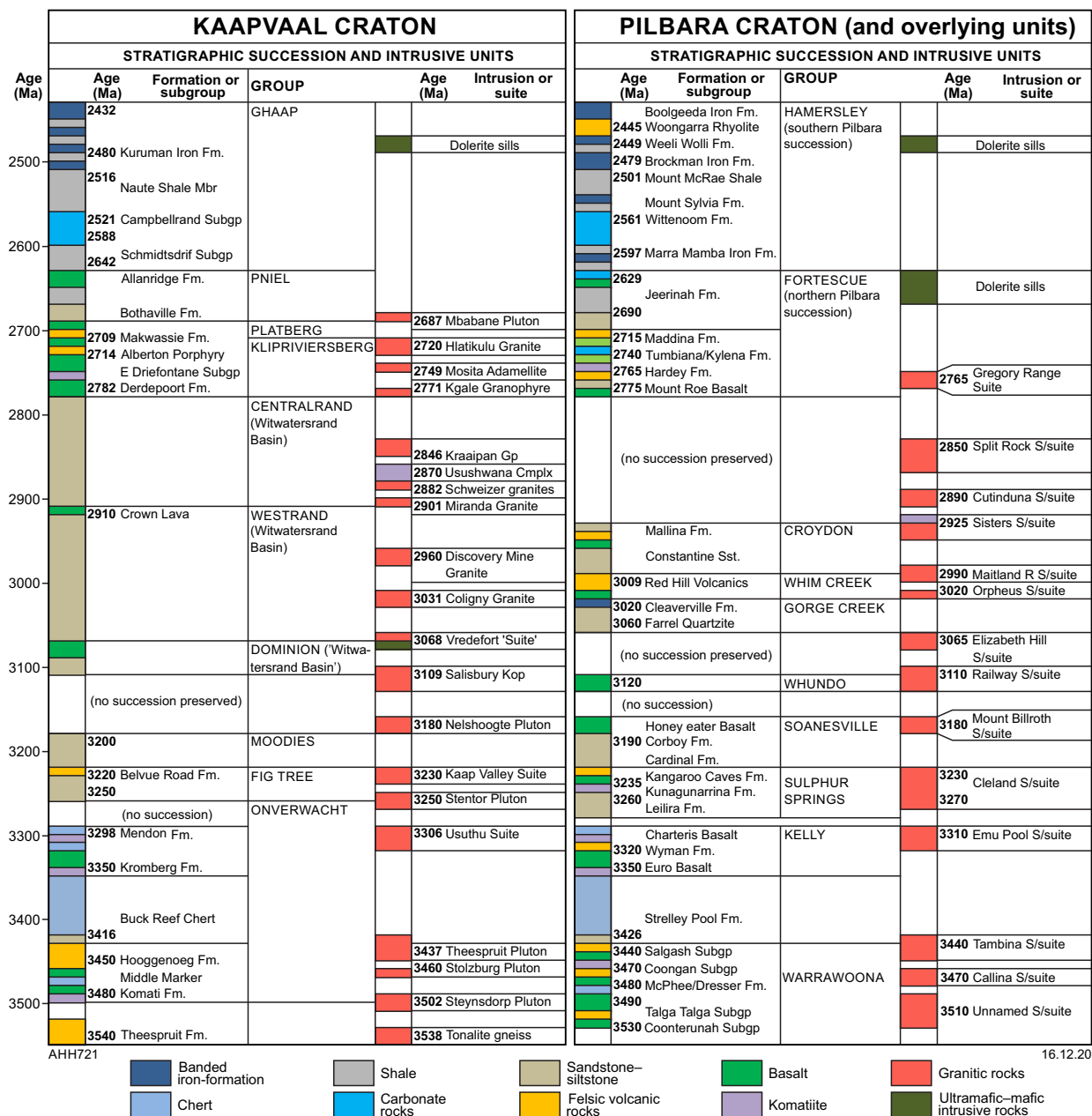


Figure 4. Stratigraphic comparison of the Pilbara and Kaapvaal successions between 3550 and 2450 Ma. Major similarities include: <2780 Ma, successions of the Fortescue and Hamersley Groups compared to the Klipriviersberg, Platberg, Pniel and Ghaap Groups; >3165 Ma, successions of the Warrawoona, Kelly, Sulphur Springs and Soanesville Groups compared to the Onverwacht, Fig Tree and Moodies Groups; 3426–3350 Ma, sedimentary deposition of the Strelley Pool Formation and Buck Reef Chert during a contemporaneous c. 75 Ma break in volcanic activity; 3500–3067 Ma, contemporaneous granitic intrusion at c. 3500, 3470–3460, 3440, 3310, 3250–3220, 3180, 3110 and 3067 Ma

As part of this Introduction, some explanation is provided on practices and conventions followed in the text of the Report:

- all U–Pb dates and ages are based on $^{207}\text{Pb}/^{206}\text{Pb}$ ratios
- all isotopic dates and ages are quoted with 95% or 2 σ uncertainties, unless noted otherwise
- an age range quoted for a geological unit (e.g. 3223–3165 Ma Soanesville Group) refers to the oldest and youngest published dates or inferred ages from that unit
- a similar practice is applied to the age ranges of tectonic units and events
- an age range quoted for cognate, xenocrystic or detrital zircons refers to the oldest and youngest published $^{207}\text{Pb}/^{206}\text{Pb}$ ages for zircons within a sample or group of related samples
- average or approximate ages of stratigraphic units, tectonic units or events are expressed by a single age (e.g. c. 3070 Ma Prinsep Orogeny)
- all ages based on Sm–Nd or Lu–Hf isotope data are two-stage depleted mantle model ages (T_{DM}^2).

Sm–Nd and Lu–Hf model ages

Whole-rock Sm–Nd isotope data (i.e. $^{143}\text{Nd}/^{144}\text{Nd}$ in combination with Sm and Nd concentrations) are commonly used to indicate ages of crustal sources. The isotope ^{147}Sm decays radioactively to ^{143}Nd , and thus the $^{143}\text{Nd}/^{144}\text{Nd}$ ratio of a rock or mineral increases over geological time at a rate proportional to the Sm/Nd ratio in the rock. A Sm–Nd model age, in its simplest form, is the time at which a sample was separated from its source in the mantle (McCulloch and Wasserburg, 1978). However, crystallizing magmas in continental settings were rarely derived from a single mantle source. Most were derived from multiple sources that had been extracted from the mantle at different times. In this situation, Nd model ages indicate only the average times from which material in samples had been resident in the continental crust (Arndt and Goldstein, 1987), and may not reveal the ages of the oldest sources.

Except for six recent Sm–Nd analyses (Gardiner et al., 2017, 2018) and Nd data on two samples from the Kurrana Terrane reported by Tyler et al. (1992), all the Nd model ages quoted in this Report (Appendix 8) were calculated and tabulated by Smithies et al. (2007a) and Champion (2013). Model ages were calculated assuming a depleted mantle (see below) and using the linear depletion model which assumes linear depletion from $\epsilon_{\text{Nd}} = 0$ at 4560 Ma to +10 today (Champion and Huston, 2016). The epsilon-Nd (ϵ_{Nd}) value is the relative deviation of the $^{143}\text{Nd}/^{144}\text{Nd}$ ratio from the chondritic ratio in parts per ten thousand (White, 2013). T_{DM}^2 ages used in this Report were calculated assuming that the first fractionation event occurred during mantle melting and a second event occurred in the crust during partial melting. The calculation of two-stage model ages is described by Champion and Huston (2016). Table 4 summarizes published Nd model ages and ϵ_{Nd} values for Paleoarchean and Mesoarchean stratigraphic units of the east Pilbara Craton. Appendix 8 lists all available Nd data from the eastern section of the northern Pilbara Craton.

Although a Nd model age might underestimate the age of the first mantle extraction event, in combination with

measured or assumed sample crystallization ages (from U–Pb zircon data), the model age nevertheless indicates the degree to which the ages of sources were greater than the crystallization age of the rock. This provides important evidence on crustal evolution. For example, if over any given period the differences between source ages and crystallization ages consistently increase with time, it can be concluded that recycling of old crust predominated over new additions of juvenile magmas. Conversely, a sudden change to only small differences between source ages and crystallization ages (as occurred in the Pilbara Craton at c. 3530 Ma, and apparently also at c. 3200 Ma) indicates a major new influx of juvenile magma.

The ϵ_{Nd} value is significant to crustal evolution studies by providing another measure of the difference between a rock's crystallization age and the time at which its sources were extracted from the mantle. A negative ϵ_{Nd} value implies that, over time, the average Sm/Nd ratio of the rock or its precursors has been lower than the chondritic ratio, indicating light rare earth element (LREE) enrichment. Negative ϵ_{Nd} values are typical of continental crust in which the Nd system has been separated from the Sm-enriched mantle for many millions of years, and indicate crustal reworking. Positive ϵ_{Nd} values indicate juvenile, mantle-derived melts, as in mid-ocean ridge basalt (MORB) and magmatic arcs produced by subduction and melting of oceanic crust.

In the context of this Report, Nd data provide part of the isotopic evidence for extensive pre-3530 Ma crust in the EPT (Van Kranendonk et al., 2006b, 2007a,b). However, the ages of crustal sources indicated by all the available whole-rock Sm–Nd analyses relate only to the currently exposed Paleoarchean and Mesoarchean Pilbara Craton rocks; the significance of Eoarchean and early Paleoarchean crust underlying the Pilbara Supergroup in the Paleoarchean is inevitably understated due to the inclusion of data from samples of Mesoarchean igneous rocks with relatively juvenile sources. The data in Table 2 and Appendix 3 suggest that Paleoarchean igneous rocks of the EPT were partly derived from 3760–3550 Ma crustal sources. However, evidence for considerably older crust (up to c. 4000 Ma) in the Pilbara Craton is provided by Hf model ages obtained from 3760–3550 Ma zircons (Kemp et al., 2015a,b); these 3760–3550 Ma zircons indicate the crystallization ages of igneous rocks within the pre-3530 Ma crust, and these 3760–3550 Ma rocks had older sources.

The lutetium–hafnium (Lu–Hf) system in zircon is capable of providing important isotopic evidence on crustal and mantle evolution. In particular, as for the Sm–Nd system, isotope values in the Lu–Hf system have been used to indicate mantle extraction ages. The Lu–Hf system in zircon has an advantage over the whole-rock Sm–Nd systematics in that it is less prone to disturbance by metamorphism and weathering. Hf isotope ratios, between ^{176}Hf (produced by decay of ^{176}Lu) and ^{177}Hf , are expressed using the ϵ -notation that was first developed for Nd. Zircon is particularly useful for measuring the initial $^{176}\text{Hf}/^{177}\text{Hf}$ ratio inherited from the melt in which it crystallized because Hf is greatly concentrated relative to Lu. This minimizes post-crystallization changes in $^{176}\text{Hf}/^{177}\text{Hf}$ by decay of ^{176}Lu . High values of $^{176}\text{Hf}/^{177}\text{Hf}$, and therefore also high (positive) ϵ_{Hf} values, indicate a juvenile or mantle-derived origin for a magma, whereas low ϵ_{Hf} values imply the reworking of old crustal material. The crystallization of zircon preserves the $^{176}\text{Hf}/^{177}\text{Hf}$ ratio of the parent magma.

Table 2. Summary of inherited zircon ages >3530 Ma in igneous rocks of the east Pilbara Craton

Sample	Analysis label	Date (Ma)	Uncertainty (1 σ) (Ma)	Rock type	Stratigraphic unit	Dome/terrane	Reference
15TKPB17	1	3535	8	rhyolite	Tambina Supersuite	North Pole	Petersson et al. (2019c)
142828	21.1	3538	3	granodiorite	Callina Supersuite	Muccan	Nelson (1998e)
178022	23.1	3538	4	granodiorite	Emu Pool Supersuite	Muccan	Nelson (2005l)
180057	8.1	3538	4	tonalite gneiss	Tambina Supersuite	Warrawagine	Wingate et al. (2009d)
180057	36.1	3541	8	tonalite gneiss	Tambina Supersuite	Warrawagine	Wingate et al. (2009d)
95NS-281	5b	3544	30	rhyolite	Duffer Formation	North Pole	Kabashima et al. (2003)
15TKPB17	n_16	3544	5	rhyolite	Tambina Supersuite	North Pole	Petersson et al. (2019c)
180057	19.1	3549	2	tonalite gneiss	Tambina Supersuite	Warrawagine	Wingate et al. (2009d)
180056	14.1	3552	3	granophyre	Shay Intrusion	Muccan	Wingate et al. (2009c)
142936	9.1	3552	5	monzogranite	Sisters Supersuite	Yule	Nelson (2000a)
180057	4.1	3553	5	tonalite gneiss	Tambina Supersuite	Warrawagine	Wingate et al. (2009d)
18APB12	7	3554	2	rhyolite	Tambina Supersuite	North Pole	Petersson et al. (2019c)
180057	20.1	3556	3	tonalite gneiss	Tambina Supersuite	Warrawagine	Wingate et al. (2009d)
15TKPB17	2	3556	6	rhyolite	Tambina Supersuite	North Pole	Petersson et al. (2019c)
96NS-430	3a	3558	45	felsic tuff	Duffer Formation	North Pole	Kabashima et al. (2003)
180057	11.1	3561	7	tonalite gneiss	Tambina Supersuite	Warrawagine	Wingate et al. (2009d)
15TKPB17	12b	3565	3	rhyolite	Tambina Supersuite	North Pole	Petersson et al. (2019c)
15TKPB17	n_39	3566	5	rhyolite	Tambina Supersuite	North Pole	Petersson et al. (2019c)
142870	22.1	3570	3	tonalite gneiss	Tambina Supersuite	Warrawagine	Nelson (1999e)
142828	25.1	3574	3	granodiorite	Callina Supersuite	Muccan	Nelson (1998e)
142870	11.1	3575	3	tonalite gneiss	Tambina Supersuite	Warrawagine	Nelson (1999e)
180057	18.1	3575	6	tonalite gneiss	Tambina Supersuite	Warrawagine	Wingate et al. (2009d)
180057	23.1	3575	7	tonalite gneiss	Tambina Supersuite	Warrawagine	Wingate et al. (2009d)
96NS-430	3b	3576	44	felsic tuff	Duffer Formation	North Pole	Kabashima et al. (2003)
178203	5.1	3577	4	granodiorite	Emu Pool Supersuite	Kurrana Terrane	Nelson (2000m)
142870	23.1	3577	5	tonalite gneiss	Tambina Supersuite	Warrawagine	Nelson (1999e)
180057	25.1	3578	3	tonalite gneiss	Tambina Supersuite	Warrawagine	Wingate et al. (2009d)
180057	28.1	3579	6	tonalite gneiss	Tambina Supersuite	Warrawagine	Wingate et al. (2009d)
15TKPB17	1b	3580	3	rhyolite	Tambina Supersuite	North Pole	Petersson et al. (2019c)
142967	15.1	3580	5	monzogranite	Sisters Supersuite	Shaw	Nelson (2000o)
142870	17.1	3582	5	tonalite gneiss	Tambina Supersuite	Warrawagine	Nelson (1999e)
178203	16.1	3582	9	granodiorite	Emu Pool Supersuite	Kurrana Terrane	Nelson (2000m)
180057	14.1	3583	3	tonalite gneiss	Tambina Supersuite	Warrawagine	Wingate et al. (2009d)
142870	21.1	3583	5	tonalite gneiss	Tambina Supersuite	Warrawagine	Nelson (1999e)
15TKPB17	21	3589	10	rhyolite	Tambina Supersuite	North Pole	Petersson et al. (2019c)
15TKPB17	4c	3589	2	rhyolite	Tambina Supersuite	North Pole	Petersson et al. (2019c)
18APB13	2	3590	3	rhyolite	Tambina Supersuite	North Pole	Petersson et al. (2019c)
142870	12.1	3593	4	tonalite gneiss	Tambina Supersuite	Warrawagine	Nelson (1999e)
142884	4.1	3600	3	syenogranite	Sisters Supersuite	Tambourah	Nelson (1998j)
142870	9.1	3601	5	tonalite gneiss	Tambina Supersuite	Warrawagine	Nelson (1999e)
18APB13	9	3601	5	rhyolite	Tambina Supersuite	North Pole	Petersson et al. (2019c)
18APB13	6	3603	3	rhyolite	Tambina Supersuite	North Pole	Petersson et al. (2019c)
18APB12	3	3605	3	rhyolite	Tambina Supersuite	North Pole	Petersson et al. (2019c)
142870	14.1	3608	5	tonalite gneiss	Tambina Supersuite	Warrawagine	Nelson (1999e)
95NS-281	5a	3609	31	rhyolite	Tambina Supersuite	North Pole	Kabashima et al. (2003)
18APB16	2	3612	3	rhyolite	Tambina Supersuite	North Pole	Petersson et al. (2019c)
178031	17.1	3621	3	granodiorite	Cleland Supersuite	Muccan	Nelson (2005f)
18APB13	1	3626	4	rhyolite	Tambina Supersuite	North Pole	Petersson et al. (2019c)
KB312	N/A	3629	35	granodiorite	Cleland Supersuite	Carlindi	Beintema (2003)

Table 2. continued

Sample	Analysis label	Date (Ma)	Uncertainty (1 σ) (Ma)	Rock type	Stratigraphic unit	Dome/terrane	Reference
142870	16.1	3631	5	tonalite gneiss	Tambina Supersuite	Warrawagine	Nelson (1999e)
15TKPB17	n_2a	3632	8	rhyolite	Tambina Supersuite	North Pole	Petersson et al. (2019c)
142870	5.1	3638	4	tonalite gneiss	Tambina Supersuite	Warrawagine	Nelson (1999e)
15TKPB17	n_1a	3640	3	rhyolite	Tambina Supersuite	North Pole	Petersson et al. (2019c)
18APB12	4	3641	3	rhyolite	Tambina Supersuite	North Pole	Petersson et al. (2019c)
142870	2.1	3641	4	tonalite gneiss	Tambina Supersuite	Warrawagine	Nelson (1999e)
18APB13	5	3650	3	rhyolite	Tambina Supersuite	North Pole	Petersson et al. (2019c)
142870	1.1	3650	6	tonalite gneiss	Tambina Supersuite	Warrawagine	Nelson (1999e)
142870	18.1	3655	3	tonalite gneiss	Tambina Supersuite	Warrawagine	Nelson (1999e)
142870	20.1	3656	4	tonalite gneiss	Tambina Supersuite	Warrawagine	Nelson (1999e)
142870	7.1	3658	3	tonalite gneiss	Tambina Supersuite	Warrawagine	Nelson (1999e)
96NS-410	80	3660	62	rhyolite	Tambina Supersuite	North Pole	Kitajima et al. (2008)
18APB13	8	3675	4	rhyolite	Tambina Supersuite	North Pole	Petersson et al. (2019c)
15TKPB17	16	3676	4	rhyolite	Tambina Supersuite	North Pole	Petersson et al. (2019c)
18APB13	3	3678	3	rhyolite	Tambina Supersuite	North Pole	Petersson et al. (2019c)
15TKPB17	13b	3681	5	rhyolite	Tambina Supersuite	North Pole	Petersson et al. (2019c)
15TKPB17	14b	3689	5	rhyolite	Tambina Supersuite	North Pole	Petersson et al. (2019c)
18APB16	1	3696	3	rhyolite	Tambina Supersuite	North Pole	Petersson et al. (2019c)
15TKPB17	10	3696	4	rhyolite	Tambina Supersuite	North Pole	Petersson et al. (2019c)
15TKPB17	n_5	3699	1	rhyolite	Tambina Supersuite	North Pole	Petersson et al. (2019c)
15TKPB17	n_1b	3704	3	rhyolite	Tambina Supersuite	North Pole	Petersson et al. (2019c)
15TKPB17	n_4b	3710	2	rhyolite	Tambina Supersuite	North Pole	Petersson et al. (2019c)
15TKPB17	n_14	3713	5	rhyolite	Tambina Supersuite	North Pole	Petersson et al. (2019c)
15TKPB17	18	3715	4	rhyolite	Tambina Supersuite	North Pole	Petersson et al. (2019c)
18APB13	7	3718	3	rhyolite	Tambina Supersuite	North Pole	Petersson et al. (2019c)
15TKPB17	6	3718	5	rhyolite	Tambina Supersuite	North Pole	Petersson et al. (2019c)
100507	AA	3724	1	rhyolite	Tambina Supersuite	North Pole	Thorpe et al. (1992a)
15TKPB17	n_15a	3729	2	rhyolite	Tambina Supersuite	North Pole	Petersson et al. (2019c)
18APB13	4	3729	4	rhyolite	Tambina Supersuite	North Pole	Petersson et al. (2019c)
15TKPB17	2b	3731	2	rhyolite	Tambina Supersuite	North Pole	Petersson et al. (2019c)
15TKPB17	n_3	3732	3	rhyolite	Tambina Supersuite	North Pole	Petersson et al. (2019c)
15TKPB17	19	3733	5	rhyolite	Tambina Supersuite	North Pole	Petersson et al. (2019c)
15TKPB17	n_15b	3735	2	rhyolite	Tambina Supersuite	North Pole	Petersson et al. (2019c)
15TKPB17	n_41	3746	3	rhyolite	Tambina Supersuite	North Pole	Petersson et al. (2019c)
15TKPB17	5	3746	4	rhyolite	Tambina Supersuite	North Pole	Petersson et al. (2019c)
18APB12	2	3753	3	rhyolite	Tambina Supersuite	North Pole	Petersson et al. (2019c)
18APB12	1	3760	3	rhyolite	Tambina Supersuite	North Pole	Petersson et al. (2019c)

Depleted or chondritic Paleoarchean mantle?

Previous interpretations of Sm–Nd and Lu–Hf isotope data from the Pilbara Craton have differed due to different interpretations of the composition of the Paleoarchean mantle (i.e. depleted or chondritic). Most workers have assumed that from the Hadean onwards there was progressive depletion of incompatible elements in the mantle due to repeated crustal extractions over time (McCulloch and Wasserberg, 1978; DePaolo, 1980, 1988; Hofmann, 1997; Griffin et al., 2000; Hasenstab et al., 2019). If Archean mantle depletion occurred at a rate similar to Phanerozoic depletion, there would have been a significantly depleted mantle by c. 3500 Ma (Bennett et al., 1993; McCulloch and Bennett, 1993; Amelin et al., 1999, 2000). On the other hand, some workers have interpreted Earth's mantle at c. 3500 Ma to be essentially chondritic (Vervoort and Blichert-Toft, 1999; Vervoort, 2011; Vervoort and Kemp, 2016; Fisher and Vervoort, 2018). Nd and Hf model ages calculated for Paleoarchean rocks or zircons from Pilbara Craton samples are likely to differ by more than 100 Ma depending on whether depleted mantle or chondritic mantle models are applied.

Kemp et al. (2015a) indicated that application of a depleted mantle model to the Hf isotope data they had obtained from c. 3600 Ma Pilbara zircons would give Hf model ages up to c. 4000 Ma. However, they rejected the concept of a significantly depleted mantle at c. 3600 Ma for two main reasons: 1) previous evidence questioning mantle depletion at this time; 2) uncertainty over the degree of Pb loss in the old zircons. They argued that significant Pb loss would cause calculated ϵ_{Hf} values to be too low, resulting in model ages that are too old. Based on studies elsewhere (e.g. Vervoort and Blichert-Toft, 1998), Kemp et al. (2015a) argued that the c. 3600 Ma Pilbara zircons had most likely crystallized from magmas extracted from a mantle of approximately chondritic composition. Under this interpretation, the Hf isotope data do not suggest sources much older than the zircon crystallization ages – that is, up to c. 3680 Ma. Izumi et al. (2017) reviewed the factors influencing the extent to which two-stage Hf model ages, as used in this Report, indicate the timing of crust generation. They noted that large uncertainties exist in the calculation, including the choice of $^{176}\text{Lu}/^{177}\text{Hf}$ for reworked crust and extrapolation of the Hf isotope evolution of juvenile continental crust. They also noted the possibility that the parental magmas of the zircons were from mixed sources; for example, a juvenile component in addition to reworked older crust.

It is likely that rates and degrees of Archean mantle depletion varied in different areas of the Earth. For example, it is questionable whether rates of mantle depletion during the operation of plate tectonic processes would have been similar to rates under different tectonic processes in the Paleoarchean and earlier. Another uncertainty is the extent of mantle depletion prior to c. 3800 Ma due to decompression melting related to major asteroid impacts (e.g. Late Heavy Bombardment), which resulted in the extraction of large volumes of basaltic melts. Even so, most interpretations of Sm–Nd and Lu–Hf data have either assumed or concluded that the mantle was depleted in the early Paleoarchean (Bennett et al., 1993; McCulloch and Bennett, 1993; Amelin et al., 1999, 2000; Belousova et al., 2010; Blichert-Toft and Puchtel, 2010; Nebel-Jacobsen et al., 2010; Guitreau et al., 2012; Champion, 2013; Griffin et al., 2014; Zeh et al., 2013, 2014; Nebel et al., 2014; Roberts and Spencer, 2015;

Champion and Huston, 2016; Kröner et al., 2016; Gardiner et al., 2017, 2018; Hasenstab et al., 2019), or even in the Hadean (Hoffmann et al., 2010). In the global database of Roberts and Spencer (2015), hundreds of >3500 Ma zircons recorded positive ϵ_{Hf} values well above the $^{176}\text{Hf}/^{177}\text{Hf}$ ratio that would apply to a chondritic mantle, CHUR (Chondritic Uniform Reservoir). Positive ϵ_{Hf} values are consistent with mantle depletion. If a Paleoarchean depleted mantle is assumed during the evolution of the EPT, the available Lu–Hf data indicate average source ages of 3700–3600 Ma for Paleoarchean rocks of the Pilbara Craton.

Mantle depletion, resulting from ongoing crustal extractions since the Hadean, has been assumed in calculating Nd model ages previously published by GSWA and Geoscience Australia. Accordingly, in this Report, Nd and Hf model ages (T_{DM}^2) are calculated based on a depleted mantle in which it is assumed that depletion occurred at a constant rate from c. 4500 Ma. However, it is recognized that these ages are likely to be inaccurate due to various unknown factors, including the unknown degree of mantle depletion in the Archean and the possibility that the parental magmas were mixtures of more than one generation of components (Arndt and Goldstein, 1987; Kemp et al., 2006).

Pilbara Craton overview

Tectonic units of the northern Pilbara Craton

Most investigations of the northern section of the Pilbara Craton have been within a 60 000 km² exposure (Fig. 3) that includes the East Pilbara, Karratha, and Kurrana Terranes, and several Mesoarchean basins unconformably overlying these terranes. Windows into the largely concealed southern part of the craton are available in the Sylvania, Milli Milli, Rocklea, and Wyloo Inliers (Fig. 2). The northern Pilbara Craton is composed of eight major tectonic units.

1. **Early crust, 3800–3530 Ma:** continental crust pre-dating the Pilbara Supergroup. Enclaves of tonalite gneiss and metagabbro within Paleoarchean granitic rocks have been dated between c. 3650 and 3580 Ma (McNaughton et al., 1988; Nelson, 1999d; Williams and Hickman, 2000; Wingate et al., 2009d; Petersson et al., 2019a). Published ages of xenocrystic zircons in igneous rocks and of detrital zircons in sedimentary rocks are locally greater than c. 3530 Ma (Thorpe et al., 1992a; Van Kranendonk et al., 2002, 2007a,b; Bagas et al., 2004b, 2008; Hickman, 2012; Kemp et al., 2015a,b; Sheppard et al., 2017; Gardiner et al., 2018b; Wiemer et al., 2018; Petersson et al., 2019c). Such pre-3530 Ma zircons were derived from older crust. Additionally, whole-rock Sm–Nd isotope data (Jahn et al., 1981; Collerson and McCulloch, 1983; Gruau et al., 1987; McCulloch, 1987; Bickle et al., 1989, 1993; Tyler et al., 1992; Van Kranendonk et al., 2002, 2007a,b; Smithies et al., 2007a; Champion, 2013; Champion and Huston, 2016; Gardiner et al., 2017, 2018a) and zircon Lu–Hf isotope data (Amelin et al., 2000; Guitreau et al., 2012; Nebel et al., 2014; Kemp et al., 2015a,b; Gardiner et al., 2017, 2018a,b) have indicated pre-3530 Ma sources for many rocks. The resulting conclusion, that

3800–3530 Ma crust formed an extensive ‘basement’ to the Pilbara Supergroup, constrains possible tectonic processes for the Paleoproterozoic crustal evolution of the craton; in particular, it precludes some previous interpretations that the Pilbara Supergroup originated as oceanic crust (Glikson, 1972; Kimura et al., 1991; Isozaki et al., 1991; Kitajima et al., 2001; Komiya et al., 2002; Kato and Nakamura, 2003; Terabayashi et al., 2003; Nijman et al., 2017). Accordingly, this Report examines all the currently available evidence on the pre-Pilbara Supergroup crust.

2. **East Pilbara Terrane (EPT), 3530–3223 Ma:** the principal Paleoproterozoic granite–greenstone terrane of the Pilbara Craton exposed across 40 000 km² of the east Pilbara Craton (Figs 3, 5). Reference to the EPT in this Report relates either to the EPT prior to c. 3220 Ma or to the exposed EPT north of the Fortescue Valley. The stratigraphic succession of the EPT comprises four volcanic groups (Warrawoona, Kelly, Sulphur Springs, and Roebourne) that together make up the Pilbara Supergroup (Fig. 6, Table 1). Spanning 300 Ma, this supergroup was deposited on a volcanic plateau (Van Kranendonk et al., 2002, 2007a,b, 2014a), the dimensions of which far exceeded the present area of the EPT. In this Report, the Warrawoona and Kelly Groups are interpreted to represent large igneous provinces (LIP; Hickman, 2012; Fig. 7). The Sulphur Springs and Roebourne Groups are not parts of a LIP because the successions are thinner, have restricted distributions, and in the case of the Sulphur Springs Group, contain a substantial sedimentary component. The Roebourne and Sulphur Springs Groups were rifted apart at c. 3220 Ma (Sun and Hickman, 1998; Hickman, 2016). The granitic rocks of the EPT were intruded during five separate magmatic events and are assigned to separate supersuites (Mulgundooona, Callina, Tambina, Emu Pool, and Cleland). The existence of the 3530–3490 Ma Mulgundooona Supersuite has recently been confirmed by geochronology in the Muccan and Carlindi Domes (Wiemer et al., 2018; Petersson et al., 2019b, 2020).
3. **Kurrana Terrane (KUT), 3530–3178 Ma:** a terrane inferred to have originated in the Paleoproterozoic EPT, but separated from that terrane during c. 3220 Ma continental breakup. The northern part of the KUT (Figs 3, 8), within the area mapped as part of the PCMP, exposes only Mesoarchean igneous and metasedimentary units. Three granitic supersuites (Mount Billroth, Cutinduna, and Split Rock) and greenstone units of uncertain age have been identified, and xenocrystic zircon ages indicate non-exposed units of the 3270–3223 Ma Cleland Supersuite. The southern part of the KUT is largely concealed by Neoproterozoic volcanic and sedimentary formations of the Fortescue and Hamersley Basins (Hickman, 2004), and the terrane therefore has an uncertain history of crustal evolution. The KUT is interpreted to include the Sylvania Inlier (Tyler et al., 1992; Bagas et al., 2004a, 2008; Hickman, 2004; Hickman and Van Kranendonk, 2008a), and Bouguer gravity data in the far southeast part of the Pilbara Craton suggest a concealed ‘dome-and-keel’ crustal architecture similar to that of the EPT. The extent of the KUT west of the Sylvania Inlier is currently unknown.
4. **Soanesville Basin and related clastic sedimentary basins, 3228–3165 Ma:** passive-margin basins formed by rifting and breakup of the pre-3220 Ma crust (Van Kranendonk et al., 2010) during the East Pilbara Terrane Rifting Event (EPTRE). Evidence of early rifting between c. 3280 and 3220 Ma includes syndepositional normal faulting in the Sulphur Springs Group (Buick et al., 2002; Van Kranendonk, 2004b) and intrusion of c. 3235 Ma gabbro along the faulted northwest margin of the EPT (Beintema, et al., 2001; Beintema, 2003; Hickman, 2016). Other passive-margin basins formed as a consequence of the rifting and plate separation were located between the EPT and the KT in the northwest Pilbara Craton (Nickol River Basin), and between the EPT and the KUT in the east Pilbara Craton (Mosquito Creek Basin).
5. **Mosquito Creek Basin, 3200–2930 Ma:** a rift basin formed between the EPT and the KUT during the EPTRE, and containing mafic volcanic and clastic sedimentary successions of the c. 3200 to 2930 Ma Nullagine Group. In ascending stratigraphic order, this group comprises the c. 3200 to 3165 Ma Coondamar Formation and the c. 2980 to 2930 Ma Mosquito Creek Formation. Geochronology is too limited to closely constrain the depositional ages of the formations.
6. **West Pilbara Superterrane, 3280–3070 Ma:** formed by the accretion of three terranes (Karratha, Regal, and Sholl) at c. 3070 Ma (Van Kranendonk et al., 2002, 2006b, 2007b; Hickman, 2004, 2016), and restricted to the northwest Pilbara Craton. The three terranes differ in age, are separated by major shear zones, and evolved in different tectonic settings. The Central Pilbara Tectonic Zone (CPTZ), which evolved as a zone of deformation, metamorphism, and magmatic intrusion between c. 3200 and 2900 Ma, is superimposed on the Regal and Sholl Terranes, and on basins of the younger De Grey Superbasin in the northwest Pilbara Craton.
7. **De Grey Superbasin, 3066–2930 Ma:** comprising three mainly sedimentary basins (Gorge Creek, Whim Creek, and Mallina Basins) and three contemporaneous, mainly granitic, supersuites (Orpheus, Maitland River, and Sisters). The distribution of these supersuites indicates progressive southeastwards migration of Mesoarchean magmatism from the northwest Pilbara Craton into the EPT (Hickman, 2016), and possibly into the KUT (this Report). Evolution of all these units was related to convergence of plates marginal to the CPTZ.
8. **Split Rock Supersuite, 2851–2831 Ma:** post-orogenic granitic intrusions (Van Kranendonk et al., 2006a).

Proterozoic to early Paleoproterozoic evolution

One of the most contentious questions for the interpretation of Archean granite–greenstone terranes has centred on the origin of the greenstones: do the greenstones represent the oldest preserved crust or were the greenstones deposited on even older crust? Many lines of evidence obtained from the PCMP combine to indicate that the 3530–3235 Ma Pilbara Supergroup was deposited on older crust, apparently at least 3800 Ma in age. The evidence is stratigraphic, geochemical, geochronological and isotopic, although the most direct evidence is provided by exposed remnants of the pre-3530 Ma crust.

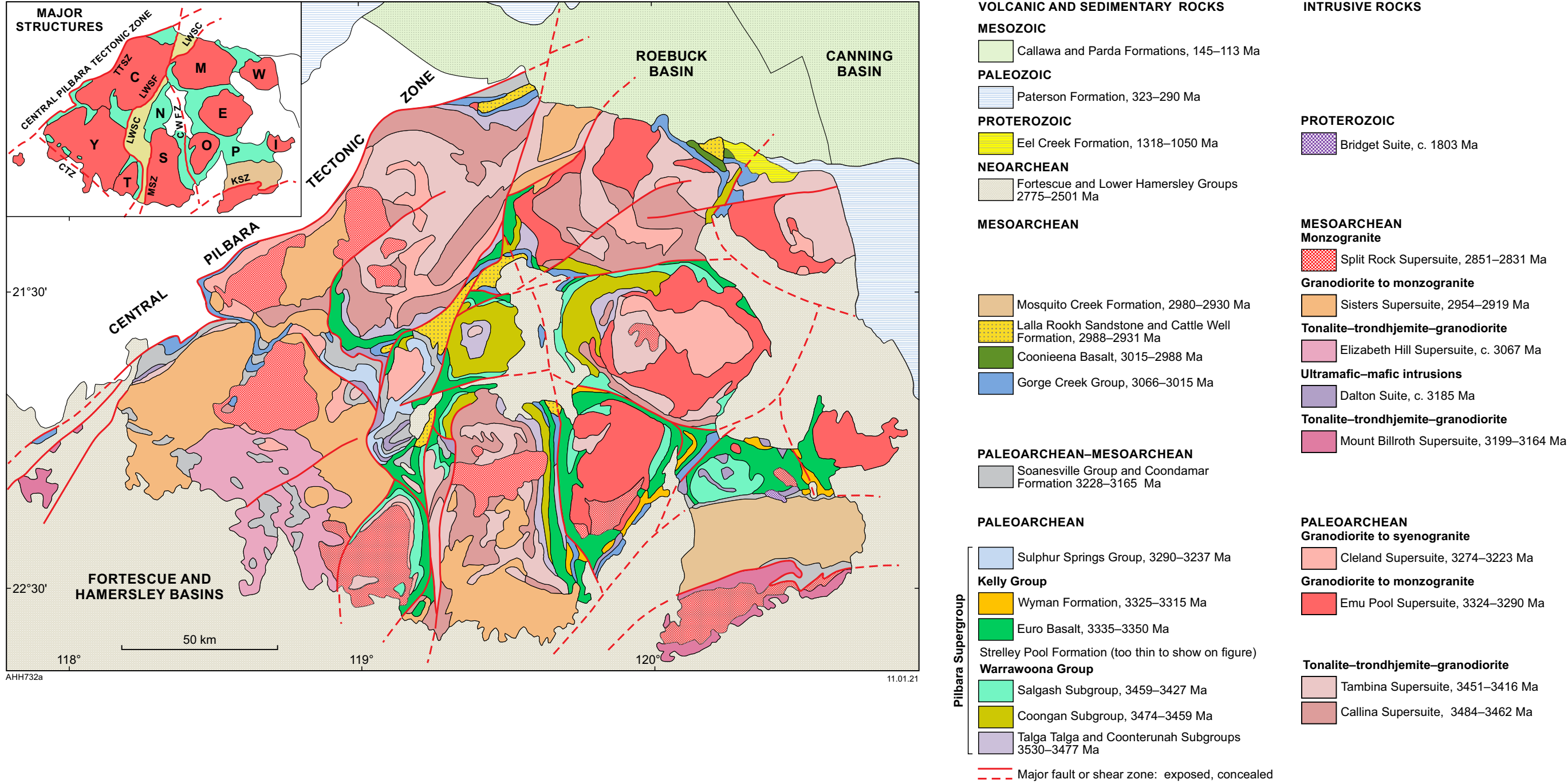


Figure 5. Simplified geological map of the east Pilbara Craton. Mainly volcanic groups and subgroups of the Paleoproterozoic EPT are unconformably overlain by mainly sedimentary Mesoproterozoic groups. Inset: domes and major structural features of the east Pilbara Craton. Dome abbreviations: C, Carlindi; E, Mount Edgar; I, Yilgalong; M, Muccan; N, North Pole; O, Corunna Downs; P, McPhee; S, Shaw; T, Tambourah; W, Warrawagine; Y, Yule. Structure abbreviations: CWFZ, Coongan–Warralong Fault Zone; CTZ, Chichester Tectonic Zone; KSZ, Kurrana Shear Zone; LWSF, Lalla Rookh – Western Shaw Structural Corridor; LWSC, Lalla Rookh – Western Shaw Fault; MSZ, Maitland Shear Zone

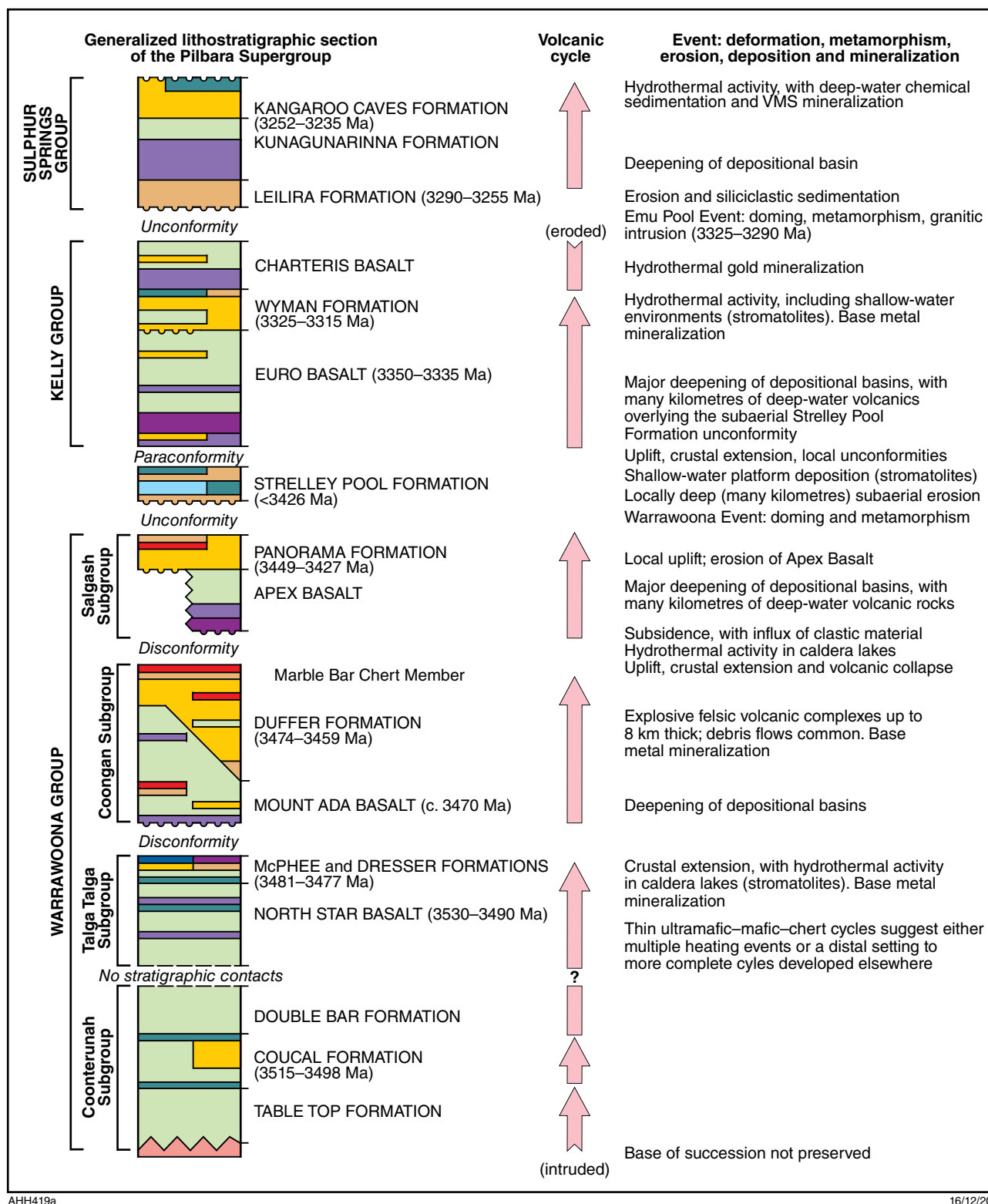
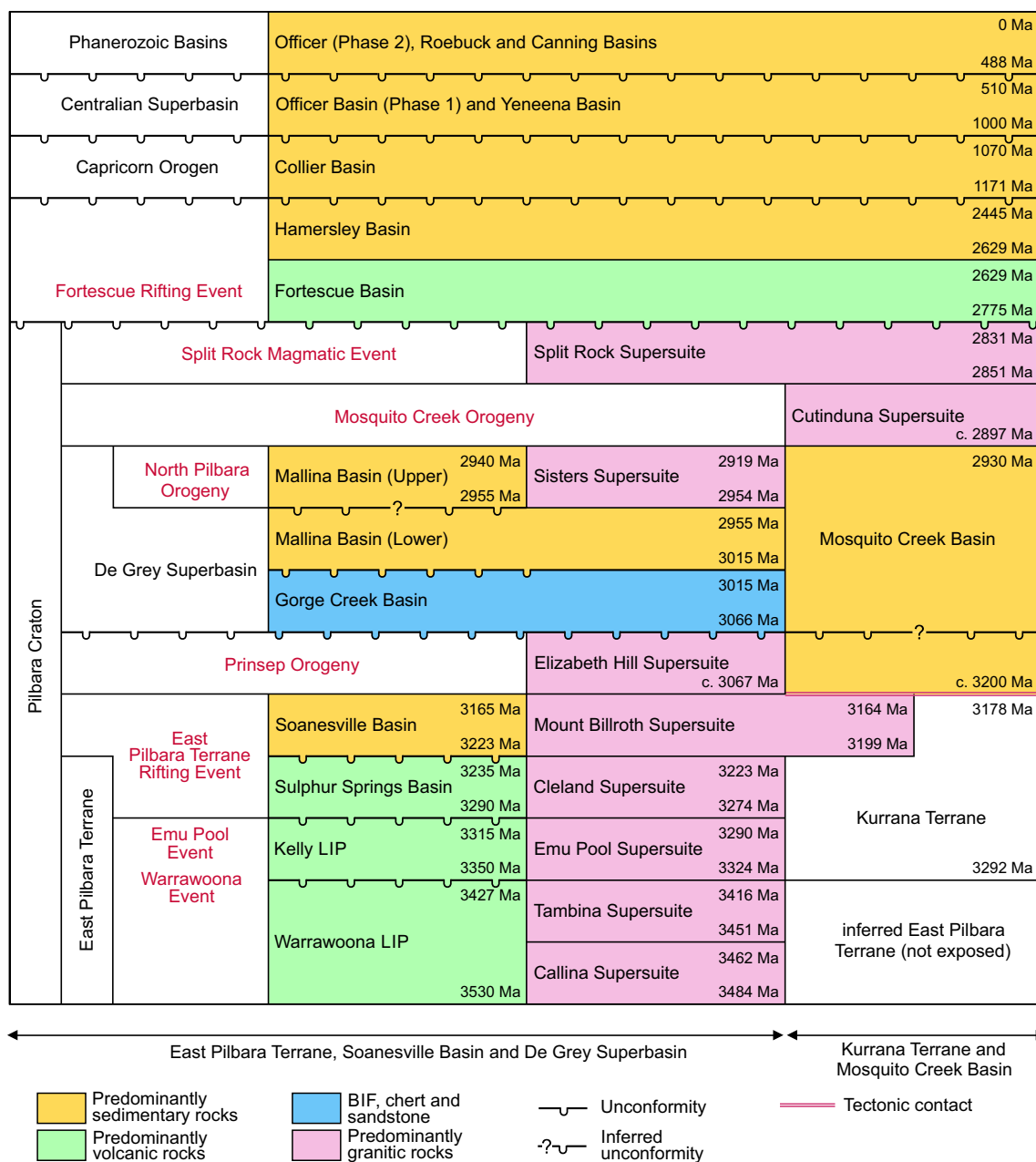


Figure 6. Generalized lithostratigraphy of the Pilbara Supergroup. The succession is composed of multiple volcanic cycles, most of which are separated by unconformities. Geochronology indicates that the Coonterunah and Talga Talga Subgroups are the same age, and each is interpreted to contain three volcanic cycles. Events of deformation, metamorphism, erosion and mineralization are noted (after Hickman, 2012)



AHH728

11.01.21

Figure 7. Diagrammatic illustration of the ages and contact relationships of terranes, basins, supersuites and events in the east Pilbara Craton. The East Pilbara Terrane Rifting Event (EPTRE) separates the Paleoarchean EPT from Mesoarchean units commencing with the Soanesville Basin and Mount Billroth Supersuite. The Mosquito Creek Basin and Kurrana Terrane have uncertain stratigraphic relationships to the successions overlying the EPT, although the Coondamar Basin (not shown), underlying the Mosquito Creek Basin, is about the same age as the Soanesville Basin

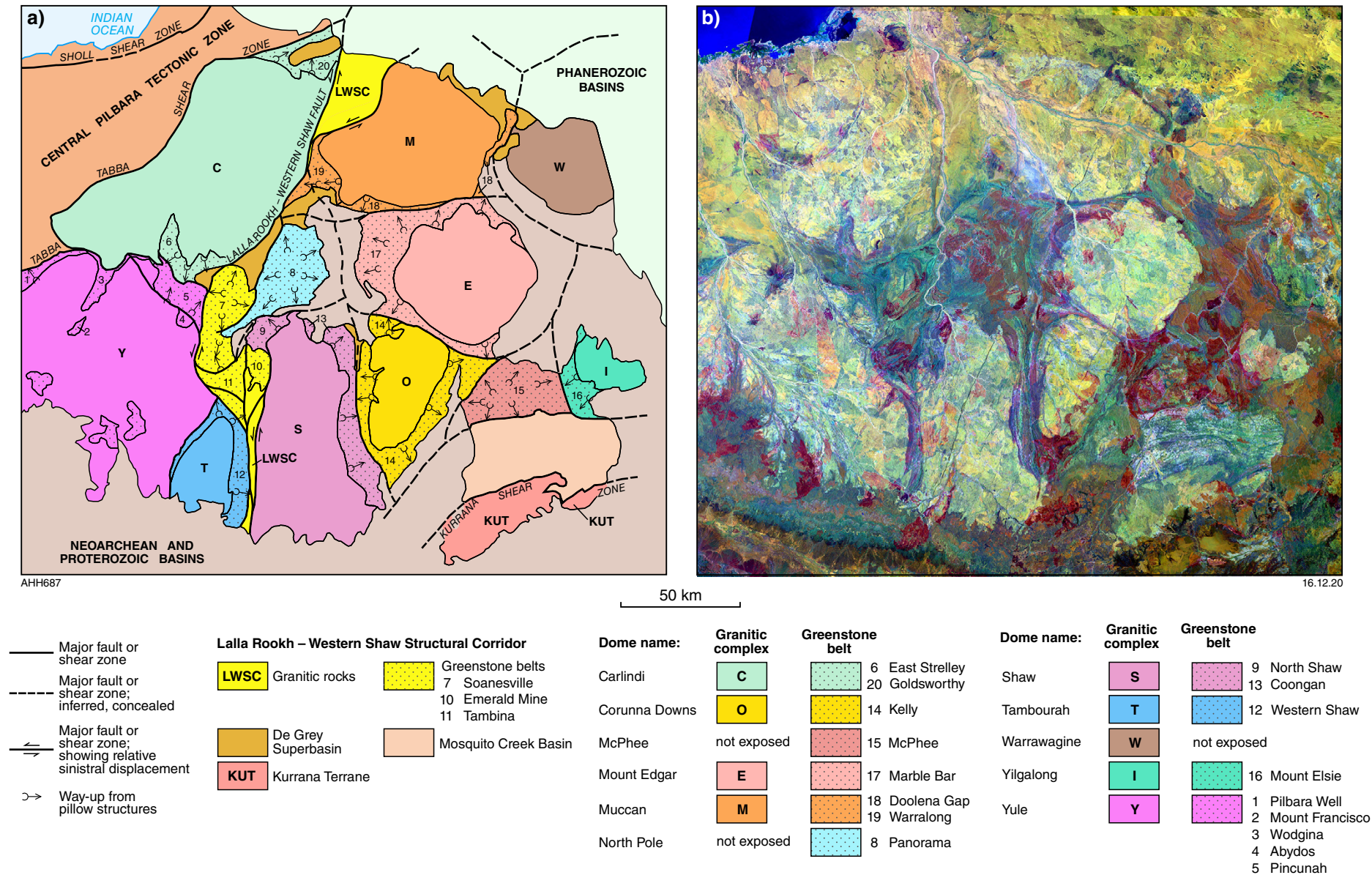


Figure 8. Granite-greenstone domes of the eastern Pilbara Craton: a) simplified structural map showing separation of domes by major faults; b) Landsat Thematic Mapper image (Bands 7, 4 and 1). Domes are composed of coupled granitic cores and greenstone belts, and are separated by major faults (Plate 1C). Colours have no age significance

Remnants of pre-3530 Ma crust

Remnants of pre-3530 Ma crust are rare owing its destruction by tectonic processes such as partial convective overturn and sagduction, and by periodic displacement and assimilation by Paleoproterozoic granitic intrusions. Even so, fragments of the pre-3530 Ma crust have been identified in several areas of the EPT: two areas in the Warrawagine Dome; an area in the Shaw Dome; and an area in the Muccan Dome. More recently, 3566–3565 Ma tonalite has been identified by U–Pb zircon dating in the Sylvania Inlier (Fig. 2) of the Kurrana Terrane (GSWA 195897, Wingate et al., 2017a; GSWA 203712, Wingate et al., 2017b). The Sylvania Inlier was not mapped during the PCMP, and is consequently not described in this Report.

Warrawagine Dome

U–Pb zircon data (GSWA 142870, Nelson, 1999e; Williams, 1999a; GSWA 180057, Wingate et al., 2009d) for xenoliths of banded tonalite gneiss in the Warrawagine Dome (Fig. 8, Plate 1) reveal mixed zircon ages: old zircons with crystallization ages between c. 3660 and 3570 Ma, and younger zircons with Paleoproterozoic ages (Fig. 9a,b). The preferred interpretation of these data (Nelson, 1999d; Williams, 1999a, 2003; Williams and Hickman, 2000; Williams, 2001; Van Kranendonk et al., 2002; Hickman and Van Kranendonk, 2012) is that the Warrawagine gneiss contains remnants of 3660–3570 Ma tonalites that were intruded, fragmented and deformed along with Paleoproterozoic granitic rocks. U–Pb zircon data for tonalite gneisses in the Ancient Gneiss Complex (AGC) of Swaziland (Kaapvaal Craton) also indicate both >3640 Ma zircons and Paleoproterozoic zircons (Compston and Kröner, 1988; Kröner

et al., 1989; Kröner and Tegtmeier, 1994; Zeh et al., 2011; Kröner et al., 2014; Van Schijndel et al., 2017). Pilbara–Kaapvaal comparisons were noted in the Introduction, and it is significant that c. 3660 Ma is the maximum age of gneisses in both the EPT and the AGC.

Shaw Dome

Gabbroic rocks dated at 3590–3580 Ma are exposed in the western Shaw Dome and are surrounded and intruded by c. 3440 Ma granitic rocks. One of these gabbroic units was first dated (U–Pb zircon) at 3578 ± 4 Ma by McNaughton et al. (1988), although published information was very limited. Subsequently, a far more detailed geochronological investigation of several large gabbroic bodies in the same area provided consistent U–Pb zircon dates of c. 3580 Ma (Petersson et al., 2019a). As evident from appendices and figures in this Report, the c. 3580 Ma date is very common among several hundred xenocrystic and detrital zircons dated from widely separated areas of the east Pilbara Craton (Figs 11–13, 15; Appendices 3, 6). This suggests a regionally significant magmatic event occurred in the Pilbara Craton at this time.

Muccan Dome

Wiemer et al. (2018) reported U–Pb zircon dates of 3591 ± 36 Ma and 3576 ± 22 Ma for samples of trondhjemite and tonalite gneiss from the southern margin of the Muccan Dome. However, as for the Warrawagine gneiss samples, zircons with much younger ages were also included in the data sets.

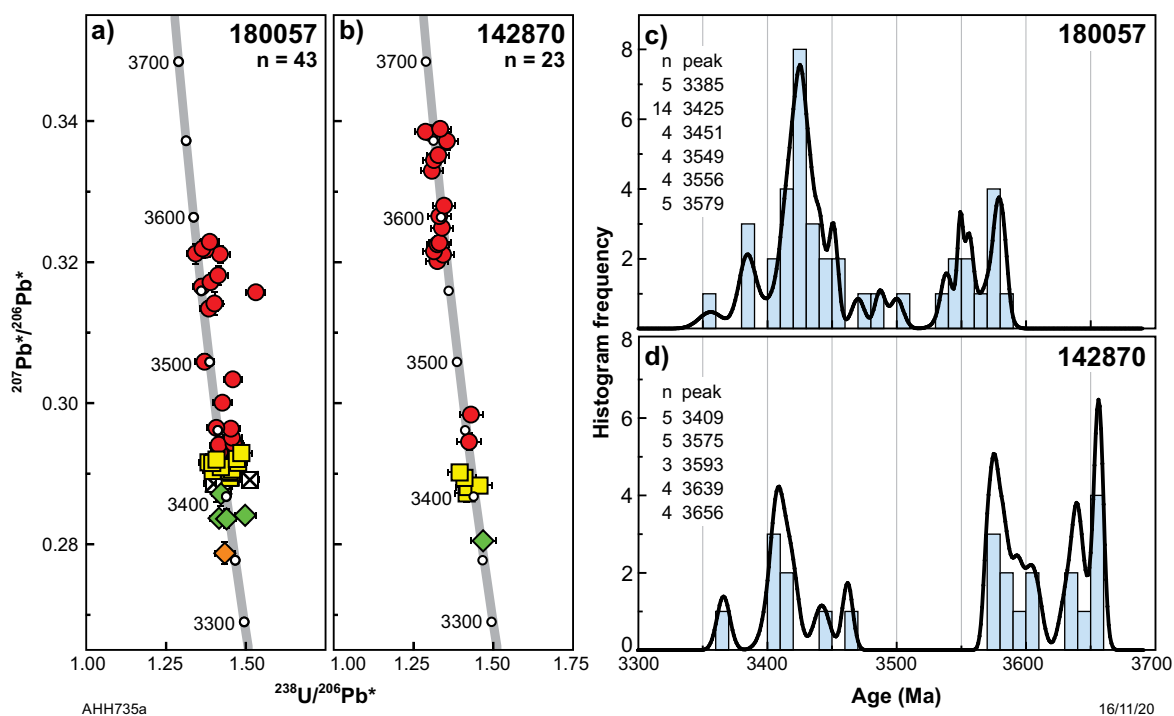


Figure 9. U–Pb analytical data for zircons from tonalite gneiss samples GSWA 180057 and 142870 from the Warrawagine Dome, revealing inheritance from Eoarchean to early Paleoproterozoic crust: a), b) concordia diagrams: n = number of analyses; yellow squares indicate magmatic zircons; green diamonds indicate metamorphic zircon rims; orange diamond indicates a younger metamorphic rim; red circles indicate xenocrystic zircons; crossed squares indicate possible core–rim mixtures; c), d) probability density histograms: n = number of ages in each significant age component (Ma, based on three or more ages)

Other evidence of pre-3530 Ma crust

Rare >3700 Ma detrital zircons are recorded in the Mosquito Creek Formation of the Mosquito Creek Basin (GSWA 178010, Nelson, 2005a), the Constantine Sandstone of the Mallina Basin (GSWA 142942, Nelson, 2000d), the Cleaverville Formation of the Gorge Creek Basin at Cleaverville (sample C91114, Kiyokawa et al., 2019), and the Farrel Quartzite of the Gorge Creek Basin in the Shay Gap greenstone belt (sample 220507-1, Sheppard et al., 2017). The wide separation of the sampling sites suggests several >3700 Ma sources. The existence of thin sandstone units low in the stratigraphy of the Warrawoona Group provided some of the first evidence that the oldest greenstones might contain detritus derived from older sialic crust (Hickman, 1981). This interpretation has been confirmed by U–Pb zircon geochronology (Van Kranendonk et al., 2002; WJ Collins, 2016, written comm., 12 October; this Report). Other sedimentary formations are also known to contain pre-3530 Ma detrital zircons (Kemp et al., 2015a,b; Sheppard et al., 2017).

Geochemical evidence has been used to suggest that the stratigraphically lowest basalts were contaminated by felsic crust (Glikson and Hickman, 1981a; Green et al., 2000; Smithies et al. 2007a), and Sm–Nd isotope evidence has been interpreted to indicate pre-3530 Ma sources for the volcanic and intrusive rocks (Jahn et al., 1981; Hamilton et al., 1981; Gruau et al., 1987; McCulloch, 1987; Bickle et al., 1989, 1993; Tyler et al., 1992; Smithies et al., 2004, 2007a; Van Kranendonk et al., 2006b, 2007a,b; Champion, 2013; Champion and Huston, 2016; Gardiner et al., 2017, 2018). Zircon Lu–Hf isotope evidence in this Report suggests crustal sources as old as c. 4000 Ma.

Indirect evidence for the existence of pre-Pilbara Supergroup crust was initially obtained through recognition that the stratigraphy of the ~15 km-thick Warrawoona Group was regionally extensive across the EPT (Hickman, 1980a,e, 1981). This lateral continuity suggested the existence of a similarly continuous older substrate or ‘basement’ onto which the Warrawoona Group was deposited (Hickman, 1983). Because the thickness and composition of the Warrawoona Group is inconsistent with it having originated as oceanic crust, it was inferred that the basement was continental crust. Moreover, it is now generally accepted that oceanic crust is rarely preserved due to its destruction by subduction.

Information on the pre-Pilbara Supergroup crust, especially regarding its thickness, extent, composition and age range, is necessary to constrain tectonic models for the crustal evolution of the EPT, and some of these questions have been addressed in previous studies (Van Kranendonk et al. 2006b, 2007a,b; Kemp et al., 2015a,b; Gardiner et al., 2017, 2018).

Isotopic evidence of pre-3530 Ma crust

U–Pb dates of xenocrystic and detrital zircons and Sm–Nd and Lu–Hf isotope data indicate the widespread existence of Eoarchean to early Paleoproterozoic continental crust in the Pilbara Craton, both prior to the 3530–3223 Ma evolution of the EPT and during the Paleoproterozoic and Mesoproterozoic. Principal lines of evidence for Eoarchean to early Paleoproterozoic crust include:

- *Ages of xenocrystic zircons in igneous rocks:* zircons significantly older than the crystallization age of a host igneous rock were inherited from older rocks. Potential sources included: 1) older igneous rocks partly assimilated during magma transport and emplacement; 2) detrital zircons incorporated from sedimentary rocks intruded during magma ascent; or 3) melting of older, deeper crust-forming new magma that was transported and emplaced higher in the crust. Most xenocrystic zircons in igneous rocks of the east Pilbara Craton are younger than 3530 Ma but, as detailed below, early Paleoproterozoic and Eoarchean zircons are also present; for example, >3700 Ma xenocrystic zircons in rhyolite on Panorama Ridge, North Pole Dome (Thorpe et al., 1992a; Petersson et al., 2019c). Xenocrystic zircons older than 3530 Ma are listed in Table 2.
- *Ages of detrital zircons in Paleoproterozoic and Mesoproterozoic metasedimentary formations:* the zircon age components in a clastic sedimentary rock provide a representative sample of the ages of felsic igneous rocks exposed in the provenance regions during deposition (Cawood et al., 2012). Recycling of xenocrystic and detrital zircons from older igneous and sedimentary rocks is also possible.
- *Whole-rock Sm–Nd model ages of igneous rocks:* these ages, and ϵ_{Nd} values, indicate the average mantle extraction ages of the sources of the melts for currently exposed igneous rocks.
- *Lu–Hf isotope data from zircons in felsic igneous and sedimentary rocks:* these data convey information on the mantle extraction ages of sources and on the relative importance of melts derived by crustal recycling vs additions of juvenile magma directly from the mantle or from recently extracted crust. Hf isotope ratios, between ^{176}Hf (produced by decay of ^{176}Lu) and ^{177}Hf , are expressed using the same ϵ -notation used for Nd. Strongly negative ϵ_{Hf} values imply reworking of significantly older crustal material whereas positive ϵ_{Hf} values suggest juvenile sources. Hf isotope ratios are therefore useful indicators of tectonic processes and settings (Gardiner et al., 2017, 2018).

Xenocrystic zircons older than 3530 Ma in igneous rocks

For igneous rocks in the east Pilbara Craton it is reasonable to infer that xenocrystic zircons older than c. 3530 Ma were derived from the early crust on which the Pilbara Supergroup was deposited (Van Kranendonk et al., 2002, 2007b; Hickman, 2004; Kemp et al., 2015a,b; Petersson et al., 2019c).

Published data for xenocrystic zircons >3530 Ma in igneous rocks of the east Pilbara Craton are summarized in Table 2, and Appendix 3 provides a detailed listing of the data for all >3490 Ma xenocrystic zircons. Cognate zircons from samples of 3530–3490 Ma igneous rocks in the Coonterunah Subgroup are not included in Table 2 and Appendix 3. The listing in Table 2 is dominated by zircon dates between c. 3760 and 3600 Ma from rhyolite outcrops along Panorama Ridge on the southern side of the North Pole Dome. This concentration is due to data from a specific study (Petersson et al., 2019c) aimed at investigating a discovery of c. 3724 Ma xenocrystic zircon

in rhyolite (Thorpe et al., 1992a) and subsequent reports of >3600 Ma zircons from the same area (Kabashima et al., 2003; Kitajima et al., 2008). Petersson et al. (2019c) established that the crystallization age of the host rhyolite is c. 3451 Ma, and on that basis interpreted it to belong to the Panorama Formation. However, this stratigraphic assignment is inconsistent with geological mapping (Hickman, 2013a) which has placed the rhyolite outcrops stratigraphically between the c. 3470 Ma Mount Ada Basalt and the c. 3459 Ma Marble Bar Chert Member of the Duffer Formation. The irregular outcrop pattern of the rhyolite suggests it is intrusive, as are similar c. 3450 Ma porphyritic rhyolite units at Miralga Creek (Goellnicht et al., 1988; Thorpe et al., 1992a) and 5 km north of Miralga Creek (Hickman and Van Kranendonk, 2008b).

In this Report, the rhyolite dated at Panorama Ridge is interpreted to be a subvolcanic intrusion of the Tambina Supersuite. Petersson et al. (2019c) reported 112 analyses of 107 zircons from four separate rock samples, with 16 analyses indicating dates between c. 3760 and 3704 Ma. They interpreted the younger dates to be due to Pb loss. An additional 17 analyses provided dates between c. 3699 and 3601 Ma. Although it is theoretically possible that xenocrystic zircons in igneous rocks were derived from assimilation of metasedimentary material lower in the crust, this may be unlikely in the EPT where clastic sedimentary rocks deposited prior to c. 3426 Ma are rare. Petersson et al. (2019c) noted the possibility of a sedimentary derivation for the >3600 Ma xenocrystic zircons in their study, but argued against this based on the abundance of xenocrystic zircons in the four rhyolite samples (29% of all analyzed zircons). They interpreted this abundance to be inconsistent with far-travelled, sporadic occurrences in a sedimentary rock. The only clastic sedimentary rocks older than c. 3451 Ma in the North Pole succession are thin sandstone units within the c. 3481 Ma Dresser Formation and in the c. 3470 Ma Mount Ada Basalt. Neither unit contains detrital zircons older than c. 3534 Ma (GSWA 180070, Wingate et al., 2009; Byerly et al., 2002). Given the large number of >3600 Ma zircons in the c. 3451 Ma rhyolite at North Pole, Petersson et al. (2019c) concluded that these zircons were inherited from underlying Eoarchean crust.

Compilation of the published xenocrystic zircon data for this Report had the following aims: 1) to determine if >3530 Ma xenocrystic zircons from different EPT domes have different age spectra, thereby suggesting regional differences in the age of the underlying pre-3530 Ma crust; 2) to examine if different igneous supersuites contain different xenocrystic zircon age components, thereby testing the possibility that different supersuites had different crustal sources; 3) to determine if the distribution of xenocrystic zircon dates suggest a series of separate crust-forming events between 3800 and 3530 Ma.

Conclusions suggested by the data for xenocrystic zircons include:

- the Tambina Supersuite contains most of the 3760–3560 Ma xenocrystic zircons, and most are from the North Pole and Warrawagine Domes. This is consistent with previous interpretations, based on other evidence, that this supersuite was substantially derived from reworking of the middle and lower crust. The Tambina Supersuite is mainly composed of banded gneiss and includes numerous enclaves of unknown age
- the Callina Supersuite and Duffer Formation, although older than the Tambina Supersuite, appear to contain no xenocrystic zircons older than c. 3576 Ma. This is consistent with the interpretation in this Report of an influx of juvenile magma at c. 3530 Ma, followed by a gradual increase in crustal reworking until c. 3420 Ma
- the Muccan Dome contains xenocrystic zircons dated between c. 3621 and 3538 Ma. This observation is supported by LA-ICP-MS zircon dates reported by Wiemer et al. (2018)
- other EPT domes have provided relatively few xenocrystic zircons older than c. 3530 Ma, and some domes (Mount Edgar, Corunna Downs, McPhee, and Yilgalong Domes) have so far provided none. However, the Corunna Downs and Yilgalong Domes expose only relatively young Paleoproterozoic stratigraphy (mainly the Emu Pool Supersuite and the Kelly Group), and almost no zircon data are available for the McPhee Dome.

Although Sm–Nd model ages (discussed below) indicate pre-3530 Ma crust in the Shaw and Mount Edgar Domes, xenocrystic zircons in felsic igneous rocks from these domes provide little or no evidence for pre-3530 Ma felsic crust. This might be evidence that the composition of the early crust in these domes was mainly mafic.

Evidence from detrital zircon ages

GSWA dating of Paleoproterozoic and Mesoproterozoic metasedimentary rocks in the northern Pilbara Craton identified many detrital zircons much older than the depositional ages of the host rocks. The sedimentary facies of rocks such as boulder conglomerate and poorly sorted sandstone, paleocurrent data (e.g. Krapež, 1984), and some depositional settings, testify to a local sedimentary provenance. In such instances, the ages of detrital zircons provide evidence of the ages of rocks within the local crust. Detrital zircon age spectra might be matched to the established ages of older felsic rocks in the same dome or adjacent to the depositional basin of the sedimentary rock. These lines of evidence were used by Kemp et al. (2015b) to argue that most of the 84 Pilbara detrital zircons with ages greater than 3550 Ma used in their study were derived locally. Data from these 84 zircons are included in this Report.

The significance of the old zircons was uncertain until the chronology of magmatic events in the crustal evolution of the craton had been established. The chronology was identified using U–Pb zircon data from more than 200 samples to recognize, define, and name eight granitic supersuites and seven granitic suites (Van Kranendonk et al., 2004b,c, 2006b). Sample numbers for different intrusions, suites, and supersuites are provided in Table 3, and Appendix 4 lists dated igneous samples from the east Pilbara Craton by U–Pb age and supersuite, noting dome location. Geochronological evidence for separation of the supersuites and suites is provided in Appendix 5, which lists published U–Pb dates for 225 samples. Data in Appendix 5 were used to compile Figure 10a and, for comparison, Figure 10b summarizes the published crystallization ages of igneous rocks (intrusive and volcanic) in the northwest Pilbara Craton (89 samples).

Table 3. Summary of geochronology of all granitic intrusions and supersuites in the east Pilbara Craton

Supersuite or suite	Dome or terrane	Intrusion	Date (Ma) [†]	Geochronology sample [‡]
Split Rock Supersuite			2851–2831	
	Mount Edgar Dome	Moolyella Monzogranite	c. 2831	169044
	McPhee Dome	Cookes Creek Monzogranite	c. 2837	178011
	Kurrana Terrane	Bonney Downs Monzogranite	c. 2838	178014
	Shaw Dome	Spear Hill Monzogranite	c. 2851	142879
	Shaw Dome	Cooglegong Monzogranite	n.d.	
	Yule Dome	Gillam Monzogranite	n.d.	
	Yule Dome	Kimmys Bore Monzogranite	n.d.	
	Yule Dome	Kadgawarrina Monzogranite	n.d.	
	Yule Dome	Minnamonica Monzogranite	n.d.	
	Corunna Downs Dome	Mondana Monzogranite	n.d.	
	Carlindi Dome	Numbana Monzogranite	n.d.	
	Carlindi Dome	Poocatche Monzogranite	n.d.	
	Tambourah Dome	Tambourah Monzogranite	n.d.	
Cutinduna Supersuite			2897–2896	
	Kurrana Terrane	Unnamed, Limestone Bore	c. 2896	178231
	Kurrana Terrane	Unnamed, Limestone Bore	c. 2897	178230
Sisters Supersuite			2954–2919*	
	Shaw Dome	Mulgandinnah Monzogranite	2934–2919	142882, 142883, 142965, 142967, T94/31 ^(s)
	Carlindi Dome	Unnamed, Pilgangoora area	c. 2923	169021
	Shaw Dome	Bamboo Springs Monzogranite	2926–2923	178047, 178049
	Carlindi Dome	Woodstock Monzogranite	2933–2927	142884, 142885
	Carlindi Dome	Unnamed granite	2944–2931	KB351 ^(b) , KB746 ^(b) , KB770 ^(b)
	Yule Dome	Cheearra Monzogranite	2937–2933	142936, 160442
	Yule Dome	Powdar Monzogranite	c. 2935	142937
	Shaw Dome	Keep It Dark Monzogranite	c. 2936	unpublished data
	Yule Dome	Mungarinya Monzogranite	c. 2938	142176
	Carlindi Dome	Petermarer Monzogranite	c. 2940	160745
	Yule Dome	Beabea Monzogranite	c. 2941	169018
	Yule Dome	Unnamed, Hong Kong Mine	c. 2942	180097
	Carlindi Dome	Unnamed aplite	c. 2944	KB351 ^(b)
	Yule Dome	Mungaroona Granodiorite	c. 2945	142938
	Carlindi Dome	Unnamed, Pilbara Well area	c. 2946	142941
	Yule Dome	Unnamed, Wodgina area	c. 2952	180038
	Yule Dome	Abydos Monzogranite	n.d.	
	Shaw Dome	Coondina Monzogranite	n.d.	
	Shaw Dome	Eley Monzogranite	n.d.	
	Yule Dome	Ellawarrina Monzogranite	n.d.	
	Yule Dome	Pilbara Creek Monzogranite	n.d.	
	Yule Dome	Pincunah Monzogranite	n.d.	
	Yule Dome	Yandearra Granodiorite	n.d.	
Elizabeth Hill Supersuite			3068–3066	
	Yule Dome	Cockeraga Leucogranite	3068–3066	169016, 169014
Mount Billroth Supersuite			3068–3066	
	Yule Dome	Flat Rocks Tonalite	3166–3164	142946, 142948
	Kurrana Terrane	Golden Eagle Orthogneiss	3199–3178	178012, 178013

Table 3. continued

Supersuite or suite	Dome or terrane	Intrusion	Date (Ma) [†]	Geochronology sample [‡]
Cleland Supersuite			3257–3223	
	Mount Edgar Dome	Bishop Creek Monzogranite	3246–3223	142980, 142983, 169034, 178076, 178078
	Strelley Dome	Strelley Monzogranite	3239–3238	RM1 ^(c) , 203366 ^(c) , 203368 ^(c)
	Yule Dome	Kavir Granodiorite	3240–3240	unpublished data
	Warrawagine Dome	Unnamed, 6 Mile Well	c. 3244	142869
	Muccan Dome	Wolline Monzogranite	3252–3244	143805, 143810
	McPhee Dome	Unnamed, Spinaway Well	c. 3245	178188
	Muccan Dome	Wolline Monzogranite	3251–3250	178031, 178032
	Carlindi Dome	Unnamed, Camel Well	c. 3252	178040
	Carlindi Dome	Unnamed, Turner River	3257–3235	KB265 ^(b) , KB264 ^(b) , KB779 ^(b) , KB810 ^(b)
	Shaw Dome	Garden Creek Monzogranite	n.d.	
	Yule Dome	Siffleetes Granodiorite	n.d.	
	Mount Edgar Dome	Bullgarina Monzogranite	n.d.	
Unnamed suite			3279–3274	
	Yilgalong Dome	Unnamed, Yilgalong Creek area	3279–3274	169260, 178007, 178089
Emu Pool Supersuite			3324–3290	
	Yilgalong Dome	Elsie Creek Tonalite	3299–3290	169261, 169262, 169263, 178008, 144682
	Mount Edgar Dome	Zulu Granodiorite	3299–3294	169036, 178008
	Mount Edgar Dome	Mullgunya Granodiorite	3308–3297	178096, 178099
	Corunna Downs Dome	Nandingarra Granodiorite	3313–3300	160208, 160209, 160210, 160212, 168922
	Mount Edgar Dome	Johansen Monzogranite	3315–3303	178075, 178077
	Muccan Dome	Unnamed, Five Mile Creek	c. 3315	178022,
	Warrawagine Dome	Unnamed, Granite Well	c. 3303	142871
	Mount Edgar Dome	Joorina Granodiorite	3321–3304	142981, 142982, 142984, LTU5472 ^(p)
	Mount Edgar Dome	Jenkin Granodiorite	3313–3307	169045, 169046, 178037
	Corunna Downs Dome	Boobina Porphyry	3324–3307	77713 ^(k) , 86473 ^(a) , 86483 ^(a) , 103279 ^(m)
	Mount Edgar Dome	Cotton Well Granodiorite	3318–3309	178034, CTW-1A ^(g)
	Mount Edgar Dome	Campbell Well Granodiorite	c. 3310	142974
	Mount Edgar Dome	Munganbrina Monzogranite	c. 3310	178095
	Corunna Downs Dome	Carbana Monzogranite	3317–3307	142978, 169027, 169028, 178001, 178002, 178003, 178084, Mond ^(a) , Carb ^(a)
	Mount Edgar Dome	Wilina Granodiorite	3324–3310	169042, N/A ^(d)
	Mount Edgar Dome	Kennell Granodiorite	3315–3312	169038, 178038, ME-28 ^(g)
	Muccan Dome	Unnamed, Don Well	c. 3313	143803
	McPhee Dome	Gobbos Granodiorite	c. 3313	180067, 86358 ^(a)
	Mount Edgar Dome	Coppin Gap Granodiorite	3317–3314	LTU5577 ^(p) , 103279 ^(m)
	Mount Edgar Dome	Chessman Granodiorite	3318–3314	169040, 169041
	Mount Edgar Dome	Chimingadgi Trondhjemite	n.d.	
	Mount Edgar Dome	Davitt Syenogranite	n.d.	
	Corunna Downs Dome	Triberton Granodiorite	n.d.	
	Mount Edgar Dome	Walgunya Trondhjemite	n.d.	
Tambina Supersuite			3451–3410	
	Warrawagine Dome	Unnamed, 6 Mile Well	c. 3410	142870
	Mount Edgar Dome	Fig Tree Gneiss	3448–3416	169031, 169041, 178036, 178079, 178100, LTU5416 ^(p) , LTU6417 ^(p) , LTU6419 ^(p) , P94-22 ^(g) P95-gran ^(g)

Table 3. continued

Supersuite or suite	Dome or terrane	Intrusion	Date (Ma) [†]	Geochronology sample [‡]
	Shaw Dome	Tambina Supersuite	3445–3417	142878, 76340 ^(l)
	Carlindi Dome	Wilson Well Gneiss	c. 3420	unpublished data
	Muccan Dome	Unnamed, Florries Well	c. 3420	178023
	Tambourah Dome	Petroglyph Gneiss	3428–3420	169019, unpublished data
	Yule Dome	Yallingarrintha Tonalite	c. 3421	142170
	Warrawagine Dome	Unnamed, Big Junction Well	c. 3423	180057
	Shaw Dome	Abyssinia Well Orthogneiss	c. 3425	142968
	Corunna Downs Dome	Bookargemoona Tonalite	c. 3427	160211
	Shaw Dome	Unnamed, Unices Well	c. 3430	142966
	Shaw Dome	South Daltons Pluton	c. 3431	UWA-98053 ^(l)
	Muccan Dome	Unnamed, Sunrise Hill	c. 3443	124755
	North Pole Dome	North Pole Monzogranite	3446–3431	NP-1 ^(f) , NP-27 ^(f) , 109711 ^(m) , unpublished data
	Muccan Dome	Unnamed, Kennedy Gap	c. 3438	143807
	Mount Edgar Dome	Unnamed, Kitty's Gap	c. 3446	JW95-001 ^(e)
	North Pole Dome	Unnamed, Miralga Creek	c. 3449	103283 ^(o)
	Mount Edgar Dome	Unnamed, West Bamboo	c. 3449	94770 ^(o)
	Mount Edgar Dome	Unnamed, Pyramid Well	c. 3449	94750 ^(o)
	Shaw Dome	Tambina Supersuite	c. 3451	T94/221 ^(s)
	Mount Edgar Dome	Lady Adelaide Orthogneiss	n.d.	
Callina Supersuite			3484–3462	
	Shaw Dome	Unnamed, Fairwick Well	c. 3462	168923
	Mount Edgar Dome	Owens Gully Diorite	3465–3462	178035, OG1 ⁽ⁿ⁾ , CTW-36 ^(g)
	Shaw Dome	Unnamed, Coondina Pool	c. 3463	T94/222 ^(s)
	Mount Edgar Dome	Homeward Bound Granite	c. 3466	142865
	Carlindi Dome	Unnamed, Strelley River	c. 3466	100698 ^(l)
	Shaw Dome	Coolyia Creek Granodiorite	3469–3467	142962, T94/227 ^(s) , A224-1 ^(h)
	Shaw Dome	North Shaw Tonalite	3469–3468	178044, T94/193 ^(s)
	Carlindi Dome	Unnamed, Coucal Ridge	3479–3468	94058, 95037 ^(l)
	Carlindi Dome	Unnamed, Wilson Well	3484–3469	153188, 153190
	Shaw Dome	Unnamed, 26 Mile Well	c. 3469	142976
	Muccan Dome	Unnamed, Fred Well	c. 3470	142828
	Carlindi Dome	Motherin Monzogranite	c. 3475	unpublished data
	Shaw Dome	Unnamed, Tambourah Creek	3485–3470	Shaw B Gneiss (large age uncertainty) ^(q,r)
	Mount Edgar Dome	Underwood Gneiss	n.d.	

Notes:

[†] Age ranges (e.g. 2934–2919) represent the range of published crystallization ages for the unit

[‡] GSWA sample unless external source cited

Abbreviation: n.d., not dated

* Maximum age of supersuite from outside east Pilbara

References for non-GSWA data: a) Barley and Pickard (1999); b) Beintema (2003); c) Buick et al. (2002); d) Collins et al. (1998); e) de Vries et al. (2006); f) Harris et al. (2009); g) Kloppenburg (2003); h) McNaughton et al. (1988); i) McNaughton et al. (1993); j) Pidgeon (1978b); k) Pidgeon (1984); l) R Buick (written comm., 2015); m) RI Thorpe (written comm., 1992); n) Stern et al. (2009); o) Thorpe et al. (1992a); p) Williams and Collins (1990); q) Williams et al. (1983a); r) Williams et al. (1983b); s) Zegers (1996)

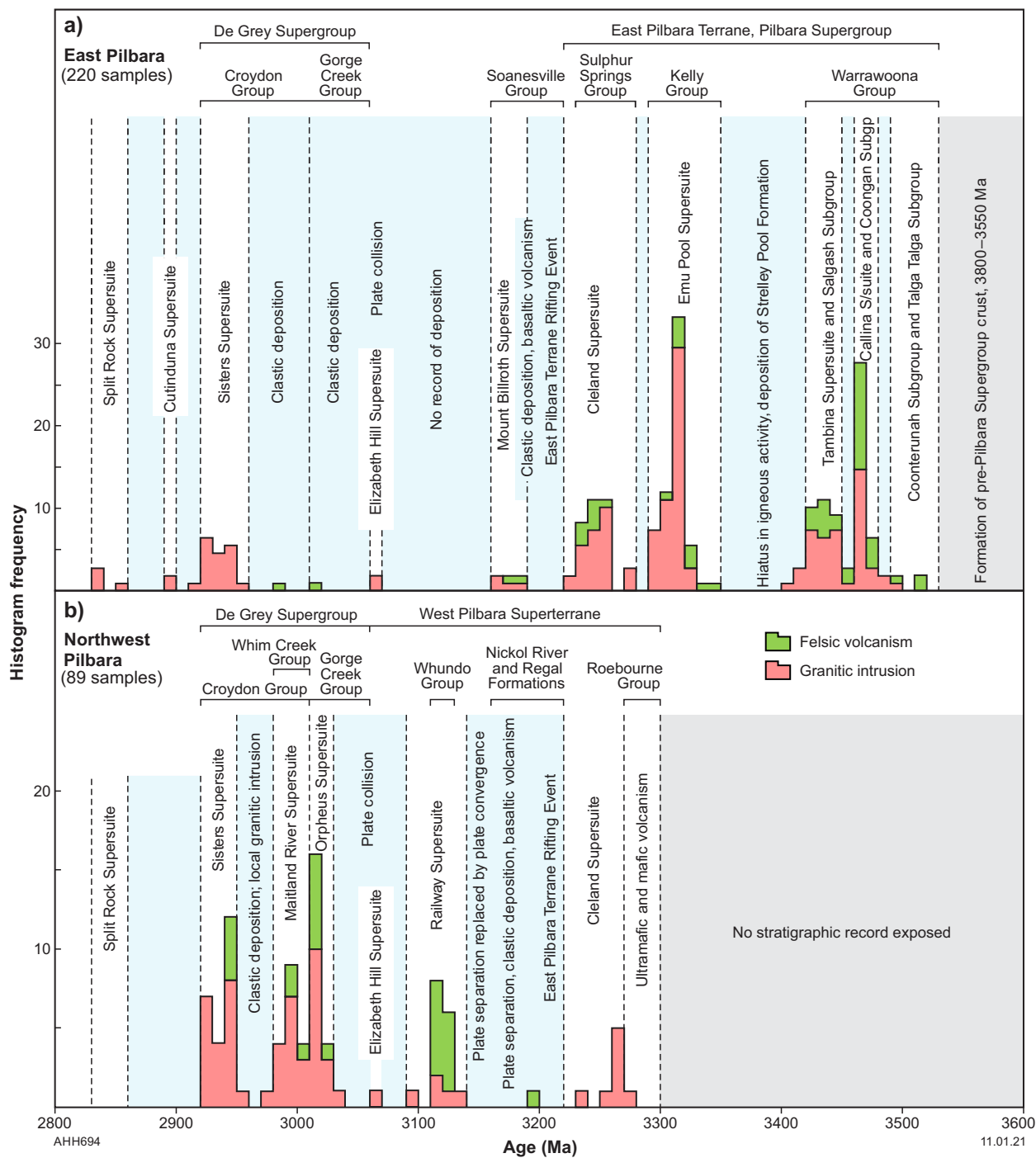


Figure 10. Comparison of the timing of episodes of granitic intrusion and felsic volcanism in the northern Pilbara Craton, based on published U–Pb zircon geochronology (309 samples): a) east Pilbara; b) northwest Pilbara

Three important observations are made from Figure 10:

1. No rocks older than c. 3280 Ma have been dated from the northwest Pilbara Craton.
2. There is no correlation between the evolution of the two areas from c. 3220 Ma (breakup of the EPT) to plate collision and reconnection of the east and northwest Pilbara Craton at 3070 Ma.
3. The 3068–3066 Ma Elizabeth Hill Supersuite and the 2954–2919 Ma Sisters Supersuite, both of which are interpreted to be related to plate collision, intruded east and northwest parts of the Pilbara Craton.

Sources of detrital zircons

The ages of detrital zircons in Paleoproterozoic and Mesoproterozoic sedimentary rocks of the east Pilbara Craton closely match the ages of established felsic magmatic events (Fig. 10a). However, many metasedimentary rocks of the Pilbara Supergroup, and of the overlying Mesoproterozoic basins (Soanesville, Gorge Creek, Mallina, and Mosquito Creek), also contain detrital zircons with ages considerably older than c. 3530 Ma (Van Kranendonk et al., 2002, 2007a,b; Kemp et al., 2015 a,b). Appendix 6 lists detrital zircon dates (discordance between 10 and –10; GSWA and non-GSWA data) determined by SHRIMP from metasedimentary rocks of the northern Pilbara Craton (n = 1479). However, detrital zircon dates published after 2016, or determined by methods other than SHRIMP, are not included. Appendix 6 is a useful database to gain insights into provenance variations through time and between depositional areas.

In most instances, the proximal sedimentary facies of coarse-grained clastic rocks in the Paleoproterozoic sedimentary units makes derivation of the detrital zircons from outside the Pilbara Craton improbable (Kemp et al. 2015b, appendix 1). Moreover, the interpreted tectonic setting of the Paleoproterozoic depositional basins, between uplifted granitic domes, is most consistent with local derivation of detritus. However, the larger Mesoproterozoic basins, in particular the Mallina and Mosquito Creek Basins, which include deep-water turbidite facies, were filled by sediments with far less certain provenance.

About 15% of the detrital zircons listed in Appendix 6 are older than 3530 Ma, which is the interpreted maximum depositional age of the Pilbara Supergroup. These pre-3530 Ma zircons were analysed in sedimentary units of the Pilbara Supergroup and in formations of overlying Mesoproterozoic sedimentary basins with depositional ages as young as 2930 Ma. Provided the detrital zircons were eroded from the pre-3530 Ma Pilbara crust, they should contribute evidence on its age, distribution and composition. This Report examines all the Pilbara detrital zircon data with these considerations in mind.

The scarcity of known outcrops of pre-3530 Ma rocks in the northern section of the Pilbara Craton, in contrast to the common occurrence of pre-3530 Ma detrital zircons in sedimentary formations, have led some workers to suggest that these old detrital zircons were derived from terranes outside the craton (Bagas et al., 2004b, 2008; Kemp et al., 2015a). However, the current rarity of exposures of pre-3530 Ma crust is not a guide to the volumetric significance of this crust in the Paleoproterozoic. Three main

processes would have progressively reduced the volume of pre-3530 Ma crust from the Paleoproterozoic onwards: doming and sagduction; intrusion by younger granitic rocks; and erosion. Second, there are no known potential alternative sources of Paleoproterozoic to early Paleoproterozoic zircons within Australia. Although the northwest Yilgarn Craton contains >3530 Ma rocks, the Pilbara and Yilgarn Cratons are interpreted to have been widely separated until their collision during the 2005–1950 Ma Glenburgh Orogeny (Sheppard et al., 2005; Spaggiari et al., 2008; Johnson et al., 2010, 2011, 2013; Smirnov et al., 2013). The Kaapvaal Craton might have been an alternative source, although pre-3530 Ma rocks have been identified over only a very small area (possibly less than 1%) of the AGC (data in Kröner et al., 2014). Additionally, Drabon et al. (2017) noted that potential >3550 Ma zircon sources in the AGC made almost no contribution to the detrital zircon content of sedimentary rocks in the immediately adjacent Barberton Greenstone Belt (BGB). Of 3410 zircons dated in various sandstone units of the BGB, only 15 are older than the Paleoproterozoic succession of the greenstone belt, and 10 of these 15 zircons were recorded from an asteroid impact-related deposit, within which the detritus might be far travelled.

There is now abundant geochemical geochronological, and isotopic evidence that the Pilbara Supergroup was deposited on older crust (Glikson and Hickman, 1981a; Hamilton et al., 1981; Jahn et al., 1981; Gruau et al., 1987; Green et al., 2000; Van Kranendonk et al., 2002, 2006b, 2007a,b, 2015; Van Kranendonk and Pirajno, 2004; Smithies et al., 2005a,b, 2007a, 2009; Tesselina et al., 2010; Champion, 2013; Nebel et al., 2014; Kemp et al., 2015a,b; Champion and Huston, 2016; Johnson et al., 2017; Gardiner et al., 2017, 2018; Petersson et al., 2019a,b). As described by Kemp et al. (2015b), the detrital zircon age spectra of particular samples are consistent with a provenance within the Pilbara Craton. The evidence falls into two main categories: specific, based on consideration of individual samples; and general, based on data from large numbers of samples.

Specific evidence on provenance

In some instances, a direct relationship might be indicated between the detrital zircons in sandstone and magmatic zircons in adjacent granitic rocks. On the northern margin of the Muccan Dome, the c. 3050 Ma Farrel Quartzite (Gorge Creek Group) contains detrital zircons with a dominant age component of 3434 ± 6 Ma (GSWA 143996, Nelson, 1998m), which is similar to the 3443 ± 6 Ma crystallization age of an underlying Tambora Supersuite granodiorite (GSWA 124755; Nelson, 1996b). A major erosional unconformity separating the sandstone from the granodiorite was described by Dawes et al. (1995a,b). Other workers in the east Pilbara Craton have also interpreted local provenance for sandstones that overlie unconformities (Buick et al., 1995; Green et al., 2000; Allwood et al., 2006, 2007a,b; Wacey et al., 2010).

Sedimentary facies commonly demonstrate local provenance, as in the example of the Duffer Formation in the Warralong greenstone belt. Sample GSWA 168996 (Fig. 11; ages recalculated from Nelson, 2002f) was collected from a tuffaceous felsic volcanoclastic rock of the Duffer Formation that overlies polymictic conglomerate containing boulders of chert up to 20 cm in diameter. This facies provides strong evidence for local derivation of the clastic material, and this

is particularly significant because the tuffaceous sample contained six older detrital zircons dated at 3571 ± 5 Ma (Fig. 11). A younger zircon age component, at 3524 ± 7 Ma, might indicate erosion of the Coonerunah Subgroup which outcrops to the east. The youngest age component, at 3479 ± 6 Ma, might represent igneous crystallization of a possibly local felsic volcanic rock, but is also consistent with erosion from the Callina Supersuite, which forms part of adjacent Muccan and Carlindi Domes, or older volcanic rocks of the Duffer Formation. Granitic rocks of the Muccan Dome contain xenocrystic zircons dated at 3621 ± 3 Ma (GSWA 178031, Nelson, 2005f) and 3574 ± 3 Ma and 3538 – 3499 Ma (GSWA 142828, Nelson, 1998e), suggesting that the granitic rocks of this dome were a probable local source.

Other types of specific evidence consistent with local provenance include:

- depositional setting: for example, sandstones deposited along growth faults, in grabens, adjacent to transpressional faults, or within intracratonic basins are evidently derived from relatively local erosion (Eriksson, 1981; Buick and Barnes, 1984; Krapež, 1984; Wilhelmij and Dunlop, 1984; Krapež and Barley, 1987; DiMarco and Lowe, 1989b; de Vries et al., 2006)
- paleocurrent data: current direction indicators, combined with geological evidence of depositional setting of a clastic unit, can suggest local provenance. Examples include evidence of deposition on the outer slopes of Paleoproterozoic volcanoes in the North Pole and Mount Edgar Domes (DiMarco and Lowe, 1989a; Olivier et al., 2012).

General evidence on provenance

The close match between detrital zircon age components and the timing of felsic magmatic events in the same terrane is evidence of a provenance within that terrane because, by definition, each terrane has a geological history different from the histories of adjacent terranes. Figure 10 uses all published dates for intrusive and extrusive felsic rocks in the northern section of the Pilbara Craton to illustrate a well-defined record of felsic magmatic events. Detrital zircon age components for Paleoproterozoic and Mesoproterozoic sandstones of the east Pilbara Craton match the ages of established Paleoproterozoic magmatic events (Figs 12, 13). Conversely, where there were lengthy breaks in EPT magmatic activity, such as between c. 3426 and 3350 Ma, during deposition of the Strelley Pool Formation (Hickman, 2008), the east Pilbara sedimentary rocks contain relatively few detrital zircons of those ages. However, it can be expected that individual formations or groups may not contain detrital zircons representative of all older or contemporaneous magmatic events in the same terrane because in many instances rocks formed by those events may not have been exposed to erosion during clastic deposition.

Another line of general evidence is the relationship between the interpreted depositional settings of formations and groups, and the detrital zircon age spectra (Figs 12–14). Cawood et al. (2012) suggested that detrital zircon spectra reflect the tectonic settings of the basins in which they were deposited.

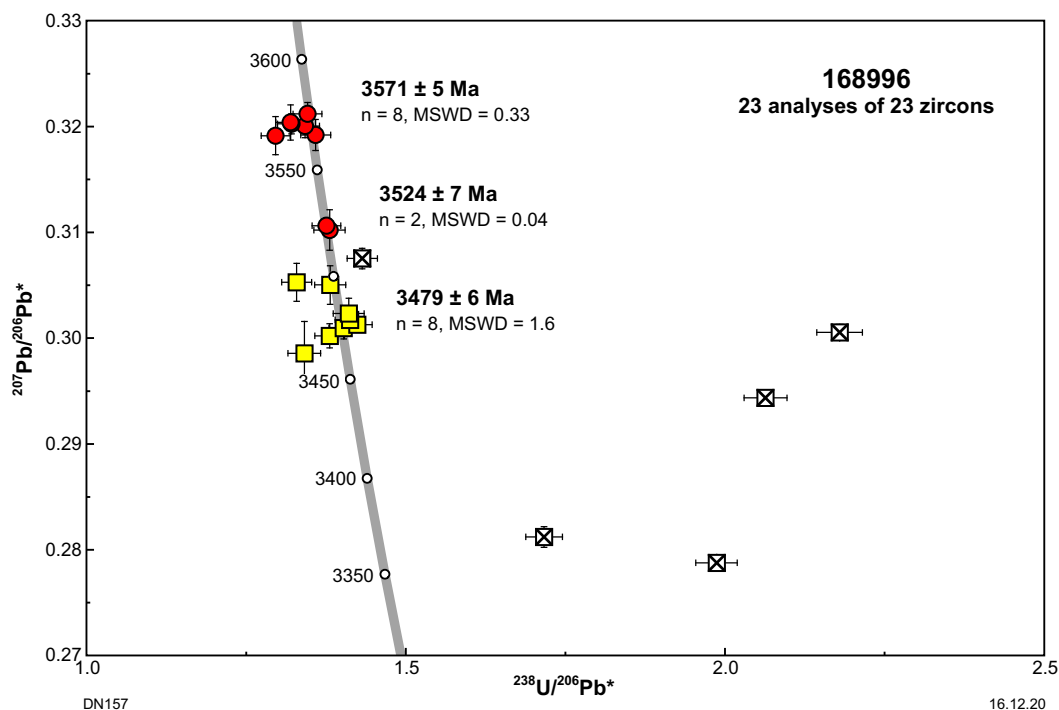


Figure 11. U–Pb analytical data for sample GSWA 168996, an altered felsic volcanoclastic rock of the c. 3470 Ma Duffer Formation, Warralong greenstone belt. The zircon age component at c. 3571 Ma indicates a felsic source of this age in either the Muccan Dome or Carlindi Dome. The c. 3524 Ma age component is consistent with derivation from the Coonerunah Subgroup currently exposed in the Carlindi Dome, or from granitic rocks of similar age. Age components in this sample are recalculated from Nelson (2002f). Yellow squares indicate magmatic (or detrital) zircons; red circles indicate inherited or detrital zircons; crossed squares indicate analyses >5% discordant. Abbreviations: n, number of analyses; MSWD, mean square of weighted deviates

They observed that convergent plate margins are characterized by a large proportion of detrital zircon dates close to the depositional age of the sediment, whereas sediments in collisional, extensional and intracratonic settings contain greater proportions of older dates that reflect the history of the underlying basement. It is evident that in the east Pilbara Craton, where geological evidence indicates that the Mesoarchean basins were intracratonic or passive-margin basins, the detrital zircon dates are very much older than the depositional ages of the sediments (Fig. 13). By contrast, in the northwest Pilbara Craton, where the Mesoarchean Mallina Basin evolved within the convergent margin setting of the CPTZ (Hickman, 2016), some detrital zircon ages are much closer to the c. 3000 to 2930 Ma depositional age (Fig. 14). Such close links between interpreted depositional and tectonic settings, and detrital zircon age spectra, add support to the interpretation that the detrital zircons in sedimentary rocks of the east Pilbara Craton were sourced from within the east Pilbara Craton itself, and not from the northwest Pilbara Craton.

Following mapping of the east Pilbara Craton in the 1970s (Hickman, 1984), it was postulated that sedimentary deposition during evolution of dome-and-keel structures in the EPT was related to erosion of uplifted domes. In this scenario, provenance would have been largely restricted to the areas of particular domes (Hickman, 2012; Wiemer et al., 2016). Exceptions might have occurred immediately

after events of regional peneplanation; for example, the Strelley Pool Formation and Leilira Formation, which overlie regional erosional unconformities (Buick et al., 1995, 2002; Van Kranendonk, 2000a; Van Kranendonk et al., 2007a,b; Hickman, 2008, 2012), and possibly the Duffer Formation and overlying Apex Basalt (DiMarco and Lowe, 1989a). In the Salgash area, 15 km south of Marble Bar (Plate 1A), a thin sandstone unit in the basal section of the Apex Basalt provides evidence of the existence of pre-Pilbara Supergroup continental crust (Hickman, 1981). Dating of detrital zircons from the sandstone (WJ Collins, 2016, written comm., 12 October) revealed age components at c. 3650 and 3592 Ma, in addition to zircon dates (19 zircons) consistent with erosion of underlying felsic volcanic rocks of the Duffer Formation and felsic volcanoclastic rocks within the lower part of the c. 3450 Ma Apex Basalt (Fig. 15). Zircons older than 3530 Ma in the sandstone were most likely derived from erosion of the uplifted Eoarchean to early Paleoproterozoic crust. If an early version of the Mount Edgar Dome already existed at c. 3450 Ma, the source is likely to have been uplifted crust within this dome. Isotope data from granitic rocks of the Mount Edgar Dome (Gardiner et al., 2017, 2018) are consistent with this possibility: 1) whole-rock Sm–Nd model ages for four samples are between c. 3650 and 3590 Ma; 2) zircon Lu–Hf model ages for 288 zircons from 41 samples are between c. 4000 and 3450 Ma (Gardiner et al., 2018, fig. 10, appendix 2).

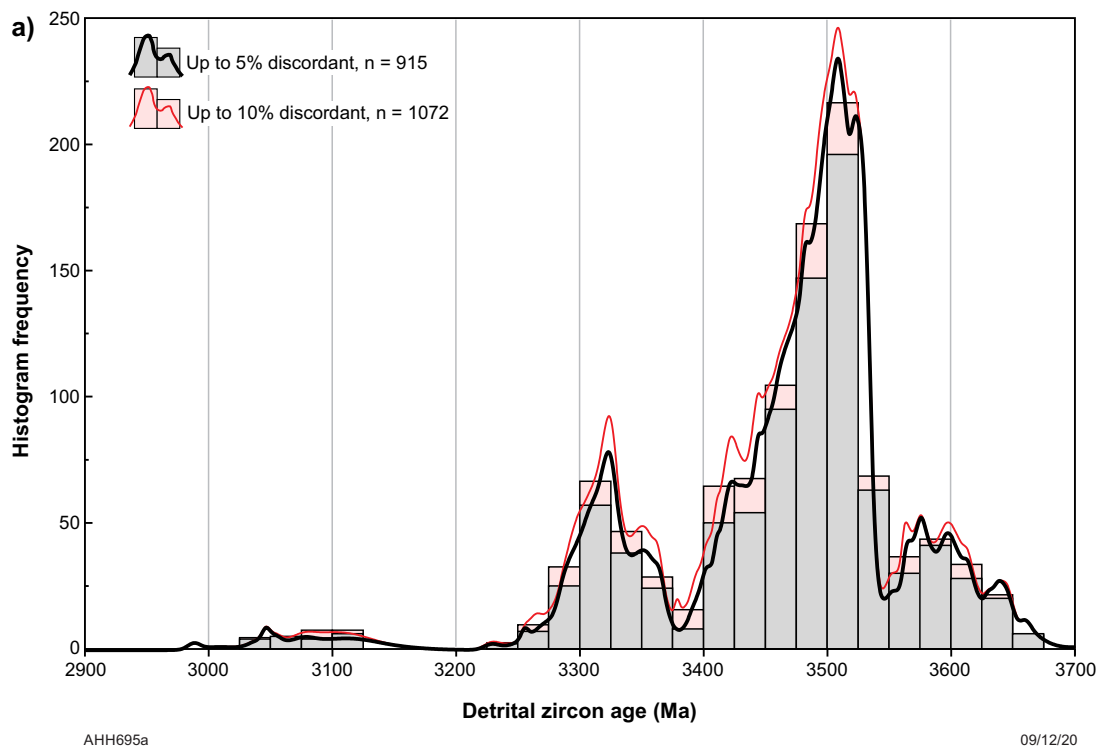


Figure 12. Histograms showing the frequencies of detrital zircon ages in sedimentary formations of the east Pilbara Craton, grouped by spatial association of samples with domes, excluding the Mosquito Creek and Mallina Formations. a) All data with three well defined peaks at 3660–3560 Ma (early crust), 3530–3400 Ma (Warrawoona Group and EPT granitic intrusions of the same age), and 3360–3280 Ma (Kelly Group and Emu Pool Supersuite). Pre-3530 Ma detrital zircons are concentrated in the Corboy and Strelley Pool Formations (d, e, f) (large sedimentary basins), although the Apex Basalt (c), and parts of the Duffer (d) and Wyman (e) Formations, also contain old zircons, presumably from more proximal sources. Differences between the zircon age spectra of different domes support relatively local derivation of detritus in most formations. Data selected from Appendix 6

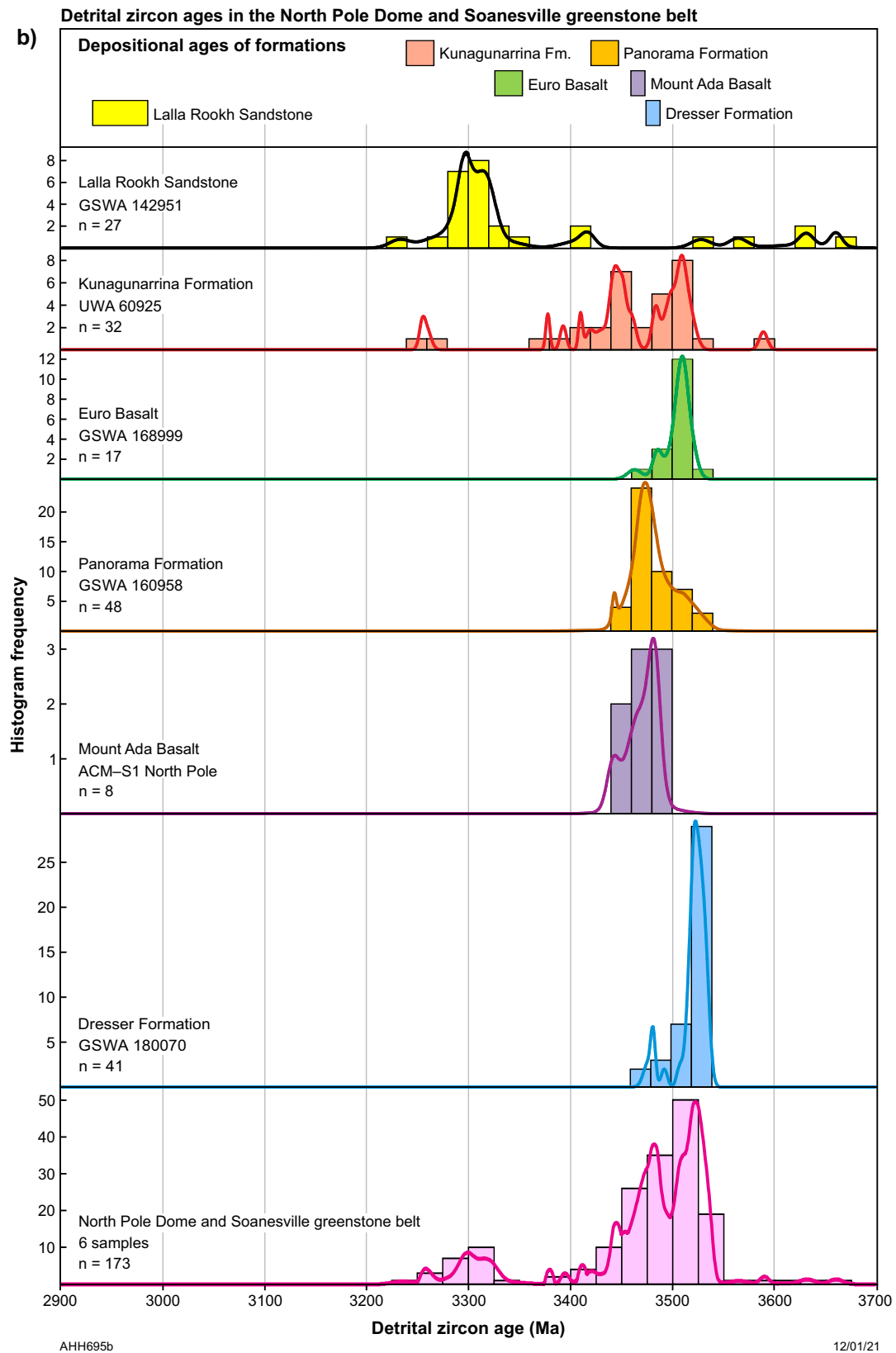


Figure 12. b) North Pole Dome and Soanesville greenstone belt

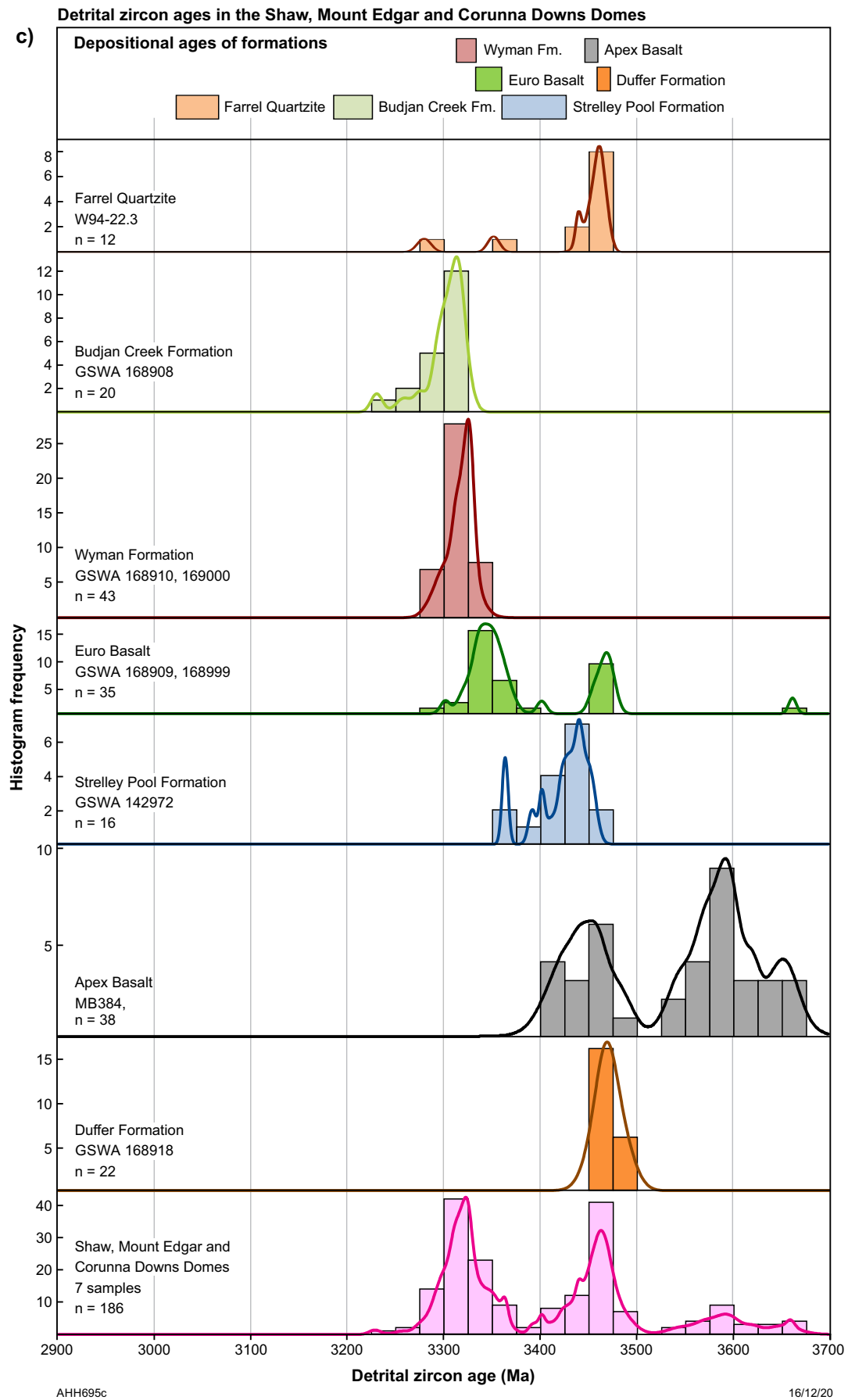


Figure 12. c) Shaw, Mount Edgar and Corunna Downs Domes

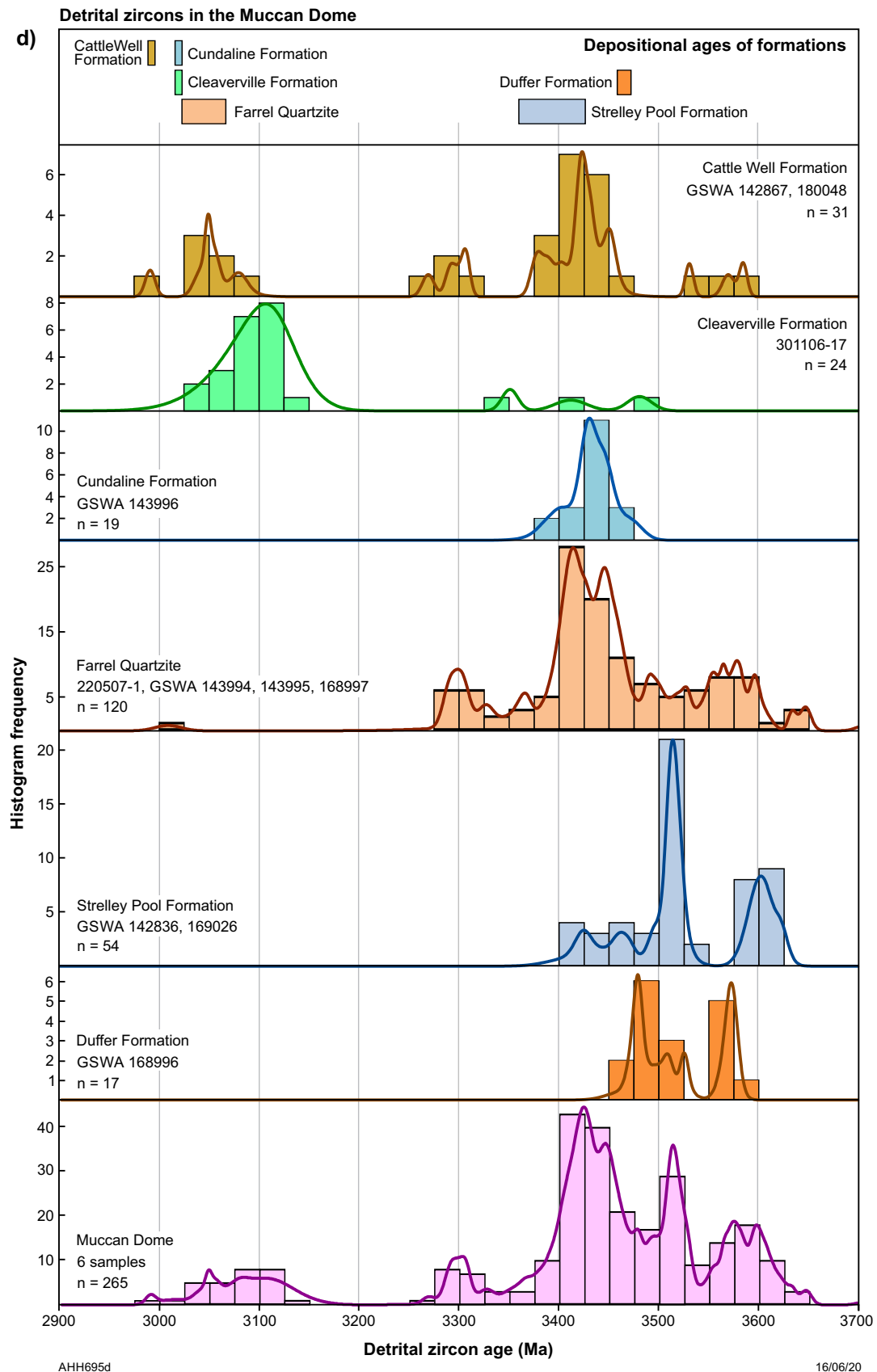


Figure 12. d) Muccan Dome

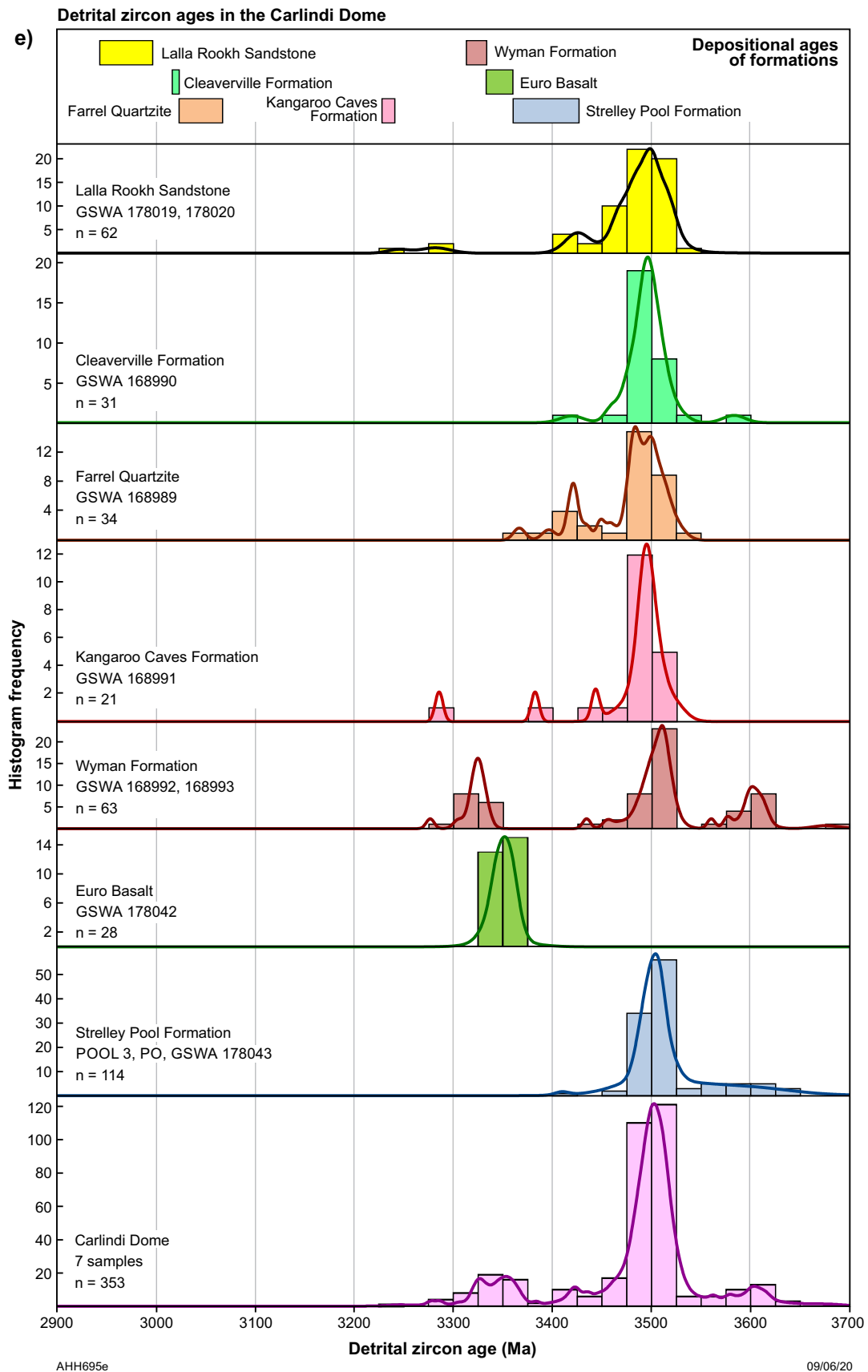


Figure 12. e) Carlindi Dome

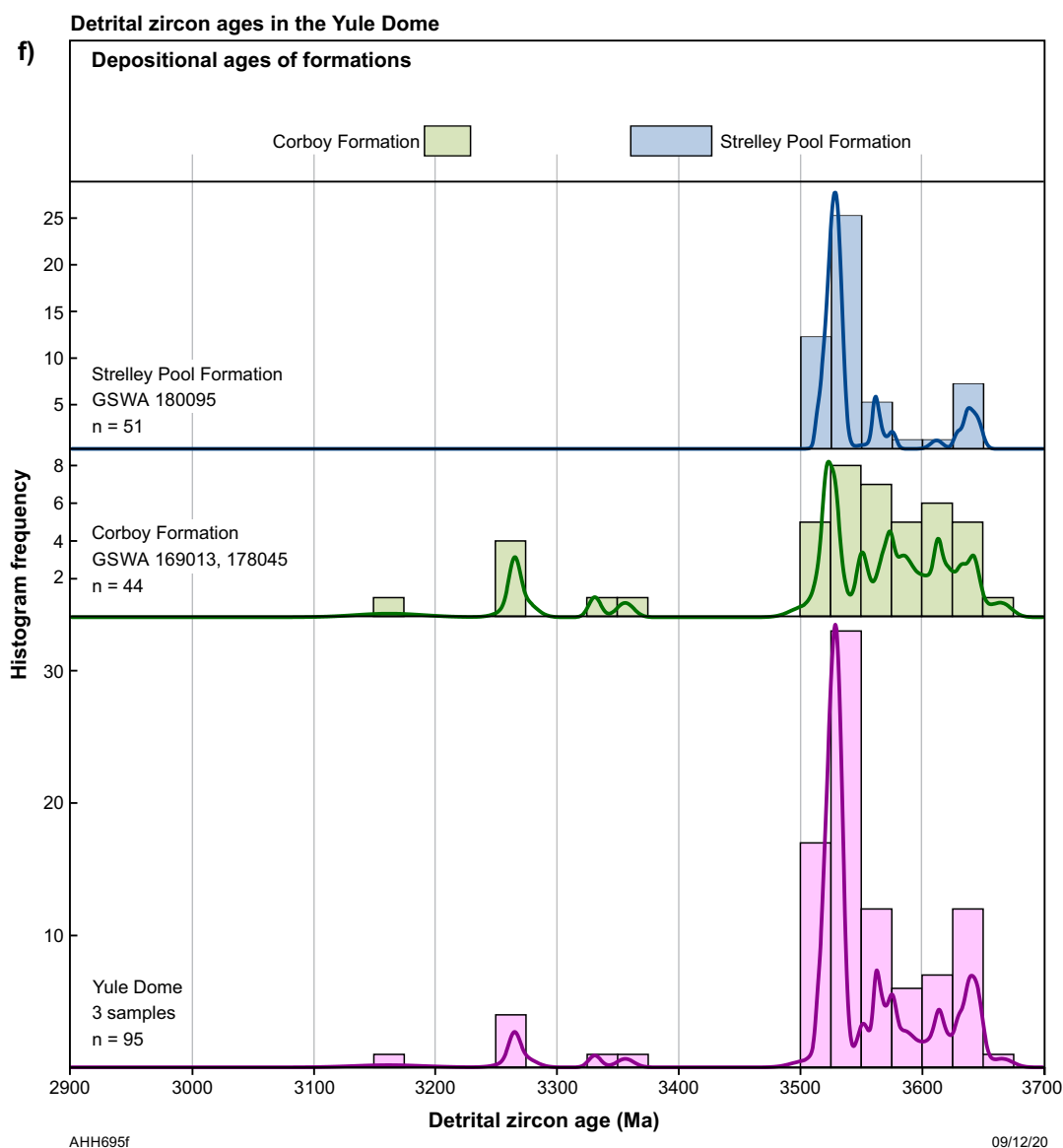


Figure 12. f) Yule Dome

Statistical analysis of data

Previous statistical analysis of Pilbara Craton detrital zircon data has been limited to the Mesoarchean Mosquito Creek Basin (Bagas et al., 2004b, 2008). Figure 12a shows the relative frequency of detrital zircon dates (1072 analyses) from the east Pilbara Craton. Several important observations are made from this histogram.

1. Almost all detrital zircons are older than 3220 Ma, indicating derivation from the EPT and older crust, despite inclusion of all zircon data from sandstones of eight different Mesoarchean formations. The marked lack of detrital zircons younger than c. 3260 Ma is surprising because granitic and felsic volcanic rocks younger than this outcrop widely in the east Pilbara Craton (e.g. Cleland, Mount Billroth, Elizabeth Hill, and Sisters Supersuites, and felsic volcanic rocks of the Sulphur Springs Group). The absence of detrital zircons from these potential felsic sources suggests non-exposure of late Paleoarchean and Mesoarchean granitic rocks during Mesoarchean deposition, whereas older rocks were still being eroded. The older rocks are interpreted to have included older crust in addition to Paleoarchean rocks (sedimentary and igneous) containing zircons derived from pre-3530 Ma crust.
2. No Mesoarchean felsic igneous rocks (3130–2919 Ma) of the northwest Pilbara Craton (e.g. granitic rocks of the Railway, Orpheus, Maitland River, or Sisters Supersuites, and felsic volcanic rocks of the Whundo and Whim Creek Groups) contributed detrital zircons to the Mesoarchean sandstones of the east Pilbara Craton. This supports the idea that the majority of detrital zircons in the east Pilbara Craton sandstones were derived from proximal sources.
3. The youngest of three well-defined zircon age components (Fig. 12a) coincides with the combined age range of the 3324–3290 Ma Emu Pool Supersuite and 3350–3315 Ma Kelly Group. Importantly, this age component is similar to the ages of volcanoclastic units in the Euro Basalt and Wyman Formation itself (Fig. 12c,e), hence most of the zircons represented by this peak are likely to have been derived from reworking

of igneous rocks of the same age. Detrital zircons dated between c. 3350 and 3290 Ma are also present in the c. 2950 Ma Lalla Rookh Sandstone (Fig. 12b) and the c. 3220 Ma Budjan Creek Formation (Fig. 12c), indicating exposure of the c. 3300 Ma stratigraphic units during deposition of some post-3290 Ma formations but not others (e.g. Farrel Quartzite, Cleaverville Formation, and Cundaline Formation of the Gorge Creek Group). In general, source rocks older than c. 3400 Ma contributed almost all detrital zircons to most of the Paleoproterozoic and Mesoproterozoic sedimentary units of the east Pilbara Craton. The Mallina and Mosquito Creek Formations were deposited in large rift-related sedimentary basins that formed after the domes of the EPT, and had multiple sources of sediment supply (Fig. 14).

4. There is a pronounced scarcity of 3400–3360 Ma detrital zircons. This interval coincides with deposition of sandstone in the Strelley Pool Formation and supports there being little or no igneous activity at this time (Hickman, 2008, 2012). If any plutonic rocks had been introduced into the crust between 3400 and 3360 Ma, some would almost certainly have been uplifted and eroded at some stage over the next 450 Ma. Major events of uplift and erosion occurred during the 3325–3290 Ma Emu Pool Event (EPE), the 3280–3165 Ma EPTRE, the c. 3070 Ma Prinsep Orogeny, and the 2955–2919 Ma North Pilbara Orogeny. The 3400–3360 Ma interval therefore marks a break in magmatic activity between the Warrawoona and Kelly Groups.
5. The major detrital zircon age component between c. 3540 and 3400 Ma (Fig. 12a) can be partly explained by erosion of 3485–3416 Ma granitic rocks of the Callina and Tambina Supersuites and felsic volcanic rocks of the Duffer and Panorama Formations. However, the 3540–3480 Ma portion of that peak indicates an additional major source of detritus that until recently has not been represented by dated felsic igneous outcrops in the EPT. Only the c. 3515 Ma Coucal Formation of the Coonterunah Subgroup (lower Warrawoona Group) was known to contain felsic igneous rocks of this age, but there are very few outcrops of this formation in the EPT. The detrital zircon data strongly suggested that a 3530–3490 Ma granitic suite or supersuite was exposed during Paleoproterozoic and Mesoproterozoic deposition (Gardiner et al., 2017). That this source is either no longer exposed or is only very poorly exposed might be explained by voluminous post-3480 Ma granitic intrusion. However, recent geochronology (Wiemer et al., 2018; Petersson et al., 2019b, 2020) has revealed outcrops of a 3530–3490 Ma granitic supersuite in two domes of the EPT. Petersson et al. (2020) named this the Mulgundoon Supersuite.
6. The 3660–3560 Ma age component is consistent with the ages of xenocrystic zircons in older magmatic rocks (Table 2, Appendix 3) that indicate pre-3530 Ma crust as old as c. 3760 Ma. Representation in the detrital zircon record indicates that this old crust was exposed and eroded during the Paleoproterozoic and Mesoproterozoic. The main exposures were probably located in the Yule, Carlindi, Muccan, and Mount Edgar Domes (Fig. 12c–f), and probably also the Warrawagine Dome (c. 3600 Ma detrital zircons in the Farrel Quartzite; GSWA 143995, Nelson, 1998l).

The detrital zircon dates are divided by dome and stratigraphic host formation in Fig. 12b–f. Two additional conclusions are reached from these histograms.

1. The various domes present different detrital zircon age spectra. For example, in the Yule Dome (Fig. 12f), almost all detrital zircons are older than c. 3500 Ma; whereas in the Shaw, Mount Edgar and Corunna Downs Domes (Fig. 12c), almost all formations except the Apex Basalt (Fig. 11) contain zircons derived from presently exposed Paleoproterozoic felsic igneous rocks. The Carlindi Dome (Fig. 12e) is dominated by 3520–3480 Ma detrital zircons irrespective of the host formation, whereas sandstones of the Muccan Dome (Fig. 12d) contain a wide range of detrital zircon dates. Sandstones of the North Pole Dome and Strelley area of the Soanesville greenstone belt (Fig. 12b) contain detrital zircons of Warrawoona Group age (c. 3530–3427 Ma), including a significant age component at c. 3520 Ma.
2. Depositional ages of the formations from which detrital zircons were extracted reveal that formations deposited after c. 3420 Ma (i.e. younger than the Warrawoona Group) contain a disproportionately large percentage of the oldest zircons. This suggests that in some domes, much of the Warrawoona Group had been eroded by c. 3420 Ma, and that this allowed erosion of underlying older crust. On this basis, most pre-3420 Ma uplift occurred in the Yule, Carlindi, and Muccan Domes, and possibly also the Warrawagine Dome.

Figure 13 illustrates the age distribution of detrital zircons in each of the main stratigraphic units. As in Figure 12, an important observation is that most detrital zircons are older than c. 3420 Ma irrespective of the depositional ages of the host deposits. Figure 13 supports previous geological interpretations of the tectonic setting of the depositional basins in the eastern Pilbara Craton. Applying the relationship between detrital zircon age spectra and the tectonic setting of the basin in which the zircons were deposited (Cawood et al., 2012), it is notable that the Leilira Formation (Sulphur Springs Group) and Strelley Pool Formation reveal a marked disconnect between depositional age and detrital zircon dates, consistent with intracratonic or extensional settings (Fig. 13d,f).

Volcaniclastic samples from the Kelly Group contain detrital zircons similar in age to the depositional age, as well as much older detrital zircons with age components at c. 3610 and 3510 Ma (Fig. 13e). This is inconsistent with convergent margin settings such as back-arc and fore-arc basins. Figure 13g might initially suggest that the tectonic setting of the Warrawoona Group was a convergent margin but closer examination argues against this interpretation. First, although the age range of the Warrawoona Group is generalized on the histogram as 3530–3420 Ma, none of the samples providing the zircon dates had a depositional age older than c. 3481 Ma, and 60% of the zircon dates are older than this. Second, most of the data in Figure 13g coincide with data in Figure 12b where both the Panorama and Dresser Formations contain zircons about 40–60 Ma older than the depositional age.

The Soanesville Group (Fig. 13c) contains a large proportion of detrital zircons older than 3500 Ma. The reason for this may lie in the depositional environment of this group –

a passive-margin, clastic basin formed immediately after rifting and breakup of the EPT at c. 3220 Ma. Crustal uplift and rifting probably exposed deep levels of the EPT crust to rapid erosion. The largest rift fault on the northwest margin

of the EPT, the Tappa Tappa Shear Zone (Fig. 3), contains sheared felsic igneous rocks of the Cleland Supersuite that locally include xenocrystic zircons dated at c. 3629 Ma (KB312, Beintema, 2003).

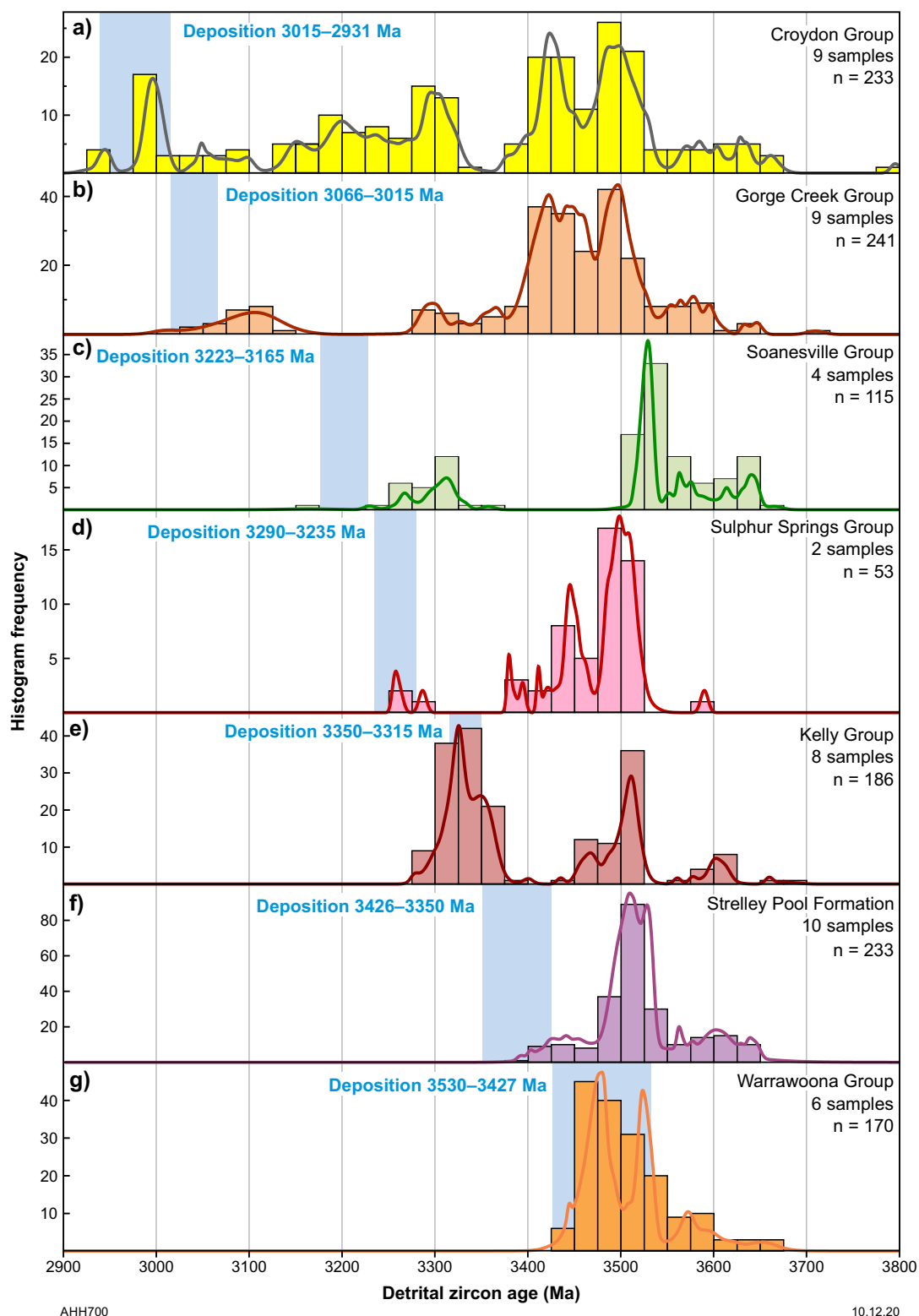


Figure 13. Histograms and normalized relative probability diagrams of detrital zircon ages in sedimentary formations arranged by lithostratigraphic group and depositional age (vertical blue bar). Difference between depositional age and average detrital zircon age increases with decreasing depositional age, and the dominant source age for all groups except the Soanesville Group is 3520–3400 Ma, indicating derivation of detritus from the Warrawoona Group and granites of the same age. Data selected from Appendix 6

Figures 12 and 13 exclude detrital zircon data for the Mallina and Mosquito Creek Basins (see Fig. 14 and Appendix 7) because sources of detritus in these rift basins are less certain than those for older sedimentary rocks in the east Pilbara Craton. Deposition in the Mallina and Mosquito Creek Basins was mainly deep water and included submarine fans and turbidites (Hickman, 1975a, 1978, 1983; Eriksson, 1982; Smithies et al., 1999, 2001b; Farrell, 2006; Bagas et al., 2008; Nijman et al., 2010; Hickman, 2016). Axial currents, parallel to the length of elongate rift basins, potentially transport detritus over considerable distances, and this might have applied to deposition in the upper stratigraphic members of the Mosquito Creek Formation (Bagas et al., 2008). Both basins contain minor Eoarchean detrital zircons, the oldest crystallization age recorded being c. 3795 Ma (GSWA 142942, Nelson, 2000d). Even so, the zircon age spectra shown in Figure 14 suggest that most detrital zircons in these basins originated from erosion of known stratigraphic units in the Pilbara Craton.

In the case of the Mallina Basin, this conclusion is supported by previous sedimentological interpretations (Eriksson, 1982), particularly those that indicate derivation of most detritus from the East Pilbara Terrane (Smithies, 1998b; Smithies et al., 1999, 2001b; Smithies and Farrell, 2000b;

Van Kranendonk et al., 2002). The Mallina Basin data show age modes at 3450–3400 Ma (Tambina Supersuite and Panorama Formation), 3240–3178 Ma (Cleland and Mount Billroth Supersuites, and Sulphur Springs and Soanesville Groups), and c. 2990 Ma (Maitland River Supersuite). There is a less prominent mode between c. 3660 and 3560 Ma, coinciding with data from the EPT (Figs 12, 13).

Most detrital zircons in the Mosquito Creek Basin have dates between c. 3620 and 3380 Ma (Fig. 14), consistent with derivation from the EPT and older crust. Prominent zircon age components are indicated between c. 3580 and 3520 Ma, and between c. 3500 and 3420 Ma. Other components are present at 3320–3280 Ma (age range of the Emu Pool Supersuite and Kelly Group) and 3200–3160 Ma (age range of the Mount Billroth Supersuite and Soanesville Group).

Bagas et al. (2004b, 2008) argued that zircons dated at c. 3540, 3360, and 3090 Ma in the Mosquito Creek samples cannot be explained by derivation of detritus from the east Pilbara Craton. However, the data indicate that these zircons are relatively uncommon in the Mosquito Creek Formation (total of 258 detrital zircon analyses <10% discordant). There are 20 detrital zircons dated within uncertainty of c. 3540 Ma with the dates ranging from c. 3554 to 3525 Ma.

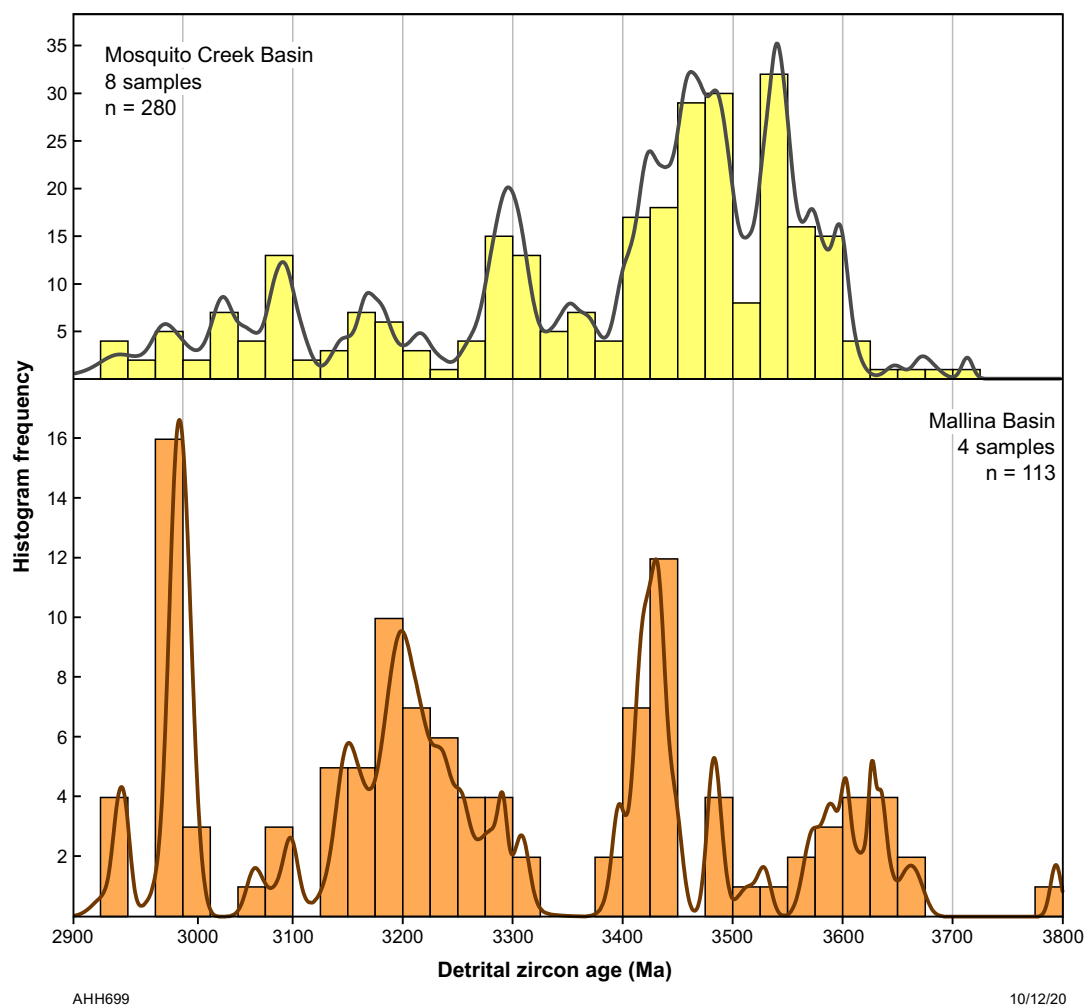


Figure 14. Histograms and normalized relative probability diagrams of detrital zircon ages in the 3015–2930 Ma Mallina and Mosquito Creek Basins. Both these large late Mesoproterozoic basins contain far more diverse zircon age components than are present in the Paleoproterozoic and rifting-related early Mesoproterozoic formations. The Mosquito Creek Basin contains the higher percentage of 3600–3400 Ma zircons. Data tabulated within Appendix 6

Most of these zircons are interpreted to have come from pre-Pilbara Supergroup crust that is no longer exposed in the EPT. Only six Mosquito Creek detrital zircons have dates close to 3360 Ma, so this is an uncommon group in the basin. The c. 3360 Ma date is consistent with derivation from the Euro Basalt; for example, in the East Strelley greenstone belt GSWA 178042 contained 16 zircon dates between c. 3374 and 3350 Ma (Nelson, 2005g).

In summary, detrital zircon dates indicate that 3660–3540 Ma felsic crust was exposed to erosion during the Paleoproterozoic and Mesoproterozoic, and that the exposures were relatively widespread across the northern half of the Pilbara Craton. Scattered remnants of 3660–3540 Ma crust are currently exposed as small enclaves within the Tambina Supersuite of the Warrawagine Dome (GSWA 142870, Nelson, 1999e; GSWA 180057, Wingate et al., 2009d).

Whole-rock Sm–Nd isotope data

The earliest Sm–Nd studies on rocks of the east Pilbara Craton were conducted in the 1980s (Hamilton et al., 1981; Jahn et al., 1981; Collerson and McCulloch, 1983; Gruau et al., 1987; McCulloch, 1987; Bickle et al., 1989, 1993). Hamilton et al. (1980) plotted data from six samples of the Talga Talga Subgroup on a Sm–Nd evolution diagram. Their analysis indicated a depositional age of 3556 ± 32 Ma, which was consistent with available U–Pb zircon data that indicated the depositional age of the overlying Duffer Formation was c. 3450 Ma (Pidgeon, 1978a). The 3556 ± 32 Ma age is within uncertainty of the currently understood maximum age of the Talga Talga Subgroup at c. 3530 Ma.

Jahn et al. (1981) used the Sm–Nd isochron method to date the North Star Basalt at 3556 ± 542 Ma; the large uncertainty reflected a limited range of $^{143}\text{Nd}/^{144}\text{Nd}$ and $^{147}\text{Sm}/^{144}\text{Nd}$ in the four samples analysed. Collerson and McCulloch (1983) reported Nd T_{CHUR} model ages (assuming the Archean mantle had a chondritic composition) from the Shaw and Mount Edgar Domes that were <3500 Ma and similar to previously reported U–Pb zircon ages; considerably older Nd model ages would have been obtained using a depleted Archean mantle model.

Gruau et al. (1987) combined basaltic samples from the North Star Basalt and Mount Ada Basalt and used the Sm–Nd isochron method to arrive at a 3712 ± 98 Ma depositional age for the lower Warrawoona Group. They also calculated the results from the two basalt formations separately and obtained ages of 3737 ± 117 Ma for the North Star Basalt and 3715 ± 170 Ma for the Mount Ada Basalt. Noting that these Sm–Nd ages are considerably older than current estimates for the depositional age of the North Star Basalt, Gruau et al. (1987) preferred an alternative interpretation that, rather than depositional ages, the isochrons represented mixing lines and the c. 3720 Ma dates reflect the time of extraction of sources from the mantle.

As part of a larger study, McCulloch (1987) analysed nine felsic igneous rocks from the east Pilbara Craton. The $^{143}\text{Nd}/^{144}\text{Nd}$ and $^{147}\text{Sm}/^{144}\text{Nd}$ results from four of these samples were interpreted by Champion (2013) to indicate Nd model ages ranging from c. 3700 to 3440 Ma and ϵ_{Nd} values of +0.45 to –6.67. Bickle et al. (1989) reported Sm–Nd data for eight granitic samples from the Shaw Dome.

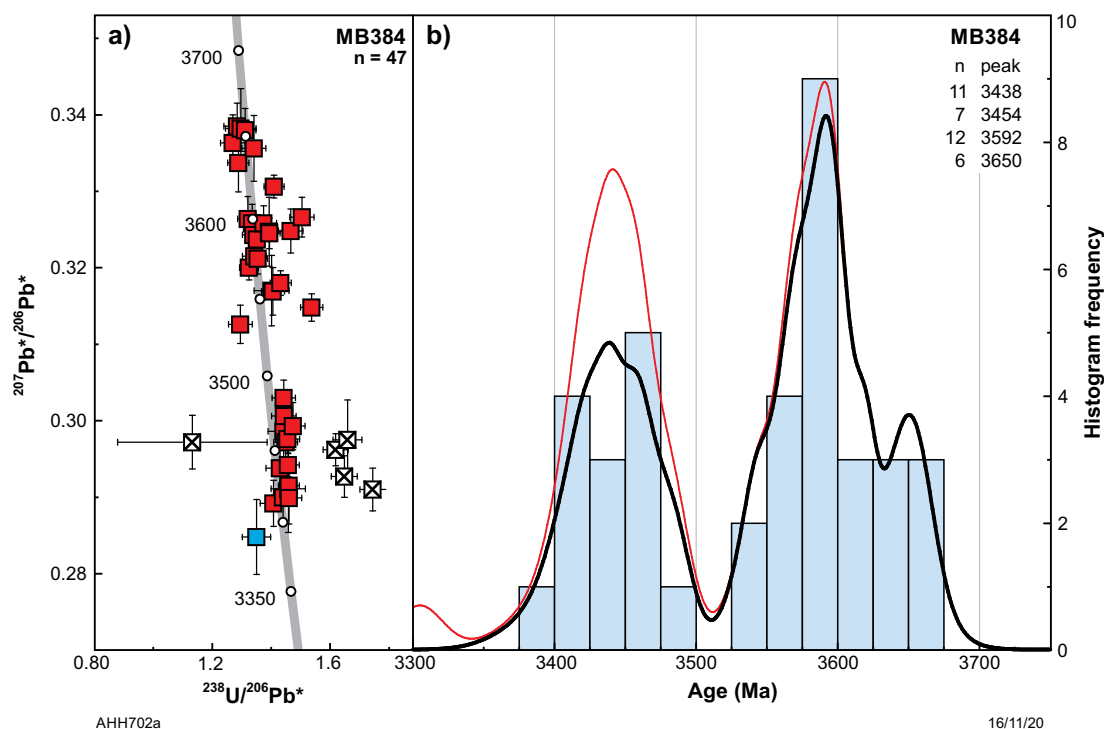


Figure 15. U–Pb analytical data for detrital zircons in a sandstone unit of the Apex Basalt, Warrawoona Group (data from sample MB384, WJ Collins, written comm.): a) concordia plot; b) histogram. Zircon age components at c. 3650 and c. 3592 Ma are consistent with zircon age peaks from other sedimentary formations in the east Pilbara, supporting crust-forming magmatic events at about these times. The c. 3454 Ma age component is interpreted to have been derived from erosion of the Duffer Formation underlying the Apex Basalt. In (a), n = number of analyses; blue square indicates the youngest detrital zircon; red squares indicate older detrital zircons; crossed squares indicate discordance >5%. In (b), n = number of dates in each significant age component (Ma, based on three or more ages)

As recalculated by Champion (2013), the oldest Nd model ages, c. 3740 and 3590 Ma, were obtained on two monzogranites of the 2851–2831 Ma Split Rock Supersuite. The ϵ_{Nd} values of these rocks were –8.01 and –6.1, suggesting partial melting of much older crust. Data from the Garden Creek Monzogranite, not dated by the U–Pb zircon method, but which Smithies et al. (2007a) interpreted to be an intrusion of the Sisters Supersuite, was recalculated by Champion (2013) to give a Nd model age of c. 3590 Ma and ϵ_{Nd} value of –5.23. Data from five other samples from the Sisters Supersuite were recalculated by Champion (2013) to give Nd model ages from c. 3530 to 3420 Ma and ϵ_{Nd} values of –4.47 to –3.31.

Bickle et al. (1989) interpreted the negative ϵ_{Nd} values as evidence for derivation of melts from older crust. Bickle et al. (1993) provided Nd model ages (T_{CHUR} and T_{DM}) and ϵ_{Nd} values for seven samples from Paleoproterozoic granitic rocks in the Shaw Dome. Assuming a crystallization age of c. 3470 Ma (Callina Supersuite) for all the samples, Champion (2013) recalculated the Nd model ages for these older granitic rocks to range between c. 3770 and 3530 Ma, and ϵ_{Nd} values to be between +1.65 and –1.53.

Tyler et al. (1992) used the Sm–Nd method to investigate granitic rocks of the Sylvania Inlier (outside the area of this Report), Kurrana Terrane, and Shaw Dome. Four of the five samples analysed from the Kurrana Terrane and Shaw Dome were from intrusions of the Split Rock Supersuite, and Champion (2013) recalculated the Nd model ages to be between c. 3490 and 3410 Ma, with ϵ_{Nd} values of –4.77 to –3.75. Champion (2013) and Champion and Huston (2016) used Nd data from the EPT to suggest that the average crustal source ages of the Paleoproterozoic rocks were c. 3600 Ma, with maximum average source ages for individual samples up to c. 3800 Ma. Gardiner et al. (2017, 2018) reached the same conclusion as Champion and Huston (2016) regarding EPT Nd model ages, and used new Hf isotope data from the Mount Edgar Dome to interpret average Hf model ages of 3.7 – 3.6 Ga.

Tessalina et al. (2010) analysed metabasalt from the c. 3481 Ma Dresser Formation to derive a Sm–Nd isochron that indicated a depositional age of 3490 ± 100 Ma. Their calculated ϵ_{Nd} value of -3.3 ± 1.0 was interpreted to indicate a much older source. Based on trace element and isotope modelling they interpreted this source to have differentiated from the mantle at >4300 Ma.

Sm–Nd model ages

Figure 16 examines the spatial distribution of Nd model ages in the northern Pilbara Craton. As observed previously (Van Kranendonk et al., 2006b, 2007a,b; Champion, 2013; Champion and Huston, 2016), Nd model ages for samples collected in the Paleoproterozoic East Pilbara Terrane (EPT) are almost invariably older than those for Mesoproterozoic rocks of the West Pilbara Superterrane and De Grey Superbasin in the northwest Pilbara Craton. Eoarchean Nd model ages (>3600 Ma, Fig. 16a) are recorded in the Warrawagine, Muccan, Mount Edgar, Shaw, Carlindi and Yule Domes (Fig. 8). By contrast, model ages younger than c. 3310 Ma (Fig. 16c) are concentrated in the Mallina Basin and Sholl Terrane. Significantly, the differences between Nd model ages and rock crystallization ages are, in most instances, far less in the northwest Pilbara Craton than in the EPT.

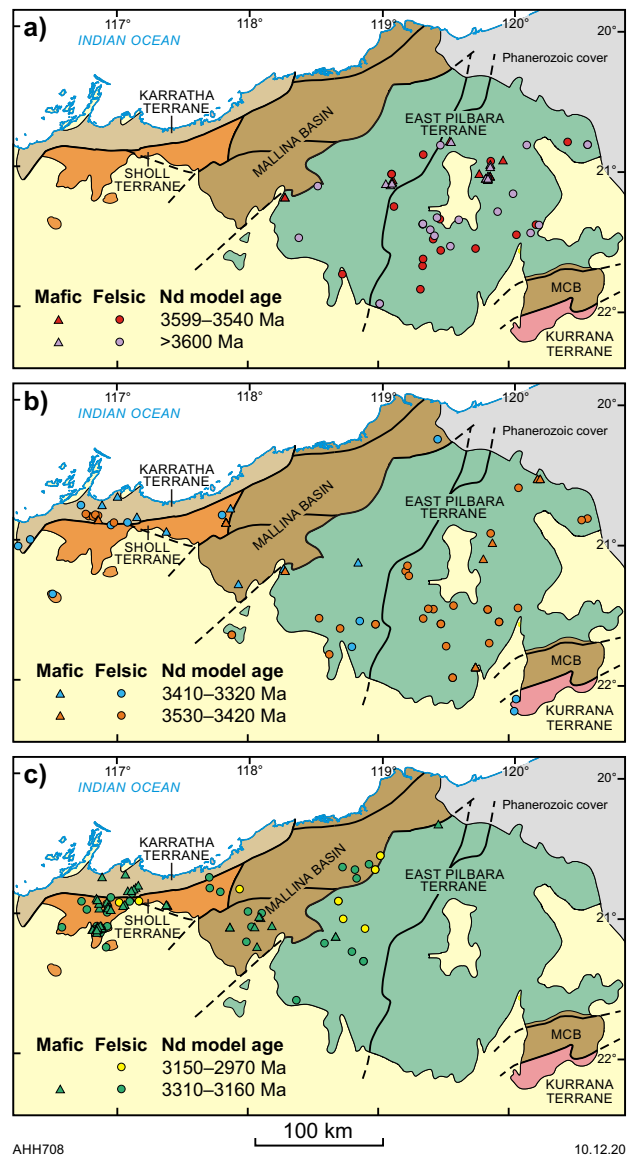


Figure 16. Sm–Nd two-stage depleted mantle model ages (T_{DM}^2) from mafic and felsic igneous rocks of the northern Pilbara Craton. Nd model ages older than the maximum depositional age of the Pilbara Supergroup (3530 Ma) have been obtained only from the EPT (a) whereas model ages <3310 Ma are mainly confined to the northwestern area of the Pilbara Craton (c). Paleoproterozoic Nd model ages in the northwest Pilbara (b) have been obtained from the Karratha Terrane and tectonic units overlying that terrane. These data have been interpreted to indicate that, apart from the Karratha Terrane, igneous formations and intrusions in the northwest Pilbara Craton were derived from juvenile Mesoproterozoic crust. Data are taken from Smithies et al. (2007a)

This is consistent with most Mesoproterozoic units in the northwest Pilbara Craton having formed as juvenile crust or from juvenile sources, whereas most Paleoproterozoic units in the EPT were derived by recycling of significantly older crust (Bickle et al., 1993; Collins, 1993; Green et al., 2000; Van Kranendonk et al., 2007a,b; Smithies et al., 2009; Champion, 2013; Champion and Huston, 2016; Gardiner et al., 2017, 2018). Nd model ages in the range 3530–3220 Ma are recorded northwest of the Mallina Basin, mostly in the Paleoproterozoic Karratha Terrane (Fig. 16b). The absence of >3530 Ma Nd model ages from the Karratha Terrane may

reflect the small number of late Paleoproterozoic rocks from that terrane (Cleland Supersuite and Roebourne Group). Even in the EPT, almost no 3270–3250 Ma rocks (Karratha Terrane age) have Nd model ages >3560 Ma (Gardiner et al., 2017). This is possibly due to average mantle extraction ages of mixed sources that included not only common EPT sources, but also more-juvenile rift-related sources (rifting during the EPTRE commenced as early as c. 3280 Ma).

Nd model ages and ϵ_{Nd} values are given in Table 4 and plotted against sample age in Figure 17. From 3530 to 3220 Ma, the EPT shows only gradually decreasing Nd model ages (Fig. 17a), a feature which indicates long-term reworking of 3700–3500 Ma crust with only minor additions of juvenile material. At c. 3200 Ma, some rocks of the Soanesville Basin (green shaded area) were derived from more juvenile, 3300–3200 Ma crust. Then, between 2950 and 2830 Ma, Mesoproterozoic granitic rocks show a wide range of Nd model ages between c. 3750 and 2950 Ma. The younger Nd model ages come from the Carlindi (CA) and northern Yule (NY) Domes (yellow shaded area, Fig. 17a), whereas samples from areas farther east in the EPT still show evidence of derivation from Eoarchean to early Paleoproterozoic sources.

Figure 17b shows that, apart from samples from the Soanesville Basin and the Yule and Carlindi Domes, rocks from the EPT show steadily decreasing ϵ_{Nd} values with decreasing magmatic age. This indicates ongoing reworking of Eoarchean to early Paleoproterozoic sources with time. However, in western areas of the EPT (CA and NY: Carlindi and Yule Domes), granitic magmas were most likely derived from melting of subducted juvenile crust of the Mallina Basin.

The relatively young Nd model ages from the Carlindi and Yule Domes led to questions about the northwestern extent of the EPT (Van Kranendonk et al., 2004c, 2007b; Smithies et al., 2007c; Champion, 2013; Champion and Huston, 2016). For example, Smithies et al. (2007c) suggested that these young Nd model ages indicate a western limit of the EPT extending northeast through the Carlindi and Yule Domes. However, the presence of c. 3250 Ma granitic, felsic volcanic and gabbroic rocks along the TTSZ (Beintema et al., 2001, 2003; Beintema, 2003; GSWA 160258, Wingate et al., 2010) indicates that the EPT extends to this major crustal structure. These c. 3250 Ma units are correlated with the Cleland Supersuite and Sulphur Springs Group of the EPT. Additionally, xenocrystic zircons in the c. 3250 Ma granitic rocks have ages consistent with derivation from much older Paleoproterozoic sources (GSWA 160745, Nelson, 2001b; KB263, 312, 770, 779, Beintema, 2003) that are not known to exist outside the EPT.

Accordingly, the northwestern boundary of the EPT remains as previously defined by geological mapping and stratigraphy (Van Kranendonk et al., 2002), and coincides with the TTSZ (Hickman, 2016). The present explanation for young Nd model ages within the Carlindi and Yule Domes is that late Mesoproterozoic granites were intruded into these Paleoproterozoic domes during convergence and collision between the EPT and the Mallina Basin. Table 3 summarizes the ranges of Nd model ages and ϵ_{Nd} values (see below) of individual stratigraphic units in the east Pilbara Craton. It is notable that extrusive and intrusive units older than c. 3200 Ma have consistently old Nd model ages. For Mesoproterozoic units, Nd model ages east of the Lalla Rookh – Western Shaw Structural Corridor (LWSC, Fig. 5) range

between c. 3700 and 3400 Ma, whereas Nd model ages in the Carlindi and northern Yule Domes are generally younger than c. 3300 Ma. Limited data from the Yule Dome indicate that the southern part of this dome, which includes tonalites of the Elizabeth Hill and Mount Billroth Supersuites, had crustal sources similar to those in the EPT east of the LWSC.

ϵ_{Nd} values

Sm–Nd isotope data from the northern Pilbara Craton reveal substantial differences in ϵ_{Nd} values between the east Pilbara Craton and most units of the northwest Pilbara Craton (Smith et al., 1998; Sun and Hickman, 1998; Arndt et al., 2001; Smithies et al., 2004a, 2007c; Van Kranendonk et al., 2007a,b; Champion, 2013; Champion and Huston, 2016; Gardiner et al., 2017, 2018). In the northwest Pilbara Craton, most stratigraphic units within the Regal and Sholl Terranes have positive ϵ_{Nd} values up to +3.5 indicating juvenile crust (Smithies et al., 2007c; Champion, 2013; Champion and Huston, 2016; Hickman, 2016), whereas many stratigraphic units of the in the EPT have moderately to strongly negative ϵ_{Nd} values consistent with crustal reworking (Champion, 2013; Champion and Huston, 2016; Gardiner et al., 2017, 2018).

In the east Pilbara Craton, two significant Nd trends are revealed by comparing rocks that vary in crystallization age from c. 3570 to 3220 Ma (Fig. 17). First, Nd model ages do not decrease with decreasing crystallization ages (Fig. 17a), indicating no significant change in the ages of crustal sources (Eoarchean to early Paleoproterozoic) with time. Only in the Carlindi Dome, and to a lesser degree the Yule Dome, is there evidence of substantial addition of juvenile magma. Second, there is a strong trend for increasingly negative ϵ_{Nd} values in younger rocks (Fig. 17b), consistent with repeated derivation of melts from the same old sources. There are few ϵ_{Nd} values from the EPT to suggest sources much older than c. 3700 Ma, although because Nd model ages indicate the average age of sources, this does not preclude contributions from sources >3700 Ma. The maximum age of crustal extraction for any particular rock is likely to be greater than the Nd model age.

The widespread distribution of samples yielding Nd model ages >3530 Ma (Fig. 16a) indicates that pre-3530 Ma crust was present in all parts of the EPT during deposition of the Pilbara Supergroup and intrusion of the Paleoproterozoic granitic supersuites. The predominant age range of this older crust is between c. 3680 and 3540 Ma (Fig. 17a, Table 4). Pilbara Craton Sm–Nd isotope data indicate widespread crustal recycling until c. 3220 Ma.

Zircon Lu–Hf data

As part of a wider study, Amelin et al. (2000) reported U–Pb and Lu–Hf data for zircons from three previously dated samples from the east Pilbara Craton (Thorpe et al., 1992a): 1) GSWA 94770, c. 3448 Ma porphyritic felsic volcanic rock from the Panorama Formation at West Bamboo, Mount Edgar Dome; 2) GSWA 103283, c. 3441 Ma porphyritic subvolcanic dacite of the Tambina Supersuite at Miralga Creek, North Pole Dome; 3) GSWA 94754, c. 3320 Ma rhyolite from the Wyman Formation at Emu Creek, Corunna Downs Dome.

Eight zircons were analysed from each of these samples, with positive ϵ_{Hf} values ranging between +4.56 (GSWA 94770) and +1.75 (GSWA 94754). These early results suggested derivation of juvenile magma from a depleted mantle at c. 3448 Ma changing to derivation from a mantle of more closely chondritic composition at c. 3320 Ma. Data in this Report (below) suggest that the strongly positive ϵ_{Hf} values obtained from zircons in the Panorama Formation and Tambina Supersuite are atypical of most of the EPT, although they are considered significant in providing evidence of a depleted Pilbara Craton mantle at c. 3450 Ma (see discussion under **Depleted or chondritic Paleoarchean mantle?**).

Kemp et al. (2011) briefly summarized unpublished Nd and Hf isotope data from a large number of Paleoarchean to Neoarchean Pilbara Craton rocks that varied in composition from komatiite to rhyolite and granite, and included many samples from the northwest Pilbara Craton. They interpreted a strong temporal trend to increasingly negative ϵ_{Hf} values in zircons from felsic igneous rocks after c. 3200 Ma, and interpreted this to indicate Mesoarchean reworking and recycling of >3500 Ma crust. They reported approximately chondritic initial $^{176}\text{Hf}/^{177}\text{Hf}$ ratios in most pre-3500 Ma zircons and, assuming an approximately chondritic mantle composition, interpreted this as evidence against reworking of >3800 Ma crust. Kemp et al. (2014) used a >3500 Ma chondritic mantle model to argue that crustal evolution in the Pilbara Craton commenced at c. 3650 Ma, and that their data provided no evidence for significantly older crust. These conclusions are significantly different from interpretations reached in other similar studies.

Whole-rock Lu–Hf data from the east Pilbara Craton

Guitreau et al. (2012) included new whole-rock and zircon Lu–Hf data from the east Pilbara Craton as part of a global study of Archean tonalite–trondhjemite–granodiorite (TTG). They concluded that, on a global scale, all continental crust was initially derived from unfractionated material from the deep mantle via mantle plumes, and that this left a depleted mantle residue in the upper mantle. The large dataset (over 12 000 samples) supported previous findings that suprachondritic ϵ_{Hf} values were present in some Archean TTGs, thus arguing for a depleted upper mantle in the Paleoarchean. They interpreted the deep mantle to have retained its primitive relative element abundances over most of Earth history because little continental material has been recycled to great depth.

Nebel et al. (2014) obtained whole-rock Hf isotope data from 21 east Pilbara Craton komatiite samples ranging in age from c. 3515 to 3200 Ma; eight komatiite samples from the northwest Pilbara Craton were also analysed. A number of strongly positive ϵ_{Hf} values (above +6.0) and initial $^{176}\text{Hf}/^{177}\text{Hf}$ ratios above depleted mantle were interpreted to provide evidence of mantle depletion from the Hadean onwards. Some negative ϵ_{Hf} values were partly attributed to crustal contamination of the hot komatiitic magmas. In contrast to the interpretation of Nebel et al. (2014), Kemp et al. (2014) interpreted the Hf–Nd systematics to indicate that the oldest Pilbara Craton komatiites and basalts were separated from mildly suprachondritic mantle – not from mantle that had been significantly depleted by older crust extractions. They argued the isotopic evidence did not support the view that 3520–3120 Ma Pilbara Craton granitic rocks were formed by

melting of significantly older crust; instead, they proposed that the granitic rocks were sourced from precursors with only short crustal residence times, and were juvenile continental additions.

Nebel-Jacobsen et al. (2018) presented whole-rock Hf isotope data from 3450–2760 Ma black shales of the Pilbara Craton (Archean Biosphere Drilling Project [ABDP] cores 2, 3, 5 and 6). Results of most relevance to the east Pilbara Craton were obtained from shale in ABDP 2 (Apex Basalt, not the Duffer Formation as stated in the paper) and the Mosquito Creek Formation (ABDP 5). Strongly positive ϵ_{Hf} values for shales of the Apex Basalt, plotting above the assumed depleted mantle array at c. 3450 Ma, were interpreted to indicate deposition during weathering of rocks from strongly depleted sources. Nebel-Jacobsen et al. (2018) commented that only komatiites from the Pilbara Craton and Barberton Greenstone Belt have comparable Hf isotope compositions, which suggests that detritus in the shales was derived from weathering and erosion of exposed juvenile komatiites rather than more evolved, reworked crustal sources. In contrast, all shale samples from the c. 2940 Ma Mosquito Creek Formation, and from the Mount Roe Basalt (ABDP 6) and Hardey Formation (ABDP 3) of the Neoarchean Fortescue Group, have negative ϵ_{Hf} values indicating evolved crustal sources in their areas of provenance. Hf model ages for these younger shales average c. 3250 Ma. Nebel-Jacobsen et al. (2018) concluded that the Hf isotope compositions of the Pilbara Craton black shales are consistent with a change from juvenile to evolved crust through the Paleoarchean to the Mesoarchean, as previously interpreted from other evidence by Smithies et al. (2007c) and Van Kranendonk et al. (2007b).

Current data

Published zircon Lu–Hf data used in this Report were derived from Kemp et al. (2015a,b), Gardiner et al. (2017, 2018), and from previously unpublished Lu–Hf data obtained by GSWA between 2010 and 2014. All these data were derived from Lu–Hf analysis of zircons on mounts previously used for SHRIMP U–Pb dating by GSWA. Individual zircon dates published in GSWA geochronology records released between 1994 and 2016 were used to select zircons most suitable for further study, and also to constrain the time at which initial $^{176}\text{Hf}/^{177}\text{Hf}$ ratios were set. To minimize any effects of zircon heterogeneity (e.g. growth zones of different ages), Lu–Hf analyses were conducted on the same analysis sites previously used for SHRIMP U–Pb geochronology. Most >3530 Ma zircons analysed are detrital, whereas the vast majority of zircons younger than c. 3500 Ma were extracted from felsic igneous rocks.

Lu–Hf analysis of detrital zircons

To investigate the possibility that the Pilbara Craton contains Hf isotope evidence of Hadean crust (>4000 Ma), Kemp et al. (2015a) analysed 84 detrital zircons (included within Appendix 9) older than 3550 Ma (representing about 50% of the pre-3550 Ma zircons previously identified by GSWA U–Pb dating). These detrital zircons came from 12 samples collected by GSWA geologists and geochronologists over a wide area of the northern Pilbara Craton. Of the 84 detrital zircons analysed, the three oldest (3795–3681 Ma) indicated negative ϵ_{Hf} values between –3 and –2, suggesting magmatic sources with very old mantle extraction ages

(4000–3800 Ma). These three detrital grains came from sandstones in the two largest Mesoarchean basins of the northern Pilbara Craton (Mallina and Mosquito Creek). The significance of these data for the age of the early Pilbara Craton crust depends on the origin of the zircons. Because data from the three oldest grains indicated significantly older sources than the other zircons analysed in their study, Kemp et al. (2015a) suggested that they might not have originated from the Pilbara Craton. However, Petersson et al. (2019b) have since reported numerous xenocrystic 3760–3600 Ma zircons in c. 3451 Ma rhyolite from the North Pole Dome, indicating that Eoarchean crust was present in the east Pilbara Craton during the Archean. Although Kemp et al. (2015a) observed that sufficiently old felsic igneous rocks exist in the Narryer Terrane of the Yilgarn Craton, the Yilgarn and Pilbara Cratons did not collide until the 2005–1950 Ma Glenburgh Orogeny (Sheppard et al., 2005; Spaggiari et al., 2008; Johnson et al., 2010, 2011, 2013), and paleomagnetic evidence suggests that the Yilgarn Craton was too remote to have provided detritus to the Pilbara Craton during the c. 2950 Ma deposition of the Pilbara Craton sedimentary

successions (Smirnov et al., 2013).

Two additional lines of evidence indicate derivation of the three oldest zircons directly from the Pilbara Craton.

1. Younger detrital zircons in the three host sandstone formations are consistent with erosion of Paleoarchean and Mesoarchean Pilbara Craton sources:
 - a) the zircon age components in the sample containing the 3795 ± 5 Ma zircon (GSWA 142942, Constantine Sandstone, Nelson, 2000d) suggest derivation by erosion of the Tambina, Mount Billroth, and Maitland River Supersuites
 - b) the 3714 ± 5 Ma zircon (GSWA 178010, Mosquito Creek Formation, Nelson, 2005a) is accompanied by zircon age components indicating derivation by erosion of the Callina, Tambina, and Emu Pool Supersuites

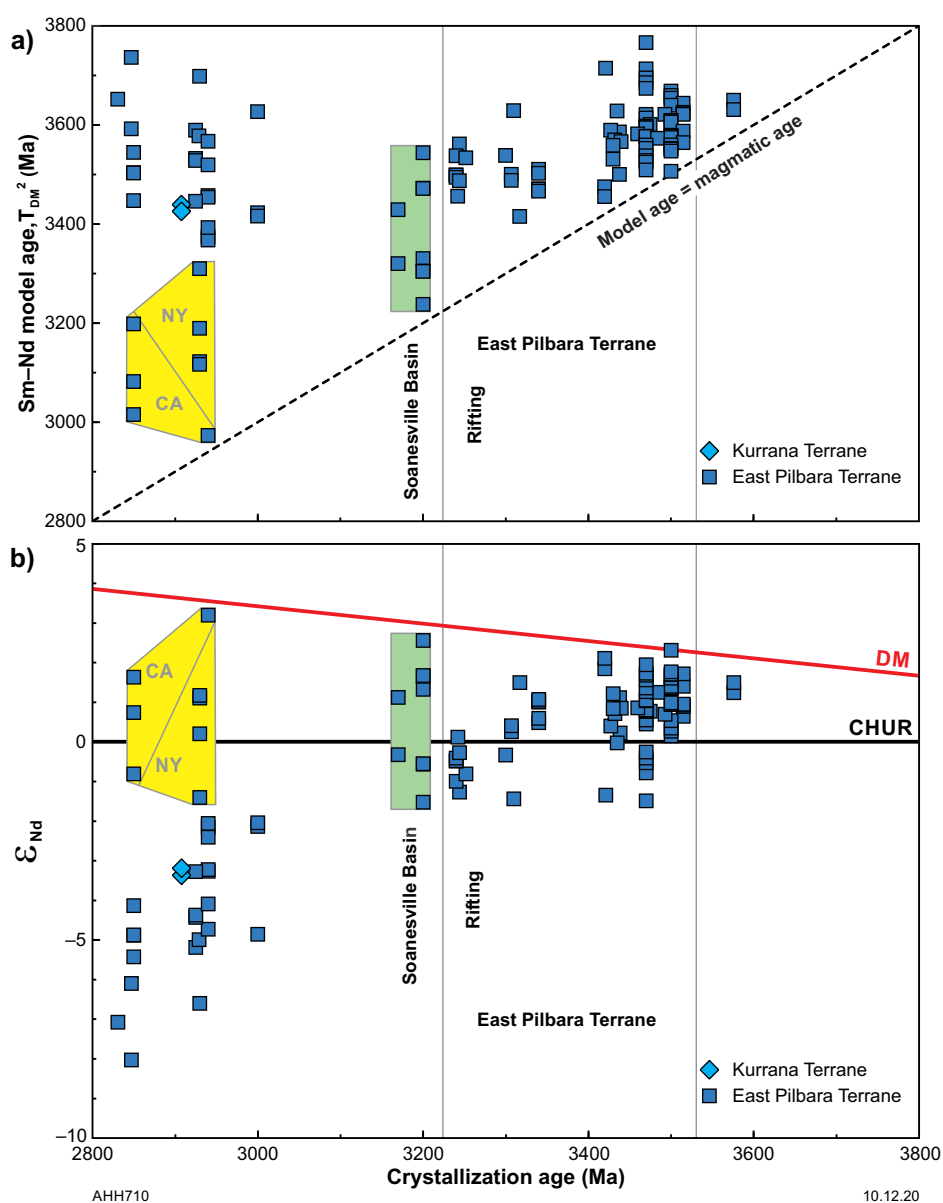


Figure 17. Sm–Nd two-stage depleted mantle model ages (T_{DM}^2) (a) and ϵ_{Nd} (b) vs magmatic age for whole-rock samples from the northern Pilbara Craton

Table 4. Nd data from igneous stratigraphic units of the east Pilbara Craton

Stratigraphic unit, age (Ga)	Lithology	Samples	ϵ_{Nd}	$T_{\text{DM}}2$ (Ga)	Data Source
PILBARA SUPERGROUP					
Warrawoona Group					
Coonterunah Subgroup					
Table Top Formation, 3.53 – 3.52	basalt	2	1.40 to 0.89	3.63 to 3.59	Smithies et al. (2007a)
Coucal Formation, c. 3.52 – 3.50	rhyolite	1	0.95	3.62	Smithies et al. (2007a)
Coucal Formation, c. 3.52 – 3.50	andesite	2	1.71 to 0.64	3.64 to 3.56	Smithies et al. (2007a)
Coucal Formation, c. 3.52 – 3.50	basalt	1	0.93	3.62	Smithies et al. (2007a)
Talga Talga Subgroup:					
North Star Basalt, 3.53 – 3.49	basalt	5	1.71 to 0.27	3.66 to 3.55	Gruau et al. (1987)
North Star Basalt, 3.53 – 3.49	komatiitic basalt	1	0.53	3.64	Gruau et al. (1987)
North Star Basalt, 3.53 – 3.49	dacite	2	1.40 to 0.94	3.61 to 3.57	Hamilton et al. (1981)
North Star Basalt, 3.53 – 3.49	andesite	1	0.98	3.61	Hamilton et al. (1981)
North Star Basalt, 3.53 – 3.49	komatiitic basalt	1	1.34	3.58	Hamilton et al. (1981)
North Star Basalt, 3.53 – 3.49	komatiite	1	2.31	3.51	Hamilton et al. (1981)
North Star Basalt, 3.53 – 3.49	dacite	3	1.60 to 0.15	3.67 to 3.56	Jahn et al. (1981)
North Star Basalt, 3.53 – 3.49	andesite	1	0.35	3.65	Jahn et al. (1981)
Dresser Formation, c. 3.48	altered basalt	8	–3.30	4.46 to 3.71	Tessalina et al. (2010)
Coongan Subgroup					
Mount Ada Basalt, c. 3.47	basalt	3	1.57 to 0.55	3.61 to 3.54	Gruau et al. (1987)
Mount Ada Basalt, c. 3.47	komatiitic basalt	2	1.95 to –0.41	3.69 to 3.51	Gruau et al. (1987)
Mount Ada Basalt, c. 3.47	basalt	1	0.77	3.60	Smithies et al. (2007a)
Duffer Formation, 3.47 – 3.46	dacite	3	1.73 to 0.76	3.60 to 3.52	Smithies et al. (2007a)
Duffer Formation, 3.47 – 3.46	andesite	1	1.05	3.58	Smithies et al. (2007a)
Duffer Formation, 3.47 – 3.46	dacite	1	0.45	3.62	McCulloch (1987)
Salgash Subgroup:					
Apex Basalt, c. 3.45	basalt	1	0.86	3.58	Smithies et al. (2007a)
Panorama Formation, 3.45 – 3.43	rhyolite	3	1.21 to 0.72	3.57 to 3.53	Smithies et al. (2007a)
Kelly Group					
Euro Basalt, 3.35 – 3.33	basalt	5	1.07 to 0.48	3.51 to 3.47	Arndt et al. (2001)
Sulphur Springs Group					
Kangaroo Caves Formation, c. 3.24	rhyolite	1	–0.48	3.50	Brauhart et al. (2000)
MESOARCHEAN FORMATIONS					
Soanesville Group					
Honeyeater Basalt, 3.18 – 3.17	basalt	5	2.56 to –1.52	3.54 to 3.24	Smithies et al. (2007a)
Empress Formation, c. 3.17	basalt	1	1.32	3.33	Smithies et al. (2007a)
DE GREY SUPERGROUP					
Coonieena Basalt, c. 3.00	basalt	2	–2.04 to –2.13	3.42 to 3.41	Smithies et al. (2007a)
GRANITIC ROCKS					
Pre-3.53 Ga gneiss, <3.66					
Warrawagine Dome	tonalite gneiss	2	1.49 to 1.24	3.65 to 3.63	Smithies et al. (2007a)
Callina Supersuite, 3.48 – 3.46					
Shaw Dome	tonalite–granodiorite	6	1.69 to –1.49	3.77 to 3.53	Bickle et al. (1993)
Shaw Dome	granite	1	–0.53	3.69	Bickle et al. (1993)
Shaw Dome	granite	1	0.70	3.62	McCulloch (1987)
Mount Edgar Dome	quartz diorite	1	0.75	3.59	Champion (2013)
Carlindi Dome	granodiorite	1	1.25	3.57	Smithies et al. (2007a)
Muccan Dome	granodiorite	1	–0.26	3.67	Gardiner et al. (2017)
Tambina Supersuite, 3.45 – 3.42					
Yule Dome	monzogranite	1	–1.34	3.71	Smithies et al. (2007a)
Mount Edgar Dome	tonalite–granodiorite	2	0.40 to –0.03	3.63 to 3.59	Gardiner et al. (2017)
Corunna Downs Dome	tonalite	2	2.11 to 1.84	3.47 to 3.45	Smithies et al. (2007a)
Carlindi Dome	monzogranite	1	–0.34	3.54	Smithies et al. (2007a)
Emu Pool Supersuite, 3.32 – 3.28					
Corunna Downs Dome	monzogranite	3	1.49 to 0.25	3.50 to 3.42	Smithies et al. (2007a)
Mount Edgar Dome	granodiorite	1	–1.44	3.63	Gardiner et al. (2017)
Cleland Supersuite, 3.27 – 3.22					
Strelley Monzogranite	diorite–monzogranite	3	–0.41 to –1.00	3.54 to 3.49	Brauhart et al. (2000)
Warrawagine Dome	granodiorite	2	0.12 to –0.28	3.49 to 3.46	Smithies et al. (2007a)
Muccan Dome	monzogranite	2	–0.81 to –1.27	3.56 to 3.53	Smithies et al. (2007a)
Mount Billroth Supersuite, 3.20 – 3.16					
Yule Dome	tonalite	2	1.13 to –0.33	3.42 to 3.31	Smithies et al. (2007a)
Elizabeth Hill Supersuite, c. 3.07					
Yule Dome	tonalite	2	–4.09 to –4.73	3.56 to 3.52	Smithies et al. (2007a)
Sisters Supersuite, 2.95 – 2.92					
Shaw Dome	monzogranite	7	–3.60 to –3.19	3.70 to 3.42	Smithies et al. (2007a)
Yule Dome	monzogranite	7	–3.27 to 0.20	3.45 to 3.18	Smithies et al. (2007a)
Carlindi Dome	monzogranite	3	3.19 to 3.10	3.12 to 2.97	Smithies et al. (2007a)
Split Rock Supersuite, 2.85 – 2.83					
Shaw Dome	monzogranite	6	–8.03 to –4.13	3.74 to 3.44	Smithies et al. (2007a)
Mount Edgar Dome	monzogranite	1	–7.08	3.65	Gardiner et al. (2018)
Carlindi Dome	monzogranite	4	–2.02 to 1.64	3.28 to 3.01	Smithies et al. (2007a)
Yule Dome	monzogranite	1	–0.81	3.19	Smithies et al. (2007a)

- c) the 3681 ± 9 Ma zircon (GSWA 169200, Mosquito Creek Formation, Nelson, 2004f) is accompanied by zircon age components consistent with erosion of the Tambina Supersuite and a number of possible c. 3000 Ma sources in both the east and west Pilbara Craton.

More evidence related to the provenances of all three samples was provided in Kemp et al. (2015b, appendix 2a).

2. Xenocrystic zircons older than 3700 Ma are recorded from felsic igneous rocks of the Pilbara Craton (Appendix 3). Thorpe et al. (1992a) reported a 3724 ± 1 Ma zircon from rhyolite in the North Pole Dome, and commented that other zircons of similar appearance were present in the sample (GSWA 100507). Subsequent investigations established that Eoarchean zircons are common in this unit (Kitajima et al., 2008; Petersson et al., 2019c). Detrital zircons dated between c. 3800 and 3700 Ma (SHRIMP U–Pb zircon data) have been recorded in the Cleaverville Formation in the Shay Gap area of the east Pilbara Craton (Sheppard et al., 2017), and at Cleaverville in the northwestern Pilbara Craton (Kiyokawa et al., 2019).

Lu–Hf analysis of cognate and xenocrystic zircons

The Hf two-stage model ages for zircons from east Pilbara Craton igneous rocks with crystallization ages corresponding to the Callina, Tambina, Emu Pool and Cleland Supersuites are shown in Figure 18. The combined model ages (Fig. 18a) suggest that the zircons were derived from sources with mantle extraction ages between c. 3750 and 3500 Ma. However, as already noted in this Report, some geochronologists have questioned model crust-formation ages based on the interpretation of a strongly depleted mantle prior to 3.5 Ga (Kemp et al. 2015a,b; Fisher and Vervoort, 2018; Petersson et al., 2019a). If the Pilbara Craton mantle at 3.5 Ga was significantly less depleted than assumed from models proposed by McCulloch and Wasserburg (1978) and DePaolo (1980), the calculated Hf two-stage model ages summarized in Figure 18 would be too old.

As might be expected, zircons from the Callina and Tambina Supersuites (Fig. 18b) had the oldest sources on average, although the gap between zircon crystallization age and Hf model age (known as the ‘crustal residence age’) increases in the younger supersuites. This indicates that the younger supersuites were derived from recycling of the same 3700–3550 Ma sources as the Callina and Tambina Supersuites, and the introduction of juvenile material to the EPT diminished after intrusion of the Tambina Supersuite. In the Emu Pool Supersuite (contemporaneous with the Kelly Group; Fig. 19), there is a range of positive ϵ_{Hf} values between CHUR and DM which suggests juvenile input from the mantle in addition to melting of older felsic crust. Mean ϵ_{Hf} values in the Callina Supersuite (contemporaneous with the pre-3460 Ma part of the Warrawoona Group) and Tambina Supersuites (contemporaneous with the post-3450 Ma part of the Warrawoona Group; Fig. 19) show no trend with time (Callina +0.6, $n = 149$; Tambina +0.7, $n = 120$). In contrast, between the Emu Pool Supersuite (contemporaneous with Kelly Group) and the Cleland

Supersuite (contemporaneous with Sulphur Springs Group) there is a trend from chondritic to negative values with time (Emu Pool +0.0, $n = 161$; Cleland –2.2, $n = 64$). The mean Callina Supersuite ϵ_{Hf} values are mainly from data in Kemp et al. (2017, Owens Gully Diorite, $n = 87$) and unpublished data ($n = 42$) from three other samples (AIS Kemp, 2018, written comm.).

Figure 20a summarizes all available zircon Hf two-stage model ages (from igneous and sedimentary rocks) from the east Pilbara Craton, including some >3.2 Ga zircons (xenocrystic or detrital) from units younger than 3.2 Ga. The minor peak on Figure 20a between 4.0 and 3.9 Ga represents zircons with crystallization ages >3540 Ma (separated in Fig. 20c). Comparison of Figure 20c with Figure 20b reveals major differences of Hf model ages between Pilbara zircons older than 3540 Ma and zircons younger than 3540 Ma. Assuming the 3700–3540 Ma zircons were mainly derived from 3700–3540 Ma felsic igneous rocks in the early crust, it is evident that these granitic rocks were derived from entirely different sources from those of almost all the <3540 Ma granitic rocks of the EPT. This suggests that the pre-Pilbara Supergroup crust formed in an Eoarchean to early Paleoarchean terrane entirely separate from the EPT. This conclusion is also suggested by Hf data in Figure 19. Negative ϵ_{Hf} values ranging between –5.9 and –1.3 indicate Hf model ages substantially older than the crystallization ages. If a depleted mantle is assumed, the Hf model ages are c. 4.0 to 3.9 Ga, depending on the $^{176}\text{Lu}/^{177}\text{Hf}$ evolution trend applied. If a chondritic mantle is assumed, the Hf T_{CHUR} model ages are c. 3800 Ma.

Figure 19 presents ϵ_{Hf} values for all east Pilbara Craton zircons and whole-rock samples that indicate crystallization ages older than c. 3160 Ma. Similar data are available for zircons and rocks younger than c. 3160 Ma but these are mainly from the northwest Pilbara Craton where Mesoarchean crustal evolution was dominated by plate tectonic processes including the subduction and melting of relatively juvenile crust (Hickman, 2016). Data used in Figure 19 (and listed in Appendix 9) permit several observations.

1. In Appendix 9, the 123 zircons older than 3540 Ma have a the mean ϵ_{Hf} value of –1.59 (SD = 0.937), and only three zircons have positive ϵ_{Hf} values. Although the >3540 Ma zircons were obtained from widely separated areas in the east Pilbara Craton (Kemp et al., 2015a,b; Petersson et al., 2019c), they are remarkably uniform with respect to ϵ_{Hf} . Assuming the existence of a depleted mantle between c. 3800 and 3540 Ma, the data suggest crustal sources with ages between c. 4050 and 3850 Ma (Fig. 20c).
2. Zircons with crystallization ages between c. 3538 and 3490 Ma ($n = 47$, Appendix 9), representing the Counterunah Subgroup (Warrawoona Group) and related granitic rocks, have a mean ϵ_{Hf} value of –0.007 (SD = 1.998). This closely chondritic value does not necessarily indicate derivation of magma from a chondritic mantle because the large standard deviation suggests mixed sources over the wide area of the east Pilbara Craton that was sampled, and possibly changing sources over 48 Ma.

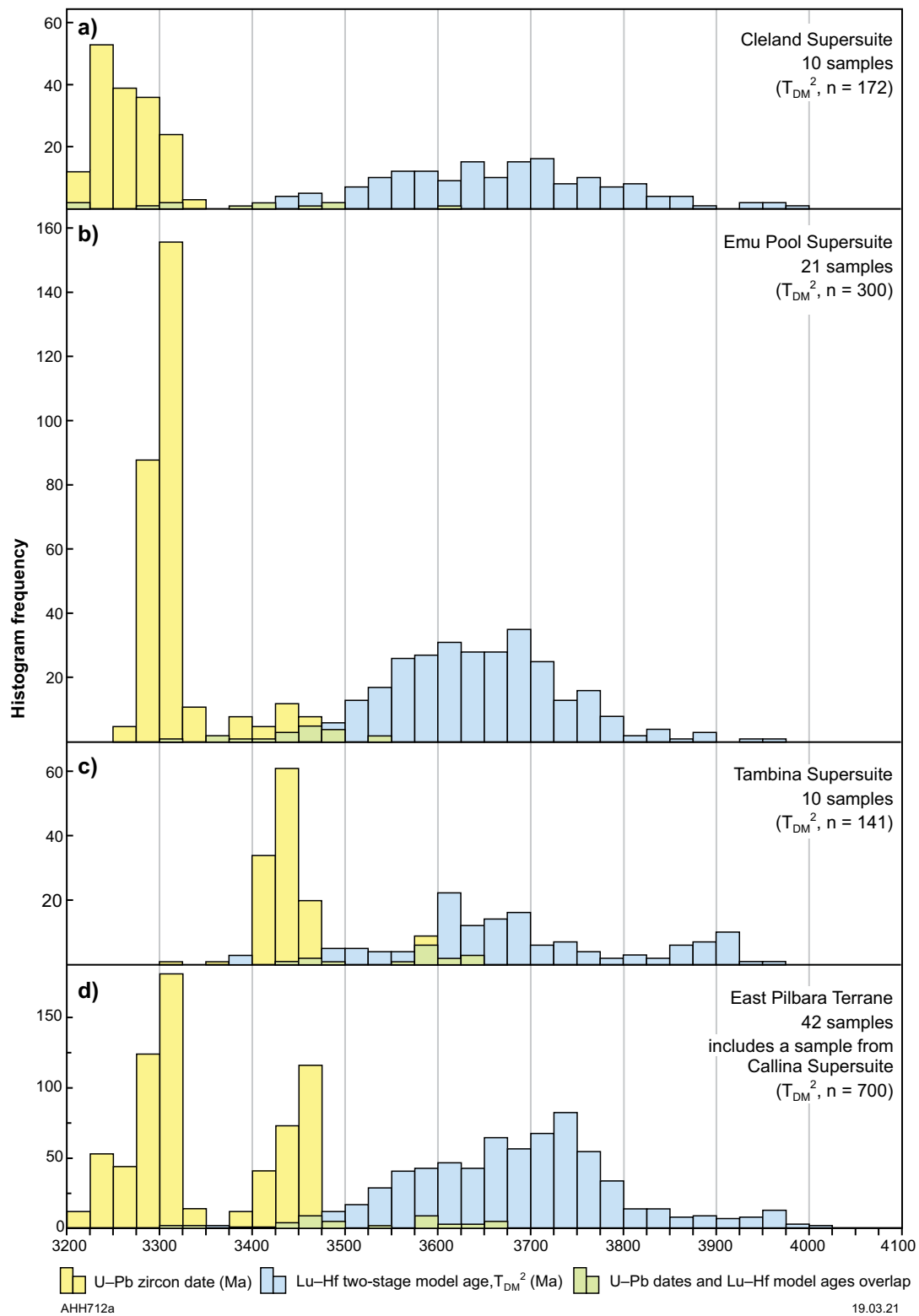


Figure 18. Histograms of zircon crystallization ages and two-stage Lu-Hf model (T_{DM}^2) ages for cognate and inherited zircons from igneous rocks of the EPT: a) Cleland Supersuite; b) Emu Pool Supersuite; c) Tambina Supersuite; d) combined data from (a), (b) and (c) plus a sample from the Callina Supersuite. Calculations used $^{176}\text{Lu}/^{177}\text{Hf}$ ratio of 0.015 after Scherer et al. (2001) ^{176}Lu decay constant (1.865×10^{-11}). The majority of model ages fall between 3750 and 3500 Ma. Difference between zircon crystallization ages (U-Pb date) and model ages increases from the older to the younger supersuites, indicating ongoing crustal recycling of similar old crustal sources with time. Data from Appendix 9; the single Callina Supersuite sample provides 87 Hf model ages ranging from 3820 to 3700 Ma

3. Figure 19 indicates no obvious isotope trend between c. 3530 and 3400 Ma. This might be due to the absence of cognate zircon Hf data from multiple intrusions of the 3484–3462 Ma Callina Supersuite, or from the 3530–3490 Ma granitic rocks. Unpublished Hf data from the 3530–3490 Ma Mulgundoona Supersuite (Petersson et al., 2020) indicate that cognate zircons from this range have approximately chondritic ϵ_{Hf} values with very limited variation. Previous investigations of EPT granitic rocks have described a secular change from TTG between c. 3485 and 3420 Ma to granodiorite and monzogranite from c. 3325 to 3223 Ma (Bickle et al., 1993; Smithies, 2000; Van Kranendonk et al., 2002, 2007a,b; Smithies et al., 2003, 2007b, 2009; Champion and Smithies, 2007; Champion, 2013; Champion and Huston, 2016; Gardiner et al., 2017, 2018). As already observed in this Report, Sm–Nd isotope data indicate increased crustal reworking during evolution of the EPT, with diminishing addition of juvenile material.

An abrupt switch to strongly positive ϵ_{Hf} values is observed at c. 3200 Ma (Fig. 19). This indicates a change from Paleoproterozoic reworking of old crustal material to an early Mesoproterozoic influx of juvenile magma. This timing coincides with breakup of the EPT, plate separation, and intrusion of the Mount Billroth Supersuite between c. 3199 and 3164 Ma. Figure 20d–f illustrates differences in the ages of early crust in those EPT domes that have provided most Lu–Hf data (Mount Edgar, Muccan and Yilgalong). Because the Yilgalong Dome is not known to contain any granitic rocks older than c. 3300 Ma (Emu Pool Supersuite), it was thought that the underlying crust might be significantly

different from that in the rest of the EPT. However, Figure 20f indicates that the Hf model ages for the c. 3300 Ma granitic rocks in the Yilgalong Dome have the same range as the older granitic rocks in the other two domes (Fig. 20d,e); that is, Hf model ages are generally >3530 Ma.

Summary

Geochronology of gneiss and metagabbro, xenocrystic zircons in felsic igneous rocks, and detrital zircons in Paleoproterozoic and Mesoproterozoic metasedimentary rocks, suggest that the pre-Pilbara Supergroup sialic crust evolved over about 250 Ma. There is some suggestion of episodic magmatic events at 3760–3700 Ma (Petersson et al., 2019c), 3650 Ma (Kemp et al., 2015a,b), and 3590–3570 Ma (McNaughton et al., 1988; Petersson et al., 2019a). The mainly negative ϵ_{Hf} values in zircons crystallized during these events (Fig. 19, Appendix 9), and Hf model ages (Fig. 20), indicate derivation of melts from considerably older sources (4000–3800 Ma). Comparison of Figures 20c and 20b reveals major differences of Hf model ages between Pilbara zircons older than 3540 Ma and zircons younger than 3540 Ma. It is evident that 3760–3540 Ma granitic rocks, from which the old zircons were derived, came from entirely different sources than those of the <3540 Ma granitic rocks of the EPT. The conclusion is that the sialic crust pre-dating the Warrawoona Group comprised one or more Eoarchean to early Paleoproterozoic terranes entirely unrelated to the EPT. Although no 3540–3530 Ma unconformity is preserved in the EPT, it follows that the Warrawoona Group was deposited unconformably on the c. 3760–3540 Ma sialic crust.

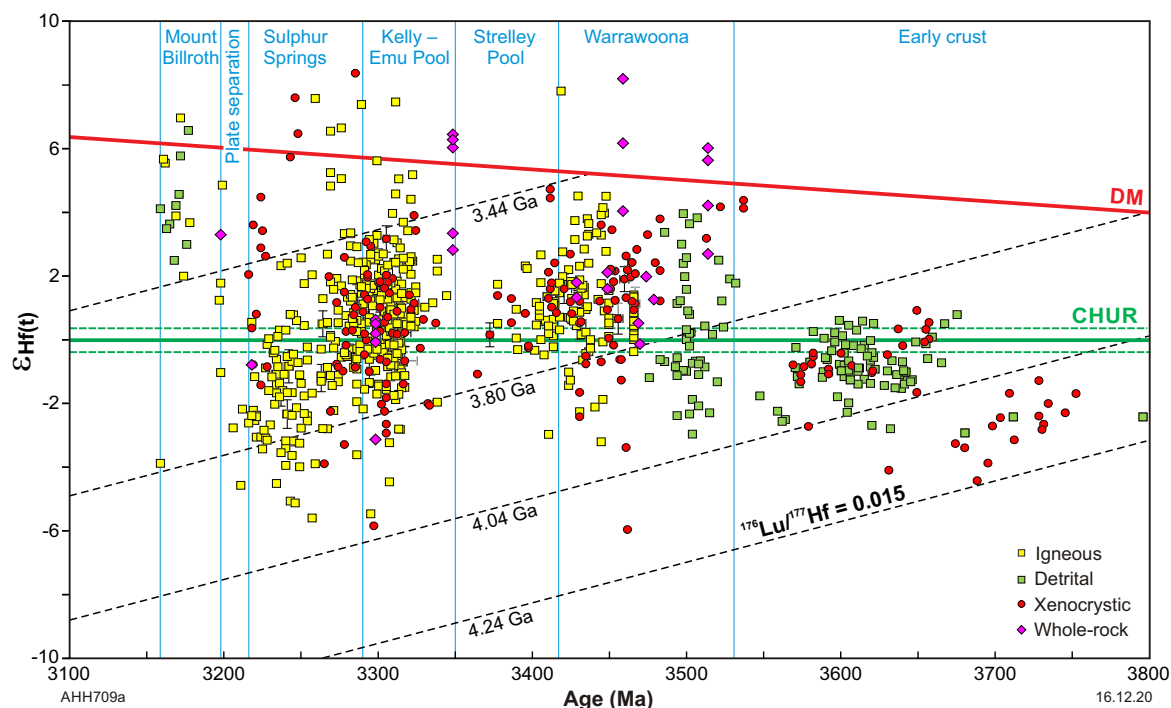


Figure 19. ϵ_{Hf} evolution diagram for analyses of igneous, inherited and detrital zircons with U–Pb ages between 3800 and 3150 Ma, and whole-rock samples (mainly komatiites) from the east Pilbara. Hf evolution lines defined by a $^{176}\text{Lu}/^{177}\text{Hf}$ ratio of 0.015 (after Scherer et al., 2001). Data for detrital and inherited zircons older than 3550 Ma are from Kemp et al. (2015b). Two abrupt changes in ϵ_{Hf} values (negative to positive) at c. 3530 Ma (initial deposition of Pilbara Supergroup) and c. 3200 Ma (intrusion of Mount Billroth Supersuite) indicate major influxes of magma from juvenile sources at these times. Increasingly negative ϵ_{Hf} values from 3530 to 3220 Ma indicate progressively more evolved sources with time (recycling of older crust). Data from Appendix 9

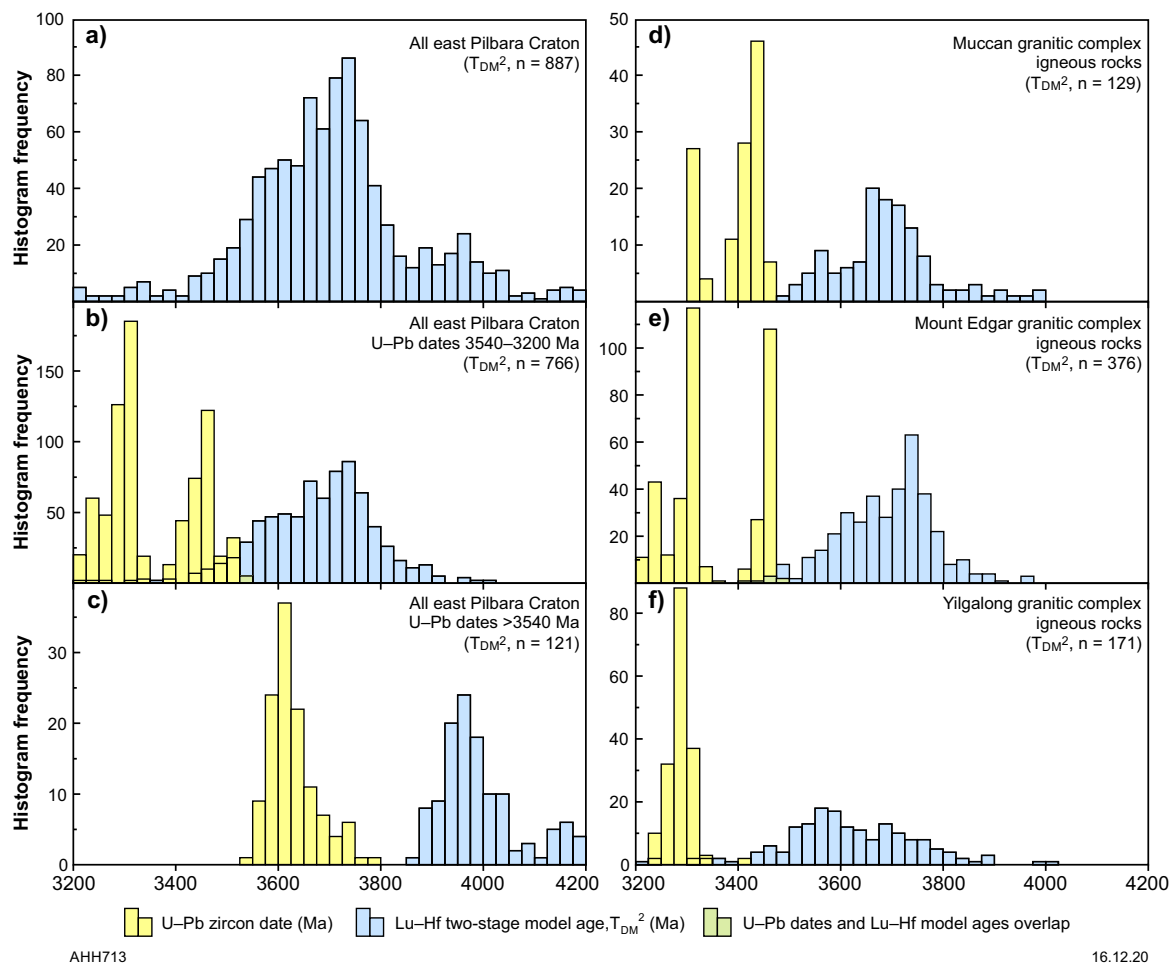


Figure 20. Histograms comparing U–Pb crystallization ages and two-stage Hf model ages (T_{DM}^2) for igneous and detrital zircons from Paleoproterozoic and Mesoproterozoic rocks of the east Pilbara Craton. Calculations used $^{176}\text{Lu}/^{177}\text{Hf}$ ratio of 0.015 (Scherer et al., 2001) ^{176}Lu decay constant (1.865×10^{-11}). a) Model ages for all detrital and igneous zircons; b) model ages for 3540–3200 Ma igneous and detrital zircons; c) Model ages for >3540 Ma zircons (note the much older model ages, and the greater separation of crystallization ages and model ages, compared to <3540 Ma zircons); d), e), f) data from three different granitic cores of east Pilbara domes, showing overall similarity of distributions of crystallization and model ages. Data from Appendix 9, excluding 2019 data

Evolution of the EPT commenced at c. 3530 Ma, and a few zircons dated between c. 3530 and 3490 Ma have moderately to strongly positive ε_{Hf} values (+2 to +4; Fig. 19). This might be considered evidence that volcanic rocks of the lower Warrawoona Group and contemporaneous granitic rocks were partly derived from juvenile sources, although negative values for other zircons suggest involvement of older crust. If, on the other hand, individual ε_{Hf} values are given less significance than mean ε_{Hf} values, the positive and negative values from the early Warrawoona Group combine to give near-chondritic values. It is most likely that the large variation in ε_{Hf} values for post-3530 Ma rocks (Fig. 19) indicates mixed sources (juvenile and evolved). This is based on geological reasoning that it is highly improbable that samples collected from different localities across a 40 000 km² terrane (EPT) had a single uniform source. Given this consideration, mean ε_{Hf} values are likely to have only limited geological significance, and it would be more informative to compare the mean ε_{Hf} values from zircon age components in individual samples. For example, the mean ε_{Hf} value of zircons from a single outcrop of the Owens Gully Diorite (Appendix 9; GSWA 178035, OG1, OGC1) is +0.775 ($n = 87$; $\text{SD} = 0.356$). The low standard deviation indicates that the individual ε_{Hf} values have relatively high precision.

The change in magma sources between c. 3540 and 3530 Ma suggests a major event in the crustal evolution of the Pilbara Craton, although the nature of this event is unknown. By analogy with the c. 300 Ma evolutionary history of the EPT, one possible cause is uplift and rifting of 3800–3540 Ma crust related to the mantle plume that was responsible for eruption of the Coonterunah and Talga Talga Subgroups (Van Kranendonk et al., 2002, 2006a, 2007a,b; Smithies et al., 2005b; Hickman, 2011). A similar c. 3530 Ma event has also been recorded in the eastern Kaapvaal Craton suggesting that, under the Vaalbara interpretation, it was significant at a continental scale.

Hf isotope data indicate another significant event in the Pilbara Craton at c. 3325 Ma (Fig. 19), after which most ε_{Hf} values changed from being approximately chondritic (Emu Pool Supersuite) to become markedly evolved between c. 3270 and 3223 Ma (Cleland Supersuite, same age as Sulphur Springs Group), indicating substantial melting of older crust. The large range of ε_{Hf} values (−6.3 to +6.9) between c. 3325 and 3290 Ma (Appendix 9) might best be explained by particularly diverse magma sources, such that positive values resulted from mantle melting and negative values reflect contemporaneous reworking of older crust.

In this scenario, the mean ϵ_{Hf} value of 0.26 ± 0.22 (2σ , $n = 255$) for these 3325–3290 Ma rocks is chondritic and does not constitute evidence of an undepleted mantle.

The overall trend of increasing crustal reworking from c. 3530 to 3220 Ma was terminated by breakup of the Pilbara Craton at c. 3220 Ma. Juvenile magma sources contributed to volcanism and granitic intrusion after c. 3200 Ma, although some post-3200 Ma igneous rocks with strongly evolved ϵ_{Hf} values and very old Hf model ages (e.g. Split Rock Supersuite) were evidently derived from recycling of much older crust.

East Pilbara Terrane

The East Pilbara Terrane (EPT) is the largest and oldest granite–greenstone terrane of the Pilbara Craton and provides exceptionally well-preserved records of Paleoproterozoic crustal evolution and early life. Its exposed area is 40 000 km² (Fig. 3), although prior to rifting and breakup of the Paleoproterozoic volcanic plateau at c. 3220 Ma (Hickman, 2001a, 2004; Van Kranendonk et al., 2002, 2007b, 2010), its area would have been considerably greater. Interpretation of gravity data (Hickman, 2004, fig. 2) suggests that the combined extents of the East Pilbara, Karratha and Kurrana Terranes, excluding any possible extensions into the southern half of the Pilbara Craton, exceed 100 000 km². Additionally, much of the Pilbara Craton was removed during late Neoproterozoic and early Paleoproterozoic breakup events. Stratigraphic and geochronological evidence suggests that the EPT and the eastern Kaapvaal Craton, including the extensively studied Barberton Greenstone Belt (BGB), evolved on the same 3530–3223 Ma volcanic plateau (Zegers et al., 1998b; Bleeker, 2003; De Kock et al., 2009; Hickman, 2012, 2016; Huston et al., 2012). Under this interpretation, the EPT and the eastern Kaapvaal Craton evolved as adjacent parts of the Archean continent Vaalbara, consistent with the extremely similar Paleoproterozoic stratigraphic sections of the EPT and the BGB (Fig. 4). If the Vaalbara interpretation is accepted, it follows that geological data from each of these terranes is relevant to improving our understanding of the other (Van Kranendonk et al., 2014b).

Geochronological evidence in this Report (e.g. Fig. 12a) indicates that evolution of the EPT commenced abruptly at c. 3530 Ma, and that the pre-3530 Ma crust was formed by entirely separate magmatic events in unknown tectonic settings. Evolution of the EPT ended at c. 3220 Ma with crustal extension, rifting, and breakup of the terrane. Major geological differences between the EPT, the West Pilbara Superterrane, and unconformably overlying sedimentary basins were progressively recognized and documented during the PCMP (Hickman, 1999, 2004; Smithies and Champion, 2000; Van Kranendonk et al., 2001a, 2002, 2004, 2006a, 2007b; Smithies et al., 2003, 2004, 2005a,b, 2007a,c; Hickman and Van Kranendonk, 2004; Sandiford et al., 2004). The overall conclusion from these investigations was that Paleoproterozoic vertical deformation and plume-related crustal growth, which had operated in the Pilbara Craton for about 300 Ma from c. 3530 Ma, was followed by Mesoproterozoic crustal evolution dominated by plate tectonic processes (Van Kranendonk et al., 2007b). Paleoproterozoic melts derived mainly from crustal recycling of older crust (Bickle et al., 1993; Collins, 1993; Van Kranendonk et al., 2007a,b; Smithies et al.,

2009) were succeeded by Mesoproterozoic juvenile, mantle-derived melts (Sun and Hickman, 1998; Smithies et al., 2004, 2007a; Van Kranendonk et al., 2007b; Hickman, 2016).

In this Report, description of the EPT is divided into sections on greenstone stratigraphy (Pilbara Supergroup), granitic supersuites, large igneous provinces, tectonic processes, tectonic settings, tectonic events and metamorphism. Mineralization is described later in the Report.

Pilbara Supergroup

Previous work has established that the 3530–3235 Ma supracrustal succession of the EPT, the Pilbara Supergroup, comprises three volcanic groups (in ascending stratigraphic order, the Warrawoona, Kelly and Sulphur Springs Groups) and one formation (Strelley Pool Formation; Fig. 6, Table 1; Hickman, 2011). Spanning about 300 Ma, this supergroup accumulated as a volcanic plateau overlying older sialic crust (Van Kranendonk et al., 2002, 2007a,b). Volcanism is interpreted to have resulted from mantle plume activity (Van Kranendonk et al., 2002, 2007a,b), establishing a 15–20 km-thick succession. The lower two volcanic groups, and contemporaneous granitic intrusions, are interpreted to represent parts of two large igneous provinces, the Warrawoona and Kelly LIPs (Fig. 7). Prior to the c. 3220 Ma breakup of the EPT (Hickman, 2004, 2012; Van Kranendonk et al., 2010), these LIPs are likely to have extended far beyond the present boundaries of the EPT (Hickman, 2012, 2016). The Sulphur Springs Group is not sufficiently extensive to rank as a LIP and is assigned to the Sulphur Springs Basin (Fig. 7).

The stratigraphic succession of the Pilbara Supergroup varies between the greenstone belts of the EPT, although there is a general continuity of its main stratigraphic divisions. Stratigraphic variations result from erosional unconformities, local nondeposition, and lateral changes of depositional thickness and facies. These variations are attributed to deposition during doming and contemporaneous basin subsidence between the domes (Hickman, 1984, 2004; Hickman and Van Kranendonk, 2004; Van Kranendonk et al., 2004a, 2007a,b).

The Pilbara Supergroup (Fig. 6, Table 1) is exposed in 18 of the 20 greenstone belts in the EPT, and parts of it are exposed in all 11 domes of the terrane (Fig. 8). The Wodgina greenstone belt, and the Cheearra greenstone belt in the far west of the EPT (outside the area of Fig. 8), expose only Mesoproterozoic formations due to removal of Paleoproterozoic stratigraphy by granitic intrusion. Two major erosional unconformities separate the three groups of the supergroup. The oldest of these unconformities, between the Warrawoona and Kelly Groups, is overlain by the 3426–3350 Ma Strelley Pool Formation (not assigned to either group). This formation is a thin, but regionally extensive, sedimentary unit deposited during a c. 75 Ma break in volcanism (Hickman, 2008). During this break, the uplifted and deformed Warrawoona Group was extensively eroded. The second major stratigraphic break, between the Kelly and Sulphur Springs Groups, is marked by an erosional unconformity overlain by the thick clastic succession of the Leilira Formation (Van Kranendonk, 2000a). This second break in volcanic activity lasted up to c. 60 Ma (3315–3255 Ma). Local erosional unconformities are also recorded within each of the three groups, as summarized in

this Report under **Tectonic processes in the EPT: Effects of doming on stratigraphy**. In most areas, an erosional unconformity separates the top of the Pilbara Supergroup from the overlying Soanesville Group.

From rare remnants of crustal material pre-dating the Pilbara Supergroup, and from a large body of isotope data described earlier in this Report, a c. 3530 Ma regional unconformity is interpreted to have once separated the Warrawoona Group from 3750–3540 Ma crust that included c. 3580 Ma gabbro, granitic rocks, and gneiss. This unconformity is no longer exposed due to repeated episodes of granitic intrusion and tectonic removal during Paleoproterozoic and Mesoproterozoic deformation.

Volcanic cycles

The stratigraphy of the Pilbara Supergroup (Fig. 6) is the product of a series of volcanic cycles. In well-preserved cycles, the earliest volcanic rocks were komatiites and komatiitic basalts derived from the lower mantle. These ultramafic volcanic rocks were overlain by thick successions of tholeiitic pillow basalt and massive basalt containing thin units of banded chert (mainly silicified fine-grained volcanoclastic and clastic sedimentary rocks). The upper parts of cycles are composed of andesite and dacite, locally overlain by rhyolite. Van Kranendonk et al. (2001, 2002) suggested that the volcanic cycles were produced by successive episodes of melting of the mantle by mantle plumes, and that volcanic compositions varied according to factors such as depths of melting in the mantle (Campbell et al., 1989) and amounts of crustal contamination. Van Kranendonk et al. (2002) also suggested that some felsic magmas were derived by melting of pre-existing basaltic crust, rather than by fractionation of the tholeiites.

Acquisition and interpretation of additional data from the 1994–2005 PCMP, including isotope data, supported the plume model and elaborated on magmatic sources (Hickman and Van Kranendonk, 2004; Smithies et al., 2005b, 2007a,b,c, 2009; Van Kranendonk et al., 2004a, 2007a,b, 2010). U–Pb zircon geochronology has revealed that felsic volcanism in individual volcanic cycles was contemporaneous with episodes of granitic intrusion into the Pilbara Supergroup (Fig. 10; Barley and Pickard, 1999; Hickman, 2001b, 2004, 2012; Van Kranendonk et al., 2001a, 2002, 2004a,c, 2006a; Hickman and Van Kranendonk, 2004). This indicates that generation of granitic magmas was related to the same plume events as the volcanic cycles, and field evidence confirms that granitic intrusions of various ages fed subvolcanic sills and overlying felsic volcanic formations (Vearncombe and Kerrich, 1999; Van Kranendonk, 1999a, 2000a; Buick et al., 2002; Van Kranendonk et al., 2002, 2006b; Bagas et al., 2004c; Van Kranendonk and Pirajno, 2004; Brown et al., 2006, 2011; Hickman and Van Kranendonk, 2008a). However, there are also instances where contemporaneous granitic intrusions and volcanic formations have trace element or isotope compositions indicative of different sources (Smithies et al., 2005b, 2007b; Van Kranendonk et al., 2007b). A likely explanation is that plume-related melting variously affected the mantle, mafic crust, and felsic crust.

The presence of volcanic cycles in the EPT was first suggested by Anhaeusser (1971b) and Ingram (1977), and was later confirmed during the PCMP (Van Kranendonk

et al., 2001a, 2002). Based on studies of the Onverwacht Group of the Kaapvaal Craton, South Africa, and in several other Archean cratons, Anhaeusser (1971b) recognized stratigraphic cyclicity on various scales involving both volcanic and sedimentary units. He described different classes of volcanic cycles, including: 1) ‘major’ cycles ranging from hundreds to thousands of metres thick and generally comprising mafic–felsic volcanic sequences; 2) ‘minor’ volcanic cycles varying from a few metres to hundreds of metres thick.

Eight volcanic cycles have been recognized in the Pilbara Supergroup (Fig. 6; Hickman and Van Kranendonk, 2004; Van Kranendonk et al., 2007a; Hickman, 2011, 2012). Within some major cycles, such as that containing the North Star Basalt, there are subsidiary ultramafic–mafic–chert cycles several hundred metres thick (Van Kranendonk et al., 2006a). Geochemical sampling traverses through formations of the Pilbara Supergroup (Glikson and Hickman, 1981a,b) revealed upwards geochemical trends within some of the individual volcanic cycles. However, because similar vertical trends are repeated in successive volcanic cycles, any overall trend across volcanic cycles of the Pilbara Supergroup would be unlikely, and the absence of such a trend was confirmed by Smithies et al. (2005b, 2007a). Geochronology indicates that most volcanic cycles lasted about 10–25 Ma, although U–Pb zircon dating has been restricted to felsic and sedimentary units. Thus, the duration of the ultramafic and mafic volcanism in a cycle can be estimated only from the difference between the age ranges of felsic formations in successive cycles. By analogy with more recent LIP (Ernst, 2014), most basaltic formations were probably erupted over periods of less than about 5 Ma.

Although no overall secular geochemical trend is evident through the entire stratigraphy of the Pilbara Supergroup, granitic rocks of the EPT do change in composition from c. 3485 to 3223 Ma; whereas granitic intrusions older than c. 3420 Ma (Callina and Tambina Supersuites) are mainly TTG, intrusions between c. 3325 and 3290 Ma (Emu Pool Supersuite) are dominated by granodiorite and monzogranite, and intrusions between c. 3270 and 3223 Ma (Cleland Supersuite) are mainly monzogranite and syenogranite (Bickle et al., 1993; Smithies, 2000; Van Kranendonk et al., 2002, 2007a,b; Smithies et al., 2003, 2007b, 2009; Champion and Smithies, 2007). There are local exceptions to this general trend within individual granitic supersuites, suggesting magmatic cycles on the same scale as in the major volcanic cycles. This would be consistent with the felsic intrusive and felsic volcanic rocks being related to the same plume events (Van Kranendonk et al., 2002, 2006b, 2007a,b), although generally not having common magmatic sources.

Under the discussion of **Eoarchean to early Paleoproterozoic evolution**, it was noted that isotopic evidence (Figs 17, 19, 20) supports previous interpretations that melting to produce the granitic rocks involved a progressive increase in crustal reworking from c. 3530 to 3223 Ma (Smithies and Champion, 2000; Champion and Smithies, 2007; Smithies et al., 2007b; Van Kranendonk et al., 2007a,b; Champion and Huston, 2016; Gardiner et al., 2017). In general, each successive supersuite was derived by more crustal recycling and less addition of juvenile material than the previous one, a feature also recorded in the Mount Edgar Dome (Fig. 8; Gardiner et al., 2017, 2018). A less well-defined secular compositional change is presented by the volcanic rocks of the Pilbara

Supergroup: the lower Warrawoona Group (Coonterunah and Talga Talga Subgroups) is dominated by ultramafic–mafic cycles, whereas the Coongan and Salgash Subgroups of the Warrawoona Group, and the Kelly and Sulphur Springs Groups, comprise ultramafic–mafic–felsic cycles in which the ratio of mafic to felsic volcanic rocks decreased with time (Smithies et al., 2007a). The very limited felsic volcanic material in the Coonterunah and Talga Talga Subgroups, and the rarity of remnants of 3530–3490 Ma granitic intrusions in the EPT, suggests that generation of felsic melts developed slowly in this terrane. Progressively increasing felsic volcanism and granitic intrusion with time is an important feature of the EPT, and coincides with a well-defined trend from sodic TTG compositions (3480–3420 Ma) to more K-rich magmas (3325–3235 Ma; Champion and Smithies, 2001, 2007; Van Kranendonk et al., 2002, 2007a,b). These changes accompanied the development of diapiric doming and sagduction.

Geochemistry

Geochemical investigations of the volcanic rocks of the northern Pilbara Craton and the Fortescue Basin were conducted through two major collaborative projects between GSWA and Geoscience Australia (formerly the Bureau of Mineral Resources [BMR]). Between 1975 and 1976, GSWA and BMR collected and analysed 442 samples from the east Pilbara Craton, with results reported and interpreted by Glikson and Hickman (1981a,b). Between 1980 and 1983, an additional 522 samples were collected from the eastern and northwestern areas of the Pilbara Craton, and from the Fortescue Basin (Glikson et al., 1986). Between 1994 and 2005 another major geochemical project formed part of the PCMP and involved collection of 438 samples, with results published by Smithies et al. (2005b, 2007a). Other geochemical studies of volcanic rocks in the northern Pilbara Craton have been those by Hallberg (1974) and Arndt et al. (2001).

An important aim of the first study described by Glikson and Hickman (1981a,b) was to examine geochemical variations in the Pilbara Supergroup by sampling at regular intervals (commonly 50–200 m, subject to outcrop) across vertical stratigraphic sections. It was found that basalts of the Pilbara Supergroup show vertical trends including progressive depletion of Fe, Ti, K, P, Ba, Rb, La, Ce, Nb, Y and Zr. Stratigraphic breaks in the volcanic succession, such as between the Talga Talga and Coongan Subgroups, across the McPhee Formation, were found to be marked by geochemical breaks followed by a repetition of the vertical geochemical trends (Fig. 21). Additionally, they observed a similar general trend from the lower to upper parts of the entire succession. Glikson and Hickman (1981a) noted that these trends are inconsistent with magmatic fractionation, and instead indicate secular mantle depletion owing to repetition of partial melting events or progressively deeper melting. Peridotitic komatiites were attributed to >50% melting of mantle peridotite, possibly representing high-temperature diapiric events.

In reviewing the geochemistry of Pilbara Supergroup basalts sampled as part of the 1994–2005 PCMP, Smithies et al. (2005b, 2007a) distinguished two contemporaneous and interbedded types: high-Ti basalts ($\text{TiO}_2 > 0.8 \text{ wt\%}$) with relatively high concentrations of high field strength elements (HFSE) and rare earth elements (REE), estimated to

constitute 65% of basalts within the Pilbara Supergroup; and low-Ti basalts ($\text{TiO}_2 < 0.8 \text{ wt\%}$) with lower concentrations of HFSE and REE. Compared to the low-Ti basalts, the high-Ti basalts are generally more Fe-rich, have very low $\text{Al}_2\text{O}_3/\text{TiO}_2$ (18.7 – 8.9) and high Gd/Yb (1.12 – 2.23) ratios. Examination of the analytical data in Smithies et al. (2007a) shows that the high-Ti basalts have considerably lower average contents of MgO, Cr and Ni than the low-Ti basalts, a feature also noted by Glikson and Hickman (1981a). Smithies et al. (2005b) observed that the composition of the high-Ti basalts did not change significantly during the c. 300 Ma evolution of the Pilbara Supergroup. In contrast, they commented that the low-Ti basalts show secular trends to lower concentrations of incompatible elements, and to lower ratios of La/Sm, La/Gd, La/Yb and Gd/Yb. Smithies et al. (2005b) interpreted this trend to indicate increasingly depleted sources over time, and to be unrelated to crustal contamination, which they considered to be of limited significance. Previously, compositional differences between low-Ti and high-Ti basalts in large igneous provinces were related to variable degrees of partial melting within mantle plumes (Campbell and Griffiths, 1990; Arndt et al., 1993).

Warrawoona Group

The Warrawoona Group (Table 1) comprises a 10–15 km-thick succession of dominantly basaltic volcanic rocks, lesser komatiitic and felsic volcanic rocks, and minor sedimentary rocks deposited between c. 3530 and 3427 Ma. The type area of the Warrawoona Group is in the Marble Bar greenstone belt, where all units except the basal Coonterunah Subgroup are well exposed and form a right-way-up, upwards-younging succession about 12 km thick. Deposition occurred as a series of ultramafic–mafic–felsic volcanic cycles, each of about 15 Ma duration. Rates of deposition are consistent with a mantle plume origin (Van Kranendonk et al., 2002, 2004c, 2006b). These volcanic cycles led to recognition of four subgroups, in ascending order: the Coonterunah, Talga Talga, Coongan, and Salgash Subgroups (Van Kranendonk et al., 2006a). Geochronology indicates that the Coonterunah and Talga Talga Subgroups are laterally equivalent. The Coonterunah Subgroup in the East Strelley greenstone belt was dated by the U–Pb zircon method at c. 3515 Ma (Buick et al., 1995), whereas in the North Shaw and Coongan greenstone belts, the Talga Talga Subgroup yielded $^{40}\text{Ar}/^{39}\text{Ar}$ hornblende ages between c. 3522 and 3518 Ma (Zegers, 1996; Davids et al., 1997). In the Marble Bar greenstone belt, the North Star Basalt of the Talga Talga Subgroup is older than c. 3490 Ma ($^{40}\text{Ar}/^{39}\text{Ar}$ hornblende cooling age obtained by van Koolwijk et al. [2001]). As illustrated in Figure 6, the Coongan and Salgash Subgroups each represent separate volcanic cycles, whereas the Coonterunah and Talga Talga Subgroups may include several incomplete cycles.

Geochronology indicates that the minimum depositional age of the group varies slightly between different domes. A U–Pb zircon date of $3424 \pm 7 \text{ Ma}$ (GSWA 169008, Nelson, 2002h) was once thought to constrain the minimum depositional age of the Panorama Formation in the Coongan greenstone belt, but the sample dated was an altered felsic (not certainly volcanic) schist and the date is now interpreted to be unreliable. In view of this uncertainty, the minimum depositional of the Panorama Formation, and the Warrawoona Group, is interpreted to be constrained by a date of $3427 \pm 2 \text{ Ma}$ (GSWA 168913, Nelson, 2001) from

dacite in the eastern part of the Kelly greenstone belt. This date is very reliable because it is supported by several very similar dates from felsic volcanic rocks of the Panorama Formation in the same area.

Individual basalt formations, typically between 3 and 5 km thick, include numerous pillow basalts that testify to subaqueous deposition, and available geochronology indicates that some individual basalt formations were erupted in less than 5 million years. Thin chert units (silicified fine-grained clastic and volcanoclastic rocks) within the basaltic sequences suggest periods of volcanic quiescence and hydrothermal activity between episodic eruptions. In some formations, such as the Dresser Formation and Apex Basalt, hydrothermal silicification of basalt immediately beneath bedded cherts was accompanied by the formation of hydrothermal chert veins (Van Kranendonk and Pirajno, 2004; Van Kranendonk, 2006) and bleaching of the basalts to resemble felsic volcanic rocks.

Together with its parent unit, the Pilbara Supergroup, the Warrawoona Group has been redefined several times since it was originally named and described by Lipple (1975). The present definition is similar to that used by Van Kranendonk et al. (2006b) in which the group is composed of four subgroups. However, the Dresser Formation, which Van Kranendonk et al. (2006b) interpreted to be c. 3525 Ma, was subsequently reinterpreted to be c. 3481 Ma (Van Kranendonk et al., 2008; GSWA 180070, Wingate et al., 2009e). This revised depositional age indicates that the Dresser Formation can be correlated with the c. 3477 Ma McPhee Formation that outcrops in several greenstone belts of the EPT (Hickman, 2011). Both formations include thick chert units, BIF, clastic rocks and basalt, although only the Dresser Formation is mineralized by hydrothermal barite and known to contain microbialites.

The Warrawoona Group displays an upwards increase in the frequency and thickness of felsic volcanic units.

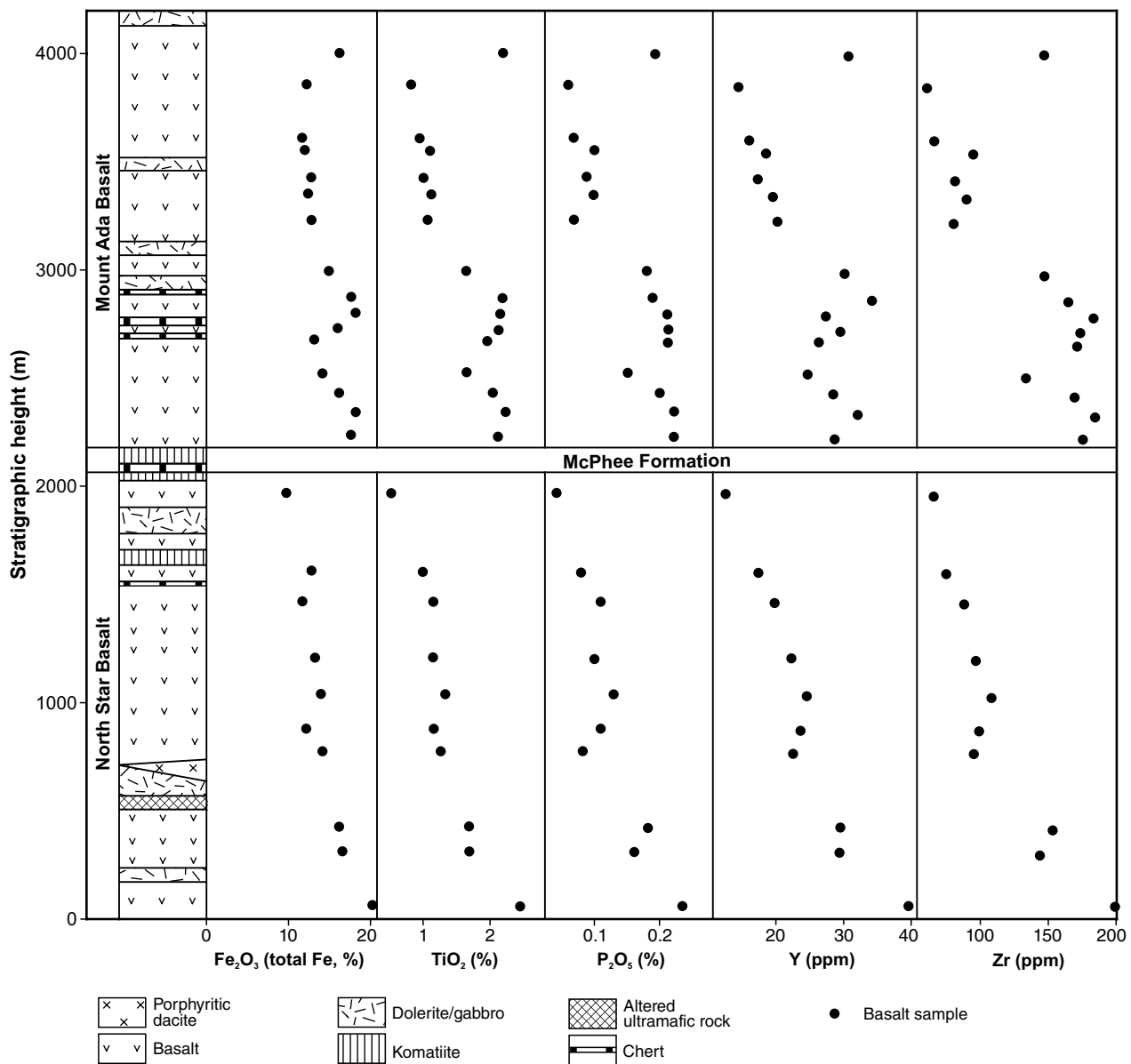


Figure 21. Vertical geochemical trends in basaltic rocks of the North Star and Mount Ada Basalts, Marble Bar greenstone belt (modified from Hickman, 1980a). The data indicate two similar volcanic cycles separated by the McPhee Formation. Geochronology establishes a continuous stratigraphic succession without structural repetition

The Coonterunah and Talga Talga Subgroups are mainly composed of ultramafic–mafic cycles, whereas the Coongan and Salgash Subgroups show better-developed ultramafic–mafic–felsic cycles. The ratio of mafic to felsic volcanic rocks decreased with time (Smithies et al., 2007a), and the frequency of komatiitic basalts and komatiites does not decrease upwards. As discussed under **Large igneous provinces of the EPT**, the Warrawoona Group is interpreted to be a remnant of a continental-scale 3530–3420 Ma LIP, another part of which may be preserved as the lower Onverwacht Group (Kaapvaal Craton). The Onverwacht Group has previously been described as a fragmented LIP (Ernst, 2007, 2014; Bryan and Ernst, 2008).

Coonterunah Subgroup

The Coonterunah Subgroup (Table 1; Van Kranendonk et al., 2006a) is a 5.9 km-thick succession of tholeiitic basalt and subordinate komatiitic and felsic volcanic rocks identified in the East Strelley greenstone belt around the southern and eastern sides of the Carlindi Dome (Plates 1A, 1C). The succession was folded and metamorphosed to amphibolite facies prior to deposition of the unconformably overlying Strelley Pool Formation. A detailed description of the subgroup, in particular its geochemistry, was provided by Smithies et al. (2007b).

The Coonterunah Subgroup succession is correlated with the Talga Talga Subgroup exposed in the Marble Bar, Panorama, Coongan and Doolena Gap greenstone belts (Hickman, 1980c,d; Van Kranendonk et al., 2006a). In this Report, the same succession is interpreted to be exposed at the base of the greenstone succession in the Pilbara Well greenstone belt, immediately adjacent to the western margin of the Yule Dome (Hickman, 1980c). U–Pb dating of detrital zircons in a metasandstone at the top of this lower succession indicated significant age components at 3639, 3575, 3563 and 3528 Ma, with a youngest zircon date of 3514 ± 2 Ma (1 σ) (GSWA 180095, Wingate et al., 2009f). These age components are similar to those for metasandstone of the 3426–3350 Ma Strelley Pool Formation in the East Strelley greenstone belt (GSWA 178043, Nelson, 2005f; cf. Fig. 12e). In that sample, 34 detrital zircons less than 5% discordant yielded dates between c. 3520 and 3467 Ma, a single age component at c. 3504 Ma, and a youngest zircon at 3467 ± 12 Ma (1 σ). The youngest date suggests a possible but minor contribution of detritus from the adjacent Callina Supersuite in the Carlindi Dome. The Strelley Pool Formation in the East Strelley greenstone belt directly overlies the Coonterunah Subgroup, and in this Report the same relationship is interpreted to be present in the Pilbara Well greenstone belt (Fig. 8).

Other evidence that the lower succession of the Pilbara Well greenstone belt is part of the Warrawoona Group is the observation that the succession was intruded by c. 3421 Ma granitic rocks (GSWA 142170, Nelson, 1999a). The granite–greenstone contact is deformed, although intrusive contacts are preserved (Blockley, 1980; Smithies and Farrel, 2000a). Blockley (1980) described the main granitic rock adjacent to the contact at Friendly Creek as comprising foliated granite, banded granitic gneiss and migmatitic granite with numerous amphibolite xenoliths, intruded by dolerite dykes and veins of pegmatite. Satellite imagery shows that this granitic unit contains a swarm of dolerite dykes. This is

relevant to its age because elsewhere in the EPT, dolerite dyke swarms are absent from granitic intrusions younger than the Callina and Tambina Supersuites (this Report). Therefore it is likely that the banded granitic gneiss and migmatitic granite at Friendly Creek belongs to one of these Paleoarchean supersuites.

In summary, by analogy with the succession of the Coonterunah Subgroup in the East Strelley greenstone belt, the metasandstone in the lower Pilbara Well succession is now correlated with the Strelley Pool Formation, and the underlying volcanic succession is most likely part of the Coonterunah Subgroup.

Following recognition of an angular unconformity between the Coonterunah Subgroup and the Strelley Pool Formation in the East Strelley greenstone belt, Buick et al. (1995) interpreted the succession of the Coonterunah Subgroup, previously mapped as part of the Talga Talga Subgroup (Hickman, 1980c), to be separate from all other parts of the Warrawoona Group. Based on the same evidence, Van Kranendonk and Morant (1998) redefined the succession as a separate group. New data from the PCMP required a revision of this interpretation to re-define the succession as a subgroup of the Warrawoona Group (Van Kranendonk et al., 2006a). U–Pb zircon and $^{40}\text{Ar}/^{39}\text{Ar}$ mineral geochronology (Buick et al., 1995; Davids et al., 1997; Zegers et al., 1999; van Koolwijk et al., 2001) indicate that the Coonterunah and Talga Talga Subgroups have the same depositional age range (3530–3490 Ma), and whole-rock Nd model ages and ϵ_{Nd} values are also similar (Table 4). Compositional differences are limited to the inclusion of thin units of well-preserved felsic volcanic rocks in the Coucal Formation of the Coonterunah Subgroup (Smithies et al., 2007b).

A significant geochemical feature of both the Coonterunah and Talga Talga Subgroups, and in the Pilbara Supergroup generally, is a progressive upwards decrease in HFSE and REE from the lowest exposed stratigraphic sections (Hickman, 1980a; Glikson and Hickman, 1981a,b; Smithies et al., 2005b, 2007a,b). One possible explanation for this geochemical trend is decreasing crustal contamination of the basaltic magmas with time. Another interpretation explains the trend as a consequence of increasingly depleted sources with time. Both processes may have influenced secular compositional changes. Relatively high levels of crustal contamination at the beginning of volcanic cycles might be explained by early wallrock interaction in conduits, or by greater contamination at the surface because the first lava flows would have most likely interacted with any underlying sedimentary or felsic igneous rocks. Geochemical data obtained from detailed vertical stratigraphic sampling traverses by Glikson and Hickman (1981a) revealed very similar geochemical trends of upwardly decreasing HFSE and large ion lithophile elements (LILE) for both the North Star and the Mount Ada Basalts. Such vertical repetition is evidence that geochemical trends were features of individual volcanic cycles represented by members or formations, rather than occurring over larger timeframes, as represented by the entire Warrawoona Group, or even the Pilbara Supergroup. This conclusion is consistent with the observation by Smithies et al. (2005b) that the composition of high-Ti basalts did not change significantly over the c. 300 Ma period of basaltic eruption of the Pilbara Supergroup.

Green et al. (2000) reported the presence of granitic boulders in the c. 3515 Ma basalts of the Coonterunah Subgroup. These boulders were most likely derived from crust underlying the Pilbara Supergroup because no 3530–3515 Ma granitic rocks have yet been identified within the Carlindi Dome or anywhere else in the EPT. Evidence for crustal contamination cited by Green et al. (2000) included upwards geochemical trends, such as relative enrichment in LILE, Th, U and LREE. Green et al. (2000) observed that the same geochemical trend is present in the Euro Basalt that immediately overlies the Strelley Pool Formation. Smithies et al. (2007b) also commented on strong geochemical similarities between the Table Top Formation and the Euro Basalt, which was deposited on the granite–greenstone continental crust of the early EPT (Hickman, 2008, 2012). These geochemical similarities imply that the Table Top Formation was also deposited unconformably on continental crust (Table 1). Extensive Paleoproterozoic granitic intrusion into the base of the Coonterunah Subgroup has removed direct evidence of its unconformable contact with the pre-3530 Ma terrane.

Table Top Formation

The oldest formation of the Coonterunah Subgroup, the Table Top Formation, is up to 3450 m thick (Van Kranendonk, 2000a) and comprises a volcanic succession of massive and pillowed tholeiitic basalt with minor komatiite, komatiitic basalt, high-Al basalt and andesite (Glikson et al., 1986; Van Kranendonk, 2000a; Smithies et al., 2007a,b), some of which are metamorphosed to amphibolite facies. Sills of dolerite and gabbro, which are common throughout the Table Top Formation succession, might be subvolcanic to overlying basaltic formations. Smithies et al. (2007a) classified the komatiites as Al-undepleted, with flat normalized trace element patterns with values typically between 0.9 to 2.4 times primitive mantle values (about 3 to 6 times chondritic) and $(\text{Ce/Yb})_{\text{PM}} \sim 0.9$. They reported $\text{Al}_2\text{O}_3/\text{TiO}_2$ ratios between 20 and 24 and noted that Gd/Yb ratios are chondritic (1.1 – 1.3). Arndt and Leshar (2004) recorded that Al-undepleted komatiites, which they referred to as 'Munro-type', typically have $\text{Al}_2\text{O}_3/\text{TiO}_2$ ratios close to 20 and near-chondritic Gd/Yb ratios, whereas Al-depleted komatiites ('Barberton-type') have ratios close to 10, with higher Gd/Yb ratios of about 1.3 – 1.5. Arndt and Leshar (2004) used the Gd/Yb ratio as a measure of relative depletion of the HREE.

Nd model ages of c. 3.63 and 3.59 Ga (Table 4) indicate derivation of the basaltic magmas from somewhat older sources, and geochemical evidence argues against significant interaction with felsic crust (Smithies et al. 2007b). ϵ_{Nd} values are moderately positive (Table 4), suggesting relatively juvenile sources.

Coucal Formation

Conformably overlying the Table Top Formation, the Coucal Formation is up to 1340 m thick (Van Kranendonk, 2000a) and comprises metamorphosed tholeiitic basalt, andesitic to dacitic volcanic and volcanoclastic units, massive porphyritic dacite, vitric tuff and sandstone. Metamorphosed chert units, varying in thickness from a few centimetres to 10 m (Bjornnes and Lindsay, 2005), are locally associated with BIF and silicified pelitic and layered carbonate rocks, and outcrop over strike lengths up to 5 km. Buick et al. (1995) dated a sample of brecciated hyaloclastic rhyolite at 3515 ± 3 Ma, whereas a quartz-phyric rhyolite was dated at 3498 ± 2 Ma

(GSWA 168995, Nelson, 2002e). The base and top of the Coucal Formation are defined by units of chert and BIF that are up to 10 m thick.

The Coucal Formation is geochemically distinct from the Table Top Formation in that the tholeiitic basalts have higher concentrations of incompatible trace elements (Th, U, Nb, Zr and LREE). Smithies et al. (2007b) recognized two geochemical series of volcanic rocks: F1 ranging from andesite to dacite and dominating the lower half of the sequence, and F2 ranging from basalt to andesite in the upper half. F1 rocks have SiO_2 contents between 55 and 65 wt%, whereas SiO_2 in F2 is between 48 and 58 wt%. Both series have relatively low K_2O (<1.0 wt%) and are Fe-rich. Compared to the F2 series, Coucal F1 rocks have slightly higher La/Sm, La/Nb and La/Yb ratios, possibly due to greater magma interaction with felsic crust. Smithies et al. (2007b) concluded that the geochemical data indicated the felsic volcanic rocks of the Coucal Formation (and the overlying Duffer Formation) were andesitic to dacitic lavas that had fractionated from tholeiitic parental magmas, variably contaminated by crustal material.

Smithies et al. (2009) used the unusual chemical compositions of the Coucal Formation basalts to explain Paleoproterozoic TTG generation in the absence of subduction. In their model, Paleoproterozoic TTG magmas were derived through infracrustal partial melting of basaltic crust that was similar in composition to the Coonterunah F2 series (enriched K, LILE, Th and LREE). They proposed that a thick mafic protocrust, dominated by F2-type basalts, formed in the Pilbara Craton between c. 3730 and 3530 Ma, possibly by melting of primitive asthenospheric mantle enriched in recycled felsic crust. This protocrust probably included more typical Archean basalts, fractionated basaltic andesite, and local intrusions of low-Al TTG (Smithies et al., 2009). Nd model ages and ϵ_{Nd} values are very similar to those of the Table Top Formation and Talga Talga Subgroup, except that komatiite in the latter is very juvenile (Table 4).

Double Bar Formation

The Double Bar Formation is up to 1870 m thick (Van Kranendonk, 2000a) and comprises a succession of tholeiitic pillow basalt, basaltic volcanoclastic rocks, massive basalt, thin chert units and dolerite sills. Folding prior to erosion and unconformable deposition of the Strelley Pool Formation has caused the formation to be absent between Sulphur Springs Creek (Zone 50, MGA 727170E 7665340N) and Strelley Pool (Zone 50, MGA 722270E 7664080N). Sericitization and silicification of the basalt to 20 m below the unconformity has been interpreted as representing a Paleoproterozoic paleosol (Altinok, 2006). Lindsay et al. (2005) interpreted hydrothermal alteration at this level, although the c. 100 Ma interval between Double Bar volcanism and deposition of the Strelley Pool Formation, and the angular nature of the unconformity, indicate that any hydrothermal alteration must have been the same age as the Strelley Pool Formation.

Talga Talga Subgroup

In the type area of the Talga Talga Subgroup around McPhee Reward mine 20 km north of Marble Bar (Marble Bar greenstone belt), the subgroup comprises the North Star Basalt and the McPhee Formation (Table 1, Plate 1A). The

succession is also exposed in the Coongan, North Shaw, Panorama and Doolena Gap greenstone belts. Two $^{40}\text{Ar}/^{39}\text{Ar}$ dates of c. 3520 Ma, for hornblende from amphibolite-facies metabasalts of the North Star Basalt in the Coongan and North Shaw greenstone belts (Davids et al., 1997; Zegers et al., 1999), suggest that the North Star Basalt and Coonterunah Subgroup have similar depositional ages. This conclusion was supported by a $^{40}\text{Ar}/^{39}\text{Ar}$ date of c. 3490 Ma for the lower North Star Basalt of the Marble Bar greenstone belt (van Koolwijk et al., 2001), indicating a minimum depositional age.

Depositional ages of the partly sedimentary McPhee and Dresser Formations are loosely constrained between c. 3500 and 3474 Ma, and U–Pb zircon dates fall within the range of 3481–3477 Ma (GSWA 148498, Nelson, 2000m; GSWA 180070, Wingate et al., 2009e). Accordingly, the formations are correlated and included within the Talga Talga Subgroup (Hickman and Van Kranendonk, 2008b; Van Kranendonk et al., 2008; Hickman, 2011). One reason for inclusion is that thick chert units, such as those in the McPhee and Dresser Formations, are commonly interpreted to mark the tops of volcanic cycles. The McPhee Formation comprises grey-and-white banded chert (possibly a silicified, fine-grained volcanoclastic or carbonate rock), iron formation, metapelite, basalt, dolerite and carbonated ultramafic rocks. Silicified felsic tuff of the formation in the Marble Bar greenstone belt was dated at 3477 ± 2 Ma (GSWA 148498, Nelson, 2000m). The Dresser Formation, which is confined to the Panorama greenstone belt, is composed of grey-and-white banded chert, basalt, and minor felsic volcanoclastic and carbonate rocks. A felsic volcanoclastic unit was dated at 3481 ± 3 Ma (GSWA 180070, Wingate et al., 2009e), although this date is based on only two analyses of a single zircon and is, therefore only a possible interpretation of depositional age. In all greenstone belts, the lower part of the subgroup is intruded by granitic rocks, removing evidence of a basal stratigraphic contact. The Talga Talga Subgroup is disconformably overlain by the Coongan Subgroup.

North Star Basalt

In well-exposed sections between the Talga Talga and Coongan Rivers 20 km north of Marble Bar (Plate 1A), the North Star Basalt is over 2000 m thick, and varies in metamorphic grade from amphibolite facies in its lower part to greenschist facies at higher stratigraphic levels. In these sections, the formation is composed of three volcanic cycles (Van Kranendonk et al., 2006b). The middle cycle is about 500 m thick and consists of a basal unit of carbonated and serpentinized olivine-cumulate peridotite overlain by metapyroxenite and metadolerite. Above the metadolerite, the remainder of the cycle is composed of less-metamorphosed, massive and pillowed tholeiitic basalt overlain by an upper unit of grey-and-white banded chert and BIF about 10 m thick. This chert unit, which is inferred to be older than c. 3490 Ma, might be similar in age to chert and BIF in the Coucal Formation, and is therefore one of the oldest sedimentary units in the Warrawoona Group. Unsuccessful attempts have been made to find evidence of early life in the Coucal Formation, but there have been no similar studies on cherts of the North Star Basalt.

Thick sills and veins of porphyritic dacite and rhyolite which intrude the basalts of the middle cycle have not been dated but are interpreted to belong to the c. 3465 Ma Homeward

Bound Granite. This granite intrudes the base of the North Star Basalt (Hickman and Van Kranendonk, 2008b).

Above the chert and BIF, the upper cycle is 400 m thick and mainly composed of komatiitic basalt and tholeiitic basalt intruded by sills of dolerite and gabbro. The stratigraphic base of this cycle is peridotitic komatiite, and the top of the cycle consists of extremely silicified basalt (hydrothermal alteration) and local lenses of dacite beneath the thick basal chert unit of the overlying McPhee Formation. The lower cycle of the North Star Basalt is a succession of metamorphosed pillow basalts and massive basalt between 1000 and 2000 m thick. Metamorphic grade increases to amphibolite facies close to contacts with the Homeward Bound Granite, and the lowermost section of the formation is a complex assemblage of sheared amphibolite intruded by numerous veins of granite and pegmatite. The lower cycle is incomplete and its thickness is uncertain due to deformation and granitic intrusion.

Bagas et al. (2004c) described the North Star Basalt of the Coongan greenstone belt (Fig. 8, Plate 1) as composed of metamorphosed tholeiitic basalt with several units of chlorite–tremolite schist and talc–carbonate rock. These Mg-rich units, which are 20–50 m thick, most likely represent komatiitic basalt and komatiite, although amphibolite-facies metamorphism has destroyed primary textures through much of the succession. The upper part of the formation locally includes a 100–200 m-thick unit of metamorphosed komatiite and komatiitic basalt overlain by banded chert, BIF and units of quartz-rich sandstone (Bagas et al., 2004c). This sandstone may be of similar depositional age to sandstone and pelite in the Coucal Formation. The ultramafic unit is lenticular, probably due to tectonic attenuation, and was mapped for only 8 km along strike (Bagas et al., 2003), but the overlying chert extends for 13 km. The sandstone is overlain by komatiitic basalt and tholeiitic basalt, which might be equivalent to the upper volcanic cycle of the North Star Basalt in the Marble Bar greenstone belt.

In the Panorama greenstone belt, the North Star Basalt occupies the core of the North Pole Dome where it is intruded by the c. 3440 Ma North Pole Monzogranite. In this area the formation is at least 2000 m thick and composed of weakly metamorphosed massive and pillowed basalt, komatiitic basalt, basaltic hyaloclastite, gabbro and dolerite. The formation is disconformably overlain by the Dresser Formation dated at c. 3481 Ma, but its stratigraphic base is not exposed. As in the North Star Basalt of the Marble Bar greenstone belt and the Double Bar Formation of the Coonterunah Subgroup of the East Strelley greenstone belt, komatiitic basalt at the top of the formation in the Panorama greenstone belt is extensively altered, and in this locality the alteration is more conclusively hydrothermal (Kitajima et al., 2001; Terabayashi et al., 2003; Van Kranendonk and Pirajno, 2004; Brown et al., 2006, 2011; Van Kranendonk, 2006; Van Kranendonk et al., 2006b, 2008). The metamorphic grade of the North Star Basalt is mainly lower greenschist facies, except close to the contact with the North Pole Monzogranite where a lower amphibolite-facies metamorphic aureole is developed (Van Kranendonk et al., 2006b).

Excluding data from one sample of komatiite, whole-rock Nd model ages on the North Star Basalt (Table 4) indicate average crustal source ages of 3670–3550 Ma. The komatiite has a high ϵ_{Nd} value of 2.31 and a Nd model age

of c. 3510 Ma suggesting that, unlike the basalts, it was a juvenile extraction from the lower mantle (Nebel et al., 2014). Basalts of the North Star Basalt are high-Ti (see above) and include a minority of rocks geochemically similar to the Coonterunah F2 series (enriched K, LILE, Th and LREE). Geochemical traverses in the Marble Bar greenstone belt (Glikson and Hickman, 1981a) revealed andesitic and dacitic rocks near the top of the North Star Basalt, although some felsic units are visibly intrusive.

Dresser Formation

The Dresser Formation arguably contains the best evidence of c. 3480 Ma life on Earth. Putative fossils include stromatolites (Walter et al., 1980; Buick et al., 1981; Groves et al., 1981; Walter, 1983; Schopf and Walter, 1983; Van Kranendonk, 2000a, 2006; Djokic et al., 2017), microfossils (Dunlop et al., 1978; Schopf and Walter, 1983; Ueno et al., 2001a,b, 2004, 2006; Philippot et al., 2007; Glikson et al., 2008, 2011; Djokic et al., 2017), microbially induced sedimentary structures (Noffke et al., 2013), and organic matter (Morag et al., 2016). Reviews of the fossil and geochemical evidence for ancient life in the Dresser Formation have been provided by Schopf (2006), Van Kranendonk (2007, 2010a), Ueno (2007), Van Kranendonk et al. (2008), and Wacey (2009). Examples of fossil evidence include domal stromatolites and bacterial mats (Fig. 22) and small carbonate stromatolites partly replaced by pyrite (Fig. 22d).

The formation also provides valuable information on the depositional processes and tectonic environment of the Warrawoona Group at c. 3480 Ma (Dunlop, 1978; Barley et al., 1979; Walter et al., 1980; Dunlop and Buick, 1981; Buick et al., 1984; Buick and Dunlop, 1990; Nijman et al., 1998a, 1999a; Van Kranendonk, 2000a, 2006, 2007; Van Kranendonk and Pirajno, 2004; Van Kranendonk et al., 2007a,b; Djokic et al., 2017). Investigations of the formation were initially related to its mineral potential following the discovery of exceptionally large deposits of barite (Hickman, 1973, 1983; Abeyasingh and Fetherston, 1997). In the early 1970s it was thought that, in addition to barite, the formation might contain significant volcanogenic massive sulfide (VMS) mineralization; however, subsequent exploration did not identify any potentially economic VMS deposits.

The origin of the barite has been controversial, with interpretations varying between primary sedimentary deposition (Hickman, 1973; Perry et al., 1975), secondary replacement of gypsum in evaporites (Dunlop, 1978; Lambert et al., 1978; Barley et al., 1979; Dunlop et al., 1978; Buick and Barnes, 1984; Dunlop and Buick, 1981; Buick and Dunlop, 1990), and syndepositional hydrothermal mineralization (Nijman et al., 1998a, 1999a; Van Kranendonk, 2000, 2006; Nijman et al., 2001; Runnegar et al., 2001; Van Kranendonk and Pirajno, 2004; Brown et al. 2006, 2011; Van Kranendonk et al., 2008; Harris et al., 2009; Djokic et al., 2017). As interpretations of the origin of the barite changed, so did interpretations of the depositional environment of the Dresser Formation. The interpretation of primary gypsum implied shallow-water, intertidal to supratidal sedimentary deposition in a series of shallow-water evaporative basins or lagoons marginal to a larger ocean; in contrast, the hydrothermal interpretation suggested deposition around hydrothermal vents, in varying water depths, and possibly within one or more actively evolving volcanic calderas.

Opinions still differ concerning the relative importance of sedimentary and hydrothermal environments for the Dresser Formation, with Noffke et al. (2013) arguing for shallow-water sedimentary deposition, whereas Djokic et al. (2017) presented evidence for a terrestrial hydrothermal hot-spring environment. In fact, the sedimentary and hydrothermal models are not mutually exclusive because large barite deposits are restricted to the Dresser Formation on the northeast side of the North Pole Dome, and in that area they are concentrated in three or four main clusters. Thus, the more recent emphasis on hydrothermal deposition is arguably biased from studies that have been focused on the most mineralized sections of the formation. The predominant depositional environment of the Dresser Formation across most of the Panorama greenstone belt was probably similar to that of the Strelley Pool Formation, which consisted of shallow-water sandstone and platform carbonate deposition during a lengthy break in volcanic activity (Hickman, 2008). Intense hydrothermal activity in the Dresser Formation was apparently restricted to zones of extensive syndepositional faulting (Nijman et al., 1998a, 1999a).

Correlation of the Dresser Formation with the c. 3477 Ma McPhee Formation favours fault control of the barite because the McPhee Formation, deposited over a much wider area of the EPT, does not contain growth faults and does not contain barite. Based on regional stratigraphy and available geochronology, the Dresser and McPhee Formations together represent a significant break in volcanism between the Talga Talga and Coongan volcanic cycles (Fig. 6). The protoliths of the secondary chert members of the Dresser Formation were most likely deposited over millions of years, as interpreted for the Marble Bar Chert Member of the Duffer Formation (Glikson et al., 2016).

The stratigraphic thickness of the Dresser Formation varies from less than 50 m to almost 1000 m. Most of the formation is composed of basalt members that are very variable in thickness, and locally absent. The formation is best known for its 'chert' units representing silicified carbonate and fine-grained clastic rocks; hydrothermal chert forms veins but does not extend far into the bedded succession. In comparison to the sedimentary protoliths of the chert, the basalts are likely to have been deposited extremely rapidly and probably represent merely a brief interruption to sedimentation that spanned 10–20 Ma (North Star Basalt >3490 Ma, Mount Ada Basalt c. 3470 Ma). The lower and upper members of the formation consist of grey-, white-, red- and black-banded chert, and additional chert units are locally present within the intervening basaltic succession. The lower chert unit, also informally referred to as the 'chert–barite unit', varies between 8 and 50 m thick (Van Kranendonk et al., 2008). This lithologically diverse member of the Dresser Formation comprises secondary chert (silicified sedimentary carbonate rocks), sandstone (including silicified carbonate grainstone), conglomerate, detrital carbonate rocks, hydrothermal chert (stratiform and in veins), veins and layers of barite, and thin felsic volcanoclastic units. Very minor sulfide mineralization (pyrite, sphalerite, and galena) is present within the chert–barite sections of the formation, with pyrite replacing carbonate.

Geoscientific drilling in 2004 provided an exceptionally well-preserved section (Van Kranendonk et al., 2006c, 2008; Van Kranendonk, 2007) that, free from the effects of near-surface alteration, has formed a basis for many subsequent studies.

The stratigraphy of the Dresser Formation around the North Pole Dome is complicated by extensive faulting. Some of the faults are growth faults (Nijman et al., 1998a), but others clearly post-date the Dresser Formation. Hickman (1973) explained these faults, which statistical analysis indicated to be approximately radial around the dome, as extensional structures related to doming. Some of these radial faults are intruded by dykes and stocks of porphyritic rhyolite (Brown et al., 2006, 2011) that have been dated at 3450–3430 Ma (Thorpe et al., 1992a; Harris et al., 2009), suggesting doming during intrusion of the c. 3440 Ma North Pole Monzogranite into the centre of the dome.

The first detailed studies of the sedimentology, mineralogy and paleontology of the formation indicated tidal to subaerial deposition, possibly along the shore of an ocean or in shallow-water evaporative basins or lagoons (Barley, 1978; Dunlop, 1978; Lambert et al., 1978; Barley et al., 1979; Dunlop et al., 1978; Dunlop and Buick, 1981; Groves et al., 1981; Buick and Barnes, 1984; Buick and Dunlop, 1990). These workers interpreted barite interbedded with chert in the Dresser Formation to have originated by diagenetic replacement of gypsum in evaporites. However, Runnegar et al. (2001) used X-ray computerized tomography to image the barite crystals and concluded that the primary

mineralogy was barite, not gypsum. Other investigations of the Dresser Formation interpreted widespread hydrothermal deposits within and adjacent to the extensional faults (Nijman et al., 1998a; Van Kranendonk, 2000a, 2006, 2010a; Ueno et al., 2001a,b; Van Kranendonk et al., 2002, 2008; Van Kranendonk and Pirajno, 2004; Pirajno and Van Kranendonk, 2005; Harris et al., 2009).

A conspicuous feature of the barite, both in discordant veins along extensional faults and in bedding-parallel deposits within the formation, is that it forms layers of crystals, generally 10–20 cm-thick, separated either by millimetre-thick stylolite seams or by chert layers of similar thickness to the barite layers (Hickman, 1973). Harris et al. (2009) interpreted geochronological evidence for pulses of hydrothermal activity during and after deposition of the Dresser Formation, with activity continuing until c. 3420 Ma. Minor barite mineralization is hosted by the c. 3470 Ma Mount Ada Basalt; although, unlike barite in the mineralized Dresser Formation, the Mount Ada barite is associated with base metals, suggesting a link to granitic intrusion. There are no known c. 3480 Ma granitic sources for barium in the Dresser Formation, although a granitic intrusion of this age at depth within the North Pole Dome cannot be discounted.

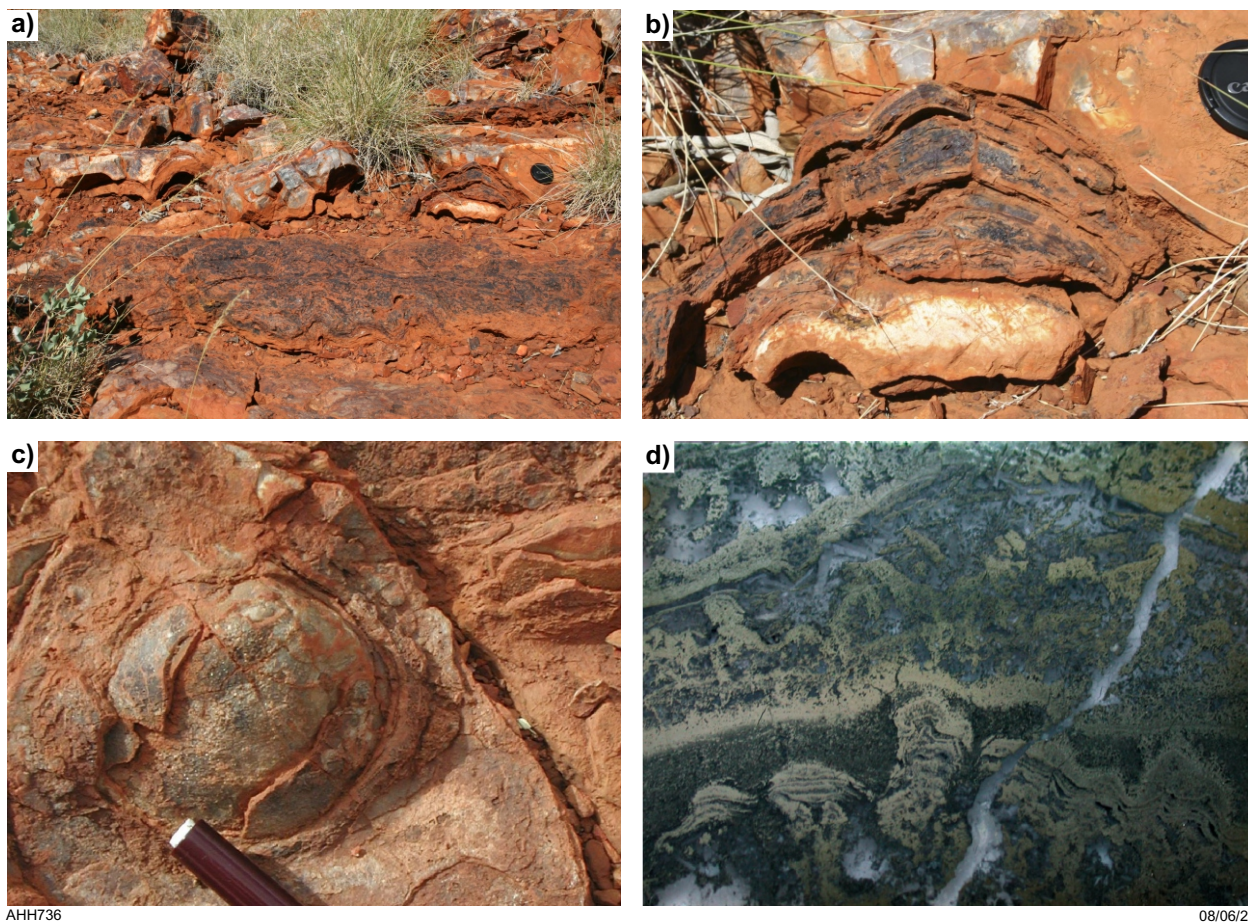


Figure 22. Stromatolites and microbial mats in the c. 3481 Ma Dresser Formation: a) outcrop section through domical stromatolite overlying a bed composed of silicified, weakly laminated microbial mats; b) domical stromatolite enlargement (centre right in (a)); c) bedding plane view of a domical stromatolite; d) thin-section view (plane-polarized light) of centimetre-scale columnar stromatolites partly replaced by hydrothermal pyrite, drillcore from the Dresser Formation (88.7 m in PDP 2B; Van Kranendonk et al., 2008)

The shallow-water depositional environment of the Dresser Formation, combined with it being immediately underlain and overlain by pillow basalt formations several kilometres thick, indicates alternating crustal uplift and subsidence during deposition of the Warrawoona Group. Syndepositional extensional faulting (Nijman et al., 1998a), and the occurrence of locally derived conglomerate in the formation (Van Kranendonk et al., 2008), testify to crustal instability and periodic high-energy depositional environments. Major lateral variations in the thickness of the Dresser Formation, and shallow-water deposition, suggest islands of older rocks within the depositional basin. The vast majority of the zircons in a sandstone of the formation were dated at c. 3525 Ma (GSWA 180070, Wingate et al., 2009e). Available geological evidence indicates that no EPT domes existed during c. 3481 Ma deposition of the Dresser Formation. Consequently, the North Star Basalt passed laterally northwest into the Coonerunah Subgroup (now forming part of the Carlindi Dome), and the Coucal Formation of this unit contains potential felsic source rocks of many of the detrital zircons in the Dresser Formation. Additionally, the recent discovery of the 3530–3490 Ma Mulgundoon Supersuite in the EPT (Petersson et al., 2020) suggests potential granitic sources.

Tessalina et al. (2010) reported geochemical and Sm–Nd isotope data from altered basalts and komatiitic basalts of the Dresser Formation. This included a mean ϵ_{Nd} value of -3.3 ± 1.0 , which indicates original mantle extraction ages far older than the depositional age of c. 3481 Ma. Nd model ages from least-altered samples, including carbonate rock, barite and vein chert, are summarized within Table 4, and suggest mafic sources older than c. 4000 Ma (Tessalina et al., 2010).

McPhee Formation

The MCPhee Formation comprises grey-and-white banded chert (silicified fine-grained volcanoclastic or carbonate rocks), iron formation, metapelite, basalt, dolerite, gabbro, and carbonated ultramafic rocks. However, it is principally a sedimentary formation that was deposited between two major volcanic cycles: those of the underlying North Star Basalt and the overlying Coongan Subgroup. The centre of the MCPhee Formation is composed of basalt, as is the Dresser Formation at North Pole. However, it is now considered likely that the ultramafic and mafic intrusions within the formation are sills that were intruded during eruption of the overlying Mount Ada Basalt.

Correlation of the c. 3477 Ma MCPhee Formation (Hickman, 1977a) and c. 3481 Ma Dresser Formation (Van Kranendonk and Hickman, 2000) followed a reinterpretation of the stratigraphy of the North Pole Dome (Van Kranendonk et al., 2007a,b; Hickman and Van Kranendonk, 2008a). At North Pole, the 5 km-thick basaltic formation immediately overlying the Dresser Formation was initially assigned to the Apex Basalt because the felsic volcanic succession of Panorama Ridge on the south side of the North Pole Dome was assigned to the Panorama Formation (Hickman, 1980b). However, the U–Pb zircon date of 3470.1 ± 1.9 Ma for an impact spherule layer in this formation (Byerly et al., 2002) is inconsistent with this correlation. This age coincides with that of the Mount Ada Basalt in the Marble Bar greenstone belt.

The MCPhee Formation is not known to contain barite mineralization, which is focused in particular areas of the

Dresser Formation. The Dresser Formation lacks peridotitic ultramafic rocks that form part of the MCPhee Formation, but alteration of these rocks makes it uncertain if they are volcanic. The ultramafic units in the MCPhee Formation might include subvolcanic sills related to the basal section of the overlying Mount Ada Basalt.

The MCPhee Formation is present in the Marble Bar, Coongan, North Shaw, and Warralong greenstones belts (Fig. 8, Plate 1) of the EPT (Van Kranendonk, 2004c, 2010c; Hickman, 2011). The distinguishing feature of the MCPhee Formation, which separates the thick basaltic successions of the North Star and Mount Ada Basalts, is its thin and lithologically mixed succession. Evidence of minor felsic volcanic activity during deposition of the MCPhee Formation is provided by silicified felsic tuff dated at 3477 ± 2 Ma (GSWA 148498, Nelson, 2000m). The lithological diversity of the MCPhee Formation in all greenstone belts, with resulting major stratigraphic variations in rock competence, allowed extensive shearing, folding and layer-parallel faulting during doming. Once established during c. 3460 Ma doming (Collins, 1989), the shear zones were later reactivated with each subsequent major deformation event. Metamorphism led to hydrothermal quartz veining, and in consequence, the formation contains numerous vein and lode-gold deposits.

Coongan Subgroup

The Coongan Subgroup (Van Kranendonk et al., 2006a) represents a single volcanic cycle in which the Mount Ada Basalt, containing komatiite, komatiitic basalt and tholeiite, passes upwards and laterally into andesite, dacite and rhyolite of the Duffer Formation (Fig. 6, Table 1). The regional geological setting of the subgroup is shown in Figure 23. U–Pb zircon dating in the Coongan and Marble Bar greenstone belts, summarized in Figure 24, indicates that felsic volcanism of the Duffer Formation commenced at c. 3474 Ma (GSWA, 142975, Nelson, 2000j) and continued until c. 3459 Ma (de Vries et al., 2006). Felsic units in the Mount Ada Basalt have been dated between c. 3470 and 3469 Ma, although these might include intrusions related to the overlying Duffer Formation. The Marble Bar Chert Member, at the top of the Duffer Formation, is inferred to have been deposited between c. 3459 and 3455 Ma, making the age range of the Coongan Subgroup 3474–3455 Ma.

In the Marble Bar greenstone belt, the maximum stratigraphic thickness of the subgroup is about 10 km, largely due to an exceptionally thick development (~8000 m) of the Duffer Formation at Marble Bar (Fig. 25). In the northern Coongan greenstone belt, 30 km southwest from Marble Bar, the subgroup is about 7000 m thick, but elsewhere the thickness is generally less than 5000 m. The Coongan Subgroup forms parts of the Marble Bar, Coongan, North Shaw, Panorama, Warralong, Doolena Gap and East Strelley greenstone belts (Fig. 8, Plate 1). The extremely limited preservation of the subgroup in the East Strelley greenstone belt is attributed to uplift and deep erosion of the Carlindi Dome before 3426 Ma (Hickman, 2008). In that dome, only remnants of the Duffer Formation (c. 3467 Ma felsic volcanoclastic rocks and high-level, porphyritic, felsic intrusive rocks) are still preserved under the unconformity at the base of the Strelley Pool Formation (Van Kranendonk, 2000a). Available stratigraphic evidence indicates that the Coongan Subgroup was deposited across at least 30 000 km² of the EPT.

Deposition of the Coongan Subgroup commenced with eruption of komatiite and komatiitic basalt. The existence of komatiite at the base of volcanic cycles provides strong evidence for a mantle plume origin because the generation of komatiitic magmas indicates mantle melting at very high temperatures (Arndt et al., 1997, 2001; Condie, 2001; Van Kranendonk et al., 2002, 2006a; Smithies et al., 2005b). Identification of komatiites uses geochemical data, although the rocks exhibit characteristic mineralogy and textures in the field. In the Marble Bar greenstone belt, Glikson and Hickman (1981a,b) identified altered peridotitic komatiite at the stratigraphic base of the Mount Ada Basalt north of Marble Bar. One of the five komatiite samples contained 31 wt% MgO (calculated on a volatile-free basis) which, owing to alteration, almost certainly understates the primary MgO content. Trace elements less mobile under alteration include Cr and Ni, and the sample contained 5650 ppm Cr and 2093 ppm Ni. Van Kranendonk (2010c) also mapped

komatiite at the base of the Mount Ada Basalt in the Marble Bar greenstone belt, north of the Talga Talga mining area.

Komatiite and komatiitic basalt also form the lower part of the Mount Ada Basalt in the Panorama greenstone belt (Brown et al., 2006, 2011), and komatiite is present in the Doolena Gap greenstone belt (Van Kranendonk, 2004c, 2010c). The apparent absence of basal komatiite in other sections of the Mount Ada Basalt may be due to komatiite having been mapped as part of the underlying McPhee Formation, or to the existence of subvolcanic sills of komatiite within the sedimentary strata of the McPhee Formation. The basal komatiites and komatiitic basalts of the Mount Ada Basalt are invariably overlain by much thicker units of pillowed tholeiitic basalt intruded by dolerite sills. Sills of porphyritic dacite and granophyre are also common in some sections, and may be subvolcanic to the overlying Duffer Formation.

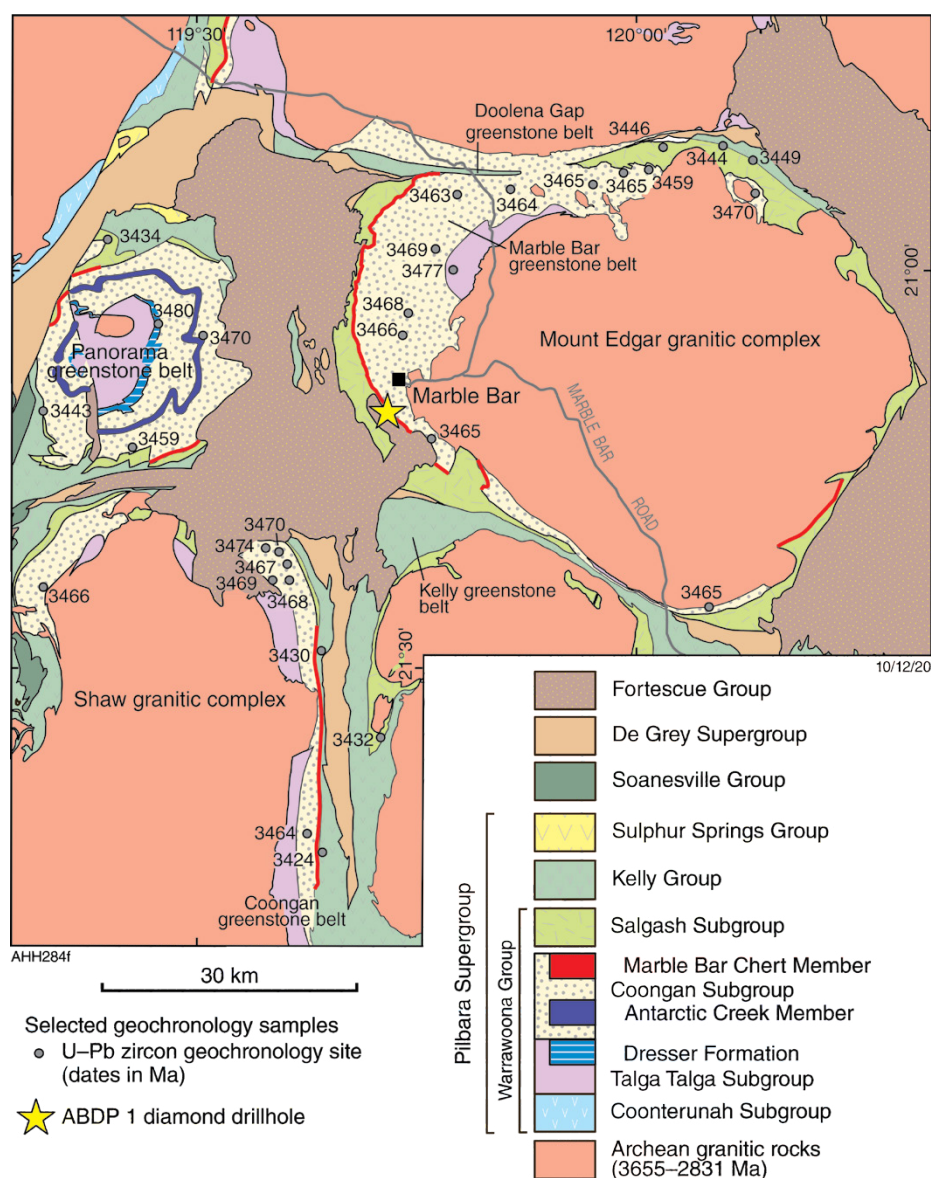


Figure 23. Geological map of part of the EPT showing outcrops of the Marble Bar Chert Member (red lines) within the stratigraphy of the Pilbara Supergroup. U–Pb zircon geochronology for units of the Pilbara Supergroup is summarized and the location of stratigraphic drillhole ABDP 1 is shown (from Glikson et al., 2016)

The contact between the Mount Ada Basalt and the Duffer Formation is conformable in most greenstone belts, although it is locally difficult to define owing to lateral intercalation of basalt and felsic volcanic rocks in some sections (Van Kranendonk et al., 2006a). In the northwestern Marble Bar greenstone belt, west and north of the Talga Talga mining area, the contact is marked by a thin unit of chert, BIF, volcanoclastic siltstone and sandstone, shale and felsic tuff up to 10 m thick (Hickman, 1983, p. 91; Van Kranendonk, 2010c). In the Doolena Gap greenstone belt (Fig. 8, Plate 1A), pillow basalts of the Mount Ada Basalt are separated from overlying felsic volcanic rocks of the Duffer Formation by a siltstone unit up to 200 m thick (Wiemer et al., 2016). At the base of this siltstone there is locally a

1 m-thick unit comprising repeated cm-thick upwards-fining graded layers of conglomerate and siltstone. The existence of this sedimentary unit indicates a brief volcanic hiatus, at least in the Marble Bar–Doolena Gap area.

Thickness and facies variations in the Duffer Formation suggest it was deposited in a major felsic volcanic complex centred on the area now situated between the Mount Edgar and Shaw Domes (Fig. 8). The maximum stratigraphic thicknesses of 8 km at Marble Bar and 5000 m in the northern Coongan greenstone belt decrease to about 1000 m on the eastern side of the Mount Edgar Dome, the southern Coongan greenstone belt, and the Panorama, North Shaw and Doolena Gap greenstone belts (Fig. 8, Plate 1A). Elsewhere the Duffer Formation is less than 100 m thick or entirely absent from the Warrawoona Group succession. Since, in most areas, the Duffer Formation is overlain by the shallow-water Marble Bar Chert Member (MBCM), the Duffer Formation must, before deposition of the MBCM, have occupied a depositional basin that subsided by at least 8000 m in the large area of greenstones west of Marble Bar. In this Report, this major basin subsidence is interpreted to be the first evidence of sagduction and, as described under **Tectonic events in the EPT**, is assigned to deformation event D₂. Accompanying 3474–3459 Ma diapiric uplift occurred in surrounding areas, now occupied by the Carlindi Dome (Hickman, 1984; Van Kranendonk, 2000a; Van Kranendonk et al., 2006a; Hickman and Van Kranendonk, 2008a), Muccan Dome (Wiemer et al., 2016), Shaw Dome (Van Kranendonk, 2000a), and Mount Edgar Dome (Collins, 1989; Hickman and Van Kranendonk, 2004).

The felsic volcanic succession of the Duffer Formation is separated from the next ultramafic–mafic–felsic volcanic cycle (Salgash Subgroup) by the MBCM of the Duffer Formation (Van Kranendonk et al., 2006a). This member was initially interpreted to be a separate formation, the 'Towers Formation' (Hickman, 1977a, 1981, 1983), and was interpreted to outcrop over a large part of the EPT. In some greenstone belts, the 'Towers Formation' was subsequently renamed as the 'Strelley Pool Chert' (obsolete name, replaced by Strelley Pool Formation) overlying the Panorama Formation (DiMarco and Lowe, 1989a,b). A regional stratigraphic revision of the northern Pilbara Craton by Van Kranendonk et al. (2006a) included renaming the 'Towers Formation' as a member of the underlying Duffer Formation.

One reason for this stratigraphic change was that volcanic cycles elsewhere are commonly 'capped' by chert units attributed to hydrothermal activity following volcanism (i.e. deposition of chert from hydrothermal vents). However, most so-called chert units in the Pilbara Supergroup are not primary hydrothermal deposits, but were formed by the silicification of sandstones, shales, carbonate rocks or fine-grained volcanoclastic rocks (Groves et al., 1981; Lowe, 1983; Barley, 1984; Buick and Barnes, 1984; Buick and Dunlop, 1990; Sugitani, 1992; Schopf, 1993; Van Kranendonk and Pirajno, 2004; Orberger et al., 2006; Van Kranendonk, 2006; Van den Boorn et al., 2007, 2010; Cammack et al., 2018). Secondary silicification was also responsible for most of the MBCM.

It can be difficult to establish if the hydrothermal activity responsible for silicification of sedimentary units was related to the underlying or overlying volcanic units. For example, Van Kranendonk and Pirajno (2004) concluded that silicification of sedimentary rocks of the Strelley Pool Formation was footwall alteration caused by eruption of the overlying Euro Basalt. Thus, it remains possible that

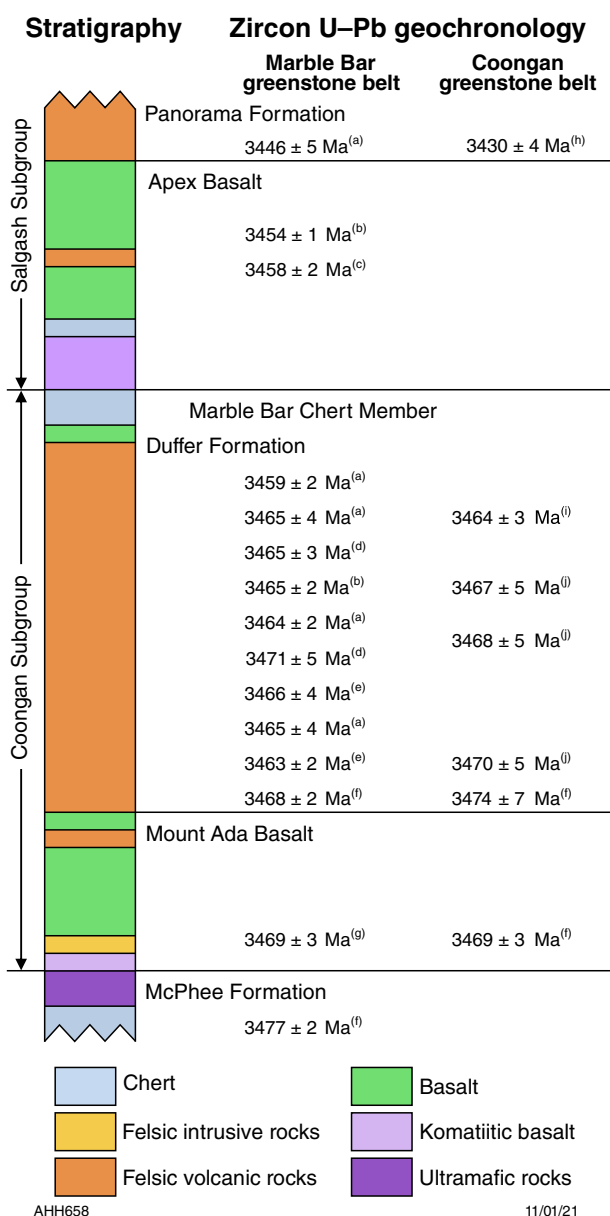


Figure 24. U–Pb zircon geochronology of igneous rocks of the Coongan and Salgash Subgroups that constrain the depositional age of the Marble Bar Chert Member. Sources of data: (a) de Vries et al. (2006); (b) RI Thorpe, written comm. (1991); (c) Thorpe et al. (1990); (d) Thorpe et al. (1992); (e) McNaughton et al. (1993); (f) Nelson (2000); (g) Nelson (1999); (h) Nelson (2002); (i) Nelson (2004); (j) Nelson (2001) (from Glikson et al., 2016)

hydrothermal silification of the MBCM occurred during deposition of the overlying Apex Basalt, at the same time as the member was intruded by numerous dolerite dykes feeding the basalt (Fig. 25). Trace element abundances indicate that the hydrothermal fluids were derived from mafic sources, which suggests an association with the dolerite dykes and sills of the overlying Apex Basalt rather than the felsic volcanic Duffer Formation. However, volcanoclastic sandstone and conglomerate forms thick units in the upper Duffer Formation, particularly north of Marble Bar (Hickman and Van Kranendonk (2008b)), and these are overlain by the silicified sandstones and conglomerates in the lower MBCM. In view of this, the stratigraphic interpretation by Van Kranendonk et al. (2006a), that the 100 m-thick silicified clastic succession is the uppermost member of the Duffer Formation, is retained.

Geochemical data from the Coongan Subgroup have been reported by Hickman and Lipple (1975), Glikson and Hickman (1981a,b), Jahn et al. (1981), Hickman (1983), Glikson et al. (1987), Barley (1993), Cullers et al. (1993), and Smithies et al. (2005a,b, 2007a,b). Hickman and Lipple (1975) presented analyses of 34 samples of dacite and rhyolite from the Pilbara Supergroup but did not interpret the data. Glikson and Hickman (1981a) described the Mount Ada Basalt in conjunction with komatiitic and basaltic rocks in the Talga Talga Subgroup. Komatiite was attributed to >50% melting of mantle peridotite and a compositional gap between the komatiites and 'high-Mg' basalts (here referred to as komatiitic basalts) was interpreted to indicate different sources. A continuous chemical spectrum between komatiitic basalts and tholeiites suggested derivation of the latter by fractionation of pyroxene, olivine, orthopyroxene and minor plagioclase. Glikson and Hickman (1981b) reported data from 50 samples of the Duffer Formation and 17 samples from the Panorama Formation. To examine vertical geochemical trends in the Duffer Formation, 41 samples were collected from a 3800 m stratigraphic section north of Marble Bar. Vertical profiles of Zr/TiO₂, Th, La, Ce (increasing), and Ni and V (decreasing) revealed a progressive upwards trend from andesite through dacite to rhyolite (Hickman, 1983). The compositional trend was also evident on a plot of Zr/TiO₂ vs Nb/Y (after Winchester and Floyd, 1977).

Jahn et al. (1981) presented REE data for 28 felsic igneous rocks from the EPT. These included felsic volcanic samples that were assigned to the upper North Star Basalt (n = 4), Duffer Formation (n = 8), Panorama Formation (n = 3) and Wyman Formation (n = 3). Based on further geological mapping, some of the samples have subsequently been stratigraphically reassigned, such that seven samples collected from the Duffer Formation and three of the four North Star Basalt samples are interpreted to be from a subvolcanic intrusion underlying the Duffer Formation. It is now evident that 10 analyses came from the Duffer Formation or related subvolcanic intrusions. All the Duffer Formation volcanic rocks exhibit fractionated REE patterns very similar to TTG of the Mount Edgar and Shaw Domes. Nine dacites have very similar chondrite-normalized REE patterns and all lack Eu anomalies; the remaining rhyolite has a negative Eu anomaly. Jahn et al. (1981) concluded that the REE data indicate magma generation by partial melting of amphibolitic or basaltic sources, followed by fractional crystallization. They ruled out derivation by direct melting of the upper mantle, and concluded that the source was basaltic crust.

Glikson et al. (1987) proposed that, in general, felsic volcanic and intrusive rocks of the EPT older than c. 3400 Ma are Na-rich, have low Rb/Sr (<0.4), no or small Eu anomalies, and near flat HREE profiles. The lack of Eu depletion was interpreted to indicate partial melting or fractional crystallization of a mafic source and no involvement of felsic sources. Barley (1993) interpreted the Mount Ada Basalt and Duffer Formation to be petrogenetically related with the basalts derived from partial melting of a mantle source enriched in the more incompatible elements (K, Rb, Zr, LREE), followed by fractional crystallization of olivine and pyroxene. The felsic rocks of the Duffer Formation were then derived from the basaltic magmas by fractional crystallization of the observed phenocryst phases (pyroxene + plagioclase + iron–titanium oxide ± amphibole). Barley (1993) observed that simple, incremental melting of mafic crust cannot explain the full range of compositions observed. Instead, the favoured a petrogenetic model involved both mantle-derived basaltic magmas and intermediate to silicic melts of mafic crust, with variable amounts of magma mixing and fractional crystallization, with or without crustal contamination.

Smithies et al. (2007a) reported geochemical data from the Mount Ada Basalt and Duffer Formation north of Marble Bar. They stated that the Mount Ada Basalt in this area is mainly composed of high-Ti tholeiites. Normalized trace element patterns for these rocks were found to be similar to those of the North Star Basalt. Low-Ti basalts have lower incompatible trace element concentrations than the high-Ti rocks and were interpreted to have been derived from a more-depleted source. Tholeiitic basalts were reported to be interleaved with felsic volcanic rocks in the lower half of the Duffer Formation, and the high-Ti tholeiites in the Duffer Formation have the same trace element concentration and normalized patterns as high-Ti tholeiites in the underlying Mount Ada Basalt. Smithies et al. (2007b) reported that the main part of the Duffer Formation is composed of two sodic (K₂O/Na₂O ≤ 0.5) basalt-to-dacite series, and that these are chemically similar to Archean TTG, with features including high La/Nb, Th/Nb and La/Yb ratios.

In contrast, rhyolites in the upper Duffer Formation have far higher K₂O/Na₂O (1.5 – 2.6), and high Fe, HREE, Zr and Nb, suggesting a strongly fractionated tholeiitic magma. Although dacites of the Duffer Formation are chemically similar to Archean TTG, a comparison between c. 3465 Ma TTG of the Shaw Dome (North Shaw Suite, Bickle et al., 1993) and the c. 3465 Ma Duffer Formation of the Mount Edgar Dome indicated differences in Nd isotopes and trace element data. This led Smithies et al. (2007b) to argue for different sources; specifically, that the Duffer Formation magmas were generated through fractionation of tholeiitic parent magma contaminated by crustal TTG, whereas the contemporaneous TTG (Callina Supersuite) was derived through melting of basaltic crust and older TTG rocks.

Whole-rock Nd model ages for 11 samples of mafic and felsic volcanic rocks of the Coongan Subgroup range between c. 3690 and 3510 Ma (Table 4). Excluding one anomalously old Nd model age from the Callina Supersuite (3.77 Ga, Bickle et al., 1993), Nd model ages from 10 Callina Supersuite samples range between c. 3710 and 3530 Ma (Table 4). These data suggest that sources for the Coongan Subgroup had approximately the same average age as sources for the Talga Talga and Coonterunah Subgroups.

The relative uniformity of source ages for volcanic and intrusive rocks of the EPT is also illustrated in Figure 17. ϵ_{Nd} values in the Coongan Subgroup (Table 4) are lower than the theoretical depleted mantle ϵ_{Nd} at 3470 Ma, which is about +2.4. This implies reworking of older material, possibly combined with juvenile additions.

Mount Ada Basalt

Komatiite, komatiitic basalt and basalt are locally interlayered in some basal sections of the Mount Ada Basalt, suggesting lateral mixing of flows from different sources. However, the Mount Ada Basalt is mainly composed of pillowed tholeiitic basalt intruded by dolerite sills. Some sections include several thin units of grey-and-white banded chert and rare units of red-and-white banded chert; for example, in the Antarctic Creek Member in the Panorama greenstone belt (Fig. 8, Plate 1A; Van Kranendonk, 2000a).

Felsic units of porphyritic granophyre and felsic tuff are less than 20 m thick, and two of units these have been dated at c. 3470 Ma (GSWA 148500, Nelson, 1999f; GSWA 142976, Nelson, 2000k). GSWA 148500 includes xenocrystic zircons up to 40 Ma older than the depositional age, suggesting zircon derivation from the underlying Talga Talga Subgroup or contemporaneous felsic intrusive rocks.

The Mount Ada Basalt contains evidence for Earth's oldest asteroid impact event. A distal ejecta layer containing impact spherules was discovered in the Antarctic Creek Member of the Mount Ada Basalt at North Pole (Lowe and Byerly, 1986). Later descriptions were provided by Byerly et al. (2002), Glikson (2004), Glikson et al. (2004), and Glikson and Pirajno (2018); the main unit containing the spherules is known as the 'ACM-1 layer'. The spherules, mainly 0.10 – 0.75 mm diameter, are contained within two 15–50 cm-thick units of chert and sandstone separated by a 200 m-thick dolerite

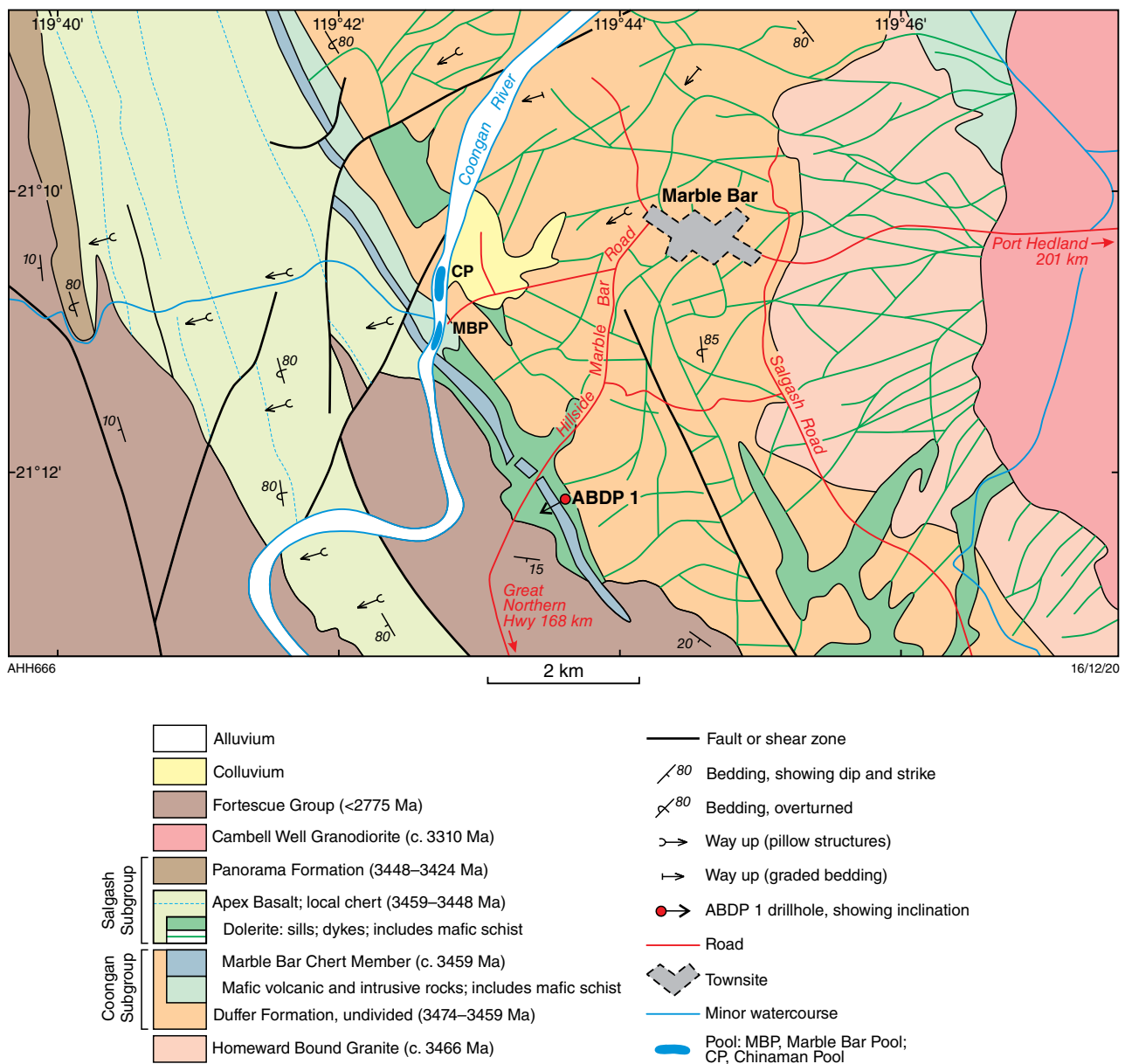


Figure 25. Geological sketch map of the Marble Bar area showing the exceptional thickness of the Duffer Formation, and a swarm of dolerite dykes and sills that were feeders to the Apex Basalt

sill (Glikson et al., 2004). The Antarctic Creek Member is underlain and overlain by thick successions of basaltic volcanic rocks. Some doubt exists as to whether the separate spherule layers in the Antarctic Creek Member were deposited from different impact events or if the upper layer represents a sedimentary reworking of the lower deposit (ACM-1 layer).

Microscopic examination shows the spherules to be microkrystites with quench textures including cloudy to opaque needle-shaped pseudomorphs, most likely replacing olivine or pyroxene, and lathlike quartz pseudomorphs probably replacing plagioclase. Devitrification features include radiating, fan-shaped aggregates of sericite. Geochemical analysis of spherule-bearing chert from the ACM-1 layer provided results consistent with an impact spherule deposit, including: Ir at 42 ppb; Pd at 9 ppb; Pt at 96 ppb; Os at 21 ppb; Rh at 16 ppb; Ru at 69 ppb; and an Ir/Pd ratio of 4.67 (unpublished data, AY Glikson, 2016, written comm., 23 May). The anomalously high platinum group element (PGE) concentrations in ACM-1 are accompanied by Ni and Cr contents (Ni at 14 ppm; Cr at 262 ppm) consistent with the basaltic environment of the Antarctic Creek Member. Based on this single analysis of the ACM-1 layer, its Ir content (an indicator of an extraterrestrial component in impact spherules) is higher than in most recorded Archean and Proterozoic spherule layers (data reviewed by Glass and Simonson, 2013). Byerly et al. (2002) dated the ACM-1 ejecta layer at 3470 ± 2 Ma.

In the Barberton Greenstone Belt of South Africa, a similar spherule layer, also dated at 3470 ± 2 Ma (Byerly et al., 2002), has been traced over a strike length of 13 km (Lowe and Byerly, 1986; Lowe, 1999; Lowe et al., 2003; Glass and Simonson, 2013). This is referred to as the 'S1 layer' and is preserved in thin sandstone and chert units within komatiite and basalt of the Hooggenoeg Formation (Lowe et al., 2003). In view of S1 and ACM-1 layers being the same age, and having other features in common (Glass and Simonson, 2013), several workers have suggested that the layers contain ejecta from the same major asteroid impact (Byerly et al., 2002; Simonson and Hassler, 2002; Glikson and Vickers, 2004; Glass and Simonson, 2013).

Duffer Formation

The lower and central sections of the Duffer Formation are composed of metamorphosed andesitic, dacitic, and rhyolitic volcanic rocks with locally variable intercalations of basalt. The upper part of the formation includes conglomerate and sandstone underlying the MBCM. Metamorphosed sedimentary rocks are also present in distal sections remote from the main centre of volcanism. Basalt intercalations are locally included in the lower half of the formation north of Marble Bar, but are absent elsewhere (e.g. northern Coongan greenstone belt, Fig. 8). Where primary textures are well preserved, many felsic units have been identified as ignimbrites (Fig. 26). Thickness variations in the Duffer Formation suggest it was deposited in a major felsic volcanic complex centred on the area now occupied by the western half of the Mount Edgar Dome and the northern Coongan greenstone belt. The apparent stratigraphic thickness of the Duffer Formation at Marble Bar is 8000 m, although this estimate relies on cumulative thicknesses of steeply inclined strata along a horizontal traverse. In a geochemical traverse 14 km north of Marble Bar (Glikson

and Hickman, 1981a), the formation is 4000 m thick, which is similar to the thickness in the northern Coongan greenstone belt (Plate 1A). On the eastern side of Mount Edgar Dome, it is only about 1000 m thick, and similar thicknesses are also present in the southern Coongan greenstone belt, and in the Panorama, North Shaw and Doolena Gap greenstone belts (Fig. 8). Elsewhere, the Duffer Formation is less than 100 m thick or entirely absent from the Warrawoona Group succession. However, present stratigraphic thicknesses may not accurately reflect depositional thicknesses, partly due to tectonic attenuation during doming, but also as a consequence of erosion of the lower Warrawoona Group prior to c. 3460 Ma (DiMarco and Lowe, 1989b; Glikson et al., 2016).

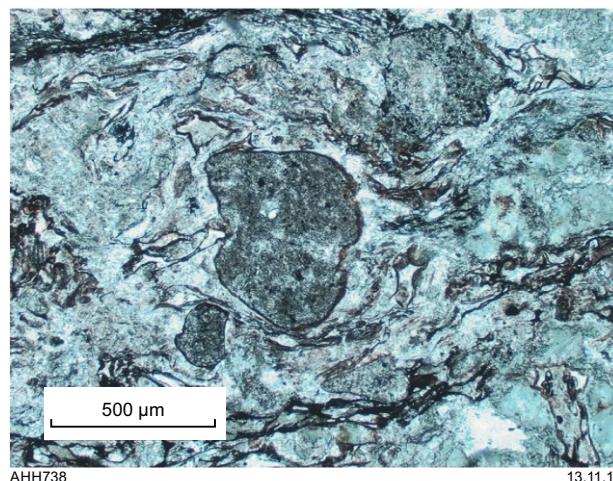


Figure 26. Photomicrograph (plane-polarized light) of ignimbrite in the upper part of the Duffer Formation north of Marble Bar. Flow lamination is deflected around a rounded fragment of porphyritic dacite

Volcanic and sedimentary facies within the Duffer Formation provide evidence on the depositional settings of individual sections. Coarse volcanoclastic facies including agglomerate are interpreted to be proximal to large volcanic vents, and this facies is restricted to the thickest sections of the formation. DiMarco and Lowe (1989b) suggested that felsic volcanic centres were located in approximately the same positions at the granitic centres of several of the domes in the EPT, although this interpretation was made assuming that the Duffer and Panorama Formations were closely related. The interpretation in this Report is that the Panorama Formation was erupted from such centres, but that the Duffer Formation pre-dated significant dome development and was centred on a major volcanic complex in the Marble Bar area. Distal facies of the Duffer Formation are represented by ashfall deposits, fine-grained volcanoclastic sedimentary rocks, quartz sandstone and shale. In the Doolena Gap greenstone belt, which is interpreted to lie close to the northern margin of the felsic volcanic complex, the Duffer Formation shows a lateral facies change from felsic lavas and pyroclastic rocks in the east to siltstones and turbidites in the west (Wiemer et al., 2016). On the southeastern side of the volcanic complex, in the Yandicoogina area of the Mount Edgar Dome, the Duffer Formation is sheared and metamorphosed (Williams and Bagas, 2007a,b) but its composition is consistent with relatively distal facies that included volcanoclastic sedimentary rocks, sandstone and shale. In the North

Shaw greenstone belt (Fig. 8, Plate 1A), where the Duffer Formation is about 1000 m thick, the formation comprises metamorphosed felsic volcanoclastic rocks, ignimbrites, sandstone and conglomerate (Van Kranendonk, 2000a). These lithologies suggest that the western margin of the Duffer Formation was located a considerable distance west of the North Shaw greenstone belt (Fig. 8; Plate 1A). The facies changes across the Duffer Formation, plus the regional continuity of the overlying Marble Bar Chert Member, suggest that the Mount Edgar, Shaw and Muccan Domes did not develop as well-defined separate structures until after c. 3460 Ma, the minimum age of the Duffer Formation.

Marble Bar Chert Member

The Marble Bar Chert Member (MBCM) (Hickman, 1977a; Van Kranendonk et al., 2006a) is the uppermost stratigraphic member of the Duffer Formation. The type section of the member is at Marble Bar Pool on the Coongan River (Fig. 25) where extensive outcrops of red, white, and grey banded chert and jaspilitic chert (Fig. 27a,b) are crosscut by irregular veins and layers of massive, dark grey, hydrothermal chert (Fig. 28). The MBCM outcrops in the Marble Bar, Coongan, Panorama and Warralong greenstone belts (Figs 8, 23). Some workers have questioned the lateral continuation of chert units between different greenstone belts (Buick and Barnes, 1984), but detailed regional mapping during the PCMP established that the MBCM (as a unit of extensively silicified clastic sedimentary rocks) is present over a wide area. Local facies changes and thickness variations along strike were consequences of the relatively shallow-water depositional setting of the sedimentary protoliths. However, these variations are regionally insignificant because the stratigraphic position of the MBCM was controlled by the 3459–3455 Ma volcanic hiatus across most of the EPT. Local thickness variations are due partly to intrusion of dolerite sills into the base of the member (Glikson et al., 2016), and partly to shearing that occurred during doming. Syndepositional extensional faulting produced locally abrupt lateral thickness and facies changes (Olivier et al., 2012; Nijman et al., 2017).

At Marble Bar Pool the MBCM is represented by a 60 m-thick stratigraphic section (Kato and Nakamura, 2003), but the base of this section is faulted against pillowed basalt and dolerite. Evidence from diamond drilling 2.5 km to the southeast of the pool (drillcore ABDP 1; Hickman, 2005; Hoashi et al., 2009) indicates that this faulting removed the lower 30 m of the member at Marble Bar Pool (Glikson et al., 2016). In the more complete stratigraphic section provided by ABDP 1 (Fig. 29), this lower part of the stratigraphy is mainly composed of silicified clastic sedimentary rocks, including diamictite and two thin layers of asteroid impact spherules (Glikson et al., 2016). In this Report, this clastic section, missing from the Marble Bar Pool outcrop, is interpreted to be exposed at Chinaman Pool (Fig. 25) where a 20 m-thick succession, previously named the Chinaman Pool Chert Member (Van Kranendonk et al., 2001a), overlies the felsic volcanic rocks and volcanoclastic sedimentary rocks of the Duffer Formation.

The Chinaman Pool Chert Member was described by Olivier et al. (2012) as including polymictic conglomerate and pebbly sandstones deposited from debris flows during erosion of the Duffer Formation. These sandstone and

conglomerate units might include the diamictites intersected in ABDP 1, and might also contain the impact spherule layers identified in ABDP 1. However, impact spherule layers are commonly lenticular due to erosion and reworking, and the <1 mm-diameter spherules are difficult to observe in outcrop. The Chinaman Pool Chert Member represents a transition sequence from high-energy, clastic deposition at the top of the felsic volcanic pile of the Duffer Formation, to low-energy deposition of fine-grained clastic sediments, carbonates and primary hydrothermal deposits exposed in the Marble Bar Pool section of the member.

The upwards-fining succession of the MBCM, from the coarse-grained clastic facies at Chinaman Pool to silicified muds and hydrothermal chemical precipitates at the top of the Marble Bar Pool section, partly explains the diversity of previous interpretations regarding its composition and origin (DiMarco and Lowe, 1989b; Sugitani, 1992; Kojima et al., 1998; Oliver and Cawood, 2001; Van Kranendonk et al., 2001a; Kato and Nakamura, 2003; Orberger et al., 2006; Van Kranendonk, 2006, 2010a; Van den Boorn et al., 2007, 2010; Hoashi et al., 2009; Van Kranendonk and Johnston, 2009; Olivier et al., 2012; Li et al., 2013; Rasmussen et al., 2014b; Glikson et al., 2016). Some interpretations have proposed oceanic depositional settings such as mid-oceanic ridge, basin plain and island arc. However, oceanic settings for the Warrawoona Group are precluded by a wide range of evidence from the PCMP and other investigations.

In the Marble Bar area, the initial depositional environment of the MBCM was similar to that interpreted by Olivier et al. (2012), marginal to an emerging landmass and including fluvial channels, deltas and submarine fans. Uplift, crustal extension and erosion were most likely related to the rising mantle plume that subsequently evolved to cause volcanism of the Salgash Subgroup. However, water depths appear to have increased during deposition of the MBCM, at least in the Marble Bar Pool area. This might have been due to gravitational collapse of the abnormally thick underlying volcanic pile of the Duffer Formation. Hoashi et al. (2009) related the upper jaspilitic section of the member in the Marble Bar Pool area to submarine hydrothermal vents, possibly in a caldera setting. In view of iron-rich layers with Fe_2O_3 (total) contents of 2–25 wt%, they interpreted this upper part of the member to be a low-grade Algoma-type (volcanic-related) BIF. Analyses by Sugitani (1992) showed that the jaspilitic chert contains up to 40 wt% Fe_2O_3 , although Fe_2O_3 <10 wt% is more typical.

The detailed structural geology of the Marble Bar Pool – Chinaman Pool area remains to be established, but a 300 m-thick unit of komatiitic basalt and dolerite that separates the outcrops of the Marble Bar and Chinaman Pool Chert Members is here interpreted to be a faulted section of the Apex Basalt rather than a basaltic unit deposited between two separate chert members, as originally interpreted (Lipple, 1975; Hickman, 1977a, 1983). Van Kranendonk et al. (2006b) noted a faulted contact between this basalt–dolerite unit and the Chinaman Pool Chert Member, and Kato et al. (2009) mapped shear zones along the lower and upper contacts of the Marble Bar Pool section of the member. The development of bedding-parallel shear zones along contacts between the basalts and the cherts is interpreted to have occurred during doming, particularly as the stratigraphy at Marble Bar Pool is overturned on the southwest side of the Mount Edgar Dome.

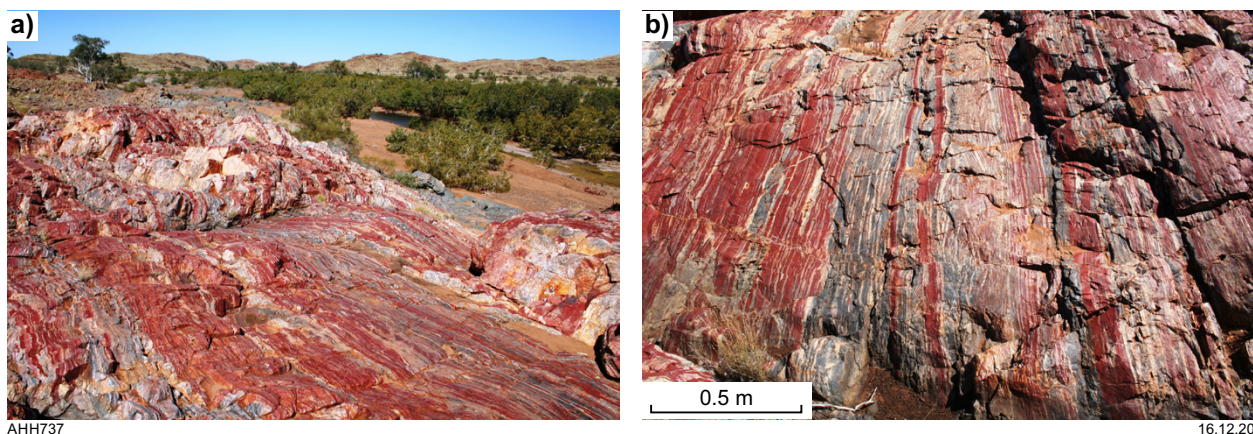


Figure 27. Outcrops of jaspilitic chert of the Marble Bar Chert Member at Marble Bar Pool: a) view (looking south) of an exposure of the upper 10 m of the member on the east bank of the Coongan River, 70 m south of Marble Bar Pool. Grey rocks to the right of the chert, and in the bed of the river, are pillowed basalt flows at the base of the Apex Basalt; b) close-up view showing alternating layers of red, white and grey chert with a central bed of fragmented chert. Notably, the grey chert (hydrothermal), and some of the white chert (partly replacing red chert), locally cuts across layers of red chert. The red chert contains fine-scale microbanding whereas the grey and white chert units are massive

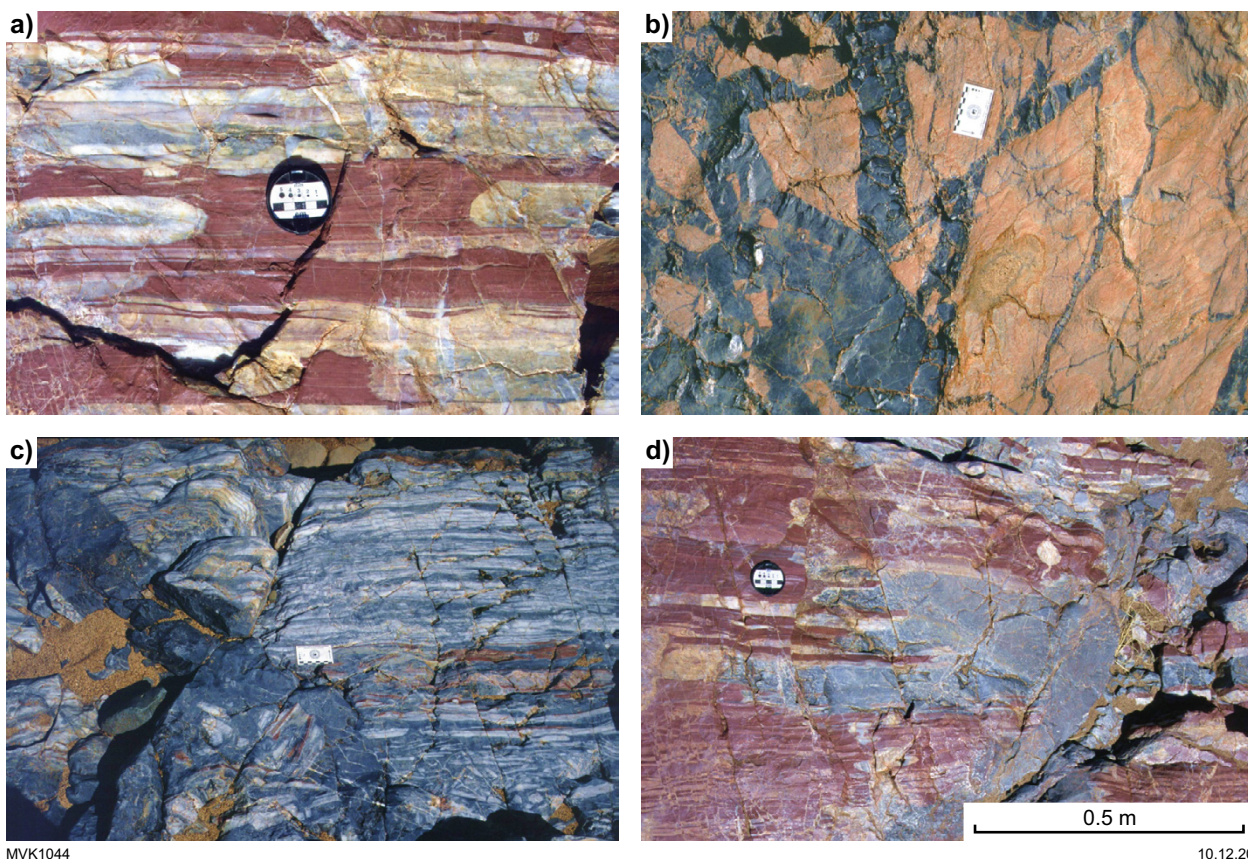


Figure 28. Hydrothermal intrusion and brecciation of the Marble Bar Chert Member and underlying altered volcanic rock of the Duffer Formation at Marble Bar Pool: a) bedded jaspilitic chert partly replaced by veins and pods of massive or weakly layered white chert; b) network of dark-grey hydrothermal chert veins intruding and fragmenting bleached basaltic rocks of the Duffer Formation immediately east of the Marble Bar Chert Member; c) dark-grey hydrothermal chert breccia cutting through layered grey and white chert; d) sills of grey and white chert emanating from a crosscutting feeder vein (from Van Kranendonk, 2010a)

The maximum depositional age of the MBCM is closely constrained by the youngest published date of 3459 ± 2 Ma (de Vries et al., 2006) for volcanic rocks of the Duffer Formation, and by other dates that are only slightly older (Fig. 24). However, the minimum depositional age of the MBCM is far less well constrained. In the Panorama greenstone belt (Fig. 8), a volcanoclastic unit correlated with the Panorama Formation was interpreted to have a maximum depositional age of 3448 ± 6 Ma (GSWA 160958, Wingate et al., 2012a). However, it was suggested that all zircons in the sample were detrital, and the total age range of the zircons is 3531–3443 Ma. In the northern Marble Bar greenstone belt, de Vries et al. (2006) dated a rhyolite of the Panorama Formation at 3446 ± 5 Ma. The Apex Basalt, which directly overlies the MBCM, has not been reliably dated; dates of c. 3458 and 3454 Ma shown for the Apex Basalt in Figure 24 relate to dates obtained on felsic intrusive rocks. Dating of a sandstone within the lower Apex Basalt yielded detrital zircon dates ranging from c. 3650 to 3441 Ma (Fig. 15). If the depositional age of the Apex Basalt is c. 3441 Ma, the potential depositional age range of the MBCM is almost 20 Ma.

Evidence of hydrothermal activity is present throughout the MBCM at Marble Bar Pool and in the ABDP 1 core. Units of layered grey-and-white chert and red-and-white chert are veined and fragmented by dark-grey chert containing numerous angular blocks of the banded chert (Fig. 28; Oliver and Cawood, 2001; Van Kranendonk et al., 2001a, 2006b; Van Kranendonk, 2006, 2010a). The outcrops show many examples of hydrothermal chert veins having injected and forced apart the layered chert to produce a mixture of angular chert fragments within a matrix of massive, cryptocrystalline, dark-grey chert. Oliver and Cawood (2001) documented rock pavements at Marble Bar Pool that display blocks of banded chert up to 10 m across within a matrix of dark-grey chert containing chert fragments down to <1 mm across.

Geochemical and petrographic investigations of the MBCM (Sugitani, 1992; Kojima et al., 1998; Kato and Nakamura, 2003; Orberger et al., 2006a,b; van den Boorn et al., 2007, 2010; Hoashi et al., 2009; Pinti et al., 2007, 2009a; Li et al., 2013; Rasmussen et al., 2014b) have been variously aimed at determining the protoliths of the member, its depositional setting, the oxygen content of Earth's Paleoarchean atmosphere, and searching for evidence of organic carbon. The majority of the studies concluded that a large part of the MBCM was deposited as fine-grained mafic and felsic detritus, and that the succession was subjected to pervasive hydrothermal alteration. Trace element abundances indicate that the hydrothermal fluids were derived from mafic sources, which suggests an association with the dolerite dykes and sills that intruded the Duffer Formation and fed into the overlying Apex Basalt. The Duffer Formation of the Marble Bar area contains thick dolerite sills that preferentially accumulated immediately beneath the MBCM, and this might have influenced fracturing and hydrothermal alteration of the member.

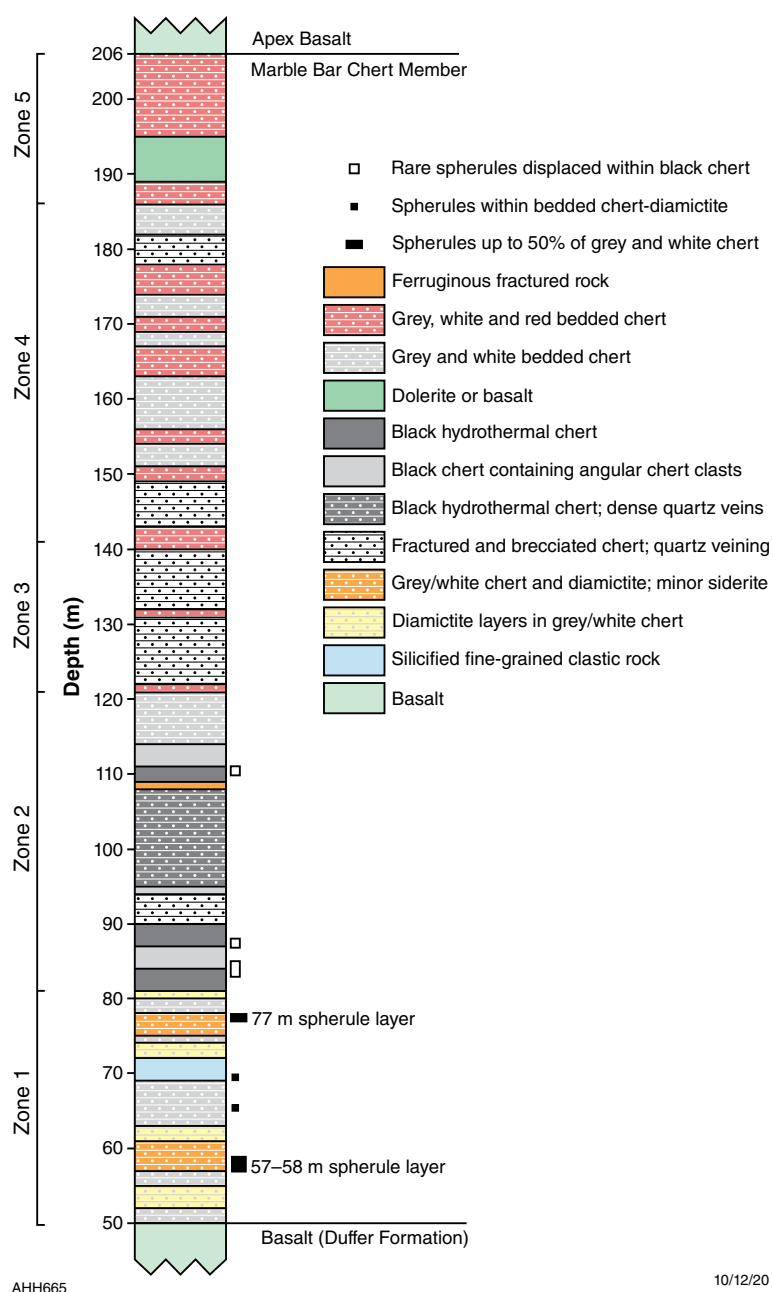
A controversial feature of the MBCM is the origin and age of the hematite in the red-and-white banded chert. Hoashi et al. (2009) provided transmission electron microscope (TEM) evidence to argue that hematite in the chert was a primary precipitate, with no evidence that it had replaced previous minerals. Hoashi et al. (2009) used this conclusion to argue for the existence of oxygenated seawater at

c. 3460 Ma. However, this conclusion conflicts with most interpretations that the Earth's atmosphere and hydrosphere were essentially anoxic until the Great Oxidation Event, an event most recently estimated to have occurred at c. 2310 Ma (Philippot et al., 2018). Based on exceptionally high $\delta^{56}\text{Fe}$ values and a low oceanic U content in the MBCM, Li et al. (2013) argued for very low levels of oxidation during its deposition. Subsequently, Rasmussen et al. (2014b) argued that the hematite was not primary but had replaced magnetite, greenalite and siderite. As noted by Hoashi et al. (2009), total iron contents in the upper part of the MBCM range between 2 and 25 wt% Fe_2O_3 , which ranks some parts of the MBCM as low-grade banded iron-formation (BIF). Recent interpretations of Archean and Proterozoic BIF elsewhere suggest it was not deposited in its present form, but that the primary lithologies (protoliths) were iron-silicate mud, Fe-rich clay such as greenalite, ferric oxyhydroxides, and Fe-rich carbonate precipitates (Rasmussen et al., 2014a, 2016; Gauger et al., 2015; Smith, 2015; Konhauser et al., 2017).

Rasmussen et al. (2014b) interpreted the lateral colour changes between white and red chert within individual mm- to cm-thick layers to have resulted from late-stage oxidation of greenalite and magnetite in the white layers to hematite, thus producing the red layers. Contrary to this interpretation, Van Kranendonk (2010a) provided photographic evidence of red chert having been replaced by massive white hydrothermal chert (Fig. 28a). In other parts of the MBCM, this hydrothermal white chert contains blocks of red-and-white banded chert (Fig. 28d) suggesting that hematite crystallization was older than hydrothermal veining. Hydrothermal veining is known to have occurred between c. 3460 and 3450 Ma because the hydrothermal veins occupy brittle fractures that penetrate the entire thickness of the MBCM but do not continue into the overlying Apex Basalt (Van Kranendonk, 2006). An explanation of these apparent inconsistencies is that two generations of white chert are present in the MBCM: an early, finely layered white chert containing magnetite and greenalite, and a younger hydrothermal white chert. However, intrusive relations still indicate that hematite in the red chert is older than the 3460–3450 Ma hydrothermal chert.

The thickest individual chert units of the Pilbara Supergroup are interpreted to be silicified sediments deposited over millions of years. As such, these units provide good targets for the detection of major asteroid impacts because ejecta fallout from these events would have been global. Examples of distal impact ejecta layers described above include the c. 3470 Ma sedimentary rocks of the Mount Ada Basalt (Antarctic Creek Member, 'ACM-1 layer'), and the c. 3470 Ma 'S1 layer' in sandstone of the Hoeggenoe Formation of the Onverwacht Group, Barberton Greenstone Belt, South Africa.

Based on their interpretation that the MBCM might have been deposited over millions of years, Glikson et al. (2016) examined the ABDP 1 core and identified two thin layers of silicified impact spherules within in the lower 30 m of the MBCM. Both spherule layers are contained within diamictites that Glikson et al. (2016) interpreted to be tsunami deposits. Unlike the polymictic conglomerates in the debris flows of the Chinaman Pool facies, the ABDP 1 diamictite is entirely composed of angular fragments of banded chert and sandstone. The diamictite is also lithologically very different from the hydrothermal chert breccia in irregular dykes and veins at higher stratigraphic levels in the MBCM.



AHH665

10/12/20

Figure 29. Stratigraphy of the Marble Bar Chert Member (MBCM) intersected in drillhole ABDP 1. Drilling intersected bedding at an angle of about 35°, indicating a true stratigraphic thickness of about 110 m. Zones shown alongside the column are from the interpretation of Hoashi et al. (2009). Zones 2 and 3 are dominated by fractured chert veined by dark-grey hydrothermal chert. In this Report, these are interpreted to have no stratigraphic significance. Notable stratigraphic features are the presence of siderite, diamictite and impact spherule layers in Zone 1, and the almost complete restriction of jaspilitic chert to Zones 4 and 5. The presence of hematite at depths below surface in excess of 200 m has been interpreted as evidence of oxygen in the Paleoproterozoic depositional environment (Hoashi et al., 2009) (figure modified from Glikson et al., 2016)

Salgash Subgroup

The Salgash Subgroup (Van Kranendonk et al., 2006a) comprises the Apex Basalt overlain by the Panorama Formation (Table 1), and was formed by a major volcanic cycle of the Pilbara Supergroup (Fig. 6). In most sections, the Apex Basalt disconformably overlies the MBCM, although an erosional contact overlain by basal conglomerate and breccia is locally present 20 km north of Marble Bar (Van Kranendonk, 2010a). Like the North Star Basalt, the Apex Basalt includes several minor volcanic cycles of ultramafic-mafic-chert sequences. The minimum age of the Apex Basalt in the Marble Bar greenstone belt is indicated by geochronology from the overlying Panorama Formation west of the Coppin Gap area (Fig. 30), where a rhyolite immediately above the Apex Basalt was dated at 3446 ± 5 Ma (de Vries, 2004). A volcanoclastic sample of the Panorama Formation in the Panorama greenstone belt was interpreted to have a maximum depositional age

of 3448 ± 6 Ma (GSWA 160958, Wingate et al., 2012a). However, detrital zircon dates (Fig. 15) from a sandstone in the lower Apex Basalt indicate a maximum depositional age of 3441 ± 12 Ma.

A c. 3441 Ma maximum depositional age for the Apex Basalt would be significant for two reasons: 1) it would imply that the 100 m-thick MBCM (Duffer Formation), which separates the volcanic part of the Duffer Formation (3474–3459 Ma) from the Apex Basalt, was deposited over almost 20 Ma; 2) it would suggest that eruption of the Apex Basalt (komatiite and basalt) and the Panorama Formation (dacite and rhyolite) of the Salgash Subgroup overlapped by at least 10 Ma (c. 3450 – 3440 Ma). Basaltic formations attributed to mantle plume events, as in the case of the Apex Basalt (Van Kranendonk et al., 2002, 2006a, 2007b; Hickman, 2011), are normally deposited quickly, typically within 1–5 Ma. A possible explanation for the apparently young maximum

depositional age of the Apex Basalt is that all the detrital zircons dated at c. 3441 Ma suffered Pb loss, and the true depositional age of the basalt is c. 3450 Ma.

U–Pb zircon geochronology of samples assigned to the Panorama Formation suggests that felsic volcanism of the Salgash Subgroup occurred in two separate stages: 3448–3446 Ma and 3434–3427 Ma (data in Appendix 5). However, there are two alternatives: 1) the apparent break in felsic volcanism might be due to c. 3440 Ma erosion of the lower Panorama Formation; 2) the few dates interpreted to represent the first stage were obtained from high-level intrusive rocks of the Tambina Supersuite, or from volcanoclastic units containing mainly detrital zircons. One line of evidence indicating that there were no breaks in felsic magmatism between c. 3448 and 3424 Ma is provided by detrital zircon dates from east Pilbara Craton sedimentary rocks (Fig. 12). Additionally, indirect evidence for felsic volcanism between c. 3448 and 3434 Ma is provided by 14 published U–Pb zircon dates between c. 3451 and 3435 Ma for granitic rocks of the Tambina Supersuite (Appendix 4). Some granitic intrusions of the Tambina Supersuite were subvolcanic, either intruding the base of the Panorama Formation or intruding the underlying Apex Basalt, and can reasonably be inferred to have been feeders to the volcanic rocks. For example, dykes and stocks of c. 3445 Ma monzogranite underlie the Panorama Formation in the North Pole Dome (Thorpe et al., 1992; Amelin et al., 2000; Harris et al., 2009) and have been interpreted to have fed volcanic rocks of the same age (Van Kranendonk, 2000a; Brown et al., 2006, 2011).

Evidence for c. 3440 Ma erosion is discussed under **Tectonic processes in the EPT**. It is notable that no dates older than c. 3434 Ma have been obtained from the thickest, and unambiguously felsic volcanic units of the Panorama Formation. In many greenstone belts of the EPT, 3434–3427 Ma felsic volcanic rocks of the Panorama Formation unconformably overlie felsic volcanic and sedimentary rocks of the 3474–3459 Ma Duffer Formation (Van Kranendonk et al., 2006a, 2007a,b; Hickman, 2011). As shown on Plate 1A, tonalite of the Tambina Supersuite immediately underlies and intrudes the Panorama Formation north of Warrery Gap on the northwest side of the Corunna Downs Dome (Hickman, 2013c). In the Tambourah Dome and the western Shaw Dome, the Tambina Supersuite, and dykes and sills emanating from it, intrude the Apex Basalt immediately beneath units of the Panorama Formation.

The maximum stratigraphic thickness of the Salgash Subgroup is 4 km in the Salgash area of the Marble Bar greenstone belt, although it is uncertain whether c. 3315 Ma shear zones that formed during development of the Warrawoona Syncline duplicated parts of the local succession. Elsewhere, the maximum thickness of the Apex Basalt is 2–3 km and the maximum thickness of the Panorama Formation is 2 km, although these maximum thicknesses do not occur together. In most greenstone belts of the EPT, any reliable estimates of original depositional thicknesses are precluded by uncertainty about the effects of c. 3440 Ma erosion associated with doming.

The Panorama Formation was erupted from several volcanic centres (Barley, 1981; Barley et al., 1984; DiMarco, 1986; DiMarco and Lowe, 1989a,b; Van Kranendonk, 1999a, 2000a; Smithies et al., 2007a; Van Kranendonk et al., 2007a,b). As with the Duffer Formation, lateral variations

of volcanic and sedimentary facies provide the best evidence for the locations of these centres, two of which are interpreted to have coincided with the McPhee Dome (Barley, 1981) and North Pole Dome (DiMarco and Lowe, 1989a,b; Van Kranendonk, 2000a). Thick successions of vent agglomerate in the northwestern and eastern section of the Kelly greenstone belt suggest a third centre was located in the Corunna Downs Dome. Conversely, sections of the Panorama Formation that are less than 500 m thick, and dominated by fine-grained felsic volcanoclastic rocks, sandstones, shales or turbidites, represent more distal successions. Distal facies are exposed around the headwaters of Warralong Creek (northwestern Marble Bar greenstone belt), south of Kittys Gap (northern Marble Bar greenstone belt), south of Yandicoogina (southeastern Marble Bar greenstone belt), and as thin units in the Goldsworthy, Warralong, Doolena Gap, North Shaw, and Coongan greenstone belts (Fig. 8). The conclusion that Panorama volcanic centres were located in areas now occupied by the granitic cores of the EPT domes (DiMarco and Lowe, 1989a,b; Hickman and Van Kranendonk, 2004; Williams and Bagas, 2007a) is consistent with the interpretation that from c. 3460 Ma onwards, Paleoproterozoic granitic intrusion was concentrated into the centres of the evolving domes (Hickman and Van Kranendonk, 2004).

Cullers et al. (1993) compared the geochemistry of the Duffer and Panorama Formations, although the samples considered to be representative of these formations came from different parts of the EPT. Based partly on high La/Lu ratios and a lack of Eu anomalies, Cullers et al. (1993) interpreted felsic volcanic rocks of the Panorama Formation in the North Pole Dome to have been derived by melting of eclogite. These North Pole data were compared with previous analyses of felsic volcanic rocks (Barley et al., 1984) interpreted to be from the Duffer Formation in the McPhee and Kelly greenstone belts (Hickman, 1980b; Barley, 1993), and Cullers et al. (1993) interpreted the latter to have been derived by fractional crystallization of basaltic magmas. However, subsequent geochronology has established that the Duffer Formation is absent from the McPhee and Kelly greenstone belts, and the geochemical comparisons were in fact with other units of the Panorama Formation. Analytical data from the PCMP confirmed that the geochemistry of the Panorama Formation is regionally variable (Smithies et al., 2005b; 2007a,b), and that the Panorama Formation was erupted from compositionally distinct volcanic centres. Although there is some compositional overlap with the Duffer Formation, the Panorama Formation volcanic rocks typically have higher K_2O/Na_2O of 0.35 – 0.70 (Smithies et al., 2007a). Smithies et al. (2007a) reported that rocks of the Panorama Formation have higher normalized La/Yb and La/Nb ratios compared to felsic rocks of the Duffer and Coucal Formations, and suggested this might reflect higher pressures of magma genesis or that the magmas had a greater contribution of a source component formed at high pressure (for example, TTG).

Tholeiitic basalts from the Apex Basalt are dominated by high-Ti compositions although minor low-Ti tholeiites are included (Smithies et al., 2007a). Normalized trace element patterns for the high-Ti basalts are very similar to those from basalts of the underlying subgroups and are up to ~15 times primitive mantle values, with wider ranges in $[La/Yb]_{PM}$ (0.87 – 2.20) and $[La/Nb]_{PM}$ (1.00 – 1.62) (Smithies et al., 2007a). In contrast, low-Ti basalts have lower incompatible

trace element concentrations (mostly less than four times primitive mantle values) and show no negative Nb anomaly on primitive mantle-normalized plots. Smithies et al. (2005b, 2007a) interpreted low $[La/Yb]_{PM}$ ratios (0.77 – 0.89) and very low $[La/Sm]_{PM}$ ratios (0.73 – 0.84) for these rocks to reflect derivation from a more depleted source than for the high-Ti basalts. Alternatively, such compositional differences between high-Ti and low-Ti basalts might be related to different degrees of partial melting of a plume or asthenospheric source (Arndt et al., 1993).

Whole-rock Nd model ages from the 3450–3440 Ma Apex Basalt and the 3448–3427 Ma Panorama Formation (Table 4) are 3580–3530 Ma, suggesting crustal recycling. ϵ_{Nd} values of +1.21 to +0.72 also suggest magma derivation involving crustal recycling. The mean ϵ_{Hf} value for 3449–3425 Ma cognate zircons ($n = 61$, Appendix 9) is $+0.75 \pm 0.23$ (1 σ) and the mean Hf model age is c. 3695 \pm 14 Ma (1 σ). These data preclude substantial contributions of magma from juvenile sources.

Apex Basalt

The Apex Basalt directly underlies the Panorama and Strelley Pool Formations in the Marble Bar, Kelly, McPhee, Warralong, Western Shaw and Tambina greenstone belts (Fig. 8, Plate 1). A thick succession of stratigraphically unassigned basaltic rocks beneath the Panorama Formation in the Goldsworthy greenstone belt is, by analogy with the East Strelley greenstone belt on the southeastern side of the Carlindi Dome, more likely to be a basaltic formation of the Coonterunah Subgroup than part of the Apex Basalt. The Apex Basalt, along with the Coongan Subgroup, is absent from the East Strelley greenstone belt (Plate 1A) due to deep erosion of the Warrawoona Group prior to deposition of the Strelley Pool Formation.

The first minor volcanic cycle of the Apex Basalt commenced with eruption of komatiite and komatiitic basalt onto the MBCM (Duffer Formation). In the Marble Bar area, Kloppenburg (2003), Van Kranendonk et al. (2006a), and Hickman and Van Kranendonk (2008a) described a major swarm of dolerite dykes and sills (informal name ‘Salgash dyke swarm’) that intruded the Coongan Subgroup and Homeward Bound Granite, and fed basaltic magma into the Apex Basalt (Figs 25, 30). About 45 km northeast of Marble Bar, large ultramafic–mafic layered intrusions include the Strutton, Gap and Nobb Well Intrusions (Williams, 1999a), which are interpreted to be subvolcanic intrusions related to the Apex Basalt, although they have not been dated. Such dykes and layered intrusions were probably widespread in the crust underlying the Apex Basalt but most were probably intruded and effectively replaced by granitic intrusions of the Tambina, Emu Pool and Cleland Supersuites.

Komatiite flows in the Warralong greenstone belt (Fig. 8) preserve olivine-spinifex texture perpendicular to flow tops above layers of cumulate-textured peridotite (Van Kranendonk, 2010c). At Salgash, 15 km south of Marble Bar, a 500 m-thick unit of metamorphosed peridotite outcrops at the base of the Salgash Subgroup (Hickman and Van Kranendonk, 2008b). This metamorphosed and deformed ultramafic unit has not been studied in detail, although remnants of thin sedimentary rocks within it suggest possible inclusion of metamorphosed komatiite flows in addition to metamorphosed dunite and peridotite sills.

West of Marble Bar Pool, in the Chinaman Creek area, the first minor volcanic cycle is mainly composed of pillowed komatiitic basalt overlain by a unit of metamorphosed sandstone, black shale, felsic volcanoclastic rocks, and hydrothermal silica. Silicification of the clastic rocks by fluids from large underlying hydrothermal dykes resulted in a stratiform unit of ‘chert’, now widely referred to as the ‘Apex chert’ (informal name). This chert received international attention following the discovery of carbonaceous microstructures that were interpreted to be early Paleoproterozoic microfossils (Schopf and Packer, 1987; Schopf, 1992, 1993). The depositional age of the Apex chert (c. 3450 Ma) meant that for almost 20 years these ‘microfossils’ were widely regarded as the oldest fossils on Earth. Subsequently, the biogenicity of these microstructures was challenged, based on several lines of evidence (Brasier et al., 2002, 2005, 2011, 2015; García-Ruiz et al., 2002, 2003; Van Kranendonk, 2006; Pinti et al., 2009b; Wacey, 2009; Marshall et al., 2011, 2014). The origin of the microstructures has remained controversial, with publication of additional evidence supporting a biological origin (Schopf et al., 2002a,b, 2007, 2017; Schopf and Kudryavtsev, 2005; Schopf, 2006; De Gregorio et al., 2009).

Meanwhile, research on the Apex chert has provided a large amount of evidence on its deposition and processes of hydrothermal alteration in thin sedimentary units of the Pilbara Supergroup. Brasier et al. (2013) discovered different evidence for bacterial life within beds of pumice interpreted to have accumulated on a c. 3460 Ma shoreline. Apart from the paleontological significance of this discovery, the evidence for shallow-water deposition of the Apex chert testifies to uplift and temporary emergence of the Apex Basalt following subaqueous deposition of up to 1000 m of pillowed komatiitic basalts and tholeiites in the first minor volcanic cycle.

The protoliths of the Apex chert were deposited at the same stratigraphic position as black shale and sandstone in the Salgash–Warrawoona area, 15 km south of Marble Bar (Fig. 30). Here, stratiform Cu–Zn deposits hosted by the metamorphosed black shales provide additional evidence of hydrothermal activity at the level of the Apex chert. Five samples of the black shale analysed by Wille et al. (2013) contained up to 13.4 wt% organic carbon (average 5.45 wt%), up to 6770 ppm Zn (average 2804 ppm), up to 1088 ppm Cu (average 562 ppm), and up to 421 ppm Ni (average 296 ppm). The shale samples have extremely high Na_2O contents (up to 9 wt%) which suggests albite alteration in a hydrothermal setting. The Apex chert outcrops over a strike length of 50 km on the western side of the Mount Edgar Dome, from the Warrawoona Syncline, where it becomes sheared out southeastwards (Hickman and Van Kranendonk, 2008b), to the Doolena Gap area 30 km north of Marble Bar. In combination with the lateral extent of the underlying MBCM (Duffer Formation), this testifies to the high degree of lateral continuity of depositional environments between volcanic cycles.

Komatiite and komatiitic basalt of the second minor cycle of the Salgash Subgroup disconformably overlie the Apex chert, although in the Marble Bar greenstone belt, komatiite is mainly restricted to the Comet and Salgash areas, 10–15 km south of Marble Bar (Hickman and Van Kranendonk, 2008b). The second minor cycle is up to 1000 m thick and capped by grey-and-white banded chert overlying hydrothermally altered pillowed basalt. The altered basalt is intruded by

hydrothermal chert dykes extending upwards to the base of the chert (Van Kranendonk and Pirajno, 2004; Van Kranendonk, 2006). Komatiitic basalt forms the greater part of the Apex Basalt in the Warralong greenstone belt, although minor komatiite is also present in the local succession (Van Kranendonk, 2004c, 2010c). The serpentized komatiite has layers of well-developed olivine-spinifex texture separated by cumulate-textured peridotite (Van Kranendonk, 2010c),

whereas the komatiitic basalt is pillowed and dominated by pyroxene-spinifex texture. The upper part of the Apex Basalt comprises minor cycles of komatiitic basalt and chert in both the Marble Bar and Warralong greenstone belts (Fig. 8).

At least two additional minor volcanic cycles are interpreted to overlie the second minor cycle in the Chinaman Creek section, and the top of the Apex Basalt is overlain by the Panorama Formation.

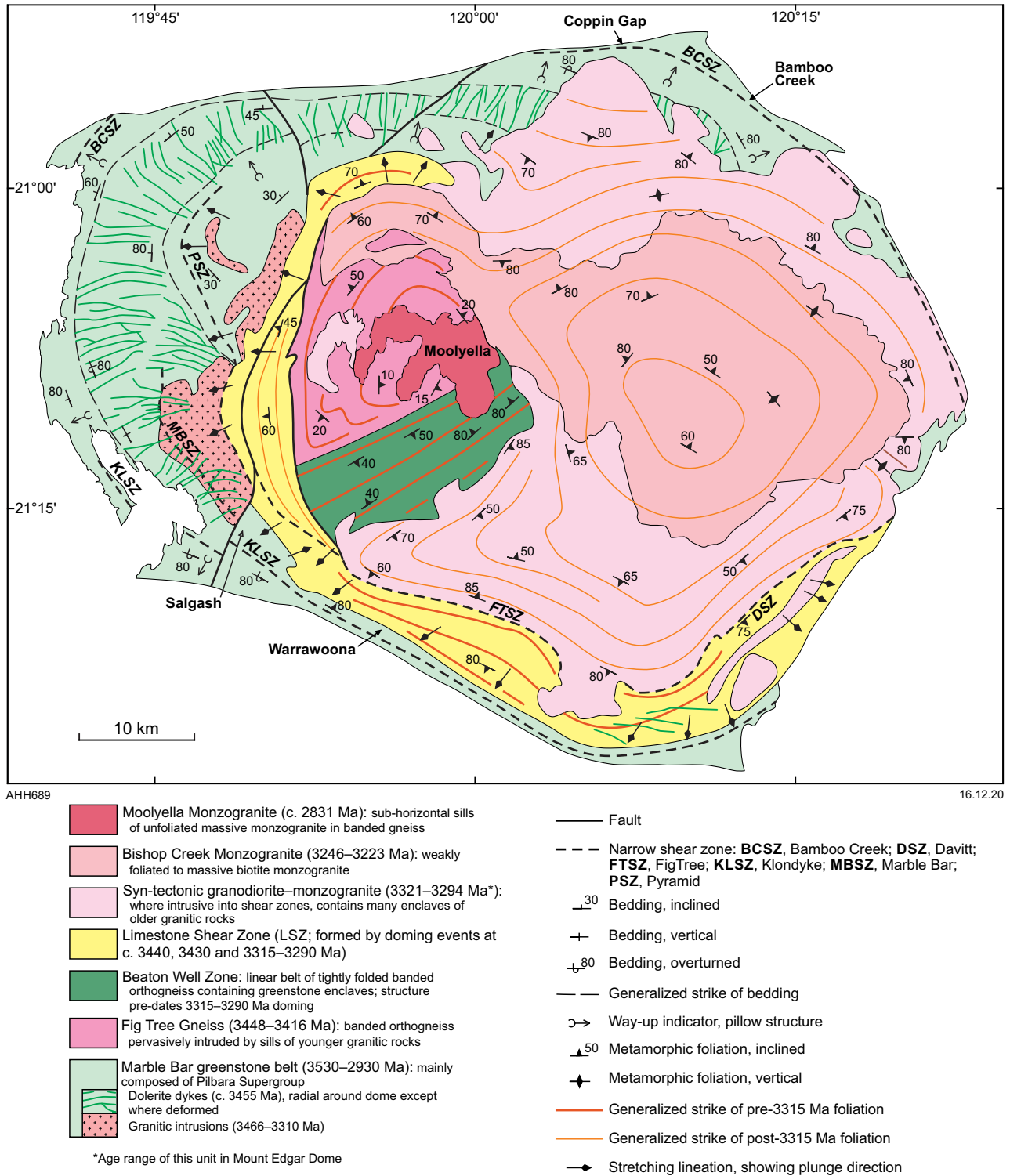


Figure 30. Tectonostratigraphic units of the Mount Edgar Dome, summarizing domal structure and ages. Structures characteristic of diapiric doming include radial outward-plunging stretching lineations within and adjacent to the 3440–3290 Ma Limestone Shear Zone (ring fault), and radial swarms of c. 3455 Ma dolerite dykes intrusive into extensional fractures formed by domal uplift. Place names (bold) are localities commonly cited in the text (from Gardiner et al., 2018)

Panorama Formation

The Panorama Formation is exposed in the Marble Bar, Panorama, Coongan, Kelly, McPhee, Doolena Gap, Warralong, Tambina and Western Shaw greenstone belts (Fig. 8, Plate 1), and comprises successions of dacitic to rhyolitic volcanic rocks and clastic sedimentary rocks. Geochronology has confirmed these correlations in seven of these greenstone belts where they have been tested. Stratigraphic sections of Panorama Formation are 500–1500 m thick in the Kelly, McPhee, Marble Bar, North Shaw and Panorama greenstone belts. The originally designated type area of the formation was Panorama Ridge in the southern Panorama greenstone belt (Lipple, 1975), but a U–Pb zircon date of 3458 ± 2 Ma at that locality (Thorpe et al., 1992a), in combination with more recent geochronology from the Warrawoona Group, led to reassignment of the lower Panorama Ridge succession to the Duffer Formation (Hickman, 2010). The first detailed descriptions of the Panorama Formation were provided by Barley (1981), Barley et al. (1984) and DiMarco (1986). Based on a regional stratigraphic interpretation by Hickman (1980b), Barley (1981) assigned thick successions of felsic volcanic rocks in the McPhee greenstone belt and the adjacent eastern Kelly greenstone belt to the Duffer Formation. Subsequent geochronology has shown that the depositional ages of the felsic successions in these areas are c. 3430 Ma, and that they therefore belong to the Panorama Formation.

In the McPhee Dome, felsic volcanic rocks overlie a succession of plagioclase-phyric basalts and andesites (Barley, 1981), and this has since been correlated with the Apex Basalt (Williams and Hickman, 2007). From the description by Barley (1981), the Panorama Formation is composed of dacitic lava overlain by felsic pyroclastic rocks that accumulated to form a volcanic centre. Debris flows and sedimentary rocks including turbidites were deposited on the flanks of this centre, and the formation is overlain by a thick chert unit (Strelley Pool Formation). Within the Kelly greenstone belt, the Panorama Formation is exceptionally well exposed along Sandy Creek in the northeastern Kelly greenstone belt. Although the lower part of the formation is intruded by c. 3311 Ma monzogranite (GSWA 178084, Nelson et al., 2006), a 1500 m-thick vertical section is preserved beneath the Strelley Pool Formation (Hickman, 1980a). Before this section of the Panorama Formation was dated at 3433 ± 2 Ma (GSWA 148502, Nelson, 2000n), it had been assigned to the Duffer Formation. Above the intrusive granitic contact, the lowest preserved part of the formation consists of interbedded dacitic and rhyolitic lavas and volcanoclastic rocks. Individual lava flows of plagioclase-phyric dacite and rhyolite up to 30 m thick are interbedded with lava breccias, clast-supported grain-flow breccias, graded pyroclastic flows, and hyaloclastic breccia (Smithies et al., 2007a). The upper Panorama Formation at Sandy Creek includes epiclastic deposits in addition to felsic volcanoclastic units, and lavas are less common. Geochemical data from the section are available in Glikson and Hickman (1981a,b) and Smithies et al. (2007a).

DiMarco (1986) investigated the stratigraphy and sedimentology of the Panorama Formation in parts of the Coongan, Kelly, Panorama, North Shaw and East Strelley greenstone belts. He interpreted the Panorama and Duffer Formations to be members of a unit that he termed the 'Coongan Formation' (obsolete name), with the result that

his descriptions of the 'Panorama Member' (obsolete name) in the Marble Bar and southern Panorama greenstone belts now apply to the Duffer Formation. DiMarco and Lowe (1989a,b) used the regional interpretation of DiMarco (1986) and, although reinstating the name Panorama Formation (from 'Panorama Member'), continued to place it directly above the Duffer Formation, thus mistakenly interpreting it to stratigraphically underlie the Marble Bar Chert Member (then referred to as the 'Towers Formation').

A detailed description of the Panorama Formation in the northwestern Panorama greenstone belt (Van Kranendonk, 1999b, 2000a; Van Kranendonk and Hickman, 2000) supported a previous conclusion that the formation was erupted from separate volcanic centres (Barley et al., 1984; DiMarco and Lowe, 1989a,b). The succession assigned to the Panorama Formation in the northwestern Panorama greenstone belt is unusual in several respects: 1) an absence of felsic lava; 2) a high proportion of sandstone units; 3) reworked, as opposed to ashfall, carbonate-bearing volcanoclastic units. A sample from the upper part of this succession, dated at 3434 ± 5 Ma (GSWA 142952, Nelson, 2000i), was interpreted to be a pervasively silicified felsic tuff, although with 85 vol% quartz and 15 vol% sericite, it could instead be a metamorphosed volcanoclastic sandstone. This succession of the Panorama Formation is also unusual in not being overlain by lithologies typical of the Strelley Pool Formation, raising the possibility that part of it might be laterally equivalent to that formation. Van Kranendonk (2000a) remarked that carbonate-bearing felsic volcanoclastic rocks of the 'Panorama volcano' (northwestern Panorama greenstone belt succession) are identical in appearance to sandstones and conglomerates in the basal Strelley Pool Formation. Retallack (2018) interpreted the succession of the Panorama Formation of this area to be a volcanic flank and floodplain facies in which layers containing barite nodules represent alluvial paleosols. The depositional environment described by Retallack (2018) is very similar to that interpreted for parts of the Strelley Pool Formation.

The sandstones and felsic tuffaceous units of the northwestern Panorama greenstone belt (North Pole Dome) overlie a 40 m-thick jaspilitic iron-formation, which was mapped as part of the Panorama Formation by Van Kranendonk (1999a) because, at that time, the underlying basalt of the North Pole Dome was interpreted to be the Apex Basalt. With later recognition that this basalt formation is the Mount Ada Basalt (Van Kranendonk et al., 2006b), the jaspilitic iron-formation might be reasonably correlated with the MBCM (Duffer Formation). Allwood et al. (2007a) interpreted the iron formation to be conformable with the underlying Mount Ada Basalt which, in view of uplift and erosion of the Apex Basalt at c. 3440 Ma, supports this correlation. Boulders and pebbles of the iron formation are included in the basal conglomerate of the overlying Strelley Pool Formation (Van Kranendonk, 2000a; Allwood et al., 2007a).

Exposures of the Panorama Formation in the northwestern Marble Bar greenstone belt are separated by faults and unconformably overlying formations of the Fortescue Group. In this area, around the headwaters of Warralong Creek, the lower part of the formation is composed of massive quartz-porphyrritic rhyolite, fine-grained felsic volcanoclastic rocks, sandstone and siltstone. The upper part of the formation comprises siltstone, shale and iron

formation overlying thin beds of pebbly sandstone and conglomerate (Van Kranendonk, 2004b). This upper unit is overlain by the Euro Basalt and might alternatively be interpreted as a facies of the Strelley Pool Formation. Near Kittys Gap, 35 km east of Warralong Creek, the Panorama Formation is mainly composed of rhyolitic agglomerate and flow-banded porphyritic rhyolite up to 800 m thick (Williams, 1999a). The rhyolitic succession is overlain by a silicified, fine-grained, volcanoclastic unit interpreted to be the Strelley Pool Formation. A porphyritic rhyolite near the base of the Panorama Formation was dated at 3446 ± 5 Ma (de Vries, 2004). Farther east in the Marble Bar greenstone belt, southwest from the Bamboo Creek mining area, lenticular units of the Panorama Formation separate the Apex and Euro Basalts along a disconformable contact (Williams, 1999a). Conventional U–Pb zircon geochronology was used to date this section of the formation at 3449 ± 3 Ma (Thorpe et al., 1990, 1992a,b).

The geochemistry of the Panorama Formation in the Kittys Gap area is distinctly different from that of the Duffer Formation in the same greenstone belt. De Vries et al. (2006) reported that dacite of the Duffer Formation has substantially higher chondrite-normalized REE contents and lower normalized La/Yb than rhyodacite of the Panorama Formation, and in contrast to the Duffer Formation, the Panorama Formation does not exhibit negative Eu anomalies. Smithies et al. (2007a) commented that normalized La/Yb and La/Nb were highest in the Panorama Formation, and their REE data indicate no negative Eu anomalies.

Syn depositional growth faulting has been interpreted in the Kittys Gap area of the northern Marble Bar greenstone belt (Nijman et al., 2001, 2017; de Vries, 2004; Nijman and de Vries, 2004; de Vries et al., 2006). The faults are visible on aerial photographs and Landsat imagery and, although younger faulting is also present in the area, lateral changes in the thicknesses of sedimentary units across the faults support an interpretation of some syn depositional movement. The interpretation in this Report is that the faults are extensional structures related to uplift of the Mount Edgar Dome. Although Nijman et al. (2017) observed that the orientations of the syn depositional faults are not consistent with the present geometry of the Mount Edgar Dome, this geometry was substantially formed by c. 3315 Ma doming (Collins et al. 1998). The absence of angular unconformities at the base of the Panorama Formation in the Mount Edgar, Corunna Downs and McPhee Domes (Hickman, 2008) suggests that these domes were not well-developed until after 3350 Ma.

Strelley Pool Formation

The 3426–3350 Ma Strelley Pool Formation is a regionally extensive sedimentary formation that overlies a regional unconformity between the two large igneous provinces represented by the Warrawoona and the Kelly Groups (Table 1). Although rarely more than 100 m thick, the formation is present in 13 greenstone belts that expose the upper Warrawoona Group (Hickman, 2008). The regional stratigraphic relations of the Strelley Pool Formation across 30 000 km² of the EPT, plus detrital zircon data, establish that it was deposited on eroded continental crust composed of the Warrawoona Group, and granitic rocks of the Callina and Tambina Supersuites. Importantly, this conclusion also

precludes interpretations (based mainly on lithology) that the overlying Euro Basalt of the Kelly Group was deposited as oceanic crust (Isozaki et al., 1997; Kitajima et al., 2001; Furnes et al., 2007, 2015). Additionally, since the chemical composition of the Euro Basalt is very similar to that of basaltic formations of the Warrawoona Group (Green et al., 2000; Smithies et al., 2007a), geochemistry-based arguments inferring oceanic tectonic settings for the lower Pilbara Supergroup are evidently unreliable.

The Strelley Pool Formation is one of the world's best sources of information on early life and depositional environments. The formation contains abundant and exceptionally well-preserved Paleoproterozoic fossils, including stromatolites (Lowe, 1980, 1983; Hofmann et al., 1999; Van Kranendonk, 2000a, 2007; Grey et al., 2002, 2010, 2012; Allwood et al., 2004a,b, 2006, 2007a,b; Hickman et al., 2011; Bontognali et al., 2012), microbial mats (Allwood et al., 2009; Duda et al., 2016), microfossils (Sugitani et al., 2010, 2013, 2015; Allee et al., 2018), and trace fossils (Wacey, 2009; Wacey et al., 2011). The scope of this Report does not extend to a review of the descriptions given in these publications. The abundance and diversity of the fossil record is attributed to widespread, favourable, depositional environments provided by the c. 75 Ma break in volcanic activity between eruption of the Warrawoona and Kelly Groups (Hickman, 2012).

Figure 31 shows locations of outcrops of the Strelley Pool Formation in nine greenstone belts within an 80 km radius of Marble Bar. More distantly, the formation is also exposed in the Tambina, Emerald Mine, Western Shaw and Goldsworthy greenstone belts (Fig. 8, Plate 1), and few of these exposures have been examined in detail. Identification of the formation across the EPT has been achieved through geochronology and mapping (Hickman, 2008), and from its stratigraphic position between the Panorama Formation and the Euro Basalt (Table 1). Lateral facies changes associated with the shallow-water depositional environments of the formation are reflected in regional lithological variations. However, in most areas, basal sandstone and conglomerate are overlain by bedded carbonate rocks or secondary chert, and these lithologies are overlain by mafic volcanoclastic rocks that form the upper part of the formation. Less common lithologies include evaporites and jaspilite.

Based on a regional review of geochronological data, Hickman (2008) estimated the maximum depositional age of the Strelley Pool Formation at c. 3426 Ma (Hickman, 2008). However, it cannot be assumed that deposition of the Strelley Pool Formation commenced at the same time in all areas of the ~30 000 km² basin. In the Kelly and Coongan greenstone belts, the Strelley Pool Formation directly overlies felsic volcanic rocks dated at c. 3430, c. 3432, and c. 3433 Ma (Fig. 31). In that area of the EPT, this collectively places a maximum depositional age limit of c. 3430 Ma on the unit. A younger maximum depositional age of c. 3414 Ma was suggested by Gardiner et al. (2019) based on dating of a sandstone sample from the type locality of the formation (Strelley Ridge, Fig. 32). They analysed 205 zircons by SIMS and LA-ICP-MS, most of which were >10% discordant. Four <10% discordant analyses were used to interpret the maximum depositional age of 3414 ± 34 Ma (2 σ), although three of the four analyses indicated dates of c. 3470 Ma. The c. 3470 Ma zircons were most likely derived from erosion of the Callina Supersuite or the Duffer Formation, and 70 analyses defined a dominant peak at 3506 ± 4 Ma

(2o), which here is considered consistent with erosion of the Mulgundoona Supersuite or the Coucal Formation. Figure 33 illustrates the lateral stratigraphic variability of the Strelley Pool Formation in this greenstone belt, so the sandstone dated by Gardiner et al. (2019) might not have been collected from the lowest stratigraphic unit of the formation in the East Strelley greenstone belt.

Assuming that deposition of the Strelley Pool Formation in the EPT commenced between c. 3430 and 3414 Ma, a 75–65 Ma break in magmatic activity has been interpreted between volcanism of the 3448–3427 Ma Panorama Formation and intrusion of the 3451–3416 Ma Tambina Supersuite, and subsequent eruption of the 3350–3335 Ma Euro Basalt (Van Kranendonk et al., 2004c, 2006a, 2007b; Hickman, 2008, 2012; Hickman et al., 2011; Hickman and Van Kranendonk, 2012; Gardiner et al., 2019). As noted by Van Kranendonk et al. (2014b), the same apparent c. 75 Ma break in volcanic activity can be recognized in the Onverwacht Group of the east Kaapvaal Craton (Fig. 4) where the Buck Reef Chert separates the Hoogenoeg Formation (equivalent to the Mount Ada Basalt, and Duffer and Panorama Formations) from komatiite and basalt of the Kromberg Formation (equivalent to the Euro Basalt). There are no igneous rocks dated between 3408 Ma and 3350 Ma in the northern Pilbara Craton (Appendix 5), and there are relatively few detrital zircon dates between 3400 and 3350 Ma (Fig. 12a). These observations are consistent with a significant break in igneous activity of at least c. 60 Ma, although there is evidence of hydrothermal activity during deposition of the Strelley Pool Formation (Van Kranendonk and Pirajno, 2004; Van Kranendonk, 2006; Cammack et al., 2018).

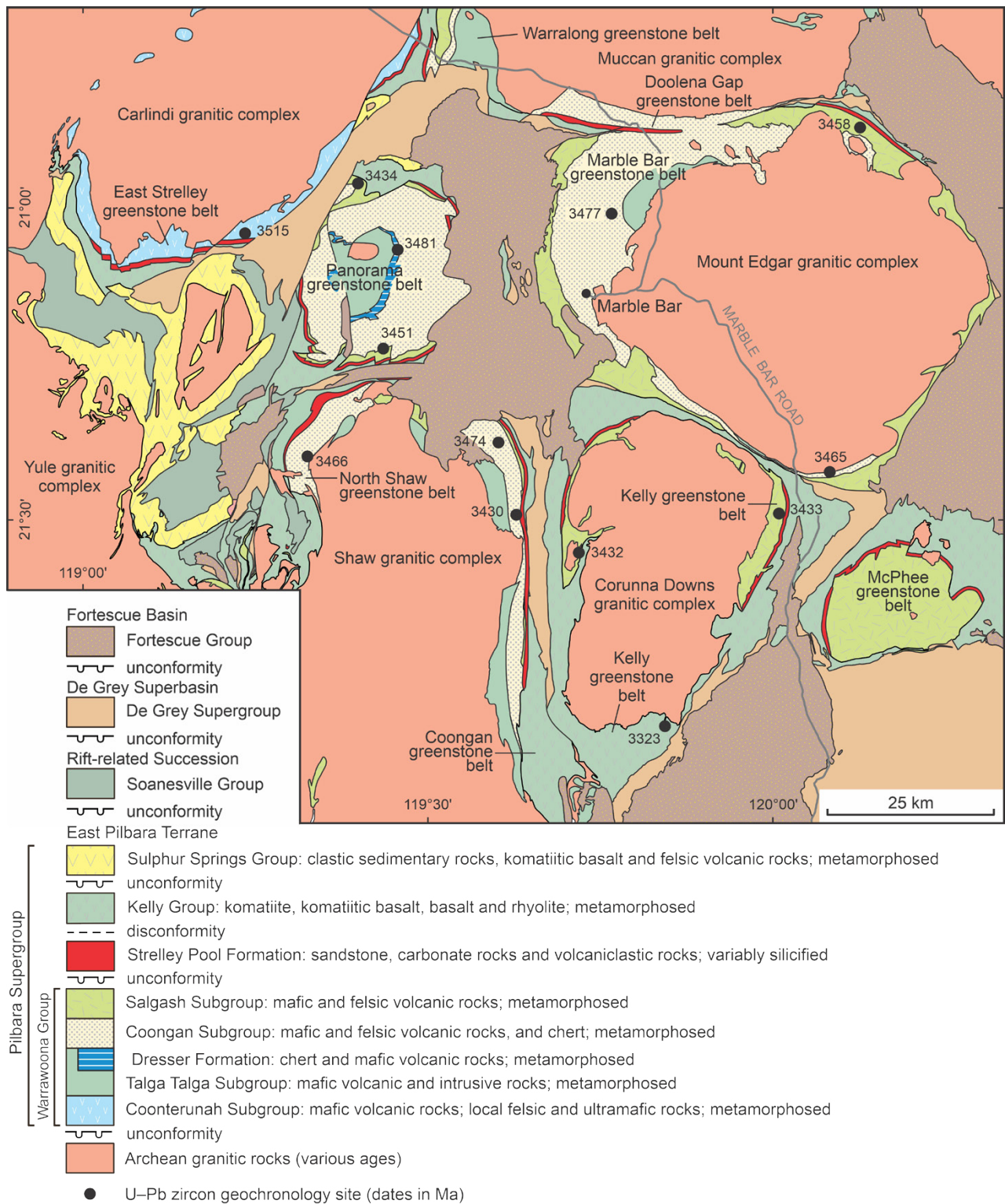
The Strelley Pool Formation unconformably overlies deformed and eroded formations of the Warrawoona Group (Buick et al., 1995), and unconformably to disconformably underlies the Kelly Group (Figs 6, 7). However, the nature of the basal unconformity varies across the EPT. In the northwestern EPT, the upper Warrawoona Group was almost entirely removed by erosion prior to deposition of the Strelley Pool Formation. This differs from the stratigraphy in the central and southeastern EPT where the Panorama Formation underlies the Strelley Pool Formation and the contact is a paraconformity (Hickman, 2008). The extent to which the Strelley Pool Formation was deposited across the granitic cores of the EPT domes is unknown because its present outcrops almost invariably overlie greenstones. However, the presence of granite pebbles in the formation 2.5 km south of the Doolena Gap Pb mine (Hickman, 1983) confirms that older granitic rocks were exposed during its deposition. On the southern side of the Carlindi Dome, the formation unconformably overlies c. 3468 Ma porphyritic microgranite (Buick et al., 1995; Van Kranendonk, 1999a), but elsewhere its visible contacts with granitic rocks are either intrusive or faulted. It is possible that deposition did not cover the centres of domes that experienced major 3455–3420 Ma uplift (Muccan, Carlindi, Shaw, Mount Edgar), or which contained substantial volcanic centres between c. 3449 and 3420 Ma (North Pole, Corunna Downs, McPhee). In these domes, the uplifted granitic rocks and remnant volcanic edifices almost certainly formed islands within the depositional basin.

Stratigraphy

The stratigraphy of the Strelley Pool Formation has been documented from the East Strelley greenstone belt (Lowe, 1983; DiMarco and Lowe, 1989b; Van Kranendonk, 2000a, 2004a,b; Wacey et al., 2010), the Panorama greenstone belt of the North Pole Dome (Lowe, 1983; DiMarco and Lowe, 1989a,b; Hofmann et al., 1999; Van Kranendonk, 2000a; Allwood et al., 2004a,b, 2006, 2007a,b), the Marble Bar greenstone belt near Kittys Gap (Nijman et al., 2001; de Vries, 2004; de Vries et al., 2006), the Kelly greenstone belt (Hickman, 1980a; Bagas, 2003; Bagas et al., 2004c), and the Doolena Gap greenstone belt (Wiemer et al., 2016). In the last of these, the formation is exceptionally thick, consisting of 1000 m of sandstone and conglomerate capped by chert (Van Kranendonk, 2007; Wiemer et al., 2016). The various sedimentary facies of the Strelley Pool Formation indicate that it was deposited in shallow-water environments that included shallow-water marine, beach, estuarine, sabkha, stromatolite reef, fluvial and lacustrine facies. Where it overlies the Panorama Formation, the Strelley Pool Formation includes reworked volcanoclastic conglomerate and sandstone.

Investigations of the Strelley Pool Formation (above cited work and Hickman, 2008; Hickman et al., 2011) have revealed not only regional stratigraphic variations but also rapid lateral variations over distances of less than a few hundred metres. Local variations were extremely well demonstrated by detailed stratigraphic studies of the formation in the western Panorama greenstone belt (Allwood et al., 2007a) and in the East Strelley greenstone belt (Wacey et al., 2010). Figure 32 shows the outcrop of the Strelley Pool Formation in the East Strelley greenstone belt and the locations of detailed stratigraphic logs made by Wacey et al. (2010). Lateral thickness and facies variations were illustrated by sections measured along a 25 km-long series of strike ridges east and west from Strelley Ridge (Figs 32, 33). Variations in the lower part of the formation are likely to reflect migrating shallow-water depositional systems (fluvial channels, sand bars, etc.) and controls by the topography of the underlying unconformity. A westerly transgression of the formation onto a previously exposed upland area of the Coonterunah Subgroup is indicated by the absence of the basal sandstone unit west of Table Top Ridge (sections P–R, Fig. 33). This western area also contains coniform stromatolites (section P) suggesting relatively shallow water, and evaporites have been recorded in this area (Lowe, 1980, 1983; Van Kranendonk and Hickman, 2000; Van Kranendonk, 2000a). Stromatolite occurrences in the Strelley Pool Formation of the Panorama greenstone belt also coincide with shallow-water environments (Hofmann et al., 1999; Van Kranendonk et al., 2003; Allwood et al., 2006, 2007a,b; Hickman et al., 2011).

Lowe (1983) divided the Strelley Pool Formation of the northwest EPT into five informal members (Table 5) and a similar subdivision was subsequently used by others (DiMarco and Lowe, 1989; Van Kranendonk, 2000a; Allwood et al., 2007a; Wacey et al., 2010). However, the same subdivision has not been applied to the formation in the central and southeastern EPT where the succession is mainly composed of metasandstone and banded chert.



AHH284e

11.01.21

Figure 31. Geological map of part of the EPT showing outcrops of the Strelley Pool Formation within the stratigraphy of the Pilbara Supergroup. Although the formation is typically less than 100 m thick, this sedimentary formation outcrops across most of the EPT, and marks a 75 Ma break between LIP-scale volcanism of the Warrawoona and Kelly Groups (from Hickman, 2008)

It is uncertain how much of the chert in these areas represents silicified carbonate and fine-grained volcanoclastic rocks, although wavy-laminated carbonate rocks are preserved in the Kelly and Coongan greenstone belts (Hickman, 1980a; Zegers, 1996; Grey et al., 2002, 2010, 2012; Bagas, 2005; Williams and Bagas, 2007a). Lowe (1983) interpreted the depositional environment in the northwestern EPT as either a large hypersaline lake or a restricted, shallow-water marine basin. He reported that basal sandstone fills channels cut into underlying parts of the Warrawoona Group. DiMarco and Lowe (1989a,b) inferred that the Strelley Pool Formation overlies an erosional unconformity, although no exposures were documented.

The c. 75 Ma period during which the formation was deposited lacked the frequent widespread events of volcanism and granitic intrusion that characterized the c. 100 Ma history of the Warrawoona Group. Although eruption of the Warrawoona Group included brief breaks in volcanic activity, represented by sedimentary successions of the Dresser and McPhee Formations, and by deposition of the Marble Bar Chert Member (Duffer Formation), deposition of the Strelley Pool Formation occurred during the first lengthy period of crustal stability.

Detrital zircon dates indicate that the maximum depositional age of the Strelley Pool Formation is c. 3426 Ma (Hickman, 2008), although deposition is likely to have commenced at slightly different times across the EPT depending on the tectonic evolution of individual domes. The minimum eruptive age of felsic volcanic rocks of the underlying Panorama Formation is c. 3424 Ma (GSWA 169008, Nelson, 2002g). The minimum depositional age of the Strelley Pool Formation is constrained by a 3350 ± 3 Ma date on the overlying Euro Basalt (GSWA 178042, Nelson, 2005g). The c. 75 Ma break in volcanism across the EPT is supported by a similar break in the ages of granitic intrusions (Fig. 10) and by a very low frequency of detrital zircon ages in the interval 3400–3360 Ma (Fig. 12a). The detrital zircon evidence from sedimentary units younger than the Panorama Formation is significant because erosion of the Pilbara Craton would likely have provided a spectrum of ages representative of principal magmatic events (Condie et al., 2009; Cawood et al., 2012, 2013). The ages of most detrital zircons in the Strelley Pool Formation indicate syndepositional erosion of the Warrawoona Group and granites of similar age. Additionally, pre-3530 Ma zircons are included in sandstone of Strelley Pool Formation of the Muccan Dome (Figs 8, 12d), providing evidence of syndepositional erosion of pre-Pilbara Supergroup felsic crust. This implies that the entire 10–15 km thickness of the Warrawoona Group had been locally removed by uplift and erosion by c. 3426 Ma, although some of this erosion was probably related to uplift and erosion prior to c. 3450 Ma. This history of uplift and erosion is consistent with detrital zircon evidence from sandstone of the Apex Basalt in the Mount Edgar Dome (Fig. 15). The total depth of erosion, and exposure of pre-3530 Ma underlying felsic crust, supports a continental setting.

Formation status

A detailed regional investigation of the stratigraphic variability of the Strelley Pool Formation would likely result in its redefinition as a group. Considerations suggesting eventual subdivision into several formations assigned to one or more groups include:

- deposition of the various sedimentary units now included within the Strelley Pool Formation spanned a time interval of c. 75 Ma, an interval of time longer than most periods of the Phanerozoic Eon
- there are no regionally continuous angular unconformities immediately below or above the formation; angular unconformities are locally present below it, but in many areas no erosional breaks have been observed at the base of the formation
- erosional breaks within the formation and rapid lateral changes of sedimentary facies and succession thickness indicate local crustal instability during deposition. Instability was probably related to late stages of the doming event between c. 3440 and 3420 Ma and to intrusion of the 3451–3416 Ma Tambina Supersuite. Ongoing granitic intrusion into the upper crust at c. 3420 Ma would probably have caused local supracrustal deformation, with resulting regional variations in uplift, possibly influencing erosion and deposition for tens of millions of years. An unconformity within the upper part of the formation in the Panorama and East Strelley greenstone belts might be due to uplift and crustal extension produced by the mantle plume that was later responsible for eruption of the Euro Basalt
- the Strelley Pool Formation is locally absent between the Warrawoona and Kelly Groups, suggesting lateral breaks in the depositional basin across upland areas of eroded Warrawoona Group
- certain distinctive components of the Strelley Pool Formation, such as the 1000 m-thick quartzite member of the Doolena Gap greenstone belt, and the laminated carbonate member of the East Strelley and Panorama greenstone belts, are mappable units that might be separated as formations.

Relationships to the Panorama Formation

The Strelley Pool Formation of the southeastern EPT is mainly composed of sandstone, and silicified fine-grained clastic rocks and laminated carbonate rocks, both outcropping mainly as laminated chert. The formation is underlain by relatively thick felsic volcanoclastic successions of the Panorama Formation, the upper parts of which include volcanoclastic sandstone and chert. Until Bagas et al. (2004c) reported local evidence of an erosional contact between the Panorama Formation and the 'Strelley Pool Chert' (obsolete name) in the Kelly greenstone belt, the units were interpreted to be conformable across the EPT (Van Kranendonk et al., 2002). Van Kranendonk (2003) interpreted the contact between the Panorama Formation and Euro Basalt to be conformable in the Western Shaw greenstone belt. Geochronology on the Panorama Formation in the eastern part of the EPT has provided dates consistently close to c. 3430 Ma, and dating of the Strelley Pool Formation has indicated very similar maximum depositional ages (Hickman, 2008). Additionally, similarity of sedimentary facies suggest that the lower parts of the Strelley Pool Formation and upper parts of the Panorama Formation were deposited in similar depositional environments. Contact relationships between the Panorama and Strelley Pool Formations in the Panorama greenstone belt have been documented by Van Kranendonk (2000a) and Allwood et al. (2007a).

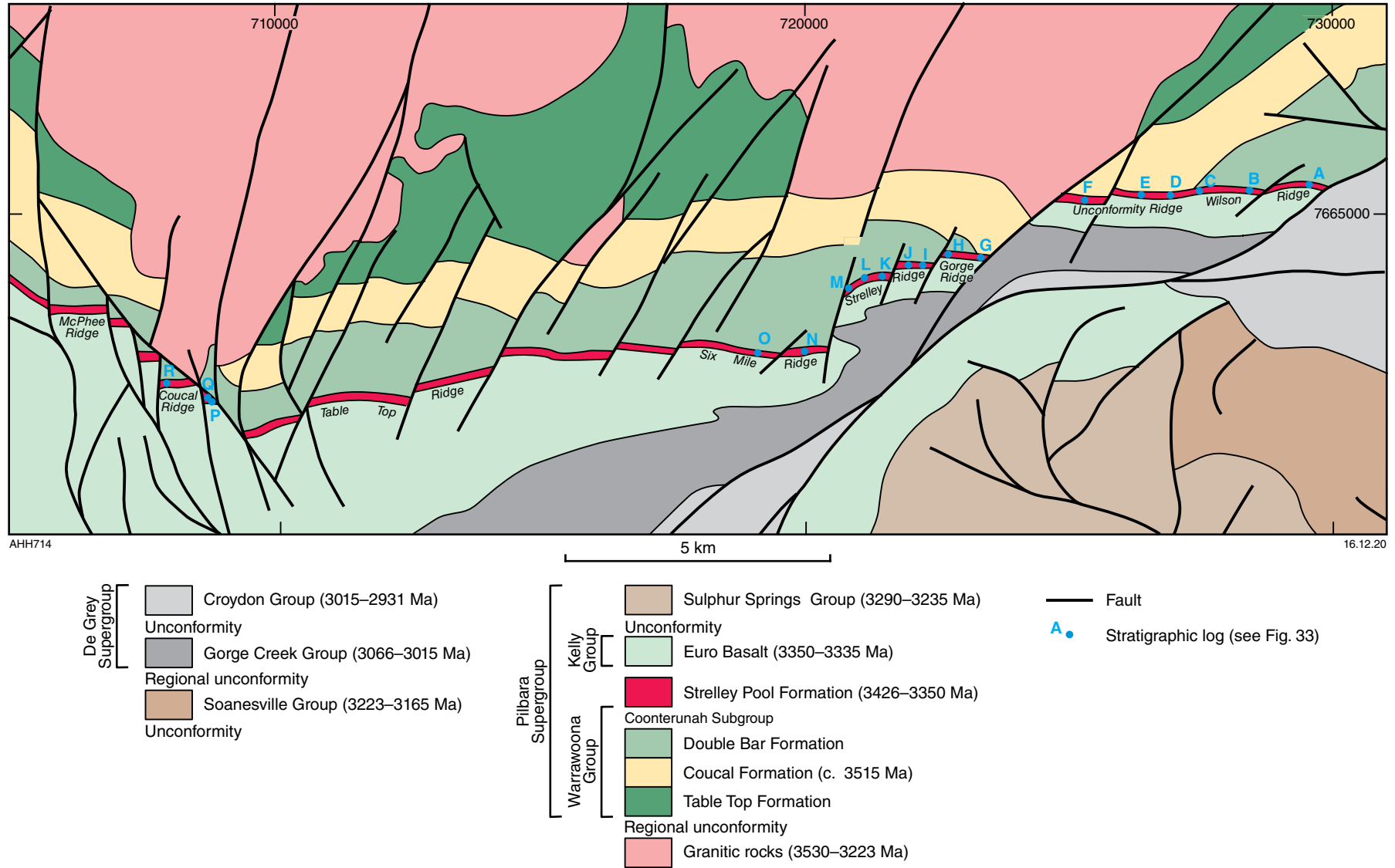


Figure 32. Outcrops of the Strelley Pool Formation in the central part of the East Strelley greenstone belt, showing locations of stratigraphic logs

Unconformities

In the Panorama greenstone belt, the Strelley Pool Formation is underlain by two unconformities: the upper unconformity overlies a thin, wedge-shaped, c. 3443 Ma unit of the Panorama Formation (Van Kranendonk, 2010a; Wingate et al., 2012a), whereas the lower unconformity separates this unit from jaspillite that might be part of either the Panorama Formation (Van Kranendonk, 1999b, 2000a) or the Marble Bar Chert Member (this Report). Consequently, in areas where the Panorama Formation is absent, it is likely that the unconformity at the base of the Strelley Pool Formation represents more than one erosional event, and there is evidence for deformation events, followed by erosion, at 3490–3460 Ma (pre-3468 Ma deformation recorded by Buick et al., 1995, Baker and Collins, 2001, and Baker et al., 2002) and 3445–3420 Ma (Kloppenburg, 2003; Pawley et al., 2004; Van Kranendonk et al., 2004a).

In the East Strelley greenstone belt, Wacey et al. (2010) recorded a westwards thinning of the basal conglomerate–sandstone unit in a northwesterly direction. Farther to the west, the entire formation is missing between the Coonterunah Subgroup and the Euro Basalt (Blewett and Champion, 2005), suggesting a northwestwards transgression of the Strelley Pool Formation onto a landmass comprising metamorphosed rocks of the Coonterunah Subgroup; this area could therefore be the northwestern margin of a depositional basin. Evidence of a third unconformity towards the top of the Strelley Pool Formation is provided by a laterally persistent unit of conglomerate in the Panorama and East Strelley greenstone belts (Lowe, 1983; Allwood et al., 2007a; Hickman, 2008; Wacey et al., 2010). This conglomerate contains boulders and pebbles eroded from the underlying parts of the formation and is overlain by mafic volcanic ash. The conglomerate and volcanic ash are conformable or paraconformable with the Euro Basalt, and probably represent a transitional sequence into the basalt.

The presence of the boulder conglomerate containing eroded blocks of the Strelley Pool Formation in the upper unit (Allwood et al., 2007a; Wacey et al., 2010) suggests a time break in which the main part of the formation was uplifted and eroded. The earliest effect of the mantle plume interpreted to have been responsible for eruption of the Euro Basalt (Van Kranendonk et al., 2004c, 2006a) was probably crustal uplift with extensional faulting. In both the East Strelley and Panorama greenstone belts, the Strelley Pool Formation is fragmented by numerous small-scale extensional faults. Zegers et al. (1996) identified pre-Euro Basalt extensional faults in the Coongan greenstone belt, and Nijman et al. (2001) and de Vries (2004) described similar structures at the same stratigraphic level in the northern Marble Bar greenstone belt. Extensional faulting of the Strelley Pool Formation would have resulted in erosion of the uplifted blocks, and lenses of conglomerate and sandstone at the base of the Euro Basalt. In this scenario, the upper clastic unit of the Strelley Pool Formation might be a basal member of the Euro Basalt.

Facies and depositional environments

Sedimentological, paleontological and geochemical features in many areas indicate shallow-water marine to subaerial depositional environments. Paleocurrent data are not recorded, although by analogy with the underlying Panorama

Formation, some of these environments were most likely marginal to partly eroded felsic volcanic piles near the centres of the EPT domes (DiMarco and Lowe, 1989a; Van Kranendonk, 2000a).

The regional facies variations of the Strelley Pool Formation indicate a broad northwest–southeast change in depositional environments, from a transgressive shoreline in the northwest, with beach and other shallow-water marine deposits, to a complex, generally shallow-water succession in the southeast. Deeper-water depositional environments may also have been present in the far southeast, as indicated by less sandstone, more flat-laminated chert, and fewer stromatolitic facies. Apparently unfossiliferous banded cherts in the southeast greenstone belts represent deposition in deeper water.

Paleontology

As already noted, the Strelley Pool Formation contains some of Earth's most abundant and best-preserved evidence of early life. In the Barberton Greenstone Belt, the Buck Reef Chert is lithologically and sedimentologically similar to the Strelley Pool Formation (de Vries, 2004; Lowe and Byerly, 2007; de Vries et al., 2010) and contains similar fossil evidence for early life (e.g. microbial mats, Tice and Lowe, 2004; Duda et al., 2016; microfossils, Oehler et al., 2017). These analogies add to stratigraphic and geochronological evidence indicating that a 3426–3350 Ma break in volcanism extended across a major part of Vaalbara.

World's oldest paleosols?

Where the unconformity at the base of the Strelley Pool Formation is angular, as in the northwestern EPT, there are 20–90 Ma breaks in the stratigraphic record: for example, between this formation and the c. 3515 Ma Coonterunah Subgroup. Although the Archean atmosphere is widely thought to have been anoxic (Holland, 2002), exposure of the Paleoarchean land surfaces for such lengthy periods of time is likely to have resulted in significant chemical alteration. Weathering might have resulted from acid rain (Heinrich, 2015) or from interaction with acidic surface waters. Alternatively, chemical weathering might have occurred under an atmosphere containing high levels of H₂ (Hao et al., 2017) related to volcanic activity (Walker, 1978). In some parts of the northwestern EPT, rocks immediately beneath the unconformity are altered to depths approaching 100 m (Buick et al., 1995; Van Kranendonk and Pirajno, 2004; Allwood, 2006, 2007a,b; Altinok and Ohmoto, 2006; Ohmoto et al., 2006; Johnson et al., 2008, 2009).

Previously, this alteration has been attributed to hydrothermal activity (Brown et al., 2006, 2011; Van Kranendonk, 2014) or to oxidation by an atmosphere containing O₂ levels similar to those of today (Ohmoto et al., 2006; Johnson et al., 2008, 2009; Hoashi et al., 2009). Hydrothermal activity immediately prior to deposition of the Strelley Pool Formation occurred during deposition of the Panorama Formation in the Panorama greenstone belt (Brown et al., 2006), but the Panorama Formation is absent in the East Strelley greenstone belt where there is also well-developed alteration beneath the unconformity (Buick et al., 1995; Altinok and Ohmoto, 2006; Wacey et al., 2010). Surface chemical weathering in the absence of atmospheric oxygen might explain much of the alteration beneath the

unconformity. Retallack (2018) interpreted the existence of paleosol horizons within the Panorama Formation of the northwestern Panorama greenstone belt; however, this succession might be at least partly equivalent to the Strelley Pool Formation.

Hydrothermal deposition?

In light of the detailed sedimentological studies of Lowe (1980, 1983) and DiMarco and Lowe (1989a,b) relatively few workers have suggested that the Strelley Pool Formation might be a hydrothermal deposit. A hydrothermal model was first proposed based on observations of dykes of massive chert that locally run into the base of the formation from underlying volcanic rocks (Van Kranendonk, 2001; Van Kranendonk and Nijman, 2001; Lindsay et al., 2003, 2005). In contrast to bedded chert, rock of these chert dykes is typically massive, generally black or dark grey, and commonly contains breccia. Where such dykes enter the bedded rocks of the Strelley Pool Formation, the chert occupies transgressive sills, irregular vein systems, or takes the form of diffuse bodies of chert breccia. Van Kranendonk (2001) advocated a hydrothermal model to explain the source of chert and carbonate laminites in the Strelley Pool Formation of the Panorama greenstone belt. He interpreted the depositional environment of the formation to be several caldera lakes developed upon the cooling, but still hydrothermally active, pile of the Panorama Formation. Likewise, Lindsay et al. (2003, 2005) interpreted the Strelley Pool Formation of the East Strelley greenstone belt to be hydrothermal, deposited in a low-energy, deep-water environment. They presented field and geochemical data to argue that the dykes represent the remnants of conduits of hydrothermal fluids from underlying volcanic and granitic rocks.

Geological objections to a hydrothermal origin include: 1) the Strelley Pool Formation is tens of millions of years younger than the granitic and volcanic rocks interpreted as the hydrothermal sources (in the East Strelley greenstone belt the age difference between the Coonterunah Subgroup

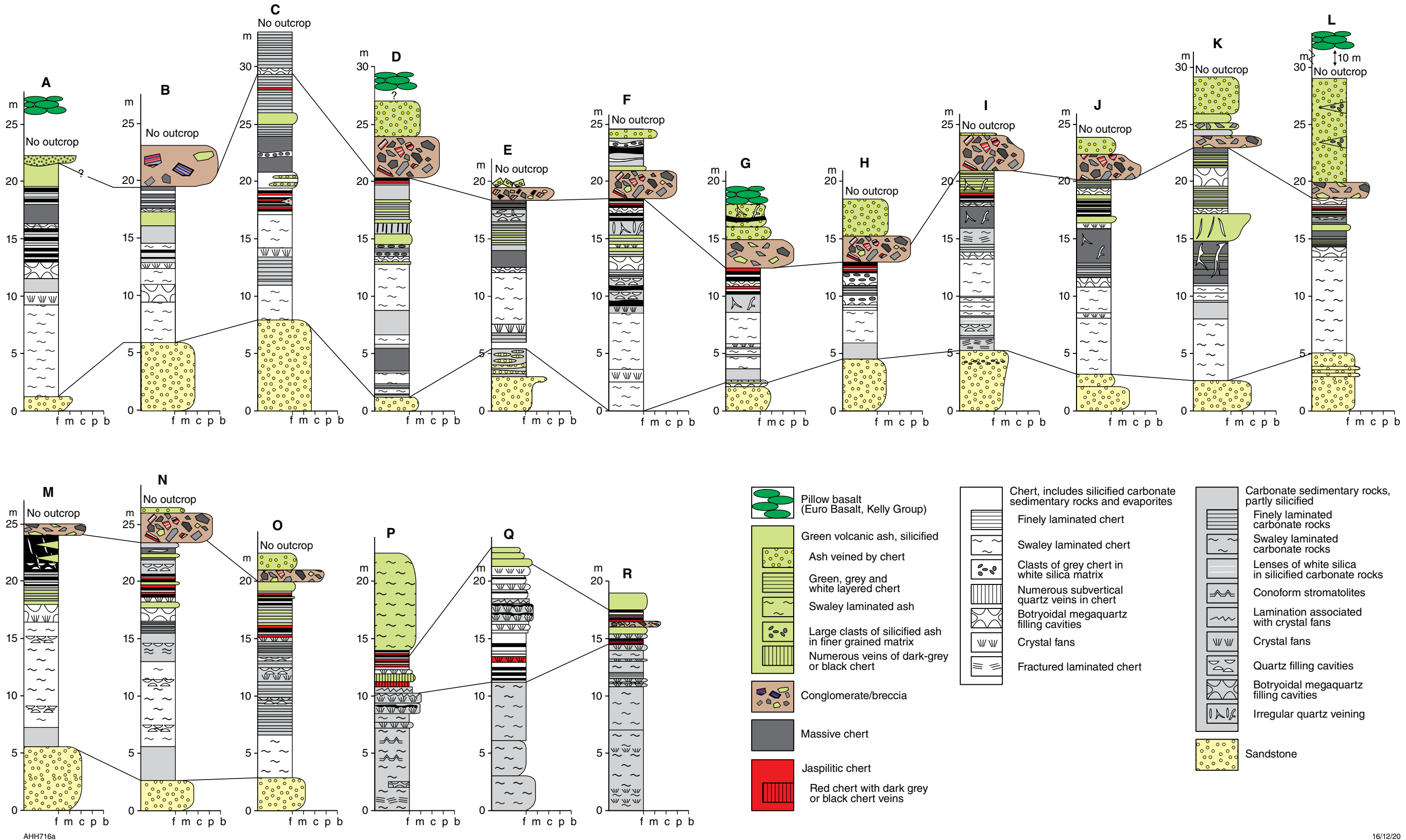
and the Strelley Pool Formation is ~90 Ma, and in the Panorama greenstone belt the age difference is ~40 Ma); 2) the underlying granitic and volcanic 'hydrothermal sources' in the East Strelley greenstone belt were deformed, metamorphosed, and eroded prior to deposition of the Strelley Pool Formation; 3) high-energy sediments, such as the conglomerate and sandstone at the base of the formation, were not mentioned or explained in the Lindsay et al. (2003) model, which invokes low-energy, relatively deep-water deposition.

The hydrothermal model was abandoned by Van Kranendonk et al. (2003) following their acquisition of geochemical data indicating marine deposition of carbonate laminites in the Panorama greenstone belt. Chondrite-normalized LREE depletion, elevated Y/Ho, and positive La, Gd and Er anomalies, all supported precipitation in the absence of hydrothermal fluids. The same conclusion was reached by Allwood et al. (2010) who reported on REE+Y patterns in both the carbonate and chert units of the Strelley Pool Formation, and in chert of formations underlying the unconformity. They found that the 'stromatolite reef' carbonate facies in the lower part of the formation has REE+Y patterns similar to other Archean marine precipitates. However, they reported that chert in the volcanoclastic facies near the top of the formation shows geochemical patterns indicative of precipitation from hydrothermal and mixed marine-hydrothermal fluids. This feature is consistent with the upper Strelley Pool Formation, above the central unconformity in the formation, being deposited in a hydrothermal environment. This suggests that this upper part of the formation is more closely related to the overlying Euro Basalt, as interpreted above.

In the East Strelley greenstone belt, the black chert dykes underlying the Strelley Pool Formation are too thin and too limited in extent to be hydrothermal feeders for the bedded chert (Wacey et al., 2010), and this is now interpreted to be the situation in all 13 greenstone belts of the EPT that contain the formation.

Table 5. Members (informal) and facies of the Strelley Pool Formation in the type section, Strelley Pool. From Lowe (1983)

Member	Depositional environment
Member 5	
Capping unit of volcanoclastic debris	Ashfall tuff and volcanoclastic, current-deposited beds (distal subaerial volcanic alluvial apron)
Member 4	
Unit of coarse, intraformational conglomerate and breccia	Debris flows and/or torrential flood deposits
Member 3	
Stratified unit of stromatolite, black chert, silicified evaporite, and evaporite-solution layers	Low-energy, clastic-starved environment subject to current activity and exposure. Modern analogues are intertidal flats and supratidal sabkhas
Member 2	
Massive-weathering cherty unit of laminated flat stromatolite, conical stromatolite and silicified evaporite	Cyclic sedimentation in a shallow, hypersaline basin
Member 1	
Basal layer of quartzose sandstone	High-energy, shallow-water conditions



Kelly Group

The Kelly Group (Table 1) comprises three formations, in ascending stratigraphic order: the 3350–3335 Ma Euro Basalt, up to 9400 m thick (Van Kranendonk, 2000a), and composed of komatiite, basaltic komatiite and tholeiite, with numerous thin chert units; the 3325–3315 Ma Wyman Formation, up to 2000 m thick, and comprising rhyolite and rhyodacite flows and intrusions, rhyolitic volcanoclastic rocks, and minor sandstone, shale and chert; and the 3325–3315 Ma Charteris Basalt, up to 2000 m thick, composed of komatiite, basaltic komatiite and tholeiite. The Euro Basalt disconformably overlies the 3426–3350 Ma Strelley Pool Formation in most greenstone belts of the East Pilbara Terrane. Where the Strelley Pool Formation is absent, the Euro Basalt overlies the Warrawoona Group across an erosional unconformity. As noted above, in the East Strelley and Panorama greenstone belts (Fig. 8, Plate 1), the upper Strelley Pool Formation contains an erosional unconformity, above which conglomerate overlain by mafic volcanoclastic rocks might belong to the first eruptive stage of the Euro Basalt. Future geochronology might resolve this question. The upper stratigraphic contact of the Kelly Group is an erosional unconformity with, in different areas, the Sulphur Springs, Soanesville or Gorge Creek Groups. This angular unconformity is a result of deep erosion following uplift during the 3325–3290 Ma EPE (Hickman and Van Kranendonk, 2008b), which is thought to explain the restricted regional extent of the Charteris Basalt.

An unresolved issue for the Kelly Group is that, whereas the Euro Basalt extends across most of the EPT, the rhyolitic Wyman Formation has been identified in only six domes in the eastern part of the EPT — the Corunna Downs, Mount Edgar, Muccan, McPhee, Yilgalong Domes, and far eastern Shaw Dome. The restricted distribution of the Wyman Formation is unlikely to be due to erosion because its intrusive equivalents, namely the 3324–3290 Ma granitic intrusions of the Emu Pool Supersuite (Bickle et al., 1993; Barley and Pickard, 1999; Bagas et al., 2004c; Van Kranendonk et al., 2006b, 2007a,b; Smithies et al., 2007b) are also confined to the same eastern part of the EPT (Van Kranendonk et al., 2004c, 2006a). These differences suggest a significant tectonic event between 3350–3335 Ma eruption of the Euro Basalt and 3325–3315 deposition of the Wyman Formation. Previous evidence for such an event is provided by the existence of unconformities between the two formations in some greenstone belts (Hickman, 1983, 1990; Barley and Pickard, 1999; Van Kranendonk, 2004b) and folding of the Euro Basalt prior to deposition of the Wyman Formation (Hickman, 1981, 1983; Van Kranendonk, 2004b). Additionally, geochemical data reveal a considerable compositional gap between the komatiites, komatiitic basalts and tholeiites of the Euro Basalt, and the rhyodacite and rhyolite of the Wyman Formation. Whereas the Euro Basalt is interpreted to have been produced by plume-related melting of the mantle (Van Kranendonk et al., 2002, 2004a,b; Hickman and Van Kranendonk, 2004; Smithies et al., 2005b; Van Kranendonk et al., 2006a, 2007a,b, 2010, 2014b), the geochemistry of the Wyman Formation indicates a strongly potassic crustal melt (Smithies et al., 2007b).

These differences cast doubt on whether the Euro Basalt and Wyman Formation should be assigned to the same group. Hickman (1990) excluded the Wyman Formation from the Warrawoona Group, which then included the

Euro Basalt, because of the erosional unconformities and structural evidence of folding between deposition of the formations. One or more deformation events between the formations had previously been interpreted on diagrammatic illustrations to interpret the crustal evolution of the northern section of the Pilbara Craton (Hickman, 1981, 1983). However, based on geological observations and interpretations from the Kelly greenstone belt, Van Kranendonk et al. (2002) combined the Euro Basalt, Wyman Formation and Charteris Basalt into a 'subgroup' of the Warrawoona Group. Reasons for this revision were given by Bagas (2003) based on local evidence in the Kelly greenstone belt. Van Kranendonk et al. (2006a) upgraded the 'Kelly Subgroup' to the Kelly Group and included the 'Strelley Pool Chert' (now Strelley Pool Formation) at its base. This revision was based on an interpretation that the three volcanic formations represent a volcanic cycle separate from underlying volcanic cycles in the Warrawoona Group. The Strelley Pool Formation was subsequently removed from the Kelly Group (Hickman, 2008) for reasons already presented in this Report.

Geochronology indicates that the Euro Basalt, Wyman Formation and Charteris Basalt were erupted during a discrete 3350–3315 Ma interval in the evolution of the Pilbara Supergroup. The compositions of the 3350–3335 Ma Euro Basalt and the undated Charteris Basalt are consistent with a mantle plume origin. The Wyman Formation and the genetically related Emu Pool Supersuite are interpreted to have been products of partial melting of older continental crust (Champion and Smithies, 1999, 2007; Bagas et al., 2003; Van Kranendonk et al., 2007a,b, 2018), with fractionation of magma resulting in the more potassic volcanic rocks (Champion and Smithies, 2007). Partial melting of the crust to produce the Emu Pool Supersuite and the Wyman Formation was almost certainly related to heating by the same mantle plume responsible for earlier eruption of the Euro Basalt. In this scenario, the Euro Basalt and the Wyman Formation originated through the same mantle plume event. Accordingly, the stratigraphy of the Kelly Group remains unchanged in this Report, with the unconformities between the Euro Basalt and the Wyman Formation interpreted as consequences of locally variable deformation during mantle plume activity. It remains unknown why the Wyman Formation and the Emu Pool Supersuite are restricted to the eastern half of the EPT, although both units appear to have a common western boundary that coincides closely with the Coongan–Warralong Fault Zone (CWFZ, Fig. 5). The exposed southern section of this structure was first referred to as the Central Coongan Shear Zone (Zegers, 1996; Zegers et al., 1999). Zegers et al. (1999) used $^{40}\text{Ar}/^{39}\text{Ar}$ dating to interpret that this shear zone was active between c. 3325 and 3197 Ma.

Whole-rock Nd model ages from the Euro Basalt range between c. 3510 and 3470 Ma, and ϵ_{Nd} values are chondritic (Table 4). No Sm–Nd analyses are available for the Wyman Formation, but granitic rocks of the contemporaneous and genetically related Emu Pool Supersuite have Nd model ages between c. 3630 and 3420 Ma, with ϵ_{Nd} values between +1.49 and –1.44 (Table 4). These data suggest various sources ranging in age from late Eoarchean to early Paleoproterozoic. Because the theoretical depleted mantle ϵ_{Nd} at 3350–3315 Ma is +2.8 (Fig. 19), isotope data from the Kelly Group and Emu Pool Supersuite indicate melting of older crust and subcontinental lithospheric mantle.

Euro Basalt

The Euro Basalt is the lowermost formation of the Kelly Group, and is the thickest and most regionally extensive basaltic formation of the Pilbara Supergroup. In most areas of the East Pilbara Terrane, the formation is between 3000 and 6000 m thick, although in the Panorama greenstone belt it is estimated to be up to 9400 m thick (Van Kranendonk, 2000a). The formation comprises a volcanic succession dominated by pillowed tholeiite interlayered with thin chert units. However, in several greenstone belts, the Euro Basalt includes basal units of komatiite or komatiitic basalt, which is a characteristic feature of the lower parts of ultramafic–mafic–felsic volcanic cycles erupted during mantle plume events.

Allowing for present-day partial concealment of the formation by younger units, the original depositional extent of the Euro Basalt across the Pilbara Craton was at least 100 000 km². Under the interpretation that the Pilbara and Kaapvaal Cratons are likely to have evolved as adjacent parts of Vaalbara (see Introduction), lithological similarities and comparable geochronology suggest the Euro Basalt might be correlated with the Kromberg Formation of the Onverwacht Group. In this scenario, the original extent of the Euro Basalt would probably have been at least 1 000 000 km². Eruption of the formation lasted at least c. 15 Ma, and was accompanied by intrusion of swarms of dolerite dykes into the underlying crust – examples intrude the Panorama Formation and Tambina Supersuite in the Corunna Downs Dome (Kloppenburg, 2003). Such dyke swarms are important features of LIPs (Ernst, 2007), and the fact that only fragments of old crust containing them are now preserved in the EPT is a consequence of intrusion by younger voluminous granitic rocks, including those of the Emu Pool Supersuite.

Based on the presence of erosional surfaces and conglomerate within the upper part of the underlying Strelley Pool Formation, the Euro Basalt was initially erupted at or slightly below sea level. However, the abnormal thickness of the formation, combined with its content of pillow basalts, establishes that it was deposited in one or more rapidly subsiding depositional basins. Deep subsidence of ultramafic–mafic volcanic basins between rising granitic domes is a key feature in the diapiric model explaining the development of the dome-and-keel crustal architecture of the EPT (Hickman and Van Kranendonk, 2004). Periodic shallowing of the basins between c. 3350 and 3335 Ma is suggested by the local presence of thin, clastic sedimentary units. The depositional extent and thickness of any eroded sections of the formation that might have been deposited across the EPT granitic domes is unknown.

Geochemistry of the Euro Basalt was investigated by Glikson and Hickman (1981a,b), Arndt et al. (2001), Smithies et al. (2005b, 2007a), and Nebel et al. (2014). Collectively, these investigations established the presence of komatiites (>18 wt% MgO) and komatiitic basalts (8–18 wt% MgO) in addition to tholeiites. Glikson and Hickman (1981a,b) identified a 400 m-thick unit of serpentinized peridotitic komatiite close to the base of the Euro Basalt in the northern Kelly greenstone belt. Most of the komatiite is massive but serpentinized olivine-spinifex texture is locally present. Geological mapping (Hickman and Van Kranendonk, 2008b) revealed that the komatiite unit extends along strike for about 30 km, suggesting it was deposited along a broad channel or in some other type of topographic

depression. Smithies et al. (2007a) classified the komatiites of this section of the Euro Basalt as Al-undepleted, with low incompatible trace element concentrations and flat normalized trace element patterns that are indistinguishable from those of the komatiites in the Table Top Formation (Coonterunah Subgroup). Nebel et al. (2014), used seven samples of komatiitic basalt analysed by Smithies et al. (2007a), to obtain whole-rock Lu–Hf isotope data that included initial ¹⁷⁶Hf/¹⁷⁷Hf ($\epsilon_{\text{Hf}(t)}$). Excluding results from one extremely altered sample, the ϵ_{Hf} values are strongly positive and plot near or above the depleted mantle ϵ_{Hf} value at 3350 Ma (Fig. 19). Nebel et al. (2014) interpreted this to indicate a component of old, melt-depleted reservoir in the mantle source.

Smithies et al. (2007a) reported that the concentration ranges of incompatible trace elements for high-Ti tholeiites from the Euro Basalt are almost identical to the high-Ti tholeiites of the Coonterunah Subgroup. Low-Ti tholeiites of the Euro Basalt were reported to have lower incompatible trace element concentrations than high-Ti tholeiites, and [La/Yb]_{PM} and [La/Sm]_{PM} ratios as low as 0.36 and 0.6, respectively. Smithies et al. (2007a) interpreted these features to indicate a strongly depleted source.

Wyman Formation

The c. 3325 to 3315 Ma Wyman Formation is up to 2000 m thick and comprises weakly metamorphosed rhyolite flows, subvolcanic rhyolite and rhyodacite intrusions, and rhyolitic volcanoclastic rocks including agglomerate, tuff and sandstone. Less-widely exposed lithologies include pillowed komatiitic basalt, banded iron-formation, ferruginous shale, pelitic schist and black chert. Chert breccia is locally present in hydrothermal veins. Sandstone, conglomerate and shale are mainly present near the base of the formation and around the margins of volcanic centres. Rhyolite in the formation is locally exceptionally potassic (6–11 wt% K₂O), and is interpreted to have been derived from melting of significantly older felsic crust. In some areas, rhyolite is interlayered with basaltic rocks, although this might be partly due to rhyolite intrusion rather than bimodal volcanism.

The Wyman Formation is exposed in six greenstone belts of the EPT, over a total area of 10 000 km². The stratigraphy of the formation across this area varies considerably because individual volcanic centres are dominated by proximal volcanic facies of rhyolite lava, subvolcanic rhyolite intrusions, and coarse-grained felsic volcanoclastic units extending laterally into more distal, finer-grained volcanoclastic rocks and clastic sedimentary rocks. Notably, clastic sedimentary lithologies are predominant in sections of the Wyman Formation close to the outer margins of the overall distribution of the formation, such as in the Warralong greenstone belt in the northwest EPT and the Mount Elsie greenstone belt in the southeastern EPT.

In the type area of the Wyman Formation, south of Wyman Well in the northwestern Kelly greenstone belt, a thin unit of chert at the base of the formation includes silicified carbonaceous shale and siltstone. This is overlain by porphyritic rhyolite and felsic volcanoclastic rocks, and lithic sandstone capped by a second thin unit of chert. Stratigraphically above this chert is a unit of pillowed komatiitic basalt up to 1000 m thick, in turn overlain by about 1000 m of rhyolite. At the top of the formation is

a 200 to 300 m-thick unit of rhyolitic agglomerate, tuff and volcanoclastic sandstone. Excellent exposures of fragmental rhyolite and rhyolite-boulder conglomerate interpreted to represent a debris-flow deposit (Zone 50, MGA 782290E 7640100N) are located 2 km south of the confluence between Camel Creek and the Coongan River. An igneous crystallization age of 3318 ± 4 Ma was reported for a dacitic volcanoclastic rock from this locality (GSWA 160220, Nelson, 2002a).

At Copper Hills, in the southeastern Kelly greenstone belt (Fig. 8, Plate 1B), and farther southwest in the Budjan Creek area, the dominant lithology is porphyritic rhyolite. This unit is up to 1500 m thick, but varies in thickness laterally due to overlying erosional unconformities with either the Soanesville Group or the Gorge Creek Group. In the area immediately south of Copper Hills, the rhyolite is conformably overlain by up to 200 m of felsic volcanoclastic rocks. The Budjan Creek and Copper Hills stratigraphy extends northeast to the Spinaway Well area where the rhyolite is up to 2000 m thick in a volcanic centre 7 km southwest from the well and 5 km west of Hales Grave Well. In this area, the rhyolite is capped by a thick unit of interlayered, fine-grained, tuffaceous volcanoclastic rocks and chert. Farther northeast, between Spinaway Well and Charteris Creek, the formation is between 500 and 1000 m thick and includes a lower unit of felsic volcanoclastic sandstone interbedded with siltstone, chert, carbonaceous mudstone and basalt.

In the McPhee greenstone belt (Fig. 8, Plate 1), the Wyman Formation consists of fine-grained to porphyritic rhyolite and rhyodacite flows, and minor felsic volcanoclastic rocks. This felsic complex is locally overlain by laminated chert with poorly preserved domal stromatolites and fuchsite-bearing silicified tuff. On the western side of Police Creek, 10 km east of Wallabirdee Ridge, laminated and stromatolitic chert is associated with barite layers up to a metre thick. Altered and silicified crystal sprays pseudomorphing barite in the chert, together with fuchsite-bearing silicified tuff or quartzite, overlie rhyolitic flows, agglomerate and tuff in this area. Black hydrothermal chert veins, many carrying open vugs lined with banded chalcedony (agate), intrude the entire felsic volcanic succession (Williams and Bagas, 2007a). The basal unit of the Wyman Formation in this greenstone belt is a thin chert that has been mapped over a strike length of 8 km (Bagas, 2005).

In the western Warralong greenstone belt (Fig. 8, Plate 1A), a succession correlated with the Wyman Formation comprises 1000 m of pillowed basalt between a basal unit of sandstone and felsic volcanoclastic rocks, and an upper unit of rhyolite and chert at the top of the formation (Van Kranendonk, 2004b). In the same general area, about 3 km north of Cooke Bluff Hill, the upper rhyolite includes ignimbrite (Hickman, 1977b).

In the southern section of the Mount Elsie greenstone belt (Fig. 8, Plate 1B), a succession overlying the Euro Basalt, and interpreted to be part of the Wyman Formation, comprises 1000 m of variably silicified variolitic and vesicular pillowed basalts containing thin chert units overlain by a 1500 m-thick unit of clastic sedimentary rocks. Without geochronology, it is unclear if this clastic succession is the same age as the Wyman Formation.

An unusual feature of the Wyman Formation is the widespread distribution of columnar-jointed, porphyritic rhyolite units (Fig. 34). The columnar jointing consists of hexagonal columns up to 40 cm diameter and 20 m long. This columnar jointing is well-developed in several areas including the Camel Creek area of the northeastern Kelly greenstone belt (Fig. 34a), the Budjan Creek area of the southeastern Kelly greenstone belt (Fig. 34b), and Wallabirdee Ridge area of the McPhee greenstone belt. The structure formed during rapid cooling of either thick rhyolite flows or subvolcanic intrusions.

Surface geology reveals that at least some felsic volcanic units of the Wyman Formation were sourced from magma chambers now preserved as monzogranite and granodiorite intrusions of the c. 3324–3290 Ma Emu Pool Supersuite. A genetic relationship between the Wyman Formation and this supersuite has been inferred for many years (Glikson et al., 1987; Collins, 1993; Barley and Pickard, 1999; Van Kranendonk et al., 2006b, 2007a,b, 2018; Champion and Smithies, 2007; Bagas et al., 2003, 2004c; Smithies et al., 2003, 2019; Hickman and Van Kranendonk, 2004, 2008a). Unlike older Paleoproterozoic granitic supersuites of the East Pilbara Terrane, most intrusions of the Emu Pool Supersuite were emplaced high into the Warrawoona Group and locally into the Kelly Group. Subvolcanic intrusions linking the granites to the volcanics are exposed in the Corunna Downs, Mount Edgar and McPhee Domes. For example, in the Copper Hills area of the Corunna Downs Dome, the subvolcanic Boobina Porphyry, part of the Emu Pool Supersuite, intrudes the lower stratigraphic levels of the Wyman Formation.

Charteris Basalt

The Charteris Basalt is the uppermost stratigraphic unit of the Kelly Group, between 1000 and 2000 m thick, and is mainly composed of komatiitic basalt and tholeiite. The formation also includes thin units of blue-black, grey and white banded chert, fine-grained felsic volcanoclastic rocks, and dolerite sills. In the McPhee greenstone belt (Fig. 8, Plate 1), about 15 km north of Lionel, the Charteris Basalt is interlayered with rhyolitic volcanic sandstone and breccia of the 3325–3315 Ma Wyman Formation.

In outcrop, the komatiitic and tholeiitic basalts of the formation are indistinguishable from those in the Euro Basalt. However, analysis of samples from the Charteris Creek area reveal that the Charteris Basalt is geochemically different from most of the Euro Basalt (data in Glikson and Hickman, 1981b; Glikson et al., 1986). Comparing both successions of komatiitic basalts and tholeiites, the Charteris Basalt has lower TiO_2 , P_2O_5 , Ce, Y, Zr and Sm, and higher K_2O , Ba, Rb, Sr, Cr, Ni and $\text{Al}_2\text{O}_3/\text{TiO}_2$ than most basalts of the Euro Basalt. These differences coincide with the differences between high-Ti and low-Ti basalts as described by Smithies et al. (2005b). The low-Ti basalts of the Charteris Basalt might have been derived from more depleted sources than the Euro Basalt. Smithies et al. (2005b) interpreted the high-Ti basalts of the Pilbara Supergroup to have been derived by plume-related partial melting of sources compositionally similar to primitive mantle, whereas low-Ti basalts were derived through melting a single source that became progressively more depleted during the evolution of the EPT.

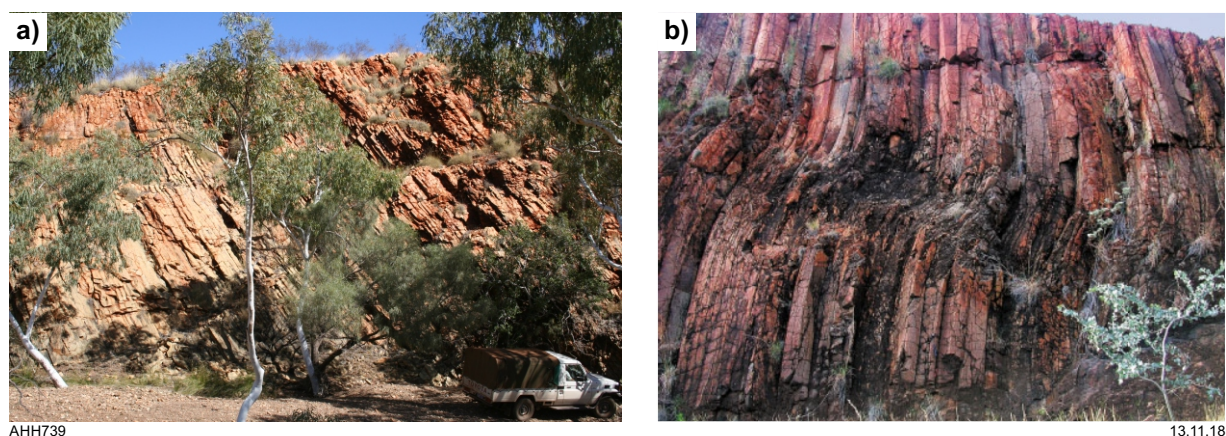


Figure 34. Columnar rhyolite in the Wyman Formation: a) Camel Creek, Kelly greenstone belt (MGA 787454E, 7640098N); b) northern McPhee greenstone belt (MGA 222200E, 7619200N). From Bagas (2005)

An alternative explanation of the geochemical differences between low-Ti and high-Ti basalts might be related to the structure and evolution of mantle plumes. Campbell and Griffiths (1990) proposed that high-Ti basalts were sourced from relatively cool, low-degree partial-melting zones in plume heads, whereas low-Ti basalts were derived from hotter axial regions of plumes with greater partial melting of less-enriched lower-mantle material. Progressively more low-Ti basalts might be erupted as the plume evolved, with flattening of the head and the introduction of more lower-mantle material into the zone of melting (Campbell and Griffiths, 1990). Crustal contamination of the low-Ti basaltic magmas of the Charteris Basalt, perhaps partly due to intrusion through the Wyman Formation and sills of the Emu Pool Supersuite, might account for relatively high levels of K_2O , Ba and Rb in these basalts. Thus, the Charteris Basalt might be a late-stage product of the same mantle plume that produced the Euro Basalt.

Sulphur Springs Group

The Sulphur Springs Group (Table 1; Van Kranendonk and Morant, 1998; Van Kranendonk, 2000a; Van Kranendonk et al., 2006a) comprises three formations, in ascending stratigraphic order:

- the 3290–3255 Ma Leilira Formation, up to 3900 m thick, composed of wacke, quartz sandstone, pebbly sandstone, volcanoclastic sandstone and shale
- the c. 3275–3255 Ma Kunagunarrina Formation up to 2400 m thick, composed of komatiite, komatiitic basalt, tholeiite and chert
- the 3253–3235 Ma Kangaroo Caves Formation, up to 1500 m thick, composed of andesite and minor basalt, overlain by dacitic to rhyolitic volcanoclastic rocks, and capped by a unit of grey-and-white banded chert up to 20 m thick.

The stratigraphy of the Sulphur Springs Group is extremely variable between different greenstone belts, so that the maximum thickness of the entire group in any one area is

about 5000 m. Of particular note is that the Kunagunarrina Formation is almost entirely absent from the northern Soanesville greenstone belt (Fig. 8, Plate 1), with the result that the Kangaroo Caves Formation directly overlies the Leilira Formation. As explained below, this might be due to locally deep erosion within the group.

Formations of the Sulphur Springs Group outcrop in six greenstone belts in the western half of the EPT: the Soanesville, Pincunah, Panorama, Abydos, East Strelley and Warralong greenstone belts (Fig. 8, Plate 1). The group might also be present in the Wodgina and Pilbara Well greenstone belts, although there is insufficient geochronology to confirm this. Felsic volcanic rocks in the TTSZ are interpreted to be deformed remnants of the group based on an igneous crystallization age of 3253 ± 4 Ma (GSWA 160258, Wingate et al., 2010) and associated VMS mineralization similar to that in the northern Soanesville greenstone belt. Most outcrops of the Sulphur Springs Group are within and adjacent to the Lalla Rookh – Western Shaw Structural Corridor (LWSC, Fig. 5).

The LWSC has previously been interpreted as a c. 2930 Ma zone of faulting (Van Kranendonk and Collins, 1998; Zegers et al., 1998a, 2001; Van Kranendonk et al., 2002, 2007a; Van Kranendonk, 2008), but this Report reviews evidence suggesting that the c. 2930 Ma deformation involved reactivation of older crustal structures formed by crustal extension and rifting during the 3280–3165 Ma EPTRE (Hickman, 2016). This extension was partly contemporaneous with deposition of the Sulphur Springs Group and followed a major event of deformation, metamorphism and granitic intrusion in the eastern half of the EPT between c. 3325 and 3290 Ma (D_6 in this Report). The D_6 event included diapiric doming and subsequent erosion, but no evidence of the deformation and granitic intrusion has been reported in the western half of the EPT. Erosion of the uplifted eastern EPT may have shed large volumes of detritus westwards into the area that later became the LWSC. This would explain deposition of the basal clastic formation of the Sulphur Springs Group, the Leilira Formation, which is locally up to 3900 m thick (Van Kranendonk and Morant, 1998).

The combined stratigraphy of the upper two formations of the group, the Kunagunarrina and Kangaroo Caves Formations, is an ultramafic–mafic–felsic volcanic cycle similar to the stratigraphic successions of older plume-related volcanic cycles of the Warrawoona and Kelly Groups. Likewise, the underlying Leilira Formation is analogous to the 3426–3350 Ma Strelley Pool Formation in that it separates two major volcanic cycles. For this reason, a case appears to exist for removing the Leilira Formation from the volcanic formations of the Sulphur Springs Group, especially since currently available geochronology suggests that the depositional age range of the Leilira Formation was most likely several tens of millions of years. However, such a revision should follow acquisition of more geochronological evidence because only the upper formation of the Sulphur Springs Group (Kangaroo Caves Formation) has been reliably dated.

The Sulphur Springs Group unconformably overlies the 3350–3335 Ma Euro Basalt of the Kelly Group in the far southwestern part of the Panorama greenstone belt, and in the Warralong and East Strelley greenstone belts (Fig. 8, Plate 1; Van Kranendonk, 1997, 2000a, 2004b). The Kangaroo Caves Formation is unconformably overlain by the 3228–3165 Ma Soanesville Group in the northern Soanesville greenstone belt (Buick et al., 2002; Hickman, 2011). However, in the western Pincunah greenstone belt, the Kangaroo Caves Formation is absent and Kunagunarrina Formation is directly overlain by the Soanesville Group (Blewett et al., 2001; Blewett and Champion, 2005), implying an unconformity. In the East Strelley greenstone belt, the Sulphur Springs Group is unconformably overlain by sandstone and conglomerate of the Farrel Quartzite (Gorge Creek Group).

Deposition of the Leilira Formation, and therefore the Sulphur Springs Group, is interpreted to have commenced at c. 3280 Ma following intrusion of the 3324–3290 Ma Emu Pool Supersuite. However, intrusion of the supersuite was accompanied by doming, and erosion probably resulted in clastic sedimentation prior to c. 3280 Ma. Dating of a felsic volcanoclastic unit near the top of the Kunagunarrina Formation indicated a maximum depositional age of c. 3255 Ma (sample 60925, Buick et al., 2002). The youngest isotopic date generally attributed to the Kangaroo Caves Formation is 3235 ± 4 Ma (Buick et al., 2002), although this rhyolite intruded the 'marker chert', so is actually younger than the formation and was most likely derived from the Strelley Monzogranite. Dacite in the TTSZ was dated at 3253 ± 4 Ma (GSWA 160258, Wingate et al., 2010), suggesting a c. 20 Ma period of felsic volcanism. This is consistent with the 3257–3223 Ma age range of the Cleland Supersuite in the EPT.

The geochemistry of the Kangaroo Caves Formation was described by Brauhart (1999), and of the Kunagunarrina Formation by Smithies et al. (2005b, 2007a). Smithies et al. (2007a) provided analyses for 27 samples from the Pincunah greenstone belt and three samples from the Abydos greenstone belt. Most samples from the Kunagunarrina Formation were komatiitic basalts, although 10 samples were classified as basalts and two samples were komatiites. All but three of the basalts are low Ti ($\text{TiO}_2 < 0.8$ wt%) and the komatiites are Al-depleted ($\text{Al}_2\text{O}_3/\text{TiO}_2$ ratios ~ 10). Trace element compositions normalized to primitive mantle show considerable variations between the basalts, more so than for older basalts of the Pilbara Supergroup (Smithies et al.,

2007a). Possible reasons include mingling of mafic and felsic melts, or variable crustal contamination. About half the basalts (low- and high-Ti varieties) show depleted LREE patterns, similar to those that characterize the rift-related Honeyeater Basalt (Soanesville Group), although there is also a group with fractionated LREE patterns and prominent negative Eu anomalies. Compared to basalts of the Kelly and Warrawoona Groups, the seven low-Ti basalts of the Kunagunarrina Formation have lower Ti, La/Sm, La/Gd, La/Yb and Gd/Yb. However, the three high-Ti basalts are compositionally similar to high-Ti basalts in the Kelly and Warrawoona Groups.

Commenting on the same dataset used by Smithies et al. (2005b), Smithies et al. (2007a) interpreted a stratigraphic trend in the low-Ti basalts from the Warrawoona Group to the Sulphur Springs Group. In this trend, La/Sm, La/Gd, La/Yb and Gd/Yb decrease to become close to primitive mantle in the Sulphur Springs Group, indicating a strongly depleted source. They explained this change in terms of the low-Ti basalts having been derived from a source that, through repeated melting events, became increasingly depleted with time (c. 3500–3250 Ma). Smithies et al. (2005b) also commented that Al-depleted komatiitic rocks appear to be more abundant in the Sulphur Springs Group than in the Warrawoona Group, and have higher Gd/Yb with decreasing age. They interpreted this to be consistent with a higher proportion of garnet in the source of the low-Ti basalts of the Sulphur Springs Group. Garnet-rich residues from high-pressure melting that produced the Al-depleted komatiites and komatiitic basalts were likely added to the bulk source of the younger low-Ti basalts (Smithies et al., 2005b).

The Kangaroo Caves Formation in the Soanesville greenstone belt (Fig. 8, Plate 1) comprises a lower succession of basalt–andesite rocks and overlying felsic volcanic rocks. In this sequence, Brauhart (1999) recognized two geochemical suites: one with $\text{Zr}/\text{Th} < 23.5$, and the other with $\text{Zr}/\text{Th} > 23.5$. Both suites are tholeiitic and were interpreted to belong to a high-K magma series derived from a common partial-melt source of felsic volcanic rocks. These tholeiitic suites were interpreted to indicate minimal influence of garnet during partial melting or fractionation, indicating shallow levels of partial melting. The intermediate to felsic volcanic rocks of the Kangaroo Caves Formation have flat HREE profiles and more-fractionated LREE profiles.

Evidence that the Sulphur Springs Group was deposited above continental crust is provided by geochemistry, detrital zircon ages and Nd model ages. Detrital zircons in the Leilira Formation in the Soanesville greenstone belt include age components at c. 3510 Ma (Coonterunah Subgroup age) and c. 3450 Ma (Salgash Subgroup age), with one date of 3589 ± 4 Ma (sample 60925, Buick et al., 2002) indicating erosion of pre-Pilbara Supergroup crust or recycling of old zircons from a sedimentary unit such as the Strelley Pool Formation. Sm–Nd isotope data obtained by Brauhart et al. (2000) are similar to Sm–Nd data from the Warrawoona and Kelly Groups, and from older granitic rocks of the EPT (Table 4). A sample of rhyolite from the Kangaroo Caves Formation has a whole-rock Nd model age of c. 3500 Ma and a ϵ_{Nd} value of -0.48 . Samples from the Strelley Monzogranite have Nd model ages from c. 3540 to 3490 Ma and ϵ_{Nd} values between -0.41 and -1.0 . Champion (2013) and Champion and Huston (2016) suggested that these data are consistent with felsic magma derivation through partial melting of early Paleoproterozoic TTG crust.

The Sulphur Springs Group has provided evidence of early life related to VMS deposition in the upper Kangaroo Caves Formation. Pyritic filaments within the VMS deposits were interpreted as microfossils (Rasmussen, 2000). Wacey (2009) commented that the pyritic filaments differ from non-biological ones in being unbranched, of constant diameter, and entangled, although no evidence for cellular organization has been reported. The filaments most likely represent remnants of thermophilic microbial communities that inhabited low-temperature marine environments around discharging hydrothermal vents. Also associated with the Sulphur Springs VMS mineralization are black seams and fragments of pyrobitumen surrounded by pyrite, chalcopyrite, sphalerite and microcrystalline silica (Rasmussen and Buick, 2000). These authors interpreted the pyrobitumen to indicate the presence of oil within the c. 3235 Ma hydrothermal fluids associated with the VMS deposits.

Leilira Formation

The Leilira Formation is locally up to 3900 m thick (Van Kranendonk and Morant, 1998), although in most areas it is only 100–500 m thick (Buick et al., 2002). The unit includes conglomerate, sandstone, wacke, shale, felsic volcanoclastic sandstone, ashfall tuff, dacite and rhyolite. However, it is uncertain if all the units mapped as rhyolite or dacite are volcanic; none has been dated, and it is possible that at least some are either sills related to the Strelley Monzogranite or felsic volcanic units older than the Sulphur Springs Group. The depositional age of the formation is loosely constrained between c. 3280 and 3255 Ma, although parts of the formation might be older, possibly up to c. 3315 Ma when doming in the EPT would have been accompanied by erosion.

The Leilira Formation unconformably overlies the Kelly Group in the far southwestern section of the Panorama greenstone belt and in the East Strelley and Warralong greenstone belts (Fig. 8, Plate 1; Van Kranendonk and Morant, 1998; Van Kranendonk, 1999a, 2000a, 2004b; Van Kranendonk et al., 2002, 2007a,b). Basal conglomerate, sandstone and wacke of the Leilira Formation are consistent with deposition above an unconformity which is interpreted to have been a consequence of erosion during and following doming contemporaneous with intrusion of the Emu Pool Supersuite. Thus, the depositional duration of the Leilira Formation might be as long as 60 Ma (Hickman, 2012).

Van Kranendonk (2004b) observed that, in the southern Warralong greenstone belt, the Leilira Formation overlies the Wyman Formation (Kelly Group) across a high-angle erosional unconformity (Fig. 35). Sandstone of the Leilira Formation in this greenstone belt includes clasts of grey and white banded chert up to 10 cm in diameter (Van Kranendonk, 2004b), and close to large hydrothermal veins of barite, the matrix of the sandstone contains ~50% barite (Hickman, 1977b). The basal unconformity is also angular in the far southwest of the Panorama greenstone belt (Van Kranendonk, 1997, 2000a).

The Leilira Formation is likely to have been deposited in environments similar to those of other major clastic units in the east Pilbara Craton; for example, the basal parts of the Soanesville and Gorge Creek Groups. Eriksson (1981, 1982) described the initial settings for these units as marine and lacustrine basins with a horst-and-graben topography.

Lateral thickness and facies changes are therefore likely to have been widespread in the Leilira Formation.

Kunagunarrina Formation

Conformably to unconformably overlying the Leilira Formation, the Kunagunarrina Formation is up to 2400 m thick (Van Kranendonk and Morant, 1998), but locally is less than 100 m thick (Buick et al., 2002) or entirely absent from the group. This formation is mainly composed of komatiitic basalt with lesser thicknesses of komatiite, tholeiitic basalt and thin units of chert and clastic and volcanoclastic rocks (Van Kranendonk and Morant, 1998). Unlike other lithologically similar formations of the Pilbara Supergroup, such as the Euro Basalt (Kelly Group), which are regionally extensive across many greenstone belts, the Kunagunarrina Formation changes thickness greatly between adjacent greenstone belts; for example, between the Pincunah greenstone belt and the northern Soanesville greenstone belt. This unusual feature has not previously been explained, although from mapping in the Warralong greenstone belt (Van Kranendonk, 2004a,b; Van Kranendonk et al., 2012) it is best explained by erosion of the Kunagunarrina Formation prior to deposition of the Kangaroo Caves Formation. In the Warralong greenstone belt, komatiitic basalt of the Kunagunarrina Formation changes thickness from 250 m to zero over a lateral distance of 500 m.

The komatiitic basalt is overlain by a 100 m-thick conglomerate composed of cobbles and pebbles of komatiitic basalt in a sandstone matrix. Van Kranendonk (2004b) described the conglomerate as having cut down through the komatiitic basalt. Above the conglomerate is a 600 m-thick clastic succession of wacke, sandstone, conglomerate (similar to the lower conglomerate), Fe-rich shale and thin, jaspilitic BIF units. This succession is disconformably overlain by an 800 m-thick succession of conglomerate, sandstone and felsic volcanoclastic rocks of the Kangaroo Caves Formation. Van Kranendonk (2004b) interpreted the cobble and pebble conglomerate and the overlying 600 m-thick clastic succession to be parts of the Kunagunarrina Formation. Alternative interpretations, which would require more detailed mapping and geochronology, are that these clastic units are parts of either the Kangaroo Caves Formation or the Corboy Formation (Soanesville Group). The lithologies described by Van Kranendonk (2004b) are more typical of the Corboy Formation.

The type section of the Kunagunarrina Formation is in the eastern Pincunah greenstone belt where a basal 500 m-thick unit of altered basalt, komatiitic basalt, thin grey and white chert units, and dolerite sills is overlain by an 850 m-thick succession of brown-weathered komatiitic basalt and minor komatiite (Van Kranendonk, 2000a). These two thick basaltic units are separated by a 10 m-thick unit of green, grey and black chert. At its base, this chert is massive but towards its top it becomes laminated. Van Kranendonk (2000a) commented that the green chert might be a silicified, fine-grained volcanoclastic unit, fining upwards and including silicified black shale towards the top.

In the southern Soanesville greenstone belt (Fig. 8, Plate 1), the Kunagunarrina Formation is composed of komatiite, komatiitic basalt and tholeiitic basalt, metamorphosed to greenschist facies. Van Kranendonk (2003) reported that, on the southern limb of the Soanesville Syncline, the formation reaches a maximum thickness of 1750 m.

However, following additional mapping, Van Kranendonk (2006) reinterpreted a thick underlying unit on the western limb of the Soanesville Syncline, previously mapped as unassigned peridotite (Van Kranendonk and Pawley, 2002), as komatiite of the Kunagunarrina Formation. This komatiite unit, locally up to 1000 m thick, was remapped (Van Kranendonk, 2006) as extending into the eastern limb of the syncline. Above the komatiite is a unit of komatiitic basalt that is about 1000 m thick that includes a central 50 m unit of carbonate-altered mafic tuff and sandstone. Above the komatiitic basalt, the top of the Kunagunarrina Formation is overlain by andesite and minor basalt of the Kangaroo Caves Formation.

In the East Strelley greenstone belt, Van Kranendonk (2000a) described the Kunagunarrina Formation as comprising a basal unit of komatiitic basalt overlain by up to 2000 m of pillowed and massive basalt and mafic schist with thin interbeds of chert. This section of the East Strelley greenstone belt is strongly faulted and distinguishing the Kunagunarrina Formation from the underlying Euro Basalt hinges on the presence of an isolated unit of wacke (Zone 50, MGA 708250E 7658500N) assigned to the Leilira Formation. In the absence of geochronology, an alternative interpretation is that the wacke is a local clastic unit within the Euro Basalt.

In the northern Soanesville greenstone the Kunagunarrina Formation is almost entirely absent, and the Kangaroo Caves Formation directly overlies the Leilira Formation. Only north of the Strelley Monzogranite, east and south of the Roadmaster base metal prospect, is a ~100 m-thick succession of komatiitic basalt and sedimentary rocks correlated with the Kunagunarrina Formation. The strike length of this unit is less than 5 km, with the lithologies being komatiitic basalt, mixed komatiite and komatiitic basalt, shale, and white, bluish-black and grey layered chert. A sample of felsic volcanoclastic sandstone from close to the top of the Kunagunarrina Formation was dated by Buick et al. (2002), and provided an interpreted maximum depositional age of c. 3255 Ma. All zircons were interpreted to be detrital, with most dated between c. 3589 and 3410 Ma. This provides additional evidence for an interval of erosion between eruption of komatiitic basalt in the Kunagunarrina Formation and deposition of the overlying felsic volcanic rocks of the Kangaroo Caves Formation.

Kangaroo Caves Formation

At the top of the Sulphur Springs Group, the Kangaroo Caves Formation has an average thickness of 1700 m. In the type area east of the Strelley Monzogranite (Soanesville greenstone belt, Plate 1), it comprises basaltic andesite, dacite, rhyolite and felsic volcanoclastic rocks, overlain by a regionally extensive 10–100 m-thick unit of chert. Buick et al. (2002) described this chert, informally known as the 'marker chert', as a silicified volcanogenic sediment, mostly felsic ash, that has been intruded by veins of black chert. Local quartz sandstone and BIF are included in the marker chert southeast of the Strelley Monzogranite (Van Kranendonk, 2000a). Most VMS Cu–Zn mineralization of the Soanesville greenstone belt is located within and immediately beneath the marker chert (Morant, 1995, 1998; Vearncombe et al., 1995). North of the Strelley Monzogranite, the marker chert is overlain by a unit of polymictic megabreccia intruded by sills of rhyodacite (Buick et al., 2002). Neptunian dykes of the

megabreccia penetrate the eroded surface of the underlying marker chert and the top of the megabreccia is silicified, forming another layer of chert (Buick et al., 2002).

In the Soanesville greenstone belt (Fig. 8), felsic volcanism producing the Kangaroo Caves Formation was genetically related to intrusion of the Strelley Monzogranite (Van Kranendonk, 2000a), a synvolcanic laccolith dated at c. 3239 Ma (Buick et al., 2002). The laccolith was emplaced as a subvolcanic magma chamber that fed the volcanic activity. Following tilting of the succession to the east, present exposures provide a cross-section through the laccolith within the stratigraphy of the Sulphur Springs Group. Intrusion of the Strelley Monzogranite drove hydrothermal circulation that silicified a unit of fine-grained, epiclastic sedimentary rocks at the top of the group, and developed several zinc–copper VMS deposits spaced at regular intervals around the monzogranite (Vearncombe et al., 1995, 1998; Brauhart et al., 1998; Morant, 1998; Brauhart, 1999; Van Kranendonk, 2000a; Pirajno and Van Kranendonk, 2005).

In the eastern Pincunah greenstone belt, the Kangaroo Caves Formation comprises andesitic tuff, quartz-porphyritic rhyolite, shale, sandstone, basalt and chert (Van Kranendonk, 2000a; Blewett and Champion, 2005). At the top of the formation is a unit of grey-blue and white banded chert (silicified felsic volcanoclastic and epiclastic detritus) up to 100 m thick. Farther west, the formation wedges out across a system of faults (Blewett and Champion, 2005).

In the Warralong greenstone belt (Fig. 8, Plate 1), Van Kranendonk, (2004b) described the Kangaroo Caves Formation as having a maximum thickness of 800 m and mainly composed of massive, felsic volcanoclastic sandstone underlain by polymictic conglomerate. The conglomerate contains numerous shards of devitrified felsic volcanic glass in addition to clasts of komatiitic basalt, altered volcanic rocks, sandstone, felsite and chert (Van Kranendonk, 2004b). In this Report, an alternative interpretation is that the Kangaroo Caves Formation in this greenstone belt is about 1500 m thick and includes a basal clastic succession that Van Kranendonk, (2004b) assigned to the Kunagunarrina Formation.

In the Panorama greenstone belt (Fig. 8, Plate 1), about 5 km southwest of the Jamesons base metal prospect, the Kangaroo Caves Formation is between 1000 and 2000 m thick, and mainly composed of rhyolite lava and pumice breccia. The rhyolite is undated and, prior to the stratigraphic revision by Van Kranendonk and Morant (1998), was correlated with the Wyman Formation of the Kelly Group (Hickman, 1980a). Other lithologies in the Kangaroo Caves Formation of this area include dacitic to rhyolitic volcanoclastic rocks, and andesitic volcanoclastic sandstone and shale. The top of the formation is defined by white-, grey-, and black-layered chert correlated with the marker chert of the Soanesville and Pincunah greenstone belts.

In the far west of the East Strelley greenstone belt (Fig. 8, Plate 1), a sample of rhyolitic volcanoclastic rock correlated with the Kangaroo Caves Formation (Hickman, 2013) was dated at 3252 ± 3 Ma (GSWA 160957, Wingate et al., 2012c). The stratigraphic relations of the formation are largely obscured by faulting and intrusion of ultramafic rocks, although mapping indicates that it overlies the Euro Basalt and underlies the Soanesville Group (Hickman, 2010; Van Kranendonk et al., 2010; Wingate et al., 2012c).

Within the EPT, the most northwesterly outcrops of the Kangaroo Caves Formation, and of the genetically related Cleland Supersuite, are in the TTSZ and along the northwestern margin of the Carlindi Dome (Fig. 5, Plate 1). Granitic rocks in this area were dated between c. 3257 and 3250 Ma (Beintema, 2003; Beintema et al., 2003) and a metamorphosed felsic volcanic rock was dated at 3253 ± 4 Ma (GSA 160258, Wingate et al., 2010). The felsic volcanic rocks of the TTSZ contain VMS mineralization, as does the Kangaroo Caves Formation in the type area east of the Strelley Monzogranite.

The geochemistry of the Kangaroo Caves Formation was described by Brauhart (1999) who recognized two geochemical suites: one with Zr/Th <23.5, and the other with Zr/Th >23.5. Both suites were tholeiitic and interpreted to belong to a high-K magma series derived from a common partial-melt source. The intermediate to felsic volcanic rocks of the Kangaroo Caves Formation have flat HREE profiles and more-fractionated LREE profiles. Brauhart et al. (1998) and Brauhart (1999) described the regional alteration system associated with mineralization in and above the Strelley Monzogranite.

Van Kranendonk and Morant (1998) and Van Kranendonk et al. (2006a) interpreted the upper Kangaroo Caves Formation as passing laterally into a 500 m-thick BIF. This was initially named the Pincunah Member but subsequently renamed as the Pincunah Banded-Iron Member (PBIM). However, for reasons discussed later in this Report, the thick BIF unit is now reinterpreted as a member of the overlying Cardinal Formation in the Soanesville Group (Table 1).

Analogies with the Fig Tree Group, Kaapvaal Craton

Although there are obvious and strong similarities between the stratigraphic successions of the Warrawoona and Kelly Groups in the Pilbara Craton and the Onverwacht Group in the Kaapvaal Craton (Fig. 4), this similarity has previously been thought to end at the Sulphur Springs Group. Whereas the Sulphur Springs Group was, until now, portrayed as mainly volcanic, the contemporaneous Fig Tree Group in the Kaapvaal Craton (Fig. 4) is described as mainly sedimentary (Glikson and Vickers, 2006; Glikson, 2014; Van Kranendonk et al., 2014b). Is this difference real and, if so, did the crustal evolution of the two cratons diverge at c. 3280 Ma?

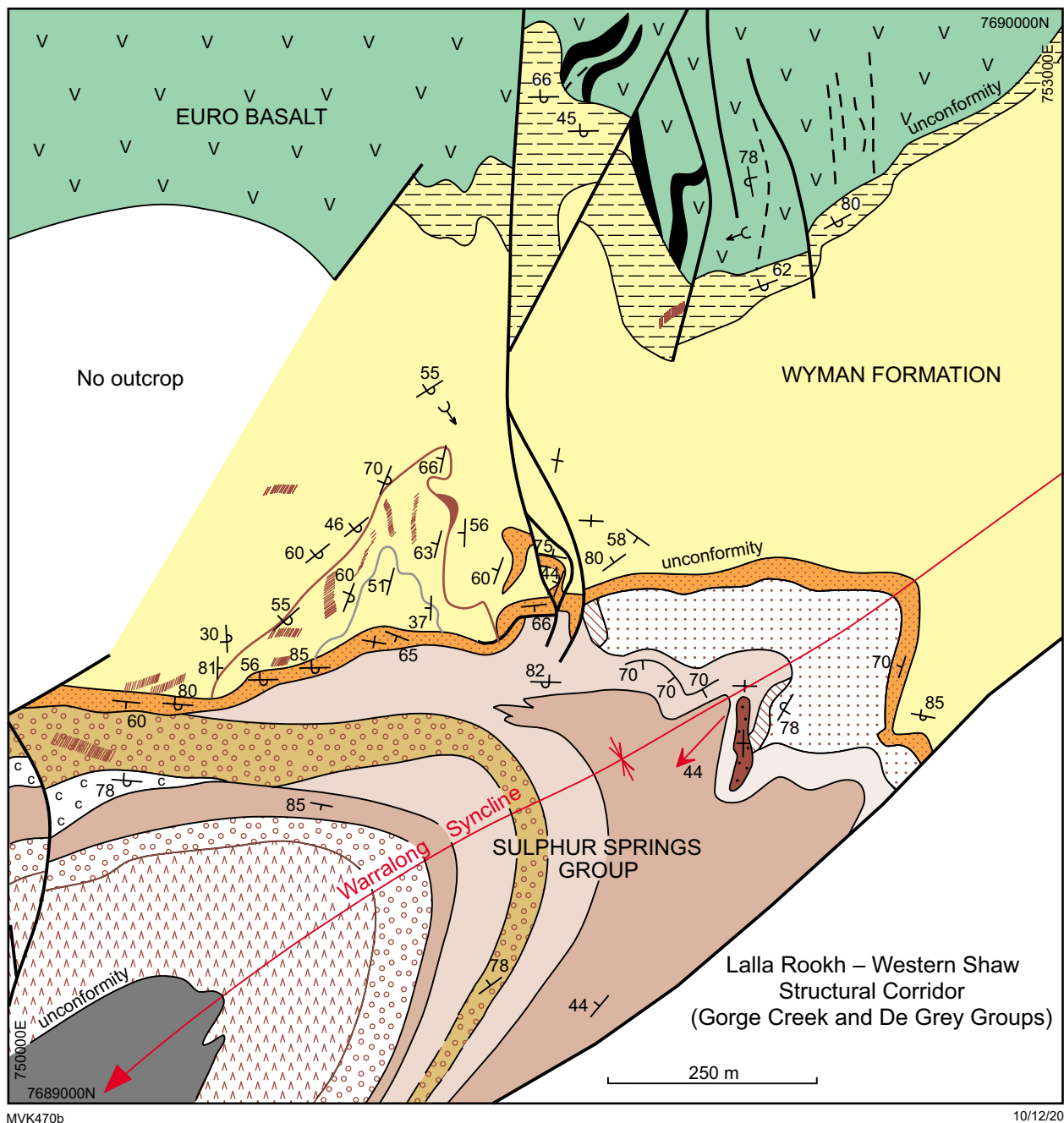
The combined age range of the Sulphur Springs Group and the Cleland Supersuite is c. 3280 to 3223 Ma (this Report), which is similar to the combined age range of c. 3260 to 3215 Ma for the Fig Tree Group and comagmatic granitic intrusions in the eastern Kaapvaal Craton (Poujol et al., 2003; Lowe and Byerly, 2007; Kisters et al., 2010). Additionally, the diverse lithological composition of the Sulphur Springs Group (conglomerate, sandstone, wacke, shale, chert, BIF, volcanoclastic rocks, komatiitic volcanic rocks and basalt-rhyolite) is similar to that of the Fig Tree Group (Lowe and Byerly, 2007). Adjacent to the Barberton Greenstone Belt (BGB) in the eastern Kaapvaal Craton, large granitic intrusions (Kaap Valley, Stentor, Nelshoogte, Badplaas, Dalmein) that were probably comagmatic with felsic volcanic rocks of the Fig Tree Group have been dated between

c. 3255 and 3215 Ma (Poujol et al., 2003; Van Kranendonk et al., 2014a). Likewise, the Cleland Supersuite, which in the EPT has been dated at 3257–3223 Ma (27 dated samples, Appendix 5), intrudes many of the domes (Van Kranendonk et al., 2006a), and was comagmatic with felsic volcanic rocks of the Sulphur Springs Group (Van Kranendonk, 2000a; Buick et al., 2002).

Deposition of the Fig Tree Group marked a major change in the crustal evolution of the BGB (Lowe and Byerly, 1999, 2007; Glikson, 2001, 2005a, 2008; Glikson and Vickers, 2006). Mainly volcanic deposition of the Onverwacht Group was replaced by mainly sedimentary deposition of the Fig Tree Group, and subsequently by coarser clastic sedimentary rocks of the Moodies Group. This is analogous to a change recognized in the Pilbara Craton between the almost entirely volcanic successions of the Pilbara Supergroup and the mainly sedimentary formations of the Soanesville Group (Van Kranendonk et al., 2002, 2006a, 2007b, 2010; Hickman, 2004, 2012). Most previous workers have interpreted the timing of these changes in the EPT and BGB to be different – c. 3225 in the EPT and c. 3260 in the BGB. However, the diverse lithological composition of the Sulphur Springs Group between EPT greenstone belts suggests that this difference may not be real. Recent detailed comparisons between the EPT and the BGB (Van Kranendonk et al., 2014a,b) concluded that the terranes were formed by the same magmatic and tectonic processes operating over the same interval of time.

Regional investigations of the stratigraphy of the Sulphur Springs Group have revealed that it is not mainly volcanic. Likewise, in the BGB, komatiitic volcanic rocks assigned to the komatiitic Weltevreden Formation overlie sedimentary rocks in part of the Fig Tree Group (Lowe and Byerly, 2007). Additionally, geochronological data reviewed by Lowe and Byerly (2007) suggest that the komatiitic Mendon Formation has an age range between c. 3298 and 3245 Ma. The sedimentary composition of the Sulphur Springs Group in some parts of the EPT is illustrated by its succession in the west Warrawoona greenstone belt (Fig. 35). Conglomerate, quartz sandstone, red-brown wacke and shale, BIF, chert and felsic volcanic rocks are predominant, with only minor komatiitic basalt (Van Kranendonk, 2004b).

Because the Fig Tree Group is composed of interlayered volcanoclastic strata (marking the final stages of volcanism) and terrigenous clastic units eroded from uplifted portions of the Onverwacht Group, Lowe and Byerly (2007) interpreted it to be a 'transitional' unit between the Onverwacht Group (volcanic) and Moodies Group (clastic sedimentary). This reasoning can also be applied to the Sulphur Springs Group, with clastic material being derived from the uplifted Warrawoona and Kelly Groups, and from erosion of pre-3290 Ma granitic supersuites. The Sulphur Springs and Fig Tree Groups were deposited in similar tectonic settings of crustal extension (Van Kranendonk et al., 2014b). Granitic intrusion between c. 3255 and 3220 Ma resulted from crustal melting associated with doming. The conclusion that both cratons were undergoing crustal extension between c. 3280 and 3220 Ma suggests that continental breakup occurred across the putative Vaalbara supercontinent at c. 3220 Ma.



MVK470b

10/12/20

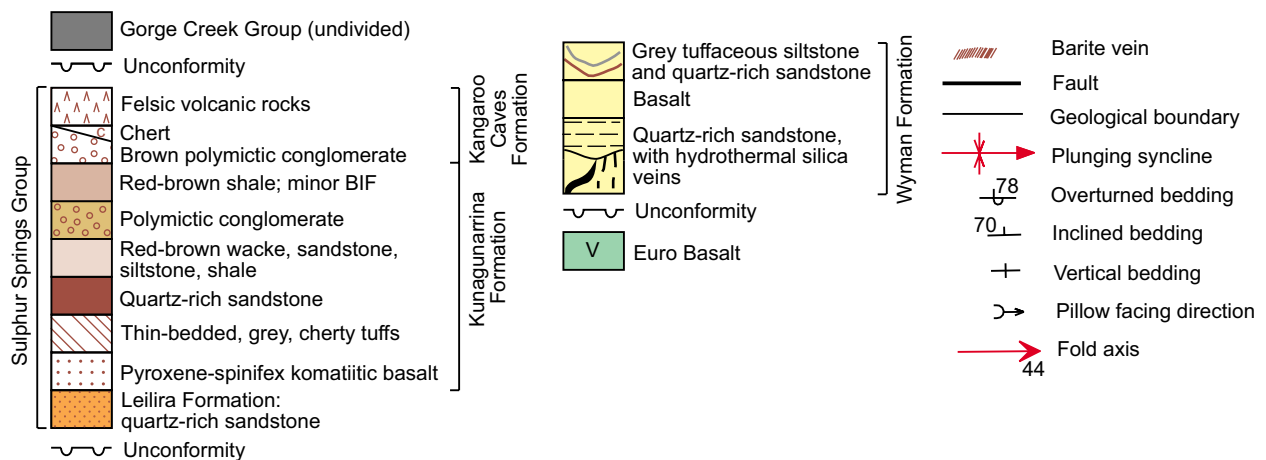


Figure 35. Geological sketch map of the southern part of the Warralong greenstone belt showing angular unconformities between the Euro Basalt and the Wyman Formation, and between the Wyman Formation and the Sulphur Springs Group (locality centred at MGA 751600E, 7688350N). From Van Kranendonk (2004b)

Large igneous provinces of the EPT

The Warrawoona and Kelly Groups are sufficiently thick and regionally extensive to be classified as large igneous provinces (LIP; Fig. 7, Plate 1C; Hickman, 2012). Ernst (2014) defined a LIP as having an aerial extent of at least 100 000 km² and an igneous volume greater than 100 000 km³. Allowing for the present-day partial concealment of the EPT by younger units, its present extent is about 100 000 km², and stratigraphic evidence indicates that both groups were deposited across this area. Moreover, the Paleoproterozoic extent of the EPT, prior to its breakup and Mesoproterozoic separation into the Karratha, East Pilbara and Kurrana Terranes, was far greater than 100 000 km².

Warrawoona LIP

The average preserved thickness of the Warrawoona Group is 10–15 km, and its original depositional extent across the EPT is interpreted to have exceeded 100 000 km². Unlike the Kelly Group, the Warrawoona Group was erupted in response to several mantle plume events (Fig. 6). Collectively, these events span c. 100 Ma which, according to LIP criteria proposed by Bryan and Ernst (2008), is too long for the formation of a single large igneous province. However, many continental LIPs are characterized by pulses of large-volume volcanic eruptions (Condie, 2001; Ernst, 2014). Available geochronology suggests that some basaltic formations of the Warrawoona Group were erupted in less than c. 5 Ma (e.g. the Mount Ada Basalt) whereas felsic volcanic formations, and contemporaneous granitic intrusions, spanned 15–30 Ma (e.g. the Duffer and Panorama Formations). The close genetic relationship between the volcanic formations and the contemporaneous granitic supersuites argues that the considerable volumes of the latter should be included in volume calculations for the Warrawoona LIP.

Because each subgroup of the Warrawoona Group was formed by a separate mantle plume event, it might be argued that each subgroup constitutes a separate LIP. However, there is insufficient exposure to assess if the subgroups meet the volume criteria for LIPs. Moreover, adoption of this interpretation would have stratigraphic implications in suggesting that the present subgroups should be redefined as 'groups', and such a significant stratigraphic revision is not proposed in this Report. One consideration is that the subgroups are separated by short intervals of time (<10 Ma) implying a close temporal relationship that is not typical of Proterozoic and Phanerozoic LIPs. It might be that the <50 Ma criterion for a single LIP, proposed by Bryan and Ernst (2008) from Phanerozoic examples formed in plate tectonic settings, is not appropriate for the early Paleoproterozoic volcanic successions of the Pilbara Craton. A precedent for this argument is that the lower Onverwacht Group of the eastern Kaapvaal Craton, which is the same age as the Warrawoona Group and is composed of a very similar volcanic succession, has been described as a 'fragmented' LIP (Ernst, 2007, 2014; Bryan and Ernst, 2008). Thus, in this Report the Warrawoona Group is assigned to the Warrawoona LIP (Fig. 7).

Mafic dyke swarms and large mafic intrusions commonly underlie eroded pre-Mesozoic continental LIPs (Ernst, 2007), and examples of these features are well exposed beneath the Apex Basalt in the Marble Bar greenstone belt.

Hundreds of closely spaced dolerite dykes intruded the >8 km-thick, c. 3470 Ma felsic crust (Callina Supersuite and Duffer Formation) underlying the Apex Basalt (Kloppenburg, 2003; Van Kranendonk et al., 2006b; Hickman and Van Kranendonk, 2008a; Hickman, 2012; Gardiner et al., 2017, 2018). The dykes cut through the MBCM at the top of the Duffer Formation and feed into the lower lava flows of the Apex Basalt. These dykes radiate from the centre of the Mount Edgar Dome (Fig. 30), but due to younger granitic intrusion and shearing, are only well preserved in relatively undeformed sections of the Marble Bar greenstone belt. This radial orientation suggests that the mafic magma intruded extensional fractures related to uplift of the dome.

Kelly LIP

The average stratigraphic thickness of the Euro Basalt is 4000 m, although it is locally up to 9400 m thick (Van Kranendonk, 2000a). The overlying Wyman Formation and Charteris Basalt have an average combined thickness of 2000 m but current evidence indicates these formations were deposited only in the eastern part of the EPT. Therefore, the Kelly LIP comprised only the Euro Basalt, which was erupted between c. 3350 and 3335 Ma. The Euro Basalt is preserved in all greenstone belts of the EPT where formations older than c. 3300 Ma are exposed, making its depositional extent similar to that of the Warrawoona Group. Given that the Pilbara and Kaapvaal Cratons may have evolved as adjacent parts of Vaalbara (Cheney et al., 1988; Cheney, 1996; Zegers et al., 1998b; Bleeker, 2003; De Kock et al., 2009; Hickman, 2012, 2016, this Report), there is a strong case to correlate the Euro Basalt with the Kromberg Formation of the Onverwacht Group. If so, the original extent of the Euro Basalt was probably at least 1 000 000 km². Eruption of the formation was accompanied by intrusion of swarms of dolerite dykes into the underlying crust; these dykes intrude the Panorama Formation and Tambina Supersuite, and are well exposed beneath the Euro Basalt, on the eastern, northern and northwestern sides of the Corunna Downs Dome (Kloppenburg, 2003; Hickman and Van Kranendonk, 2008a; Hickman, 2012). Several large mafic intrusions into the Panorama Formation of the McPhee Dome are also now interpreted to have been feeders to the overlying Euro Basalt, although they have not been dated.

Granitic supersuites of the EPT

About 70% of the exposed area of the EPT is composed of granitic intrusions that were initially mapped according to lithology and field observations of intrusive relationships. During the PCMP, the granitic intrusions were distinguished on the basis of their location in particular granite–greenstone domes and on any available geochronology. By 2004, sufficient geochronology and geochemistry had been obtained to establish a stratigraphic scheme in which all the intrusions were assigned to suites or supersuites that were common to multiple domes (Van Kranendonk et al., 2004b,c, 2006b). Eventually, the PCMP acquired U–Pb zircon crystallization ages for about 200 granitic samples collected from across the northern Pilbara Craton. Within the EPT, intrusions older than c. 3220 Ma were assigned to four granitic supersuites (Figs 5, 7, Appendices 4, 5). Recent geochronology (Petersson et al., 2019b, 2020) has revealed an additional 3530–3490 Ma supersuite. Geochronology

indicates that the four main supersuites were emplaced contemporaneously with the four major felsic volcanic formations of the Pilbara Supergroup. From oldest to youngest, the supersuites are: Callina Supersuite, emplaced during volcanism of the Duffer Formation; Tambina Supersuite, emplaced during volcanism of the Panorama Formation; Emu Pool Supersuite, intruded at the time that the Wyman Formation was erupted; and the Cleland Supersuite, emplaced during volcanism of the Kangaroo Caves Formation.

Although it has been suggested that geochemical data call into question a direct genetic link between the older supersuites and the volcanic rocks (Champion and Smithies, 2007), this Report describes several instances where particular granitic intrusions immediately underlie, and transition upwards into, felsic volcanic formations of the same age. Where there is no such visible genetic link, the relationship might be indirect. An explanation for the close coincidence between episodes of granitic intrusion and felsic volcanism is that, in different ways, both were related to the same mantle plume events as magma sources (Van Kranendonk et al., 2002, 2006b, 2007a,b). Much EPT felsic volcanism, particularly prior to c. 3420 Ma, occurred within plume-related ultramafic–mafic–felsic volcanic cycles in which magma was derived by melting of the mantle (Van Kranendonk et al., 2002, 2007a,b). For reasons noted above, subvolcanic granitic rocks probably had the same mantle origin but the majority of EPT granitic magmas were derived by melting of older mafic and TTG crust (Collins, 1993; Smithies et al., 2003, 2009). Crustally derived magmas were products of temperature increases beneath rapidly thickening volcanic successions and sagduction, both features directly related to mantle plumes. This conclusion is also consistent with previous observations that granitic intrusion was essentially synchronous with major episodes of deformation (Williams and Collins, 1990; Collins et al., 1998; Collins and Van Kranendonk, 1999; Van Kranendonk and Collins, 2001; Kloppenburg, 2003; Hickman and Van Kranendonk et al., 2004).

Each supersuite is composed of numerous individual intrusions (Table 3), most of which had been mapped and described prior to 2004. For example, the Emu Pool Supersuite comprises 24 named and unnamed intrusions ranging in age from c. 3324 to 3290 Ma, and varying in composition from tonalite to syenogranite (Table 3). Additionally, each of the supersuites is represented by intrusions in several EPT domes. The varying ages and compositions of the intrusions within individual supersuites, and their regional distributions, are important considerations before making any generalizations on subjects such as their magmatic sources. General geochemical and isotope trends are evident between the Callina and Cleland Supersuites but the degree of data scatter within these isotope trends (e.g. Figs 17, 19) might result from mixed juvenile and evolved sources for the different intrusions within any particular supersuite. In this scenario, mean isotope values, such as mean ϵ_{Hf} , are more likely to fall close to CHUR.

Once the early model of solid-state diapiric doming (Hickman, 1975a, 1981, 1983, 1984) had been modified to include syntectonic granitic intrusion (Collins, 1989; Collins et al., 1998), it became recognized that there is a strong correlation between the timing of doming events and episodes of granitic intrusion. To quote Collins et al. (1998), ‘age determination of the granitic sheets should

constrain the timing of dome and keel formation’. Thus, it can reasonably be inferred that intrusion of each granitic supersuite was accompanied by some degree of doming, and that the ages of granitic supersuites within individual domes indicates which doming events occurred in which domes. Once the granitic intrusions of the northern Pilbara Craton had been assigned to supersuites (Van Kranendonk et al., 2006a), the distribution of these supersuites revealed major regional changes in granitic intrusion through time, lending support to an earlier conclusion that different domes developed at different times (Hickman, 1984). A remarkably good example of a regional variation in the distribution of a particular supersuite is provided by the Emu Pool Supersuite (Van Kranendonk et al., 2006a).

Mulgundoona Supersuite (3530–3490 Ma)

By analogy with the Callina Supersuite and all subsequent EPT supersuites, it has been suggested that felsic volcanism in the Coonterunah and Talga Talga Subgroups was accompanied by granitic intrusion between c. 3530 and 3490 Ma (Gardiner et al., 2017, 2018). A diorite gneiss in this age range was identified in the Muccan Dome (Allen et al., 2016). Until recently the main evidence for a 3530–3490 Ma supersuite was an abundance of 3530–3490 Ma detrital zircons in Paleoproterozoic and Mesoproterozoic sedimentary rocks of the east Pilbara Craton (Figs 12–14). Because exposures of felsic volcanic rocks are relatively rare in the preserved outcrops of the Coonterunah and Talga Talga Subgroups, it is likely that most of the 3530–3490 Ma detrital zircons were derived by erosion of contemporaneous granitic rocks. Prior to voluminous granitic intrusions of the Emu Pool, Cleland and Sisters Supersuites, which collectively engulfed most pre-3420 Ma intrusions, the inferred 3530–3490 Ma granitic rocks were, based on the detrital zircon evidence, extensively exposed in some EPT domes.

Dating of granitic rocks in the Muccan and Carlindi Domes has revealed four separate outcrops of 3530–3490 Ma granitic rocks. A unit of quartz diorite gneiss in the southern part of the Muccan Dome was dated between c. 3510 Ma (Allen et al., 2016) and c. 3503 Ma (Wiemer et al., 2018). Petersson et al. (2019b) interpreted their identification of c. 3500 Ma intrusions in the Muccan and Carlindi Domes to represent parts of a supersuite contemporaneous with felsic volcanic rocks of the Coucal Formation in the Coonterunah Subgroup. A more detailed description of these intrusions is provided by Petersson et al. (2020). In the southern Muccan Dome, these workers dated a granodiorite gneiss at 3523 ± 2 Ma and a tonalite gneiss at 3502 ± 3 Ma, and in the eastern Carlindi Dome, they dated a quartz diorite gneiss at 3501 ± 1 Ma. Additionally, in the northwestern Muccan Dome a c. 3312 Ma lithologically complex gneiss included eight zircons with large rounded cores collectively dated at 3496 ± 7 Ma. Petersson et al. (2020) interpreted the four separate granitic intrusive rocks to belong to a 3530–3490 Ma supersuite, and named this the Mulgundoona Supersuite.

The present scarcity of exposed 3530–3490 Ma granitic rocks is here attributed to the process of diapiric doming in which successive granitic supersuites were intruded into the central granitic cores of each dome (Hickman and Van Kranendonk, 2004). Each intrusion displaced older supersuites outwards, towards the margins of the granitic cores, while episodic sagduction progressively dragged

down the oldest, outermost granitic rocks, along with adjacent basal greenstones, into the crust. Consequently, most remnants of pre-3490 Ma granitic rocks, and of pre-3530 Ma crust, have been discovered in sheared granite–greenstone contacts at the western margin of the Shaw Dome (McNaughton et al., 1988; Petersson et al., 2019a) and southern margin of the Muccan Dome (Wiemer et al., 2018). The present geology of the southern half of the Mount Edgar Dome (Plate 1A, Fig. 30) illustrates an example of the increasing age of granitic rocks towards a sheared granite–greenstone contact.

Callina Supersuite (3484–3462 Ma)

The Callina Supersuite is composed of sodic metagranitic rocks that outcrop in the Carlindi, Shaw, Mount Edgar, Yule and Muccan Domes (Figs 5, 8, Table 3, Plate 1). The dominant composition is mafic granodiorite, although other compositions include hornblende diorite, biotite tonalite, and less commonly monzogranite and alkali granite. Alkali granite (c. 3466 Ma Homeward Bound Granite) forms well-preserved subvolcanic intrusions in the Marble Bar area of the Mount Edgar Dome (Hickman and Lipple, 1978a,b; Van Kranendonk et al., 2006b; Hickman and Van Kranendonk, 2008a). However, many intrusions of the Callina Supersuite elsewhere are migmatized and sheared in more-strongly deformed zones near granite–greenstone contacts. Arguably, the most studied components of the supersuite outcrop in the northern Shaw Dome, and include the North Shaw Suite (Bettenay et al., 1981; Bickle et al., 1983, 1985; Van Kranendonk, 2000a; Pawley et al., 2004) which comprises the North Shaw Tonalite (Hickman and Lipple, 1978a) and the Coolyia Creek Granodiorite (Van Kranendonk et al., 2001a).

Champion and Smithies (2007) considered the Callina and Tambina Supersuites together in reaching conclusions on the granitic petrogenesis of TTG in the EPT domes. They recognized two geochemical groups: 1) low-Al granites with low Al_2O_3 , Na_2O , Sr, LREE/HREE, and high FeO^* , HREE, Y, $(\text{Gd}/\text{Yb})_N$; 2) high-Al granites with high Al_2O_3 , Na_2O , Sr, LREE/HREE, and low FeO^* , HREE, Y, $(\text{Gd}/\text{Yb})_N$. They argued that the lack of significant Eu anomalies, especially in the high-Al subgroup, coupled with a lack of correlation between Eu/Eu^* (measured Eu divided by Eu calculated from interpolation between Sm and Gd; Henderson, 1984) and MgO or SiO_2 , was inconsistent with significant fractional crystallization. Champion and Smithies (2007) commented that moderate to high Mg# in these granitic supersuites also argued against significant fractional crystallization, and that similar conclusions had been reached for TTG in other Archean terranes. They concluded that the TTG were derived by partial melting of mafic crust, although LILE- and Th-rich TTG would have also required more enriched source components, such as intermediate and felsic rocks.

Tambina Supersuite (3451–3416 Ma)

The Tambina Supersuite is mainly composed of TTG gneiss and is well exposed along the western and eastern sides of the Shaw Dome and on the south and west sides of the Mount Edgar Dome (Figs 5, 8, Plate 1). Less well-exposed sections of the supersuite form parts of the Carlindi, Muccan, Warrawagine, North Pole, Corunna Downs, Tambourah and Yule Domes. The North Pole

Dome contains only monzogranite and small subvolcanic intrusions of porphyritic rhyolite and dacite. Monzogranite and leucogranite also form parts of the Shaw, Mount Edgar and Yule Domes. Outcrops of some less-deformed intrusions of the Tambina Supersuite that are unconformably overlain by the Euro Basalt (Kelly Group) contain swarms of dolerite dykes representing feeders into the basalt. In the centre of the Warrawagine Dome and on the western side of the Shaw Dome, the Tambina Supersuite contains xenoliths of granitic and mafic intrusive rocks that pre-date the EPT by between c. 135 and 48 Ma. Belts containing numerous greenstone xenoliths are also a feature of the Tambina Supersuite in the Mount Edgar, Muccan, Shaw, Yule and Carlindi Domes. In some instances, these xenolith belts pass laterally into greenstone belts suggesting that they are the synformal root zones of eroded greenstone keels (Hickman, 1975a, 1983, 1984). This interpretation implies that some granitic cores of EPT domes contain 'second order' domal structures (Van Kranendonk et al., 2001a).

Previous investigations of the Tambina Supersuite in the Shaw Dome have revealed that its composition is mainly sodic, including tonalite and granodiorite. In the Shaw Dome, this supersuite does not display extensive migmatization and deformation, although it is cut by swarms of leucogranite veins. Widespread leucogranite in the Tambina Supersuite of the Shaw Dome represents melt derived from the Callina Supersuite (Van Kranendonk, 2000a; Pawley et al., 2004; Van Kranendonk et al., 2004a). In the Mount Edgar Dome, the Fig Tree Gneiss is compositionally banded and strongly deformed, and is interpreted to have been emplaced at mid-crustal levels and subsequently buried to depths approaching 25 km with metamorphism at upper amphibolite facies. Most workers have interpreted that TTG magmas for the Tambina Supersuite were derived by partial melting of older felsic crust, as in the case of leucogranite in the Shaw Dome (Pawley et al., 2004) or, more generally, infracrustal melting of enriched basaltic crust (Champion and Smithies, 2007; Smithies et al., 2009; Van Kranendonk et al., 2014b).

Emu Pool Supersuite (3324–3290 Ma)

The Emu Pool Supersuite comprises 3324–3290 Ma intrusions of monzogranite, granodiorite, and rare tonalite within that part of the EPT east of the CWFZ (Figs 5, 8, Plate 1). Tonalite is largely confined to the Yilgalong Dome. No intrusions of this supersuite have been identified in the Shaw and North Pole Domes. This is unlikely to be explained by insufficient dating because, with one exception, the genetically related Wyman Formation is almost entirely absent from the greenstone successions of these two domes. The exception is restricted to the eastern boundary of the Coongan greenstone belt in the Shaw Dome where the Wyman Formation is mapped (Hickman and Van Kranendonk, 2008b). Since doming was accompanied by granitic intrusion (Collins et al., 1998; Hickman and Van Kranendonk, 2004), these anomalies suggest that there was no significant c. 3315 Ma deformation in the Shaw and North Pole Domes.

The supersuite consists of widespread and voluminous granitic rocks emplaced into the granitic cores of the domes during the c. 3315 Ma doming (Hickman and Van Kranendonk, 2004) of the EPE. Except in the Yilgalong Dome (Fig. 8, Plate 1B) and adjacent Mosquito Creek Basin (Fig. 3),

all intrusions of the supersuite are older than c. 3294 Ma and most have U–Pb zircon crystallization ages between c. 3321 and 3300 Ma (Appendices 4, 5). Monzogranite intrusions in the Yilgalong Dome, dated between c. 3279 and 3274 Ma, are probably unrelated to c. 3290 Ma tonalite intrusions assigned to the Emu Pool Supersuite in this dome. Their ages follow the final stage of deformation and metamorphism between deposition of the Kelly and Sulphur Springs Groups (3325–3290 Ma EPE). The maximum age of the Emu Pool Supersuite is currently defined by a date of 3324 ± 6 Ma for the Wilina Granodiorite (unpublished data, Collins et al., 1998; Appendix 4, Table 3) in the southeast part of the Mount Edgar Dome (Plate 1). This date is questionable because Collins et al. (1998) described the intrusion as post-kinematic, which is inconsistent with the main deformation in this dome occurring at c. 3315 Ma (Van Kranendonk et al., 2001a, 2002, 2004a; Hickman and Van Kranendonk, 2004). Other geochronology on the Wilina Granodiorite indicates that the date of 3310 ± 8 Ma (GSWA 169042, Nelson, 2004d) most likely represents its crystallization age.

The full compositional range of the Emu Pool Supersuite is diorite to syenogranite. Several distinct compositional and textural phases, and plutons, have been identified in the Corunna Downs, Mount Edgar, Muccan, Warrawagine and Yilgalong Domes (Fig. 8, Plate 1). For example, many intrusions of granodiorite and monzogranite exhibit porphyritic texture in which abundant plagioclase or microcline phenocrysts are up to 5 cm long. Early mapping of the EPT recognized that feldspar phenocrysts were far more common within intrusions intermediate in age between the foliated TTGs and late-stage, post-tectonic granites associated with tin mineralization (Hickman, 1983). Work during the PCMP established that porphyritic granitic rocks of this kind are mainly confined to the Emu Pool and Cleland Supersuites.

Intrusion of the Emu Pool Supersuite accompanied volcanic eruption of the Wyman Formation (Kelly Group), and in the Mount Edgar and Corunna Downs Domes there are examples of granodiorite intrusions immediately underlying hypabyssal felsic intrusions and volcanic units. All intrusions of the supersuite are only moderately to weakly foliated because the EPT experienced relatively little deformation and metamorphism between the EPE and the North Pilbara Orogeny at c. 2.95 Ga.

The Emu Pool Supersuite is composed of both high-Al and low-Al granitic rocks, similar to the pre-3420 Ma supersuites (see **Callina Supersuite**). High-Al granitic rocks are dominant in the Mount Edgar Dome (Collins, 1993; Davy and Lewis, 1986), whereas low-Al granites are more common in the Corunna Downs Dome (Champion and Smithies, 2007). Average SiO_2 and K_2O contents are higher than in the pre-3420 Ma granitic rocks, and highest in the low-Al group. In this group, Na_2O is <4.5%, and $\text{Na}_2\text{O}/\text{K}_2\text{O}$ varies from c. 2.0 to 0.5. Unlike the high-Al group, the low-Al group has pronounced negative Eu anomalies (Eu/Eu* mostly 0.8 to <0.2). The high-Al granitic rocks exhibit a trend of increasingly negative ϵ_{Nd} values with higher K_2O , but this negative correlation is absent in the low-Al granitic rocks due to more compositional variations (Champion and Smithies, 2007). The geochemical data suggest that the high-Al granites were most likely derived by partial melting of thickened mafic crust, whereas derivation of the low-Al granites probably involved some fractional crystallization,

especially for silica-rich granites. Nd and Hf isotope data indicate more recycling of older crust in the Emu Pool Supersuite than in the Callina Supersuite (Champion, 2013; Champion and Huston, 2016; Gardiner et al., 2017). ϵ_{Nd} values for the supersuite vary from +1.49 to –1.44 and Nd model ages range between c. 3630 and 3420 Ma (Table 4).

Cleland Supersuite (3270–3223 Ma)

In the EPT, the Cleland Supersuite comprises numerous granitic intrusions with crystallization ages between c. 3257 and 3223 Ma (Table 3, Appendix 5). However, in the Karratha Terrane (KT) of the northwest Pilbara Craton, the supersuite is represented by only two intrusions: the c. 3270–3261 Ma Karratha Granodiorite and the c. 3236 Ma Tarlwa Pool Tonalite. The presence of the supersuite in the KT is consistent with its intrusion accompanying the early stage of the plume-related 3280–3165 Ma EPTRE during which the Sulphur Springs Group was deposited. Three 3279–3274 Ma monzogranite and granite intrusions in the Yilgalong Dome and adjacent Mosquito Creek Basin (Table 3) are thought to belong to a magmatic event in the far southeast EPT that was separate from intrusion of the Cleland Supersuite.

Most intrusions of the Cleland Supersuite are composed of monzogranite, although granodiorite and syenogranite are also locally present. One intrusion, the c. 3238 Ma Strelley Monzogranite, is a subvolcanic laccolith (Van Kranendonk, 2000a), and is atypical in that it exhibits rapakivi textures that are interpreted as evidence for mingling between basaltic and felsic magmas (Brauchart, 1999). Heat from the intrusion drove hydrothermal circulation that precipitated volcanogenic massive sulfide (Cu–Zn) deposits (Morant, 1998; Vearncombe et al., 1998; Huston et al., 2001d; Van Kranendonk, 2006).

Felsic magmas for the Cleland Supersuite were largely derived from melting of older granitic crust (Barley and Pickard, 1999; Smithies et al., 2003; Champion and Smithies, 2007; Van Kranendonk et al., 2007a,b; Champion and Huston, 2016). High- and low-Al granites have similar characteristics to those of the Emu Pool Supersuite (Champion and Smithies, 2007). ϵ_{Nd} values for the supersuite vary from 1.49 to –1.44 and Nd model ages range between c. 3630 and 3420 Ma (Table 4).

Granitic intrusion and felsic volcanism

Figure 10 and Plate 1C illustrate strong correlations between the ages of the four established Paleoproterozoic supersuites and those of felsic volcanic formations: the Callina Supersuite was intruded during volcanism of the Duffer Formation; the Tambina Supersuite was intruded during eruption of the Panorama Formation; the Emu Pool Supersuite was emplaced contemporaneously with eruption of the Wyman Formation; and the Cleland Supersuite was intruded at the same time as volcanism of the Kangaroo Caves Formation. So, was there a direct genetic relationship between granitic intrusion and felsic volcanism? There is widespread field evidence of instances where granitic intrusions can be traced stratigraphically upwards into subvolcanic felsic intrusions and overlying felsic volcanic formations.

Geological mapping has provided direct evidence that some granitic intrusions originated as magma chambers that fed subvolcanic laccoliths, and that these in turn released magma into overlying felsic volcanic centres. Detailed accounts of individual relationships are outside the scope of this review, but some previously described examples are as follows.

1. The c. 3466 Ma Homeward Bound Granite (Callina Supersuite) was subvolcanic to 3474–3459 Ma felsic volcanic rocks of the Duffer Formation at Marble Bar (Hickman and Lipple, 1975; Van Kranendonk et al., 2006b; Hickman and Van Kranendonk, 2008b).
2. The c. 3446 Ma North Pole Monzogranite (Tambina Supersuite) has peripheral dykes of porphyritic dacite that fed into the overlying Panorama Formation (Van Kranendonk, 1999a, 2000a; Brown et al., 2006, 2011).
3. The 3317–3314 Ma Coppin Gap Granodiorite (Emu Pool Supersuite) fed upwards into the c. 3317 Ma Spinifex Ridge Cu–Mo porphyry and 3325–3315 Ma Wyman Formation at Coppin Gap (Hickman, 1983; Van Kranendonk et al., 2006b).
4. The c. 3314 Ma Carbarua Monzogranite (Emu Pool Supersuite) is subvolcanic to the c. 3315 Ma Boobina Porphyry and the 3325–3315 Ma Wyman Formation at Copper Hills (Bagas et al., 2004c).
5. The c. 3239 Ma Strelley Monzogranite (Cleland Supersuite) is subvolcanic to the 3253–3235 Ma Kangaroo Caves Formation at Sulphur Springs (Vearncombe and Kerrich, 1999; Van Kranendonk, 2000a; Buick et al., 2002; Van Kranendonk et al., 2002; Van Kranendonk and Pirajno, 2004).
6. In the northern part of the Shaw Dome, the c. 3468 Ma North Shaw Tonalite (Callina Supersuite) intruded through the lower part of the Warrawoona Group to the stratigraphic level of the 3474–3459 Ma Duffer Formation (Plate 1A; Bickle et al., 1983, 1993; Van Kranendonk, 1999a).

The field relations of these examples establish that many granitic intrusions originated as subvolcanic magma chambers.

Geochemical data have been used to argue against direct petrogenetic relationships between some of the granitic rocks and potentially correlative volcanic formations (Collins, 1993; Champion and Smithies, 2007; Smithies et al., 2007a,b, 2019; Van Kranendonk et al., 2007a, 2014b, 2019), particularly for the Callina and Tambina Supersuites and the contemporaneous felsic volcanic formations of the Warrawoona Group. In these instances, the similar timing of granitic intrusion and felsic volcanism might be due to both being linked to individual mantle plume events (Van Kranendonk et al., 2002, 2006b, 2007a,b), with felsic magmas being derived either by fractionation of basaltic magmas or by partial melting of older continental crust (Champion and Smithies, 2001, 2007, 2019; Bagas et al., 2003; Smithies et al., 2003, 2007, 2019). Nd and Hf isotope data indicate that crustal recycling became increasingly prevalent during the evolution of the EPT (Champion, 2013; Champion and Huston, 2016; Gardiner et al., 2017, 2018).

Secular trends

From c. 3530 to 3220 Ma, the compositions of EPT granitic rocks exhibit a secular change from mainly TTG before c. 3420 Ma to granodiorite–monzogranite and syenogranite at c. 3325 to 3220 Ma (Smithies, 2000; Smithies and Champion, 2000; Champion and Smithies, 2001, 2007; Smithies et al., 2003; Van Kranendonk et al., 2002, 2006a, 2007a,b). This trend has mostly been attributed to increased crustal recycling with time (Bickle et al., 1993; Collins, 1993; Van Kranendonk et al., 2007a,b; Smithies et al., 2009). Most isotope data support this generalization, with relatively juvenile Nd and Hf isotope signatures between c. 3530 and 3420 Ma and more evolved signatures in granitic rocks younger than 3325 Ma (Champion, 2013; Champion and Huston, 2016; Gardiner et al., 2017, 2018; this Report, Figs 17, 19).

The interpretation that the geochemical trends observed in EPT Paleoproterozoic granitic rocks are due to increased magma generation by remelting of older crust with time, rather than to ongoing episodic additions of new juvenile magma, argues against Phanerozoic-style subduction. Additionally, the Paleoproterozoic TTGs have lower Mg# (mostly 10–45), Cr (mostly <50 ppm) and Ni (<40 ppm) contents than younger TTG (Smithies et al., 2009), and thus provide no evidence for interaction with a mantle component (i.e. mantle wedge; Smithies, 2000; Martin et al., 2005). Smithies et al. (2009) commented that these relationships suggest partial melting of older mafic crust rather than derivation of melts from a subducted slab. Nd model ages (Champion, 2013) calculated from data obtained by McCulloch (1987) and Bickle et al. (1993) from the 3485–3420 Ma TTG suggest that the mafic source was up to 200 Ma older than the Pilbara Supergroup (Smithies et al., 2009; Gardiner et al., 2017, 2018).

Breakup of the EPT at c. 3220 Ma appears to have interrupted, although not terminated, crustal recycling. The next granitic rocks to intrude the EPT were TTGs of the 3199–3164 Ma Mount Billroth Supersuite that have isotope signatures indicating juvenile sources.

Tectonic processes in the EPT

Before publication of data from the 1994–2005 PCMP, some tectonic interpretations of the EPT were based on Phanerozoic plate tectonic paradigms (Bickle et al., 1980, 1985, 1993; Kimura et al., 1991; Isozaki et al., 1991; Barley 1993, 1997; Zegers et al., 1996, 2001; Barley et al., 1998; van Haaften and White, 1998; Barley and Pickard, 1999; Vearncombe and Kerrich, 1999; Kitajima et al., 2001; Kloppenburg et al., 2001; Blewett, 2002; Komiya et al., 2002; Kato and Nakamura, 2003; Kloppenburg 2003; Terabayashi et al., 2003). The PCMP provided evidence requiring a revised interpretation of the geology and evolution of the EPT (Smithies, 2000; Smithies and Champion, 2000; Van Kranendonk et al., 2001a, 2002, 2004a, 2006a, 2007a,b; Huston et al., 2002; Smithies et al., 2003, 2005b, 2007a,b,c, 2009; Hickman, 2004; Hickman and Van Kranendonk, 2004; Champion and Smithies, 2007). Extensive data obtained from the project, and from research outside the project (Sandiford et al., 2004; Thébaud and Rey, 2013; François et al., 2014; Johnson et al., 2017), supported earlier conclusions that important features of the EPT did not originate through Phanerozoic-style plate tectonic processes (Hickman, 1981, 1983, 1990; Collins, 1989; Van Kranendonk, 1997, 1998; Collins et al., 1998).

The most obvious feature of the EPT without any close modern analogues is its regional-scale dome-and-keel crustal architecture. Although there have been suggestions that this distinctive crustal structure originated as a metamorphic core complex and was modified by younger deformation (Zegers, 1996; Zegers et al., 1996, 2001; Kloppenburg et al., 2001; Kloppenburg, 2003), there are many lines of evidence inconsistent with this suggestion (Hickman and Van Kranendonk, 2004; Pawley et al., 2004; Van Kranendonk et al., 2004a).

Doming and sagduction

A major constraint on tectonic models for the EPT is provided by its dome-and-keel crustal architecture (Fig. 8, Plate 1). Stratigraphic and geochronological lines of evidence establish that development of the dome-and-keel structure was integral to the Paleoproterozoic evolution of the EPT (Hickman, 1980e, 1981, 1984; Hickman and Van Kranendonk, 2004; Pawley et al., 2004; Van Kranendonk et al., 2004a, 2007a,b). Interpretations that the dome-and-keel structure originated in the Mesoproterozoic (Bickle et al., 1980, 1985, 1989; Bettenay et al., 1981; Boulter et al., 1987; Zegers, 1996; Zegers et al., 1996, 2001; White et al., 1998; Blewett, 2002) took no account of the link between doming and the Paleoproterozoic stratigraphy of the EPT. They are also inconsistent with geochronological data from the PCMP (Van Kranendonk et al., 2002, 2004a,b, 2006a, 2007a; Hickman and Van Kranendonk, 2004, 2008a). Detailed descriptions of the doming process, and explanations of why the domes could not have been produced by horizontal tectonic processes, have already been published (Hickman, 1984; Collins et al., 1998; Hickman and Van Kranendonk, 2004; Sandiford et al., 2004; Van Kranendonk et al., 2004a; Thébaud and Rey, 2013; François et al., 2014), and are not repeated in this Report. However, various additional observations are made.

The major vertical uplifts that occurred during episodes of Paleoproterozoic deformation in the EPT effectively preclude tectonic models other than diapiric doming. For example, metamorphic evidence, in conjunction with geochronology, indicates 20–25 km vertical uplift of some dome cores between c. 3445 and 3280 Ma (Délor et al., 1991; Collins and Van Kranendonk, 1999; Pawley et al., 2004; Van Kranendonk et al., 2004a; François et al., 2014). In other instances, relative vertical displacements between adjacent domes, as measured by stratigraphic mis-matches across boundary faults, exceed 10 km (Hickman, 2001b).

Domal uplift of the granitic cores was accompanied by adjacent greenstone basin subsidence because the doming and basin sinking (sagduction) are interrelated parts of a mass transfer process (Thébaud and Rey, 2013). At the same time that the granitic cores of the EPT domes were uplifted by many kilometres, the adjacent greenstones were sagducted deep into the crust (Collins, 1989; Collins et al., 1998; Hamilton, 2007; Bedard et al., 2013; Thébaud and Rey, 2013), and probably to the base of the crust (François et al., 2014). Generation of magmas of TTG composition by partial melting of mafic sources (Glikson, 1971, 1972, 1978; Smithies, 2000; Smithies et al., 2003, 2009; Van Kranendonk et al., 2014b) raises the possibility that TTG sources included basalts of the Pilbara Supergroup, as suggested by Smithies et al. (2007b, 2009). A consequence of sagduction is likely to have been that the basaltic sources for TTGs included

basaltic formations of the Warrawoona Group (Hickman, 1983, p. 174) in addition to partial melting of older mafic crust. Some Nd model ages younger than c. 3530 Ma indicate sources within the age range of the Warrawoona Group.

Granite–greenstone relationships

A notable feature of EPT granitic intrusions is that those exposed in the apices of domes preserve primary, discordant, intrusive contacts with overlying formations of the Pilbara Supergroup, whereas those exposed on steep sides of domes do not. Many of the former intrusions pass upwards into subvolcanic intrusions and overlying felsic volcanic formations. Additionally, unlike granitic intrusions exposed on the sides of domes, where they typically have well-developed metamorphic fabrics and are strongly sheared at greenstone contacts, those in dome apices are typically massive, compositionally homogeneous, even-grained, and contain little or no tectonic foliation. These differences are consistent with the interpretation that the domes formed as diapiric structures (Hickman, 1984; Collins et al., 1998; Hickman and Van Kranendonk, 2004; Van Kranendonk et al., 2004a).

Conversely, these well-preserved intrusive relationships are difficult to reconcile with metamorphic core complex models that have been proposed for formation of the EPT domes (Bickle et al., 1980, 1985; Boulter et al., 1987; Zegers, 1996; Zegers et al., 1996; van Haaften and White, 1998, 2001; Kloppenburg et al., 2001; Kloppenburg, 2003). In a core complex model, the main granite–greenstone contact around the entire profile of a dome should be a major shear zone produced by mid-crustal detachment and lateral movement; primary intrusive relationships at such a contact would have been destroyed. Examples of well-preserved intrusive relationships at dome apices include:

- the c. 3468 Ma North Shaw Tonalite in the northern Shaw Dome (Hickman and Lipple, 1975; Bettenay et al., 1981; Bickle et al., 1983, 1993; Van Kranendonk, 1999a, 2000a)
- the c. 3466 Ma Homeward Bound Granite in the northwestern Mount Edgar Dome (Hickman and Lipple, 1975; Hickman, 1983; Van Kranendonk et al., 2006b; Hickman and Van Kranendonk, 2008a,b)
- the c. 3446 Ma North Pole Monzogranite in the North Pole Dome (Van Kranendonk, 1999a, 2000a; Brown et al., 2006, 2011)
- the c. 3427 Ma Bookargemoona Tonalite in the Corunna Downs Dome (Bagas et al., 2004c; Hickman and Van Kranendonk, 2008a)
- the 3315 Ma Coppin Gap Granodiorite in the Mount Edgar Dome (Hickman, 1983; Van Kranendonk et al., 2006b)
- the c. 3314 Ma Carvana Monzogranite and related c. 3315 Ma Boobina Porphyry in the Corunna Downs Dome (Hickman and Lipple, 1975; Lipple, 1975; Barley and Pickard, 1999; Bagas et al., 2004c)
- the c. 3313 Ma Gobbos Granodiorite in the McPhee Dome (Barley, 1982; Barley and Pickard, 1999; Bagas, 2005).

Timing and magnitude of doming

The first indications that the 11 individual domes of the EPT (Fig. 8, Plate 1) were not formed at precisely the same times, and were not developed to the same extents during individual doming events, came from stratigraphic comparisons between greenstone belt successions (Hickman, 1981, 1984). More direct evidence on the timing of deformation events became available with the extensive acquisition of isotopic ages from 1994 onwards, in particular from U–Pb zircon geochronology conducted during the PCMP. There is now general agreement that EPT granitic intrusions younger than c. 3450 Ma were synkinematic (Collins, 1989, 1993; Williams and Collins, 1990; Zegers et al., 1996; Collins et al., 1998; Van Kranendonk et al., 2002, 2004a; Kloppenburg, 2003; Hickman, 2004; Hickman and Van Kranendonk, 2004; Pawley et al., 2004; Sandiford et al., 2004), and therefore peak periods of granitic intrusion coincided with deformation which, in the EPT, was doming.

Another line of evidence is provided by the age ranges of plume-related groups and subgroups of the Pilbara Supergroup (Fig. 6). Stratigraphic and geochronological evidence indicate that major deformation events occurred towards the end of each volcanic cycle. Lastly, angular unconformities in the succession indicate erosion following uplift.

Current evidence on the timing of tectonic events (see **Tectonic Events in the EPT and East Pilbara Terrane Rifting Event, 3280–3165 Ma**) indicates doming at 3490–3477 Ma (towards the end of Talga Talga Subgroup deposition), 3470–3459 Ma (towards the end of the Coongan Subgroup), 3455–3440 Ma (early Salgash Subgroup), c. 3420 Ma (late Salgash Subgroup), 3360–3325 Ma (between the Euro Basalt and the Wyman Formation in the Kelly Group), 3325–3290 Ma (at the end of Kelly Group deposition), c. 3240 Ma (at the end of Sulphur Springs Group deposition), and c. 2950 Ma (during the North Pilbara Orogeny). However, it is emphasized that from c. 3460 Ma, the various domes of the EPT developed at different rates, and some domes preserve little or no evidence of some events, particularly after c. 3335 Ma. The event histories of all the EPT domes are briefly examined later in the Report (**Event history of EPT domes**).

The evidence on the timing of doming is not consistent with a recent suggestion of c. 100 Ma growth cycles in the evolution of the EPT (Wiemer et al., 2018). This proposed cyclicity was based on a concept that there were three events of ‘crustal overturn’, namely at 3460–3413 Ma, 3325–3300 Ma, and 3250–3200 Ma. These times of doming, or ‘partial convective overturn’ (PCO, Collins et al., 1998), were previously inferred during compilation of evidence from the PCMP (Van Kranendonk et al., 2002, 2004a, 2006a, 2007a,b). Importantly, these early conclusions were based largely on data from only two of the eleven domes (the Mount Edgar and Shaw Domes), in combination with an assumption that each doming event extended across the EPT. This assumption was influenced by the recognition of closely contemporaneous volcanic cycles in the greenstone belts of different EPT domes, and by the explanation that the cycles were related to mantle plumes (Van Kranendonk et al., 2002). Since the volcanic products of plumes typically extend for 2000 km or more, it was thought that related deformation would have a similar extent.

However, a review of the event history of EPT domes in this Report shows that the stratigraphic development of the individual domes after c. 3335 Ma was different. Additionally, the magnitude of doming during any given event was not the same in all domes. Major differences in relative uplift of adjacent domes are locally revealed across the boundary faults that separate them (Van Kranendonk, 1998; Hickman, 2001b; Hickman and Van Kranendonk, 2004). Tectonic activity in the domes was triggered by regional events, but responses differed between the domes. The available evidence indicates that some doming events were localized and had little or no impact on the evolution of some of the domes.

For example, there is little evidence for 3325–3300 Ma granitic intrusion or significant uplift in the Shaw and North Pole Domes, or anywhere else in the western half of the EPT. Zegers (1996) and Zegers et al. (1996) recorded no $^{40}\text{Ar}/^{39}\text{Ar}$ evidence for c. 3300 Ma metamorphism in the Shaw Dome, whereas a significant metamorphic event of this age was identified in the Mount Edgar and Corunna Downs Domes (Zegers, 1996; Zegers et al., 1996, 1999; Kloppenburg, 2003). The Emu Pool Supersuite, which was intruded during this event, has been identified in only six domes of the EPT (Corunna Downs, Mount Edgar, Muccan, Warrawagine, Yilgalong and McPhee Domes; Van Kranendonk et al., 2006a), which is important in view of the tectonic model introduced by Collins et al. (1998), and adopted by subsequent workers, that Paleoproterozoic doming was accompanied by major granitic intrusion. At present, it is unknown why the Emu Pool Supersuite, the Wyman Formation and the 3325–3290 Ma doming event did not extend west from the Mount Edgar, Corunna Downs, and Muccan Domes into the Shaw and North Pole Domes.

Sense of movement on ring faults and shear zones

Based on plate tectonic models, it has been suggested that Paleoproterozoic granitic intrusion in the Shaw and Mount Edgar Domes was contemporaneous with horizontal deformation (Bickle et al., 1983, 1985, 1993; Bettenay et al., 1981; Zegers, 1996; Zegers et al., 1996, 2001; White et al., 1998; Kloppenburg et al., 2001, 2003). In particular, the ‘metamorphic core complex model’ applied by Zegers (1996) and a few others (White et al., 1998; Kloppenburg et al., 2001) interpreted major shear zones around the margins of the Shaw and Mount Edgar Domes to have originated as regionally extensive horizontal structures. However, these models are inappropriate for the EPT for reasons previously documented (Collins et al., 1998; Van Kranendonk et al., 2001a,b, 2002, 2004a; Hickman and Van Kranendonk, 2004). Evidence that the deformation accompanying granitic intrusion was vertical is:

- structural (Hickman, 1975a, 1981, 1984; Collins, 1989, 1993; Collins et al., 1998; Van Kranendonk et al., 2001a,b, 2002, 2004a, 2007a,b)
- metamorphic (Délor et al., 1991; Collins and Van Kranendonk, 1999; Hickman and Van Kranendonk, 2004; Van Kranendonk et al., 2004a; François et al., 2014)
- geochemical (Smithies and Champion, 2000; Champion and Smithies, 2007; Van Kranendonk et al., 2007a,b)
- isotopic (Van Kranendonk et al., 2007a,b; Kemp et al., 2011; Champion, 2013; Champion and Huston, 2016; Gardiner et al., 2017, 2018).

On the southwestern side of the Mount Edgar Dome, major vertical uplift on the 3440–3300 Ma Limestone Shear Zone (Fig. 30) is indicated by kyanite in felsic schist of the Duffer Formation. Based on pressure–temperature estimates of 5.5 – 6.0 kbar and 500–600 °C (Délor et al., 1991), Collins and Van Kranendonk (1999) argued for diapiric uplift from burial depths of ~25 km. François et al. (2014) reported data from garnet-bearing metasedimentary rocks and metabasalts from the same shear zone. The data indicated equilibration pressures and temperatures of 9–11 kbar and 450–550 °C, and they concluded that these units had been subject to rapid diapiric uplift from lower levels of the crust. Several lines of evidence establish that changes of metamorphic grade across these shear zones are not mid-crustal detachments formed as parts of metamorphic core complexes. In particular, the shear zones are not regional structures extending around all the individual domes; rather, they were formed in individual domes, and only along those granite–greenstone contacts where relative movement exceeded several kilometres. None of the domes contains Paleoproterozoic shear zones extending over more than 40% of dome circumference, and some domes (e.g. Corunna Downs Dome) have no shear zones.

Excellent structural data are available from the Mount Edgar, Corunna Downs and Shaw Domes, including stretching lineations within the 3440–3300 Ma tectonic foliations rimming the domes. In the Mount Edgar Dome (Fig. 30), these lineations consistently plunge steeply to vertically around the sides of the dome (Hickman, 1984), testifying to stretching associated with uplift rather than folding of horizontal lineations as suggested by Kloppenburg et al. (2001). The lineations have a radial orientation around the Mount Edgar (Fig. 30), Shaw and Corunna Downs Domes (Collins, 1989; Collins and Van Kranendonk, 1998; Van Kranendonk et al., 2002, 2004a, 2007a,b, 2014b; Hickman and Van Kranendonk, 2004; Gardiner et al., 2017, 2018), which is consistent with diapiric doming.

On a regional scale, the EPT domes are separated by major faults and shear zones (Fig. 8, Plate 1), across which stratigraphic displacements between adjacent greenstone belts indicate relative vertical movements of up to 10 km (Van Kranendonk, 1998; Hickman, 2001b; Hickman and Van Kranendonk, 2004). These faults and shear zones were produced by different rates and amounts of uplift between adjacent domes. Sections of Paleoproterozoic shear zones parallel to Mesoproterozoic faults were reactivated in the Mesoproterozoic, and probably influenced the location of major Mesoproterozoic structures.

Certain of the faults, such as two separating the Mount Edgar Dome from the Muccan and Corunna Downs Domes, and another separating the Corunna Downs and Shaw Domes, were intruded by large ultramafic–mafic intrusions assigned to the Dalton Suite (Hickman 2010; Hickman and Van Kranendonk, 2012). These intrusions are interpreted to have been emplaced during the regional crustal extension of the 3280–3165 Ma EPTRE (Fig. 7) that commenced during deposition of the Sulphur Springs Group. The mylonite fabric in the shear zone that separates the Shaw and Corunna Downs Domes is overgrown by crosscutting rosettes of actinolite that Zegers et al. (1999) dated at 3197 ± 44 Ma ($^{40}\text{Ar}/^{39}\text{Ar}$). This result indicates that older movement in the greenstones between the domes was Paleoproterozoic, and that the large ultramafic–mafic intrusion containing the shear zone was emplaced before c. 3200 Ma. The TTSZ, which

was also originally a product of the rifting event, contains a large intrusion of gabbro dated at c. 3235 Ma (Beintema et al., 2001; Beintema, 2003).

Effects of doming on stratigraphy

Evidence that the Paleoproterozoic stratigraphy of the Pilbara Supergroup was greatly influenced by syndepositional doming is provided by erosional unconformities and lateral changes of volcanic facies and formation thicknesses.

Erosional unconformities

Unconformities within the Pilbara Supergroup (Fig. 6, Table 1) record times when parts of the EPT plateau were uplifted and subjected to subaerial erosion. Paleoproterozoic uplift is interpreted to have resulted either from uplift above mantle plumes or from the diapiric doming that produced the dome-and-keel crustal architecture of the terrane. Plume-related uplift is normally regionally extensive (area diameter >1000 km) and moderate (maximum uplift of 1–2 km; Condie, 2001), whereas diapiric uplift is localized to individual domes (area diameter <100 km) and involves much greater vertical movement (up to 20 km; Délor et al., 1991; Collins and Van Kranendonk, 1999; François et al., 2014).

The first deformation event in the EPT occurred at c. 3480 Ma, resulting in unconformities at the level of the Dresser and McPhee Formations (GSWA 148498, Nelson, 2000m; GSWA 180070, Wingate et al., 2009e). These erosional breaks separate the correlated Coonterunah and Talga Talga Subgroups from the overlying Coongan Subgroup (Fig. 6, Table 1), and define a hiatus between major volcanic cycles. Notably, the c. 3481 Ma Dresser Formation contains a large detrital zircon age component at c. 3520 Ma (GSWA 180070, Wingate et al., 2009e; Figure 12b) that indicates erosion of the Coonterunah Subgroup at c. 3480 Ma.

A second, more regionally extensive erosional event is indicated between deposition of 3474–3459 Ma felsic volcanic rocks of the Duffer Formation and the overlying MBCM and Apex Basalt (DiMarco and Lowe, 1989b). Clastic and chemical deposition formed the 100 m-thick MBCM which is regionally extensive in the EPT (Glikson et al., 2016; Fig. 23, Plate 1). Clastic sedimentary units exposed at this stratigraphic level contain detrital zircons dated at 3650–3570 Ma (see Fig. 15), suggesting exposure of felsic crust considerably older than the Warrawoona Group (Van Kranendonk et al., 2002).

Evidence for two subsequent erosional events between c. 3445 and 3420 Ma is provided by stratigraphic and geochronological data. Erosion of the Apex Basalt prior to deposition of the upper Panorama Formation (Hickman, 2011) indicates uplift and erosion at 3445–3440 Ma. A younger unconformity, at c. 3426 Ma (Hickman, 2008), separates the upper Panorama Formation from the Strelley Pool Formation (Van Kranendonk, 2010a).

In the northwestern EPT these separate erosional events are represented by an erosional unconformity at the base of the Strelley Pool Formation (Buick et al., 1995). There is at least one unconformity within the Strelley Pool Formation (Allwood et al., 2007a), most likely reflecting c. 3360 Ma plume-related uplift and erosion prior to the Kelly Group volcanic cycle (see **Strelley Pool Formation**).

In the eastern half of the EPT, local unconformities are present between the Euro Basalt and the Wyman Formation (Hickman and Lipple, 1975; Hickman, 1983; Barley and Pickard, 1999; Van Kranendonk, 2004b), indicating uplift and erosion prior to deposition of the 3325–3315 Ma Wyman Formation. In this part of the EPT, the Emu Pool Event (Hickman and Van Kranendonk, 2008b) was a major event of diapiric doming, metamorphism, and granitic intrusion that was followed by deep erosion. The Leilira Formation (Sulphur Springs Group) was deposited across the resulting erosional unconformity (Van Kranendonk, 2000a; Buick et al., 2002; Van Kranendonk et al., 2002, 2006b, 2007a,b).

Regional extension and rifting of the Paleoproterozoic volcanic plateau increased during deposition of the Sulphur Springs Group until breakup of the EPT between c. 3220 and 3200 Ma (Hickman, 2004; Van Kranendonk et al., 2006b, 2007b, 2010). During plate separation, a clastic passive-margin succession (Soanesville Group) was deposited on the eroded Sulphur Springs Group, resulting in an angular unconformity (Buick et al., 2002).

Unconformities within the Pilbara Supergroup testify to episodic uplift, erosion and subsidence of the volcanic plateau. These unconformities are either local and confined to particular domes, or regional with variable magnitude and style (angular erosional to disconformity) across the terrane. This is consistent with lateral variations in crustal uplift during diapiric doming.

Lateral changes of facies and thickness

Owing to the geodynamic evolution of the EPT dome-and-keel structure, the presently exposed greenstones are unlikely to include the deepest basin successions that were deposited between the rising domes. Such central basin successions are now either concealed by younger successions in the greenstone belts, or were sagducted during Paleoproterozoic diapirism. The presently exposed greenstone successions represent only those parts of the Pilbara Supergroup that were not sagducted and not eroded from the tops of the domes. Therefore, the most likely depositional setting of the exposed successions was on the flanks of the domes, although some greenstone sections might include successions that slid off the tops of the domes during uplift (Gorman et al., 1978; Collins, 1989; Van Kranendonk and Collins, 1998). If granite doming and basin subsidence were contemporaneous, all formations would change thickness laterally between the margins and centres of the depositional basins. As the amplitude of the domes progressively increased, younger formations would tend to be thickest farther into the basins (Van Kranendonk et al. 2004a, 2007b, 2014b).

There appears to be at least one exception to the generalization that deep-water basin successions are not preserved and exposed. The greenstone-dominated North Pole Dome (Fig. 8, Plate 1A) is a low amplitude dome and exposes sections of three basaltic formations (North Star Basalt, Mount Ada Basalt and Euro Basalt) that were most likely deposited remote from surrounding areas of major diapiric uprise (Shaw, Yule, Carlindi, Muccan, Mount Edgar and Corunna Downs Domes). In this area, the North Star Basalt is at least 3 km thick (base not exposed), the Mount Ada Basalt is about 5 km thick, and the Euro Basalt is 9.4 km thick (Van Kranendonk, 2000a). Significantly, the Mount Ada Basalt and Euro Basalt thicknesses are greater than anywhere else in the EPT.

By contrast, the thickest felsic volcanic successions are located close to granite contacts on the flanks of the domes. This feature is exemplified by the Duffer Formation in the Mount Edgar, Shaw and Muccan Domes, the Panorama Formation in the McPhee and Corunna Downs Domes, and the Kangaroo Caves Formation in the Soanesville greenstone belt. Such abnormally thick felsic sections have previously been explained as representing parts of felsic volcanic centres (Hickman and Lipple, 1975; Barley et al., 1979, 1998; Hickman, 1980a, 1981, 1983; Barley, 1981, 1984, 1993; DiMarco, 1986; DiMarco and Lowe, 1989a,b; Van Kranendonk, 1998; Van Kranendonk et al., 2002), with felsic magmas sourced from subvolcanic intrusions within or immediately above the granitic cores of the domes (Barley, 1981; Vearncombe and Kerrich, 1999; Van Kranendonk, 2000a; Buick et al., 2002; Van Kranendonk et al., 2002, 2006b; Bagas et al., 2004c; Van Kranendonk and Pirajno, 2004; Hickman and Van Kranendonk, 2008a). Lateral changes of volcanic and sedimentary facies outwards from the felsic volcanic centres (Barley, 1981, 1984, 1993; DiMarco, 1986; DiMarco and Lowe, 1989a,b) also imply lateral volcanic facies changes down the sides of the domes and into the basins.

Tectonic setting of the EPT

Evidence from the PCMP indicates that the EPT evolved as an extensive Paleoproterozoic volcanic plateau (Van Kranendonk et al., 2002, 2007a,b, 2014a), consistent with an earlier interpretation that the Pilbara Supergroup was deposited on older sialic crust as a 15–20 km-thick, laterally continuous succession (Hickman, 1975a, 1981, 1983). Nd isotope data obtained in the 1980s (Hamilton et al., 1981; Jahn et al., 1981; Gruau et al., 1987) are consistent with pre-3530 Ma crustal sources for the Talga Talga Subgroup. A large body of subsequent evidence confirming the existence of Eoarchean to early Paleoproterozoic crust is collated in this Report.

One interpretation of the EPT plateau has been that the tectonic setting was similar to that of a modern oceanic plateau such as the Kerguelen Plateau (Arndt et al., 2001; Van Kranendonk and Pirajno, 2004; Van Kranendonk et al., 2007a,b, 2014b). This interpretation is partly based on the Pilbara Supergroup including thick units of subaqueous basalt (Arndt, 1999; Van Kranendonk and Pirajno, 2004). However, evidence in this Report indicates that the tectonic setting of thick, subaqueous basaltic successions in individual greenstone belts was most likely basins subsiding between simultaneously rising domes, and not deep submergence of the entire terrane in an oceanic setting. From c. 3470 Ma onwards, the increasing volume of felsic igneous rocks in the EPT, combined with felsic components in the underlying pre-3530 Ma sialic crust, would have made it too buoyant for complete oceanic submergence, yet the 3350–3335 Ma Euro Basalt is locally up to 9400 m thick (Van Kranendonk, 2000a).

Features of the EPT that are inconsistent with an oceanic plateau model include:

- its evolution over about 300 Ma compared to an average duration of about 100 Ma for most modern oceanic plateaus
- stratigraphic and geochronological evidence that for about half the evolution of the EPT, it was subject to

subaerial erosion and shallow-water sedimentation (Dresser and McPhee Formations, 3500–3474 Ma; Strelley Pool Formation, 3426–3350 Ma; Leilira Formation, 3290–3255 Ma)

- modern oceanic plateaus do not have dome-and-keel crustal architectures, which establishes that the EPT evolved by different tectonic processes
- modern oceanic plateaus do not contain greater volumes of granitic rocks than basaltic volcanic rocks
- assuming the Pilbara Craton was part of Vaalbara (see **Introduction**), the probable area of the plateau was >1 000 000 km², which is considerably greater than most modern oceanic plateaus (50 000 to 150 000 km²; Harris et al., 2014).

Two other considerations argue against an oceanic plateau model to explain the evolution of the EPT. First, in modern oceanic plateaus that are interpreted to be underlain by continental crust, this crust is interpreted to have originated by plate tectonic processes (continental breakup and plate separation). However, evidence from the Pilbara Craton indicates that the onset of plate tectonic processes occurred after c. 3220 Ma. Smithies et al. (2018) used Th/Yb vs Nb/Yb plots (Pearce, 2008) to suggest that fully developed modern-style plate tectonic processes did not play any significant role in the Archean before c. 2650 Ma. Second, it is unknown if there were any Paleoproterozoic oceans of sufficient size to accommodate a >1 000 000 km² oceanic plateau (Vaalbara), especially in view of evidence that Archean plates were most likely microplates, and much smaller than Phanerozoic oceanic plates (Komiya and Maruyama, 2007). All these lines of evidence strongly suggest that the Paleoproterozoic volcanic plateau which included the EPT was a continental plateau. Parts of this plateau were periodically submerged as a result of sagduction during vertical deformation.

Tectonic events in the EPT

In this Report, tectonic events during the c. 300 Ma evolution of the EPT are numbered D₁, D₂, etc., according to absolute chronological age. It is important to note that not all deformation events affected all 11 granite–greenstone domes, and that individual events might have commenced and finished at slightly different times in different domes. The numbering of events is similar to the approach used in most previous descriptions of deformation in the EPT (Kloppenburg et al., 2001; Van Kranendonk et al., 2002, 2007a,b; Hickman, 2004; Hickman and Van Kranendonk, 2008a). The same method has been used in the northwest Pilbara Craton (Krapež and Eisenlohr, 1998; Smithies, 1998b; Hickman and Smithies, 2001; Hickman et al., 2001, 2010; Hickman and Strong, 2003; Hickman, 2016). However, because the northwest Pilbara Craton does not expose Paleoproterozoic rocks older than c. 3280 Ma, and the first deformation recognized there was Mesoproterozoic (Hickman, 2016), no correlation of deformation events is possible prior to the 3280–3165 Ma East Pilbara Terrane Rifting Event.

D₁, 3530–3477 Ma

In this Report, D₁ refers to deformation between c. 3530 and 3477 Ma, corresponding to the period of deposition of the Coonterunah and Talga Talga Subgroups. D₁ deformation can be recognized only in those domes that expose this basal part of the Pilbara Supergroup (Carlindi, Muccan, Mount Edgar, Shaw, North Pole and Yule Domes). Structures formed during D₁ include:

- tectonic foliation (S₁) in tonalite gneiss of the Carlindi Dome that was intruded by, and therefore pre-dates, undeformed equigranular granodiorite dated at 3484 ± 4 Ma (GSWA 153188, Nelson, 1999g)
- metamorphic foliation (S₁) in amphibolite-facies metabasalt of the >3515 Ma Table Top Formation in the Carlindi Dome
- tight to isoclinal folds (F₁) and gravitational slides in the McPhee Formation of the Mount Edgar Dome that are intruded by the 3466 ± 2 Ma Homeward Bound Granite (GSWA 142865, Nelson, 1998h)
- syndepositional extensional faults in the c. 3481 Ma Dresser Formation of the North Pole Dome.

Additionally, one or more ⁴⁰Ar/³⁹Ar dates older than c. 3477 Ma from the Talga Talga and Coonterunah Subgroups might mark events of deformation and metamorphism. These dates include:

- a 3522 ± 13 Ma hornblende plateau age (>60% of ³⁹Ar released) for the North Star Basalt of the North Shaw greenstone belt in the Shaw Dome (Zegers, 1996)
- a 3518 ± 16 Ma ⁴⁰Ar/³⁹Ar hornblende isochron age for the North Star Basalt of the Coongan greenstone belt in the Shaw Dome (Davids et al., 1997)
- a 3490 ± 15 Ma ⁴⁰Ar/³⁹Ar hornblende metamorphic age for the North Star Basalt of the Mount Edgar Dome (Van Koolwijk et al., 2001).

Folds and faults indicative of gravitational sliding off the rising Mount Edgar Dome were initially interpreted to have formed at c. 3465 Ma (Collins, 1989), which would classify them as D₂ in this Report. However, the structures in the McPhee Formation, here interpreted as F₁ and S₁, are crosscut by the unfoliated c. 3466 Ma Homeward Bound Granite (Hickman and Van Kranendonk, 2008b). This undeformed granite also intrudes a pre-existing, northwest-plunging anticline on the northwest side of the Mount Edgar Dome. Accordingly, this anticline might be a remnant of part of an early dome formed at c. 3477 Ma, and later partly replaced by the main 3455–3290 Ma dome to the southeast.

Evidence of deformation and metamorphism prior to deposition of the Coongan Subgroup between c. 3474 and c. 3450 Ma is limited, partly due to relatively few greenstone belts preserving rocks older than c. 3477 Ma, and partly as a result of overprinting by younger events. However, an abundance of detrital and xenocrystic zircons dated between c. 3530 and 3490 Ma in younger Paleoproterozoic and Mesoproterozoic rocks suggests widespread granitic

intrusion into and beneath the Coonterunah Subgroup (see **Mulgundoona Supersuite**). U–Pb zircon dating (Allen et al., 2016; Wiemer et al., 2018; Petersson et al., 2019, 2020) revealed granitic intrusions similar in age to the Coonterunah Subgroup (which includes c. 3515 Ma felsic volcanic rocks; Buick et al., 1995). A quartz diorite gneiss in the Muccan Dome was first dated at c. 3510 Ma (Allen et al., 2016), and subsequently the date was revised to c. 3503 Ma (Wiemer et al., 2018).

Following intrusion of the Mulgundoona Supersuite (Petersson et al., 2020), numerous intrusions of the Callina Supersuite were intruded into the EPT between 3484 and 3462 Ma. A biotite granodiorite in the Carlindi Dome was dated at 3484 ± 4 Ma (GSWA 153188, Nelson, 1999g) and a tonalite gneiss in the Shaw Dome gave a less precise date of 3485 ± 30 Ma (Williams et al., 1983b). Bickle et al. (1983) obtained a Pb–Pb isochron age of 3499 ± 22 Ma for foliated granodiorite of the North Shaw Suite in the Shaw Dome. This result was subsequently corroborated by a U–Pb zircon date of 3493 ± 4 Ma from another locality (McNaughton et al., 1988). Because the intrusive ages of younger Paleoproterozoic granites in the EPT are closely similar to events of deformation and metamorphism, similar events are likely to have accompanied pre-3477 Ma granitic intrusions.

D₂, 3477–3459 Ma

Stratigraphic, sedimentological, paleontological and geochronological evidence indicate a significant event of basin subsidence and adjacent crustal uplift during deposition of the Coongan Subgroup. The largest single area of greenstone exposure in the EPT lies between the Mount Edgar, Muccan, Carlindi, Shaw and Corunna Downs Domes (Figs 3, 8, Plate 1A), and includes the abnormally thick greenstone succession of the North Pole Dome. In this 4500 km² area, preserved sections of the Mount Ada Basalt are up to 5 km thick and the Duffer Formation is up to 8 km thick. However, this thick, subaqueous, volcanic pile (ubiquitous pillow basalts) is underlain and overlain by shallow-water sedimentary deposits. Underlying the Mount Ada Basalt, the c. 3481 Ma Dresser Formation includes evaporites, stromatolitic carbonates and clastic units with microbially induced sedimentary structures (MISS; Noffke et al., 2013). Overlying the Duffer Formation, the 3459–3450 Ma MBCM includes conglomerate and sandstone deposited in deltas and shallow-marine fans.

These relationships indicate that the 3481–3477 Ma plateau surface subsided by at least 5 km, and possibly by more than 10 km, before a return to subaerial erosion and shallow-water deposition at c. 3459 Ma. Such major subsidence of the plateau is likely to have been accompanied by uplift of surrounding areas; a process similar to sagduction and doming. The Carlindi and Muccan Domes, and the western Shaw and eastern Mount Edgar Domes, preserve evidence of relative stability and erosion during this period. In these areas, the Duffer Formation is <1 km thick and is mainly sedimentary, and the Mount Ada Basalt is 0–2 km thick. Evidence of 3477–3459 Ma uplift in these domes (Van Kranendonk, 1997, 2000a; Hickman and Van Kranendonk, 2004; Van Kranendonk et al., 2006a; Hickman and Van Kranendonk, 2008a; Wiemer et al., 2016) is supported by detrital zircon evidence of deep erosion of the lower Warrawoona Group to expose Eoarchean crust (see **Eoarchean to early Paleoproterozoic evolution**).

If extensional faulting in the c. 3481 Ma Dresser Formation was syndepositional (Nijman et al., 1998, 1999; Van Kranendonk and Hickman, 2000; Van Kranendonk, 2006), these faults are D₁ structures. Alternatively, if the faults formed as extensional structures above the mantle plume that led to eruption of the Coongan Subgroup, they are D₂ structures. Similar extensional faulting is a feature of other thick sedimentary units deposited at the end of major volcanic cycles in the EPT. For example, the MBCM was fractured and intruded by dolerite at the beginning of the Salgash volcanic cycle, and the Strelley Pool Formation was faulted in advance of the Kelly volcanic cycle. Nijman et al. (2017) related the extensional faulting in the Dresser Formation and other sedimentary units of the EPT to arching above hot spots, although they assumed a plate tectonic setting.

Structures more certainly formed during D₂ include gneissic foliation developed in c. 3465 Ma TTG of the Callina Supersuite in the Shaw Dome (Van Kranendonk, 2000a; Hickman and Van Kranendonk, 2008a). The age of this foliation is older than crosscutting leucogranite dated at 3445 ± 3 Ma (GSWA 142878, Nelson, 1998i; Van Kranendonk, 2000a). Because the gneissic foliation is parallel to a sheared granite–greenstone contact on the eastern side of the Shaw Dome, it is interpreted to have formed during doming (Van Kranendonk, 2000a). Based on U–Pb zircon dating of three samples, Zegers (1996) and Zegers et al. (2001) interpreted the Split Rock Shear Zone (SRSZ) to have formed at c. 3468 Ma, with reactivation between c. 3451 and 3420 Ma. Zegers (1996) did not relate the shear zone to diapiric deformation, but it is interpreted here to have formed by early vertical deformation that initiated the Shaw Dome.

Tight to isoclinal folds (F₂) in the Coonterunah Subgroup of the Carlindi Dome are crosscut by undeformed, c. 3469 Ma granitic rocks of the Callina Supersuite (Buick et al., 1995; Van Kranendonk, 2000a, 2010a). In the Mount Edgar Dome, Kloppenburg (2003) dated a syntectonic gabbro sill within the Limestone Shear Zone at 3462 ± 4 Ma. In the Shaw Dome, upper stratigraphic levels of the Duffer Formation are affected by extensional faulting, with associated fault-scarp sandstones and conglomerates (Zegers, 1996; Wiemer et al., 2016). Wiemer et al. (2016) attributed the extensional faulting in the Muccan Dome to uplift during doming at c. 3470 Ma.

D₃, 3455–3420 Ma

The Salgash Subgroup records up to three stages of deformation, with most evidence indicating final diapiric uplift at c. 3420 Ma. Intrusive relations and geochronology in the Callina and Tambina Supersuites indicate deformation, as well as metamorphic and melting events, between c. 3450 and 3410 Ma. The first deformation affecting the Salgash Subgroup (D_{3A}) occurred at 3455–3450 Ma during initial deposition of the Apex Basalt. Extensional faulting fractured the underlying Coongan Subgroup and Callina Supersuite, allowing a major swarm of dolerite dykes and sills to feed basaltic magma onto the MBCM and upwards into the lower section of the Apex Basalt (Kloppenburg, 2003; Van Kranendonk et al., 2006b; Hickman and Van Kranendonk, 2008a,b; Hickman, 2012; Gardiner et al., 2018). The orientations of the dolerite dykes are radial on the northeast, northwest, and southwest sides of the Mount Edgar Dome (Fig. 30), which is consistent with extensional fracturing in an

actively developing diapiric structure (Van Kranendonk et al., 2006b; Gardiner et al., 2018). The dykes are also present on the south and southeastern sides of the dome but have been rotated to become subparallel to a strong, c. 3315 Ma tectonic foliation (S_5 in this Report). Radially plunging stretching lineations in the dome (Collins, 1989; Collins et al., 1998; Hickman and Van Kranendonk, 2004, 2008a; Van Kranendonk et al., 2006b) provide additional evidence of diapiric uplift, although the precise timing (D_3 , D_4 or D_5) is difficult to establish.

The 'Apex chert' (informal name), which was deposited as a thin unit of sandstone, shale and felsic volcanoclastic sediments 500–1000 m above the base of the Apex Basalt, testifies to a period of uplift and shallow-water deposition (Brasier et al., 2013). Large dykes of hydrothermal chert immediately underlying and feeding into the Apex chert provide evidence of syndepositional extension and hydrothermal activity (Brasier et al., 2011). In another area, sandstone correlated with the Apex chert contains detrital zircon age components of c. 3650 and 3592 Ma (Fig. 15) indicating c. 3450 Ma erosion of (at that time) exposed Eoarchean to early Paleoproterozoic crust.

In northeastern and central parts of the EPT (e.g. Carlindi, Muccan, North Pole and Shaw Domes), stratigraphic evidence indicates that the Apex Basalt and part of the Duffer Formation were extensively eroded between c. 3445 and 3430 Ma (Bagas et al., 2004c; Hickman, 2011), with the likelihood that this erosion continued during deposition of the 3426–3350 Ma Strelley Pool Formation. In contrast, preservation of the Apex Basalt in the Mount Edgar, Corunna Downs and McPhee Domes indicates lack of uplift and erosion in those southeastern areas. Crustal stability in the southeastern EPT continued during deposition of the Panorama Formation, Strelley Pool Formation and Euro Basalt. A lack of visible deformation in the Corunna Downs and McPhee Domes between c. 3445 and 3335 Ma is consistent with observations of paraconformable to disconformable relations between the above-mentioned formations in these areas (Bagas, 2003, 2005; Hickman, 2008).

In the Shaw Dome, Zegers (1996) interpreted a metamorphic event at c. 3450 Ma which coincided with the crystallization age of the protolith of a unit referred to as 'grey gneiss' (sample T94/221). Additionally, a sample of monzogranite from the Shaw Dome was dated at 3445 ± 3 Ma (GSWA 142878, Nelson, 1998j). Wiemer et al. (2016) interpreted a major event of deformation and metamorphism at 3470–3430 Ma in the Muccan Dome, and ascribed most tectonic structures to this event. Several granitic intrusions of the Tambina Supersuite in the North Pole Dome have been dated between c. 3449 and 3431 Ma, and five intrusions in the Mount Edgar Dome have crystallization ages between c. 3449 and 3443 Ma (Table 3). François et al. (2014) dated monazite inclusions within garnet from a metasedimentary rock on the southwestern side of the Mount Edgar Dome at 3443.4 ± 4.5 Ma and interpreted this to define a discrete metamorphic event. On the basis that periods of granitic intrusion are likely to coincide with deformation and metamorphism, a tectonic event can be inferred between c. 3450 and 3440 Ma.

Based on available dating of the Panorama Formation, there were two separate periods of volcanism: the first is interpreted to have been between 3449 and 3445 Ma,

which is supported by the oldest dates from the Tambina Supersuite between c. 3451 and 3443 Ma (10 dated intrusive samples, Appendix 4); the second occurred between 3435 and 3427 Ma (seven dated volcanic samples, Appendix 5). These dates suggest two tectonic events within those domes covered by the dating, although there are insufficient data to determine if this applied to most EPT domes. Support for two magmatic events is provided by the recognition of two unconformities, separated by part of the Panorama Formation, between the Mount Ada Basalt and the Strelley Pool Formation in the North Pole Dome (Van Kranendonk, 2010a). The lower unconformity indicates erosion after eruption of the Duffer Formation and Apex Basalt, whereas the upper unconformity (directly underlying the Strelley Pool Formation) provides evidence of uplift and erosion after deposition of the Panorama Formation. Therefore, at least in the area of the North Pole Dome, there were separate events, here distinguished as D_{3B} and D_{3C} .

Warrawoona Event (D_{3C})

The final stage of D_3 deformation, D_{3C} , occurred between c. 3430 and 3410 Ma following eruption of the Panorama Formation, and has been referred to as the Warrawoona Event (Hickman, 2010). This event had limited impact on areas of the southeastern EPT now occupied by the Corunna Downs, McPhee and Yilgalong Domes. However, deformation and melting occurred in the Muccan Dome (Wiemer et al., 2016), Shaw Dome (Van Kranendonk, 1997, 2000a, 2010a; Pawley et al., 2004; Van Kranendonk et al., 2004a, 2006a), Warrawagine Dome (Williams, 2003), and Mount Edgar Dome (Kloppenburg, 2003). In the Mount Edgar Dome, the Beaton Well Zone (Kloppenburg, 2003; Gardiner et al., 2018) was formed at c. 3420 Ma, and is exposed as a tight to isoclinal synformal belt in the 3448–3416 Ma Fig Tree Gneiss (Fig. 30). The D_{3C} age of the Beaton Well structure is indicated by it being abruptly truncated by the c. 3320 Ma Joorina Granodiorite in the northeast and by the c. 3315 Ma Limestone Shear Zone to the southwest. The Beaton Well Zone is interpreted to separate two early domes within the Mount Edgar Dome (Hickman, 1975a, 1983).

The angular unconformity at the base of the 3426–3350 Ma Strelley Pool Formation in the Carlindi Dome (Buick et al., 1995; Green et al., 2000; Van Kranendonk, 2000a; Van Kranendonk et al., 2002, 2006a, 2007a,b; Hickman, 2008; Wacey et al., 2010), North Pole Dome (Van Kranendonk, 2000a; Allwood et al., 2007a; Hickman, 2008), and Muccan Dome (Van Kranendonk, 2010a; Wiemer et al., 2016) was the result of major uplift and erosion prior to c. 3426 Ma. The almost complete absence of the Coongan and Salgash Subgroups in the Carlindi Dome, combined with the limited age range of detrital zircons in the Strelley Pool Formation (Fig. 12e), makes it uncertain if this uplift was mainly D_2 or D_3 .

D_4 , 3360–3350 Ma

A relatively minor deformation event, here assigned to D_4 , includes extensional faulting of the Panorama and Strelley Pool Formations in the Kelly and Marble Bar greenstone belts. In the Corunna Downs Dome, many of the extensional faults contain mafic and ultramafic dykes which served as magmatic conduits into the Euro Basalt (Kloppenburg, 2003; Bagas et al., 2004c). Like the D_{3A} dolerite dykes in the Mount

Edgar Dome, the D₄ dykes are radial around the northern half of the Corunna Downs Dome, and the extension is therefore likely to have been a consequence of domal uplift in advance of the mantle plume that was responsible for eruption of the Kelly Group. An erosional unconformity within the upper Strelley Pool Formation in the North Pole Dome (Allwood et al., 2007a; Hickman, 2008) suggests uplift related to the Kelly Group plume commenced slightly prior to the earliest isotopic date of c. 3350 Ma on the Euro Basalt.

A different explanation for extensional faulting of the Strelley Pool Formation in the Mount Edgar Dome was proposed by Nijman et al. (2001, 2017) and Nijman and de Vries (2004). This interpretation, which envisaged the operation of c. 3400 Ma plate tectonic processes in the EPT, was that crustal uplift above a hotspot, related to subduction of slabs of cooled, water-saturated basalt, had been followed by crustal collapse. However, the substantial evidence against Paleoproterozoic plate tectonic processes in the Pilbara Craton prior to c. 3200 Ma (e.g. Van Kranendonk et al., 2002), and further reviewed in this Report, precludes the model proposed by Nijman et al. (2001, 2017) and Nijman and de Vries (2004).

D₅, 3335–3325 Ma

Locally exposed angular unconformities between the 3350–3335 Ma Euro Basalt and the 3325–3315 Ma Wyman Formation (Lipple, 1975; Hickman, 1981, 1983; Barley and Pickard, 1999; Van Kranendonk, 2004b, 2010a) are evidence of deformation between deposition of these formations, although in some areas they have been described as conformable or paraconformable. The Wyman Formation unconformably overlies the Euro Basalt in the McPhee greenstone belt (Barley and Pickard, 1999), and also in the western Warralong greenstone belt (Van Kranendonk, 2004b). In the southeastern Kelly greenstone belt, there is an angular discordance of 20–30° between the formations, suggesting an unconformity (Van Kranendonk et al., 2002, fig. 8). Bagas et al. (2004c) explained this angular relationship as a consequence of the rhyolite flows of the Wyman Formation having a primary dip on the slopes of a volcano. Other researchers accepted a depositional break between the Euro Basalt and the Wyman Formation; for example, Krapež (1993) and Barley and Pickard (1999) who assigned the formations to different sequences.

The geochemical composition of the Wyman Formation indicates a strongly potassic crustal melt (Smithies et al., 2007b), which is not consistent with fractionation from tholeiitic magma (Euro Basalt). This differs from older mafic–felsic volcanic cycles (e.g. Mount Ada Basalt to Duffer Formation) where tholeiitic basalts are overlain by andesitic to dacitic volcanic successions. Previously, eruption of the 3325–3315 Ma Wyman Formation and intrusion of the 3324–3290 Ma Emu Pool Supersuite have been interpreted to mark a major influx of felsic magmas derived from partial melting of TTG crust (Glikson et al., 1987; Collins, 1993; Barley and Pickard, 1999; Champion and Smithies, 1999; Bagas et al., 2003; Smithies et al., 2003; Van Kranendonk et al., 2007a,b). Van Kranendonk and Collins (2001) suggested that the event was triggered by a heat source additional to that related to the mantle plume that produced the Euro Basalt. Barley and Pickard (1999) interpreted an extensional setting for the post-3325 Ma felsic magmatic

activity, and it is notable that most outcrops of the Wyman Formation are close to the faulted boundaries of various domes. The Wyman Formation was erupted at local volcanic centres whereas the Euro Basalt is essentially a plateau basalt succession that extends across most of the EPT (Van Kranendonk et al., 2002). In summary, there are several lines of evidence to indicate a significant tectonic event between c. 3335 and 3325 Ma. Because field observations do not support a regional unconformity at the base of the Wyman Formation, it is currently retained within the Kelly Group.

Structures produced during D₅ include tight, upright folds in the Euro Basalt that were eroded prior to deposition of clastic sedimentary rocks of the Wyman Formation in the western Warralong greenstone belt (Van Kranendonk, 2004b). In this Report, other D₅ structures are interpreted to include the folds, foliations and lineations that were designated by Bagas et al. (2004c) as 'D2a' in the Warrery Anticline on the west side of the Corunna Downs Dome. Bagas et al. (2004c) interpreted two phases of deformation within the event that they assigned to 'D₂' (their classification) at c. 3315 Ma. In the rocky bed of the Coongan River at Warrery Gap, a strong tectonic foliation in the Euro Basalt is crosscut by veins of massive monzogranite (Fig. 36), which are likely to be part of the Emu Pool Supersuite. Cooper et al. (1982) recognized two generations of structures in this area, the earliest of which is represented by refolded minor folds in the Panorama Formation. The depositional age of the Panorama Formation at Warrery Gap is 3432 ± 2 Ma (GSWA 168915, Nelson, 2001e). Satisfactory separation of D₅ from D₆ requires the identification of additional areas where deformed Euro Basalt is overlain by undeformed Wyman Formation or intruded by undeformed granitic rocks of the Emu Pool Supersuite, as appears to be the situation at Warrery Gap.



Figure 36. View of a rock platform in the bed of the Coongan River at Warrery Gap showing granitic veins intruding metamorphosed pillow structures in strongly foliated Euro Basalt (MGA 784100E 7612300N). Hammer in centre of outcrop provides scale. Modified from Bagas et al. (2004c)

D₆, 3325–3290 Ma

D₆ deformation occurred during the Emu Pool Event (EPE; Hickman and Van Kranendonk, 2008b), a major event of 3325–3290 Ma diapiric doming, rifting, metamorphism and granitic intrusion in the eastern part of the EPT.

Emu Pool Event

Doming during the Emu Pool Event (EPE) resulted in uplift and erosion of the Kelly Group, Strelley Pool Formation, Warrawoona Group, and pre-3530 Ma crust. An erosional unconformity is exposed between the Kelly Group and the Sulphur Springs Group in the Soanesville greenstone belt (Van Kranendonk, 1997, 2000a; Van Kranendonk et al., 2004c, 2006a), and in the west Warralong greenstone belt (Fig. 35), where sandstone of the Leilira Formation unconformably overlies tightly folded units of the Wyman Formation (Van Kranendonk, 2004b). Detrital zircon ages in the Leilira Formation range up to c. 3589 Ma (Buick et al., 2002), indicating exposure of the early crust of the Pilbara Craton during the EPE.

The EPE included the first event of diapiric doming to be isotopically dated through the application of U–Pb zircon geochronology (Williams and Collins, 1990; Collins et al., 1998). Collins et al. (1998) concluded that the dome-and-keel crustal architecture of the Pilbara Craton was formed between c. 3320 and 3310 Ma. However, subsequent geochronology has shown this to be an over-simplification; instead, there were multiple doming events during the crustal evolution of the EPT. Additionally, there is no geochronological evidence for D₆ doming, or related granitic intrusion (Emu Pool Supersuite), west of the Muccan, Mount Edgar and Corunna Downs Domes; for example, in the Shaw Dome (Zegers, 1996; Zegers et al., 1999; Pawley et al., 2004).

Intrusion of the Emu Pool Supersuite and deposition of the Wyman Formation occurred during the EPE. The local angular unconformities between the Euro Basalt and the Wyman Formation testify to deformation between c. 3335 and 3325 Ma. More significant deformation followed at c. 3315 Ma (Collins et al., 1998). On the interpretation that doming was accompanied by granitic intrusion (Collins et al., 1998; Van Kranendonk et al., 2002, 2007a,b; Hickman and Van Kranendonk, 2004), the range of crystallization ages from the Emu Pool Supersuite (Appendix 5) provides evidence that different domes were uplifted at slightly different times, with the last doming occurring after c. 3300 Ma in the Yilgalong Dome. Several published estimates of the age of the doming at this time have been 3315–3310 Ma (Williams and Collins, 1990; Collins et al., 1998; Van Kranendonk et al., 2002; Kloppenburg, 2003; François et al., 2014), although this estimate is entirely derived from geochronology in the Mount Edgar Dome.

Coongan–Warralong Fault Zone

The distribution of the Emu Pool Supersuite (Fig. 37) suggests that crustal thickening associated with the formation of the domes was restricted to the eastern half of the EPT. The western boundary of the supersuite coincides with the Coongan–Warralong Fault Zone (CWFZ; Fig. 5). This zone of faulting and shearing, first identified and named in this Report, extends from the Coongan greenstone belt northwards under the Fortescue Group as the concealed

tectonic boundary between the Mount Edgar and North Pole Domes. Farther north, in the Warralong greenstone belt, the CWFZ joins the Lalla Rookh – Western Shaw Fault to form the faulted contact between the Muccan and Carlindi Domes (Hickman, 2001b, 2011).

The compilation of all U–Pb zircon dates from EPT granitic rocks (Appendices 4, 5 and Table 3) reveals that, of 55 samples dated between c. 3325 and 3290 Ma, none came from the Shaw or North Pole Domes, or from any of the other domes farther west in the EPT. Most came from the Mount Edgar Dome (n = 26) and the Corunna Downs Dome (n = 18), with a total of 11 samples from the Yilgalong, Muccan, McPhee, Warrawagine and Yilgalong Domes. The stratigraphic significance of the CWFZ is considerable, and it is likely to have a tectonic explanation that is not yet understood. The CWFZ displaces the pre-3325 Ma stratigraphy of the EPT but does not otherwise interrupt it. Accordingly, the zone does not represent a c. 3325 Ma terrane boundary, although it might be evidence of a failed rift. If 3325–3290 Ma crustal uplift was mainly east of the CWFZ, this zone might have formed a north–south trending fault scarp at c. 3290 Ma. Barley and Pickard (1999) related the felsic magmatic activity between c. 3325 and 3310 Ma to crustal extension, and it is possible that the tectonic setting was somewhat similar to that of a Phanerozoic volcanic rifted margin, as described by Menzies et al. (2002). In many of these margins, substantial silicic volcanism follows the development of a basaltic LIP, and the Euro Basalt has the characteristics of a LIP. Bimodal basalt–rhyolite successions are present in some volcanic rifted margins (Menzies et al., 2002), and the Wyman Formation is locally a mix of rhyolitic and basaltic members (e.g. northern Kelly greenstone belt). The c. 2940 Ma Lalla Rookh – Western Shaw Structural Corridor (LWSC) also has an early history dating from c. 3325 Ma (see **North Pilbara Orogeny, 2955–2919 Ma**).

Limestone Shear Zone

D₆ structures of the Mount Edgar Dome provided much of the early evidence that the domes of the EPT were formed by gravity-driven vertical deformation (Hickman, 1975a, 1981, 1984; Collins, 1989; Collins et al., 1998), rather than by cross-folding (Noldart and Wyatt, 1962). In this regard, the most important D₆ structure of the Mount Edgar Dome is the Limestone Shear Zone (LSZ; Fig. 30). Separating the granitic core of the dome from the Marble Bar greenstone belt, this 2–6 km-wide shear zone is an arcuate belt of mylonite, schist and strongly foliated granitic rocks of various intrusions of the Callina, Tambina and Emu Pool Supersuites. The width of the shear zone and the degree of deformation within it increase southwards on the western and eastern sides of the Mount Edgar Dome. The adjacent Marble Bar greenstone belt shows the same southerly increase of shearing, such that the 15 km-thick stratigraphic succession at Marble Bar is attenuated to 1–2 km thickness north of the Warrawoona Syncline. Hornblende ⁴⁰Ar/³⁹Ar plateau ages from the LSZ indicate a maximum cooling age of c. 3340 to 3300 Ma, but also indicate that the zone was reactivated several times between then and c. 2950 Ma (Kloppenburg, 2003). Detailed mapping of the LSZ has revealed a well-developed radial orientation of stretching lineations, consistent with diapiric doming (Collins, 1989; Collins et al., 1998; Van Kranendonk et al., 2002, 2004a, 2006b, 2007a,b, 2014b; Hickman and Van Kranendonk, 2004; Gardiner et al., 2018).

Evidence supporting major vertical uplift across the LSZ on the southwest side of the Mount Edgar Dome is provided by kyanite in felsic schist. Based on pressure–temperature estimates of 5.5 – 6.0 kb and 500–600 °C (Délor et al., 1991), Collins and Van Kranendonk (1999) argued for diapiric uplift from burial depths of ~25 km. This depth estimate is consistent with other evidence that the 3451–3416 Ma TTG protoliths of the Tambina Supersuite were emplaced at crustal depths of ~15 km. From c. 3350 to 3335 Ma, all rocks at this crustal level were overlain by a new addition to the upper crust – the 5–10 km-thick Euro Basalt. François et al. (2014) reported that data from garnet-bearing metasedimentary rocks and metabasalts from the southwest and southeast sections of the LSZ indicated equilibrium pressures and temperatures of 9–11 kb and 450–550 °C, and concluded that these units had been subject to rapid diapiric uplift from lower levels of the crust. Kloppenburg (2003) applied $^{40}\text{Ar}/^{39}\text{Ar}$ dating to numerous samples from the LSZ and confirmed significant events of intrusion and metamorphism between c. 3325 and 3280 Ma. The first of these events recorded by $^{40}\text{Ar}/^{39}\text{Ar}$ dating coincides with intrusion of the Emu Pool Supersuite.

The horseshoe-shaped outcrop of the LSZ can be explained in two ways. First, if the LSZ is a major c. 3315 Ma ring fault, as proposed by Van Kranendonk et al. (2001a, 2004a), tectonic foliations within it indicate that the uplifted central granitic core of the dome is steeply inclined to the southwest. In this scenario, and under the diapiric model in which shearing of dome margins increases with crustal depth (Hickman, 1975a, 1984), erosion in the southwestern part of Mount Edgar Dome has exposed a much deeper crustal level of the dome than exposed in the northeast (Coppin Gap – Bamboo Creek area; Fig. 30). Second, absence of the LSZ along the granite–greenstone contact on the northeastern side of the dome is partly due to 3315–3223 Ma granitic intrusion in this area. However, on the northeastern side of the dome, D_6 vertical uplift is likely to have been partly focused in a shear zone that extends west from Bamboo Creek along the northern margin of the Marble Bar greenstone belt.

Bamboo Creek Shear Zone

The Bamboo Creek Shear Zone (BCSZ) was originally described as an arcuate fault extending 70 km from southeast of Bamboo Creek mining area in the Marble Bar greenstone belt to the Pear Creek area in the Doolena Gap greenstone belt (Hickman, 1983). More detailed mapping by de Vries (2004) and Van Kranendonk (2004c) confirmed its westward extent as far as the Talga River, about 50 km from Bamboo Creek (Fig. 30). Over this strike length, one constraint on the maximum age of the BCSZ is provided by the fact that it deforms the 3350–3335 Ma Euro Basalt (Williams, 1998, 1999a; de Vries, 2004; de Vries et al., 2006). An additional constraint is that, about 8 km east of the Talga River, a body of porphyritic rhyolite within deformed rocks of the BCSZ has been dated at 3318 ± 4 Ma (sample W95-36, de Vries, 2004; de Vries et al., 2006), consistent with it being part of the 3325–3315 Ma Wyman Formation. If the Wyman Formation of this area is contained within a tectonic lens, the maximum age of the BCSZ is c. 3318 Ma. This maximum age is important because Zegers et al. (2002) incorrectly identified the host formation as the c. 3450 Ma Apex Basalt, and interpreted c. 3415 Ma galena Pb–Pb ages as evidence

of its age. Huston et al. (2001a) used the same Pb-isotope data to interpret the age of gold mineralization within the BCSZ. However, the stratigraphic interpretation by Williams (1998, 1999a) has since been confirmed by U–Pb zircon geochronology.

At Kitty's Gap, half way between Bamboo Creek and the Talga River, deformed Euro Basalt within the BCSZ is stratigraphically underlain by the 3426–3350 Ma Strelley Pool Formation (Hickman, 2008) and, beneath that, by the Panorama Formation locally dated at 3446 ± 5 Ma (sample JW95-001, de Vries, 2004; de Vries et al., 2006). The minimum age of the BCSZ is constrained to c. 3300 Ma because it is intruded by the c. 3300 Ma Chimingadgi Trondhjemite (Williams, 1999a; Zegers et al., 2002). In summary, U–Pb zircon geochronology has established that the BCSZ was formed between c. 3318 and 3300 Ma. Accordingly, the BCSZ is a D_6 structure, and was most likely geodynamically related to the same doming event as the LSZ on the opposite side of the Mount Edgar Dome.

Other D_6 structures

Large-scale D_6 structures related to doming have been documented from the Corunna Downs and Mount Edgar Domes. Van Kranendonk et al. (2001a) interpreted major anticlines and synclines with axes parallel to the margin of the Corunna Downs Dome; the main examples are the Warrery Anticline, Spinaway Anticline and Cookkindina Syncline (Bagas et al., 2004c). All these folds deform the Euro Basalt, although only the Cookkindina Syncline visibly folds the Wyman Formation (Bagas et al., 2004c). Sections of the Euro Basalt in the eastern Kelly greenstone belt are repeated by steep reverse faults.

Other important D_6 structures of the Mount Edgar Dome include a strongly developed tectonic foliation (S_6) which is concentric in the greenstones around the dome (Hickman, 1984) and ring faults in the greenstones parallel to the LSZ (Collins et al., 1998; Van Kranendonk, 1998; Collins and Van Kranendonk, 1999; Hickman, 2001b; Van Kranendonk and Collins, 2001; Hickman and Van Kranendonk, 2004, 2008a; Van Kranendonk et al., 2006b). Steeply plunging mineral lineations within S_6 are radial around the dome (Collins, 1989; Van Kranendonk et al., 2006b; Hickman and Van Kranendonk, 2004, 2008a; Gardiner et al., 2018).

Metamorphism in the EPT

Van Kranendonk (2010b) summarized the main metamorphic features of the EPT, noting that it is characterized by low-P, contact-style metamorphism. Isograds are distributed concentrically around the domes, and vary from high-temperature (amphibolite facies) adjacent to granite–greenstone contacts to low grade (prehnite–pumpellyite facies) in the central areas of greenstone belts. In the Shaw Dome, $^{40}\text{Ar}/^{39}\text{Ar}$ dating has revealed that contact metamorphism occurred in several events over hundreds of millions of years (Zegers et al., 1999). Various $^{40}\text{Ar}/^{39}\text{Ar}$ studies (Wijbrans and McDougall, 1987; Davids et al., 1997; Zegers, 1996; Zegers et al., 1999) have indicated metamorphism at c. 3200 Ma that is interpreted here to have been related to the 3280–3165 Ma EPTRE during breakup of the EPT.

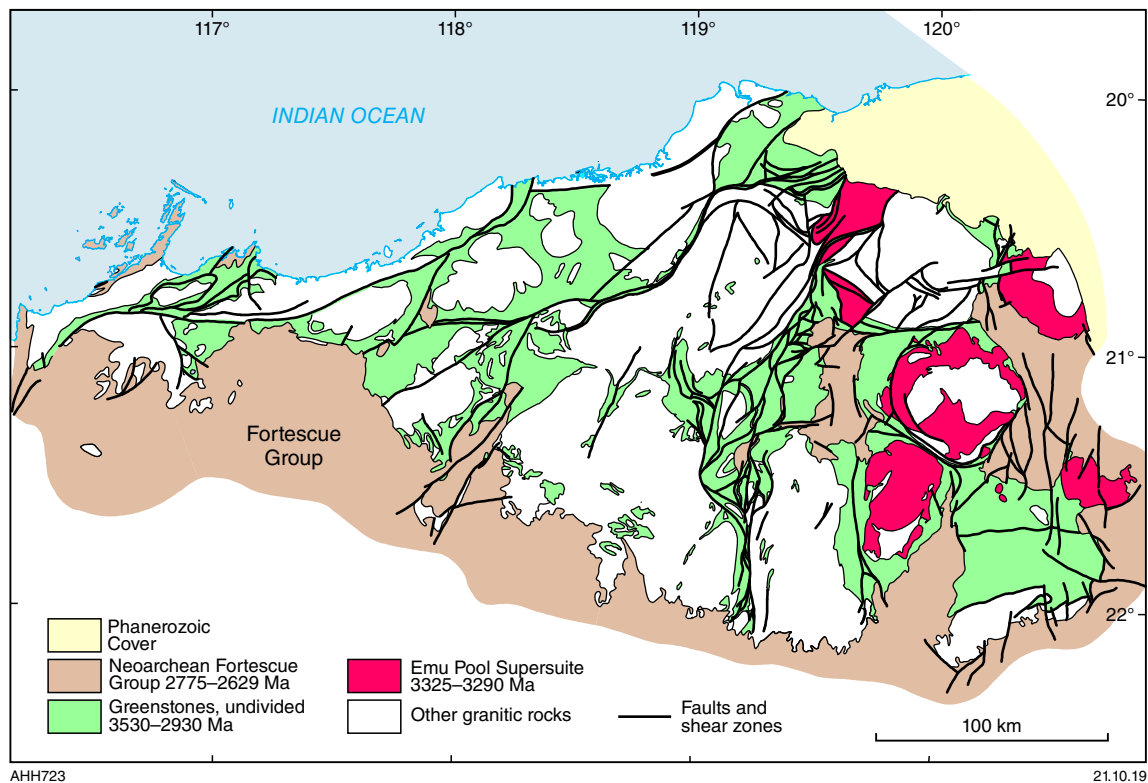


Figure 37. Simplified geological map of the northern Pilbara Craton showing the distribution of the Emu Pool Supersuite

This event is the same age as an important event of deformation and metamorphism in the eastern Kaapvaal Craton (Moyen et al., 2006; Van Kranendonk, 2011; Van Kranendonk et al., 2014a,b). There, as in the Pilbara Craton, c. 300 Ma of Paleoarchean volcanic deposition was replaced by Mesoarchean deposition in mainly sedimentary basins, marking a major change in crustal evolution (Van Kranendonk et al., 2010).

$^{40}\text{Ar}/^{39}\text{Ar}$ dating in the Mount Edgar and Corunna Downs Domes (Kloppenburg, 2003) supports interpretations from U–Pb zircon data that there were significant events of intrusion, deformation, and metamorphism in the EPT at 3325–3290 and 3250–3200 Ma. The first of these events coincides with the EPE, and supports previous interpretations of a major doming event in these domes at c. 3315 Ma (Williams and Collins, 1990; Collins et al., 1998; Van Kranendonk et al., 1999a, 2002; Hickman and Van Kranendonk, 2004). $^{40}\text{Ar}/^{39}\text{Ar}$ data for samples from the LSZ (referred to by Kloppenburg [2003] as the 'Mount Edgar Shear Zone') provided no evidence for displacement at 3470–3420 Ma, even though U–Pb zircon dating (Williams and Collins, 1990) indicated the shear zone originated at about this time. The lack of older dates from argon–argon dating may be due to resetting of the isotope system by extensive intrusion of c. 3315 Ma synkinematic granitic rocks (Kloppenburg, 2003).

Other $^{40}\text{Ar}/^{39}\text{Ar}$ dates reported by Kloppenburg (2003) were interpreted to indicate Mesoarchean metamorphic events at c. 3150, 3080, 2930, 2850, and 2800 Ma. The c. 3150 Ma event coincides with the 3160–3140 Ma Karratha Event recognized in the northwest Pilbara Craton (Kiyokawa, 1993; Kiyokawa and Taira, 1998; Smith et al., 1998; Beintema, 2003; Hickman, 2016). This marked a change from plate separation, following the 3280–3165 Ma EPTRE, to convergence involving obduction and subduction, interpreted to be due to collision with another plate northwest of the Pilbara Craton (Hickman, 2016). The c. 3080 Ma event closely coincides with the 3068–3066 Ma Prinsep Orogeny, produced by collision between the EPT and the West Pilbara Superterrane. The interpreted age range of the Prinsep Orogeny is based only on U–Pb zircon dating of the Elizabeth Hill Supersuite, and Hickman (2016) noted that U–Pb zircon data (igneous and detrital zircons) suggest a longer age range for this orogeny between c. 3080 and 3060 Ma. The c. 2930 and 2850 Ma events coincide with intrusion of the Sisters and Split Rock Supersuites, and the c. 2800 Ma event may coincide with first rifting of the Pilbara Craton prior to deposition of the Fortescue Group.

Kurrana Terrane

Exposures of the Kurrana Terrane (KUT) in the southeast of the northern Pilbara Craton (Fig. 3) are interpreted to represent only a small fraction of its total extent. Due to poor exposure and limited geological investigation, the precise composition of the KUT remains to be established. Recognition and description of the terrane by Tyler et al. (1992) indicated that, unlike the Paleoarchean EPT (as later defined by Van Kranendonk et al., 2006a), the KUT includes Mesoarchean granitic rocks as young as the c. 2838 Ma Bonney Downs Monzogranite. Until more data are obtained, the definition of the KUT by Tyler et al. (1992) is used here.

Regional gravity and magnetic data (Blewett et al., 2000) indicate that most of the KUT is concealed by parts of the Fortescue and Hamersley Basins (Hickman, 2004). In addition to the granitic rocks of the KUT that are exposed immediately south of the Mosquito Creek Basin, the granite–greenstone terrane of the Sylvania Inlier (Fig. 2), and smaller exposures of granitic rocks and greenstones in the intervening Cooninia, Billinooka, Turkey, Rooney, Springo and Rat Hill Inliers, provide windows into this 50 000 km² Paleo–Mesoarchean terrane. Evidence for continuity of the KUT from the southern margin of the Mosquito Creek Basin to the Sylvania Inlier was first provided by Tyler et al. (1992) who used isotope and REE data to indicate that granitic rocks exposed in the northern KUT are geologically similar to granitic rocks in the Sylvania, Cooninia and Billinooka Inliers.

Recent U–Pb zircon dating of granitic rocks in the Sylvania Inlier indicates that three supersuites (Cleland, Mount Billroth and Cutinduna) are common to both areas. A monzogranite dated at 3239 ± 6 Ma (GSWA 195899, Wingate et al., 2018b) has a crystallization age and composition consistent with being part of the 3270–3223 Ma Cleland Supersuite that is widespread in the EPT. This age is similar to that of xenocrystic zircons in the Mount Billroth Supersuite of the northern KUT (GSWA 178013, Nelson, 2005b). A second monzogranite from the Sylvania Inlier was dated imprecisely at c. 3.2 Ga (GSWA 216542, Wingate et al., 2019a). One zircon from this sample was dated at 3222 ± 14 Ma (1 σ), within uncertainty of the age range of the Cleland Supersuite, whereas two other zircons gave dates within the range of the 3199–3164 Ma Mount Billroth Supersuite. A rhyolite from the Sylvania Inlier was dated at 3193 ± 11 Ma (GSWA 216598, Wingate et al., 2019d), consistent with it being a volcanic unit erupted during intrusion of the Mount Billroth Supersuite. Finally, two monzogranite samples from the Sylvania Inlier were dated at 2892 ± 6 Ma (GSWA 216546, Lu et al., 2018) and 2886 ± 8 Ma (GSWA 195898, Wingate et al., 2018a); GSWA 195898 also contained two zircons dated at 2918 ± 3 and 2901 ± 3 Ma (both $\pm 1\sigma$). These dates are similar to the c. 2897 Ma age of the Cutinduna Supersuite in the Cooninia Inlier (GSWA, Nelson, 2005j; GSWA 178231, Nelson, 2005k). Accordingly, the evolution of the KUT included granitic intrusion, with at least some volcanism, between c. 3239 and 2886 Ma before the terrane was intruded by the 2851–2831 Ma Split Rock Supersuite.

Calculation of Nd model ages from data reported by Tyler et al. (1992) indicates that the c. 2838 Ma Bonney Downs Monzogranite in the northern KUT was derived from sources with average mantle extraction ages of 3410–3360 Ma (samples 76339 and 76338, Champion, 2013), and four samples from the Sylvania Inlier (85313, 85320, 85332 and 85338), inferred to have been intruded at c. 2950 Ma,

provided Nd model ages between c. 3400 and 3310 Ma (Champion, 2013). Xenocrystic zircons in a c. 3.2 Ga monzogranite in the Sylvania Inlier have crystallization ages between c. 3564 and 3476 Ma (GSWA 216542, Wingate et al., 2019a). Two samples of metatonalite from the Sylvania Inlier were dated at 3566 ± 5 Ma (GSWA 216594, Wingate et al., 2019c) and 3565 ± 3 Ma (GSWA 216545, Wingate et al., 2019b), establishing the existence of pre-3530 Ma felsic crust in the KUT.

Northern KUT stratigraphy

Only those parts of the KUT covered by the NULLAGINE and EASTERN CREEK 1:100 000 sheet areas were mapped geologically and described as part of the PCMP (Bagas, 2005; Farrell, 2006). Additional areas were mapped geologically, without accompanying descriptions, on the NOREENA DOWNS sheet area (Farrell and Smithies, 2005). All these areas are informally referred to as parts of the northern KUT. The northern KUT is dominated by the 3199–3178 Ma Golden Eagle Orthogneiss and the c. 2838 Ma Bonney Downs Monzogranite. Only very limited U–Pb zircon geochronology has been conducted.

The oldest stratigraphic unit so far identified in the northern KUT is the Golden Eagle Orthogneiss (Bagas, 2005). The orthogneiss includes a variety of granitic lithologies apparently ranging in age from c. 3225 (GSWA 178013, Nelson, 2005b) to 3178 Ma (GSWA 178012, Nelson, 2004g). The dominant protoliths of the gneiss were tonalite and quartz diorite, although the gneiss also contains layers of biotite-bearing monzogranite that might have been intruded from the c. 2838 Ma Bonney Downs Monzogranite. Alternatively, some of the monzogranite layers might be deformed remnants of the Cleland Supersuite. A third possibility is that the monzogranite layering originated during emplacement of the c. 2895 Ma Cutinduna Supersuite, intrusions of which are exposed farther south in the KUT (Van Kranendonk et al., 2006a). The Golden Eagle Orthogneiss contains deformed units of amphibolite, ultramafic schist and quartz–mica schist. These units, interpreted to be remnants of a greenstone succession, are largest and most numerous 3–5 km east of Haystack Well, 5 km east-northeast of Dinkum Well, and 1–2 km south of Quartz Bore. The tonalite precursor of the orthogneiss was metamorphosed at amphibolite facies before retrogression to greenschist facies (Williams, 1989).

The Bonney Downs Monzogranite is mainly composed of weakly foliated, fine- to medium-grained, sparsely porphyritic, biotite monzogranite with local pegmatitic zones and sparse aplite veins. Xenoliths of the Golden Eagle Orthogneiss are locally present. Where the monzogranite is interleaved with the Golden Eagle Orthogneiss, it is a strongly foliated, providing evidence of deformation after c. 2838 Ma.

EPT ancestry of the KUT?

In the first regional stratigraphic description of the northern Pilbara Craton, the northern KUT was interpreted to be part of the EPT (Hickman, 1983). However, Tyler et al. (1992) used Rb–Sr, Sm–Nd and REE data to conclude that the KUT is fundamentally different from the EPT. The two terranes are separated by the Mosquito Creek Basin, which contains a mainly sedimentary succession that is younger

than most of the greenstones. This relationship is evident from the unconformity between the basin succession and the dome-and-keel structures of the McPhee and Mount Elsie greenstone belts in the EPT immediately to the north. Accordingly, basement to the Mosquito Creek Basin was initially interpreted to be granite–greenstone crust of the EPT, as illustrated in a diagrammatic section (Thom et al., 1980). Based on later, more-detailed geological mapping during the PCMP, similar sections were drawn for the NULLAGINE and EASTERN CREEK 1:100 000 Series maps (Bagas et al., 2004a; Farrell, 2005). However, the southern contact of the Mosquito Creek Basin is a major shear zone (Kurrana Shear Zone, Fig. 3) against c. 3200 Ma granitic gneiss of the Mount Billroth Supersuite in the KUT. Tyler et al. (1992) interpreted the two terranes to have evolved separately until being brought together and amalgamated between c. 3000 and 2760 Ma. In this interpretation, the Kurrana Shear Zone was regarded as a suture zone joining the amalgamated terranes.

The current interpretation, based on the PCMP, is that the KUT was originally part of the EPT but became separated from it during the 3280–3165 Ma EPTRE; Hickman, 2016). This situation is analogous to the Karratha Terrane (KT) having separated from the EPT by continental breakup that occurred at c. 3220 Ma (Hickman, 2001c, 2004, 2012, 2016; Van Kranendonk et al., 2002, 2004c, 2006a, 2007b, 2010; Hickman and Van Kranendonk, 2008a, 2012). The EPT and the KT are separated by the Mallina Basin, and there are strong geological similarities between the Mosquito Creek and Mallina Basins suggesting similar origins: both directly overlie c. 3200 Ma mafic crust (juvenile in the Mallina Basin, not tested in the Mosquito Creek Basin); both contain an upper succession of mainly deep-water clastic sedimentary facies, including turbidites; both are structurally complex, with several generations of tight to isoclinal folding related to strike-slip movements and basin closure; both are bounded by major faults and faulted unconformities; and both contain economically significant, orogenic, lode-gold deposits.

Interpretations that the Mosquito Creek Basin originated as an extensional basin (Bagas et al., 2008; Hickman, 2012; Hickman and Van Kranendonk, 2012), or as a complex faulted synclinal zone within the EPT (Hickman, 1975a,b, 1978, 1983; Nijman et al., 2010) imply a common ancestry of the EPT and KUT. This conclusion is consistent with the interpretation that the Pilbara Craton evolved as part of the larger Vaalbara continent. U–Pb detrital zircon dating of sandstone and quartzite in the EPT and Sylvania Inlier, and in the eastern Kaapvaal Craton, has revealed very similar age ranges of pre-greenstone detrital zircons (3650–3550 Ma). Data from the Sylvania Inlier (GSWA 195897, Wingate et al., 2017a; GSWA 203712, Wingate et al., 2017b) suggest that pre-3530 Ma sialic crust was present in all these terranes during the Paleoproterozoic.

Kurrana Shear Zone

Based on geological mapping of the KUT and the Mosquito Creek Basin, Bagas et al. (2004a), Bagas (2005), and Farrell (2005, 2006), recognized six deformation events (D_{MB1} – D_{MB6}) that followed intrusion of the protoliths of the 3199–3178 Ma Golden Eagle Orthogneiss. Structures formed by these events were described from both the orthogneiss and the Mosquito Creek Formation, and in the latter, partly coincide with deformation events interpreted from other work (Hickman, 1975a; Blewett, 2002; Nijman

et al., 2010). Events directly related to evolution of the Kurrana Shear Zone (KSZ) were D_{MB2} , D_{MB4} and D_{MB5} , indicating a relatively complex history. Evidence from the PCMP suggests that the KSZ probably originated as an extensional fault during the EPTRE, much like the Tabba Tabba and Sholl Shear Zones of the northwest Pilbara Craton, although no structural evidence for this has been documented. Regional-scale tight folding of the KSZ was assigned to D_{MB4} by Bagas (2005) and Farrell (2006). Thrusting of the Mosquito Creek Basin against the KUT is likely to have occurred during the Mosquito Creek Orogeny when a large amount of crustal shortening took place across the Mosquito Creek Basin. This major orogenic event is interpreted to have occurred at c. 2905 Ma (Van Kranendonk et al., 2002, 2006a), based on a 2905 ± 9 Ma Pb–Pb galena model age for galena associated with epigenetic gold mineralization at the Mosquito Creek gold mine (Huston et al., 2002; Bagas, 2005). However, as noted by Farrell (2006), the c. 2838 Ma Bonney Downs Monzogranite was strongly deformed immediately adjacent to the eastern section of the KSZ, indicating younger movement. Because the shear zone is unconformably overlain by undeformed units of the 2775–2630 Ma Fortescue Group, most deformation of the monzogranite is likely to have occurred at c. 2800 Ma. This deformation event was designated D_{MB5} by Farrell (2006). The KSZ might have been reactivated again during the Paleoproterozoic Capricorn Orogeny because pegmatite veining within the western exposures of the shear zone was dated at 1793 ± 17 Ma (GSWA 178232, Bodorkos et al., 2006).

Mafic and ultramafic rocks along the KSZ at the northern boundary of the KUT have not been dated, but are likely to be either c. 3185 Ma intrusions of the Dalton Suite (Hickman and Van Kranendonk, 2012) or c. 3200 Ma remnants of the Coondamar Formation. These mafic rocks are closely associated with thin units of chert and BIF, which might be parts of the Coondamar Formation. Some of these units might alternatively be recrystallized mylonites formed when the Mosquito Creek Formation was thrust against the KUT; no definitive studies have been reported.

The beginning of plate tectonics in the Pilbara Craton

Evidence gained from the 1994–2005 Pilbara Craton Mapping Project (PCMP) revealed a major change in the crustal evolution of the northern Pilbara Craton between c. 3280 and 3165 Ma. Although a vertical stratigraphic change from volcanic to sedimentary successions had been recognized previously (Hickman and Lipple, 1975; Hickman, 1983), the cause of the change was unknown. Evidence from the PCMP indicated that between c. 3280 and 3165 Ma, the Paleoproterozoic plume-related volcanic cycles, gravity-driven vertical deformation, and crustal recycling of the EPT ceased and were followed by Mesoproterozoic processes of crustal evolution characteristic of Phanerozoic plate tectonic settings, as best revealed in the northwest Pilbara Craton (Hickman, 2001a, 2004, 2012; Van Kranendonk et al., 2002, 2006a, 2007a,b, 2010; Smithies et al., 2005a).

Additional geochemical evidence for the change was provided by Smithies et al. (2018b) who applied the Th/Yb vs Nb/Yb plot of Pearce (2008) to investigate the origin of greenstones in the Yilgarn Craton. As part of the study, they

also investigated Pilbara Craton greenstones and found that the Paleoproterozoic basaltic units have high (Th/Yb)/(Nb/Yb) trends (i.e. variable Th/Nb). This was attributed to mixing of low-Th/Nb mantle-derived melts and high-Th/Nb crust. Smithies et al. (2018b) pointed out that those trends reflect interaction of mantle-derived magmas and older crust, and are inconsistent with formation of greenstones by subduction. Smithies et al. (2018b) reported that Pilbara Craton greenstones formed between c. 3130 and 2950 Ma have constant Th/Nb, more typical of modern-style subduction settings, which is consistent with boninite-like lavas and calc-alkaline andesites in this time interval (Smithies et al., 2005a). The most likely trigger for the 3280–3165 Ma change in crustal evolution of the Pilbara Craton was crustal extension above the mantle plume responsible for eruption of the Sulphur Springs Group and intrusion of the Cleland Supersuite (Van Kranendonk et al., 2006a). Continental breakups are commonly attributed to mantle plumes (Condie, 2016).

Previous publications have presented evidence that during the c. 150 Ma interval between the formation of the mainly volcanic 3530–3223 Ma East Pilbara Terrane and the development of the mainly sedimentary 3066–2919 Ma De Grey Superbasin, the evolution of the northern Pilbara Craton was controlled initially by plate separation, and then by plate convergence and collision (Hickman, 2001a,c, 2004, 2012, 2016; Van Kranendonk et al., 2002, 2006a, 2007b, 2010; Hickman and Van Kranendonk, 2012). Although the precise sizes of the continental plates produced by the c. 3220 Ma breakup of the EPT are indeterminate, preserved geological evidence indicates that they were ‘microplates’ (<1 000 000 km²; Van Kranendonk et al., 2002, 2007b), and certainly not comparable in size to most Phanerozoic continents. Additionally, the two basaltic basins (Regal and Mosquito Creek Basins) that opened up between the separating plates of the Karratha, East Pilbara and Kurrana Terranes are here interpreted to have been no more than 400 km wide, and therefore comparable in size to the Red Sea today.

A metamorphic event in the northwest Pilbara Craton between c. 3160 and 3140 Ma (Kiyokawa, 1993; Kiyokawa and Taira, 1998; Smith et al., 1998; Beintema, 2003) is interpreted to mark the end of plate separation and the start of convergence, most likely as a result of collision of the northwest-moving KT with a plate converging from the northwest (Hickman, 2016). Following this collision the northwestern plate is here interpreted to have begun to push the KT southeast, back towards the EPT. This interpretation is based on evidence that, from c. 3160 Ma, the Regal Basin became compressed between the KT and the EPT. Resulting crustal failure within the Regal Basin led to formation of a subduction zone above which the mafic–felsic volcanic Whundo Group accumulated in a 3130–3110 Ma volcanic arc (Smithies et al., 2005a; Van Kranendonk et al., 2006a, 2007b). During the same post-3160 Ma convergence, parts of the Regal Formation were obducted as ophiolites onto the Karratha Terrane across the Regal Thrust (Sun and Hickman, 1998, 1999; Hickman et al., 2000, 2001, 2006, 2010; Hickman, 2001c, 2002, 2012, 2016; Hickman and Smithies, 2001; Van Kranendonk et al., 2002). In this Report, it is suggested that similar obduction occurred along the southeastern margin of the basin, involving thrusting of juvenile, MORB-like basaltic crust onto the East Pilbara Terrane. However, more mapping, structural analysis, geochemistry, and geochronology are required in

the Pilbara Well and Wodgina greenstone belts to examine this interpretation.

Once established between c. 3200 and 3160 Ma, the belt of thin mafic crust of the Regal Basin, separating the thicker, more rigid continental plates of the East Pilbara and Karratha Terranes, acted as a zone of weakness during subsequent plate interactions along the northwestern margin of the Pilbara Craton. It subsequently developed into a zone of episodic tectonic and magmatic activity named the Central Pilbara Tectonic Zone (CPTZ, Fig. 3; Hickman, 1999, 2001a, 2004; Smithies and Farrell, 2000b; Beintema et al., 2001, 2003; Hickman et al., 2001; Van Kranendonk et al., 2002; Beintema, 2003).

East Pilbara Terrane Rifting Event, 3280–3165 Ma

As indicated by the c. 100 Ma duration of the East Pilbara Terrane Rifting Event (EPTRE), the change from vertical to horizontal tectonics occurred gradually between c. 3280 and 3165 Ma; that is, during deposition of the Sulphur Springs and Soanesville Groups, and during eruption of the 3200–3160 Ma Regal Formation within the area of the CPTZ (Fig. 3). Accordingly, most evidence for the nature of the change has been derived from the stratigraphy, depositional environments, geochemistry and structural geology of these units. Progressively increasing crustal extension during deposition of the Sulphur Springs Group, most likely above a mantle plume, led to rifting, and eventual continental breakup and plate separation.

The 3280–3165 Ma EPTRE is interpreted to have developed in three main stages.

1. During deposition of the Sulphur Springs Group, plume-related volcanism and diapiric doming characteristic of the Pilbara Supergroup was accompanied by progressively increasing crustal extension and rifting with significant clastic sedimentation (Leilira Formation). Ultramafic–mafic sills and dykes were intruded in some of the extensional faults.
2. At c. 3220 Ma, rifting evolved into full-scale continental breakup and fragmentation of the of the pre-3220 Ma volcanic plateau of the EPT into three plates (East Pilbara, Karratha and Kurrana Terranes), which then commenced separation (Hickman, 2001a, 2004, 2012, 2016; Van Kranendonk et al., 2002, 2006b, 2007b, 2010; Hickman et al., 2010). Oceanic-like basaltic crust (3200–3160 Ma Regal Formation) was erupted in a spreading rift basin (Regal Basin) between the post-3220 Ma EPT and the newly formed KT.
3. Following plate separation, mantle plume activity and diapiric doming ceased and initially clastic sedimentary basins were formed on the margins of the three separating plates (Van Kranendonk et al., 2006a, 2007b; Hickman et al., 2010; Hickman, 2012, 2016). At c. 3185 Ma, clastic sedimentation in the Soanesville Basin was followed by eruption of basaltic volcanic rocks (Honeyeater Basalt) and intrusion of ultramafic–mafic sills and dykes (Dalton Suite). In this basin, volcanism increased northwest towards the margin of the Regal Basin. In the Mosquito Creek Basin, clastic sedimentation of the Budjan Creek Formation (Eriksson,

1981; Bagas et al., 2004c) was followed by mixed sedimentary and volcanic deposition of the Coondamar Formation (Bagas, 2005; Farrell, 2006).

Each stage involved various types of deformation, here assigned to D₇, D₈ and D₉.

D₇, 3280–3220 Ma

Following the EPE, the Sulphur Springs Group was deposited during a period of increasing crustal extension leading to the eventual rifting and breakup of the EPT, representing the first stage of the EPTRE. Crustal extension during deposition of the Sulphur Springs Group resulted in syndepositional normal faulting within both the Leilira Formation (Van Kranendonk, 2004b) and the Kangaroo Caves Formation (Vearncombe et al., 1995, 1998; Buick et al., 2002). Additionally, a c. 3235 Ma gabbro which intruded into the TTSZ along the northwest margin of the EPT (Beintema, et al., 2001; Beintema, 2003; Hickman, 2016) was most likely related to the extension.

Available geochronology indicates two periods of granitic intrusion between c. 3280 and 3223 Ma: a local event in the Yilgalong Dome at c. 3277 Ma (average age of rocks from three intrusions; Table 3, Appendix 4), and a regional event between c. 3257 and 3223 Ma elsewhere in the EPT (Table 3, Appendix 4). The existence of the c. 3277 Ma intrusions in the Yilgalong Dome suggests a tectonic event southeast of the exposed EPT that had little effect on the greater part of the terrane. Evidence of 3280–3270 Ma metamorphism includes a c. 3270 Ma Rb–Sr date on the Emu Pool Supersuite (Cooper et al., 1982). The volcanic rocks of the Sulphur Springs Group are contemporaneous with 3257–3223 Ma K-rich monzogranites of the Cleland Supersuite (Table 3, Appendix 4). In the northern Soanesville greenstone belt, the Sulphur Springs Group was arched upwards by intrusion of the Strelley Monzogranite laccolith (Van Kranendonk, 1997).

D₈, c. 3220 Ma

The main structures originating at c. 3220 Ma during breakup of the EPT were major faults such as the Tabba Tabba and Sholl Shear Zones (Beintema et al., 2001, 2003; Hickman, 2001b, 2004, 2016; Hickman et al., 2001; Van Kranendonk et al., 2002; Beintema, 2003), the Lalla Rookh – Western Shaw Structural Corridor (LWSC), and possibly the Kurrana Shear Zone (Hickman, 2012). The Tabba Tabba and Sholl Shear Zones are described later in the Report, but because c. 3220 Ma faulting along the trend of the LWSC is now interpreted to have greatly influenced deposition of the 3223–3165 Ma Soanesville Group, evidence for the c. 3220 Ma development of this structure is described here. A major fault zone similar to that of the LWSC is the Coongan–Warralong Fault Zone (CWFZ; Figs 5, 8, Plate 1C). Based on ⁴⁰Ar/³⁹Ar cooling ages between c. 3260 and 3200 Ma in the Coongan greenstone belt, Davids et al. (1997) suggested that an inferred linear structure, here named as the CWFZ (D₆ deformation), was active during D₈. Zegers et al. (1999) dated actinolite porphyroblasts that grew across the mylonite fabric of the CWFZ at 3197 ± 44 Ma, providing a minimum age for movement.

Lalla Rookh – Western Shaw Structural Corridor (early development)

One of the most important structures of the EPT is the Lalla Rookh – Western Shaw Structural Corridor (LWSC; Figs 5, 8, Plate 1C). Faulting within and along the margins of this zone were recognized in early geological mapping (Hickman and Lipple, 1978; Hickman, 1980c), although the significance of the structure was unknown. With the advent of satellite imagery in the 1980s, several major north-northeasterly trending lineaments were observed across the northern Pilbara Craton (Krapež and Barley, 1987; Krapež et al., 1990; Blake, 1993; Krapež, 1993; Eriksson et al., 1994; Krapež and Eisenlohr, 1998), and one of these coincides with the LWSC. Krapež (1993) interpreted the lineaments to have a long history of development and reactivation. Krapež and Eisenlohr (1998) referred to the LWSC as the 'Lalla Rookh Strike-Slip Orogen' (obsolete name) and their stratigraphic interpretation of the northern Pilbara Craton suggests that it formed sometime between c. 3325 and 3000 Ma. The first detailed description of the LWSC was by Van Kranendonk and Collins (1998) who initially referred to the LWSC as the 'Central Pilbara structural corridor' (obsolete name). Based on structural observations within the LWSC, they interpreted it to be a c. 2950 Ma structure superimposed on the Paleoproterozoic dome-and-keel crustal architecture of the EPT. Van Kranendonk et al. (2002) and Van Kranendonk (2008) re-interpreted the LWSC to be c. 2940 Ma zone of sinistral strike-slip movement resulting from compression across the CPTZ.

Several lines of evidence suggest that the LWSC, also described under **North Pilbara Orogeny, 2955–2919 Ma**, was superimposed on a zone of extensional faulting that originated during the EPTRE.

1. The regional distributions of the Sulphur Springs and Soanesville Groups suggest depositional control by a structural feature located along the trend of the LWSC. The Sulphur Springs Group is largely restricted to within the LWSC, although it is also present in the rifting zone now represented by the TTSZ. The Soanesville Group was deposited within the LWSC and across the western part of the EPT as far as the TTSZ. East of the LWSC, deposition between 3323 and 3165 Ma was limited to the Budjan Creek Formation on the northwest margin of the Mosquito Creek Basin. Paleocurrent and sedimentary facies evidence in the Soanesville Group indicate that the faulted eastern boundary of the LWSC coincided with a shoreline. In terms of stratigraphic units younger than the Soanesville Group, the Sisters Supersuite is almost entirely restricted to the area west of the LWSC (Van Kranendonk et al., 2006a, fig. 12); exceptions are several intrusions in the Shaw Dome. The post-3060 Ma structural geology of the areas east and west of the LWSC also differ, suggesting that the LWSC overlies a significant crustal boundary. However, the LWSC is not a suture because stratigraphic units older than c. 3325 Ma (Warrawona Group and Euro Basalt; Callina and Tambina Supersuites) outcrop both east and west of the LWSC, confirming a laterally continuous stratigraphy prior to the 3325–3315 Ma Wyman Formation.
2. Ultramafic–mafic intrusions of the c. 3185 Ma Dalton Suite are concentrated within the LWSC, and are interpreted to have been emplaced as a result of rifting

during regional extension (Van Kranendonk et al., 2010). Geochemical and Nd isotope data indicate that the Honeyeater Basalt of the Soanesville Group, also within and to the west of the LWSC, was likely fed from the same rift-related conduits as the Dalton Suite. These mafic igneous rocks were derived from juvenile crust, albeit with variable crustal contamination (Soanesville Basin). This suggests that the LWSC was a zone of crustal extension and rifting at c. 3200 Ma, although it failed to develop into a rift basin.

3. Rifting of the upper Sulphur Springs Group within the LWSC at c. 3235 Ma was accompanied by Cu–Zn VMS mineralization (Vearncombe et al., 1995, 1998; Brauhart et al., 1998; Van Kranendonk, 2000a, 2006; Huston et al., 2001d, 2007). Extension of the ‘marker chert’ (informal name) at the top of the Kangaroo Caves Formation was accompanied by intrusion of c. 3235 Ma rhyolite (Buick et al., 2002) and brecciation of the chert prior to deposition of the Corboy Formation (lower Soanesville Group).

D, 3220–3165 Ma

In the Pincunah greenstone belt, horst-and-graben block faulting of the Sulphur Springs Group was prevalent during deposition of the Corboy Formation (Wilhelmij and Dunlop, 1984; Van Kranendonk et al., 2010). Similar syndepositional extensional faulting produced graben-like basins in the Budjan Creek Basin (Eriksson, 1981). Deformation during deposition of the Soanesville Group in the Soanesville greenstone belt included extensional faulting of the Cleland Supersuite allowing mafic intrusion of the c. 3185 Ma Dalton Suite (Hickman, 2004; Van Kranendonk et al., 2006a, 2010). Eriksson (1981, 1982, 1983) interpreted clastic deposition of the Soanesville Group to have occurred during rifting and erosion of the Pilbara Supergroup on an ‘east Pilbara protocraton’. His geotectonic model involved an early intracratonic rift stage that evolved into a rifted continental margin. In the Soanesville and Pincunah greenstone belts, he interpreted a platform (alluvial) to trough (marine) transition towards the southwest, whereas in the Budjan Creek – Mosquito Creek area on the southeast side of the EPT, the same type of transition was towards the southeast.

Cause of the change in crustal evolution

Evidence from the PCMP indicates the geodynamic trigger for the EPTRE was crustal uplift, extension and thinning above the same mantle plume that led to volcanism of the Sulphur Springs Group and intrusion of the Cleland Supersuite (Van Kranendonk et al., 2002, 2006a,b, 2007b, 2010; Hickman, 2004, 2012). Mantle plumes are widely accepted to have caused Phanerozoic continental breakups (White and McKenzie, 1989; Storey, 1995; Ernst, 2014) and, within the Pilbara, the Neoarchean rifting and breakup of the Pilbara Craton during deposition of the Fortescue Group has been attributed to mantle plume activity (Arndt et al., 2001; Condie, 2001, 2004; Ernst et al., 2004; Pirajno, 2007; Pease et al., 2008). Moreover, convection related to a mantle plume is a likely cause of plate separation after continental breakup.

It has been suggested that an alternative cause of the change in the crustal evolution of the Pilbara Craton was a

cluster of asteroid impacts between c. 3260 and 3225 Ma (Glikson and Vickers, 2006, 2010; Glikson, 2007a). Although no evidence has been found in the Pilbara Craton for asteroid impacts during this time interval, impact spherule layers reported from the Barberton Greenstone Belt in South Africa and Swaziland (Lowe and Byerly, 1986, 1999, 2007, 2010; Lowe et al., 1989, 2003, 2014; Glass and Simonson, 2013) establish that major impacts did occur somewhere on Earth at this time. With respect to the evolution of the Kaapvaal Craton, Lowe et al. (2003) suggested that the transition from mainly basaltic and komatiitic volcanism of the Onverwacht Group to clastic and volcanoclastic deposition of the Fig Tree Group might be a direct consequence of these impacts. However, if the change in crustal evolution was a consequence of continental breakup leading to plate tectonics, the issue is that asteroid impacts are not generally considered to be capable of breaking up continents. For example, large impact craters on Precambrian continental crust, such as Vredefort, South Africa, and Sudbury, Canada, were not associated with continental breakup, or even significant rifting. Additionally, the chemistry of the Barberton spherules indicates oceanic impacts (Glikson, 2005b), and it appears even less likely that asteroids impacting oceanic crust could have led to fragmentation of adjacent continents.

Two other lines of evidence cast doubt on any relationship between the 3260–3225 Ma asteroid impacts recorded in South Africa and the change in crustal evolution in the Pilbara Craton. First, the EPTRE evolved over c. 100 Ma, commencing at c. 3280 Ma, before the asteroid cluster. Secondly, the Cleland Supersuite, which is the same age as c. 3240 Ma Barberton granitic rocks that have been cited as possible products of the impacts, represents the final K₂O-rich stage of granitic evolution in a c. 300 Ma process of crustal recycling (Bickle et al., 1993; Collins, 1993; Smithies, 2000; Champion and Smithies, 2001, 2007; Van Kranendonk et al., 2002, 2007a,b; Smithies et al., 2003, 2007b, 2009; Champion, 2013; Champion and Huston, 2016; Gardiner et al., 2017, 2018). Furthermore, the composition of the Cleland Supersuite is inconsistent with magma derivation from mantle melting, as would apply in an asteroid impact scenario. The first significant influxes of juvenile magma into the EPT after c. 3225 Ma occurred between c. 3199 and 3164 Ma (Mount Billroth Supersuite), nearing the end of plate separation.

Early Mesoarchean basins

Early Mesoarchean basin successions of the northern Pilbara Craton (Soanesville Group and the Nickol River, Budjan Creek and Coondamar Formations) were deposited in three basins – Nickol River, Soanesville and Mosquito Creek Basins – on the margins of the separating continental microplates (Van Kranendonk et al., 2010; Hickman, 2012, 2016). These tectonic settings are consistent with passive-margin successions (Hickman et al., 2010; Hickman, 2012, 2016; Hickman and Van Kranendonk, 2012). At c. 3200 Ma, the Mosquito Creek Basin included an early eruption of mafic volcanic rocks (Coondamar Formation) indicative of a deep rift transitioning into an ‘oceanic-like’ basin. The Nickol River Basin (marginal to the Karratha Terrane in the northwest Pilbara Craton) was described by Hickman (2016), and is not discussed further here.

Soanesville Basin

The 3223–3165 Ma Soanesville Basin unconformably overlies the volcano-sedimentary basin of the Sulphur Springs Group, and is unconformably overlain in turn by the sedimentary Gorge Creek Basin (Fig. 7). The stratigraphic succession of the Soanesville Group (Van Kranendonk et al., 2006a) is summarized in Table 1. In ascending stratigraphic order, this group comprises the following formations: 1) Cardinal Formation (shale and BIF, up to 1000 m thick); 2) Corboy Formation (sandstone, conglomerate, wacke, and shale, 2500 m thick); 3) Paddy Market Formation (BIF and Fe-rich clastic sedimentary rocks, 1000 m thick); 4) Honeyeater Basalt (komatiitic and tholeiitic basalt, 1000 m thick); 5) Pyramid Hill Formation (BIF and chert, up to 900 m thick); 6) Hong Kong Chert (chert, basalt, and siliciclastic sedimentary rocks); 7) Empress Formation (komatiitic basalt, komatiite, and thin chert units). Additionally, the 3223–3190 Ma Budjan Creek Formation in the southeastern Kelly greenstone belt is assigned to the Soanesville Group (Table 1), although it was deposited on the northwestern margin of the Mosquito Creek Basin.

The c. 3185 Ma Dalton Suite, consisting of numerous ultramafic–mafic sills and dykes intruding the lower Soanesville Group, was genetically related to the Honeyeater Basalt (Van Kranendonk et al., 2010).

Parts of the Soanesville Group are preserved in the Soanesville, Pincunah, Abydos, Wodgina, Pilbara Well, Cheearra, Tambina, Emerald Mine, Western Shaw and Kelly greenstone belts, (Fig. 8, Plate 1). Sinistral strike-slip faulting at c. 2940 Ma displaced the Soanesville greenstone belt relative to the Pincunah greenstone belt by at least 18.5 km (Van Kranendonk and Collins, 1998; Van Kranendonk, 2000a, 2008). This displacement might partly explain stratigraphic differences between these greenstone belts; in particular, the absence of thick BIF within the Cardinal Formation of the Soanesville greenstone belt.

Depositional age

Geochronology has established that the Soanesville Basin and two other late Paleoproterozoic–early Mesoproterozoic depositional basins of the northern Pilbara Craton (Mosquito Creek and Nickol River) formed during the late stages of the 3280–3165 Ma EPTRE. In the northern Soanesville greenstone belt, Rasmussen et al. (2007) reported a date of 3190 ± 10 Ma for xenotime interpreted as diagenetic in the Corboy Formation, and therefore indicating a minimum depositional age. In the same area, a U–Pb zircon date of 3185 ± 2 Ma was obtained for a gabbro sill of the Dalton Suite (GSWA 178185, Wingate et al., 2009a). If the interpretation that Dalton Suite intrusions were feeders to the overlying Honeyeater Basalt is correct, this result also indicates the age of that formation. Additionally, Van Kranendonk et al. (2010) described a unit of rhyolitic tuff dated at 3176 ± 2 Ma within basalts in the Pilbara Well greenstone belt (GSWA 180098, Wingate et al., 2009g). This suggests that the central part of the thick basaltic succession of this greenstone belt correlates with the Honeyeater Basalt.

The maximum depositional age of the Soanesville Group is constrained by two lines of evidence. First, in the Soanesville greenstone belt, the underlying Kangaroo

Caves Formation of the Sulphur Springs Group is well dated at 3253–3235 Ma, with most volcanism occurring between c. 3238 and 3235 Ma (Buick et al., 2002). This timing coincides with intrusion of the underlying Strelley Monzogranite at c. 3239 Ma (Buick et al., 2002). Buick et al. (2002) concluded that the Strelley Monzogranite was consanguineous with the felsic volcanic rocks of the Kangaroo Caves Formation, and described the monzogranite as a subvolcanic intrusion emplaced within its own volcanic edifice. Considered in isolation, it might therefore be interpreted that c. 3235 Ma is the maximum depositional age of the Soanesville Group.

A second constraint on the maximum depositional age of the Soanesville Group is that regional stratigraphic and sedimentological evidence indicates that it was deposited in a subsiding extensional basin after rifting and breakup of the EPT (Van Kranendonk et al., 2010; Hickman, 2012; Hickman and Van Kranendonk, 2012). Breakup and plate separation, resulting in marginal-basin successions, followed the final magmatic event in the EPT that was responsible for intrusion of the 3270–3223 Ma Cleland Supersuite (Van Kranendonk et al., 2006a, 2007b). This suggests an alternative maximum depositional age of c. 3223 Ma for the Soanesville Group.

Closer examination of the geochronology obtained by Buick et al. (2002) on the Kangaroo Caves Formation and Strelley Monzogranite raises the possibility that magmatic and hydrothermal activity related to the monzogranite continued after c. 3235 Ma. Thick mounds of coarse breccia overlying the ‘marker chert’ at the top of the Kangaroo Caves Formation contain intrusive rhyodacite. At the Kangaroo Caves prospect, the main zircon age component in the rhyodacite was dated at 3235 ± 3 Ma (sample 94002, Buick et al., 2002). A sample of rhyolite from the Kangaroo Caves Formation beneath the ‘marker chert’ was dated at 3238 ± 3 Ma, with no zircon dates younger than c. 3231 Ma (sample 72081, Buick et al., 2002). This geochronology is similar to the age of c. 3239 Ma for the adjacent Strelley Monzogranite (Buick et al., 2002).

Although the geochronological data from the Kangaroo Caves Formation and Strelley Monzogranite are dominated by 3239–3235 Ma zircons, there are also slightly younger outliers dated at c. 3220 Ma. Data from two of the three dated samples of Strelley Monzogranite (RM1 and 203368) included four near-concordant zircon analyses indicating dates between c. 3225 and 3213 Ma (Buick et al., 2002). Further data from the rhyodacite above the ‘marker chert’ included two near-concordant zircon analyses indicating dates (1σ) of 3217 ± 8 and 3214 ± 4 Ma (sample 94002, Buick et al., 2002). While these younger dates might be results of Pb loss, it is equally possible that there was late phase of monzogranite intrusion at c. 3220 Ma. This would be significant in terms of more closely constraining the depositional age of the overlying Corboy Formation (lower Soanesville Group). As determined by Rasmussen et al. (2007), the minimum depositional age of the Corboy Formation is c. 3190 Ma.

Sedimentology

Several sedimentological studies have investigated the Soanesville Group in the Soanesville and Pincunah greenstone belts, although until the regional stratigraphic revision by Van Kranendonk et al. (2006a), it was considered

a subgroup of the Gorge Creek Group. Eriksson (1981) studied the sedimentology of the Soanesville Group succession in the Pincunah greenstone belt, and that of the Budjan Creek Formation in the Budjan Creek area of the southeastern Kelly greenstone belt. He also studied the Lalla Rookh Sandstone that he interpreted to be contemporaneous, but which is now known to be c. 200 Ma younger than the Soanesville Group and is assigned to the Croydon Group (Table 1). In both successions, Eriksson (1981) interpreted deposition to have commenced with intracontinental rifting that produced horst-and-graben structures. Based on upward-changing lithofacies, he interpreted the depositional settings to have evolved from intracratonic continental rifting to deposition on a rifted continental margin. Eriksson (1981) presented evidence that with continued rifting, and possibly spreading, the Soanesville Group was deposited in two different environments: a continental platform, and a submarine deep-water trough along the western margin of the East Pilbara Terrane.

The lateral transition from the platform to the trough was interpreted to have been abrupt, with no intervening shallow-water marine shelf. The absence of a shallow-marine facies was interpreted to indicate a continental to marine transition across a narrow continental shelf. Thereafter, contemporaneous platform (alluvial) to trough (submarine fan) sedimentation prevailed. In the trough, clastic submarine fans prograded across basal, finer-grained sediments containing BIF protoliths. There is general agreement that BIF was not deposited in its present form, with nearly all the rock-forming minerals of BIF being secondary products of diagenesis or metamorphism. Suggested primary lithologies (protoliths) include iron-silicate mud, Fe-rich clay such as greenalite, ferric oxyhydroxides, and Fe-rich carbonate precipitates (Rasmussen et al., 2014a, 2016; Gauger et al., 2015; Smith, 2015; Konhauser et al., 2017). The sedimentary rocks, now exposed in the Pilgangoora Syncline of the Pincunah greenstone belt, include conglomerate, sandstone, shale, chert and BIF.

Tectonic setting

The first detailed sedimentological investigation of Mesoarchean Pilbara Craton basins was by Eriksson (1981, 1982), who interpreted an initial 'cratonic rift stage' in which sedimentation was governed by crustal extension and localized in grabens. This resulted in successions of sandstone, siltstone, shale and BIF. Much of the evidence for this tectonic model was derived from detailed observations in the Budjan Creek Formation of the southeastern Kelly greenstone belt (Eriksson 1981). A second study of the Soanesville Group was conducted by Wilhelmij and Dunlop (1984), who investigated the sedimentology of the Cardinal and Corboy Formations in the Pincunah greenstone belt. Wilhelmij and Dunlop (1984) interpreted a tectonically active basin, with deposition in fault-bounded sub-basins. Relatively thin, and laterally discontinuous, sandstone, siltstone, and shale units at the base of the succession were interpreted as wave- or tide-dominated, transgressive shelf deposits. On the southern side of the greenstone belt, an 800 m-thick unit of BIF and chert (named in this Report as the Pincunah Banded-Iron Member of the Cardinal Formation) was described as unconformably overlying volcanic rocks of the Warrawoona

Group' (in the Pincunah greenstone belt, these volcanic rocks are now assigned to the Sulphur Springs Group). With deepening of the basin, the lower sandstone, shale and BIF were overlain by coarse sandstone and turbidites that were deposited in submarine fans with migrating proximal channels. Wilhelmij and Dunlop (1984) interpreted the basin to have been rapidly subsiding, and deepening to the southwest. Coarse-grained sediment was deposited in submarine fans, with aggradational facies stacking in an uplapping fan-wedge system. The tectonic setting was interpreted to be an unstable continental margin.

The Soanesville Group is now interpreted to be a passive-margin succession that was deposited during stage 3 of the EPTRE (see **East Pilbara Terrane Rifting Event, 3280–3165 Ma**). Rifting across the EPT is likely to have commenced at different times in different areas. Under regional crustal extension, any pre-existing deep crustal fractures, such as the faulted boundaries of the EPT domes and major fault zones associated with earlier rifting, would have been likely to open sufficiently to allow mafic intrusions. This is thought to explain the concentration of ultramafic–mafic intrusions (Dalton Suite) along the boundaries of the EPT domes, and along basin boundary faults such as the Tabba Tabba and Kurrana Shear Zones. Owing to the relative difficulty of dating mafic and ultramafic rocks, only two closely associated mafic units have been directly dated from a shear zone. Metadiorite and gabbro in the TTSZ were dated by LA-ICP-MS at 3238 ± 10 Ma (metadiorite sample KB779, Beintema, 2003) and 3234 ± 9 Ma (gabbro sample KB810, Beintema, 2003). These dates suggest intrusion during rifting in stage 1 of the EPTRE. Additionally, ultramafic–mafic intrusions along the faulted boundary of the Coongan and Kelly greenstone belts (Central Coongan Shear Zone) are younger than c. 3315 Ma and older than c. 3197 Ma, based on the age of actinolite porphyroblasts that grew across the mylonite fabric of the shear zone (Zegers et al., 1999).

Soanesville Group

Stratigraphy

Within a revision of Pilbara Craton stratigraphy (Van Kranendonk et al., 2006a), the 6000 m-thick succession of the newly named Soanesville Group included three formations that had previously been assigned to the 'Soanesville Subgroup' of the Gorge Creek Group (Lipple, 1975); namely the Corboy Formation, Paddy Market Formation, and Honeyeater Basalt. Two formations added to the Soanesville Group by Van Kranendonk et al. (2006a) were the Cardinal Formation (shale underlying the Corboy Formation) and the Pyramid Hill Formation (BIF, chert and shale) overlying the Honeyeater Basalt in the Soanesville greenstone belt. The Soanesville Group was later separated from the newly defined Gorge Creek Group following the recognition of an erosional unconformity between the groups.

Basal unconformity of the Soanesville Group

Disconformities and angular unconformities are present at the base of different successions of the Soanesville Group. In greenstone belts where the Sulphur Springs Group is absent, the Soanesville Group unconformably overlies the Kelly Group or granitic rocks older than c. 3220 Ma.

An excellent example of the former situation is exposed in the southeastern Kelly greenstone belt where the Budjan Creek Formation overlies the Wyman Formation and Euro Basalt across an angular unconformity. A similar situation is present in the Cheearra greenstone belt where the Corboy Formation unconformably overlies various Paleoproterozoic granitic intrusions of the Yule Dome. These contacts, at the base of the Soanesville Group or its lateral equivalents, are major unconformities. Only where the Sulphur Springs Group is well preserved, as in the Soanesville greenstone belt, has the nature of the basal contact of the Soanesville Group been more controversial. However, the basal unconformity is of major importance in the stratigraphy of the northern Pilbara Craton because it marks not only the top of the Pilbara Supergroup, but also the breakup of the EPT and the unambiguous beginning of plate tectonic processes. The unconformity is situated at a stratigraphic level coinciding with a major change from volcanic deposition of the Pilbara Supergroup to mainly sedimentary deposition of the Soanesville Group, and subsequently in the Gorge Creek and Croydon Groups. The unconformity also marks a tectonic change from gravity-driven vertical deformation associated with episodic mantle plume events (3530–3220 Ma) to horizontal deformation involving plate separation and convergence (3220–2900 Ma; Van Kranendonk et al., 2010).

The contact between the Soanesville Group and the underlying Sulphur Springs Group has mostly been described as an unconformity (Hickman and Lipple, 1975; Hickman, 1981, 1983; Wilhelmij and Dunlop, 1984; Morant, 1995, 1998; Glikson, 2001; Buick et al., 2002; Glikson and Vickers, 2006, 2010; Rasmussen et al., 2007). However, in the Soanesville greenstone belt, Van Kranendonk (1997, 2000, 2003) interpreted the contact to vary from conformable to disconformable, locally involving an onlap of the Soanesville Group across the Sulphur Springs Group. Van Kranendonk et al. (2006a) also described the contact as a disconformity, and commented that the onset of deposition of the Soanesville Group directly followed deposition of the Sulphur Springs Group. One reason given for this interpretation was that hydrothermal alteration associated with VMS mineralization in the Sulphur Springs Group is also present in the base of the Soanesville Group. However, as already noted, felsic magmatic activity related to the underlying Strelley Monzogranite might have continued through and above the 'marker chert' until c. 3220 Ma, about c. 15 Ma after deposition of the Sulphur Springs Group. This is consistent with the 3270–3223 Ma age range of the Cleland Supersuite.

Geochemistry

Geochemical studies of the Soanesville Group have been limited to the Honeyeater Basalt and the Empress Formation (Glikson and Hickman, 1981a,b; Glikson et al., 1986; Smithies et al., 2007a). Glikson and Hickman (1981a) analysed 28 volcanic samples from the Honeyeater Basalt in the Soanesville Syncline of the southern Soanesville greenstone belt, and Glikson et al. (1986) provided more-accurate REE and HFSE analyses for four of these samples. Smithies et al. (2007a) provided analyses of five samples of the Honeyeater Basalt from the northern Soanesville greenstone belt. These five samples were all low-Ti basalts with strongly LREE-depleted normalized trace element patterns. Glikson and Hickman (1981) reported low-Ti basalts with relatively high K_2O (>0.5 wt%), Ba (400 ppm) and Rb (20 ppm). Data from

Glikson et al. (1986) revealed LREE enrichment, probably resulting from either crustal contamination or a crustal component in the source. Similar LREE enrichment was recorded by Van Kranendonk et al. (2010) from basalts in the lower Pilbara Well greenstone belt succession. In contrast, samples from the upper Pilbara Well succession (Empress Formation; Fitton et al., 1975), and from the Wodgina greenstone belt (Fig. 8), have depleted LREE profiles with no evidence of crustal contamination.

Whole-rock Nd model ages and ϵ_{Nd} values from basalt samples from the Pilbara Well greenstone belt (Smithies et al., 2007a) support geochemical evidence that the lower and upper parts of the succession were formed in different tectonic settings. Two basalt samples from the Honeyeater Basalt, collected close to the c. 3176 Ma rhyolitic tuff, yielded Nd model ages of c. 3540 and 3470 Ma and ϵ_{Nd} values of -1.52 and -0.57 , suggesting Paleoproterozoic bulk sources. However, a basalt collected from the Empress Formation has a Nd model age of c. 3320 Ma and a ϵ_{Nd} value of $+1.32$, indicating a more juvenile source (Van Kranendonk et al., 2010). The Nd data from this sample are similar to data from juvenile basaltic crust of the Regal Formation, which underlies the Mallina Basin northwest of the Pilbara Well greenstone belt. Two basalt samples collected from the Wodgina greenstone belt are isotopically similar to the upper basalt of the Pilbara Well greenstone belt.

The basaltic successions of the Wodgina and Pilbara Well greenstone belts have been correlated with the Honeyeater Basalt (Plate 1A; Hickman, 2010), although the isotopic evidence of far more juvenile basalt in the Empress Formation suggests that this is a separate stratigraphic formation. Evidence from mapping (Smithies and Farrell, 2000a) indicates that the Hong Kong Chert (Fitton et al., 1975), which conformably underlies the Empress Formation, includes a basal conglomerate (Smithies and Farrell, 2000b). Therefore, it remains possible that the contact between the Honeyeater Basalt and the Hong Kong Chert is either an unconformity or a tectonic contact.

Cardinal Formation

The Cardinal Formation (Van Kranendonk et al., 2006a), is a unit of red-weathering grey shale, siltstone, chert, BIF and minor felsic volcanoclastic rocks, up to 1000 m thick, which forms the base of the Soanesville Group in several greenstone belts. The shale was previously part of the 'Pincunah Hill Formation', which included the 800–1000 m-thick BIF unit at the base of the group in the Pincunah greenstone belt (Van Kranendonk and Morant, 1998). Sedimentological studies (Eriksson, 1981; Wilhelmij and Dunlop, 1984) indicated that the BIF and shale are facies variations of the same formation. Wilhelmij and Dunlop (1984) observed that several shale units are included within the BIF in the eastern section of the Pincunah greenstone belt, and they interpreted a west to east change from BIF to shale before the onset of submarine-fan deposition (Corboy Formation). The BIF of the Cardinal Formation is formally named as the Pincunah Banded-Iron Member (PBIM). In the Pincunah greenstone belt (Fig. 8, Plate 1A), the basal 10–40 m-thick succession of the Cardinal Formation is locally composed of metamorphosed and partly mylonitized quartz sandstone. Wilhelmij and Dunlop (1984) named this unit the 'Tank Pool quartzite' (informal). This unit was mapped by Hickman and Lipple (1978a) as an unnamed

quartzite extending laterally along a strike length of about 15 km in the vicinity of Tank Pool. Blewett and Champion (2005) described it as a mylonitized quartzite including units of semipelitic schist and BIF. Wilhelmij and Dunlop (1984) observed trough cross-bedding and cross-lamination in the metasandstone, and noted that is intercalated with, and grades laterally into, the 800 m-thick BIF unit (PBIM). Wilhelmij and Dunlop (1984) and Blewett and Champion (2005) identified a lithologically similar unit including sandstone and conglomerate underlying the Corboy Formation near the northern boundary of the Pincunah greenstone belt. This suggests that the unit is a tectonically attenuated fluvial sandstone that was locally deposited at the base of the Soanesville Group.

Pincunah Banded-Iron Member

The PBIM is 800–1000 m thick in the Pincunah greenstone belt (Fig. 8, Plate 1A), and mainly composed of red and black, thinly bedded BIF, with minor purplish-red to purplish-grey shale, chert, siltstone and sandstone. The BIF is highly magnetic, and contains a magnetite resource in the eastern Pincunah greenstone belt (Iron Bridge magnetite project). The member partly overlies, and is partly laterally transitional into, a 10–40 m-thick unit of sheared sandstone. The sandstone preserves trough cross-bedding and cross-lamination, suggesting deposition from currents carrying detritus eroded from the EPT. The PBIM is interpreted to be a submarine fan to basin plain unit that was deposited west of the EPT. Contemporaneous basaltic volcanism in the oceanic-like spreading centre of the Regal Basin is likely to have increased levels of iron in the ocean during deposition of the Soanesville Group.

Apart from its presence in the Pincunah greenstone belt, the PBIM forms part of the Cardinal Formation in the Western Shaw, Emerald Mine, Tambina, Panorama and North Shaw greenstone belts (Fig. 8, Plate 1B). Additionally, thin BIF units in the Cardinal Formation of the Soanesville greenstone belt are likely to be related to the member. In the southern section of the Western Shaw greenstone belt, BIF of the PBIM is composed of millimetre- to centimetre-thick layers of red-brown iron formation and microcrystalline quartz (Van Kranendonk, 2003). This BIF is overlain by light grey siltstone and quartz sandstone passing up into red and grey shales, and interbedded grey shales and siltstones, of the Cardinal Formation.

Stratigraphic status of the PBIM

During a regional revision of the stratigraphy of the northern Pilbara Craton, Van Kranendonk et al. (2006a) recognized a major unconformity within the succession previously assigned to the Gorge Creek Group (Lipple, 1975). Accordingly, they divided this succession into the Soanesville Group (previously 'Soanesville Subgroup') and the Gorge Creek Group. As part of the revision, Van Kranendonk et al. (2006a) assigned the thick BIF unit, previously named as the 'Pincunah Hill Formation' (obsolete; now Pincunah Banded-Iron Member) as a member of the Kangaroo Caves Formation of the Sulphur Springs Group. This changed a previous interpretation that this BIF is part of the Soanesville Group (Hickman, 1980b, 1983; Wilhelmij and Dunlop, 1984; Van Kranendonk and Morant, 1998; Van Kranendonk, 2000a, 2003; Van Kranendonk et al., 2002; Blewett and Champion, 2005). There are several important considerations requiring

reinstatement of the PBIM to the Soanesville Group.

1. In the Pincunah greenstone belt, the PBIM stratigraphically overlies the 'marker chert', which defines the top of the Kangaroo Caves Formation (Van Kranendonk, 1999; Blewett et al., 2001; Buick et al., 2002; Blewett and Champion, 2005).
2. According to Wilhelmij and Dunlop (1984), the basal BIF of the Pincunah greenstone belt was part of the succession then assigned to the Gorge Creek Group, and Van Kranendonk et al. (2006a) re-assigned that succession to the Soanesville Group. Wilhelmij and Dunlop (1984) observed that the BIF unconformably overlies volcanic rocks of the succession that Van Kranendonk et al. (2006a) assigned to the Sulphur Springs Group.
3. As described by Buick et al. (2002), the Kangaroo Caves Formation is mainly volcanic and contains no BIF. A minor exception to this generalization is that, southeast of the Strelley Monzogranite, a silicified unit correlated with the 'marker chert' locally includes BIF of hydrothermal origin (Van Kranendonk, 2000a).
4. In the Pincunah greenstone belt, the PBIM conformably underlies the Corboy Formation (Eriksson, 1983; Wilhelmij and Dunlop, 1984; Blewett and Champion, 2005), and in the Soanesville greenstone belt, the Corboy Formation unconformably overlies the Kangaroo Caves Formation (Morant, 1995, 1998; Glikson, 2001; Buick et al., 2002; Rasmussen et al., 2007; Glikson and Vickers, 2010).
5. In the Pincunah greenstone belt, BIF of the PBIM is intercalated with shale correlated with the Cardinal Formation, which is the basal formation of the Soanesville Group in the Soanesville greenstone belt (Van Kranendonk et al., 2006a).
6. The thickness, lateral extent, lithology, and facies associations of the PBIM are similar to BIF units that elsewhere form parts of large sedimentary basins such as the Hamersley, Transvaal, and Animikie Basins. These Precambrian BIFs were deposited over many hundreds of kilometres, in areas remote from the hydrothermal input of iron to the oceans (Konhauser et al., 2017). As for other stratigraphic units of the Soanesville Group, the distribution of the PBIM is almost entirely restricted to the LWSC and the western half of the EPT. Even so, its minimum north–south extent in the LWSC is 100 km, its east–west extent is at least 60 km, and it is 800–1000 m thick. In contrast, BIF units in mainly volcanic successions, referred to by some authors as 'Algoma-type' iron formations (Gross, 1980), rarely have lateral extents greater than 10 km and are normally less than 50 m thick (Bekker et al., 2010, 2014). The volcanic stratigraphy of the Kangaroo Caves Formation is therefore inconsistent with including a BIF of the PBIM type.

Corboy Formation

The Corboy Formation is the thickest (2500 m) and most widespread formation of the Soanesville Group. The formation was deposited in tectonically active basins during crustal extension, and is mainly composed of

submarine-fan deposits (Eriksson, 1981). In the Pincunah greenstone belt, Wilhelmij and Dunlop (1984) described the succession of the Corboy Formation (above the basal BIF member of the Cardinal Formation) as comprising shales, siltstones, and sandstones, and multiple thin units of chert and BIF. The succession was interpreted to be dominated by turbidites and pelagic shales. Eriksson (1981) included lenticular channel deposits containing conglomerate and sandstone locally up to 500 m thick and 1500 m wide, and separated from the turbidites by levees of laminated shale and siltstone. In the southern Pincunah greenstone belt, the basal unit of the Corboy Formation is a 100 m-thick unit of quartzite, siltstone, wacke, and conglomerate that overlies the PBIM (Van Kranendonk, 2000a). Above this basal unit is a homogeneous unit of brown-weathering lithic sandstone or greywacke almost 1000 m thick. An overlying thin unit of shale and polymictic conglomerate is succeeded by an upper succession of siltstone, shale and sandstone of uncertain thickness (Van Kranendonk, 2000a). In the western Pincunah greenstone belt, the Corboy Formation is overlain by a unit about 200 m-thick of quartz sandstone and sandstone assigned to the Farrel Quartzite (Hickman, 2010).

The Corboy Formation is the basal formation of the Soanesville Group in the Sulphur Springs area of the northern Soanesville greenstone belt, although in the south of this greenstone belt, and in the Pincunah, Tambina and Emerald Mine greenstone belts, it is underlain by the Cardinal Formation. At Sulphur Springs, the Corboy Formation has a maximum thickness of 475 m but this thickness varies across a mass of breccia and intrusive rhyodacite above the 'marker chert' which formed a topographic high during its deposition (Van Kranendonk, 2000a). Basal polymictic conglomerate includes large pebbles of black chert derived from erosion of the 'marker chert' at the top of the underlying Sulphur Springs Group (Van Kranendonk, 2000a). Above the conglomerate, the main part of the formation is an upwards-fining sequence of graded beds of pebbly sandstone overlain by graded sandstone-siltstone beds. The depositional setting was probably a series of shallow-marine deltas and fans (Wilhelmij, 1986), which contrasts with the deep-water submarine-fan setting of the Corboy Formation in the Pincunah greenstone belt. The Corboy Formation also forms parts of the Tambina and Emerald Mine greenstone belts (Fig. 8, Plate 1B), although most of the Soanesville Group in these areas is shale and iron formation facies assigned to the Cardinal and Paddy Market Formations.

The Corboy Formation was previously interpreted to underlie the Cleaverville Formation in the East Strelley greenstone belt (Hickman, 1980b; Wilhelmij and Dunlop, 1984). However, data from the PCMP led to a revision of the stratigraphy in this area: the formation previously correlated with the Corboy Formation is now correlated with the Farrel Quartzite of the Gorge Creek Group (Hickman, 2010; Van Kranendonk et al., 2010). This revision was based on regional continuity of the Gorge Creek Group from the type area of Gorge Creek (Warralong greenstone belt). In the Warralong greenstone belt, a clastic sedimentary succession unconformably underlying the Farrel Quartzite and overlying the Sulphur Springs Group (Van Kranendonk, 2004b) is interpreted to be a local remnant of the Soanesville Group (Fig. 35).

Quartzite and metasandstone of the Cheearra greenstone belt, preserved in isolated outliers and enclaves across the granitic core of the Yule Dome (Fig. 38), are tentatively assigned to the Corboy Formation, although no stratigraphic

or sedimentological studies have been undertaken. Most detrital zircons in the metasandstones have Eoarchean to early Paleoeoarchean U–Pb ages (GSWA 169013, Nelson, 2004c; GSWA 178045, Nelson, 2005i; Kemp et al., 2015a,b). It is currently inferred that detritus comprising the Corboy Formation in this greenstone belt included material derived from erosion of the EPT and underlying Eoarchean rocks east of the Lalla Rookh – Western Shaw Structural Corridor; no rocks older than the Tambina Supersuite have yet been identified from sparse geochronology in the Yule Dome.

Paddy Market Formation

The Paddy Market Formation conformably overlies the Corboy Formation in the Soanesville greenstone belt and is distinguished from that formation by being mainly composed of units of BIF intercalated with ferruginous clastic sedimentary rocks. Lipple (1975) estimated the total thickness of the formation as 1000 m and described it as comprising units of BIF, ferruginous shale, and ferruginous siltstone and sandstone. Van Kranendonk (2000a, 2008) reported the distribution of the Paddy Market Formation as extending through the Soanesville, East Strelley, Panorama, North Shaw, Emerald Mine and Tambina greenstone belts (Fig. 8, Plate 1B). Southwest from Shaw Gorge in the North Shaw greenstone belt, the base of the formation is composed of finely layered chert overlain by thinly bedded BIF, red and green shale, black, white, and brown banded chert (after shale), up to 10 m of sandstone, up to 100 m of jaspilite, and chert. Van Kranendonk (2000a) interpreted the stratigraphically highest chert to contain felsic volcanic breccia and silicified, well-bedded, felsic volcanoclastic tuff overlain by 200 m of massive to spherulitic dacite. These felsic rocks have not been dated and it is uncertain if the dacite is extrusive or intrusive. Cenozoic silicification of ferruginous shale and siltstone has formed secondary chert and BIF on the tops of ridges. Van Kranendonk (2003) recorded similar silicification of ferruginous shale in the Emerald Mine greenstone belt (Fig. 8, Plate 1B).

Honeyeater Basalt

The Honeyeater Basalt was first recognized and defined in the Soanesville greenstone belt (Lipple, 1975) where it is up to 1000 m thick and is composed of komatiitic and tholeiitic basalt (Gliksun and Hickman, 1981a,b; Van Kranendonk, 2000a; Van Kranendonk et al., 2006a; Smithies et al., 2007a). This unit conformably or disconformably overlies the Paddy Market Formation. The depositional age of the basalt in this greenstone belt is c. 3185 Ma based on SHRIMP U–Pb zircon dating of a gabbro sill that is interpreted to be one of many subvolcanic feeders to the formation (GSWA 178185, Wingate et al., 2009a; Van Kranendonk et al., 2010). A stratigraphic section through the Honeyeater Basalt in the southern Soanesville greenstone belt (Gliksun and Hickman, 1981b, fig. 2.1d) indicates that komatiitic basalt is confined to the lower half of the formation, pillow basalts are restricted to the central and upper parts of the formation, and dolerite and gabbro sills are present throughout the entire formation.

Basalt formations that have been correlated with the Honeyeater Basalt of the Soanesville greenstone belt are exposed in the North Shaw greenstone belt (Van Kranendonk, 2000a) and in the Wodgina and Pilbara Well greenstone belts (Hickman, 2010; Van Kranendonk et al.,

2010). Van Kranendonk et al. (2010) also assigned tholeiitic pillow basalt in the far western East Strelley greenstone belt (Fig. 8) to the Soanesville Group. Alternatively, since this basalt unit is not underlain by the Sulphur Springs Group or lower formations of the Soanesville Group, it might be part of the Euro Basalt (Hickman, 2010). Limited Sm–Nd isotope data from basaltic rocks of the Wodgina and Pilbara Well greenstone belts suggest evolved and juvenile sources, making the volume of Honeyeater Basalt in these areas uncertain. Geochronology in the Pilbara Well greenstone belt (Van Kranendonk et al., 2010) indicates a thick basalt succession of approximately the same age as the Honeyeater Basalt of the Soanesville greenstone belt, and the basalts of both areas are stratigraphically overlain by the Gorge Creek Group.

Pyramid Hill Formation

The Pyramid Hill Formation is composed of red to black shale, grey-and-white banded chert, and red to brown BIF. The formation outcrops in the Soanesville Syncline in the southern Soanesville greenstone belt, and on Agrippa Ridge between the Panorama and North Shaw greenstone belts. In the Soanesville Syncline, the Pyramid Hill Formation conformably overlies the c. 3185 Ma Honeyeater Basalt and is unconformably overlain by the Mount Roe Basalt of the Fortescue Group. At Agrippa Ridge, BIF, chert and shale correlated with the Pyramid Hill Formation conformably overlie the Honeyeater Basalt and unconformably underlie the c. 2950 Ma Lalla Rookh Sandstone. However, there are no geochronological data from any units at Agrippa Ridge to test stratigraphic correlations with the Soanesville Group.

In the Soanesville Syncline, the Pyramid Hill Formation is 100–200 m thick based on outcrop width, although the top of the formation is not exposed. The maximum depositional age of the Pyramid Hill Formation is c. 3185 Ma, the interpreted maximum depositional age of the underlying Honeyeater Basalt (GSWA 178185, Wingate et al., 2009a). In the Soanesville area, the Pyramid Hill Formation conformably overlies the Honeyeater Basalt and comprises red to black shale, grey and white banded chert, and red to brown BIF. The BIF is composed of alternating centimetre-thick layers of hematite-rich chert and silica-rich chert.

At the southern end of Sunset Ridge (Zone 50, MGA 735200E 7653600N), 3 km north of Honeyeater Creek, BIF and shale underlying the Lalla Rookh Sandstone were previously interpreted to be parts of the Pyramid Hill Formation (Van Kranendonk and Morant, 1999; Van Kranendonk, 1999a, 2000a). This correlation is no longer preferred because aeromagnetic imagery, combined with geological mapping to the north and west of Sunset Ridge, indicates that the Lalla Rookh Sandstone is underlain by the Cleaverville Formation throughout the Lalla Rookh Synclinorium. The Sunset Ridge outcrop of BIF is separated from the Honeyeater Basalt by a large fault, preventing an interpretation that this BIF is conformable with the basalt. An alternative interpretation, which would require testing by more detailed mapping and geochronology, is that the BIF at Sunset Ridge is silicified and Fe-rich shale at the base of the Lalla Rookh Sandstone.

Conformably overlying the Honeyeater Basalt, and relatively restricted in its distribution, the Pyramid Hill Formation might

be a relatively proximal hydrothermal deposit rather than a sedimentary BIF that was deposited over a large area. At present, there is insufficient lithological and geochemical evidence to test this possibility.

Hong Kong Chert

The Hong Kong Chert (Fitton et al., 1975) is apparently restricted to the Pilbara Well greenstone belt, although it occupies the same stratigraphic position, immediately overlying the Honeyeater Basalt, as the Pyramid Hill Formation in the Soanesville Syncline of the east Pilbara Craton. In this Report, the formation is tentatively included in the Soanesville Group based on dating of the underlying Honeyeater Basalt at 3176 ± 3 Ma (GSWA 180098, Wingate et al., 2009g; Van Kranendonk et al., 2010) and a minimum depositional age of c. 3166 Ma for the overlying Empress Formation.

The Hong Kong Chert comprises two units of grey-and-white banded chert separated by silicified basalt, komatiitic basalt, gabbro and clastic sedimentary rocks including conglomerate, breccia and sandstone. When first named (Fitton et al., 1975), the formation was interpreted to be a single chert formation folded by a major northeast-plunging isoclinal anticline. This structure was mapped in the core of a larger anticline that formed the northwestern part of a fold pair that dominated the structural geology of the Pilbara Well greenstone belt. Southeast of the anticline, Fitton et al. (1975) interpreted a more open northeast-plunging syncline (John Bull Syncline). Following new geological mapping (Smithies and Farrell, 2000a,b; Van Kranendonk et al., 2010), the revised interpretation is that the Hong Kong Chert includes two chert members located along a major northeast-striking fault that bisects the Pilbara Well greenstone belt. In this Report, this fault is interpreted to be a major thrust and is referred to as the Kangaroo Flat Thrust. It tectonically removed the northwestern, southeast-facing limb of the John Bull Syncline, transporting the upper Honeyeater Basalt, the Hong Kong Chert and the Empress Formation over older greenstone units to the southeast. Pillow structures in the Honeyeater Basalt on both sides of the thrust indicate younging to the northwest; moreover, Van Kranendonk et al. (2010) emphasized that the metamorphic grade of greenstones in the succession northwest of the thrust is lower greenschist facies, whereas the greenstone succession to the southeast is metamorphosed to amphibolite and upper greenschist facies.

This revised structural interpretation is stratigraphically important because the greenstone succession northwest of the Kangaroo Flat Thrust is younger than the succession to the southeast. In describing the lithology of the Hong Kong Chert, Smithies and Farrell (2000b) combined evidence from the Hong Kong Chert near Hong Kong mine northwest of the thrust with observations on a chert and sandstone unit north of Pilbara Well on the southeast limb of the John Bull Syncline. This southeastern unit is now correlated with the 3426–3350 Ma Strelley Pool Formation. Detrital zircon data from sandstone of the southeast unit are very similar to data from the Strelley Pool Formation at the type locality in the East Strelley greenstone belt. Additionally, basalt overlying the Strelley Pool Formation includes komatiite units with peridotite compositions, which is characteristic of the Euro Basalt in other greenstone belts.

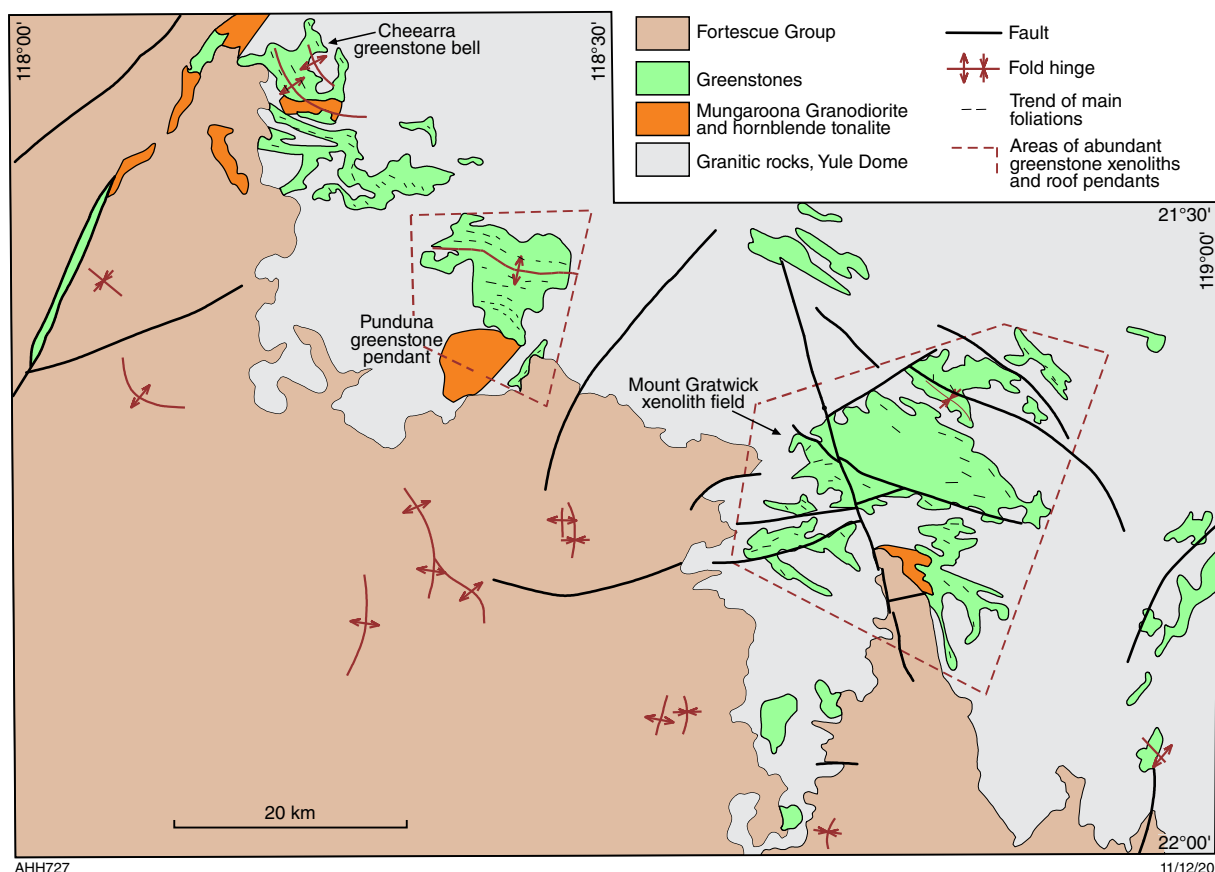


Figure 38. Simplified structural geology of the southern Yule Dome showing outcrops of high-Mg diorite and granodiorite, and hornblende tonalite. The east-southeast trend of fold structures, foliations, greenstone xenoliths, and amphibolite facies metamorphism is at a high angle to structural trends farther north in the Yule Dome, and transects the dome-and-keel architecture of the EPT. Modified from Smithies (2003)

In the vicinity of the Hong Kong mine, the Hong Kong Chert includes a silicified basal sequence of mafic volcanoclastic breccia, conglomerate and sandstone (Smithies and Farrell, 2000b). Smithies and Farrell (2000b) described the overlying succession as comprising a lower chert 'zone', an intervening succession of basalt, silicified metagabbro, and strongly silicified mafic and sedimentary rocks, and an upper chert 'zone'. The chert zones rank as members of the formation, although there is currently insufficient detail to name and define them. The colour of the chert varies from off-white to black, and the degree of layering is variable. Layers are between 0.1 and 40 mm thick, and most of the thicker layers have fine-scale internal laminae or microbanding. The upper chert member contains alternating dark-grey and cream or pale-grey layers up to about 700 mm thick.

The formation has a stratigraphic thickness of 150 m and outcrops in a northeast–southwest direction over a strike length of 13 km, and is unconformably overlain by younger formations at both ends of this exposure. In addition to grey-and-white banded chert, the Hong Kong Chert contains a basal unit of conglomerate, sandstone and basaltic volcanoclastic breccia (Smithies and Farrell, 2000a).

Empress Formation

The Empress Formation (Fitton et al., 1975) outcrops along the northwest side of the Pilbara Well greenstone

belt over a total strike length of 60 km, although between Hong Kong mine and Nunyerry Gap it is largely concealed by the Fortescue Group. The formation is 1500–2000 m thick and comprises komatiitic basalt and komatiite with sills or flows of peridotite and numerous thin chert units. In the northern Pilbara Well greenstone belt, the Empress Formation conformably overlies the Hong Kong Chert and is unconformably overlain by the Gorge Creek and Croydon Groups. Inclusion of the Empress Formation within the Soanesville Group is new in this Report, and is based on apparently conformable contacts with the underlying Hong Kong Chert, and its depositional age being closely similar to that of the Honeyeater Basalt. Limited geochemical and isotope data from the Pilbara Well greenstone belt indicate significant differences from some parts of the Honeyeater Basalt, but not from others.

In the vicinity of Nunyerry Gap, the Empress Formation is intruded by the c. 3165 Ma Flat Rocks Tonalite, constraining its minimum depositional age. The maximum age of the formation is constrained by the 3176 ± 3 Ma date on the underlying Honeyeater Basalt (GSWA 180098, Wingate et al., 2009g).

The geochemical and isotope compositions of the juvenile basalt of the Empress Formation (Smithies et al., 2007a; Van Kranendonk et al., 2010), combined with its deformation by recumbent folding and thrusting (Blewett, 2002; Blewett

and Champion, 2005; Van Kranendonk et al., 2010), suggest it may be part of an ophiolite succession obducted southeastwards from c. 3200 Ma juvenile basaltic crust (Regal Basin) onto the EPT. If such obduction occurred, it is likely to have been between c. 3160 and 3070 Ma during convergence of the East Pilbara and Karratha Terranes, and before the Prinsep Orogeny. This scenario is analogous to the northwestwards obduction of the Regal Formation onto the Karratha Terrane in the northwest Pilbara Craton (Hickman, 2001c, 2004, 2016; Hickman et al., 2010). The 3066–3015 Ma Gorge Creek Group, deposited following plate collision (Prinsep Orogeny), unconformably overlies the interpreted obducted juvenile crust on both sides of the Mallina Basin.

Budjan Creek Formation

The Budjan Creek Formation is well exposed along a southwest–northeast strike length of 60 km in the eastern Kelly greenstone belt (Fig. 8, Plate 1). The formation unconformably overlies the Wyman Formation and Euro Basalt and is an upwards-fining succession of conglomerate, sandstone, siltstone and shale, with coarse felsic volcanoclastic rocks locally deposited at the top of the formation (Bagas et al., 2004c). In the southwest of this linear outcrop, the basal part of the formation is a 1200 m-thick succession starting with a matrix-supported boulder conglomerate. The conglomerate fines upwards into a succession of pebble conglomerate interbedded with arkosic sandstone, siltstone and shale (Bagas et al., 2004c). Clasts in the conglomerate include vein quartz and chert with rare felsic volcanic rocks, consistent with derivation from the underlying Kelly Group. The arkosic composition of the sandstone suggests derivation from granitic rocks, most likely those of the Corunna Downs Dome to the west. Sandstone beds in the basal unit contain planar cross-beds and rare trough cross-beds that indicate paleocurrents trending towards the south and southeast (Bagas et al., 2004c). This basal clastic unit is conformably overlain by a 600 m-thick unit of lithic wacke, siltstone, minor conglomerate, felsic tuff and fine-grained volcanogenic sandstone (Bagas et al., 2004c).

The stratigraphically highest units in the formation are felsic volcanoclastic rocks. Detrital zircons in a fine-grained sample collected near Copper Hills (GSWA 168908, Nelson, 2001c) have a dominant age component at 3308 ± 5 Ma, consistent with derivation from the Boobina Porphyry, Wyman Formation, or the Carbara Monzogranite. GSWA 168908 also contained a single, near-concordant younger zircon dated at 3228 ± 6 Ma (1 σ). If this date does not reflect loss of radiogenic Pb, this zircon could have been eroded from the Cleland Supersuite. The youngest granitic intrusion of the Cleland Supersuite in the EPT was dated at 3223 ± 3 Ma (GSWA 178076, Bodorkos et al., 2006). If intrusion of the Cleland Supersuite pre-dated breakup and plate separation of the EPT, the minimum age of the Cleland Supersuite provides a maximum depositional age for the Budjan Creek Formation.

Tectonic setting

Deposition of the Budjan Creek Formation commenced with intracontinental rifting that produced horst-and-graben

structures (Eriksson, 1981). The formation was deposited along the southeastern margin of the EPT during separation of the KUT from the EPT (Hickman, 2012). Paleocurrent data and facies changes indicate that the depositional basin became deeper to the south or south-southeast (Eriksson, 1981; Bagas et al., 2004c), suggesting deposition on the north-northwestern margin of the rift basin that developed into the Mosquito Creek Basin (Fig. 3). In this interpretation, the Budjan Creek Formation was a passive-margin succession on the southeastern side of the EPT, similar to the Corboy Formation on the western margin of the EPT, where the Soanesville Basin deepened to the west or southwest.

Mosquito Creek Basin

In the southeast of the northern Pilbara Craton, between the EPT and the KUT, the Mosquito Creek Basin (Fig. 39) contains the successions of the Coondamar and Mosquito Creek Formations, which together make up the c. 3200–2930 Ma Nullagine Group. Due to an absence of felsic volcanic rocks in the Nullagine Group, the estimated depositional ages of the formations rely on dating of detrital zircons and inferred relations to igneous intrusions. Maximum depositional ages for different units of the Mosquito Creek Formation are c. 2980–2930 Ma (data in Bagas et al., 2008). The theoretical maximum depositional age of the Coondamar Formation is constrained by the interpretation that the Mosquito Creek Basin was formed by 3220–3200 Ma separation of the KUT from the EPT during the EPTRE. Additionally, the 3199–3178 Ma Golden Eagle Orthogneiss contains greenstone enclaves possibly acquired during intrusion into the Coondamar Formation; if so, part of the Coondamar Formation is older than c. 3178 Ma. The formation is extensively intruded by sills of peridotite, pyroxenite and gabbro. These intrusions, which are absent from the Mosquito Creek Formation, are likely to have been emplaced during the EPTRE, in which case they are probably of similar age to c. 3185 Ma Dalton Suite (Hickman, 2012).

The present 30 km width of the basin is the result of major south–north compression of the succession during the 2930–2900 Ma Mosquito Creek Orogeny. Reconstruction of the deformation, including upright isoclinal folding and thrusting, suggests that the depositional width of the basin probably exceeded 100 km. The present uniform width of the basin along its exposed length of 60 km, and its formation as a rift basin, suggest an original east–west length of at least several hundred kilometres. Gravity data indicate that south and southwest of Nullagine the basin strikes southwest for another 100 km beneath the unconformably overlying Fortescue Group (Bagas et al., 2004b; Hickman, 2004). Evidence for a greater lateral extent was provided by Bagas et al. (2008) who noted that a number of detrital zircon age components in the Mosquito Creek Formation have no apparent provenance in the northern Pilbara Craton. Since there is no evidence that the Mosquito Creek Basin extended into the southern area of the Pilbara Craton, it is possible that the basin extended west, rather than southwest, under the area now occupied by the Fortescue Valley. In this scenario, the Chichester Tectonic Zone in the southern Yule Dome might be related to closure of a western continuation of the Mosquito Creek Basin.

Coondamar Formation

The Coondamar Formation (Van Kranendonk et al., 2004c) comprises a metamorphosed succession of komatiitic basalt, tholeiitic basalt, chloritic sedimentary rocks, mafic volcanoclastic sandstone, and chert underlying the Mosquito Creek Formation (Bagas, 2005; Farrell, 2006). On the northern side of the Mosquito Creek Basin (Figs 3, 5, 8), mafic and ultramafic rocks of the Coondamar Formation occupy a 1 km-wide, east–west-striking Mesoarchean belt that cuts across the Paleoproterozoic stratigraphy and structures of the McPhee and Yilgarn Domes. Therefore, the Coondamar Formation was deposited after the Paleoproterozoic dome-and-keel architecture of the McPhee and Yilgarn Domes had been formed; that is, after c. 3220 Ma. Contacts between the Coondamar Formation and the underlying EPT stratigraphy are either unconformities or faulted unconformities. The Nullagine Group was thrust northwards onto the EPT during the 2930–2900 Ma Mosquito Creek Orogeny (Farrell, 2006; Nijman et al., 2010).

The southern boundary of the Coondamar Formation, against the KUT, is the Kurrana Shear Zone (KSZ; Figs 5, 8). This major zone of faulting, separating the Coondamar Formation from the Golden Eagle Orthogneiss, has been recognized in all detailed studies of the Mosquito Creek Basin (Hickman, 1975a, 1978; Tyler et al., 1992; Blewett, 2002; Bagas et al., 2004a,b, 2008; Bagas, 2005; Farrell, 2006; Nijman et al., 2010). Geochronology indicates that tonalite and granodiorite protoliths of the Golden Eagle Orthogneiss were emplaced between c. 3199 and 3178 Ma. The orthogneiss contains numerous enclaves of greenstone and chert that might be parts of the Coondamar Formation. Ultramafic and mafic sills within the Coondamar Formation adjacent to the KSZ might belong to the Dalton Suite (Hickman, 2012).

The high proportion of metamorphosed basaltic rocks in the Coondamar Formation is consistent with an origin as juvenile crust within a c. 3200 Ma rift basin (Hickman,

2012). Geochemical and isotopic evidence is lacking for the Coondamar Formation, but there is ample evidence that the lithologically similar Regal Formation of the northwest Pilbara Craton originated in this way (Ohta et al., 1996; Kiyokawa and Taira, 1998; Sun and Hickman, 1998, 1999; Beintema, 2003; Smithies et al., 2007a; Hickman et al., 2010; Hickman, 2012, 2016).

Mosquito Creek Formation

The Mosquito Creek Formation (Hickman, 1975b) is composed of metamorphosed sandstone, siltstone and shale with well-preserved graded bedding, local cross-bedding, and sole marks. Graded bedding is typically part of well-developed Bouma sequences (Bouma, 1962) showing a complete gradation from massive coarse-grained sandstone, through parallel-laminated and convolute-laminated siltstones, to shale (A, B, C and E Bouma divisions). Tabular beds of sandstone with massive or cross-bedded bases and thin, silty tops may be channel deposits. Siltstone and shale are metamorphosed to slate or phyllite, depending on local metamorphic grade and protolith composition, whereas sandstone is partly recrystallized and foliated. Farrell (2006) recorded that the slate and phyllite consist of fine-grained chlorite, illite/white mica, albite, carbonaceous matter (probably graphite), and quartz. Sandstone is composed of detrital white mica, quartz and clasts of grey or black chert, and in many areas is poorly sorted and matrix supported. Petrographically, the sandstones can be classified as lithic wacke or lithic arenite, but may range through to quartz wacke or subarkosic wacke.

Following mapping in the 1970s, Hickman (1975b, 1978) estimated the total stratigraphic thickness of the Nullagine Group to be 5000 m. The preserved thickness of the Mosquito Creek Formation in the eastern part of the basin might be less than 2000 m. Here, Farrell (2006) interpreted east–west striking sandstone and conglomerate ridges within the outcrop of the Mosquito Creek Formation as being narrow windows of the underlying Coondamar Formation

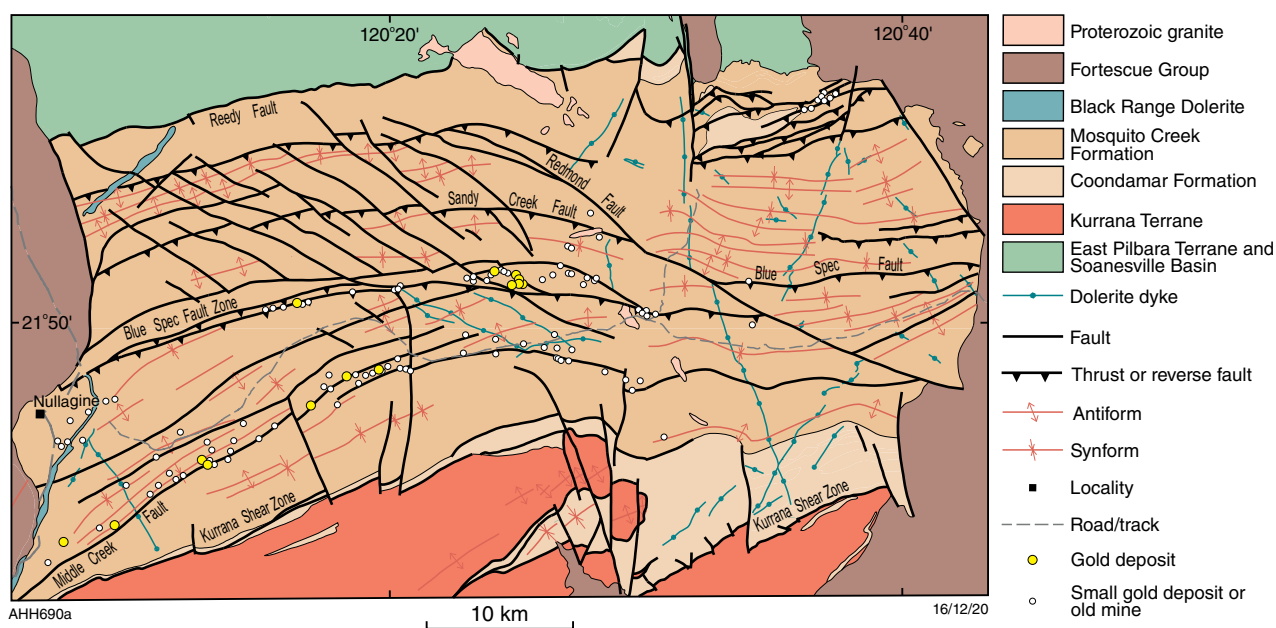


Figure 39. Geological setting of the Mosquito Creek Basin showing major structures and areas of gold mineralization

exposed along anticlinal hinge zones. A thicker succession is preserved in the western part of the basin where the 30 km basin width, and high-amplitude upright folding with only marginal exposure of the Coondamar Formation, suggests a thickness in excess of 3000 m. As in the Mallina Basin of the northwest Pilbara Craton, there has been no detailed stratigraphic subdivision due to structural complexity, lateral facies changes, a lack of distinctive stratigraphic marker units, and discontinuous exposure.

Nijman et al. (2010) subdivided the formation into several informal stratigraphic units, and presented an interpretation of the evolution of the Mosquito Creek Basin. Their interpretation agreed with that of Bagas et al. (2008), that the basin fill was derived from the EPT along its northern margin, whereas in the south it was derived from the KUT. Conglomerate facies are present along both margins. The central part of the basin is mainly composed of distal turbidite units. Bagas et al. (2004b, 2008) used detrital zircon ages to suggest derivation of detritus from distant sources with longitudinal transport along the length of the basin. Conglomerate units outcropping about 10 km southeast of Nullagine, and previously referred to as the 'Dromedary Formation' (Noldart and Wyatt, 1962), overlie unconformities, but Bagas (2005) did not interpret these conglomerates to be the youngest part of the total succession.

Basin evolution

The gap in the estimated depositional ages of the Coondamar and Mosquito Creek Formations implies a major stratigraphic break, although an unconformity has not been documented between the formations. The Coondamar Formation is interpreted to have been deposited during regional extension during the latter stage of the EPTRE, and its deposition is likely to have been terminated when plate separation changed to convergence between c. 3165 and 3160 Ma. Significantly, tonalite intrusions of the Mount Billroth Supersuite (see below) were intruded when this change occurred, and might have originated through partial melting of the juvenile mafic crust along the margins of the Mosquito Creek and Regal Basins. Application of $^{40}\text{Ar}/^{39}\text{Ar}$ chronology in the EPT and KT indicated a metamorphic event in the northern half of the Pilbara Craton between c. 3160 and 3140 Ma (Kiyokawa, 1993; Kiyokawa and Taira, 1998; Smith et al., 1998; Beintema, 2003; Kloppenburg, 2003). Hickman (2016) named this the Karratha Event, and it is inferred to mark a c. 3160 Ma collision with another plate northwest of the Pilbara Craton. However, in view of the intrusion of the diorite, tonalite and granodiorite protoliths of the Golden Eagle Orthogneiss in the southeastern Pilbara Craton, the KUT might have been thrust against the Coondamar Formation of the Mosquito Creek Basin slightly before c. 3160 Ma.

Evidence from the northern Pilbara Craton indicates that convergence lasted until c. 3070 Ma, likely preventing much further deposition in the Mosquito Creek Basin. No c. 3100 Ma felsic volcanic or granitic rocks analogous to those of the Sholl Terrane (northwest Pilbara Craton) have been recognized in the Mosquito Creek Basin, or in the adjacent KUT.

Nijman et al. (2010) recognized local unconformities in the southwest of the basin near the Golden Eagle mine, and in the North Dromedary and South Dromedary Hills.

They interpreted a unit of sandstone and conglomerate, informally referred to as the 'Cajuput Spring sandstone' to unconformably overlie the Coondamar Formation and to be unconformably overlain by the main part of the Mosquito Creek Formation. Dating detrital zircons from the 'Cajuput Spring sandstone' might better constrain the maximum depositional age of the Mosquito Creek Formation.

The orientation of thrusts and isoclinal folds in the basin (Fig. 39; Bagas et al., 2004a; Bagas, 2005; Farrell, 2005, 2006; Nijman et al., 2010) suggests 2930–2900 Ma north–south or northwest–southeast compression, which resulted in south-directed thrusting of the Mosquito Creek Formation onto the northwestern margin of the KUT, and north to northwest thrusting against the southeastern margin of the EPT. However, local preservation of unconformities along the southeastern margin of the EPT, most notably in the east, is evidence against regional-scale thrusting of the basin onto the EPT – that is, the basin is not an allochthonous tectonic unit. The north–south cross-sectional structure of the basin (see **Mosquito Creek Orogeny**) consists of north-verging folds in the north and south-verging folds in the south (Bagas et al., 2004a, 2008; Farrell, 2005; Williams and Hickman, 2007; Nijman et al., 2010). Thrust faults related to the folds are approximately parallel to their axial planes and the combination of these features suggests a positive flower structure produced by uplift of the basin between the converging continental plates of the EPT and KUT (Nijman et al., 2010).

Tectonic interpretations of the Mosquito Creek Basin that differ from the rift-basin interpretation in this Report include: 1) an allochthonous fragment of a fore-arc basin lithotectonic complex (Krapež, 1993; Eriksson et al., 1994); 2), an upper sedimentary component of a synclinal greenstone belt (Nijman et al., 2010). Bagas et al. (2008) proposed a rift-related passive-margin origin.

Krapež (1993) divided the succession into two packages: a northern submarine-fan sequence with an arc provenance that was thrust northwards onto greenstones of the McPhee and Yilgalong Domes and, to the south, a younger fan-delta sequence with a mainly chert and iron formation provenance. The KUT, south of the basin, was interpreted to be either an accreted terrane unrelated to the EPT, as suggested by Tyler et al. (1992), or an assemblage of collision-related granitic intrusions representing a subduction complex. Tight to isoclinal folding in the basin was related to synsedimentary deformation in a fore-arc setting followed by deformation in a foreland thrust belt.

Nijman et al. (2010) summarized the basin fill as consisting of coarsely clastic, fan-delta marginal facies with stacked unconformities, rimming the centre of the basin, in which mainly finer-grained mass-flow sediments dominated by turbidites were deposited. They interpreted the basin fill as a single, major, fining-upwards sequence from fan-delta sandstone to distal turbidites that unconformably overlies an older, partially preserved clastic sequence. Nijman et al. (2010) interpreted the Mosquito Creek Basin to be an underfilled, compressional, intramontane, clastic sedimentary basin unconformably superposed on a stratigraphically underlying greenstone belt. In this interpretation, the geological setting of the Mosquito Creek Basin was regarded as similar to that of most other EPT greenstone belts.

Dalton Suite

Although currently available geochronological evidence indicates that the Dalton Suite intruded the EPT during eruption of the Honeyeater Basalt, intrusions assigned to the suite are far more extensive across the EPT than the basalt formation. Therefore, the suite is not considered to be part of the Soanesville Group. The single available crystallization age of 3185 ± 2 Ma for a metagabbro sill (GSWA 178185, Wingate, 2009a) was obtained in the northern Soanesville greenstone belt, and might not be representative of the entire suite. For example, a gabbro dyke which intruded the early extensional rift fault of the Tabba Tabba Shear Zone was dated at 3235 ± 9 Ma (KB 810, Beintema, 2003), and large ultramafic–mafic intrusions into the Coongan–Warralong Fault Zone (CWFZ) were emplaced prior to c. 3200 Ma (see below). The need for more geochronology on intrusions of the Dalton Suite outside the Soanesville greenstone belt is an issue for future Pilbara Craton studies.

The regional distribution of intrusions assigned to the Dalton Suite includes:

- sills in the Soanesville Syncline in the southern Soanesville greenstone belt
- dykes and sills intruding the Soanesville Group in the northern Soanesville greenstone belt
- dykes and sills intruding the McPhee greenstone belt and the Coondamar Formation in the Mosquito Creek Basin
- sills intruding boundary faults separating the Shaw, Corunna Downs, Mount Edgar, Yule, and Carlindi Domes.

As described by McCall (1971), the Soanesville Syncline sills include dunite, harzburgite, wehrlite, lherzolite, clinopyroxenite, two-pyroxene pyroxenite, gabbro and diorite. Based on geological setting, large units of metaperidotite at Lionel (western McPhee greenstone belt) and in the Pincunah greenstone belt are currently assigned to the Dalton Suite (Plates 1A, 1C), although no dating has been reported. The Dalton Suite was mined for asbestos at Soanesville and Lionel in the first half of the twentieth century, and relatively thin intersections of nickel sulfides were reported during exploration from 1970 onwards.

Evidence that the age range of the suite extends to at least c. 3200 Ma was obtained from $^{40}\text{Ar}/^{39}\text{Ar}$ dating of metamorphism of intrusive ultramafic rocks in the CWFZ between the Coongan and Kelly greenstone belts (Davids et al., 1997). Additionally, Zegers et al. (1999) dated actinolite porphyroblasts that grew across the mylonite fabric of the shear zone at 3197 ± 44 Ma, providing a minimum age for movement on the shear zone, and a local age for metamorphism of the Dalton Suite.

Mount Billroth Supersuite

Tonalitic intrusions of the 3199–3165 Ma Mount Billroth Supersuite were emplaced towards the end of the EPTRE. In the KUT, the Golden Eagle Orthogneiss has been dated between c. 3199 and 3178 Ma (GSWA 178012, Nelson, 2004g; GSWA 178013, Nelson, 2005b). In the western margin of the EPT, the Flat Rocks Tonalite was dated at c. 3166 and c. 3164 Ma (GSWA 142946, Nelson, 2000f; GSWA 142948,

Nelson, 2000g). These age differences might be due to slightly different timing of tectonic events between the terranes or reflect variable contents of older crustal material. For example, Nelson (2005b) dated a sample of five zircons in GSWA 178013 at 3225 ± 5 Ma, suggesting a granitic protolith component in the gneiss equivalent in age to the Cleland Supersuite.

In stark contrast to the mainly monzogranitic and syenogranitic compositions of the preceding Cleland Supersuite, intrusions of the Mount Billroth Supersuite are diorites, tonalites and granodiorites. The compositional change demonstrates an abrupt departure from the secular trend of increasingly potassic granites through the Paleoproterozoic, and isotopic evidence indicates a marked change in the crustal evolution of the northern Pilbara Craton at this time. Zircon Hf isotope values in the Mount Billroth Supersuite are extremely variable; for example, 6 of 17 ϵ_{Hf} values from the Yule Dome have an average value of +4.45, whereas the other 11 ϵ_{Hf} values average -1.66 (Appendix 9). In the KUT, 11 ϵ_{Hf} values average +0.86. The inclusion of positive ϵ_{Hf} values in the Mount Billroth Supersuite marks a major change from consistently negative ϵ_{Hf} values at the end of the Paleoproterozoic trend (Fig. 19). The range of whole-rock Nd model ages from the Flat Rocks Tonalite is 3420–3310 Ma (Table 4), suggesting an influx of juvenile material in addition to reworking of more evolved sources in the EPT. A whole-rock Nd model age from the Golden Eagle Orthogneiss of the KUT was calculated at c. 3369 Ma, assuming an intrusive age of c. 3285 Ma (Champion, 2013). If the intrusive age is assumed to be younger at c. 3199 Ma, the calculated Nd model age is c. 3405 Ma.

Flat Rocks Tonalite

The c. 3165 Ma Flat Rocks Tonalite outcrops on the Pyramid 1:250 000 sheet (Smithies and Hickman, 2004) at the southwestern end of the Pilbara Well greenstone belt, and is the most westerly exposure of Mesoarchean granitic rocks southeast of the TTSZ (Fig. 5). The predominant rock type is biotite-bearing tonalite, which is strongly foliated and locally interleaved with K-feldspar porphyritic monzogranite (Van Kranendonk et al., 2006a). The unit was not mapped during the PCMP and it might extend to include various undated granitic outcrops farther northeast in the western Yule Dome. This possibility arises if the tonalitic composition of the intrusion is due to partial melting of basaltic crust of the Regal Basin subducted beneath the EPT. The Flat Rocks Tonalite, or a related volcanic rock, is also likely to underlie the southeastern margin of the Mallina Basin near Nunyerry Gap. This is based on the ages of 10 xenocrystic zircons dated between c. 3196 and 3164 Ma (GSWA 142945, Nelson, 2000e), extracted from a c. 2946 Ma porphyritic andesite sill in the Constantine Sandstone.

Samples of the Flat Rocks Tonalite were dated at 3166 ± 5 Ma (GSWA 142948, Nelson, 2000g) and 3164 ± 4 Ma (GSWA 142946, Nelson, 2000f), indicating an average crystallization age of c. 3165 Ma. Both samples included older zircon age components corresponding to the Emu Pool and Cleland Supersuites. GSWA 142948 also included a c. 3496 Ma zircon probably derived from felsic volcanic rock of the Coonterunah Group, or by recycling of detrital zircons from either of the Strelley Pool or Corboy Formations.

Golden Eagle Orthogneiss

Protoliths of the Golden Eagle Orthogneiss were tonalite and quartz diorite (GSWA 178012, Nelson, 2004g; GSWA 178013, Nelson, 2005b), and the gneiss is tectonically interleaved with granodiorite and monzogranite. The Golden Eagle Orthogneiss also contains lenses and sheets of amphibolite, ultramafic schist and quartz–mica schist, suggesting intrusion or interfolding of greenstone material, possibly including the Coondamar Formation. The undated monzogranite layers might have been introduced during intrusion of the c. 2838 Ma Bonney Downs Monzogranite (Split Rock Supersuite), although alternatively some might be remnants of the >3220 Ma Cleland Supersuite.

U–Pb zircon dating indicates that the early Mesoarchean components of the unit originated between c. 3199 (GSWA 178013, Nelson, 2005b) and 3178 Ma (GSWA 178012, Nelson, 2004g). Sm–Nd isotope analysis of the Golden Eagle Orthogneiss is limited to one sample collected by Tyler et al. (1992, sample 76338). Recalculation of the isotope data indicates a Nd model age of c. 3369 Ma and an ϵ_{Nd} value of +1.75 (Champion, 2013). The mineral assemblage of the orthogneiss suggests that it was metamorphosed at amphibolite facies with retrogression to greenschist facies (Bagas, 2005).

Tectonic interpretation

The compositional and isotopic data from the Mount Billroth Supersuite suggest that the intrusions had a mix of both very juvenile and considerably evolved sources. The TTG composition of the supersuite, and the locations of the intrusions, suggest that it was partly derived by partial melting of juvenile basaltic crust along the margins of the EPT and KUT. The timing of its intrusion coincides with the end of the EPTRE, and is similar to that of 3160–3140 Ma metamorphism during the D_{10} Karratha Event. This event is interpreted to mark a reversal from crustal extension and plate separation to regional compression and plate convergence. Under convergence, the major rift faults along the northwestern margin of the EPT (Tabba Tabbas Shear Zone) and the north-northwestern margin of the KUT (Kurrana Shear Zone) are likely to have been reversed to form zones of subduction of the recently formed mafic crusts of the Regal and Coondamar Formations.

In addition to magma derived from partial melting of juvenile basaltic crust, intrusions of the Mount Billroth Supersuite included magma derived from recycling of older crust. Xenocrystic zircons in the c. 3165 Ma Flat Rocks Tonalite (GSWA 142946, Nelson, 2000f; GSWA 142948, Nelson, 2000g) include dates consistent with derivation from the 3324–3290 Ma Emu Pool and 3270–3223 Ma Cleland Supersuites, and one zircon was dated at c. 3496 Ma. Nd model ages varying between 3420 and 3310 Ma, and negative ϵ_{Hf} values for some zircons (Fig. 19), also indicate crustal recycling, either of the Paleoproterozoic EPT or of sedimentary rocks derived from erosion of the EPT. The Golden Eagle Orthogneiss contains xenocrystic zircons inherited from the 3270–3223 Ma Cleland Supersuite, and a Nd model age of c. 3369 Ma (Champion, 2013) indicates partial melting of Paleoproterozoic crust. These data indicate some degree of crustal recycling.

Tectonic events in the early Mesoarchean basins

D_{10} Karratha Event, 3160–3140 Ma

Application of $^{40}\text{Ar}/^{39}\text{Ar}$ dating of biotite and muscovite in the Mount Edgar Dome indicated a metamorphic event at c. 3150 Ma (Kloppenburger, 2003), which coincides with the 3160–3140 Ma Karratha Event in the northwest Pilbara Craton (Kiyokawa, 1993; Kiyokawa and Taira, 1998; Smith et al., 1998; Beintema, 2003; Hickman, 2016). The Karratha Event ended plate separation of the EPTRE and is interpreted to mark a c. 3160 Ma collision of the Karratha Terrane with an inferred plate northwest of the Pilbara Craton (Hickman, 2016). D_{10} of the east Pilbara Craton correlates with D_1 in the northwest Pilbara Craton (Hickman, 2016), a difference that highlights the separate evolutionary histories of the northern Pilbara Craton east and west of the TTSZ between c. 3220 Ma and 3170 Ma.

Effects of the Karratha Event in the east Pilbara Craton are interpreted to include intrusion of the Mount Billroth Supersuite near parts of the western margin of the EPT (Flat Rocks Tonalite) and along the northern margin of the KUT (Golden Eagle Orthogneiss). The TTG composition of this supersuite, in combination with Nd isotope data, suggest that it was partly derived by partial melting of juvenile basaltic crust along the convergent margins of the EPT and KUT.

It is likely that post-3160 Ma deformation and metamorphism impacted the northwestern margin of the EPT because both subduction and obduction are recorded in the adjacent Regal Basin. This included development of the volcanic arc of the Whundo Group (Smithies et al. 2005a, 2007c; Van Kranendonk et al., 2007b) and thrusting of the Regal Formation across 3000 km² of the Karratha Terrane (Hickman, 2001a, 2004, 2012, 2016; Hickman and Smithies, 2001; Hickman and Strong, 2003; Hickman et al., 2010). Large-scale refolded isoclinal folds in the Honeyeater Basalt of the Pilbara Well greenstone belt, as defined by the outcrop of the Hong Kong Chert and other structures visible on satellite imagery, might be products of the post-3160 Ma convergence. However, large, refolded, isoclinal folds in the Wodgina greenstone belt (Fig. 8) deform not only the Honeyeater Basalt, but also the c. 3020 Ma Cleaverville Formation (Van Kranendonk et al., 2010).

A major northeast-striking fault that bisects the Pilbara Well greenstone belt (Fig. 8; Smithies and Farrell, 2000a; Van Kranendonk et al., 2010) is likely to be a D_{10} thrust related to partial closure of the Regal Basin. This Kangaroo Flat Thrust removed the northwest limb of the John Bull Syncline, transporting the upper Honeyeater Basalt, the Hong Kong Chert and the Empress Formation across older greenstone units to the southeast. Van Kranendonk et al. (2010) emphasized that greenstones northwest of this fault have lower greenschist-facies mineral assemblages whereas greenstones to the southeast are metamorphosed to amphibolite and upper greenschist facies. Geological mapping establishes that the fault post-dates the 3185–3165 Ma Honeyeater Basalt, but it does not appear to have displaced or otherwise affected any formations of the <3066 Ma De Grey Supergroup.

The structural history of greenstones and granitic rocks close to the TTSZ along the northwestern margin of the EPT, and close to the Kurrana Shear Zone along the northern margin of the KUT, is relatively complex suggesting the possibility of local deformation along each shear zone related to post-3160 Ma convergence. Xenocrystic zircons of this age are present in 2950–2930 Ma granitic rocks of the TTSZ (KB 746, KB 770, Beintema, 2003).

In summary, the structural geology and geochronology of the northwestern margin of the EPT indicates deformation and metamorphism between >3165 Ma deposition of the Soanesville Group and the c. 3070 Ma Prinsep Orogeny, although no definitive structural studies have been published.

Prinsep Orogeny

North–south or northwest–southeast plate convergence following the 3160–3140 Ma Karratha Event (Hickman, 2016) eventually led to c. 3070 Ma accretion of three terranes (Karratha, Regal and Sholl) to form the West Pilbara Superterrane (WPS; Van Kranendonk et al., 2006a, 2007b, 2010), and collision of the WPS with the EPT. These collisions resulted in deformation, metamorphism and granitic intrusion during an event referred to as the Prinsep Orogeny (Van Kranendonk et al., 2006a). Most of the c. 3070 Ma orogenic deformation is interpreted to have occurred in the Central Pilbara Tectonic Zone (CPTZ) between the EPT and Karratha Terrane because this part of the northern Pilbara Craton contained the thinnest crust (mafic crust of the Regal Basin). However, the western part of the EPT also had relatively thin crust due to extension and local rifting during the EPTRE. Mesoarchean Nd model ages are restricted to this part of the EPT (Figs 16c, 17a) and this has been related to thin or missing Paleoproterozoic crust (Van Kranendonk et al., 2004c, 2007b; Smithies et al., 2007c; Champion, 2013; Champion and Huston, 2016). Relatively thin Paleoproterozoic crust in this section of the EPT might also explain the locally complex history of Mesoarchean horizontal deformation described by Blewett (2002).

It is unlikely that all four terranes were amalgamated at precisely the same time, but there has been insufficient geochronology along the contacts to indicate a sequence. At present, the process of accretion is interpreted to have occurred between c. 3080 and 3060 Ma. Additionally, there have been no studies to precisely date the structures formed during the convergence and collision, including thrusting of the Regal Formation across the Karratha Terrane. Therefore, distinguishing D_{10} from D_{11} structures is not always possible, and some structures, such as the Regal Thrust, might have formed over a protracted interval between c. 3160 and 3060 Ma. For some other structures, such as the Maitland Shear Zone, there is stratigraphic evidence to constrain the age to D_{11} .

Timing of the Prinsep Orogeny

One of the first unconformities to be recognized in the northwest Pilbara Craton was that between amphibolite-facies metabasalt of the Whundo Group (Sholl Terrane) and overlying greenschist-facies metabasalt of the Whim Creek Group (Fitton et al., 1975; Hickman, 1977a, 1983; Horwitz, 1979; Barley, 1987; Smithies, 1998a; Hickman

et al., 2000, 2001; Pike et al., 2006). The depositional age of the Whundo Group in this area is indicated by dates for felsic volcanic rocks of 3116 ± 3 Ma (GSWA 144210, Nelson, 1998n) and 3118 ± 2 Ma (GSWA 144256, Nelson, 1998o), whereas the Whim Creek Group has been dated at 3009 ± 4 Ma (GSWA 141936, Nelson, 1998c). Metamorphism of the Whundo Group was younger than the 3093 ± 4 Ma intrusion of a genetically related monzogranite of the Railway Supersuite of the Sholl Terrane (GSWA 118965, Nelson, 1997a). Between c. 3093 Ma and deposition of the 3022–3015 Ma Cleaverville Formation, which also unconformably underlies the Whim Creek Group, the monzogranite was metamorphosed and deformed to gneiss.

Isotopic evidence for a significant tectonic event such as the collision of the EPT and the WPS might be preserved in older rocks, particularly in major faults such as the Sholl, Maitland and Tappa Tappa Shear Zones. Felsic tuff of the Whundo Group south of the Sholl Shear Zone was dated at 3115 ± 5 Ma, although it contained a significantly younger zircon (concordant analysis) dated at 3066 ± 14 Ma (1σ) (GSWA 114305, Nelson, 1996a). A sample of c. 3265 Ma granodiorite close to the Sholl Shear Zone recorded a resetting event dated at 3031 ± 6 Ma (JS 43, Smith et al., 1998) and a c. 3114 Ma granodiorite in the Maitland Shear Zone contained four zircons dated between 3086 and 3052 Ma (JS 33, Smith et al., 1998). Dating of tonalite gneiss in the Maitland Shear Zone south of Whundo indicated that shearing and metamorphism was younger than 3107 ± 9 Ma (GSWA 142835, Nelson, 1999c). A possible maximum age of the orogeny is suggested by a zircon dated at 3079 ± 6 Ma (1σ), although the analysis is 12% discordant. In c. 3250 Ma granitic rocks within the TTSZ, Beintema (2003) recorded zircon dates of 3069 ± 41 and 3045 ± 24 Ma, which were interpreted as disturbance events.

In the EPT, the c. 3066 Ma Cockeraga Leucogranite was intruded across a large area in the southern Yule Dome (Smithies, 2003a). Although named as a leucogranite, this stratigraphic unit is a complex mix of granitic rocks ranging widely in age and composition. It also contains numerous large rafts and xenoliths of metamafic, meta-ultramafic, and metasedimentary rocks. The leucocratic phase of the Cockeraga Leucogranite, which has the composition of a quartz diorite, was dated at 3066 ± 4 Ma (GSWA 169016, Nelson, 2002j). A dark-grey diorite phase of the unit, which forms xenoliths, was dated at 3068 ± 22 Ma (GSWA 169014, Nelson, 2002i). Based on the established ages of granitic supersuites elsewhere in the EPT, the data from GSWA 169014 indicate that the Cockeraga Leucogranite includes remnants of the Tambina, Emu Pool, Cleland and Mount Billroth Supersuites. Smithies (2003a) interpreted the c. 3068 and 3066 Ma dates, plus unpublished geochemical data, to indicate the approximate time of disequilibrium melting, with other lithologies in the Cockeraga Leucogranite representing restite. Farther east in the EPT, $^{40}\text{Ar}/^{39}\text{Ar}$ plateau ages, and K/Ar ages between c. 3075 and 3028 Ma on blue-green hornblende in the Shaw Dome, (Wijbrans and McDougall, 1987; Zegers et al., 1999) suggest that metamorphism related to the EPT–WPS collision also extended to this area. Additionally, Kloppenburg (2003) obtained an $^{40}\text{Ar}/^{39}\text{Ar}$ age of c. 3080 Ma from the Mount Edgar Dome.

In summary, geochronological data from the northern Pilbara Craton indicate a metamorphic event after evolution of the 3130–3093 Ma Sholl Terrane and before intrusion of the 3024–3012 Ma Orpheus Supersuite and deposition

of the c. 3020 Ma Cleaverville Formation. Intrusion of the c. 3067 Ma Elizabeth Hill Supersuite probably coincided with this metamorphic event.

D₁₁ during the Prinsep Orogeny

The regional unconformity at the base of the De Grey Supergroup has been attributed to erosion of the northern area of the Pilbara Craton due to uplift during the Prinsep Orogeny (Van Kranendonk et al., 2004c, 2006a), although in the eastern Pilbara Craton the unconformity is partly a product of earlier erosion related to Paleoarchean doming. The youngest stratigraphic units underlying the unconformity in the east Pilbara Craton are 3185–3165 Ma basaltic formations of the Soanesville Group, whereas in the northwest Pilbara Craton, the supergroup unconformably overlies the 3130–3093 Ma Sholl Terrane. Although there is no exposed unconformity between the c. 3067 Ma Elizabeth Hill Supersuite and the De Grey Supergroup, evidence of an erosional unconformity between these units is provided by numerous detrital zircons dated between c. 3085 and 3054 Ma in the c. 3020 Ma Cleaverville Formation (GSWA 127330, Nelson, 1998a; GSWA 142842, Nelson, 1998f; GSWA 136899, Nelson, 1998b; Hickman, 2004).

D₁₁ deformation included low-angle thrusting of the 3130–3110 Ma Whundo Group along the Maitland Shear Zone (Hickman and Kojan, 2003; Hickman, 2016). This was probably contemporaneous with major sinistral strike-slip movement on the Sholl Shear Zone that was responsible for the terrane boundary between the Sholl and Karratha Terranes (Smith et al., 1998; Hickman, 2001c, 2004, 2016; Van Kranendonk et al., 2002). Deformation on both shear zones was accompanied by amphibolite-facies metamorphism in adjacent parts of the Whundo Group and Railway Supersuite (Fig. 10). Since the Railway Supersuite was intruded between c. 3130 and 3093 Ma, D₁₁ metamorphism must have occurred after 3093 Ma. The prevalence of sinistral strike-slip on the generally east-northeasterly striking Sholl Shear Zone suggests oblique north–south convergence. During the same period, the EPT interacted with the Sholl Terrane and with the underlying c. 3200 Ma basaltic crust of the Regal Formation. Crustal melting associated with collision resulted in intrusion of the 3068–3066 Ma Elizabeth Hill Supersuite, both in the WPS and in the western EPT (Van Kranendonk et al., 2006a, 2010; Hickman, 2016).

Between the c. 3160 Ma Karratha Event and plate collision marked by the Prinsep Orogeny at c. 3070 Ma, early Mesoarchean ophiolites of the c. 3200 Ma Regal Formation were obducted onto the Paleoarchean Karratha Terrane across the Regal Thrust (Sun and Hickman, 1998; Hickman, 2001a, 2004, 2012, 2016; Hickman and Smithies 2001; Hickman et al., 2001, 2010; Van Kranendonk et al., 2006). Accordingly, the Regal Thrust, now exposed as a zone of deformation and metamorphism up to 1 km wide and extending across an area of at least 3000 km² (Hickman, 2016), separates the Regal and Karratha Terranes. Structures within the thrust zone include recumbent folds and layers of mylonite. No successful geochronological investigations of the Regal Thrust have been reported. Obduction of the Regal Formation onto the Karratha Terrane suggests the possibility of similar obduction onto the EPT as the Regal Basin was compressed (Hickman, 2016, and see **D₁₀ Karratha Event, 3160–3140 Ma**).

It is evident from differences in metamorphic grades between units formed before and after the Prinsep Orogeny that metamorphism was mainly at amphibolite facies, although it locally reached granulite facies. Units affected by the higher metamorphic grades include parts of the Whundo Group, and most of the Railway and Elizabeth Hill Supersuites. Amphibolite-facies metamorphism in the Whundo Group was restricted to units within 5–10 km of major deformation zones, such as the Sholl and Maitland Shear Zones in the northwest Pilbara Craton.

In the Caines Well Granitic complex south of the Sholl Shear Zone, Smithies (1998a) recorded that c. 3093 Ma gneiss of the Railway Supersuite includes ultramafic xenoliths containing assemblages of either hornblende–plagioclase–clinopyroxene or cummingtonite–orthopyroxene–olivine. The latter assemblage indicates conditions close to the amphibolite–granulite transition. Development of gneissic segregations and migmatization within the gneiss suggests that the ultramafic xenoliths and the biotite monzogranite protolith to the gneiss might have been metamorphosed together. Combined with the contrast in metamorphic grades between amphibolite-facies metabasalt of the 3130–3110 Ma Whundo Group, and unconformably overlying greenschist-facies rocks of the c. 3010 Ma Whim Creek Group on the southern side of the Caines Well Granitic complex, this indicates a significant metamorphic event at about the time of the Prinsep Orogeny.

The Whundo Group was also metamorphosed to amphibolite facies above the Maitland Shear Zone between Whundo copper mine and the Maitland River (Hickman and Kojan, 2003), and intruded post-metamorphism by the non-foliated South Whundo Monzogranite dated at 3013 ± 4 Ma (JS 35, Smith et al., 1998). These relationships indicate a metamorphic event between c. 3110 and 3013 Ma. In the Cherratta Granitic complex, tonalite and granodiorite of the Railway Supersuite have also been metamorphosed to amphibolite facies.

The c. 3066 Ma Cockeraga Leucogranite of the Elizabeth Hill Supersuite outcrops over much of the southern part of the Yule Dome, and constituted far more of the granitic core of the dome prior to intrusion by younger granites. This leucogranite is interpreted to be a product of disequilibrium melting, in which a very low-degree partial melt was rapidly extracted from a proximal source (Smithies, 2003a). The Cockeraga Leucogranite invaded, disaggregated and included greenstones on all scales. Greenstone assemblages and gneiss are locally swamped, or net-veined, and some outcrops containing a large proportion of leucogranite were described as injection migmatite by Smithies (2003a). The available geochronology suggests that melting of source rocks to produce the Cockeraga Leucogranite occurred at or before c. 3065 Ma (Smithies, 2003a).

Elizabeth Hill Supersuite

The Elizabeth Hill Supersuite was first identified by geochronology in the northwest Pilbara Craton (GSWA 142661, Nelson, 1998d) where it is apparently restricted to a relatively small area (70 km²) of the Sholl Terrane (Fig. 3). Subsequent mapping and geochronology in the Yule granitic complex of the EPT (Fig. 8, Plate 1B) indicated widespread intrusion of the c. 3066 Ma Cockeraga Leucogranite, a subunit of the Elizabeth Hill Supersuite. Numerous undated

greenstone and metasedimentary xenoliths in the Cockeraga Supersuite, probably from the Soanesville Group, were metamorphosed to at least amphibolite facies, then strongly retrogressed (Smithies, 2003a). This is in contrast to the type area of the Soanesville Group where metamorphic grade is prehnite–pumpellyite to lower greenschist facies.

In the southern Yule Dome, the Cockeraga Leucogranite includes biotite(–hornblende) tonalite and granodiorite with minor monzogranite (Smithies, 2003a). The interpreted extent of the Cockeraga Leucogranite is >1500 km², although this remains to be confirmed by geochronology and geochemistry. Prior to it being extensively intruded by the c. 2950 Ma Sisters Supersuite, the Cockeraga Leucogranite is likely to have formed an east-southeast trending belt along what is now the northern limit of the Fortescue outcrop in the Chichester Range. Since the Elizabeth Hill Supersuite was intruded during the Prinsep Orogeny (Van Kranendonk et al., 2006a), the supersuite may, in the Yule Dome, mark the northern margin of an east-southeast trending collision zone now concealed by the Fortescue Group in the Chichester Range. Smithies (2003a) interpreted the source of melting for the Cockeraga Leucogranite to be close to its present position. Whole-rock Nd model ages of 3560–3520 Ma and negative ϵ_{Nd} values (Table 4) indicate inclusion of old crustal sources. Some hornblende tonalite and hornblende granodiorite units within the Cockeraga Leucogranite might be high-Mg diorite lithologically similar to the c. 2940 Ma Mungaroona Granodiorite (Smithies, 2003a), in which case, these intrusions support the interpretation of a zone of collision and subduction south of the present outcrop of the EPT that was active during a period of at least 100 Ma.

Chichester Tectonic Zone

Structural and metamorphic evidence has established the existence of an east-southeast – west-northwesterly trending zone of deformation, metamorphism, granitic intrusion, and alignment of greenstone enclaves in the southern Yule Dome between Cheearra and White Springs (Fig. 38; Smithies, 2003b). Previously, this zone of greenstone enclaves within the Yule Dome was interpreted to represent the base of an eroded greenstone keel (Hickman, 1983, fig. 4). However, more recent evidence from the PCMP, and from regional geophysical imagery, suggests this zone might be the northern section of an east-southeasterly striking linear crustal structure concealed beneath the Fortescue Group in the Chichester Range and the Hamersley Group in the Fortescue Valley. South of this inferred structure, faults and fold axes in the southern Pilbara Craton strike east-southeast, whereas north of it, the dominant structural trend is north-northeast. Major Proterozoic faults with the same east-southeast alignment in the Fortescue Valley and Chichester Range include the 180 km-long Poonda Fault (Tyler et al., 1991; Williams and Tyler, 1991; Fowers et al., 2013) in the east, and the 60 km-long Portland Fault in the west (Hickman and Kojan, 2003). Although structural trends in the southern Pilbara Craton are products of Proterozoic deformation (Ophthalmia and Capricorn Orogenies), these trends might have been influenced by older structures in the underlying Pilbara Craton.

The east-southeasterly trending belt of deformation exposed in the Yule Dome is referred to as the Chichester Tectonic Zone (CTZ), and it is tentatively inferred that this zone is part of a larger east-southeasterly trending crustal structure underlying the Fortescue Valley. Smithies and Farrell (2000b) noted a progressive southerly increase in metamorphic grade to amphibolite facies across this zone in the Cheearra greenstone belt. This pattern is similar to the increasing grade in the Coondamar Formation north of the Kurrana Shear Zone (KSZ) in the southeastern Pilbara Craton. The KSZ is interpreted to have originated as a c. 3200 Ma extensional fault that was reactivated when the Kurrana Terrane was thrust against the Mosquito Creek Basin between 2930 and 2900 Ma (Mosquito Creek Orogeny). Features of the Cheearra area described by Smithies and Farrell (2000b) include east-southeasterly trending fold axes, widespread banded gneiss, and diatexitic injection migmatite in the Cheearra Monzogranite (Fig. 40).

At Cheearra, the CTZ was intruded by c. 2945 Ma high-Mg diorite components of the Mungaroona Granodiorite. High-Mg diorite intrusions (sanukitoids, Indee Suite) in the CPTZ of the Mallina Basin were derived from melting of a mantle source with a crustal component enriched in Th, Zr and LREE (Smithies and Champion, 2000; Smithies, 2002a; Smithies et al., 2004). Mantle enrichment in those high-Mg diorites has been attributed to a previous subduction event (Smithies and Champion, 2000; Smithies et al., 2004, 2007c; Martin et al., 2005). Therefore, the Mungaroona Granodiorite might provide evidence of a similar subduction event prior to c. 2945 Ma in the CTZ. Hornblende tonalite 40 km southeast of Cheearra is possibly part of the Mungaroona Granodiorite (Smithies, 2003b), although no geochemical data are available.

The CPTZ was completed during the c. 2950 Ma closure of the Mallina Basin which overlies mafic crust of the c. 3200 Ma Regal Basin. The Regal Basin was formed by rifting and plate separation during the EPTRE (Hickman, 2016). The c. 3200 Ma Regal Basin evolved into the 3015–2930 Ma Mallina Basin via a 3160–3070 Ma stage of plate convergence that included subduction (Smithies et al., 2005a, 2007c; Van Kranendonk et al., 2006a, 2007b). This suggests that the CTZ might also be related to a belt of Mesoarchean crust that included a subduction event. The orientation of structures in the CTZ, and the belt of hornblende tonalite and granodiorite intrusions within it, might be evidence of a Mesoarchean convergent margin orthogonal to that in the Mallina Basin.

The east-southeast trend of structures in the CTZ is not confined to the area between Cheearra and White Springs. Near the western limit of the EPT, 25 km south of Nunyerry Gap, the c. 3165 Ma Flat Rocks Tonalite contains a strongly developed east–west to northwest–southeasterly trending tectonic foliation orthogonal to the main northeast–southwest structural trends in the Pilbara Well greenstone belt to the north. The tectonic foliation in Flat Rocks Tonalite is also orthogonal to the CPTZ to the northwest. About 150 km farther west, in the northwest Pilbara Craton, granitic rocks in the southern Cherratta granitic complex contain east–west striking tectonic foliations in the 3006–2982 Ma Maitland River Supersuite (Hickman et al., 2006). This orientation is anomalous in the northern part of

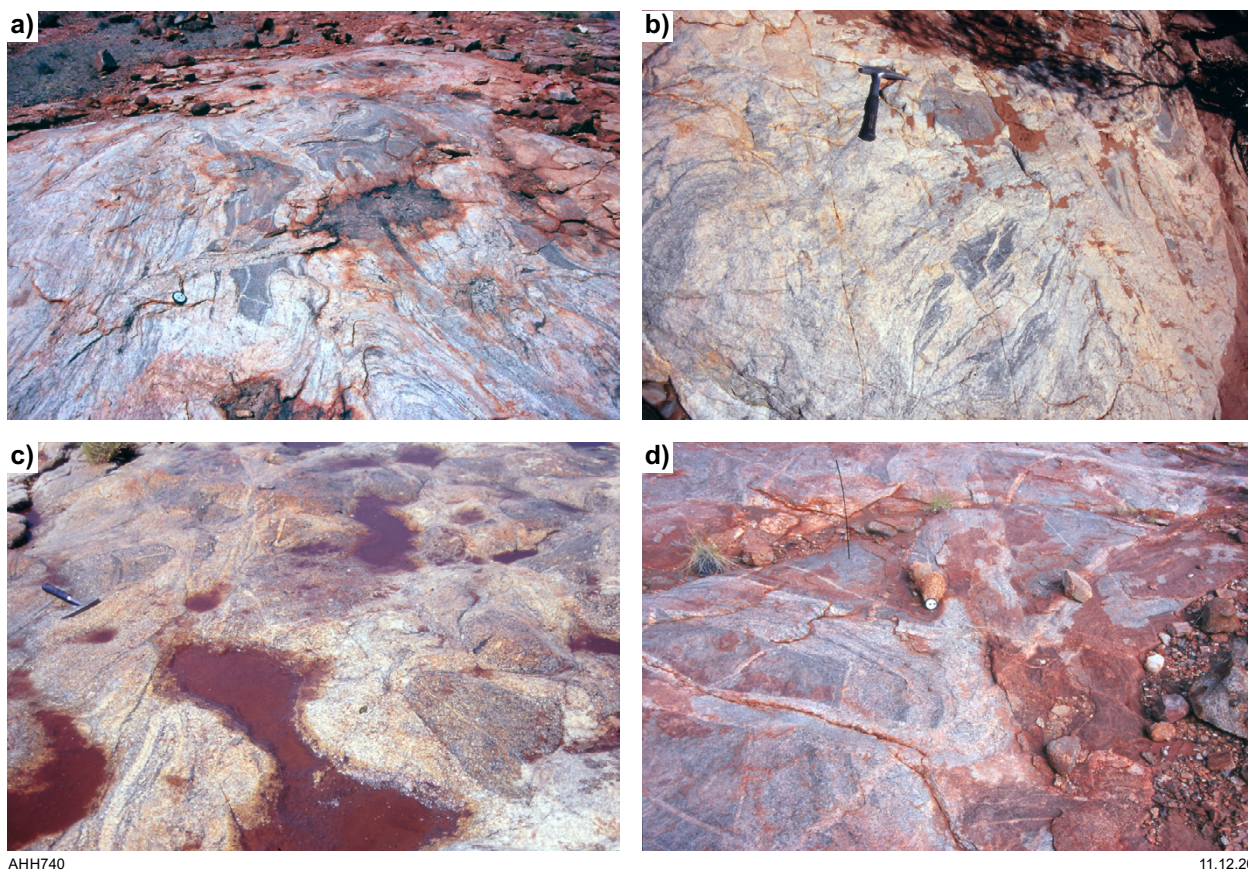


Figure 40. Gneiss and diatexite in the Chichester Tectonic Zone: a) banded gneiss of the Cockeraga Leucogranite. Scale, lens cap 4 cm diameter; b) diatexite developed in the Cheearra Monzogranite, showing disaggregated xenoliths. Scale, hammer; c) diatexite in the Cheearra Monzogranite consisting of rounded blocks of granitic gneiss surrounded by flow-banded leucogranite forming an injection migmatite. Scale, hammer; d) schlieric leucogranite veins of the Cockeraga Leucogranite in granitic gneiss. Scale, lens cap 4 cm diameter. Photos and interpretations from Smithies (2003) and Smithies and Farrell (2000)

the complex, where north- and northeast-striking foliations trend parallel to lithological boundaries. About 50 km south of the Cherratta granitic complex, the Mingah Inlier exposes the c. 3236 Ma Turlwa Pool Tonalite, which also contains an east–west tectonic foliation beneath the Fortescue Group (Hickman et al., 2006). All these areas lie along an east-southeast – west-northwest zone that was intruded by the Mount Billroth and Elizabeth Hill Supersuites (Fig. 41).

Structures within the CTZ are younger than c. 3165 Ma (Flat Rocks Tonalite) and might include c. 3060 Ma synmagmatic shear zones in the Cockeraga Leucogranite (Smithies, 2003a). More than one deformation event is indicated by the observation that foliations striking east–west in the Maitland River Supersuite of the northwest Pilbara Craton are younger than c. 2982 Ma. The minimum age of CTZ deformation is c. 2935 Ma because the zone is crosscut by large intrusions of the Powdar Monzogranite (Smithies and Farrell, 2000a,b; Smithies, 2003b) dated at 2935 ± 3 Ma (GSWA 142937,

Nelson (2000b). Additionally, the southeast end of the CTZ in the Yule Dome is truncated by the north-striking c. 2940 Ma LWSC. Thus, deformation within the CTZ might correlate with D_{11} and D_{13} .

The regional significance of the CTZ within the Pilbara Craton would be considerable if it formed as part of an east-southeasterly trending terrane boundary (Mesoarchean convergent margin) separating the northern half of the craton from its southern half. In this scenario, c. 3220 Ma breakup of the EPT produced a third rift basin to the south of the presently exposed EPT. Crustal extension, rifting and continental breakup above mantle plumes commonly results in diverse rift orientations (Condie, 2016). Further investigation of the CTZ between White Springs, Cheearra, and the Nunyerry Inlier is required; in particular, geochemical analysis of hornblende tonalites and hornblende granodiorites to identify additional sanukitoids.

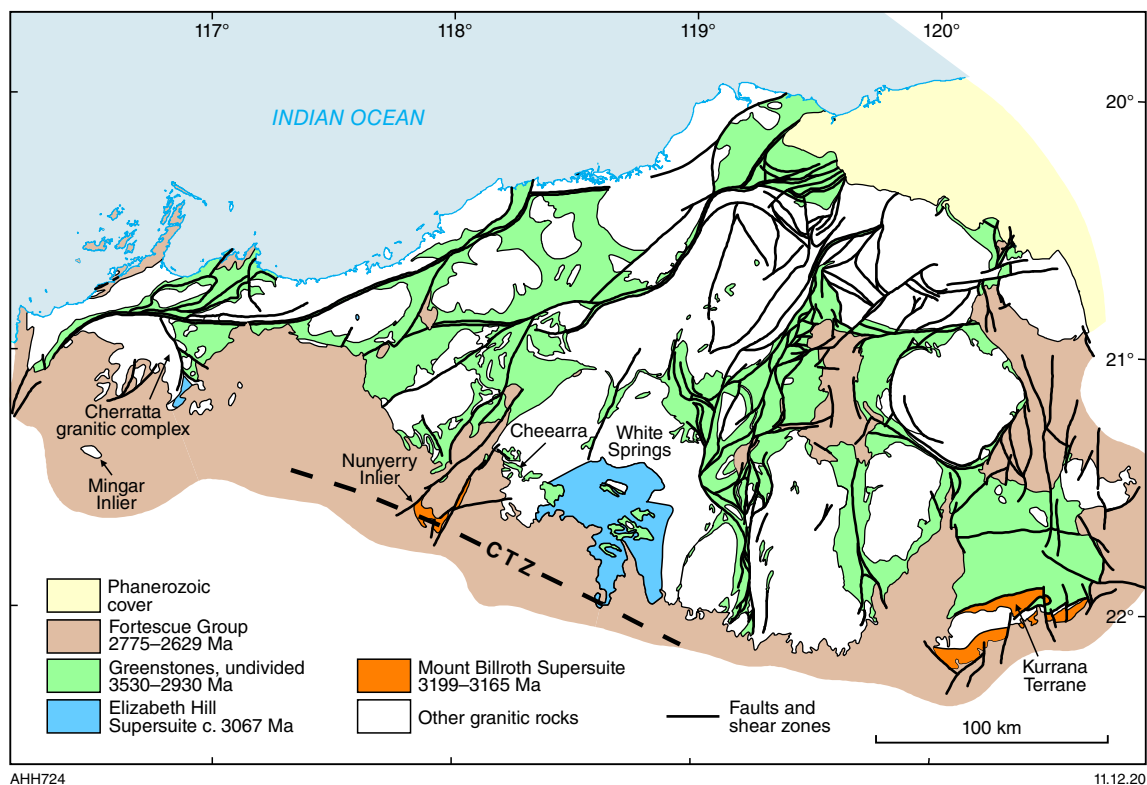


Figure 41. Simplified geological map of the northern Pilbara Craton showing the distribution of the Mount Billroth and Elizabeth Hill Supersuites. The Elizabeth Hill Supersuite was more continuous in an east-southeast – west-northwest orientation prior to being intruded by the Sisters Supersuite. Both supersuites are interpreted to be related to plate margins, suggesting that the east-southeast trending Chichester Tectonic Zone is evidence of a concealed terrane boundary underlying the Chichester Range or Fortescue Valley

De Grey Superbasin

Van Kranendonk et al. (2006a) defined the De Grey Superbasin as a major tectonic unit that unconformably overlies Paleoproterozoic and early Mesoproterozoic crust across the northern Pilbara Craton. In this definition, the superbasin comprised the Gorge Creek, Whim Creek, Mallina, and Mosquito Creek Basins. However, the Mosquito Creek Basin is now excluded from the superbasin because, as defined by Van Kranendonk et al. (2006a), it includes the Coondamar Formation (Fig. 7, Table 1). Although the Coondamar Formation directly underlies the Mosquito Creek Formation, available evidence suggests that it was deposited at c. 3200 Ma (Hickman, 2012), whereas the maximum age range of the De Grey Superbasin is c. 3066 to 2930 Ma. This age range requires some qualification because the maximum age is inferred from the interpretation that deposition of the Gorge Creek Group followed the Prinsep Orogeny. The maximum depositional age of the Farrel Quartzite, at the base of the Gorge Creek Group, has not yet been directly dated isotopically, although detrital zircons in the unit have been dated (Fig. 12c,d,e), and it is possible that this formation is not significantly older than the overlying c. 3020 Ma Cleaverville Formation.

The Gorge Creek Basin is the oldest and most laterally extensive basin of the De Grey Superbasin. The succession of this basin, the Gorge Creek Group, is exposed across the northern part of the craton (Fig. 42). The stratigraphy of the Gorge Creek Group (Van Kranendonk et al., 2006a)

comprises, in ascending order, the Farrel Quartzite, Cleaverville Formation and Cundaline Formation, although most mapping prior to Van Kranendonk et al. (2006a) did not distinguish all three formations. In the northwest Pilbara Craton, deformation during strike-slip movement along the Sholl Shear Zone occurred between deposition of the Gorge Creek Group and the 3015–2990 Ma Whim Creek Group (Whim Creek Basin, Hickman, 2016), resulting in an unconformable contact. With the exception of an interpretation by Horwitz (1990), the Whim Creek Basin has not been recognized in the east Pilbara Craton.

The 3015–2931 Ma Mallina Basin, containing the Croydon Group, overlies the Gorge Creek Basin and is divided into three northeast–southwesterly trending zones (Hickman, 2016), of which only the southeastern zone is represented in the east Pilbara Craton:

- a central deep-water trough (Constantine Sandstone and Mallina Formation) deposited between c. 3015 and 2931 Ma
- a northwestern shallow-water shelf (Bookingarra Group) unconformably overlying the Whim Creek Basin, and deposited between c. 2955 and 2931 Ma
- a southeastern shallow-water shelf (Cattle Well Formation and Lalla Rookh Sandstone) unconformably overlying the East Pilbara Terrane (EPT), Soanesville Basin and Gorge Creek Basin, and deposited between c. 3015 and 2931 Ma.

Tectonic models

Early tectonic models to explain the development of the De Grey Superbasin envisaged continental rifting (Krapež, 1984; Barley, 1987; Krapež and Barley, 1987; Smithies et al., 1999, 2001b; Smithies and Champion, 2000; Smithies, 2002a). Van Kranendonk et al. (2007b) developed a second model in which the Gorge Creek Group was deposited in a subsiding, post-orogenic, extensional basin overlying the EPT and the three amalgamated terranes (Karratha, Regal and Sholl) of the West Pilbara Superterrane (WPS). Subsequently, a northwest to southeast migration of granitic intrusions from c. 3000 to 2920 Ma was attributed to the break-off of a subducted slab (Van Kranendonk et al., 2006a, 2007b). According to Van Kranendonk et al. (2007b), the likely origin of this slab was related to the c. 3130 Ma Sholl subduction event, and the c. 3000 Ma Whim Creek Group was a result of magmatism related to rupture of a hinge in the slab. Younger magmatic events (Sisters Supersuite) were related to influx of hot new mantle material during sinking of the detached slab.

A third tectonic model interpreted the Whim Creek Group and the genetically related Maitland River Supersuite to be parts of a c. 3000 Ma magmatic arc situated southeast of a subduction zone that lay to the northwest of the Pilbara Craton (Krapež and Eisenlohr, 1998; Smith et al., 1998; Blewett, 2002; Pike and Cas, 2002; Beintema, 2003; Smith, 2003; Pike et al., 2006; Hickman, 2012, 2016).

The third model provides the basis for the present interpretation. Magmatic arcs of the 3024–3012 Ma Orpheus Supersuite, the 3006–2982 Ma Maitland River Supersuite, and the 2954–2919 Ma Sisters Supersuite, all of which are exposed close to the northwest Pilbara coast, formed as a result of subduction of the northwestern plate under the Pilbara Craton. Southeast of the Orpheus arc, the Gorge Creek Basin developed between the arc and the eastern EPT. The stratigraphic succession of this basin is mainly sedimentary (sandstone, BIF, shale and chert), although close to the Orpheus Supersuite, it is intruded by mafic and felsic sills, and locally includes thin units of felsic tuff. The Gorge Creek Basin overlies continental crust of the Pilbara Craton and extends 200 km southeast of the arc. Parallel to the Pilbara coast, the preserved west-southwest – east-northeast length of the basin is at least 500 km. In this Report, the basin is interpreted to occupy a tectonic setting similar to that of a retro-arc foreland basin.

The Mallina Basin overlies the Gorge Creek Basin, and developed between c. 3015 and 2931 Ma, closely contemporaneous with the volcanic arc of the 3015–2990 Ma Whim Creek Group, 3006–2982 Ma granitic intrusions of the Maitland River Supersuite, and 2954–2919 Ma igneous intrusions (mafic and felsic) of the Sisters Supersuite. The northwest–southeast width of the Mallina Basin is about 150 km, and its preserved west-southwest – east-northeast length is the same as that of the Gorge Creek Basin. The basal stratigraphy of the Mallina Basin is transitional from the stratigraphy of the Gorge Creek Basin (Hickman, 2016), and therefore it might be argued that the two basins would be better interpreted as a single basin. Reasons for separating the basins are partly historical, although the Mallina Basin differs from the Gorge Creek Basin in being more structurally and stratigraphically complex due to tectonic processes during its compression and closure at the time of the 2955–2919 Ma North Pilbara Orogeny. Previous tectonic interpretations of the Mallina

Basin succession have suggested a back-arc or retro-arc basin setting (Krapež, 1993; Krapež and Eisenlohr, 1998; Smith et al., 1998; Smith, 2003), and a similar interpretation is made in this Report.

East–west extent of the superbasin

Gorge Creek Basin

Prior to the 1994–2005 PCMP, most stratigraphic evidence suggested that east–west correlations of the Gorge Creek Group, in particular the exceptionally thick, BIF-dominated Cleaverville Formation, were reasonably well established across the northern Pilbara Craton (Ryan and Kriewaldt, 1964; Fitton et al., 1975; Hickman, 1981, 1983, 1990; Horwitz, 1990). The PCMP provided additional evidence supporting this conclusion (Van Kranendonk et al., 2006a, 2007b, 2010; Hickman and Van Kranendonk, 2008a, 2012). Even so, in the absence of regionally definitive geochronological data from BIF in the east Pilbara Craton, various aspects of the correlations have been questioned in the literature (Krapež, 1993; Krapež and Eisenlohr, 1998; Van Kranendonk and Morant, 1998; Williams, 1999a; Van Kranendonk, 2000a; Van Kranendonk et al., 2002, 2010; Sheppard et al., 2017). A significant factor in the debate has been the difficulty in dating the Gorge Creek Group in the east Pilbara Craton. In this Report, this difficulty is attributed to an absence of Mesoarchean felsic igneous sources in the east Pilbara Craton which might have provided 3200–3070 Ma detritus or ashfall, containing datable zircons, to the sedimentary formations of the group. However, at two east Pilbara Craton localities (Nunyerry Gap and Shay Gap), which are close to Mesoarchean felsic magmatic activity in the northwest Pilbara Craton, dating has revealed that Mesoarchean zircons were added to the Gorge Creek Basin. Elsewhere in the east Pilbara Craton, correlation with the Gorge Creek Group of the west Pilbara Craton currently relies on stratigraphic and geochemical criteria. Several lines of evidence establish the degree of stratigraphic continuity of the Gorge Creek Group across the east and west Pilbara Craton.

1. The Gorge Creek Group overlies the same regional unconformity in the east Pilbara Craton that it overlies in the northwest Pilbara Craton (Van Kranendonk et al., 2006a, 2007b; Hickman and Van Kranendonk, 2008a, 2012). This unconformity is related to the collision between the EPT and the WPS, marked by the Prinsep Orogeny and intrusion of the c. 3067 Ma Elizabeth Hill Supersuite. Prior to the collision, the EPT, Sholl, and Karratha Terranes were separated by oceanic-like basaltic crust of the c. 3200 Ma Regal Formation (Hickman, 2004; Smithies et al., 2005a; Van Kranendonk et al., 2004c, 2006a, 2007b, 2010). Following the collision, the Gorge Creek Group was deposited across all the terranes.

Various lines of evidence indicate that the Prinsep Orogeny and intrusion of the Elizabeth Hill Supersuite occurred at c. 3070 Ma. Therefore, all groups and formations in the De Grey Supergroup across the northern Pilbara Craton must be younger than c. 3070 Ma. Geochronological data from the northwest Pilbara Craton are consistent with this interpretation, and include dates on samples of the Cleaverville

Formation indicating a c. 3020 Ma depositional age, and dates on samples of the Orpheus Supersuite indicating intrusion at various times between 3024 and 3007 Ma. Geochronological data from the Nunyerry Gap and Shay Gap samples from the Gorge Creek Group of the east Pilbara Craton include many individual zircons apparently younger than c. 3070 Ma, implying the same interpretation for at least the northwestern and northeastern parts of the east Pilbara Craton east of the TTSZ. The Nunyerry Gap sample has a published maximum depositional age of 3016 ± 6 Ma (GSWA 142842, recalculated from Nelson, 1998f). However, as discussed below, the interpreted maximum depositional age of the Shay Gap sample is more contentious.

2. In several greenstone belts of the east Pilbara Craton, there are two regional unconformities younger than the Paleoproterozoic Pilbara Supergroup: the Soanesville unconformity at the base of the Soanesville Group, and the Gorge Creek unconformity at the base of the Gorge Creek Group (Table 1). Both these unconformities are present in the Soanesville, Pincunah, East Strelley, Kelly, McPhee, Wodgina and Pilbara Well greenstone belts (Plates 1A, 1B). In other east Pilbara greenstone belts, due to non-deposition of the Soanesville Group, the Gorge Creek unconformity directly overlies Paleoproterozoic rocks (Warralong, Panorama, Marble Bar, Goldsworthy, Shay Gap and Coongan greenstone belts). A third unconformity is locally present at the base of a shallow-water shelf succession of the Mallina Basin in the southeast where either the Lalla Rookh Sandstone or the Cattle Well Formation (Table 1) unconformably overlies the Gorge Creek Group.
3. In relation to the question of how many different Mesoarchean BIF units might be present in the east Pilbara Craton (Sheppard et al., 2017), it is significant that BIF units more than 200 m thick are restricted to two stratigraphic levels: 1) above the Soanesville unconformity (3223–3190 Ma Pincunah Banded-Iron Member [PBIM], Cardinal Formation, Table 1); 2) above the Gorge Creek unconformity (c. 3020 Ma Cleaverville Formation). Figure 42 shows the regional distribution and thickness variations of the Gorge Creek Group. East of the TTSZ each stated thickness comprises approximately equal thicknesses of the BIF-dominated Cleaverville Formation and the Farrel Quartzite. West of the TTSZ the recorded thickness are almost entirely composed of the Cleaverville Formation. Figure 42 does not show the PBIM which is restricted to a much smaller area of the northern Pilbara Craton, with outcrops in the Pincunah, Soanesville, Emerald Mine, Tambina, and Western Shaw greenstone belts (Fig. 8, Plate 1). No greenstone belt contains more than one thick quartzite–BIF succession above the Gorge Creek unconformity, a situation strongly supporting stratigraphic correlation of all these thick quartzite–BIF successions.
4. Studies of the sedimentary facies and geochemistry of east Pilbara BIF units in the Ord Range, Wodgina, East Strelley, Coongan, and Kelly greenstone belts (Fig. 8) indicate that deposition occurred in a single, southeast-deepening basin at least 200 km across (Duuring et al., 2016). Trace element patterns of the BIF units indicate deposition under similar marine conditions (Duuring et al., 2016).

Geochronological evidence for east–west correlations

The depositional age of the Cleaverville Formation at three different localities in the northwest Pilbara Craton is indicated by dates between c. 3022 and 3015 Ma (GSWA 127330, Nelson, 1998a; GSWA 136899, Nelson, 1998b; GSWA 142830, Nelson, 1998f). However, there is no reason to believe that the dated samples are fully representative of the formation regionally. The minimum depositional age of the Cleaverville Formation at Mount Ada is indicated by the intrusive age of a crosscutting granophyre dated at 3014 ± 6 Ma (95% confidence; GSWA 127320, Nelson, 1997b).

The maximum depositional age of the Cleaverville Formation in the northwest Pilbara Craton is less well constrained than its minimum age. The volcanoclastic sandstone with an interpreted maximum depositional age of 3022 ± 12 Ma (95% confidence; GSWA 127330, Nelson, 1998a), has an alternative maximum depositional age of 3058 ± 7 Ma (95% confidence; Nelson, 1998a). The older maximum depositional age is younger than the c. 3070 Ma Prinsep Orogeny, and the related c. 3067 Ma Elizabeth Hill Supersuite (Van Kranendonk et al., 2006a; Hickman, 2016), supporting the interpretation that the Gorge Creek Basin was formed after collision of the East Pilbara Terrane with the West Pilbara Superterrane (Van Kranendonk et al., 2006a, 2010; Hickman et al., 2010; Hickman, 2016). The detrital zircons in GSWA 127330 are interpreted to have been derived from erosion of the Elizabeth Hill and Orpheus Supersuites. Thirteen samples of the Orpheus Supersuite from the northwest Pilbara Craton were dated between c. 3024 and 3007 Ma. The dates do not agree within uncertainty and cannot be averaged, implying a lengthy period of magmatic activity. Two samples of the Gorge Creek Group in the EPT, at Nunyerry Gap and Shay Gap, have provided data indicating a Mesoarchean depositional age.

Dating at Nunyerry Gap

At Nunyerry Gap (NY, Fig. 42), close to the western margin of the EPT, a 400 m-thick felsic volcanoclastic sandstone immediately underlying a 400 m-thick BIF and chert was dated at 3016 ± 6 Ma (GSWA 142842, recalculated from Nelson, 1998g). The sample contains several zircon age components, including:

- c. 3016 Ma, most likely derived from the Orpheus Supersuite in the northwest Pilbara Craton
- c. 3068 Ma, derived from either the c. 3067 Ma Elizabeth Hill Supersuite or a magmatic arc close to the northwest margin of the Pilbara Craton
- c. 3106 Ma, consistent with derivation from the 3130–3093 Ma Sholl Terrane in the adjacent Regal Basin
- c. 3141 Ma, possibly derived from felsic magmatic activity related to the 3160–3140 Ma Karratha Event
- c. 3171 Ma, consistent with derivation from underlying 3185–3165 Ma formations of the Soanesville Group or intrusions of the c. 3165 Ma Flat Rocks Tonalite in the Pilbara Well greenstone belt.

The felsic volcanoclastic sandstone dated at Nunyerry Gap unconformably overlies a thick succession of 3176–3165 Ma komatiitic basalt and komatiite (Empress Formation) in the southern Pilbara Well greenstone belt.

Along strike in the northern Pilbara Well greenstone belt, about 50 km northeast of Nunyerry Gap, a similar BIF and chert unit about 800 m thick is underlain by 200 m of felsic volcanoclastic sandstone (locality PB, Fig. 42). Notably, the volcanoclastic sandstones at Nunyerry Gap and Pilbara Well each contain abundant clasts of trachytic lava (GSWA 142842, Nelson, 1998g; Smithies and Farrell, 2000a). Trachyte has not been recorded elsewhere in Archean rocks of the northern Pilbara Craton, strengthening the case for correlation of the Nunyerry and Pilbara Well successions. Aeromagnetic imagery between Nunyerry Gap and the northern Pilbara Well greenstone belt suggests continuity of the BIF–chert units.

Smithies and Farrell (2000a) correlated the BIF and chert at Pilbara Well with the Cleaverville Formation, as Fitton et al. (1975), Hickman (1980b) and Horwitz (1990) had done previously. This correlation has wider implications in the east Pilbara Craton because the BIF and chert of the northern Pilbara Well greenstone belt is laterally contiguous with BIF and chert in the Wodgina greenstone belt, and with BIF and chert in the TTSZ along the northwestern margin of the EPT. The TTSZ unit comes close to connecting with thick BIF and chert in the Ord Ranges in the Goldsworthy greenstone belt. There is stratigraphic and geochemical evidence that the BIF of the Ord Range and Wodgina are parts of the same formation (Duuring et al., 2016). Moreover, BIF and chert of the Ord Range have been correlated with very similar BIF and chert units in the Goldsworthy and Shay Gap greenstone belts (Plate 1A; Hickman, 1980c, 1990; Hickman and Gibson, 1982; Hickman, et al., 1983; Horwitz, 1990; Williams, 1999a, 2003; Smithies, 2002b, 2004; Van Kranendonk and Smithies, 2006; Sheppard et al., 2017).

Dating at Shay Gap

Near Shay Gap (SH, Fig. 42), a thick unit of BIF, chert and shale has been correlated with the Cleaverville Formation of the northwest Pilbara Craton (Plate 1A; Hickman, 1980c, 1983, 1990; Hickman et al., 1983; Horwitz, 1990; Dawes et al., 1995a,b). During geological mapping for the PCMP, it was renamed by Williams (1999a, 2003) as the 'Nimingarra Iron Formation' pending more evidence on its depositional age and stratigraphic relationships to other Pilbara BIF units. The name Cleaverville Formation was re-introduced by Van Kranendonk et al. (2006a) based on regional stratigraphic evidence and a new tectonic interpretation of the Archean crustal evolution of the northern Pilbara Craton. Van Kranendonk et al. (2006a) declared the name 'Nimingarra Iron Formation' obsolete.

Correlation of the BIF at Shay Gap with the Cleaverville Formation was challenged by Sheppard et al. (2017) based on U–Pb zircon dating of a <1 mm-thick layer of interpreted felsic tuff in a <70 m-thick shale unit. Several zircon age components were identified (sample 301106-17, Sheppard et al., 2017), and 14 of the least discordant analyses (<5% discordant) were used to calculate a weighted mean date of 3104 ± 16 Ma. Sheppard et al. (2017) argued that this result indicates the maximum depositional age of the formation because they considered that the distribution of analyses, together with the euhedral to subhedral shape of the zircons and the presence of angular quartz fragments, is more consistent with a volcanic rock than a sedimentary rock. Sheppard et al. (2017) assumed this date of c. 3104 Ma was close to the true depositional age. This interpretation requires close examination because, if correct, it would

mean that the formation can no longer be correlated with the c. 3020 Ma Cleaverville Formation. It would also mean that the only BIF formation in the Gorge Creek Group of the east Pilbara Craton (Fig. 42) has a depositional age closely similar to that of the 3130–3110 Ma Whundo Group in the northwest Pilbara Craton (Smithies et al. 2005a; Van Kranendonk et al., 2006a). This would be difficult to reconcile with the interpretation that the Whundo Group is an intra-oceanic arc succession (Smithies et al. 2005a, 2007a,c; Van Kranendonk et al., 2006a, 2007a,b), whereas the Gorge Creek Group of the east Pilbara Craton is continental (Hickman, 1981, 1983, 2004; Dawes et al., 1995a,b; Williams, 1999a, 2000; Van Kranendonk, 2000a; Van Kranendonk et al., 2002, 2006a).

There are several geological issues for the interpretation that the depositional age of the BIF at Shay Gap is close to c. 3104 Ma. An immediate problem is that, as accepted by Sheppard et al. (2017), the thick BIF formation at Shay Gap is correlated with lithologically very similar thick BIF formations in the Goldsworthy greenstone belt (GO, Fig. 42) and the Ord Range greenstone belt (OR, Fig. 42; Hickman and Gibson, 1982; Horwitz, 1990; Williams, 1999a, 2003; Smithies, 2002b, 2004; Van Kranendonk and Smithies, 2006; Sheppard et al., 2017). BIF in the Ord Range immediately underlies the 3015–2931 Ma Croydon Group in the Mallina Basin (Van Kranendonk and Smithies, 2006), and inliers of this same BIF are present farther southwest in the Mallina Basin (north of NY and northwest of PB on Fig. 42; Hickman, 2016, figure 25). Throughout the Mallina Basin, this BIF has been correlated with the c. 3020 Ma Cleaverville Formation of the northwest Pilbara Craton (Smithies, 1998a,b; Smithies and Farrell, 2000a; Smithies and Hickman, 2003, 2004; Hickman, 2016). The same c. 3020 Ma BIF is exposed at Nunyerry Gap (NY, Fig. 42) where it extends from the Mallina Basin onto the northwestern margin of the EPT, and where sandstone conformably underlying it has been dated at 3016 ± 6 Ma (GSWA 142842, recalculated from Nelson, 1998g). Sheppard et al. (2017) agreed that the BIF at Nunyerry Gap is the same BIF as that in the Mallina Basin. They questioned previous interpretations that the BIF at Nunyerry Gap is the same BIF as in the Pilbara Well area (PB, Fig. 42) (Smithies and Farrell, 2000a,b; Smithies and Hickman, 2003, 2004), but this correlation has no bearing on the correlations from Shay Gap to the Ord Range, and from there to the Mallina Basin and Nunyerry Gap.

The BIF units of the Ord Range and Mallina Basin have not been dated, so without reference to other regional data it might be argued that they could be as old as c. 3104 Ma. However, this is improbable for the BIF in the Mallina Basin southwest from the Ord Range. The maximum depositional age of the immediately overlying Croydon Group in the Mallina Basin is c. 3015 (Hickman, 2016), and the stratigraphic contact with the underlying Cleaverville Formation is a lithological transition sequence. Geochronology on the Constantine Sandstone (sampled above the basal contact of the Croydon Group) indicated a maximum depositional age of 2997 ± 20 Ma (95% confidence; GSWA 118969, Nelson, 1997).

Five additional lines of evidence question a c. 3104 Ma depositional age for the BIF at Shay Gap.

1. The spread of zircon dates within the 14 analyses used by Sheppard et al. (2017) to calculate the 3104 ± 16 Ma age is 3146–3027 Ma. This large spread of dates is

not explained by Sheppard et al. (2017), and here it is considered to be inconsistent with a single volcanic source. Additionally, the individual analyses are imprecise, resulting in age uncertainties averaging about 25 Ma.

2. There are no known potential sources of c. 3104 Ma zircons in the east Pilbara Craton, and the only potential source in the northwest Pilbara Craton is the 3130–3093 Ma Sholl Terrane (Van Kranendonk et al., 2006a; Hickman, 2016). In the northwest Pilbara Craton, and at Nunyerry Gap on the western margin of the EPT, samples of the Cleaverville Formation have detrital zircons with dates consistent with derivation from the Sholl Terrane. Extensive erosion of the Sholl Terrane is likely to have followed its uplift and deformation related to the c. 3070 Ma Prinsep Orogeny.
3. The zircons dated by Sheppard et al. (2017) were extracted from graded beds <1 mm thick, and were described as stubby or elongate, euhedral to subhedral crystals with aspect ratios up to 3:1, and typically 20–50 µm long. Fine-scale graded bedding in the shale suggests deposition from turbidity currents. Duuring et al. (2016) reported turbidites in the Cleaverville Formation at Wodgina (WO, Fig. 42), and turbidites are components of other Pilbara BIFs; for example, in the Hamersley Basin (Krapež et al., 2003; Pickard et al., 2004). Limited abrasion of the zircons in the Shay Gap shale might be a consequence of rapid transport in suspension by turbidity currents rather than indicating ashfall deposition of tuff. Nine of the 14 zircon dates from the Shay Gap shale are consistent with derivation of the detritus from the Sholl Terrane. Another four of the 14 zircon dates, between c. 3078 and 3068 Ma, were most likely eroded from felsic igneous rocks (e.g. Elizabeth Hill Supersuite) related to the c. 3070 Ma Prinsep Orogeny.
4. Sheppard et al. (2017) suggested that the stratigraphy of the Gorge Creek Group is very variable across the east Pilbara Craton, and that in the northwest Pilbara Craton the group is represented only by the Cleaverville Formation. This suggestion is misleading because it is based on first-edition 1:100 000- scale geological mapping by several different geologists many years before the first regional synthesis of PCMP data (Van Kranendonk et al., 2006a). For example, the Cundaline Formation was distinguished only by Williams (1998, 1999a,b, 2000), who did not distinguish the Farrel Quartzite (by name), even though it is now recognized in the area mapped. The Farrel Quartzite was first named and described by Van Kranendonk et al. (2006a), with a distribution initially described as restricted to an area of about 75 x 50 km, mainly on COONGAN and CARLINDI (Van Kranendonk, 2004c, 2010c). However, the Farrel Quartzite is now recognized in all east Pilbara Craton greenstone belts containing the Cleaverville Formation (Plate 1). Likewise, siltstone, sandstone and conglomerate underlie the Cleaverville Formation in various areas of the northwest Pilbara Craton (Hickman, 2016), although the mapping pre-dated the 2006 PCMP synthesis so the name Farrel Quartzite was not applied. Remapping the numerous Cleaverville Formation outcrops in the northern Pilbara Craton is likely to reveal more clastic units in the upper part of

the Gorge Creek Group that lack BIF, and that would now be correlated with the Cundaline Formation. In summary, the stratigraphy of the Gorge Creek Group across the northern Pilbara Craton is far less variable than suggested by Sheppard et al. (2017), and supports the interpretation of one major depositional basin in which outcrops of the Cleaverville Formation can be correlated for hundreds of kilometres.

5. Evidence in this Report suggests that the Gorge Creek Basin formed as a retro-arc foreland basin southeast of a c. 3066–3007 Ma magmatic arc, the formation of which was triggered by collision of the EPT and WPS at c. 3070 Ma. The Gorge Creek Basin underlies, and is transitional into, the Mallina Basin (Hickman, 2016), for which most tectonic interpretations favour a back-arc or retro-arc setting (Krapež and Eisenlohr, 1998; Smith et al., 1998; Blewett, 2002; Beintema, 2003; Smith, 2003; Pike et al., 2006; Hickman, 2012, 2016).

Therefore, although the c. 3104 Ma date obtained by Sheppard et al. (2017) provides a maximum depositional age for the BIF at Shay Gap, there is compelling geological evidence that this age is not close to the true depositional age of the BIF. The present interpreted link between formation of the Gorge Creek Basin and the c. 3024–3007 Ma magmatic arc (Orpheus Supersuite) precludes a depositional age of the Cleaverville Formation close to c. 3104 Ma. The Gorge Creek Basin was formed after the c. 3070 Ma Prinsep Orogeny (Van Kranendonk et al., 2006a, 2007b, 2010; Hickman, 2012, 2016), which constrains the maximum depositional age of the Gorge Creek Group to c. 3070 Ma. The presence of a c. 3070 Ma zircon age component (four zircon dates) within the shale also suggests deposition after c. 3070 Ma. The single zircon date of c. 3027 Ma, although in itself not statistically reliable, suggests there may be a younger zircon age component within the shale.

Extent of the Mallina Basin

Regarding the extent of the Mallina Basin, the southeastern, shallow-shelf zone of this basin (Hickman, 2016) unconformably overlies pre-3000 Ma units of the EPT, Soanesville Group, and Gorge Creek Group. The most widespread formation of the shelf succession is the Lalla Rookh Sandstone, which is interpreted to have been deposited within intracratonic sub-basins (Krapež, 1984; Krapež and Barley, 1987; Krapež and Furnell, 1987; Van Kranendonk and Collins, 1998; Van Kranendonk, 2000a; Van Kranendonk et al., 2002, 2006a, 2007b). Due to deep erosion of the eastern section of the northern Pilbara Craton following the North Pilbara Orogeny, it is uncertain to what extent these local basins were physically connected during deposition of the formation. However, some of the basins first mapped as containing formations of sandstone and conglomerate that were given different names (Paradise Plains Formation in the Goldsworthy greenstone belt, and Cooragoora Formation in the Shay Gap greenstone belt) have been renamed as the Lalla Rookh Sandstone (Van Kranendonk et al., 2006a). At the contact between the southeast shelf and the central deep-water trough of the Mallina Basin, it is likely that the Lalla Rookh Sandstone was locally laterally connected to the Constantine Sandstone (Hickman, 2016).

Gorge Creek Basin stratigraphy

The Gorge Creek Basin comprises three formations of the Gorge Creek Group, in ascending stratigraphic order: the Farrel Quartzite (Van Kranendonk et al., 2006a) — a basal formation of metamorphosed sandstone and conglomerate; the Cleaverville Formation (Ryan and Kriewaldt, 1964; Hickman, 1980a) — a central formation of BIF, chert, carbonaceous shale, siltstone and sandstone; and the Cundaline Formation (Williams, 1999a) — an upper formation of conglomerate, sandstone, wacke and shale. The type area of the Gorge Creek Group is Gorge Creek in the Warralong greenstone belt where the group unconformably overlies the Sulphur Springs Group (Van Kranendonk, 2004a; Van Kranendonk et al., 2006a). However, formations of the group, in particular the lithologically distinctive Cleaverville Formation, have been mapped in areas as far apart as the Devil Creek greenstone belt in the northwestern Pilbara Craton (Hickman and Strong, 2000; Hickman, 2016), the northern Isabella Range in the northeastern Pilbara Craton (Williams, 2001a), and Budjan Creek in the southeastern section of the EPT (Fig. 42; Hickman, 2013b).

Farrel Quartzite

The Farrel Quartzite overlies the regional unconformity at the base of the De Grey Supergroup. Until a major lithostratigraphic revision of the northern Pilbara Craton arising from results of the GSWA–GA PCMP (Van Kranendonk et al., 2006a), all conglomerate–sandstone units immediately overlying this unconformity had been assigned to the Corboy Formation. This interpretation followed the first formal definition of the Gorge Creek Group (Lipple, 1975; Hickman and Lipple, 1975, 1978b). Accordingly, many descriptions and interpretations of the Corboy Formation that were published prior to 2006 now apply to the Farrel Quartzite. Exceptions are descriptions of the Corboy Formation in the Soanesville and Pincunah greenstone belts.

U–Pb zircon geochronology on the Farrel Quartzite has provided important evidence on the exposed geology of the east Pilbara Craton after the c. 3070 Ma Prinsep Orogeny. Data in Figure 12c–e show that the ages of individual detrital zircons are mainly 3600–3340 Ma, indicating widespread exposures of early Paleoarchean crust. The almost complete absence of 3340–3070 Ma zircons suggests that younger felsic crust such as granitic rocks of the Emu Pool, Cleland and Mount Billroth Supersuites, and felsic volcanic formations including the Wyman and Kangaroo Caves Formations, were not exposed, at least in the northeast Pilbara Craton in the vicinity of the Muccan, Carlindi and Mount Edgar Domes. A likely explanation is that much of the EPT was submerged between c. 3070 and 3015 Ma, when the Gorge Creek Group was being deposited, and islands were dominated by pre-3400 Ma crust. The Farrel Quartzite remains to be dated in the Yule, Shaw, Corunna Downs and McPhee Domes. Most sedimentological evidence on the depositional environment of the Farrel Quartzite has been obtained from the Goldsworthy, Warralong and East Strelley greenstone belts.

Goldsworthy greenstone belt

Sugitani et al. (2003, 2006, 2007) interpreted the depositional environment of the Farrel Quartzite at Goldsworthy as fluvial and coastal plain, including evaporite deposits of coastal

salinas. Microprobe analyses and crystallographic studies indicated evaporitic gypsum, nahcolite (NaHCO_3) and barite, later pseudomorphed by silica. One bed of black chert containing microfossils (Sugitani et al., 2007, 2009a,b), and associated with evaporite minerals, was traced laterally for 7 km. Sugahara et al. (2010) analysed the microfossiliferous black chert and detected positive La anomalies, HREE enrichment, slightly positive europium anomalies, and chondritic to slightly super-chondritic Y/Ho ratios. They interpreted these features as evidence of freshwater deposition, possibly influenced by geothermal water, but not high-temperature hydrothermal solutions. Retallack et al. (2016) supported the interpretation of a coastal-plain setting including evaporites, and interpreted other features as evidence of sandy and silty paleosols.

Warralong greenstone belt

Deposition of the Farrel Quartzite in the Warralong greenstone belt was accompanied by crustal extension accommodated by normal growth faults. These faults extend to the top of the formation, but do not penetrate the overlying Cleaverville Formation (Van Kranendonk, 2004b, 2010c; Van Kranendonk et al., 2006a). The growth faults separate along-strike panels of similar lithology but markedly different sedimentary thicknesses (Van Kranendonk, 2004a,b). The tectonically active setting resulted in beds of polymictic conglomerate locally 20 m thick and containing clasts up to 30 cm in diameter (Van Kranendonk, 2010c). Quartz sandstone higher in the formation contains ripple marks and cross-bedding. In combination with its well-sorted composition, this was interpreted by Van Kranendonk (2010c) as evidence of deposition in a nearshore, high-energy, probably beach environment. Interbedded quartz-rich sandstone and siltstone at the top of the formation in some sections indicate an upwards-fining transition into deeper-water facies of the overlying Cleaverville Formation.

East Strelley greenstone belt

In the East Strelley greenstone belt, the Farrel Quartzite is about 500–650 m thick and is an upwards-fining succession commencing with coarse- to medium-grained sandstone overlying an erosional unconformity that was developed on formations of the Kelly and Sulphur Springs Groups. Wilhelmij and Dunlop (1984) divided the succession into lower and upper parts, with a distinctive unit of siltstone, shale, and beds of tuffaceous green chert 30–60 m above the base of the formation. They interpreted this part of the formation, with soft-sediment deformation, symmetrical ripple marks, climbing ripple cross-lamination, and lenticular and flaser bedding, as a wave- or tide-dominated, transgressive shallow-shelf deposit. The 600 m-thick upper division comprises alternating units of regularly bedded sandstone, siltstone and shale with minor chert that Wilhelmij and Dunlop (1984) interpreted as thin-bedded and proximal turbidites. The thin-bedded turbidites contain middle and upper sections of the typical Bouma sequence, whereas the proximal turbidites are represented by >10 cm-thick graded sandstone layers stacked or separated by thin shale partings (Wilhelmij and Dunlop, 1984). The depositional environment of the upper division was interpreted as a submarine fan with migrating proximal channels. The Farrel Quartzite grades upwards into the Cleaverville Formation via a transitional succession of siltstone, shale, chert and BIF.

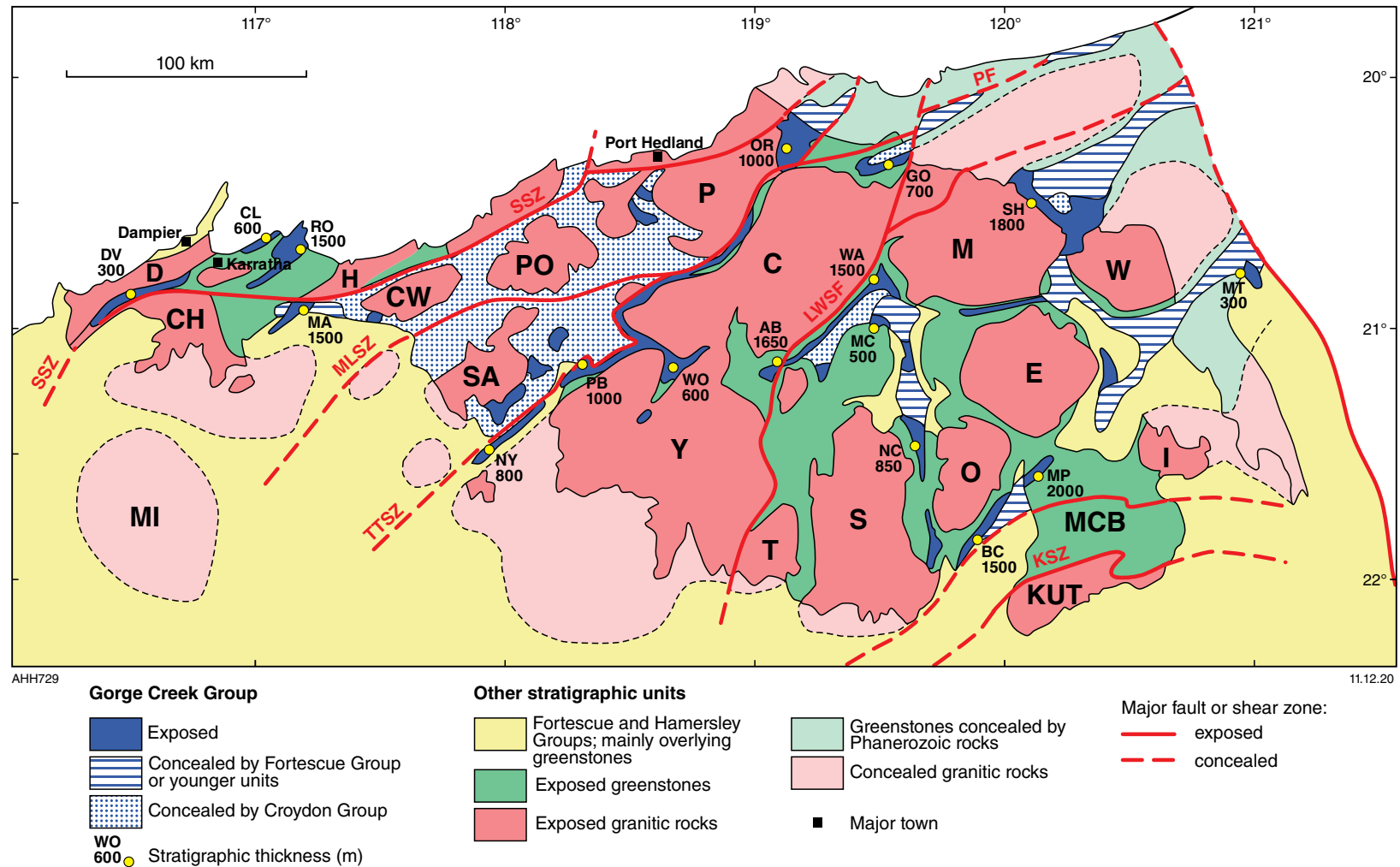


Figure 42. Simplified geological map of the northern Pilbara Craton showing outcrops and exposed thicknesses of the Gorge Creek Group. Interpreted concealed sections of the group (from magnetic imagery) illustrate the minimum extent of its depositional basin. Thickness data indicate that the basin extended well beyond the present outcrop areas. Abbreviations: see Figures 5 and 8 for domes, terranes and basins. Granites and granitic complexes west of the TTSZ: CH, Cherratta granitic complex; CW, Caines Well granitic complex; D, Dampier granitic complex; H, Harding granitic complex; MI, Mingar granitic complex; P, Pippingarra granitic complex; PO, Portree, granitic complex; SA, Satirist Granite. Major faults and shear zones: KSZ, Kurrana Shear Zone; LWSF, Lalla Rookh – Western Shaw Fault; MLSZ, Mallina Shear Zone; PF, Pardoo Fault; SSZ, Sholl Shear Zone; TTSZ, Tappa Tappa Shear Zone. Section locations: AB, Abydos; BC, Budjan Creek; CL, Cleaverville; DV, Devil Creek; GO, Goldsworthy; MA, Mount Ada; MC, Miralga Creek; MP, McPhee Creek; MT, Mount Cecelia; NC, North Coongan; NY, Nunyerry Gap; OR, Ord Range; PB, Pilbara Well; RO, Roebourne; SH, Shay Gap; WA, Warralong; WO, Wodgina

Wodgina greenstone belt

In the Wodgina greenstone belt, the Farrel Quartzite is represented by a succession of metamorphosed sandstone and siltstone conformably overlain by the Cleaverville Formation (Van Kranendonk et al., 2010; Duuring et al., 2016). Duuring et al. (2016) described units that are here correlated with the Farrel Quartzite as comprising a basal unit of volcanogenic sedimentary rocks (possibly tuffaceous), overlain by siltstone and chert, overlain in turn by quartz arenite and quartzite.

Pilbara Well greenstone belt

A mixed clastic succession of conglomerate, sandstone, siltstone and shale, along with felsic volcanoclastic sandstone and minor felsic lava, is conformably overlain by BIF and ferruginous chert of the Cleaverville Formation in the Pilbara Well greenstone belt (Smithies and Farrell, 2000a,b). The stratigraphic thickness of this succession is difficult to measure due to isoclinal folding and faulting, but is estimated to be about 200 m. Van Kranendonk et al. (2010) noted a similar clastic succession at Nunyerry Gap in the southwestern part of the greenstone belt. Smithies and Farrell (2000a,b) reported trachyte and trachytic fragmental rocks in the sandstone succession of the northern Pilbara Well greenstone belt, and trachytic volcanoclastic material is included in the sandstone at Nunyerry Gap (GSWA 142842, Nelson, 1998g).

Facies variations

Facies differences exposed in these five greenstone belts are here interpreted to provide evidence of lateral changes in the Farrel Quartzite from subaerial coastal-plain to submarine-fan settings. The different sections of the transition now exposed are most likely fortuitous combined results of deformation and erosion and might, therefore, have no regional paleogeographic significance. However, it is notable that felsic volcanoclastic sandstone is a significant component of the Farrel Quartzite in only the Pilbara Well greenstone belt. Following the Prinsep Orogeny, deposition of the Farrel Quartzite in areas close to the collisional contact (approximately coinciding with the TTSZ) probably included detritus eroded from either the 3130–3093 Ma Sholl Terrane of the northwestern Pilbara Craton, or the c. 3067 Ma Elizabeth Supersuite. Detrital zircons in a sample of the Farrel Quartzite from Nunyerry Gap included age components dated at 3106 ± 5 Ma and 3068 ± 9 Ma (recalculated from GSWA 142842, Nelson, 1998g).

Cleaverville Formation

The Cleaverville Formation is composed of BIF, chert, shale and siltstone, with minor volcanoclastic rocks and sandstone. Near-surface silicification of Fe-rich shales has locally formed cherty, BIF-like cappings which have been mapped as BIF. Such silicification is evident in some cliff exposures or in drilling below near-surface alteration. Some units of BIF and chert include silicified carbonate rocks, as revealed by rare occurrences of ooids (Van Kranendonk, 2004b). The name 'Nimigarra Iron Formation' was briefly applied to the Cleaverville Formation in the northeast Pilbara Craton pending clarification of regional stratigraphy through the PCMP. Evidence presented by Van Kranendonk et al. (2006a) indicated that the collision between the WPS and the EPT

at c. 3070 Ma, resulting in the Prinsep Orogeny, closed the rift basin that had existed since c. 3200 Ma. Since mapping had established that the Gorge Creek Group was deposited across all the terranes of the northern Pilbara Craton, its maximum age was thereby constrained to c. 3070 Ma. This meant that the 'Nimigarra Iron Formation' was deposited in the same basin as the Cleaverville Formation; accordingly, Van Kranendonk et al. (2006a) declared the name 'Nimigarra Iron Formation' obsolete.

Whereas the stratigraphic thickness of the Farrel Quartzite is regionally extremely variable (0–1500 m), the thickness of the conformably overlying Cleaverville Formation is more constant between 500 and 1000 m (Hickman, 1983; Williams, 1999a; Bagas et al., 2004c; Duuring et al., 2016, 2017). Even so, isoclinal folding and faulting within the BIF–shale succession caused local structural duplication and tectonic thickening, giving a false impression of original stratigraphic thickness. For the same reason, it is locally difficult to exclude the possibility that some lenticular units of sandstone or shale, apparently in the centre of the Cleaverville Formation, are displaced from either its base or top. The average background composition of least-altered BIF within the formation is 57 wt% Fe_2O_3 and 41 wt% SiO_2 (Duuring et al., 2016). By comparison, seven analyses of BIF in the Dales Gorge Member of the Brockman Iron Formation average 42 wt% Fe_2O_3 and 50 wt% SiO_2 (data in Trendall and Blockley, 1970). Compositional differences are partly due to BIF of the Dales Gorge Member containing more MgO, CaO and CO_2 .

Evidence for the depositional environment of the Cleaverville Formation is partly stratigraphic and partly geochemical. The stratigraphic evidence indicates a regionally extensive depositional basin across the northern Pilbara Craton that progressively subsided during deposition of the Gorge Creek Group. The total stratigraphic thickness of the Gorge Creek Group in the east Pilbara Craton is about 2000 m, suggesting this was the minimum amount of subsidence. Any reactivation of the EPT dome-and-keel crustal architecture during deposition of the Cleaverville Formation would have deepened the basin above greenstone keels. Turbidites in the upper Farrel Quartzite (Wilhelmij and Dunlop, 1984), the Cleaverville Formation (Duuring et al., 2016), and the Cundaline Formation (Williams, 1999a) might be evidence of syndepositional tectonic activity, and the Cundaline Formation is locally unconformable on the Cleaverville Formation (Williams, 1999a), indicating uplift and erosion. Fine-scale graded bedding in the Cleaverville Formation is present in most greenstone belts, although its origins are uncertain.

Smithies (2004) reported field evidence for hydrothermal activity during deposition of the Cleaverville Formation in the Goldsworthy greenstone belt. The formation contains layers of dark-grey, fine-grained silica up to 0.5 m thick that were fed from fracture zones with hydrothermal brecciation. Similar hydrothermal features have not been described from the Cleaverville Formation in greenstone belts farther south in the EPT. This is consistent with syndepositional intrusion of the Orpheus Supersuite in the northwestern Pilbara Craton, close to the interpreted magmatic arc at c. 3020 Ma (Hickman, 2016). Sugahara et al. (2010) analysed black chert and BIF from the Cleaverville Formation of the Goldsworthy greenstone belt, and reported a vertical trend of increasing Y/Ho with HREE enrichment and positive La anomalies. These results were interpreted to indicate a

change from non-marine deposition in the Farrel Quartzite to marine deposition of the Cleaverville Formation. They also noted increasingly positive Eu anomalies upwards into the Cleaverville Formation, and interpreted this as evidence of increasing syndepositional hydrothermal activity. This trend is consistent with southeast migration of the Orpheus arc (Hickman, 2016).

Cundaline Formation

At different localities in the Shay Gap and Marble Bar greenstone belts, the contact between the Cleaverville Formation and the overlying Cundaline Formation (Williams, 1999a) has been described as conformable (Williams and Hickman, 2000), disconformable (Williams, 1999a, 2000, 2003), or unconformable (Williams, 1999a; Williams and Hickman, 2000; Sheppard et al., 2017). In most areas, the contact is visibly an erosional unconformity, which suggests that the Cundaline Formation should be removed from the Gorge Creek Group. An attempt to date the depositional age of the Cundaline Formation was unsuccessful, indicating only a maximum depositional age of 3398 ± 15 Ma (GSWA 143996, Nelson, 1998m). An interpretation of the Shay Gap greenstone succession by Sheppard et al. (2017) indicates that there are no unconformities between the Cundaline Formation and the overlying Cattle Well Formation. This latter formation has an interpreted maximum depositional age of 2988 ± 5 Ma (1 σ) (GSWA 180048, Wingate et al., 2009b), although this date was based on a single analysis of a high-uranium zircon, and could reflect loss of radiogenic Pb.

As defined by Williams (1999a), the Cundaline Formation is about 800 m thick and consists of reddish Fe-rich shale, grey-green shale, siltstone, wacke, sandstone, immature pebbly sandstone, and pebble conglomerate. Lithic clasts are mainly chert, jasper and minor devitrified felsic volcanic rock. Thick, coarse-grained clastic units locally contain graded bedding. Intercalated thin units of komatiitic basaltic rock are present in the Shay Gap greenstone belt, suggesting sills related to the overlying Coonieena Basalt. In the northeastern Marble Bar greenstone belt, the Cundaline Formation unconformably overlies the Cleaverville Formation and includes basal conglomerate and breccia derived from that unit (Williams, 1999a). Erosion of the Cleaverville Formation during deposition of the Cundaline Formation suggests areas of uplift in the Gorge Creek Basin. The Cundaline Formation was interpreted to overlie the 'Nimingarra Iron Formation' (obsolete name) at Mount Cecilia (Williams, 2001), suggesting that it was deposited across the Muccan and Warrawagine Domes (Fig. 8, Plate 1A).

Regional continuity of stratigraphic succession

Based on an interpretation of the maximum depositional age of BIF in the Shay Gap greenstone belt, Sheppard et al. (2017) questioned the regional continuity of the stratigraphic succession of the Gorge Creek Group across the northern Pilbara Craton. There have been no previous assessments of the regional stratigraphy of the group, and impressions of stratigraphic differences between greenstone belts might originate from the very brief local descriptions of the group in the GSWA Explanatory Notes for first-edition 1:100 000-scale geological maps. This Report addresses this deficiency by comparing the successions of the various

greenstone belts, particularly in the EPT. Figure 42 provides estimates of the total thickness of the Gorge Creek Group (Farrel Quartzite plus Cleaverville Formation) at most localities across the northern Pilbara Craton. The conclusion is that the succession of the Gorge Creek Group is present in all greenstone belts that expose this stratigraphic level, despite thickness variations of the basal Farrel Quartzite and local erosion of the top of the group prior to deposition of overlying units, such as the Lalla Rookh Sandstone. The depositional extent of the group is consistent with the interpretation that it was deposited in a single, regionally extensive retro-arc foreland basin.

Mapping in the Devil Creek greenstone belt (Strong et al., 2000) suggests that the Cleaverville Formation there is up to 300 m thick, although measurement of stratigraphic thickness is complicated by folding and shearing adjacent to the Sholl Shear Zone. At Cleaverville (CL, Fig. 42), the formation is between 300 and 600 m thick (Kiyokawa et al., 2012; Ryan and Kriewaldt, 1964), whereas south of Roebourne the Cleaverville Formation is 1500 m thick (Hickman, 1997). At Nunyerry Gap (NY, Fig. 42), the Cleaverville Formation is 400 m thick (Smithies, 1998b) and overlies a volcanoclastic sandstone unit, interpreted to be part of the Farrel Quartzite, that is also about 400 m thick. The Farrel Quartzite is also present in the Pilbara Well greenstone belt (PB, Fig. 42) where the 800 m-thick Cleaverville Formation is conformably underlain by a 200 m-thick succession of conglomerate, sandstone, shale and felsic volcanoclastic rocks (Smithies and Farrell, 2000b). In the Ord Range (OR, Fig. 42), the total thickness of the Cleaverville Formation is 1000 m, and the thickest individual BIF is 500 m thick (Duuring et al., 2016). The reported thickness of the Cleaverville Formation in the Wodgina greenstone belt (WO, Fig. 42) is 600 m, and in the Abydos area of the East Strelley greenstone belt (AB, Fig. 42) the estimated thickness is 1000 m (Duuring et al., 2016). The underlying Farrel Quartzite in the Abydos area is up to 650 m thick (Wilhelmij and Dunlop, 1984).

In the northeastern Panorama greenstone belt at Miralga Creek, mapping by Van Kranendonk et al. (2012) indicated that BIF of the Cleaverville Formation is about 500 m thick, and the formation maintains this thickness northwards into the Warralong and Doolena Gap greenstone belts. In the Warralong greenstone belt (WA, Fig. 42), the Farrel Quartzite is up to 1000 m thick (Van Kranendonk, 2004c, 2010c) and the Cleaverville Formation is up to 500 m thick. In the northern Coongan greenstone belt (NC, Fig. 42), the Cleaverville Formation is 750 m thick (Duuring et al., 2016) and the Farrel Quartzite, largely tectonically removed, has an original thickness of at least 100 m (Hickman and Van Kranendonk, 2008b). At Goldsworthy (GO, Fig. 42), the Cleaverville Formation is over 400 m thick (Neale, 1975) and the Farrel Quartzite is about 300 m thick. In the Shay Gap area (SH, Fig. 42) of the Muccan Dome, the Cleaverville Formation is 1000 m thick, with the overlying Cundaline Formation being 800 m thick (Williams 2000). Aeromagnetic data indicate that BIF of the Cleaverville Formation underlies Proterozoic and younger rocks up to 30 km northeast of Shay Gap, and possibly as far as the faulted contact between the Pilbara Craton and the Paterson Orogen (Fig. 42).

North of Nullagine, in the McPhee Creek area (MP, Fig. 42), the Cleaverville Formation is at least 500 m thick (Bagas et al., 2004a) and the underlying Farrel Quartzite is up to 1500 m thick. Here, the Gorge Creek Group unconformably

overlies the <3223 Ma Budjan Creek Formation, and the same relationship is present to the southeast, in the Copper Hills – Budjan Creek area (BC, Fig. 42) of the Kelly greenstone belt, where the Farrel Quartzite is up to 1000 m thick and the Cleaverville Formation is at least 500 m thick (Hickman, 2013b). East of Nullagine, in the Mount Elsie greenstone belt (Fig. 8, Plate 1B), the Cleaverville Formation is not preserved, apparently as a result of erosion to the level of the Kelly Group. In the far northeast of the east Pilbara Craton, at Mount Cecilia (MT, Fig. 42) in the northern Isabella Range, the Cleaverville Formation is faulted and tightly folded, but outcrop width suggests a minimum stratigraphic thickness of 300 m. Aeromagnetic data indicate not only that this outcrop is an eastern extension of the Cleaverville Formation between the Mount Edgar and Warrawagine Domes (Williams, 2003), but also that the Cleaverville Formation is thickly developed on the northeastern side of the EPT (Fig. 42).

BIF of the Gorge Creek Group is a different type of sedimentary unit from BIF in mainly volcanic successions, which is referred to in some publications as Algoma-type iron formation (Gross, 1980). Volcanic-hosted BIF is locally present in the Warrawoona Group (for example, in the c. 3515 Ma Coucal Formation, in the 3530–3490 Ma North Star Basalt, and in the c. 3477 Ma McPhee Formation), but these BIF units are no more than 20 m thick and have very limited lateral extents. Bekker et al. (2010, 2014) commented that Algoma-type iron formations elsewhere in the world rarely have lateral extents greater than 10 km and are typically less than 50 m thick, whereas BIF units in extensive sedimentary basins extend for hundreds of kilometres and are typically hundreds of metres thick. Konhauser et al. (2017) noted that dissolved hydrothermal Fe(II) can be transported >2000 km from seafloor hydrothermal systems, such as at mid-ocean ridges or in arc or back-arc settings, and precipitated by various oxidative mechanisms far from the source in relatively shallow-water photic zones. Thus, thick BIF units in Archean and Paleoproterozoic sedimentary basins are likely to have been deposited over hundreds of kilometres.

Stratigraphic continuity of Gorge Creek Group between greenstone belts

Pilbara Well and Wodgina greenstone belts

Stratigraphic continuity of the Cleaverville Formation from the type area on the Cleaverville Peninsula, southeast across the Karratha and Sholl Terranes and the Mallina Basin, to the boundary of the EPT, is demonstrated by inliers of the formation within the Mallina Basin (Hickman, 2016). Accordingly, the Cleaverville Formation is interpreted to underlie the Croydon Group in all parts of the Mallina Basin except areas of granitic intrusion (Fig. 42). Eastward continuation of the formation onto the EPT is established by a succession of BIF and underlying clastic rocks on the western margin of the Pilbara Well greenstone belt (Fitton et al., 1975; Smithies and Farrell, 2000b). The Cleaverville Formation of the Pilbara Well greenstone belt is continuous with BIF and chert in the Wodgina greenstone belt through outcrops within the Kangan Syncline. This outcrop continuity indicates that the quartzite–BIF–shale succession of the Wodgina greenstone belt is part of the Gorge Creek Group.

A basaltic succession underlying the Gorge Creek Group in both belts is assigned to the 3185–3165 Ma Honeyeater Basalt of the Soanesville Group.

A U–Pb zircon date of 3016 ± 6 Ma was obtained on the volcanoclastic sandstone under BIF of the Cleaverville Formation at Nunyerry Gap (GSWA 142842, recalculated from Nelson, 1998g). This date is consistent with published maximum depositional ages of the Cleaverville Formation at three widely spaced localities in the northwest Pilbara Craton (GSWA 127330, Nelson 1998a; GSWA 136899, Nelson, 1998b; GSWA 142830, Nelson, 1998f). In the Pilbara Well greenstone belt, the Gorge Creek Group is up to 1000 m thick and consists of basal conglomerate, sandstone and felsic volcanoclastic rocks that are stratigraphically overlain by BIF and chert (Smithies and Farrell, 2000a,b). In this greenstone belt, the upper Gorge Creek Group was removed by erosion during deposition of the unconformably overlying Constantine Sandstone (Croydon Group). The succession of the Gorge Creek Group at Wodgina is at least 600 m thick (Duuring et al., 2016) and includes a basal unit of siltstone, chert and quartzite. This basal unit is overlain by the main BIF unit which is, in turn, overlain by a turbidite succession including sandstone, siltstone, shale and BIF (Duuring et al., 2016). Sheared BIF within the TTSZ on the western side of the Carlindi Dome indicates continuation of the formation northwards to the Strelley area (Smithies et al., 2001a).

Ord Range greenstone belt

Inliers of the Cleaverville Formation within the Mallina Basin include a 100 km² outcrop in the Ord Ranges, 20 km west of Mount Goldsworthy (Plate 1; Van Kranendonk and Smithies, 2006; Duuring et al., 2016). Exposure of the Gorge Creek Group in this inlier is a consequence of local folding and unroofing through the 3015–2931 Ma Croydon Group. Although the BIF–shale succession is tightly to isoclinally folded, detailed mapping by Smithies (2002b) indicated that it consists of sandstone and siltstone overlain by chert (silicified shale) that are, in turn, overlain by a thick unit of BIF and variably silicified black shale. The Cleaverville Formation is about 1000 m thick and comprises several BIF–shale units, all of which are conformably overlain by units of shale, siltstone and chert. The basal sandstone–siltstone unit is interpreted to be the Farrel Quartzite and, the alternating succession overlying the Cleaverville Formation is correlated with the Cundaline Formation.

Goldsworthy and Shay Gap areas

The stratigraphic successions of the De Grey Supergroup in the Goldsworthy and Shay Gap areas are extremely similar, consisting of a basal unit of quartzite and chert overlain by a thick BIF–shale unit. This is, in turn, overlain by turbidite-dominated sandstone, wacke, siltstone, shale, and minor chert and BIF. Despite the 60 km separation of these greenstone belts, most researchers have correlated the successions, with an additional stratigraphic correlation to the Ord Range greenstone belt (Dawes et al., 1995a,b; Williams, 1999a, 2000; Smithies, 2004; Van Kranendonk and Smithies, 2006; Sheppard et al., 2017). The Ord Range and Goldsworthy outcrops were mostly likely adjacent prior to c. 2940 Ma sinistral displacement along the TTSZ and its eastern continuation, the Pardoo Fault (Fig. 3; Hickman, 2016).

Stratigraphic correlation of the quartzite–BIF–shale successions in these three greenstone belts provides an important link between the Gorge Creek Group of the northeast Pilbara Craton and successions of the group that underlie the Mallina Basin and outcrop in the northwest Pilbara Craton. This implies that the depositional age of the Gorge Creek Group in the northeast Pilbara Craton is the same as that in the northwest Pilbara Craton – that is, between c. 3066 and 3015 Ma (Hickman, 2016).

Marble Bar, Doolena Gap, Warralong and East Strelley greenstone belts

From the northern Marble Bar greenstone belt to the southwestern East Strelley greenstone belt, geological mapping and aeromagnetic imagery indicate continuity of the BIF-dominated Cleaverville Formation over a distance of 120 km. TMI imagery supports continuation of the Cleaverville Formation to Mount Cecelia in the northern Isabella Range (Hickman, 1980b; Williams and Trendall, 1998), south to the Coongan and Kelly greenstone belts (Hickman, 1980b; Bagas et al., 2004c; Hickman and Van Kranendonk, 2008b; Duuring et al., 2016), and southeast through the Oakover Syncline to the Meentheena area.

The succession in the Marble Bar greenstone belt between Kittys Gap and Bamboo Creek is a continuation of the Gorge Creek Group in the Shay Gap greenstone belt (Dawes et al., 1995a,b; Williams, 1999a, 2003). Conglomerate and sandstone of the Farrel Quartzite unconformably overlie the Euro Basalt. The sandstone contains clasts of fuchsitic quartzite derived from quartzite units in the Euro Basalt (Williams, 1999a). BIF and shale of the Cleaverville Formation conformably overlies the Farrel Quartzite forming a 400–1000 m-thick unit. Locally unconformably overlying the Cleaverville Formation, the 1000 m-thick Cundaline Formation is composed of polymictic pebble to cobble conglomerate grading up into sandstone, wacke, siltstone, shale and chert. Clasts in the conglomerate include BIF, jaspilite, and chert derived from erosion of the immediately underlying Cleaverville Formation. The Coonieena Basalt unconformably overlying the Cundaline and Cleaverville Formations in the Marble Bar greenstone belt is lithologically similar to the Coonieena Basalt in the Shay Gap greenstone belt (Williams, 1999a). In summary, the entire succession of the Gorge Creek Group in the Shay Gap greenstone belt continues south into the Marble Bar greenstone belt. Excellent exposures of the Cleaverville Formation are accessible at Coppin Gap (Fig. 30).

Semi-continuous outcrops of the Gorge Creek Group extend from Bamboo Creek in the northeastern Marble Bar greenstone belt through the Doolena Gap, Warralong and East Strelley greenstone belts (Fig. 8) to north of Glacier Valley (Plate 1A; Van Kranendonk, 1999a, 2000a, 2004a,b,c, 2010c; Williams, 1999a; de Vries, 2004; Van Kranendonk and Smithies, 2006; Van Kranendonk et al., 2006b; Hickman, 2010). The type area of the group is at Gorge Creek in the Warralong greenstone belt where the combined thickness of the Farrel Quartzite and Cleaverville Formation is about 1500 m. The Cundaline Formation has not been mapped separately from the Cleaverville Formation, but is likely to be represented by quartz sandstone, siltstone and shale in the upper part of the group north of Cooke Bluff Hill.

At different localities in the Warralong greenstone belt, the Farrel Quartzite overlies various formations of the Warrawoona, Kelly, and Sulphur Springs Groups across angular erosional unconformities. The Soanesville Group has not been identified in any of these greenstone belts, most likely due to its depositional basin being confined to the Lalla Rookh – Western Shaw Structural Corridor and areas extending west to the TTSZ. The base of the Farrel Quartzite typically includes beds of polymictic conglomerate up to 50 m thick, in which boulders and pebbles are composed of a range of lithologies including quartzite, vein quartz, grey-and-white banded chert, green chert, jaspilitic BIF, and altered volcanic rocks. Most of the formation consists of quartz-rich sandstone. The Cleaverville Formation is composed of BIF, Fe-rich chert, grey-and-white banded chert, and metamorphosed shale, siltstone and minor volcanogenic sedimentary rocks.

Coongan, Kelly and McPhee greenstone belts

Quartzite–BIF–shale successions of the Gorge Creek Group occupy two large outcrops in faulted synclines in the Coongan and Kelly greenstone belts, between the Shaw and Corunna Downs Domes (Fig. 8, Plate 1), and in the Kelly and McPhee greenstone belts, between the Corunna Downs and McPhee Domes. Inliers of BIF and quartzite within the Fortescue Group between the Mount Edgar and North Pole Domes (Hickman and Van Kranendonk, 2008b) confirm that the Cleaverville Formation and Farrel Quartzite underlie the Fortescue Group. The Cleaverville Formation exposed in the syncline between the Shaw and Corunna Downs Domes is extensively faulted and preserves very few original stratigraphic contacts. However, in the northern area of the belt, southwest of Blue Bar mine, the BIF and silicified shale of the formation are stratigraphically underlain by quartzite and grey-and-white banded chert (Hickman and Van Kranendonk, 2008b). On the western limb of the syncline, the BIF unconformably overlies rhyolite of the Wyman Formation. Duuring et al. (2016) recorded volcanoclastic sandstone, siltstone and chert in the lower part of the succession, and BIF and jaspilitic chert in the central and upper parts of the succession. About 30 km south of these exposures, south of Triberton Creek, the Gorge Creek Group is mainly composed of Fe-rich shale which does not have a strong magnetic signature.

Two long outcrops of the Gorge Creek Group in the eastern Kelly greenstone belt are separated by a 1–2 km-deep depositional basin of the lower Fortescue Group and several major north-striking normal faults. These structures interrupt the linear magnetic anomaly associated with the northeast–southwest striking Cleaverville Formation. In the southwestern outcrop of the Gorge Creek Group, between Copper Hills and Cookindina Pool, polymictic conglomerate, sandstone, siltstone and shale, correlated with the Farrel Quartzite (Hickman, 2013b), unconformably overlie the Budjan Creek Formation (Bagas et al., 2004c). The conglomerate contains cobble- to pebble-sized clasts of chert, porphyritic dacite or rhyolite, and rare mafic volcanic rocks, indicating derivation from the underlying Kelly Group. This clastic succession fines upwards, and is conformably overlain by BIF, carbonaceous shale and chert (Bagas et al., 2004c). Outcrop width and bedding inclination suggest this upper unit is between 200 and 500 m thick.

The stratigraphic top of the group is concealed by the Fortescue Group, but a high magnetic anomaly 8 km southeast of Copper Hills suggests a substantial unit of BIF is present. The northeastern outcrop of the Gorge Creek Group, from McPhee Creek northeast to Yandicoogina Creek, is characterized by a thick basal succession of the Farrel Quartzite. Around the headwaters of Yandicoogina Creek, the formation is estimated to be 1500 m thick (Williams and Bagas, 2007a), and is composed of metamorphosed sandstone, polymictic conglomerate, and grey, black and Fe-rich chert. Clasts in the conglomerate include quartzite, chert and vein quartz. Farther south, the Farrel Quartzite is about 500–1000 m thick and is composed of metamorphosed sandstone containing lenticular units of conglomerate, siltstone, shale, and banded chert that is locally Fe-rich. Contacts with the underlying Budjan Creek Formation are unconformable (Bagas, 2005). The Cleaverville Formation is at least 200 m thick and composed of thinly bedded quartz–magnetite BIF interbedded with ferruginous chert and variably silicified shale.

The Farrel Quartzite also outcrops in the northern McPhee Dome (Fig. 8, Plate 1A) where it unconformably overlies the Kelly Group (Williams and Bagas, 2007a). No exposures of the Cleaverville Formation are known from this area, almost certainly due to concealment by the Fortescue Group in the Meentheena Centrocline.

Extent of the Gorge Creek Basin

Outcrops and interpreted subcrop of the Gorge Creek Group indicate that its minimum depositional extent was 500 km from west-southwest to east-northeast and 200 km from northwest to southeast (Fig. 42). However, four lines of evidence suggest that the Gorge Creek Basin was larger than this.

1. If, as interpreted in this Report, the Gorge Creek Basin formed as a retro-arc foreland basin southeast of a subduction zone, it is likely to have been many hundreds of kilometres in length. This interpretation is similar to previous back-arc or retro-arc basin interpretations for the Mallina Basin (Krapež, 1993; Krapež and Eisenlohr, 1998; Smith et al., 1998; Beintema, 2003; Smith, 2003; Pike et al., 2006; Hickman, 2012, 2016). The Mallina Basin directly overlies the Gorge Creek Basin via a transitional succession (Hickman, 2016). The c. 3025 Ma magmatic arc of the Orpheus Supersuite provides evidence of a subduction zone on the northwest margin of the Pilbara Craton. In the Roebourne–Karratha area, the Cleaverville Formation is intruded by felsic rocks of this supersuite (GSWA 142830, Nelson, 1998f) and layers of c. 3025 Ma felsic ash are present within the BIF and shale (GSWA 136899, Nelson, 1998b).
2. As indicated by stratigraphic thickness data in Figure 42, the east-northeast extent of the basin was truncated by Proterozoic deformation (faulted contact with Paterson Orogen). The west-southwest extent of the basin is concealed by the unconformably overlying Fortescue and Hamersley Basins.
3. The width of the basin was greater than 200 km because the thickness of the Cleaverville Formation in the Ord Range is similar to its thickness at Budjan Creek

and McPhee Creek (Fig. 42). These thicknesses suggest that the northwestern and southeastern basin margins are not exposed.

4. Northwest–southeast crustal shortening during the 2955–2919 Ma North Pilbara Orogeny is estimated to have reduced the width of the overlying Mallina Basin by at least 100 km (Hickman, 2016). The underlying Gorge Creek Basin would have been compressed by the same amount, implying that its pre-2955 Ma width was at least 300 km.

The Cleaverville Formation ranges in thickness from 300 m to over 1000 m. Although the formation includes local shale units, its thickest BIFs are thicker than the thickest BIF in the Hamersley Group, the 335 m-thick Joffre Member of the Brockman Iron Formation. In most east Pilbara sections of the Gorge Creek Basin, the formation comprises two or more BIF members separated by thinner members of shale and siltstone. Between areas of outcrop, aeromagnetic data confirm lateral continuity of up to 200 km, unbroken by granitic intrusions, stratigraphic concealment or tectonic displacement. For example, the Cleaverville Formation of the Shay Gap greenstone belt (SG, Fig. 42) is the same BIF as in the northern Marble Bar greenstone belt (Fig. 8, Plate 1A) because in both it is overlain by the Cundaline Formation and the Coonieena Basalt (Williams, 1999a). The Marble Bar greenstone belt is contiguous with the Warralong, East Strelley, Panorama and Coongan greenstone belts, all of which contain the same BIF (locations WA, AB, MC and NC, Fig. 42), and aeromagnetic data (Blewett et al., 2000) support this interpretation. Northwest from Shay Gap, most interpretations have correlated the BIF at Shay Gap with BIF at Goldsworthy and Ord Range (GO and OR, Fig. 42). Hickman (2016) recorded that in the northwest Pilbara Craton the Cleaverville Formation outcrops intermittently across a west–east distance of >300 km (DV to OR, Fig. 42).

Conclusions regarding the Gorge Creek Basin

There are multiple lines of evidence supporting the interpretation that the Gorge Creek Group was deposited in a single, laterally continuous basin across the northern Pilbara Craton. Formation of the basin is interpreted to have followed collision of the EPT and WPS at c. 3070 Ma, and the subsequent development of a subduction zone along the northwest margin of the craton. Previously published evidence (Van Kranendonk et al., 2006a, 2007b) indicates that from c. 3025 to 2920 Ma, a succession of magmatic arcs migrated southeast across the northern Pilbara Craton, as inferred from the decreasing ages of granitic intrusions in this direction (Fig. 43; Hickman, 2016). The oldest arc exposed on land is that of the 3024–3007 Ma Orpheus Supersuite, although remnants of 3070–3024 Ma arcs might be preserved within a 150–200 km-wide offshore Pilbara Craton that is concealed by the Northern Carnarvon Basin (Fig. 2). Therefore, the Gorge Creek Basin is likely to have formed as a retro-arc basin southeast of one or more subduction-related magmatic arcs. A back-arc or retro-arc setting has long been interpreted for the Mallina Basin (Krapež, 1993; Krapež and Eisenlohr, 1998; Smith et al., 1998; Beintema, 2003; Smith, 2003; Pike et al., 2006; Hickman, 2012, 2016), and it is now evident that the Mallina Basin evolved from the underlying Gorge Creek Basin. Stratigraphic

evidence (Smithies, 1998b; Hickman, 2016) has revealed that the Gorge Creek Group has a transitional contact with the Croydon Group in the Mallina Basin. Thus, the retro-arc tectonic setting and the subduction related to both basins extended from c. 3070 to 2919 Ma.

Throughout the east Pilbara Craton, the earliest sedimentation in the Gorge Creek Basin was sandstone and conglomerate of the 3066–3022 Ma Farrel Quartzite. In some areas, the Farrel Quartzite is over 1000 m thick. By contrast, only thin units of sandstone and siltstone underlie the Cleaverville Formation in the northwest Pilbara Craton. This is consistent with the absence of a basal angular unconformity in the northwest Pilbara Craton (Hickman, 2016). Deposition of the Farrel Quartzite commenced in subaerial to shallow-water environments including coastal plain, river channel, coastal salina, delta, supratidal and tidal flats, and shallow shelf. Although there have been no paleocurrent studies, it is likely that the topography of the depositional basin was complicated by shallow horst-and-graben structures and islands composed of mainly Paleoproterozoic rocks. Some sections through the Farrel Quartzite have provided evidence of progressive basin subsidence, including upwards-fining sequences, introduction of turbidites, and transitions into the Cleaverville Formation with increases in the amounts of siltstone, shale, chert and BIF (Wilhelmij and Dunlop, 1984).

Based on investigations of BIFs elsewhere (Rasmussen et al., 2014a, 2016; Gauger et al., 2015; Smith, 2015; Konhauser et al., 2017), the principal protoliths of BIF in the Cleaverville Formation are likely to have been iron-silicate mud, Fe-rich clays such as greenalite, ferric oxyhydroxides, and Fe-rich carbonate precipitates. The thicknesses of the BIF–shale successions in the Cleaverville Formation, locally exceeding 1000 m, testify to deposition in a large basin, which is consistent with the retro-arc foreland basin environment interpreted in this Report. Prior to breakup of the Pilbara Craton at c. 2590 Ma (Blake and Barley, 1992; Martin et al., 1998a,b; Muller et al., 2005), the Gorge Creek Basin apparently extended in an east-northeast – west-southwest direction for more than 500 km, and in a southeast direction for at least 200 km. In contrast to the Farrel Quartzite, the Cleaverville Formation was deposited in relatively deep water remote from significant terrigenous influx. However, in the northwest Pilbara Craton, where the Cleaverville Formation was deposited adjacent to felsic volcanism of the Orpheus Supersuite, the formation includes felsic tuff and volcanoclastic sandstone.

The Cundaline Formation unconformably overlies the Cleaverville Formation (Williams, 1999a), and differs lithologically from the Cleaverville Formation by containing more wacke, sandstone and conglomerate, but no BIF. Above the basal unconformity in the northeastern Marble Bar greenstone belt, the Cundaline Formation contains clasts of BIF, jaspilite and chert derived from erosion of the underlying Cleaverville Formation. In the central trough of the Mallina Basin, there is a lithologically similar transitional succession between BIF of the Gorge Creek Group and the Constantine Sandstone (Smithies, 1998b; Hickman, 2016), raising the possibility that the Cundaline Formation is laterally equivalent to the 3015–2970 Ma lower part of the Croydon Group. The lithological composition of the Cundaline Formation indicates shallowing and local emergence of the Gorge Creek Basin following deposition of the Cleaverville Formation.

Coonieena Basalt

Outcrops of the Coonieena Basalt (Williams, 1999a) are restricted to the Shay Gap and Marble Bar greenstone belts where the formation comprises a c. 1500 m-thick succession of pillowed tholeiitic and komatiitic basalt lava flows intruded by dolerite sills. The formation unconformably to disconformably overlies the Gorge Creek Group and is disconformably overlain by the Cattle Well Formation of the Croydon Group (Williams, 1999a). Williams (1999a, 2003) observed that the Gorge Creek Group underlying the Coonieena Basalt is intruded by numerous mafic and ultramafic dykes and sills that were feeders to the basalt; none of the dykes continues into the overlying Cattle Well Formation. This suggests crustal extension during eruption of the Coonieena Basalt, consistent with contemporaneous rifting in the Mallina Basin (Smithies et al., 1999, 2001b; Van Kranendonk et al., 2002).

The Coonieena Basalt is intruded by the Shay Intrusion, although ages of zircons from a granophyre at the top of the intrusion indicate inheritance from the Cattle Well Formation (GSWA 180056, Wingate et al., 2009c). The Cattle Well Formation of the Croydon Group has a maximum depositional age of c. 2988 Ma (GSWA 180048, Wingate et al., 2009b), although, because the overlying Lalla Rookh Sandstone is conformable with the Cattle Well Formation, the depositional age of the latter might be closer to c. 2950 Ma. Therefore, geochronological data from the Shay Gap greenstone belt do not constrain the eruptive age of the Coonieena Basalt, except to suggest an age between c. 3015 and 2950 Ma.

Geochemical data from the Coonieena Basalt and mafic volcanic and intrusive rocks in the central trough of the Mallina Basin suggest they were derived from very similar LREE-enriched mantle sources (Smithies et al., 2004, 2005b, 2007a; Van Kranendonk et al., 2006a, 2007b). Additionally, the c. 2950 Ma Loudon Volcanics and Mount Negri Volcanics of the Bookingarra Group (Hickman, 2016) have similar compositions (Smithies et al., 2004). On the basis of these geochemical similarities, Van Kranendonk et al. (2006a) assigned the Coonieena Basalt to the Croydon Group, despite outcrops of the Coonieena Basalt and the Loudon and Mount Negri Volcanics being separated by more than 200 km. Smithies et al. (2007a) noted that other komatiitic basalt units overlying the Gorge Creek Group in the Goldsworthy and Ord Range greenstone belts (Fig. 8, Plate 1A) are also chemically very similar to the Coonieena Basalt. Like the Loudon Volcanics and Mount Negri Volcanics, the approximate eruptive age of these basalts is c. 2950 Ma (Hickman, 2016). Identical whole-rock ϵ_{Nd} values of -2.00 and Nd model ages of c. 3.4 Ga for the Coonieena Basalt, and the Loudon Volcanics and Mount Negri Volcanics (Smithies et al., 2007a), also favour the stratigraphic correlation suggested by Van Kranendonk et al. (2006a). Arndt et al. (2001) argued that magmas for the Loudon and Mount Negri Volcanics were derived by melting of continental lithosphere due to a mantle plume, although adopting this interpretation for the Coonieena Basalt would require it to have been eroded from most areas prior to deposition of the Lalla Rookh Sandstone. Smithies et al. (2005b) referred to high La/Nb and La/Sm ratios of the Coonieena Basalt as evidence against simple crustal contamination and more consistent with magma derivation from a refractory mantle source that was enriched by a subduction-derived component.

Mallina Basin

The Mallina Basin trends southwest northeast and, as preserved today, is up to 100 km wide and 300 km long. Prior to orogenic northwest–southeast crustal shortening and closure of the basin during the 2955–2919 Ma North Pilbara Orogeny, the central Mallina Basin was likely to have been at least 200 km wide. Regional gravity and aeromagnetic data indicate that the total length of the rift basin, including concealed sections in the southwest and northeast, exceeds 600 km (Hickman, 2004). The Mesoproterozoic extent of all linear tectonic units such as the Mallina Basin would have been greater before Neoproterozoic–Paleoproterozoic continental breakup.

The sedimentary fill of the central trough and southeast shelf of the Mallina Basin is assigned to the Croydon Group (Van Kranendonk et al., 2006a). The southeast shallow-water shelf of the Mallina Basin unconformably overlies the EPT, Soanesville Basin and Gorge Creek Basin, and was deposited between c. 3015 and 2931 Ma. In a tectonic model that interpreted the Mallina Basin as a back-arc or retro-arc basin (Krapež, 1993; Krapež and Eisenlohr, 1998; Smith et al., 1998; Blewett, 2002; Beintema, 2003; Smith, 2003; Pike et al., 2006; Hickman, 2012, 2016), the southeast shelf occupied the southeastern margin of the basin adjacent to erosional areas that exposed the EPT and older crust. The main stratigraphic unit of the shelf is the Lalla Rookh Sandstone which, in the northeastern Pilbara Craton, was given two local names, now obsolete: 'Cooragoora Formation' (Shay Gap greenstone belt, Williams, 1999a) and 'Paradise Plains Formation' (Smithies, 2004). Underlying the Lalla Rookh Sandstone in the Shay Gap greenstone belt is another clastic unit, the c. 2988 Ma Cattle Well Formation. The northwest shelf of the basin is mainly volcanic and is assigned to the Bookingarra Group (Hickman, 2016).

Croydon Group

In the east Pilbara Craton, the Croydon Group comprises the Cattle Well Formation and Lalla Rookh Sandstone, whereas in the northwest Pilbara Craton the group includes the Constantine Sandstone and the Mallina Formation (Hickman, 2016). Evidence from the central and northwestern sections of the Mallina Basin in the northwest Pilbara Craton indicates that deposition of the Croydon Group was in two main stages separated by granitic intrusion of the Sisters Supersuite at c. 2950 Ma (Smithies, 1998a,b; Smithies et al., 1999, 2001b; Smithies and Farrell, 2000b). The maximum depositional age of the Croydon Group in the central Mallina Basin is indicated by a transitional contact between the Cleaverville Formation and the overlying Constantine Sandstone (Hickman, 2016). This sedimentary transition indicates that the basal Constantine Sandstone is only slightly younger than the Cleaverville Formation, and the youngest date on the Cleaverville Formation is 3015 ± 5 Ma (GSWA 136899, Nelson, 1998b). This minimum depositional age of the Cleaverville Formation is supported by the crystallization age of crosscutting granophyre dated at 3014 ± 6 Ma (95% confidence; GSWA 127320, Nelson, 1997b). Based on the ages of intrusive granitic rocks in the central Mallina Basin, most of the Croydon Group was deposited prior to c. 2940 Ma (Smithies et al., 1999, 2001b).

Cattle Well Formation

The Cattle Well Formation (Williams, 1999a) is a mixed epiclastic and volcanoclastic succession deposited in a shallow-marine basin or on a shelf. Hickman (1980c) interpreted the succession of this unit to be part of the Lalla Rookh Sandstone, and it is notable that the Cattle Well Formation has not been recognized outside the Shay Gap greenstone belt. In the type area around Cattle Well, the formation comprises a lower unit of thinly bedded sandstone, feldspathic sandstone, and lithic and feldspathic wacke, locally intercalated with siltstone and shale. Thinly bedded, grey-white dolomitic carbonate and calcareous shale are present near the base of the formation. Middle and upper units of the formation contain layers of felsic tuffaceous and volcanoclastic material. As there are no 2988–2950 Ma felsic volcanic formations overlying the EPT, any felsic volcanic sources must have been in the northwest Pilbara Craton, and possibly included late volcanic activity along the Whim Creek volcanic arc. The minimum age of the Whim Creek Group is poorly constrained and felsic volcanism may have contributed volcanic ash to the Cattle Well Formation. Williams (1999) noted that the nature of the contact with the underlying Coonieena Basalt was uncertain due to intrusion of a mafic sill, but that regional evidence suggested a disconformity.

Felsic volcanic lithologies in the Cattle Well Formation, not reported in any outcrops of the Lalla Rookh Sandstone, include bedded blue-grey tuff, welded tuff and re-sedimented tuffaceous sandstone, siltstone, wacke and chert. Williams (1999a) reported that some tuffs carry abundant shards of devitrified volcanic glass. An isolated outcrop of blue and white chert and chert breccia, interpreted to be a silicified carbonate unit, contains poorly preserved columnar stromatolites up to 10 cm high and 5 cm wide (Williams, 2000). U–Pb detrital zircon dating of a quartzofeldspathic sandstone provided a majority of dates ranging from c. 3583 to 3289 Ma (GSWA 142867, Nelson, 1999d). Three other analyses (<5% discordant) indicated dates of c. 3053, 3048, and 3038 Ma. Dating of a volcanoclastic sandstone from the same formation indicated a possible maximum depositional age of 2988 ± 5 Ma (1σ), although this is based on a single analysis of a high-uranium zircon, and the younger age could reflect loss of radiogenic Pb (GSWA 180048, Wingate et al., 2009b).

Lalla Rookh Sandstone

In the type area east of Lalla Rookh mine, the Lalla Rookh Sandstone (Lipple, 1975) is a 3000 m-thick succession of feldspathic sandstone, conglomerate and shale (Hickman and Lipple, 1975; Hickman, 1983; Krapež, 1984; Krapež and Barley, 1987; Van Kranendonk and Collins, 1998; Van Kranendonk, 2000a). In this area, the formation is strongly deformed by tight to isoclinal upright folds and faults in a synclinal structure that has been referred to as the Lalla Rookh Syncline (Hickman and Lipple, 1975; Eriksson et al., 1988) or Lalla Rookh Synclinorium (Van Kranendonk et al., 2002). The northwestern margin of this northeast–southwesterly trending syncline is partly replaced by the Lalla Rookh – Western Shaw Fault (Fig. 5), although sinistral strike-slip movement on this fault post-dates deposition of the Lalla Rookh Sandstone because the formation is also exposed northwest of the fault in the East Strelley

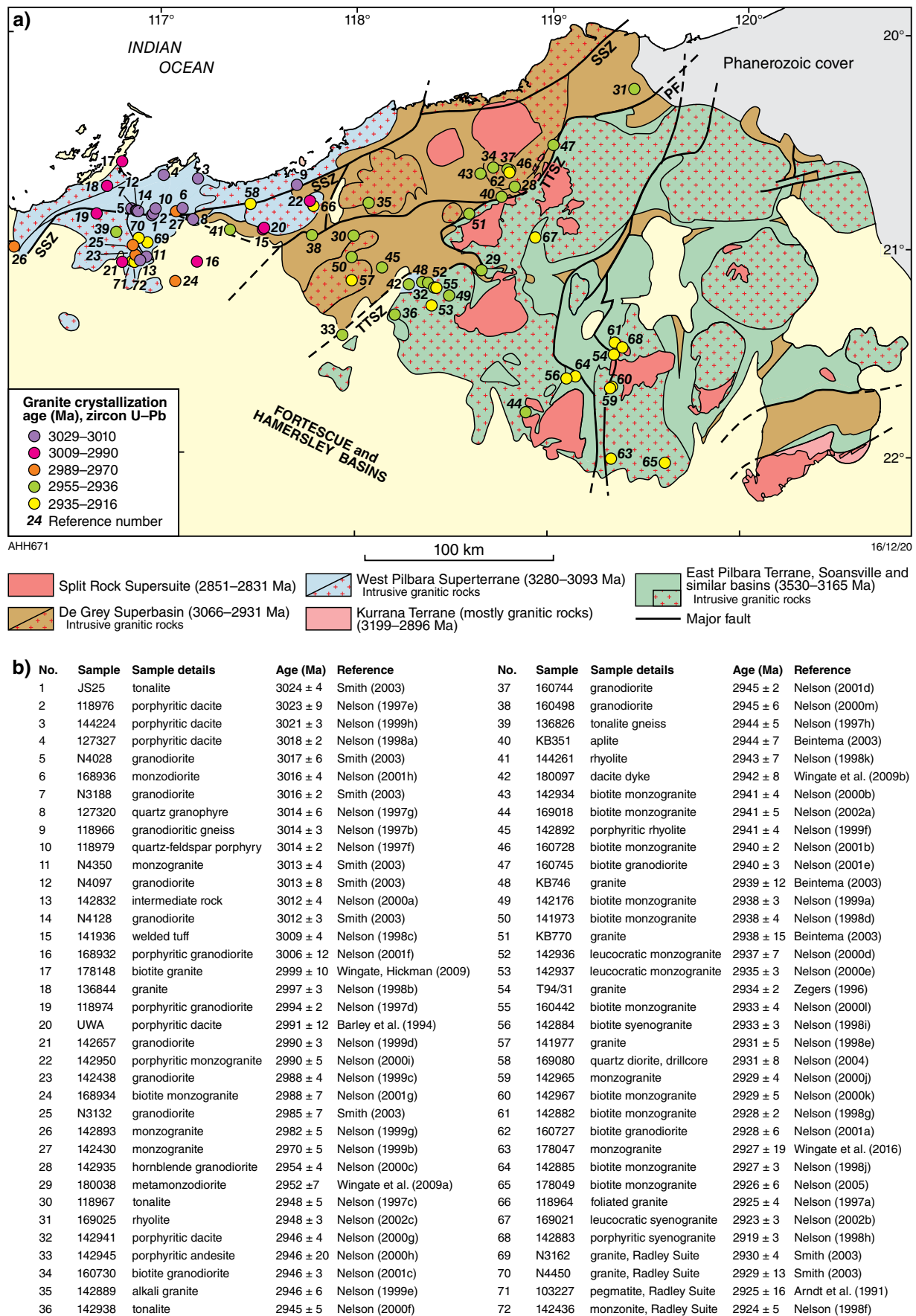


Figure 43. Southeasterly migration of granitic intrusions in the northern Pilbara Craton from c. 3024 Ma to 2919 Ma, demonstrated by trends in geochronology data: a) sites from which geochronology samples and data were obtained; b) SHRIMP U-Pb zircon granite crystallization ages with sample information, age and source reference, by site number shown in (a). Full references for age data given in Appendix 10

greenstone belt (Plate 1B; Hickman, 2010). The southeastern side of the syncline is faulted by a late structure that, to the northeast, cuts across the central axis of the syncline (Plate 1A). East of Cooke Bluff Hill, the Lalla Rookh Sandstone outcrop continues east of this fault where it occupies the core of a major east-trending syncline between the North Pole and Muccan Domes. Farther east, the Lalla Rookh Sandstone is concealed by the Fortescue Group but is interpreted to continue in the centre of the greenstones between the North Pole and Mount Edgar Domes.

Therefore, deposition of the Lalla Rookh Sandstone was not, as interpreted by Krapež (1984) and Van Kranendonk and Collins (1998), confined to a relatively small intracratonic basin bounded by major northeast-striking faults. Thick conglomerate–sandstone units are present at the same stratigraphic level in other greenstone belts in the east Pilbara Craton (East Strelley, North Shaw, Tambina, Coongan, Kelly, Goldsworthy and Shay Gap). Following detailed mapping during the PCMP (Williams, 1998, 1999b; Van Kranendonk, 1999a, 2004a; Smithies, 2002b,c; Hickman and Van Kranendonk, 2008b), all these sandstone–conglomerate units were correlated with the Lalla Rookh Sandstone (Van Kranendonk et al., 2006a). This correlation, implying widespread deposition of the formation across the east Pilbara Craton, is consistent with the present interpretation that the Mallina and Gorge Creek Basins evolved in much the same tectonic settings (retro-arc basins), and that both overlay large areas of the EPT. The present restricted exposures of the formation to synformal structures between the EPT domes is due to its erosion from uplifted areas during and following the North Pilbara Orogeny.

Sandstone and conglomerate unconformably overlying the Cleaverville Formation in the Pilbara Well greenstone belt might link the Lalla Rookh Sandstone of the east Pilbara Craton with the Constantine Sandstone in the central Mallina Basin. In most areas of the east Pilbara Craton, the Lalla Rookh Sandstone disconformably or unconformably overlies the Gorge Creek Group, which was also downfolded prior to c. 2940 Ma strike-slip faulting. This unconformable relationship indicates that D_{15} doming occurred both before and after deposition of the Lalla Rookh Sandstone.

Detrital zircon ages indicate that detritus for feldspathic sandstone in the upper Lalla Rookh Sandstone came from relatively distal sources. U–Pb zircon dating of a sandstone east of the Shaw River revealed a wide range of zircon dates from c. 3660 to 3233 Ma (GSWA 142951, Nelson, 2000h). In particular, four zircons older than c. 3600 Ma have no known sources in the adjacent Carlindi and North Pole Domes. Similar results were obtained from U–Pb zircon dating of sandstone and conglomerate of the then-named ‘Paradise Plains Formation’ (obsolete name, Van Kranendonk et al., 2006a) in the Goldsworthy greenstone belt (GSWA 178019, Nelson, 2005d; GSWA 178020, Nelson, 2005e), and dating of quartzofeldspathic sandstone of the Cattle Well Formation (GSWA 142867, Nelson, 1999d; GSWA 180048, Wingate et al., 2009b) in the Shay Gap greenstone belt. It is possible that the Cattle Well Formation is laterally equivalent to the lower Lalla Rookh Sandstone succession in other areas of the east Pilbara Craton. Williams (1999a, 2000) noted that the Cattle Well Formation is conformably overlain by the ‘Cooragoora Formation’ (obsolete name, Van Kranendonk et al., 2006a), which is now interpreted to be part of the Lalla Rookh Sandstone. The Cattle Well Formation differs lithologically from that of the Lalla Rookh

Sandstone only by containing some units interpreted from field observations to be either felsic lava or volcanic ash. However, some of these units might be fine-grained quartzofeldspathic sandstone, as suggested by lithological descriptions and petrography accompanying geochronology records (GSWA 142867, Nelson, 1999d; GSWA 180048, Wingate et al., 2009b). The depositional setting of the Lalla Rookh Sandstone is consistent with lateral changes of sedimentary facies and suggests that its basal contact is likely to be diachronous across the east Pilbara Craton.

In the Soanesville greenstone belt, the basal contact of the Lalla Rookh Sandstone is an unconformity that, from northwest to southeast, cuts down 950 m through underlying BIF (either Cleaverville Formation or Pyramid Hill Formation) and through most of the Honeyeater Basalt (Van Kranendonk, 2000a). Beneath the unconformity, ridges of resistant chert (Soanesville Group) up to 200 m high are flanked by scree deposits (Van Kranendonk, 2000a).

A large outcrop of the Lalla Rookh Sandstone in the East Strelley greenstone belt lies outside the LWSC, and is displaced sinistrally by the Lalla Rookh – Western Shaw Fault. This establishes that deposition of the Lalla Rookh Sandstone was not confined to basins within the LWSC, and that at least part of the formation pre-dated the c. 2940 Ma late structures of the LWSC. The stratigraphic thickness of the Lalla Rookh Sandstone in the East Strelley greenstone belt is 1500 m (Wilhelmij and Dunlop, 1984), and the formation overlies the Cleaverville Formation across an erosional unconformity. The lower 600–1300 m of the formation comprises interfingering packages of conglomerate and trough cross-bedded sandstone, pebbly sandstone and cobbly sandstone (Wilhelmij and Dunlop, 1984). This lower part of the formation was deposited in interfingering alluvial fans of upwards-fining sandstones in which detritus was derived from the underlying Cleaverville Formation, quartzite (Farrel Quartzite) and greenstones. Higher in the succession, increasingly sericitic sandstones were interpreted to indicate a change to granitic sources. The present interpretation is consistent with progressively increasing exposure of the granitic cores of rising domes during deposition of the Lalla Rookh Sandstone.

The Shaw Gorge outcrop of the Lalla Rookh Sandstone is 10 km long and up to 2 km wide, located in the centre of a faulted synclinal zone between the North Pole and Shaw Domes. Mapping by Van Kranendonk (1999a, 2000a) indicates a succession at least 500 m thick consisting of coarse-grained sandstone and pebble to boulder conglomerate. The Lalla Rookh Sandstone also outcrops at the southern end of the Keep It Dark Synclinorium between the Shaw Dome and the LWSC (Van Kranendonk and Pawley, 2002; Van Kranendonk, 2003). The succession is dominated by polymictic conglomerate interbedded with pebbly to coarse-grained feldspathic sandstone. The formation unconformably overlies the Kelly and Soanesville Groups and is unconformably overlain by the Fortescue Group.

In the Goldsworthy and Ord Range greenstone belts, the Lalla Rookh Sandstone is composed of fine- to coarse-grained sandstone and conglomerate with local mafic volcanic and volcanoclastic units (Smithies, 2004). Clastic rocks are mainly of fluvial origin, but subaqueous debris-flow deposits are abundant near the base of the formation. In the Ord Range, the basal contact of the Lalla Rookh Sandstone with the underlying Cleaverville Formation (Gorge Creek Group)

is an angular unconformity, whereas in the Goldsworthy greenstone belt, it is a disconformity. Units of vesicular and pillowed basalt, mafic volcanoclastic debris-flow deposits, mafic breccia, and dolerite sills are assigned to the Salt Well Member. The upper part of the formation is composed of medium- to coarse-grained, trough cross-bedded sandstone, arkosic sandstone and polymictic conglomerate.

In the Shay Gap greenstone belt, Williams (2003) recorded that the 'Cooragoora Formation' (now Lalla Rookh Sandstone) includes units of polymictic conglomerate containing cobbles and pebbles derived from the underlying Cleaverville Formation, and interpreted these as channel deposits. The sandstones in the upper part of the formation exhibit trough cross-bedding and both upwards-fining and upwards-coarsening sequences. Williams (2003) interpreted the formation to be a high-energy, fluvial-deltaic deposit prograding into a shallow-marine or lacustrine basin.

In the northern Coongan greenstone belt, the Lalla Rookh Sandstone is at least 1000 m thick and unconformably overlies the Cleaverville Formation in a synclinal structure between the Shaw and Corunna Downs Domes (Fig. 8, Plate 1A). The formation is composed of sandstone with beds of conglomerate, and minor siltstone and shale. The formation is unconformably overlain by the Fortescue Group, preventing an estimate of its total thickness where it is interpreted to occupy a syncline between the Mount Edgar and North Pole Domes (Fig. 8, Plate 1).

A suggested stratigraphic correlation between the Constantine Sandstone of the central Mallina Basin and the Lalla Rookh Sandstone (Fitton et al., 1975) remains possible, especially since the Constantine Sandstone has a large range of maximum and minimum depositional ages (3015–2948 Ma). Paleocurrent and detrital zircon data indicate that much of the sedimentary fill of the Mallina Basin was derived from erosion of the EPT; in that case, the Constantine Sandstone might be a deep-water lateral equivalent of the shallow-water Lalla Rookh Sandstone. The depositional age of the Lalla Rookh Sandstone is loosely constrained between c. 3015 Ma (minimum depositional age of underlying Cleaverville Formation) and 2940 Ma (deformation by strike-slip faults).

Sisters Supersuite

In the northwest Pilbara Craton, the Sisters Supersuite was initially intruded into the Mallina Basin, where it includes alkaline granite, hornblende granodiorite, high-Mg diorite (sanukitoid), and ultramafic-mafic layered intrusions of various types. Geochronology (Fig. 43) has established that, from c. 2954 to 2919 Ma, magmatic activity migrated east across the TTSZ and into the east Pilbara Craton, where intrusions were mainly composed of leucocratic high-K monzogranite derived from partial melting of older basement rocks. The regional distribution of the Sisters Supersuite (Fig. 44) suggests not only subduction of the Mallina Basin and underlying Mesoarchean crust eastwards under the EPT (Hickman, 2016), but also northerly subduction of a concealed terrane underlying the Fortescue Group in the Chichester Range (see **Chichester Tectonic Zone**). Figure 44 shows an arcuate intrusive front trending northwest from the southern Shaw Dome, through the eastern margin of the Yule Dome, and into the western side of the Carlindi

Dome. Northeast of this front, the EPT was not intruded by Mesoarchean granitic rocks other than the Split Rock Supersuite. The Split Rock Supersuite is c. 100 Ma younger than the Sisters Supersuite and, based on its chemical composition, unrelated to subduction.

Most of the dated rocks of the Sisters Supersuite in the southwestern and western Yule Dome contain a minority of old xenocrystic zircons, including zircons dated between c. 3552 and 3409 Ma (GSWA 142176, Nelson, 1999b; GSWA, 142936, Nelson, 2000a; GSWA 142937, Nelson, 2000b; GSWA 142938, Nelson, 2000c). This indicates that the Sisters Supersuite intruded early Paleoproterozoic crust in the western parts of the Yule Dome. Direct evidence of this is provided by the c. 3421 Ma Yallingarrintha Tonalite exposed near Kangan Homestead (GSWA 142170, Nelson, 1999a).

Whole-rock Nd isotope data indicate that sources within the central trough of the Mallina Basin were younger than c. 3300 Ma (Van Kranendonk et al., 2006a, 2007a,b), and likely included the 3130–3093 Ma Sholl Terrane and the 3199–3164 Ma Mount Billroth Supersuite. Whole-rock Nd model ages <3300 Ma continue into the northwest margin of the EPT (Table 4; Van Kranendonk et al., 2004c, 2007b; Smithies et al., 2007c; Champion, 2013; Champion and Huston, 2016). These relatively young Nd model ages in the northwest EPT do not define the northwest limit of Paleoproterozoic crust because other geochronological data reveal the presence of this crust within and adjacent to the TTSZ. Rather, the <3300 Ma Nd model ages from the Sisters Supersuite in the western parts of the Carlindi and Yule Granitic Domes suggest melting of Mallina Basin crust subducted beneath the EPT during the North Pilbara Orogeny. Closer to the LWSC, particularly in the eastern Yule Dome, and in the Shaw Dome, the Sisters Supersuite is characterized by high K_2O/Na_2O , generally high Rb/Sr, variable HREE enrichment, and moderate to strong negative Eu anomalies (Champion and Smithies, 2001). Whole-rock Nd model ages >3500 Ma in the Shaw Dome (3700–3420 Ma, Table 4) indicate partial melting of Paleoproterozoic and Eoarchean felsic crust.

Cutinduna Supersuite

The Cooninia Inlier of the Kurrana Terrane (Fig. 2) includes porphyritic biotite monzogranite and granodiorite dated at c. 2897 Ma (GSWA 178230, Nelson, 2005j; GSWA 178231, Nelson, 2005k). Van Kranendonk et al. (2006a) assigned these granitic rocks to the Cutinduna Supersuite. Information on this supersuite is limited because the Cooninia Inlier was not within the area remapped during the 1994–2005 Ma PCMP. Williams (1989) described the granites as post-orogenic, based mainly on composition and a lack of tectonic foliations. He recorded that they have been metamorphosed to lower greenschist facies, and that all granitic rocks of the Cooninia Inlier and adjacent inliers of the Kurrana Terrane are unconformably overlain by the Fortescue Group. The published U–Pb zircon age of these granitic rocks suggests intrusion after the 2930–2900 Ma Mosquito Creek Orogeny. Both dated samples of Cutinduna Supersuite were altered and many zircons that were analysed showed effects of Pb loss. However, the least discordant zircons are close to c. 2900 Ma in age, indicating that the intrusions are distinct from those of the 2851–2831 Ma Split Rock Supersuite.

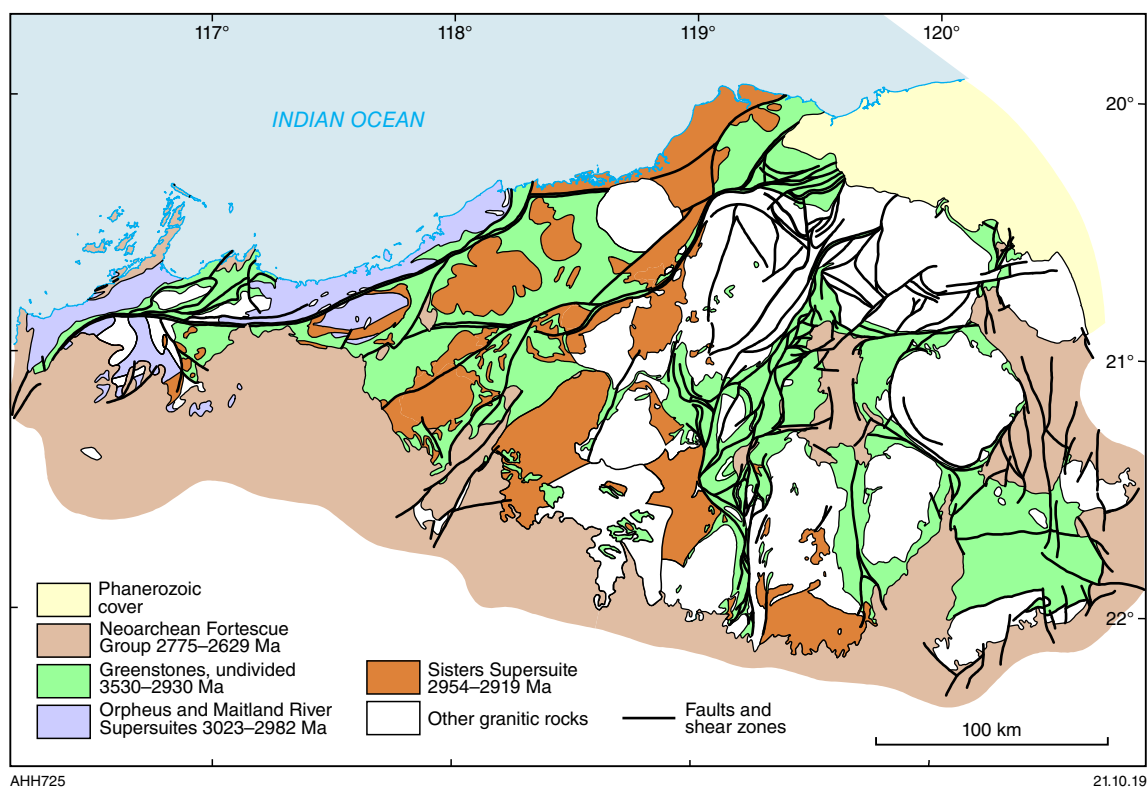


Figure 44. Simplified geological map of the northern Pilbara Craton showing distribution of the Sisters Supersuite

Rare-metal pegmatites dated between 2890 and 2880 Ma (Kinny, 2000; Sweetapple and Collins, 2002) suggest that granitic intrusions of similar age to the Cutinduna Supersuite might be present in the Carlindi and Yule Domes. Kinny (2000) dated tantalite in a Sn-Ta-Li pegmatite at Pilgangoora at 2879 ± 5 Ma. Additionally, the timing of gold mineralization in the Pilgangoora area of the East Strelley greenstone belt, adjacent to some of the rare-metal pegmatites, was c. 2890 Ma (Neumayr et al., 1998; Huston et al., 2001c, 2002; Baker et al., 2002), indicating local deformation and hydrothermal activity at this time (Blewett and Champion, 2005).

Split Rock Supersuite

The Split Rock Supersuite comprises multiple intrusions of highly fractionated, Sn-Ta-Li-bearing, post-orogenic monzogranites that were emplaced in a broad, northwest-trending linear belt across the KUT and EPT, and into the northeastern Mallina Basin (Fig. 45; Van Kranendonk et al., 2006a, 2007b). Dating of the Split Rock Supersuite has been limited to intrusions in the southeastern EPT and in the KUT, where ages of 2851–2831 Ma are recorded. However, as noted in the description of the Cutinduna Supersuite, there is evidence suggesting that some granitic intrusions in the Carlindi and Yule Domes might have been emplaced at c. 2880 Ma. Intrusions assigned to the Split Rock Supersuite in the Carlindi and Yule Dome (Kadgawarrina, Kimmys Bore, Minnamonica, Pooatche, Gillam and Numbana Monzogranites) have not been dated by the U-Pb zircon method. Some of these intrusions are weakly foliated, whereas others are non-foliated, suggesting different

intrusive events. In the Carlindi Dome, the Minnamonica Monzogranite is interpreted to have been intruded by the Pooatche Monzogranite (Smithies et al., 2002).

In the Corunna Downs Dome, a sample from a thin wedge of the Mondana Monzogranite, which locally intrudes the Boobina Porphyry and the Carban Monzogranite, was dated at 3317 ± 2 Ma (Barley and Pickard, 1999). This age of intrusion conflicts with a previous interpretation that the Mondana Monzogranite is a post-orogenic intrusion (Hickman and Lipple, 1975, 1978b; Blockley, 1980; Davy and Lewis, 1981; Hickman, 1983). Early attempts to date the Moolyella Monzogranite gave results similar to that for the Mondana Monzogranite, with an initial conclusion that the Moolyella Monzogranite was emplaced at 3313 ± 2 Ma (GSWA 142977, Nelson, 2000l). However, the highly fractionated chemical composition of the Moolyella Monzogranite, its massive unfoliated texture, and its geological relationship to nearby tin-bearing pegmatites with an interpreted age of 2830 ± 30 Ma (Pidgeon, 1978b) suggested that all the zircons dated (GSWA 142977, Nelson, 2000l) might have been xenocrysts. Subsequent U-Pb zircon dating of the Moolyella Monzogranite indicated a date of 2831 ± 12 Ma (GSWA 169044, Nelson, 2004e). Consequently, the c. 3317 Ma date on the Mondana Monzogranite might represent xenocrystic zircons inherited from the adjacent Boobina Porphyry and Carban Monzogranite (average age c. 3315 Ma).

Geochemical data (Bagas et al., 2003) indicate that the Mondana Monzogranite does not belong to the Emu Pool Supersuite. Differences include its greater fractionation (higher SiO_2 , K_2O , Rb, Y, Th), large negative Eu anomalies,

and somewhat flatter chondrite-normalized REE patterns (Bagas et al., 2003). On K:Th:U gamma-ray spectrometric imagery (Blewett et al., 2000), the Mondana Monzogranite is indicated to have high contents of all three elements, which is a characteristic feature of established post-orogenic granites of the east Pilbara Craton.

Geochemical features of the supersuite and whole-rock Nd model ages up to c. 3.74 Ga (Table 4) indicate magma derivation from partial melting of much older granitic crust (Blockley, 1980; Davy and Lewis, 1986; Bickle et al., 1989; Champion and Smithies, 2000, 2001; Smithies et al., 2003; Gardiner et al., 2017, 2018). Much younger Nd model ages in the Carlindi and Yule Domes (Table 4) suggest far more juvenile sources, although ϵ_{Nd} values are moderately negative to chondritic. Champion and Smithies (2000) described the supersuite as consisting of silica-rich granitic rocks (>73% SiO_2), with high LILE and moderate to large negative Eu anomalies, that are depleted in Sr and undepleted in Y. They interpreted moderate to high Rb, Rb/Sr, Rb/Ba, Ca/Sr and $\text{K}_2\text{O}/\text{Na}_2\text{O}$, and low K/Rb ratios as consistent with crystal fractionation. Fluorite is a common accessory mineral in most of the dated intrusions.

Field evidence indicates that some of the granites and pegmatites were intruded as subhorizontal sheets into the older granites and greenstones of the craton. This is the situation in the Mount Edgar Dome where the Moolyella Monzogranite includes a subhorizontal sheet of monzogranite underlain and overlain by banded orthogneiss of the Tambina Supersuite. Likewise, field exposures of the Cooglegong Monzogranite in the Shaw Dome reveal this to be a subhorizontal, sheet-like intrusion (Van Kranendonk et al., 2001a). At Wodgina, on the boundary between the Yule and Carlindi Domes, almost horizontal Sn–Ta–Li-bearing

pegmatites cut across folded strata of the Soanesville Group (Van Kranendonk et al., 2006b). Intrusion of horizontal sheets suggests reduced vertical pressures within the crust, possibly due to rapid erosion after the Mosquito Creek and North Pilbara Orogenies.

The distribution of the post-orogenic intrusions in a northwest-trending zone across the east Pilbara Craton (Fig. 45) suggests either some form of structural control or a process producing a succession of intrusions along this trend. One possible explanation is that intrusion of the supersuite occurred as the Pilbara Craton crust drifted southeast to northwest across a hot spot (Hickman, 2016). In this scenario, the northwest intrusions might have been emplaced at c. 2880 Ma, about 30 Ma older than the dated intrusions in the southeast. A drift rate of 150 km in c. 30 Ma (5 cm/yr) would be consistent with modern rates of plate movement.

Tectonic events in the De Grey Superbasin

Although most deformation in the De Grey Superbasin occurred during the 2955–2919 Ma North Pilbara Orogeny, various parts of the northwest Pilbara Craton and the northwestern margin of the east Pilbara Craton record evidence of deformation events between c. 3060 and 2955 Ma (Hickman, 2016). The interpretation that this deformation, and that of the subsequent North Pilbara Orogeny, occurred during northwest–southeast convergence of the Pilbara Craton with another plate northwest of the craton (Krapež and Eisenlohr, 1998; Smith et al., 1998; Blewett, 2002; Van Kranendonk et al., 2002; Beintema, 2003; Smith, 2003; Hickman, 2004, 2012, 2016; Pike

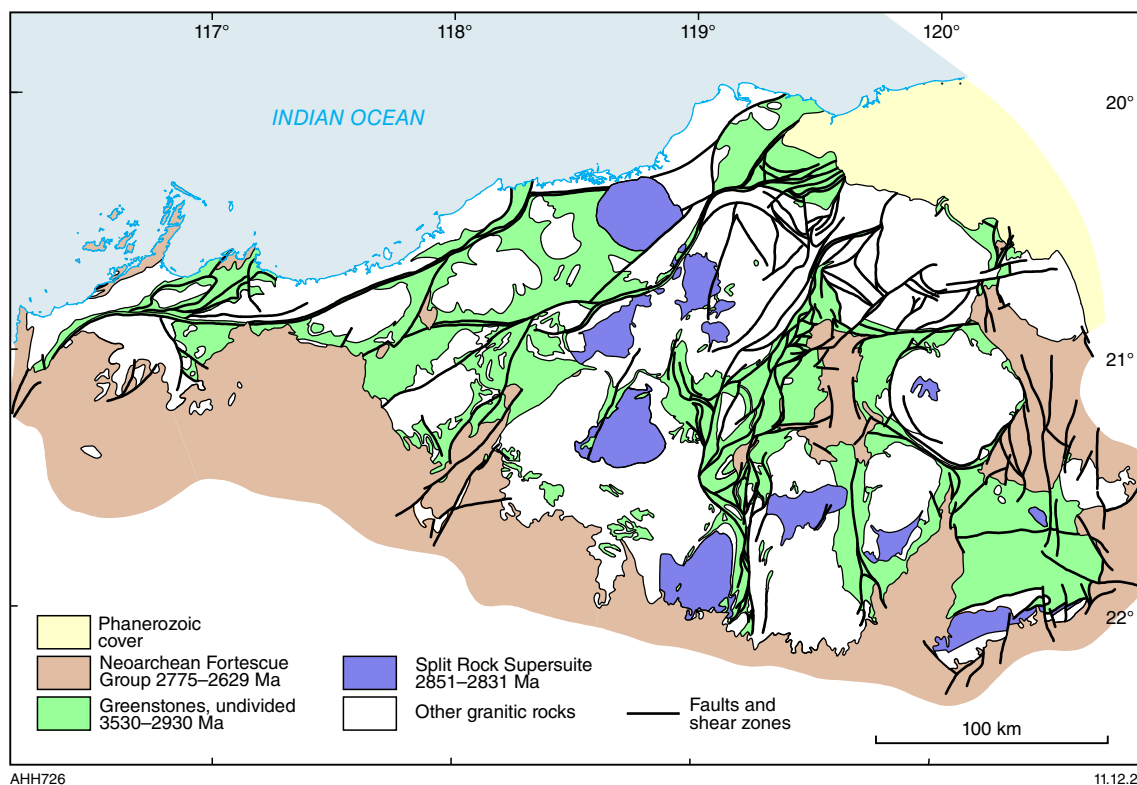


Figure 45. Simplified geological map of the northern Pilbara Craton showing distribution of the Split Rock Supersuite

et al., 2006; Hickman et al., 2006, 2010) is supported by southeast migration of belts of igneous activity between c. 3023 and 2919 Ma (Hickman, 2016). Subduction of the northwestern plate under the northwestern margin of the Pilbara Craton implies the subducted plate was less buoyant than the craton. Igneous products of the subduction included the Orpheus and Maitland River Supersuites, and volcanic rocks of the Whim Creek Group (Hickman, 2016). Whole-rock Nd model ages obtained on these units range between c. 3391 and 3350 Ma (Smithies et al., 2004, 2007a; Hickman, 2016). This suggests either that melting of the northwestern plate included melting of Paleoproterozoic crust, or that melts of juvenile crust in the subducted plate were extensively contaminated by the Paleoproterozoic crust of the Karratha Terrane.

Post-3200 Ma tectonic events in the east Pilbara Craton can be correlated with some events in the northwest Pilbara Craton. All tectonic activity during this period is interpreted as a consequence of interaction between the Pilbara Craton and the converging northwestern plate. The earliest deformation event recognized in the northwest Pilbara Craton, there referred to by Hickman (2016) as D_{11} , is the Karratha Event. This corresponds to D_{10} in the east Pilbara Craton. To avoid confusion when referring to deformation events in the northwest and east Pilbara Cratons, the earliest deformation event in the northwest Pilbara Craton is referred to as D_{1NW} . The second event in the northwest Pilbara Craton was the Prinsep Orogeny, so that D_{2NW} is equivalent to D_{11} in the east Pilbara Craton. D_{12} in the east Pilbara Craton is interpreted to be equivalent to D_{3NW} dykes and sills intruded along extensional structures in the Gorge Creek Basin of the northwest Pilbara Craton. D_{13} of the east Pilbara Craton is correlated with D_{4NW} folding of the Cleaverville Formation in the northwest Pilbara Craton. Six younger deformation events in the northwest Pilbara Craton D_{5NW} to D_{10NW} (Hickman, 2016) are restricted to the Central Pilbara Tectonic Zone (Fig. 3) and correlations with deformation in the east Pilbara Craton are less evident.

1. D_{5NW} (3015–2970 Ma): isoclinal folds in the Mallina Basin that deformed the Cleaverville Formation and Constantine Sandstone, formed under north–south compression.
2. D_{6NW} (2970–2955 Ma): north-trending tight, upright, and locally overturned folds in the central Mallina Basin, formed under east–west compression. Refolded D_{5NW} folds. Possibly equivalent to D_{14} of the east Pilbara Craton.
3. D_{7NW} (2955–2945 Ma): thrusts, folds and axial planar slaty cleavage in the Whim Creek greenstone belt (Krapež and Eisenlohr, 1998). Not recognized in the Mallina Basin.
4. D_{8NW} (2940–2930 Ma): major northeast-trending transpressional folds in the Mallina Basin and WPS, formed under regional north-northwest – south-southeast compression. Fold axes are oblique to major sinistral strike-slip faults and shear zones. Correlated with D_{16} in the east Pilbara Craton.
5. D_{9NW} (c. 2930 Ma): north- to northwest-striking shear zones and parallel tectonic foliation superimposed on D_{8NW} folds in the WPS.

6. D_{10NW} (c. 2920 Ma): dextral displacement of stratigraphy and isoclinal folding of mylonite lamination along the Sholl Shear Zone. Metamorphic disturbance event recorded in zircons. Correlated with D_{17} in the east Pilbara Craton.

Apart from minor syndepositional tectonic activity during deposition of the Gorge Creek Group (D_{12}), most deformation in the eastern area of the northern Pilbara Craton, in the time between the Prinsep Orogeny and the end of the North Pilbara Orogeny, was confined to the area west of the LWSC. There are two likely explanations for this: 1) the northwestern EPT is closest to the CPTZ in which most convergence-related deformation was concentrated; 2) the EPT crust between the TTSZ and the LWSC was less rigid than EPT crust east of the LWSC, possibly due to extensional thinning and fracturing during the EPTRE.

An exception to this generalization that most later deformation occurred west of the LWSC, was the reactivation and amplification of the EPT domes, most evidence for which comes from the eastern half of the EPT. Renewed doming might have commenced as early at c. 3015 Ma and continued until strike-slip faulting and transpressional folding at c. 2940 Ma.

D_{12} , c. 3060–3015 Ma

Crustal relaxation after the Prinsep Orogeny led to local extensional faulting during deposition of the Farrel Quartzite and the Cleaverville Formation (Van Kranendonk et al., 2010; Hickman and Van Kranendonk, 2012). Deposition of the Farrel Quartzite was locally accompanied by growth faults producing graben-like structures containing thicker units of conglomerate and sandstone than on intervening horsts (Van Kranendonk, 2004a).

D_{13} , 3015–2970 Ma

The Soanesville Group and Cleaverville Formation are tightly to isoclinally folded in the Wodgina greenstone belt (Blewett, 2002; Blewett and Champion, 2005; Van Kranendonk et al., 2010; Duuring et al., 2016), Pilbara Well greenstone belt (Smithies and Farrell, 2000b; Van Kranendonk et al., 2010), and in the western East Strelley greenstone belt (Van Kranendonk et al., 2010).

Other areas of the western half of the EPT that contain structures correlated with D_{13} are the Cheearra greenstone belt (Fig. 41; Smithies and Farrell, 2000b; Van Kranendonk et al., 2010) and the Pincunah greenstone belt (Blewett, 2002; Blewett and Champion, 2005). Between the southwest Carlindi Dome and the northwest Yule Dome (Fig. 8), the Kangan Syncline of the Mallina Basin is also likely to contain structures of this type and age, although no structural studies have been published. In the northeast Pilbara Craton, in the Goldsworthy greenstone belt, the northeast-trending Goldsworthy Syncline deforms minor folds within the Cleaverville Formation that contain an axial plane cleavage (Smithies, 2004). The minor folds pre-date the Lalla Rookh Sandstone and are correlated with D_{13} in this Report. The Goldsworthy Syncline deforms the Lalla Rookh Sandstone and is therefore most likely a D_{16} structure. Van Kranendonk et al. (2010) recorded that, at Wodgina, the deformation designated D_{13} in this Report

occurred under lower amphibolite- to greenschist-facies conditions and was accompanied by development of a strong planar foliation (S_{13}).

The original orientation of D_{13} structures indicates north-south or north-northeast – south-southwest compression at a time when the Pilbara Craton is interpreted to have converged and collided with another plate to the north or northwest (Krapež and Eisenlohr, 1998; Smith et al., 1998; Blewett, 2002; Beintema, 2003; Smith, 2003; Hickman, 2016). It is notable that all D_{13} deformation was confined to those parts of the EPT west of the Lalla Rookh–Western Shaw Structural Corridor (LWSC).

D_{14} , 2970–2955 Ma

D_{14} folds and faults deform D_{13} structures in greenstone belts west of the LWSC. The folds trend north-northeast and are upright, open to tight, and have subvertical axial planes (Van Kranendonk et al., 2010). A crenulation cleavage is locally developed where D_{14} deforms S_{13} . Based on a correlation with D_{6NW} folds in the Mallina Basin, the age of D_{14} structures is interpreted to be 2970–2955 Ma. Examples described by Van Kranendonk et al. (2010) include folds in the Wodgina, East Strelley, Cheearra, and Pilbara Well greenstone belts. The difference between the trend of D_{13} and D_{14} indicates a change in the direction of compression to west-northwest – east-southeast, but the reason for this is unknown.

D_{15} dome reactivation, 3015–2940 Ma

BIF of the Cleaverville Formation encircles and separates several of the EPT domes, indicating reactivation and amplification of these Paleoproterozoic structures following final deposition of the formation at c. 3015 Ma. In some greenstone belts, the Cleaverville Formation is inclined moderately to steeply away from the centres of domes, but in others it is subvertical within narrow and deep graben-like structures of the type described by Hickman (2001b). An excellent example of this is at Coppin Gap (Fig. 30) where subvertical and tight to isoclinally folded beds of the Cleaverville Formation occupy the faulted boundary between the Mount Edgar and Muccan Domes. Additional evidence for timing of the deformation is that, although the Lalla Rookh Sandstone unconformably overlies the Cleaverville Formation (providing evidence of another episode of uplift and erosion), it also is deformed into narrow and deep graben-like structures between several of the EPT domes. In both situations (Cleaverville Formation and Lalla Rookh Sandstone) the down-faulted formations are much younger than the surrounding greenstones, indicating downthrow of many kilometres. Such extreme vertical displacement in the axial zones between diapiric domes is predicted by centrifuge models (Dixon and Summers, 1983).

The minimum age of D_{15} is constrained by the fact that associated faults and folds are crosscut by 2940–2920 Ma north-northeasterly trending strike-slip faults of the D_{16} event. This relationship exists south of the Warralong greenstone belt where the LWSC is superimposed on the arcuate synclinal graben containing the Lalla Rookh Sandstone. The graben pre-dates the LWSC because, as illustrated by Van Kranendonk (2004c), the Lalla Rookh Sandstone is interpreted to continue east under the Fortescue Group of the Pear Creek area of the Doolena Gap greenstone belt

(Fig. 8), well outside the eastern boundary of the LWSC. A similar crosscutting relationship is exposed 60 km southwest, west of the Strelley Monzogranite, where the Lalla Rookh Sandstone outcrops in a faulted syncline west of the LWSC. The Lalla Rookh – Western Shaw Fault, which forms the western boundary of the LWSC, offsets the Lalla Rookh Sandstone and underlying Gorge Creek Group by about 10 km of sinistral strike-slip displacement.

The maximum age of D_{15} is c. 3015 Ma, the interpreted youngest depositional age of the Cleaverville Formation. Deposition of the Gorge Creek Group provided the first significant addition to those greenstone successions of the EPT east of the LWSC since deposition of the Kelly Group. This sudden increase in loading of the upper crust might have triggered basin subsidence and adjacent crustal uplift. Evidence of uplift and erosion is provided by a c. 3015 Ma erosional unconformity between the Cleaverville Formation and the Cundaline Formation in the Marble Bar greenstone belt (Williams, 1999a). In the same greenstone belt, the Cundaline Formation is unconformably overlain by the Coonleena Basalt (Williams, 1999a), suggesting additional uplift and erosion at 3000–2990 Ma. If the succession assigned to the Cattle Well Formation (Williams, 1999) is a member of the Lalla Rookh Sandstone (Hickman, 1980c), deposition of this formation in the northeast Pilbara Craton commenced at c. 2988 Ma. Other evidence that deposition of the Lalla Rookh Sandstone might have spanned a considerable time is the presence of lithologically distinctive lower and upper divisions of this unit in some greenstone belts (Wilhelmij and Dunlop, 1984). The lower part of the formation typically contains detritus derived from erosion of underlying greenstones, whereas the upper part is more quartzofeldspathic, suggesting erosion of the granitic cores of the EPT domes (Van Kranendonk and Collins, 1998; Van Kranendonk, 2000a; Van Kranendonk et al., 2002). This change might have closely followed a regional metamorphic event at c. 2950 Ma (Oversby, 1976; Bickle et al., 1985, 1989; Wijbrans and McDougall, 1987; Zegers, 1996) that is likely to have coincided with the main phase of doming. Greater uplift would have exposed the domes to deeper erosion. In the northwest Pilbara Craton, a major event of deformation and erosion at 2955–2950 Ma established an unconformity in the middle of the Mallina Basin succession, and an unconformity between the Whim Creek Group and the Bookingarra Group (Hickman, 2016).

The descriptions of D_{13} – D_{15} imply that plate convergence prior to the North Pilbara Orogeny produced different styles of deformation west and east of the LWSC over the same time period. Whereas two near-orthogonal sets of upright folds were formed west of the LWSC, east of the LWSC the EPT crust was deformed only by minor uplift and basin subsidence. Significant doming probably did not eventuate until the North Pilbara Orogeny at c. 2950 Ma. Domes in the eastern EPT were not produced by refolding on orthogonal, subhorizontal axes because the geometry of the structures is very different from that of Type 1 fold interference patterns (Ramsay, 1967), and because the c. 2950 Ma doming was an amplification of pre-existing Paleoproterozoic domes. It is unknown if any D_{15} doming occurred west of the LWSC, mainly due to poor exposure across the mainly granitic Yule and Carlindi Domes. Some expansion of these domes probably occurred through intrusion of the Sisters Supersuite after c. 2950 Ma.

North Pilbara Orogeny, 2955–2919 Ma

The North Pilbara Orogeny marked final accretion of the WPS to the EPT, driven by ongoing northwest–southeast convergence and subduction of the northwestern plate. In this Report, the orogeny includes the final stages of D_{14} and D_{15} , together with D_{16} and D_{17} , reflecting regional differences in the nature and timing of deformation.

D_{16} , 2940–2920 Ma

The D_{16} event, comprising c. 2940 Ma northeast-trending strike-slip faulting and transpressional folding, was an important tectonic event in the northwest Pilbara Craton (Krapež and Eisenlohr, 1998; Smithies, 1998a; Smithies et al., 2002; Van Kranendonk et al., 2002, 2006a; Beintema, 2003). Hickman (2016) reviewed previous observations and interpretations concerning these structures in the northwest Pilbara Craton and assigned them to D_8 (D_{BNW} in this Report). The same deformation extended into the western part of the east Pilbara Craton as far as the LWSC. However, D_{16} structures are rare east of the LWSC; some examples are strike-slip faults in the Warralong greenstone belt immediately east of the LWSC (Van Kranendonk, 2004c, 2010c). Many northeast-trending strike-slip faults east of the LWSC either displace the Fortescue Group or pre-date the Croydon Group (Krapež, 1993).

Major D_{16} transpressional folds in the east Pilbara Craton include the John Bull Syncline in the Pilbara Well greenstone belt (Fitton et al., 1975; Smithies and Farrell, 2000b), the Goldsworthy Syncline in the Goldsworthy greenstone belt (Smithies, 2004), northeast-plunging folds in the west Warralong greenstone belt (Van Kranendonk, 2004b), open, northeast-trending folds across the prevailing northwest strike of the Pincunah greenstone belt (Hickman, 1983, p. 169), and numerous northeasterly and east-northeasterly trending folds within the LWSC (Van Kranendonk and Collins, 1998; Van Kranendonk, 2000a, 2003, 2008). D_{16} folding of the Tambourah Dome is indicated by U–Pb zircon dating of synkinematic monzogranite (Van Kranendonk, 2003) at 2933 ± 3 Ma (GSA 142884, Nelson, 1998j).

There are numerous northeast- to north-trending D_{16} strike-slip faults and shear zones within the LWSC (Van Kranendonk, 1997, 2000a, 2003, 2008; Van Kranendonk and Collins, 1998). Along the eastern boundary of the LWSC, the Mulgandinnah Shear Zone (MUSZ) separates the granitic core of the Shaw Dome from the Western Shaw greenstone belt (Zegers, 1996; Zegers et al., 1996, 1998a, 2001; Van Kranendonk and Collins, 1998; Van Kranendonk et al., 2002, 2004a; Van Kranendonk, 2003, 2008). The TTSZ on the northwestern margin of the EPT was also a focus of c. 2940 Ma strike-slip movement (Blewett, 2000; Beintema et al., 2001, 2003; Hickman et al., 2001; Smithies et al., 2001a, 2002; Beintema, 2003).

Lalla Rookh – Western Shaw Structural Corridor (late development)

Almost all the exposed major faults and folds that make up the Lalla Rookh – Western Shaw Structural Corridor (LWSC, Figs 5, 8, Plate 1C) were mapped in the 1970s (e.g. Hickman and Lipple, 1978b, fig. 3). Van Kranendonk and Collins (1998) identified the LWSC as a corridor of linked

fold structures and shear zones, developed in response to c. 2950 Ma sinistral transpression. The timing of the compression and deformation was subsequently revised to between 2940 and 2930 Ma (Van Kranendonk et al., 2002; Van Kranendonk, 2008). Van Kranendonk and Collins (1998) argued that the continuity of greenstone stratigraphy east and west of the LWSC precluded it being a terrane boundary, a previous interpretation by Krapež (1993). The age of the visible deformation within the LWSC has been interpreted from U–Pb zircon dating of synkinematic granitic rocks in the MUSZ along the eastern margin of the LWSC (Zegers, 1996; Zegers et al., 1998a, 2001).

The post-2950 Ma structural geology of the central part of the LWSC was described in detail by Van Kranendonk (2008) and is not repeated in this Report. Several lines of evidence indicating that the visible deformation within the LWSC was superimposed on an older zone of extensional faulting related to the EPTRE are described earlier in the Report (see **D_8 deformation, c. 3220 Ma**).

The LWSC is not simply a 2940–2920 Ma zone of sinistral strike-slip deformation superimposed on a previously uniform stratigraphy across the east Pilbara Craton; instead, it was preceded by a linear extensional structure formed during the EPTRE. Thereafter, as a zone of crustal weakness, it is likely to have been reactivated during convergence of the EPT and KT between c. 3160 and 3070 Ma, and during doming of the Gorge Creek Group between c. 3015 and 2955 Ma. However, the apparent absence of Mesoarchean felsic igneous rocks older than 2940 Ma within the LWSC is likely to impede dating of such tectonic events.

Tabba Tabba Shear Zone

The southeast boundary of the CPTZ (Fig. 3) is defined by a zone of intense faulting and shearing up to 3 km wide. Protoliths of strongly foliated to mylonitic units within the shear zone include granitic and ultramafic–mafic intrusive rocks, felsic and mafic volcanic rocks, and sedimentary rocks including the Cleaverville Formation and the Mallina Formation. From northeast to southwest, this zone includes the Pardoo Fault (PF, Fig. 3), the Tabba Tabba Shear Zone (TTSZ), and the faulted northwest margin of the Pilbara Well greenstone belt, which is interpreted to be a southeast extension of the TTSZ (Fig. 8). The Pardoo Fault is very poorly exposed, and is mainly interpreted from magnetic data. Shearing along the northern TTSZ was recognized by Hickman and Gibson (1982). Subsequently, the structure was described as one of a number of major lineaments seen in Landsat imagery extending across the northern Pilbara Craton (Krapež and Barley, 1987; Krapež, 1993; Barley 1997; Krapež and Eisenlohr, 1998). In the absence of any structural investigations, the significance of these lineaments was uncertain and contentious (Hickman, 1999, 2001c, 2004; Zegers, 1996; Smithies et al., 1999; Hickman et al., 2000; Van Kranendonk et al., 2002). Smith et al. (1998) mapped and dated units within and adjacent to the Sholl Shear Zone whereas Beintema et al. (2001) and Beintema (2003) investigated the TTSZ. The TTSZ is now understood to be a major crustal structure of the northern Pilbara Craton that originated as a rift fault during the 3280–3165 Ma EPTRE, and was reactivated several times during episodes of plate convergence between c. 3160 and 2920 Ma.

The origins, geological history, and tectonic significance of the TTSZ are closely linked to the evolution of the CPTZ (Hickman, 2016). Evidence that the TTSZ originated as a c. 3235 Ma extensional fault includes the presence of c. 3235 Ma gabbroic intrusions within the shear zone (Beintema, 2003; Beintema et al., 2003). Farther east within the EPT, rift-related intrusion of dolerite and gabbro continued until c. 3190 Ma (Van Kranendonk et al., 2010; Hickman, 2012). On the southeast side of the TTSZ, the c. 3235 Ma gabbros intruded c. 3257 and 3250 Ma granodiorite and granite (Beintema, 2003; Beintema et al., 2003; GSWA 160745, Nelson, 2001b) and 3253 ± 4 Ma felsic metavolcanic rock (GSWA 160258, Wingate et al., 2010). The granitic rocks are part of the Cleland Supersuite and the felsic volcanic rocks are correlated with the Sulphur Springs Group. Both correlations are important because they imply that, prior to rifting and separation of the Tabba Tabba and Sholl Shear Zones, the Sulphur Springs Group and Cleland Supersuite of the EPT were probably contiguous with the Roebourne Group and Karratha Granodiorite of the Karratha Terrane (Sun and Hickman, 1998).

Geochronology has also established that the Carlindi Dome includes the c. 3430 Ma Tambina and c. 3465 Ma Callina Supersuites (Van Kranendonk et al., 2006a; Van Kranendonk and Smithies, 2006; Hickman and Van Kranendonk, 2012). Furthermore, xenocrystic zircons in the c. 3250 Ma granitic rocks of the TTSZ have ages consistent with derivation from similarly older Paleoproterozoic sources (GSWA 160745, Nelson, 2001b; KB 263, 312, 770, 779, Beintema, 2003). By contrast, granitic intrusions in the Mallina Basin immediately northwest of the TTSZ contain no xenocrystic zircons older than c. 3246 Ma (GSWA 160727, Nelson, 2001a), and the single 3246 Ma grain detected was most likely inherited from sedimentary rocks of the Mallina Formation rather than from basement rocks. Thus, the TTSZ coincides with, and defines, the northwestern edge of the EPT, and a major change in the composition of the Pilbara Craton crust.

The second episode of deformation along the TTSZ occurred after c. 3160 Ma when separation of the EPT and KT was reversed, and these terranes re converged until 3070 Ma. A metamorphic event occurred in the KT at c. 3160 Ma (Kiyokawa, 1993; Beintema, 2003) and c. 3165 Ma tonalite (Flat Rocks Tonalite) was intruded at the southwestern end of the Pilbara Well greenstone belt. Based on ages of xenocrystic zircon within granitic rocks (KB 746, 770, Beintema, 2003), the TTSZ records 3160–3070 Ma movement and associated igneous activity. Beintema et al. (2001, 2003) described evidence of early dextral movement on the shear zone and suggested this occurred at or before c. 3115 Ma.

Structural studies of the TTSZ have reported evidence of major c. 2940 Ma strike-slip movement (Beintema et al., 2001, 2003; Hickman et al., 2001; Smithies et al., 2002; Smithies et al., 2002; Beintema, 2003). Mesoscopic structures, such as C–S fabrics and rotated feldspar phenocrysts, indicate a sinistral component of displacement. Additionally, northwest-plunging mineral and stretching lineations indicate normal movement consistent with juxtaposition of the Croydon Group in the Mallina Basin against Paleoproterozoic rocks of the EPT to the southeast. The intrusion of gabbro and high-Mg diorite along the TTSZ reveals that it was a deep crustal structure controlling the migration and emplacement of mantle-derived magmas (Smithies and Champion, 2000).

The Pardoo Fault is a northeast continuation of the TTSZ, and relative sinistral displacement of the Cleaverville Formation between the Ord Ranges and Goldsworthy is at least 30 km. In this area, the Pardoo Fault separates the Mallina Formation from the Warrawoona Group (Smithies, 2004), suggesting downthrow of at least 5 km on the northern side of the fault.

D₁₇ c. 2920 Ma

Evidence of late dextral movement on the TTSZ is provided by crenulations and steeply southwest-plunging folds that overprint the main shear foliation related to the c. 2940 Ma sinistral movement (Beintema et al., 2001; Hickman et al., 2001). Beintema et al. (2001) interpreted this to be post-2930 Ma, which suggests it could have occurred at the same time as c. 2920 Ma dextral movement on the Sholl Shear Zone (D_{10NW}). No equivalent of D_{9NW} has been recorded in the east Pilbara Craton.

Mosquito Creek Orogeny, $D_{18} - D_{20}$ between c. 2930 and 2900 Ma

In the Mosquito Creek Basin of the southeast Pilbara Craton (Fig. 3), the 2980–2930 Ma Mosquito Creek Formation is deformed by thrusting and tight to isoclinal upright folding attributed to the 2930–2900 Ma Mosquito Creek Orogeny (Hickman, 1990; Van Kranendonk et al., 2006a, 2007b). The combined evidence from previous structural investigations suggests that the orogeny evolved in three events, D_{18} to D_{20} .

The east–west trend of the Mosquito Creek Basin, and of virtually all the folds and thrusts within it, suggests that the orogeny reflected north–south or northwest–southeast compression of the basin. Gravity data indicate that the orientation of the concealed section of the basin south of Nullagine is northeast–southwest (Hickman, 2004). The interpreted timing of compression of the Mosquito Creek Basin is about 30 Ma younger than the 2955–2919 Ma North Pilbara Orogeny in the Mallina Basin. This suggests that the Mosquito Creek Orogeny was a delayed response to the same collision between the northwest Pilbara Craton and a plate converging from the north or northwest (Hickman, 2016). Until c. 2930 Ma, tectonic effects of the collision might initially have been absorbed by compression within the Mallina Basin but, with final closure of the Mallina Basin, deformation in the Pilbara Craton transferred to the relatively thin crust of the Mosquito Creek Basin. From c. 2930 Ma, the EPT and KT were driven together and the sedimentary succession of the Mosquito Creek Basin, probably >100 km wide at c. 2930 Ma, was progressively compressed into a 30–35 km-wide synclinorium. Basin inversion and reactivation of c. 3200 Ma extensional faults into c. 2905 Ma thrusts probably evolved along the lines of experimental laboratory models testing the transformation of graben into basin inversions (Del Ventisette et al., 2006).

Geological mapping of the Mosquito Creek Basin has revealed that the orogeny evolved through a number of stages, culminating in significant deformation and accompanying epigenetic gold mineralization at c. 2905 Ma. The clearest evidence of polyphase deformation is provided by regional-scale tight folding of the Kurrana Shear Zone (KSZ) along the southeast margin of the basin (Hickman, 1975a,b). The north-dipping KSZ is interpreted to be a

reactivated major normal fault formed during the c. 3200 Ma rifting that developed the graben-like Coondamar Basin. However, the main mylonitic foliation of the KSZ is likely to have been produced by c. 2905 Ma thrusting of the Mosquito Creek Formation (and underlying Coondamar Formation) southwards over the Golden Eagle Orthogneiss in the KUT.

Structural interpretations of the Mosquito Creek Formation have recognized up to five phases of deformation (Hickman, 1975a, 1978; Huston et al., 2001a; Blewett, 2002; Bagas et al., 2004b; Bagas, 2005; Farrell, 2006; Nijman et al., 2010), although some of the deformation within the formation occurred after the Mosquito Creek Orogeny. In most structural interpretations of the Mosquito Creek Basin and adjacent KUT, 'D₁' structures are restricted to the Coondamar Formation and the Golden Eagle Orthogneiss and probably belong to an event prior to c. 3000 Ma. Accordingly, the 'D₁' structures mentioned by Huston et al. (2001a), Blewett (2002), Bagas (2005) and Farrell (2006) were not part of the Mosquito Creek Orogeny and are not described here. The fifth deformation event described by Bagas (2005) and Farrell (2006) was in response to east–west crustal shortening that occurred after the Mosquito Creek Orogeny.

D₁₈ – D₂₀ structures

The first deformation during the 2930–2900 Ma Mosquito Creek Orogeny produced a strong foliation in the Mosquito Creek and Coondamar Formations, and in the northern KUT. This D₁₈ deformation is equivalent to D_{MB2} of Bagas (2005) and Farrell (2006), and to mD₂ of Huston et al. (2001a). S₁₈ (mS₂ of Huston et al., 2001a) is a penetrative slaty cleavage striking east-northeast across the basin. In the eastern half of the basin, S₁₈ also strikes east (Farrell, 2006). Associated D₁₈ folds are tight to isoclinal and plunge shallowly east-northeast or east. In contrast, folds assigned to D₁₉ were described by Huston et al. (2001a) as north-trending and north-plunging mD₃ folds, producing a crenulation cleavage (S₁₉ in this Report) superimposed on S₁₈. Huston et al. (2001a) interpreted D₁₉ to indicate a regional east–west shortening event. Bagas (2005) commented that these folds (D_{MB3}: Bagas, 2005; Farrell, 2006) are rare in the western half of the basin, and Farrell (2006) was unable to identify them in the east. D₂₀ folds (D_{MB4}: Bagas, 2005; Farrell, 2006) are tight, upright structures that trend east to east-northeast and have an axial plane foliation (S₂₀). D₂₀ structures (mD₄ in the scheme of Huston et al., 2001a) are dominant over earlier structures in most parts of the Mosquito Creek Basin. Two major folds of this generation deform the KSZ and all D₁₈ structures in the southeast section of the basin (Hickman, 1975a; Bagas, 2005). Huston et al. (2001a) included reverse faulting and shearing in D₂₀ (mD₄), commenting that shearing was particularly intense along the Middle Creek Shear Zone. Huston et al. (2002) suggested that gold mineralization occurred at this time (c. 2905 Ma).

Structures post-dating D₂₀ were assigned to D_{MB5} and D_{MB6} by Bagas (2005) and Farrell (2006), and to mD₅ and mD₆ by Huston et al. (2001a). The age of these structures is uncertain, but Blewett (2002) interpreted mD₅ and mD₆ to have formed after c. 2800 Ma. Farrell (2006) noted that D_{MB5} occurred after intrusion of the c. 2838 Ma Bonney Downs Monzogranite. This timing suggests a relationship to the evolution of the Fortescue Group.

Post-orogenic events

The North Pilbara and Mosquito Creek Orogenies effectively completed cratonization of the Pilbara Craton (Hickman, 2012). However, the EPT was not entirely inactive during this c. 120 Ma period. Deformation, metamorphism and pegmatite intrusion occurred between 2890 and 2880 Ma, and the Split Rock Supersuite of post-orogenic granitic and pegmatitic rocks was emplaced between c. 2851 and 2831 Ma.

D₂₁, c. 2880 Ma

North-northeasterly trending folds and shear zones deform older structures in the Pilgangoora area of the East Strelley greenstone belt. Baker et al. (2002) recorded that the shear zones are intruded by synkinematic Sn–Ta–Li-bearing granitic pegmatite dykes, and that north-northeasterly trending pegmatite dykes were dated at 2879 ± 5 Ma (Kinny, 2000). Baker et al. (2002) interpreted most of the hydrothermal gold mineralization at Pilgangoora to have been introduced during the D₂₁ event, and gold mineralization in the Mount York area south of Pilgangoora was dated at 2888 ± 6 Ma (Neumayr et al., 1998; Huston et al., 2001a). Major D₂₁ folds include the McPhees Syncline (Baker et al., 2002) and several unnamed anticlines and synclines close to the western margin of the East Strelley greenstone belt at Pilgangoora. In this Report, a major strike-slip fault zone forming the western boundary of the greenstone belt in this area, and extending north-northeast for at least 30 km into the centre of the Carlindi Dome (Fig. 8), is interpreted to be a D₂₁ structure. Based on the geometry of adjacent D₂₁ folding, the dominant sense of movement is dextral.

D₂₂, 2851–2831 Ma

Intrusion of the post-orogenic Split Rock Supersuite into older granitic rocks and greenstones in the east Pilbara Craton is evidence of a tectonic event, although the type of event is uncertain. There is evidence that certain intrusions evolved in multiple stages; for example, the Cooglegong Monzogranite (Van Kranendonk and Pawley, 2002; Van Kranendonk, 2003). Apart from igneous flow banding defined by phenocryst alignment, some of the Split Rock intrusions contain a weakly developed tectonic foliation (S₂₂) formed during or after intrusion. Examples include: a tectonic foliation in the Numbana Monzogranite in the Yule Dome (Blewett and Champion, 2005); a foliation in the Bonney Downs Monzogranite in the KUT (Bagas, 2005); and foliations in the Kadgewarrina, Minnamonica, and Poocatche Monzogranites in the Carlindi Dome (Smithies et al., 2002).

Whereas parts of some intrusions were emplaced as subhorizontal sills (Moolyella and Cooglegong Monzogranites), other intrusions appear to be vertical stocks (Cokes Creek and Spear Hill Monzogranites). This apparent variation might be partly due to present erosion levels; for example, if horizontal emplacement occurred towards the tops of otherwise vertical intrusions.

D₂₃, 2775–2750 Ma

Deformation during deposition of the lower Fortescue Group included rifting of the Pilbara Craton due to crustal extension above a mantle plume (Nelson et al., 1992; Barley et al., 1998; Arndt et al., 2001; Eriksson et al., 2002; Hickman et al., 2010; Hickman, 2012; Hickman and Van Kranendonk, 2012; Mole et al., 2018; Pirajno and Huston, 2018). This formed new faults in the underlying granite–greenstone terrane, and these are locally filled by Neoproterozoic dolerite dykes, felsic dykes or quartz veins. Reactivation of the Paleoproterozoic–Mesoproterozoic dome-and-keel structures, possibly gravity driven as the thick succession of the Fortescue Group accumulated, steepened bedding in the greenstone successions. In areas where the Fortescue Group has been completely removed by erosion, the Neoproterozoic age of such structures is normally difficult to establish without geochronology.

Event history of EPT domes

An important conclusion from data obtained during the Pilbara Craton Mapping Project (PCMP) is that the 11 granite–greenstone domes of the East Pilbara Terrane (EPT) evolved at different rates and have slightly different stratigraphic successions, particularly after c. 3335 Ma. Therefore, the event history of any individual dome does not precisely correspond to that of any of the other domes. The boundary faults between the domes (Van Kranendonk, 1998; Hickman, 2001; Hickman and Van Kranendonk, 2004) are evidence of partly independent dome evolution. Even so, regional events that affected the entire EPT did, to varying degrees, influence the evolution of all the domes. In the Paleoproterozoic, such events included the successive mantle plumes which controlled magmatic activity and influenced doming; whereas in the Mesoproterozoic, the stratigraphy was controlled by plate movements and plate interaction.

Figure 46 compares the volcanic, intrusive and sedimentary components of all 11 EPT domes (see Fig. 8) to examine the extent to which they differ stratigraphically. Differences in stratigraphy should relate to any differences in the evolutionary history of the individual domes. In some domes (Warrawagine and Yilgalong), the volcanic and sedimentary units of the greenstone belts are extensively covered by the Fortescue Group, which obscures the geological record. In other domes (McPhee and Corunna Downs), only the upper stratigraphy has been exposed by erosion; the early geological records of these domes are concealed. Even so, a number of important observations are made.

1. The stratigraphic record between c. 3530 and 3335 Ma is remarkably uniform across the EPT, with all of the better exposed domes revealing thick, mafic volcanic successions of the Warrawoona and Kelly Groups, widespread granitic intrusions of the Callina and Tambina Supersuites, and the regionally extensive

sedimentary deposition of the Strelley Pool Formation. This establishes that volcanic and intrusive events during the first c. 200 Ma of construction of the Paleoproterozoic volcanic plateau (Pilbara Supergroup) were widespread and relatively uniform. This is consistent with the greenstone successions of the Warrawoona and Kelly Groups being erupted as two large igneous provinces (Warrawoona and Kelly IAP) separated by a c. 75 Ma break in volcanism when the sedimentary Strelley Pool Formation was deposited.

2. The regional uniformity of the 15 km-thick greenstone succession across the Paleoproterozoic volcanic plateau implies the existence of a thick and relatively stable 'basement'. Geochemical, geochronological and isotope evidence reviewed in this Report supports the existence of 3800–3530 Ma sialic crust.
3. The eastern half of the EPT contains granitic intrusions of the 3324–3290 Ma Emu Pool Supersuite, whereas the western half does not. Since Paleoproterozoic doming was accompanied by granitic intrusion, this indicates that the major c. 3315 Ma doming event in the east did not affect the western domes.
4. Clastic sedimentary successions of the 3223–3165 Ma Soanesville Group were deposited onto the far west and far east of the EPT, but not between the LWSC and the southeastern side of the Corunna Downs Dome. This is consistent with passive-margin deposition either side of elevated upland on the post-rifting EPT continental plate.
5. No volcanic activity, granitic intrusion or sedimentation occurred in any domes of the EPT between c. 3160 and 3070 Ma.
6. The 3066–3015 Ma Gorge Creek Basin was developed across the entire east Pilbara Craton, with the possible exception of the far southeast (Yilgalong Dome). The regional extent of the basin in the east Pilbara Craton (Fig. 42) is consistent with continuation of the basin into the northwest Pilbara Craton.
7. Clastic deposition of the c. 2950 Ma Lalla Rookh Sandstone is recorded in most domes of the Pilbara Craton. This indicates widespread erosion during doming but, unlike doming in the Paleoproterozoic, this was not accompanied by granitic intrusion.
8. Post-orogenic granites intruded most domes between c. 2851 and 2831 Ma.

The scope of this Report does not permit separate detailed interpretations of the history of events in each of the domes. However, an example of the relative complexity of events is provided with reference to the Mount Edgar Dome (Table 6). Gardiner et al. (2017, 2018) provided other information on the tectonic evolution of this dome.

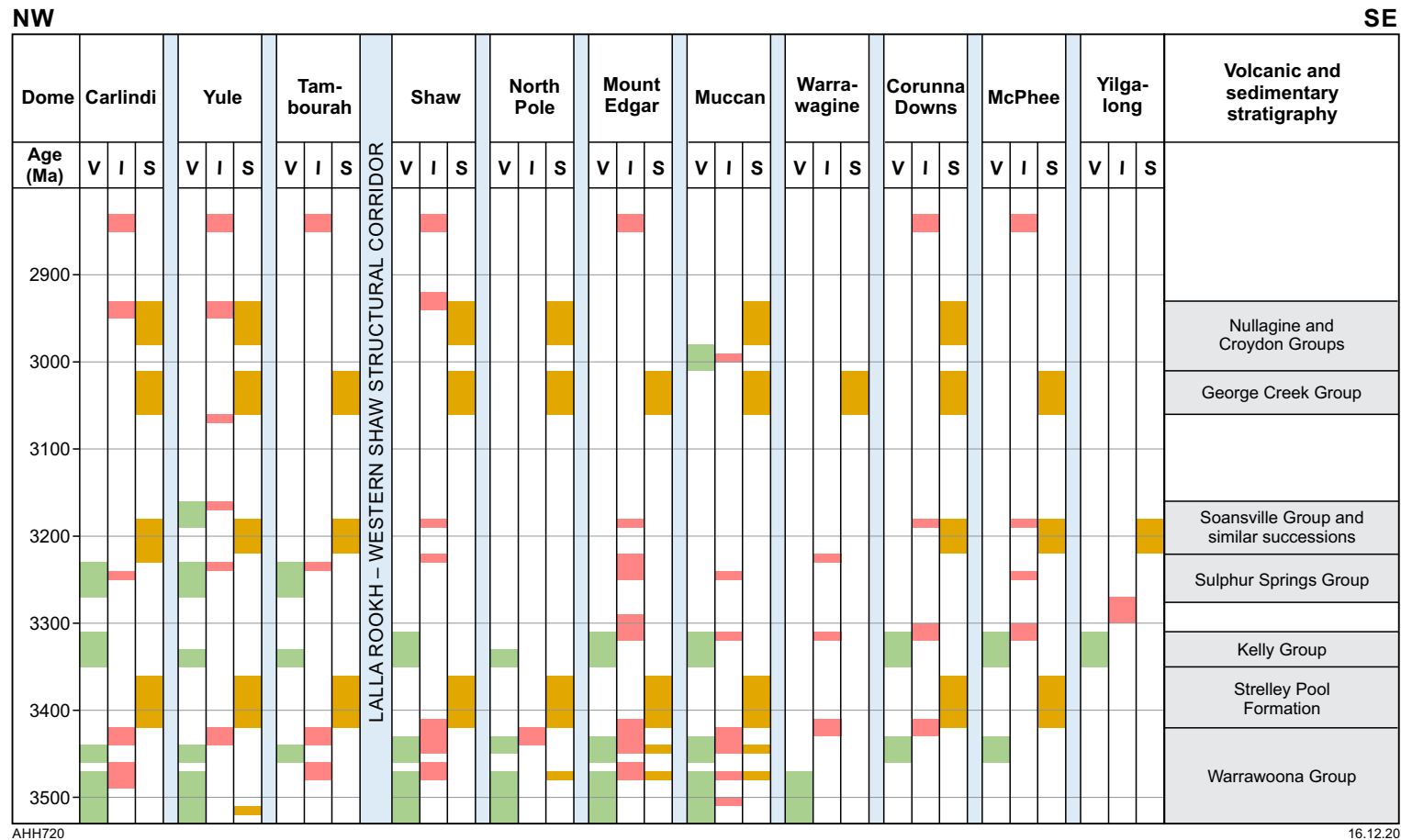


Figure 46. Event history (V, volcanism; I, granitic intrusion; S, sedimentation) of the 11 domes of the EPT. Correlations between domes provide evidence of the regional extent of individual events. Significant differences between the domes are evident from c. 3330 Ma, coinciding with intrusion of the Emu Pool Supersuite, possibly marking early rifting of the EPT. A strong degree of correlation was re-established with collision of the EPT and West Pilbara Superterrane at c. 3070 Ma and subsequent deposition of the Gorge Creek Group

Table 6. Outline of the evolution of the Mount Edgar Dome

Age (Ma)	Event	Evidence (source of data)
2851–2831	Post-orogenic intrusion of the Split Rock Supersuite (monzogranite) derived from partial melting of granitic crust	a) Age range of the Split Rock Supersuite defined by U–Pb zircon ages in several east Pilbara domes ^(7, 37) b) Derivation of supersuite from melting of older crust based on geochemistry ^(39, 40) and Nd model ages to 3700 Ma ^(6, 41, 42)
2955–2919	Regional compression during the North Pilbara Orogeny: re-activation of all east Pilbara Paleoproterozoic domes, increasing amplitudes, folding the Gorge Creek Group, and resulting in deep erosion with clastic deposition of the Croydon Group	a) Folding of the Gorge Creek Group around the Mount Edgar Dome ⁽²⁹⁾ b) Age of North Pilbara Orogeny ^(35, 37) c) Deep erosion indicated by pre-Pilbara Supergroup detrital zircon ages in sandstone of the Croydon Group ⁽³⁸⁾
3066–3015	Deposition of conglomerate, sandstone, shale, and BIF of the Gorge Creek Group above a regional erosional unconformity	a) Regional unconformity c. 3067 Ma ^(32, 35, 37) b) Minimum age of Gorge Creek Group c. 3015 Ma ⁽³⁷⁾
3280–3176	Rifting of the East Pilbara Terrane with emplacement of ultramafic–mafic intrusions of the Dalton Suite	a) Regional intrusion of the Dalton Suite during crustal extension ^(19, 35) b) Dalton Suite dated at c. 3185 Ma ⁽³⁶⁾
3270–3223	Plume event: Intrusion of Cleland Supersuite (chiefly monzogranite) during deformation. Partial melting of the mid- to lower crust	a) Cleland Supersuite contains a tectonic foliation broadly parallel to the margins of the dome ^(19, 27, 29) b) Monzogranite derived by partial melting of older granitic crust ^(13, 34)
3290–3275	Erosion of the dome; clastic depositionprior to intrusion of the Cleland Supersuite	a) Regional unconformity across the East Pilbara Terrane ⁽³²⁾ b) Sandstone in the adjacent Corunna Downs Dome has a maximum depositional age of c. 3278 Ma ⁽³³⁾
3324–3290	Intrusion of Emu Pool Supersuite during doming and metamorphism. Associated sinking (sagduction) of the Warrawoona Group around the margins of the dome. Granites (chiefly granodiorite) derived by anatexis in the mid- to lower crust	a) Intrusion of 3324–3304 Ma granites into the Limestone Shear Zone ^(10, 21, 25) b) Tectonic foliation and metamorphism in Limestone Shear Zone dated at 3320–3305 Ma ^(9, 10, 21, 22) c) Structural evidence for sagduction of the Warrawoona Group ^(12, 19, 21, 23, 26, 27, 28, 29, 30) d) Anatexis of older crust during doming ^(21, 22, 31)
3350–3315	Plume event: Deposition of Euro Basalt overlain by Wyman Formation; intrusion of early granites of Emu Pool Formation	U–Pb zircon dating of volcanic and granitic units ^(7, 10)
3426–3350	Hiatus in volcanism and no recorded granitic intrusion between 3416 and 3324 Ma; regional erosion with deposition of the Strelley Pool Formation	a) Regional unconformity across the East Pilbara Terrane ⁽²⁴⁾ b) Geochronology provides evidence of a break in magmatic activity ⁽²⁴⁾
3435–3427	Deposition of felsic volcanic rocks in upper Panorama Formation; contemporaneous late intrusions of the Tambina Supersuite	U–Pb zircon dating of volcanic and granitic units ^(7, 10)
c. 3440 Ma	Deformation and metamorphism: doming and erosion of the Apex Basalt in adjacent domes	a) Metamorphic event recorded by monazite in garnet ⁽²²⁾ b) Apex Basalt absent in several adjacent greenstone belts ⁽²³⁾
3450–3445	Intrusion of the Tambina Supersuite (TTG) as sheets into basal section of the ~15 km-thick Warrawoona Group; felsic volcanic and volcanoclastic rocks deposited to form the lower Panorama Formation	a) Timing established by geochronology on the Tambina Supersuite and the Panorama Formation ^(6, 9, 15) b) depth of intrusion indicated by the 15 km-thickness of the Warrawoona Group at 3450 Ma and by the metamorphic grades (amphibolite–granulite facies) in the Tambina Supersuite and intruded greenstones ^(19, 20, 21)
c. 3450	Plume event: Deposition of Apex Basalt after or during doming and extensional faulting. Basin subsidence and possible sagduction of the Warrawoona Group between domes	a) Basaltic volcanism after or during doming indicated by radial dolerite feeder dykes around the southwest, northwest, and northeast sides of the Mount Edgar Dome ⁽¹⁸⁾ b) Basin subsidence of at least 3 km indicated by the thickness of Apex Basalt above shallow-water sedimentary rocks
3459–3450	Hiatus in volcanism, uplift, erosion and deposition of Marble Bar Chert Member across a regional erosion surface	a) Depositional age constrained by geochronology on immediately underlying and overlying felsic formations ⁽¹⁷⁾ b) Regional extent from geological mapping ⁽¹²⁾ c) Erosion surface from sedimentological evidence ⁽¹⁸⁾
c. 3460	Deformation: synvolcanic doming, extensional faulting	a) Sandstone at the top of the Duffer Formation (Muccan Dome contains detrital zircons dated at 3575–3522 Ma ⁽¹⁴⁾ indicating erosion of the lower Warrawoona Group and older crust in the area of the Muccan Dome b) Syn-depositional extensional structures in the Duffer Formation interpreted in the northern part of the Mount Edgar Dome ^(15, 16)
3474–3459	Plume event: Deposition of Mount Ada Basalt and Duffer Formation and intrusion of the Callina Supersuite (granite to quartz diorite) derived from partial melting of older crust. Thickness of the Warrawoona Group became 10–15 km	a) Extensive U–Pb zircon dating of volcanic and granitic units ⁽⁷⁾ ; b) Stratigraphic thickness from exposed geology ⁽¹²⁾ c) Partial melting of older crust (mafic) based on geochemical evidence ⁽¹³⁾
c. 3477	Deposition of the McPhee Formation	U–Pb zircon age of silicified felsic tuff unit ⁽¹¹⁾
3530–3490	Inferred intrusion of granitic rocks (no outcrops identified in Mount Edgar Dome)	a) Inherited zircons in Callina Supersuite, 3523–3512 ⁽⁸⁾ b) Inherited zircon in Callina Supersuite, 3492 Ma ⁽⁹⁾ c) Inherited zircon in McPhee Formation, 3492 Ma ⁽¹⁰⁾
3530–3490	Plume event: Deposition of the North Star Basalt; three ultramafic–mafic volcanic cycles	a) Maximum age from correlation with Coonterunah Subgroup ⁽⁷⁾ b) Lower cycle metamorphosed prior to c. 3490 Ma (Ar–Ar hornblende cooling age) ⁽⁸⁾
3750–3538	Formation of pre-Pilbara Supergroup crust	a) Inherited 3750–3700 Ma zircons in Tambina Supersuite of adjacent North Pole Dome ⁽¹⁾ b) 3650–3570 Ma zircons in composite orthogneiss in the adjacent Muccan and Warrawagine Domes ^(2, 3) c) Detrital zircon age (c. 3566 Ma) in c. 3050 Ma quartzite on the northern margin of the Mount Edgar Dome ⁽⁴⁾ d) Nd model ages for four felsic volcanic rocks from the North Star Basalt (3670–3550 Ma) ⁽⁵⁾ indicating mantle extraction ages of sources e) Nd model ages for four samples of felsic volcanic rocks of the Duffer Formation (3620–3550 Ma) ⁽⁶⁾

References: 1) Petersson et al., 2019; 2) Nelson, 1998 (GSWA 142828); 3) Nelson, 1999 (GSWA 142870); 4) Nelson, 1998 (GSWA 143994); 5) Champion, 2013 (recalculation of data in Jahn et al., 1981); 6) Smithies et al., 2007; 7) Van Kranendonk et al., 2006; 8) van Koolwijk et al., 2001; 9) Williams and Collins, 1990 (LTU 6417); 10) Kloppenburg, 2003 (CTW-36); 11) Nelson, 2000 (GSWA 148498); 12) Hickman, 1983; 13) Champion and Smithies, 2007; 14) Nelson, 2002 (GSWA 16896); 15) Nijman et al., 1998; 16) De Vries, 2003; 17) Glikson et al., 2016; 18) DiMarco and Lowe, 1998; 19) Hickman and Van Kranendonk, 2008; 20) Delor et al., 1991; 21) Collins et al., 1998; 22) Francois et al., 2014; 23) Hickman, 2011; 24) Hickman, 2008; 25) Williams and Collins, 1990 (LTU 5472); 26) Collins, 1989; 27) Hickman, 1984; 28) Collins and Teyssier, 1990; 29) Hickman and Van Kranendonk, 2004; 30) Thébaud and Rey, 2013; 31) Collins, 1993; 32) Hickman, 2012; 33) Nelson, 2002 (GSWA 169000); 34) Smithies et al., 2003; 35) Van Kranendonk et al., 2010; 36) Wingate et al., 2009 (GSWA 178185); 37) Hickman, 2016; 38) Kemp et al., 2015; 39) De Laeter and Blockley, 1972; 40) Champion and Smithies, 2001; 41) Bickle et al., 1989; 42) Tyler et al., 1992.

Mineralization

Mineralization styles in the Paleoproterozoic East Pilbara Terrane (EPT) differ from those in the overlying Mesoproterozoic basins. However, some tectonic and depositional environments were repeated through the Paleoproterozoic and Mesoproterozoic, such as those dominated by the hydrothermal activity at the end of each volcanic cycle in the Pilbara Supergroup. Mineralization during evolution of the EPT was influenced by increasing crustal recycling within vertical tectonic processes. The secular changes revealed in the composition of granitic rocks would have affected magmatic fluids involved in mineralization. Additionally, it is generally accepted that the EPT crust was progressively thickened as the volcanic plateau developed and successive granitic supersuites were intruded. One consequence of the growth of the crust is interpreted to have been the first appearance of Cu–Mo mineralization at c. 3315 Ma, some c. 200 Ma into the evolution of the EPT. In contrast to the TTG composition of most pre-3420 Ma granitic rocks, the 3324–3290 Ma Emu Pool Supersuite is mainly composed of porphyritic granodiorite and monzogranite derived either by partial melting of older felsic crust, or through fractionation of mafic magma. Subvolcanic porphyritic dacite stocks at the tops of the 3324–3290 Ma intrusions were the first in the EPT to contain Cu–Mo mineralization.

During breakup of the EPT, crustal extension established new tectonic settings including local continental rift systems followed by passive-margin basins (see **East Pilbara Terrane Rifting Event**). Extensional faulting above c. 3235 monzogranite of the Cleland Supersuite provided the environment for hydrothermal Cu–Zn mineralization (Sulphur Springs, Orchard Tank). Clastic sedimentary basins of the 3223–3165 Ma Soanesville Group included units of BIF up to 1000 m thick, and in places these were subsequently enriched to form large iron ore deposits (e.g. Mount Webber and Iron Bridge). At c. 3160 Ma (see **D₁₀, Karratha Event**), plate divergence of the previous c. 60 Ma was replaced by convergence, and the Mount Billroth Supersuite was intruded. The influx of magma from juvenile sources at this time might have introduced convergent margin mineralization. Although no east Pilbara mineral deposits of this age have been identified, it is possible that gold mineralization in the Pilbara Well and East Strelley greenstone belts, and copper mineralization in the Wodgina greenstone belt, were introduced at this time. Using the method of Thorpe et al. (1992b), which compares $^{206}\text{Pb}/^{204}\text{Pb}$, $^{207}\text{Pb}/^{204}\text{Pb}$, and $^{208}\text{Pb}/^{204}\text{Pb}$ ratios, a Pb–Pb model age of c. 3142 Ma was obtained from galena in an auriferous quartz vein at the McPhees gold deposit (Huston et al., 2001a,c, 2002; Blewett and Champion, 2005). The east Pilbara Craton contains no stratigraphic record from c. 3160 Ma to 3070 Ma, at which time plate collision resulted in the Prinsep Orogeny. Gold and minor copper mineralization in the Pilbara Well, Wodgina and East Strelley greenstone belts, and along the TTSZ, might be related to this event.

From c. 3060 to 2900 Ma, the eastern section of the northern Pilbara Craton evolved through alternating phases of crustal tension and compression as the northwestern margin of the Pilbara Craton interacted with a converging plate (Hickman, 2016). The clastic sedimentary Gorge Creek Basin that formed across the northern Pilbara Craton included a thick BIF (Cleaverville Formation) which, following enrichment

during younger events (Duuring et al., 2016), was host to large iron ore deposits (Mt Goldsworthy, Nimingarra, Sunrise Hill, Yarrie, Pardoo, Wodgina, Abydos, Corunna Downs, McPhee Creek). Plate collisions and basin closures between c. 2955 and 2900 Ma (North Pilbara and Mosquito Creek Orogenies) produced some of the largest gold deposits in the east Pilbara Craton (Golden Eagle, Blue Spec, and other deposits in the Mosquito Creek Basin). Post-tectonic granites and associated pegmatites containing Sn–Ta (Moolyella, Cooglegong, Wodgina, Pilgangoora), Li (Pilgangoora), and W (Big Hill at Cookes Creek) mineralization were intruded from c. 2895 to 2830 Ma.

General reviews of mineralization in the east Pilbara Craton (Witt et al., 1998; Ferguson and Ruddock, 2001; Huston et al., 2001a,c, 2002, 2007) have summarized the styles and ages of mineralization, and provided references to investigations that were focused on particular mineral commodities. In the following, important mineralization events are summarized with reference to tectonic units, suites, supersuites and deformation events.

Mineralization in the East Pilbara Terrane (3530–3223 Ma)

Rocks of the EPT host a variety of mineralization styles related to volcanic activity and magmatic intrusion (Fig. 47), including:

- sediment-hosted, hydrothermal massive sulfates, Dresser Formation
- volcanogenic massive sulfides (VMS), Duffer Formation
- black shale-hosted Cu–Zn, Apex Basalt
- vein and hydrothermal base metals, Panorama Formation
- base and speciality metal mineralization at c. 3315 Ma
- precious metals, mainly c. 3315 Ma.

Sediment-hosted, hydrothermal massive sulfates, Dresser Formation

The oldest known economic mineralization of the EPT is hydrothermal barite in the c. 3481 Ma Dresser Formation of the North Pole Dome (Hickman, 1973, 1983). Minor amounts of sphalerite and galena are included in the deposits. Between 1970 and 1990, 129 505 t of barite were mined at the Dresser mining area (Plate 1A), which still contains substantial mineralization. A review of the North Pole deposits and their origin was presented by Abeysinghe and Fetherston (1997). The main barite deposits outcrop in an 8 km-long zone within and immediately underlying the Dresser Formation. Mineralization takes the form of either stratabound layers and mounds, or veins of coarsely crystalline barite within hydrothermal chert–barite veins. The veins intrude extremely altered metabasalt immediately underlying chert of the Dresser Formation. Barite is also present as pebbles in basal diamictite layers, as finely laminated rock containing stromatoloid laminae (Buick et al., 1981), and as coarsely crystalline mounds adjacent to synsedimentary growth faults (Nijman et al., 1998a).

The main deposits are located where the Dresser Formation is thickest and consists of three stratigraphic horizons of chert–barite interlayered with metabasalt. The three mineralized beds are bound by an array of extensional normal growth faults, the main set of which passes just south of and through the Dresser mining centre. The geometry of the faults and their close relation to barite mineralization (Nijman et al., 1998a) indicates that the barite was deposited during extensional faulting. Newmont Pty Limited (1979) inferred that the deposits formed by exhalative chemical precipitation. In this model, the chert–barite veins were interpreted to represent the footwall vein-stockwork system of bedded chert–barite rocks of the Dresser Formation, a conclusion supported by subsequent studies (Nijman et al., 1998a; Van Kranendonk, 2006) that documented variations in both lithofacies type and thicknesses of barite and chert adjacent to growth faults, and showed contemporaneous development. The interpreted environment of deposition was a shallow-marine setting, with precipitation of barite, and diagenetic replacement of carbonate rocks by barite, during low-temperature hydrothermal volcanic emissions (Van Kranendonk, 2006).

Volcanogenic massive sulfides, Duffer Formation

Volcanogenic massive sulfide (VMS) Zn–Pb mineralization is present in 3474–3459 Ma felsic volcanic rocks of the Duffer Formation on the southwest and southeast sides of the Mount Edgar Dome. The best documented deposits are at the Big Stubby prospect (Plate 1A), 6 km south of Marble Bar, and at Lennons Find (Plate 1A), 50 km southeast of Marble Bar. South of Marble Bar, Reynolds et al. (1975) interpreted the VMS mineralization to be associated with seven rhyolite domes, although Barley (1992) interpreted most of the ‘rhyolite’ to be pyroclastic or volcanoclastic sedimentary material. In the interpretation of Reynolds et al. (1975), the rhyolite domes occupy a zone of statabound mineralization 1 km long and several hundred metres thick in the upper Duffer Formation. Rhyolite within the domes is likely to have been directly derived from a large underlying magma chamber that is now preserved as the c. 3466 Ma Homeward Bound Granite (Hickman and Van Kranendonk, 2008). This alkali granite, very atypical of the Callina Supersuite which is mainly composed of TTG, is a large laccolith-like intrusion included in ‘Granite intrusions (3466–3310 Ma)’ (Fig. 30) on the western side of the Mount Edgar Dome (Plate 1A). The small rhyolite domes within the upper Duffer Formation are capped by red, black and white banded chert and lenses of massive pyrite.

The flanks of the domes contain zinc, lead, silver and barite mineralization. The Zn–Pb mineralization, which includes barite, stratigraphically overlies a copper-rich zone. Barite and gypsum are also located in the lateral extensions of the lenses. Sphalerite, galena, pyrite and barite are the principal ore minerals. Silver occurs as acanthite. The mineralized zones are thin and discontinuous, with chlorite and carbonate alteration. Drilling intersections reported by Reynolds et al. (1975) included 4.7 m at 14.7% Zn, 3.2% Pb, 0.3% Cu and 840 g/t Ag (DDH 21B), and 2.52 m at 21.0% Zn, 5.7% Pb, 0.1% Cu, 28 g/t Ag and 10% Ba (DDH 16). Total resources (non-JORC*) at Big Stubby have been estimated as

0.1 to 0.2 Mt at 13.8% Zn, 4.5% Pb, 0.2% Cu and 305 g/t Ag (Reynolds et al., 1975; Davies and Blockley, 1990; Barley, 1992). Barley et al. (1998) interpreted the mineralization to be similar to that of the Miocene Kuroko deposits of Japan. Kuroko-style VMS mineralization is most commonly associated with felsic submarine volcanism in back-arc rift settings, although intracontinental extensional environments are also known (Pirajno, 2009). Reviews of the mineralization are provided by Van Kranendonk (2006), Huston et al. (2007) and Pirajno (2009).

The Lennons Find VMS mineralization is more deformed and metamorphosed than the mineralization at Big Stubby. Lenses of Zn–Pb–Cu mineralization are located in five mineralized zones over a strike length of 4.3 km. The Duffer Formation is locally represented by quartzofeldspathic schist overlain by clastic sedimentary rocks, which are in turn overlain by quartz–muscovite schist. Sulfide minerals are mainly sphalerite, chalcopyrite, galena and pyrite. Associated minerals are barite, chlorite, carbonate, tourmaline, muscovite and biotite. The mineralization is zoned, with a zinc-, lead- and barium-rich zone at the top, and a copper-rich zone at the base. The largest sulfidic zone (Hammerhead deposit) is 400 m long, 300 m wide and 2 m thick, and massive barite occupies the contact with the overlying Apex Basalt.

Pb–Pb dating of galena in the mineralization has given ages of c. 3469 Ma at Big Stubby (Thorpe et al., 1992b) and c. 3472 Ma at Lennons Find (isotope data from Richards et al. [1981]; recalculated by Thorpe et al. [1992b]). Several U–Pb zircon dates on the Duffer Formation and Homeward Bound Granite in the Marble Bar area indicate an age for the host rocks at Big Stubby of c. 3464 Ma, consistent with a U–Pb zircon date of c. 3465 Ma (Thorpe et al., 1992a) for felsic schist at Yandicoogina on strike with the stratigraphy at Lennons Find (Plate 1A). The close agreement between Pb-isotope ages and igneous crystallization ages suggests little contribution of Pb from older crustal material. Whole-rock Nd model ages from the Duffer Formation elsewhere in the Marble Bar greenstone belt are 3620–3520 Ma and ϵ_{Nd} values are slightly positive (Table 4), suggesting inclusion of juvenile sources.

Black shale-hosted Cu–Zn, Apex Basalt

Metamorphosed black shale in the lower Apex Basalt contains minor stratabound Cu–Zn mineralization at Salgash (Plate 1A), 15 km south of Marble Bar. The shale is part of a sedimentary unit that outcrops intermittently over a strike length of 80 km on the western side of the Mount Edgar Dome, from Doolena Gap in the north, through the Marble Bar greenstone belt west of Marble Bar, southwards to Salgash, Warrawoona and Yandicoogina. Mid-way along this strike length, the unit is exposed as the ‘Apex chert’ (informal name, Schopf, 1993) west of Marble Bar Pool. At Salgash it comprises metamorphosed carbonaceous shale and sandstone, mafic and ultramafic breccia, and ultramafic sills. The copper content of the shale is locally sufficiently high at Salgash to have supported small-scale mining. Drilling beneath old copper workings, referred to as the ‘Salgash Copper Prospect’ by Marston (1979), intersected wide zones with anomalous Cu values. Gossanous material on spoil tips includes malachite, chalcocite, chalcopyrite, and bornite (Marston, 1979).

* The Joint Ore Reserves Committee (JORC) sets out minimum standards, recommendations, and guidelines for public reporting of Exploration Results, Mineral Resources, and Ore Reserves. The JORC code is updated periodically.

In 2003, the Salgash shale–sandstone unit was drilled during the Archean Biosphere Drilling Project (ABDP) to obtain samples of c. 3450 Ma carbonaceous black shale. ABDP 2, about 3 km southeast of Salgash Copper Prospect, intersected a thick succession of metamorphosed and sheared sulfidic black shale and sandstone. Five samples of black shale from ABDP 2 contained up to 13.4 wt% organic carbon (average 5.45 wt%) up to 6770 ppm Zn (average 2804 ppm), up to 1088 ppm Cu (average 562 ppm), and up to 421 ppm Ni (average 296 ppm) (Wille et al., 2013). Irregular layers of sulfide minerals in the core were not analysed but the background levels in the shale suggest the presence of chalcopyrite and sphalerite. The Salgash mineralization is distinctly different from VMS mineralization in the underlying Duffer Formation (Cu–Zn in black shale as opposed to Zn–Pb in felsic volcanic rocks), and is similar to Besshi-type mineralization, as described by Pirajno (2009). Where fully developed, the deposits are conformable, stratiform, blanket-like sheets of massive pyrrhotite or pyrite, or both, with variable contents of chalcopyrite, minor sphalerite and rare galena. Host rocks are typically mafic volcanic rocks and associated marine sedimentary rocks including wacke, sandstone and shale. Copper is the principal economic metal, and there is subordinate zinc, cobalt, silver or gold (Peter and Scott, 1997). Besshi-type deposits are known from a range of tectonic settings with crustal extension in common.

The black shale in ABDP 2 has extremely high Na₂O contents (up to 9.03 wt%, averaging 6.08 wt% Na₂O). Analyses of 10 additional samples of the ABDP 2 black shale (H Ohmoto, 2014, written comm.) confirmed abnormally high Na₂O levels (average 4.17 wt% Na₂O). Such high Na₂O contents suggest hydrothermal alteration, most likely leading to introduction of albite in the shale. Van Kranendonk and Pirajno (2004) recorded hydrothermal propylitic alteration beneath the bedded ‘Apex chert’ (silicified black shale), which stripped alkalis from the underlying Apex Basalt. At Salgash, the lower Apex Basalt beneath the shale–sandstone unit was tectonically removed by major c. 3315 Ma shearing on the northern limb of the Warrawoona Syncline.

Vein and hydrothermal base metals, Panorama Formation

Pb–Zn mineralization at Quartz Circle (Plate 1B) in the McPhee Dome, and at Breens Copper and Miralga Creek (Plate 1A) in the North Pole Dome, is associated with felsic volcanic rocks and related porphyritic granodiorite and monzogranite intrusions of the Panorama Formation. At Quartz Circle, both massive and vein-type base metal mineralization are present, possibly with epithermal affiliations (Ferguson and Ruddock, 2001). At Miralga Creek, gold, zinc, lead and copper mineralization (Goellnicht et al., 1988) is associated with a felsic porphyry stock intruded into the Mount Ada Basalt on the southeast side of the North Pole Dome. Thorpe et al. (1992a) reported a U–Pb zircon crystallization age for this intrusion of 3449 ± 2 Ma. Galena in the Miralga Creek mineralization gave a range of Pb isotope model ages between c. 3447 and 3451 Ma (Groves, 1987). The stock includes an outer zone of marginal intrusive breccia with disseminated, stringer, vein and hydrothermal mineralization in association with porphyritic felsic dykes. Van Kranendonk (1999, 2000) related the mineralization to emplacement of the c. 3446 Ma North Pole Monzogranite

in the core of the North Pole Dome. Elsewhere in the dome, the porphyritic felsic dykes radiate from the North Pole Monzogranite to feed into the Panorama Formation (Brown et al., 2006).

The Breens Copper deposit in the west-central part of the North Pole Dome is a complex, northeasterly striking belt of stratabound massive sulfide mineralization (pyrite, chalcopyrite, chalcocite, covellite, and neodiginite) and native copper, 500 m wide, consisting of stockworks and silicified breccia zones (Ferguson and Ruddock, 2001). Mineralization is associated with a small dyke of porphyritic felsic rock related to the North Pole Monzogranite (Van Kranendonk, 1999). Gold mineralization is locally associated with the hydrothermal copper mineralization (Finucane, 1936).

Copper and molybdenum mineralization at c. 3315 Ma

A porphyry copper–molybdenum system is developed at Spinifex Ridge (Plate 1A) where the northern tip of the Coppin Gap Granodiorite intrudes the Marble Bar greenstone belt. Similar deposits are located at Gobbos, Lightning Ridge and Reedies (Plate 1B) where stocks of the Gobbos Granodiorite intrude the McPhee greenstone belt. Copper mineralization (without Mo) is associated with the c. 3315 Ma Boobina Porphyry at the Copper Hills and Kelly mining areas (Plate 1B) on the eastern margin of the Corunna Downs Dome (Barley and Pickard, 1999).

The Spinifex Ridge Cu–Mo deposit has been the subject of several investigations (Marston, 1979; Barley, 1982; Hickman, 1983; De Laeter and Martyn, 1986; Jones, 1990; Van Kranendonk et al., 2006b; Huston et al., 2007, 2017; Stein et al., 2007; Cummins and Cairns, 2017) but no mining has yet occurred. Combined measured and indicated resources are 652.3 Mt at 0.05% Mo and 0.08% Cu (JORC 2004) reported by Moly Mines Ltd. (2012). Cummins and Cairns (2017) reported that the deposit also contains 40 Moz Ag. The higher grade mineralization (up to 0.18% Mo and 0.30% Cu) is located at the top of a long, narrow stock of porphyritic dacite and microgranodiorite that intruded the Apex Basalt, Panorama Formation and Euro Basalt from the underlying Coppin Gap Granodiorite. The narrow stock is 1000 m long, and in the main mineralized zone is 200 m thick and 50–80 m wide (Cummins and Cairns, 2017). Drilling by Australian Anglo American Limited from 1970 to 1973 intersected a grade of 0.13% Mo and 0.23% Cu over 75.6 m (Marston, 1979).

The c. 3314 Ma Coppin Gap Granodiorite represents one of several subvolcanic magma chambers contemporaneous with eruption of the 3325–3315 Ma Wyman Formation of the Kelly Group, and it is likely that the porphyritic microgranodiorite stock was emplaced as a late-stage vent structure. Prior to steep tilting of the greenstone succession on the northern side of the Mount Edgar Dome, the stock was approximately vertical. Mineralization within and around the porphyritic microgranodiorite is in the form of a stockwork of quartz and quartz–carbonate veins containing sulfide minerals, particularly molybdenite, chalcopyrite, pyrrhotite, pyrite and scheelite. Scheelite is concentrated in a zone on the northeast side of the Cu–Mo mineralization (Cummins and Cairns, 2017). Historic mining of tungsten is recorded from ‘Talga Talga’, which was the station property that included the area containing the Spinifex

Ridge mineralization. Production of 162 kg of wolframite concentrate containing 95.2 kg WO_3 was attributed to 'Talga Talga' prior to 1977 (Hickman, 1983). Potassic alteration introduced potassium feldspar into veins containing Mo and Cu, and within the dacite has altered oligoclase to potassium feldspar (Huston et al., 2007). Biotite alteration is present in the porphyritic dacite and intense sericite alteration surrounds and overprints the potassic alteration throughout the deposit.

Other subvolcanic granitic intrusions of the Emu Pool Supersuite also contain either Cu–Mo mineralization or Cu mineralization lacking Mo. Examples of Cu–Mo mineralization are located within and adjacent to several c. 3313 Ma granodiorite stocks in the McPhee Dome (Gobbos, Lightning Ridge and Reedies prospects; Marston, 1979; Barley, 1982; Barley and Pickard, 1998; Bagas 2005; Huston et al., 2007; Williams and Bagas, 2007a). A similar relationship between the Emu Pool Supersuite and Cu–Mo mineralization is present in the Warrawagine Dome where Williams (2000) identified disseminated molybdenite grains and weak Cu mineralization in leucocratic, muscovite-bearing monzogranite 2 km east of 17 Mile Well. No further investigation is recorded.

Copper mineralization in the Copper Hills and Kelly mining areas on the east side of the Corunna Downs Dome is directly associated with the subvolcanic 3324–3307 Ma Boobina Porphyry. This intrusion, which outcrops over an area of 100 km², is essentially a laccolith that in its central outcrop, between the Copper Hills and Kelly mines, is 2000 m thick and was emplaced along the stratigraphic contact between the Euro Basalt and the Wyman Formation. North of Copper Hills, and in the southern area between Kelly and Ryans mines, the laccolith was intruded at lower stratigraphic levels. The northern area is almost devoid of mineralization, whereas close to the upper limit of its intrusion level, between Copper Hills and Kelly, there are numerous copper deposits. This central area of the intrusion includes by far the largest copper mine, Copper Hills; between discovery of the deposit in 1952 and mine closure in 1963, this produced 49.2 t of copper ore and concentrates averaging 35.08% Cu, and 15 455.67 t cupreous ore and concentrates averaging 12.68% Cu (Marston, 1979). Most of the ore consisted of supergene malachite, azurite, chalcocite and bornite. Features of the Cu mineralization at Copper Hills, including sericitization of feldspar, alteration of rare biotite phenocrysts to chlorite and sericite, and groundmass recrystallization to very fine-grained quartz, sericite, carbonate, chlorite and rutile (Bagas et al., 2004c), indicate a low-temperature, epithermal mineralization system.

At the southern end of its intrusion, the c. 3315 Ma Boobina Porphyry splits into several thin transgressive sills within the Euro Basalt. These southern sills are associated with relatively minor copper mineralization along faults. Minerals mined at Kelly included malachite, chrysocolla, azurite, bornite, cuprite and chalcocite. In contrast to the Cu–Mo mineralization at Spinifex Ridge and Gobbos, quartz stockworks are absent at both Copper Hills and the Kelly mining area.

The stratigraphy and structure of the Corunna Downs Dome suggest that it was mainly formed at c. 3315 Ma. In this interpretation, the Euro Basalt would have been relatively flat-lying when the Boobina Porphyry was intruded, although

south of Copper Hills there is a low-angle unconformity between the Euro Basalt and the Wyman Formation. The Boobina Porphyry, which intrudes volcanic rocks of the Wyman Formation between Copper Hills and Kelly, was therefore intruded very close to the c. 3315 Ma land surface, consistent with epithermal mineralization.

Precious metals, mainly c. 3315 Ma

A minority of gold and silver deposits in the EPT include minor galena that has been dated by the Pb–Pb method to indicate ages between c. 3430 and c. 3400 Ma (Thorpe et al., 1992b; Huston et al., 2001a, 2002; Zegers et al., 2002). However, very little EPT gold mineralization is now interpreted to be this old. For example, several >3400 Ma Pb isotope ages were obtained from the Bamboo Creek mining area on the northeast side of the Mount Edgar Dome (Fig. 30). Because the gold mineralization at this mining centre is hosted by a shear zone that cuts the 3350–3335 Ma Euro Basalt, the Pb isotope ages indicate derivation of Pb from older crust. This interpretation is consistent with Sm–Nd and Lu–Hf isotope evidence that most Paleoarchean Pilbara rocks were derived from evolved crustal sources (Champion and Smithies, 2007; Champion, 2013; Champion and Huston, 2016; Gardiner et al., 2017, 2018). The true age of the Bamboo Creek gold mineralization is here interpreted to be c. 3315 Ma, when gold-bearing hydrothermal fluids were introduced during major diapiric uplift of the Mount Edgar Dome.

Hydrothermal fluids were most likely derived by metamorphic devolatilization of greenstones (Phillips and Powell, 2010) sagducted vertically during the c. 3315 Ma event. If so, this explains the relatively small size of the EPT gold deposits because limited volumes of source material would have been available compared to source-rock volumes possible during horizontal tectonic processes such as subduction. Precipitation of gold from silica-rich hydrothermal fluids was influenced by wallrock compositions, with ultramafic rocks and carbonaceous shale and chert being particularly favourable. In the Warrawoona Syncline, about 20 km southeast from Marble Bar, the Warrawoona Group is exceptionally attenuated and sheared between the Mount Edgar and Corunna Downs Domes. Historically, gold mining at Warrawoona (Fig. 30) was concentrated along a few narrow shear zones, in particular the Klondyke and Copenhagen Shear Zones (Jones, 1938; Hickman, 1983; Huston et al., 2001a, 2002; Kloppenburg, 2003).

Gold mineralization during doming

Gold mineralization in the EPT is mostly contained in hydrothermal quartz veins hosted by faults and shear zones. Since evolution of the EPT was dominated by doming and sagduction, gold mineralization coincided with doming events and was focused along dome-boundary faults or ring faults. For example, the mineralized Bamboo Creek Shear Zone (BCSZ) on the northeast side of the Mount Edgar Dome (Fig. 30) developed on a major ring fault during D_6 at c. 3315 Ma. The hydrothermal fluids responsible for the gold mineralization along the BCSZ were most likely derived during the event that introduced felsic magma of the Emu Pool Supersuite through metamorphism of older crust.



Figure 47. Mineralization in the east Pilbara in relation to stratigraphy and tectonic events

The main mineralized structure at Warrawoona is the Klondyke Shear Zone (KLSZ, Fig. 30) that includes historically important mines such as Klondyke Boulder, Klondyke Queen, and Comet (Plate 1A). Galena samples from the Klondyke group of workings yielded Pb isotope model ages of c. 3385, 3374, and 3050 Ma (Huston et al., 2001a, 2002). The c. 3385 and 3374 Ma model ages are unlikely to indicate the age of the mineralization because these ages fall within the c. 75 Ma year period of crustal stability during deposition of the Strelley Pool Formation. The present interpretation is that these ages are too old due to inclusion of Pb from recycling of older crust, and that the true age of the KLSZ mineralization is c. 3315 Ma. The c. 3050 Ma Pb model age might be due to renewed hydrothermal activity on the KLSZ during the Prinsep Orogeny, or reactivation of the shear zone during the c. 2950 Ma North Pilbara Orogeny, again with introduction of older crustal Pb.

Mineralization during EPTRE rifting (3280–3165 Ma)

The East Pilbara Terrane Rifting Event (EPTRE) commenced during deposition of the Sulphur Springs Group and resulted in several different types of mineralization. For example, extensional faulting influenced syngenetic VMS Cu-Zn mineralization at Sulphur Springs and Kangaroo Caves (Plate 1A; Vearncombe et al., 1995, 1998; Brauhart et al., 1998; Brauhart, 1999; Van Kranendonk, 2000a, 2006; Huston et al., 2019; Pirajno and Huston, 2019). As the continental rifting evolved into breakup of the EPT, mineralization styles changed to those associated with mafic volcanism and intrusion, and passive-margin deposition of the Soanesville Group.

Sulphur Springs Group

VMS Cu–Zn mineralization, Sulphur Springs

VMS Cu–Zn mineralization at the top of the Sulphur Springs Group is attributed to hydrothermal circulation through extensional faults above intrusions of the c. 3239 Ma Strelley Monzogranite (Brauhart et al., 1998; Van Kranendonk, 2000a, 2006; Huston et al., 2001d, 2007, 2019). Regional crustal extension across the EPT commenced at c. 3280 Ma and intrusion of the laccolith occurred within that tectonic environment. Sulfide mineralization is vertically zoned, from Cu rich at the base to Zn (\pm Pb) and barite at the top. Most of the mineralization is either immediately beneath or within the formerly named 'Marker chert' at the top of the Kangaroo Caves Formation. Chlorite alteration of the Sulphur Springs Group 1000–2000 m beneath the VMS mineralization caused about 80% loss of ore-related metals, in particular Zn, Pb, Cu and Mo, from which it is inferred that this chloritized zone was the source of the metal in the overlying mineralization (Huston et al., 2001d, 2007, 2019). The last reported JORC 2012 mineral resource estimate at Sulphur Springs was 13.8 Mt at 3.8% Zn, 1.5% Cu and 18.0 g/t Ag, and at Kangaroo Caves 3.6 Mt at 6.0% Zn, 0.8% Cu, 0.32% Pb and 15.2 g/t Ag (Venturex Resources, 2020). Sulfide minerals include pyrite, chalcopyrite, sphalerite and galena. Abundant barite is present at the top of several of the deposits (Vearncombe et al., 1995). Minor molybdenum, tin and gold mineralization was also associated with emplacement of the intrusion.

Hydrothermal barite mineralization at c. 3240 Ma

In the western Warralong greenstone belt, the Sulphur Springs Group contains large hydrothermal veins of barite discovered during GSWA mapping of the Port Hedland 1:250 000 map sheet (Hickman, 1977b). Based on surface exposures north of Cooke Bluff Hill (Plate 1A), Hickman (1977b) estimated that the larger veins contain about 10 400 t of massive barite to a depth of only 10 m. The mineralization is adjacent to the faulted northwest margin of the LWSC which originated during extension and rifting of the East Pilbara Terrane from c. 3280 Ma onwards. Hydrothermal veins of barite also intrude the western margin of the Warralong greenstone belt 20 km northeast of the Cooke Bluff Hill deposits (Van Kranendonk, 2010c), suggesting a zone of hydrothermal activity during early rifting. Abundant hydrothermal barite of the same age is also present in the rifting-related VMS deposits of the c. 3240 Ma Kangaroo Caves Formation in the Soanesville greenstone belt (Vearncombe et al., 1995). Analysis of the barite and gossans at Cooke Bluff Hill did not reveal any significant base metal or gold anomalies, and a possible explanation is that the mineralization was distal to sulfide-bearing hydrothermal sources.

In the context of the correlation between the Sulphur Springs Group and the Fig Tree Group of South Africa, suggested earlier in this Report, it is notable that there are large sediment-hosted barite deposits in the 3260–3230 Ma Mapepe Formation in the Barberton Greenstone Belt (BGB). Descriptions of these deposits by Gutzmer et al. (2006), indicate that the BGB barite mineralization is similar to that in the sedimentary succession in the Warralong greenstone belt (Van Kranendonk, 2004b).

Chert–barite veins and sills at the top of the Kelly Group in the northern McPhee greenstone belt (Williams and Bagas, 2007a) might have been introduced at c. 3240 Ma rather than during the final stages of Wyman Formation volcanism at c. 3315 Ma. Approximately the same stratigraphic level is intruded by barite veins at Lionel North (Plate 1B) between the McPhee and Corunna Downs Domes (Thorn et al., 1978; Bagas, 2005). The host rocks (chert and sandstone) are undated but stratigraphically overlie the Wyman Formation.

VMS Cu–Zn mineralization, Tabba Tabba Shear Zone

The TTSZ contains two deposits of c. 3250 Ma VMS Zn–Pb mineralization within the Orchard Well project (De Grey Mining Ltd., 2020): Orchard Tank and Discovery (Plate 1A). Mineralization is associated with felsic volcanic and granitic rocks dated at c. 3250 Ma (Beintema, 2003; GSWA 160258, Wingate et al., 2010), although primary relationships have been destroyed by strong deformation. The Orchard Well project (also known as Turner River VMS) has a reported total mineral resource (JORC 2012) of 3.5 Mt at 3.2% Zn, 1.3% Pb, 0.8 g/t Au and 110 g/t Ag (De Grey Mining Ltd., 2020). Local drilling intersections at both deposits suggest the presence of higher grade zones: at Orchard Tank, 5.4 m at 11.59% Zn, 6.63% Pb, 300.55 g/t Ag and 2.3 g/t Au; and at Discovery, 10 m at 6.27% Zn, 2.31% Pb, 154.6 g/t Ag and 0.99 g/t Au (De Grey Mining Ltd., 2014). Drilling has indicated that the Orchard Tank lenses are stacked (De Grey Mining Ltd, 2014), suggesting tectonic duplication.

Soanesville Group

Iron ore, supergene enrichment of banded iron-formation

The passive-margin setting of the lower Soanesville Group after breakup of the EPT included deposition of banded iron-formation (BIF) protoliths, in particular within the succession that became the c. 800 m-thick Pincunah Banded-Iron Member (PBIM) of the Cardinal Formation. Other clastic sedimentary formations of the Soanesville Group (Corboy, Paddy Market and Pyramid Hill Formations) also contain BIF, although these are either much thinner than the PBIM or have not been sufficiently enriched to warrant mining. The depositional setting of the PBIM is interpreted to have been similar to that of Neoproterozoic–Paleoproterozoic BIF units of the Hamersley Group (Marra Mamba Iron Formation and Brockman Iron Formation; see **Stratigraphic status of the PBIM**). It is generally agreed the Hamersley Group was deposited on a continental margin platform during breakup of the Pilbara Craton (Morris and Horwitz, 1983; Tyler and Thorne, 1990; Blake and Barley, 1992; Blake, 1993; Martin et al., 1998a; Zegers et al., 1998b; Thorne and Trendall, 2001; Krapež et al., 2003; Bekker et al., 2010, 2014). Current iron ore mining of Soanesville Group BIF is restricted to the Mt Webber deposits (Plate 1B) in the Emerald Mine greenstone belt (Fig. 8). Published measured iron ore resources at Mt Webber (JORC 2012, Atlas Iron Limited, 2018), are 37.5 Mt at 57.7% Fe. Duuring et al. (2017) reported that the Mt Webber deposits were developed by supergene enrichment of quartz–magnetite BIF units where these are thickened in the hinge areas of tight synclines. In contrast to the steeply inclined BIFs, the supergene goethite \pm martite ores are flat-lying, extend to depths of about 80 m, and are locally capped by nodular laterite.

Other potentially mineable iron ore deposits hosted by the PBIM are present in the Pincunah greenstone belt, and are mainly unenriched BIF at the North Star, Eastern Limb, Glacier Valley and West Star deposits (Plate 1A), collectively referred to as the Iron Bridge Magnetite Project. Reported total resources of these deposits (JORC 2012, Fortescue Metals Group Limited, 2020) were 5448 Mt at about 30.4% Fe. The mineralization extends along a strike length of >10 km on the eastern limb of the major syncline that forms the Pincunah greenstone belt. Drilling has confirmed that the mineralization extends to a depth of >600 m.

Ni–Cu and PGE mineralization, Dalton Suite

Ultramafic–mafic intrusions of the c. 3185 Ma Dalton Suite (Van Kranendonk et al., 2006a) were intruded during the 3280–3165 Ma EPTRE (Hickman, 2012). The intrusions include layered sills in the Soanesville greenstone belt, vertical intrusions along some EPT boundaries, and sills between the Mosquito Creek Basin and the EPT and KUT. In the northwest Pilbara Craton, c. 2930 Ma ultramafic–mafic intrusions contain Ni–Cu and PGE mineralization: Radio Hill (mined for Ni, Cu and Co); Munni Munni (large PGE resources); and Mount Sholl (Ni–Cu resources) (Hickman, 2016). No Ni–Cu or PGE deposits sufficiently large for mining have been identified in the east Pilbara Craton, but the large number of <3200 Ma intrusions suggests the possibility of economic mineralization.

Drilling of differentiated sills and layered intrusions at Soanesville (Plate 1B) intersected nickel sulfides in serpentinized peridotite. Marston (1979) reported that 11 diamond drillholes intersected low-grade disseminated sulfides and two adjacent drillholes intersected narrow widths (0.4 m) of high-tenor massive sulfides (20–26% nickel). Average intersections for two drillholes were 3.50 m at 2.55 wt% Ni and 1.16 wt% Cu, and 3.66 m at 2.41 wt% Ni and 0.61 wt% Cu. Up to 0.55% Co was reported in these intersections (Ferguson and Ruddock, 2001).

Convergence-related mineralization (3160–3070 Ma)

Between c. 3160 and 3070 Ma, plate separation following breakup of the EPT was replaced by convergence. In the northwest Pilbara Craton, this was marked by a metamorphic event at 3160–3140 Ma (Karratha Event, Hickman, 2016), subduction forming the Sholl Terrane, and obduction of part of the Regal Formation (c. 3200 Ma juvenile basaltic crust) onto the Paleoproterozoic Karratha Terrane. Although the main part of the EPT was unaffected by the convergence until closure of the Regal Basin at c. 3070 Ma, the northwestern margin of the EPT, and the relatively thin EPT crust as far east as the Lalla Rookh – Western Shaw Structural Corridor (LWSC), was impacted by 3160–3070 Ma events within the Central Pilbara Tectonic Zone (CPTZ). Early effects of the convergence included intrusion of the Flat Rocks Tonalite near the northwestern margin of the EPT. The TTG composition of this intrusion, in combination with Nd isotope data (this Report), suggests that it was partly derived by partial melting of subducted juvenile basaltic crust. It is significant that the structural geology of the EPT close to its northwestern margin is far more complex than farther east. Blewett (2002) recognized nine deformation events within 50 km of the northwest

margin of the EPT: all nine events, D₁ to D₉, in the Pilgangoora area of the East Strelley and Pincunah greenstone belts; six events, D₂ to D₇, in the Abydos greenstone belt; and six events, D₃ to D₈, in the Wodgina greenstone belt. Beintema (2003) obtained evidence of a 3160–3090 Ma event in the TTSZ based on ages of xenocrystic zircon in 2950–2930 Ma granitic rocks (KB 746, KB 770, Beintema, 2003).

Gold mineralization

Formation of the structures described by Blewett (2002) are likely to have been associated with gold mineralization of the type developed during orogenic events.

Gold mineralization in the area where the TTSZ is crossed by the Turner River (Plate 1A) has not been dated but, based on the interpreted 3160–3070 Ma event in the TTSZ, might include mineralization related to convergence at this time. A 3069 ± 41 Ma event in the shear zone is indicated by U–Pb zircon dating of Mesoarchean granitic rocks, and xenocrystic zircons in granitic rocks of the Sisters Supersuite were dated at 3123–3108 Ma (Beintema, 2003; Beintema et al., 2003).

Based on a c. 3142 Ma Pb isotope model age (Huston et al., 2001a), gold mineralization at Pilgangoora (Plate 1A) in the East Strelley greenstone belt (Fig. 8) might include 3160–3070 Ma deposits, although previous interpretations in this area have recognized only c. 2890 Ma mineralization (Neumayr et al., 1998; Huston et al., 2001c; Baker et al., 2002). In the Pilbara Well greenstone belt (Fig. 8), gold mineralization in the Hong Kong mining area (Sullivan, 1939) is hosted by thin quartz veins in 3176–3165 Ma juvenile basaltic crust of the Empress Formation. The Empress Formation is likely to have been obducted from the Regal Basin between c. 3160 and 3070 Ma (see **Soanesville Group, Empress Formation**), a process that included thrusting and isoclinal folding. Alternatively, the deformation and gold mineralization might have occurred during the 2955–2919 Ma North Pilbara Orogeny.

Galena from the Lalla Rookh gold mine in the East Strelley greenstone belt gave a Pb isotope model age of c. 3188 Ma (data from Richards et al. [1981], recalculated by Huston et al. [2001a]). The mine is close to the Lalla Rookh – Western Shaw Fault, which is interpreted to have originated during the 3280–3165 Ma EPTRE and was reactivated during subsequent deformation events. Since the host rocks at Lalla Rookh mineralization are Paleoproterozoic, it is likely that the Pb isotope model age is somewhat older than the true age of the mineralization due to inclusion of old crustal Pb in the hydrothermal fluids.

Mineralization in the De Grey Superbasin (3166–2930 Ma)

In the central and western parts of east Pilbara Craton, the De Grey Superbasin is represented by the Gorge Creek and Croydon Groups, whereas in the southeast it is represented by the Mosquito Creek Formation. The Gorge Creek and Croydon Groups were deformed by the North Pilbara Orogeny whereas the Mosquito Creek Formation was deformed and metamorphosed by the Mosquito Creek Orogeny. Intrusion of the Sisters Supersuite accompanied the North Pilbara Orogeny but no Mesoarchean igneous activity was associated with the Mosquito Creek Orogeny.

Gorge Creek Basin

Iron ore, supergene enrichment of banded iron-formation

In terms of past and current production, and demonstrated resources, iron ore is by far the most important mineral commodity in the northern Pilbara Craton. Mining of 60 wt% Fe hematite–goethite iron ore from deposits within the Cleaverville Formation commenced in the east Pilbara Craton in the mid-1960s and continues to the present. Important mines have been located at Mount Goldsworthy, Nimingarra, Shay Gap – Sunrise Hill, Yarrie, and in the Wodgina and Pardoo project areas (Plate 1A). Deposits under development are located at McPhee Creek (Plate 1B) and Corunna Downs (Plate 1A) and in the Abydos project area (Plate 1A). The Pardoo iron project in the Ord Ranges (Plate 1A) includes several deposits (including Ridley, South Limb, Bobby and Emma) and is within an inlier of the Gorge Creek Group in the Mallina Basin, and was briefly described by Hickman (2016).

It is notable that almost all of the mined iron ore deposits in the northern Pilbara Craton are supergene enrichments of BIF immediately underlying a Mesozoic–Cenozoic peneplain named by Campana et al. (1964) as the ‘Hamersley Surface’. North of the Fortescue River, this old land surface is preserved as isolated flat-topped hills capped by ferricrete (Hickman, 1983, fig. 1). From the Neogene onwards, the surface was deeply dissected by northerly flowing river systems and is now best preserved above those lithologies most resistant to erosion, including chert, BIF and quartzite. Duuring et al. (2017) commented that all iron ore deposits of the northern Pilbara Craton display broad, near-surface, supergene goethite ± martite ores that constitute the bulk of the high-grade mineralization. In most deposits, the high-grade ores are limited to depths of between 50 and 200 m from the surface.

Conglomerate-hosted gold mineralization

In the Marble Bar greenstone belt, boulder conglomerate at the base of the Cundaline Formation east of Coppin Gap contains up to 0.158 g/t Au (Weir, 1989a). At Shay Gap, in the Shay Gap greenstone belt, analyses of conglomerate from the same stratigraphic level provided gold contents up to 0.05 g/t Au (Weir, 1989a). Since relatively few samples were analysed, these results suggest potential for further exploration for conglomerate-hosted gold in the Cundaline Formation, especially in the northeastern Marble Bar greenstone belt where Paleoproterozoic gold deposits along the Bamboo Creek Shear Zone might have contributed detritus to the Cundaline Formation.

Mallina Basin

Conglomerate-hosted gold mineralization

Although no potentially economic gold deposits have been identified in the Lalla Rookh Sandstone, the formation is known to contain minor conglomerate-hosted gold mineralization in the following areas: the Lalla Rookh – Western Shaw Structural Corridor (Carter, 1981; Krapež and Groves, 1984; Hickman and Harrison, 1986; Krapež and Furnell, 1987; Carter and Gee, 1988); the Goldsworthy

greenstone belt (Guj et al., 1983, 1984; Taylor, 1985); and in the Shay Gap greenstone belt (Weir, 1989b). The Lalla Rookh Sandstone has sedimentological features in common with auriferous conglomerate–sandstone sequences in the Witwatersrand Basin of South Africa. These include braided-stream deposits, stacked and telescoped sequences above low-angle intraformational unconformities, fining-upwards sequences, heavy-mineral concentrations, and sedimentary reworking (Krapež and Groves, 1984).

The Lalla Rookh Sandstone is likely to have been deposited across most of the preserved northern EPT, rather than having been restricted to small, intracratonic fault-bounded basins. For example, the restricted outcrop of the formation within the Lalla Rookh Syncline (Hickman and Lipple, 1975) is primarily structurally controlled between the Carlindi and North Pole Domes, and the present boundaries of the formation do not coincide with those of an intracratonic depositional basin. Although this was not the interpretation of Krapež (1984), his sedimentary facies and paleocurrent data are consistent with evolution of the basal stratigraphy of the formation between rising domes, with mainly axial southwest-to-northeast sediment transport. The uppermost stratigraphy of the Lalla Rookh Sandstone is not preserved in the Lalla Rookh area, but the formation also outcrops in other synclinal positions northwest of the Strelley Monzogranite, between the North Pole and Shaw Domes, north of Soanesville, and in the northern Coongan greenstone belt (Plate 1A). This distribution indicates that, due to erosion between c. 2940 and 2775 Ma, the Lalla Rookh Sandstone is preserved in the cores of synclines between the domes, and that it was far more extensive before D₁₅.

Evidence from the PCMP indicates that the Lalla Rookh Sandstone was deposited in shallow-water, fluvial to marine shelf settings marginal to the central deep-water trough of the Mallina Basin. This shelf had an area of at least 20 000 km², which is not greatly different from the 50 000 km² area of the Witwatersrand Basin, although the tectonic settings are interpreted to be different. Until the North Pilbara Orogeny at c. 2950 Ma, the shelf was relatively stable with moderate vertical movements producing local erosional unconformities. Banks (1981) identified five erosional unconformities within the 3000 m-thick Lalla Rookh Sandstone succession preserved in the Lalla Rookh Syncline between the Carlindi and North Pole Domes. Intraformational unconformities were also reported by Hickman (1983) and Van Kranendonk (2000a). These breaks in the succession provide evidence of a lengthy period of deposition interrupted by local uplift, erosion, and sedimentary reworking on the shelf.

Detrital zircon age spectra in sandstone of the Lalla Rookh area reveal that the dominant source of detritus was the EPT, and paleocurrent data from various localities indicate that the dominant direction of transport was from south to north or southwest to northeast (Hickman, 1983; Krapež, 1984; Van Kranendonk, 2000a). Dating of a sample from the Lalla Rookh Syncline indicates that most zircons in that area have ages between c. 3330 and 3290 Ma (GSWA 142951, Nelson, 2000h). This age range corresponds to an important period of epigenetic gold mineralization in the EPT. In the Goldsworthy greenstone belt, the available detrital zircon age data (GSWA 178019, Nelson, 2005d; GSWA 178020, Nelson, 2005e) indicate an older EPT provenance. In that area, visible detrital grains of gold in conglomerate, and small nuggets in

recent alluvial deposits derived from its erosion (Guj et al. 1983, 1984; Taylor, 1985), demonstrate the availability of gold sources during deposition. Nearby abandoned gold workings on auriferous quartz veins in the underlying Warrawoona Group (Smithies, 2004) suggest one local source.

Exploration of the Lalla Rookh Sandstone in the Lalla Rookh area of the LWSC revealed pyritic and auriferous conglomerate units in a 3000–5000 m-thick succession sedimentologically similar to units in the Witwatersrand Basin (Banks, 1981; Furnell, 1982). Banks (1981) recognized six vertically stacked conglomerate–sandstone sequences separated by five unconformities and disconformities, each of which is immediately overlain by a paleoplacer of oligomictic conglomerate. The majority of samples with anomalous gold contents assayed 0.05 – 0.5 g/t Au, with a maximum recorded value of 20 g/t Au (Banks, 1981). Of 472 surface rock samples analysed in that study, 2% contained more than 1 g/t Au, and 60% contained more than 0.01 g/t Au. Apart from gold and pyrite, heavy minerals include chromite, leucoxene, rutile, tourmaline, apatite, ilmenite and zircon. Follow-up diamond drilling detected less than 1 g/t Au in seven holes (Furnell, 1982).

The Lalla Rookh Sandstone of the Goldsworthy greenstone belt contains auriferous boulder- and pebble-conglomerate units at Amphitheatre (Plate 1A). The conglomerate overlies basal and intraformational erosional unconformities (Guj et al. 1983, 1984; Taylor, 1985). Guj et al. (1983) divided the formation into lower and upper associations, with the main auriferous conglomerate located at the base of the upper association, 300–500 m above the top of the underlying Cleaverville Formation. Most analyses of rock samples from this conglomerate unit contain approximately 0.1 g/t Au, although some intervals average more than 0.5 g/t Au. The maximum gold content reported by Guj et al. (1984) was 44.6 g/t Au. The conglomerate contains abundant detrital pyrite which locally forms up to 20% of the rock. Boulder conglomerate in the lower association was reported to contain up to 6.11 g/t Au, although contents were otherwise less than 0.5 g/t Au. Paleocurrent data from cross-bedded sandstone units indicate paleoslopes directed towards the east-northeast, which suggests higher potential for well-sorted mid-fan facies in that direction.

Based on limited exploration, auriferous pyritic conglomerate in the Lalla Rookh Sandstone of the Shay Gap greenstone belt is apparently concentrated in the central part of the formation. Analyses of surface samples from a synclinal structure 9.3 km northeast of Shay Gap revealed a weakly mineralized unit extending along a strike length of 1300 m. The most anomalous gold content reported was 0.2 g/t Au (Weir, 1989b), and subsequent drilling intersected no mineralization above 0.016 g/t Au.

Mosquito Creek Basin

Historical production from mines in the Mosquito Creek Basin (Fig. 8) has exceeded 12 t gold, with almost all of this production coming from mines along two parallel, east-trending shear zones: the Middle Creek Fault and Blue Spec Fault Zone (Fig. 39; Huston et al., 2001a; Blewett et al., 2002; Bagas et al., 2008; Huston et al., 2017). Mineralization is hosted by sections of the Mosquito Creek Formation that

contain unusually large amounts of carbonaceous pelitic schist (Hickman, 1983). A structural interpretation by Nijman et al. (2010) suggests that the schist is stratigraphically high in the formation, and might be a single stratigraphic unit duplicated by folding. Both shear zones are interpreted to have developed along major thrust structures formed during c. 2905 Ma convergence of the EPT and KUT (see **Mosquito Creek Orogeny, D₁₈ – D₂₂ at 2930–2900 Ma**). Gold was most likely derived from metamorphism of mafic rocks of the Coondamar Formation or from metamorphism of c. 3200 Ma oceanic-like mafic crust interpreted to underlie the Mosquito Creek Formation. The Middle Creek Shear Zone coincides with a linear magnetic anomaly that might be due to magnetite in psammitic units (Blewett et al., 2002).

The mine geology of the principal deposits on both shear zones was reviewed by Hickman (1983). Results of more recent exploration and mining have been described by Huston et al. (2001b), Blewett et al. (2002), and Bagas (2005).

Post-orogenic mineralization (2895–2830 Ma)

Mineralization in the Pilbara Craton following the Mosquito Creek Orogeny includes rare-metal pegmatite mineralization associated with post-orogenic granites of the Split Rock Supersuite. Mineral commodities include lithium, tin, tantalum, beryllium and tungsten, all of which have been mined. Additionally, geochronology suggests that gold mineralization in the Mount York area, south of Pilgangoora, was introduced after the Mosquito Creek and North Pilbara Orogenies.

Lithium-bearing pegmatites (c. 2880 Ma)

Spodumene is the principal lithium mineral in moderately dipping Sn–Ta–Li-bearing pegmatite sheets at Pilgangoora (Plate 1A) on the western margin of the East Strelley greenstone belt. Available information indicates that the pegmatite sheets emanated from one or more intrusions of massive, non-foliated granite and syenogranite in the Carlindi Dome. Tantalite in a Pilgangoora pegmatite was dated at 2879 ± 5 Ma (Kinny, 2000). This result suggests an intrusive age between intrusion of the Cutinduna and Split Rock Supersuites. However, more geochronology is required because the age of the Split Rock Supersuite in the Carlindi and Yule Domes has not been isotopically established. The lithium-bearing pegmatites at Pilgangoora are up to 70 m thick and form a north-trending swarm within mafic and ultramafic units correlated with the Euro Basalt and the Dalton Suite. Megacrystic spodumene and microcline are contained within a fine- to coarse-grained albite–quartz matrix. The strike length of the swarm is about 5 km and some individual pegmatites are more than 1 km long (Huston et al., 2017; Sweetapple et al., 2017). Lithium resources at Pilgangoora have been reported from tenements held by Pilbara Minerals Ltd and Altura Mining Ltd. Pilbara Minerals Ltd (2020) reported a mineral resource (JORC 2012) of 222.5 Mt at 1.26% Li₂O (spodumene) and Altura Mining Ltd (2019) reported a mineral resource (JORC 2012) of 45.7 Mt at 1.08% Li₂O.

Pegmatite of the 2851–2831 Ma Split Rock Supersuite

The Split Rock Supersuite, intruded at 2851–2831 Ma, consists of post-tectonic, sheet-like granitic plutons distributed in a northwest-trending belt across the northern half of the Pilbara Craton. These highly fractionated intrusions are typically fringed by pegmatite veins containing tin–tantalum–lithium mineralization (Blockley, 1980; Hickman, 1983; Sweetapple and Collins, 1998, 2002; Sweetapple, 2000; Huston et al., 2001a; Sweetapple et al., 2001), and locally fluorite–barite mineralization (Bagas, 2005). Three main types of pegmatite were described by Hickman (1983): 1) simple pegmatite, with cassiterite and tantalite–columbite minerals, rarer lithium, and beryllium compounds; 2) layered albite pegmatites with a wider variety of mineral species and cassiterite concentrated at finer albitic margins; 3) complex rare-earth pegmatites that mainly intrude greenstones (Ferguson and Ruddock, 2001). A more detailed classification was provided by Sweetapple et al. (2001). Mining in the Shaw Dome recovered tin and tantalum mineralization from alluvial workings in recent drainage basins (Van Kranendonk, 2002). In addition to alluvial mining, local underground mining took place in the Mount Edgar Dome where cassiterite occupies the margins of layered albite-pegmatite veins emplaced along the western side of the Moolyella Monzogranite. Pegmatite-hosted tantalite mineralization has been mined from the Wodgina project area (Plate 1A) where there are thick, shallow-dipping pegmatite sheets (Ferguson and Ruddock, 2001; Sweetapple et al., 2001). Fluorite is a common accessory mineral in most of the post-tectonic granites, and veins containing fluorite and barite fringe the southwestern margin of the Cookes Creek Monzogranite (Hickman, 1983; Bagas, 2005).

Tungsten mineralization is associated with the supersuite in several areas of the northern Pilbara Craton, and small-scale mining has been recorded at Cookes Creek and Burrows Well (Plate 1B) and the Friendly Creek and Wodgina project areas (Baxter, 1978; Hickman, 1983). At all these localities, tungsten mineralization is present where intrusions of the Split Rock Supersuite have intruded greenstones, as opposed to older granitic rocks (Hickman, 1975a). Based on DMIRS records, Hickman (1983) reported that most of the recorded production came from Cookes Creek in 1951 and 1952, and was 26.6 t of wolframite and scheelite concentrate containing 17.6 t WO₃. The workings were on quartz-pegmatite veins within the margin of the Cookes Creek Monzogranite, and in greenstones to the southwest and south of the intrusion (Hickman, 1983). The largest undeveloped tungsten deposit is also at Cookes Creek, and is hosted by metamorphosed pyroxenite and dolerite at the Big Hill deposit (Plate 1B) adjacent to the southern contact of the monzogranite. This mineralization comprises scheelite in veins of quartz, aplite and pegmatite, and is the same age as the monzogranite, locally dated at 2837 ± 16 Ma (GSWA 178011, Wingate et al., 2015a). Tungsten Mining NL (2020) reported Big Hill's mineral resource (JORC 2012) as 11.5 Mt at 0.15% WO₃ (0.10% WO₃ cutoff).

Gold mineralization (c. 2880 Ma)

Gold mineralization in the Mount York area south of Pilgangoora was dated at 2888 ± 6 Ma (Pb–Pb isochron of alteration minerals; Neumayr et al., 1998; Huston et al., 2001a). The mineralization is hosted by shear zones

interpreted to be related to late-stage strike-slip movement in the Pilgangoora and Wodgina areas. Baker et al. (2002) interpreted most of the hydrothermal gold mineralization at Pilgangoora to have been introduced at this time.

Summary and conclusions

This Report traces the crustal evolution of the Pilbara Craton through a series of events.

Formation of Eoarchean – early Paleoproterozoic sialic crust between c. 3.80 and 3.53 Ga

Summary

U–Pb zircon ages and Nd and Hf isotope data presented in this Report are used to expand on previous interpretations that the 3.53 – 3.22 Ga East Pilbara Terrane (EPT) developed on Eoarchean to early Paleoproterozoic crust (Van Kranendonk et al., 2002, 2007a,b; Kemp et al., 2015a,b; Gardiner et al., 2017, 2018; Petersson et al., 2019a,b). If Hf isotope data from >3.53 Ga detrital zircons (Kemp et al., 2015a) or >3.70 Ga xenocrystic zircon in felsic igneous rocks are interpreted using a depleted-mantle model, 3.75 – 3.53 Ga igneous rocks were likely derived by melting of sources with mantle extraction ages between c. 4.0 and 3.8 Ga. Data available prior to 2020 are provided in Appendix 9. On the other hand, if an Eoarchean chondritic mantle is assumed (Kemp et al., 2015a; Petersson et al., 2019a,c, 2020), the sources are interpreted to have been extracted from the mantle after 3.8 Ga. Hf isotope data from a substantial number of <3.53 Ga zircons indicate juvenile sources not represented in the data from older zircons (Fig. 19). These differences suggest an abrupt influx of juvenile magma at c. 3.53 Ga, although the Hf data from most <3.53 Ga zircons still indicate old crustal sources. Data from xenocrystic and detrital zircons dated between c. 3.8 and 3.7 Ga (Thorpe et al., 1992a; GSWA 142942, Nelson, 2000d; Beintema et al., 2003; GSWA 178010, Nelson, 2005a; Kemp et al., 2015a,b; Petersson et al., 2019c) suggest that >3.7 Ga felsic igneous rocks were locally produced by partial melting of older crust.

It is widely accepted that the Earth, like the Moon, was subjected to the Late Heavy Bombardment between c. 4.0 and 3.8 Ga (Rhyder, 1991; Dalrymple and Rhyder, 1993; Cohen et al., 2000; Glikson, 2001, 2004; Lowe and Byerly, 2010; Glikson and Pirajno, 2017). This would have generated an extensive cover of new mafic crust by widespread melting of the mantle. Once formed, this crust would have been subject to reworking, most likely by melting related to mantle plumes, and in the Pilbara Craton this probably produced some 3.8 – 3.7 Ga felsic crust. A detrital zircon from the Mosquito Creek Formation, where this formation overlies an erosional unconformity with the EPT, was dated at 3714 ± 5 Ma (1 σ , zero discordance) (GSWA 178010, spot 15.1, Nelson, 2005a), and has an Hf model age of c. 4.14 Ga (Appendix 9). Assuming the analysis is reliable, and the zircon originally crystallized in a c. 3.7 Ga rock, this suggests a source >4.0 Ga (assuming a depleted mantle at c. 3.7 Ga). Lu–Hf analyses (Kemp et al., 2015a,b) of c. 3.65 Ga xenocrystic zircons extracted from a gneiss

xenolith in the Tambina Supersuite of the Warrawagine Dome (GSWA 142870, Nelson, 1999e) indicate Hf model ages of c. 3.95 – 3.92 Ga (Appendix 9). However, the ϵ_{Hf} values of these xenocrystic zircons are only weakly negative, allowing the interpretation of younger model ages if a c. 3.65 Ga chondritic mantle is assumed.

The recent publication of U–Pb, Lu–Hf and O isotope analyses of numerous xenocrystic 3.76 – 3.60 Ga zircons in c. 3.45 Ga rhyolite of the North Pole Dome (Petersson et al., 2019c) has provided more definite evidence of Eoarchean crust in the east Pilbara Craton. Depending on assumptions regarding either a depleted mantle or a chondritic mantle, the mantle extraction ages of the sources from which this crust was derived were between c. 4.0 and 3.8 Ga. Petersson et al. (2019c) assumed that c. 3.75 – 3.70 Ga crust was very limited in extent, although the wide separation of c. 3.70 Ga detrital zircons in three different basins of the northern Pilbara Craton (see **Other evidence of pre-3530 Ma crust**) does not support this conclusion. The interpretation that the North Pole >3.70 Ga xenocrystic zircons were derived from a relatively small ancient nucleus in the Pilbara Craton, and that this might have been connected to the Narryer Terrane of the Yilgarn Craton (Petersson et al., 2019c), is not supported by available evidence. This indicates that the Pilbara Craton was remote from the Yilgarn Craton in the Paleoproterozoic (Smirnov et al., 2013) and did not collide with the Yilgarn Craton until the 2002–1947 Ma Glenburgh Orogeny (Sheppard et al., 2005; Spaggiari et al., 2008; Johnson et al., 2010, 2011, 2013). However, an Eoarchean connection cannot be ruled out, which would imply an event of continental breakup and separation of the Pilbara and Yilgarn proto-crusts after c. 3.7 Ga. This is an interesting possibility because it would require some form plate tectonic activity in the late Eoarchean or early Paleoproterozoic.

Conclusions

Exposed remnants of the pre-Pilbara Supergroup crust establish that it was composed of greenstones and granitic rocks. Based on dating of xenocrystic zircons in igneous rocks, this crust appears to have formed during three main episodes of magmatic activity at c. 3.75, 3.65, and 3.59 – 3.57 Ga. Nd and Hf model ages suggest derivation of the 3.75 – 3.57 Ga crust from sources with mantle extraction ages between c. 4.0 and 3.8 Ga. However, these model ages depend on the condition that the Earth's mantle was significantly depleted by c. 3.7 Ga, and as yet there is no direct evidence (preserved crust, or xenocrystic or detrital zircons) for crust >3.8 Ga in the Pilbara Craton. If Earth's crust was extensively reworked during the Late Heavy Bombardment, it is doubtful if much >3.8 Ga sialic crust survived.

Paleoproterozoic evolution of a volcanic plateau

Summary

Previous reviews of the Paleoproterozoic evolution of the EPT (Van Kranendonk et al., 2002, 2006a, 2007a,b; Hickman, 2004; Hickman and Van Kranendonk, 2008a) have been revised based on new data, in particular additional U–Pb

zircon geochronology and acquisition of Nd and Hf isotope evidence. For example, the Pilbara Supergroup no longer includes the Soanesville Group, which was deposited after rifting and breakup of the EPT (Van Kranendonk et al., 2010; Hickman, 2011). Additionally, new isotopic evidence indicates that, following an introduction of juvenile material at c. 3.53 Ga, over the next 300 Ma the EPT crust evolved by crustal reworking with only very limited subsequent additions of juvenile material (Champion, 2013; Champion and Huston, 2016; Gardiner et al., 2017, 2018; Smithies et al., 2019).

The ϵ_{Hf} values of some 3.53 – 3.42 Ga xenocrystic and detrital zircons are strongly positive (+6.0 to +2.6) whereas others are as negative, as are the ϵ_{Hf} values of pre-3.53 Ga zircons (Fig. 19). This is interpreted to be evidence of mixed sources of granitic melts at c. 3.5 Ga. Although mean ϵ_{Hf} values at any given crystallization age between c. 3.53 and 3.42 Ga are approximately chondritic, this is unlikely to be geologically significant because the zircons came from samples collected over a wide area of the EPT. By analogy with the lateral lithological variability of the Paleoproterozoic EPT crust, it is likely that the pre-3.53 Ga crust was also laterally variable. In the case of granitic rocks intruded between c. 3.42 to 3.22 Ga, there is a general trend of increasingly negative values consistent with progressively more crustal reworking. Zircons that crystallized between 3.53 and 3.22 Ga have relatively uniform Hf model ages of c. 3.6 Ga.

Whole-rock Nd isotope data also indicate increased crustal reworking during crustal evolution of the EPT, with increasingly limited evidence for addition of juvenile material towards c. 3.22 Ga. These trends support previous conclusions from the PCMP that the EPT evolved by vertical tectonic processes involving the remelting of older crust (Van Kranendonk et al., 2002, 2007a,b; Champion and Smithies, 2007; Smithies et al., 2009), and did not involve horizontal processes such as plate convergence, subduction and collision. Previous suggestions that the Paleoproterozoic greenstone successions of the Pilbara Craton originated in oceanic basins, along volcanic arcs, or in marginal basins (Barley, 1993; Krapež, 1993; Krapež and Eisenlohr, 1998) are inconsistent with these and other lines of evidence.

The strong similarity between the stratigraphy of the EPT and the Onverwacht Group and contemporaneous granitic rocks in South Africa (Fig. 4), means that this conclusion also has important implications for the Paleoproterozoic evolution of the Barberton Greenstone Belt (BGB). The BGB was previously interpreted in terms of Phanerozoic-style plate tectonic processes (De Wit, 1991; De Wit et al., 1992), which substantially influenced interpretations of greenstone belts in other Archean cratons (Shackleton, 1995; Windley, 1995; Daigneault et al., 2004; Barley et al., 2008). However, major reinterpretations of its stratigraphy and crustal evolution (Lowe and Byerly, 2007; Van Kranendonk et al., 2014, 2015) now indicate the BGB evolved in the same way as the EPT.

Evidence from the PCMP supports earlier interpretations (Hickman, 1975a, 1981, 1984) that the dome-and-keel crustal architecture of the EPT resulted from gravity-driven vertical deformation. However, the 1970s model, which interpreted solid-state diapirism unrelated to granitic intrusion, was modified to include syntectonic granitic intrusion (Collins et al., 1998; Hickman, 2004; Hickman and Van Kranendonk, 2004; Sandiford et al., 2004; Van Kranendonk et al., 2004a;

Bodorkos and Sandiford, 2006). Gravitational instability in the upper crust increased from c. 3.53 to 3.32 Ga due to deposition of relatively dense ultramafic–mafic formations of the Warrawoona and Kelly Groups upon a less-dense, mainly felsic, substrate. Volcanism was directly related to melting of the mantle and lower crust by a succession of mantle plumes (Van Kranendonk et al., 2002, 2007a). In response to the resulting density inversion, greatest diapiric uplift of the felsic crust commenced between c. 3.49 and 3.46 Ga. Thereafter, diapiric uplift was episodic and followed each major mafic volcanic eruption; in particular, the 3.45 – 3.44 Ga Apex Basalt of the Warrawoona Group, and 3.35 – 3.33 Ga Euro Basalt of the Kelly Group. Uplift in the diapiric domes was between 10 and 20 km in some parts of the EPT and is likely to have been accompanied by equal or greater sagduction of the mafic volcanic cover (greenstones) in the relatively narrow zones between the domes. Some of the granitic magmas which intruded the domes might have been derived by partial melting of greenstones sagducted to the lower crust and mantle, although most granitic magmas were probably derived from melting related to the mantle plumes.

Geochemical evidence supporting the 3.53 – 3.22 Ga continental growth of the East Pilbara Terrane has been presented and reviewed in several key papers (Smithies, 2000; Smithies and Champion, 2000; Smithies et al., 2003, 2005b, 2007a,b, 2009; Van Kranendonk et al., 2006a, 2007a,b; Champion and Smithies, 2007; Van Kranendonk, 2010a). This geochemical evidence, derived from analysis of hundreds of samples collected from many greenstone belts and granitic supersuites of the EPT, is not consistent with derivation of the volcanic and granitic rocks of the EPT from the very juvenile sources applying to oceanic basins or oceanic volcanic arc settings. Additionally, Smithies et al. (2009) found that the c. 3.51 Ga basalts and andesites near the base of the Pilbara Supergroup (Coonterunah Subgroup) are enriched in K, LILE, Th, and LREE relative to typical Archean basalt. They argued that these c. 3.51 Ga volcanic rocks must have been derived from a mantle source enriched in felsic crustal components through previous episodes of crustal recycling. They further suggested that crustal material chemically similar to these enriched c. 3.51 Ga volcanic rocks could have been the source for the <3.5 Ga TTG of the EPT.

Important constraints on the tectonic setting of the EPT are provided by the thicknesses, stratigraphy and age range of the Pilbara Supergroup. As an example, preserved thicknesses of the Pilbara Supergroup in different greenstone belts of the EPT are generally between 10 and 15 km, and depositional ages span up to c. 300 Ma. The measured thicknesses can considerably understate total depositional thicknesses owing the presence of Paleoproterozoic erosional unconformities, faulting and granitic intrusion. The Pilbara Supergroup succession in the North Pole Dome (North Star Basalt to Sulphur Springs Group), which has been interpreted as Archean oceanic crust (Kitajima et al., 2001, 2008; Komiya et al., 2002; Terabayashi et al., 2003), is 22 km thick with a depositional age range >250 Ma. In contrast, modern oceanic crust is 6–7 km thick and vertical sections have a very limited age range due to lateral growth from a spreading centre.

The successive ultramafic–mafic–felsic volcanic cycles of the Pilbara Supergroup are inconsistent with oceanic crust. Features characteristic of oceanic crust, such as a thick

basal gabbro layer and sheeted dyke complexes, are absent from the Pilbara Supergroup. Where mafic dyke swarms were emplaced, they intruded granitic crust. The existence of major regional-scale erosional breaks in the succession (Buick et al., 1995; Van Kranendonk, 2000a), combined with the presence of shallow-water sediments and stromatolites at several stratigraphic levels (Dunlop 1978; Barley et al., 1979; Walter et al. 1980; Lowe 1983; DiMarco and Lowe 1989a,b; Hofmann et al., 1999; Hickman, 2008; Hickman et al., 2011), provide strong evidence against oceanic tectonic settings such as a mid-ocean ridge or oceanic island. Key papers were those by Barley et al. (1979), who first recognized widespread shallow-water deposition in the c. 3480 Ma Dresser Formation of the North Pole area, and Buick et al. (1995), who recognized and documented Earth's oldest erosional unconformity at the base of the Strelley Pool Formation.

Conclusions

Paleoproterozoic crustal evolution was dominated by a series of mantle plume events and vertical tectonic processes that developed the dome-and-keel crustal architecture of the EPT. There is no evidence for plate tectonic processes between c. 3.53 and 3.22 Ga, and in the absence of subduction, no new crust was introduced for crustal rejuvenation. This resulted in repeated reworking of the crust formed at 3.53 – 3.49 Ga, leading to intrusion and eruption of igneous rocks with progressively increasing K₂O contents. By c. 3.33 Ga, the accumulation of volcanic cycles had formed a c. 15 km-thick volcanic succession overlying the pre-3.53 Ga crust. However, this succession is separated into two parts by a thin but laterally extensive sedimentary formation (3.42 – 3.35 Ga Strelley Pool Formation) overlying a regional unconformity. The two divisions of the 15 km-thick volcanic succession, the Warrawoona Group and the Kelly Group, represent large igneous provinces (Warrawoona and Kelly LIPs) which originally extended far outside the area of the presently preserved EPT. A major 3.33 – 3.29 Ga event of doming and granitic intrusion (Emu Pool Event) in the eastern half of the EPT coincided with a change in the evolution of the terrane. In the west, the Emu Pool Supersuite and its volcanic equivalent the Wyman Formation are absent, although both are important components of the eastern half of the EPT. The boundary between these stratigraphically different parts of the EPT is a narrow zone of faulting and shearing (Coongan–Warralong Fault Zone) that probably represents an important crustal break.

Mesoproterozoic crustal evolution

Summary

Crustal extension and rifting from c. 3.28 Ga onwards, most likely related to the mantle plume responsible for deposition of the Sulphur Springs Group and intrusion of the Cleland Supersuite (Van Kranendonk et al., 2002, 2006a, 2007b), led to breakup of the EPT at c. 3.22 Ga. Breakup was followed by northwest–southeast plate separation that persisted until c. 3.16 Ga. The separation formed two basins of juvenile basaltic crust (Regal and Mosquito Creek Basins) separating three Paleoproterozoic continental microplates (East Pilbara, Karratha and Kurrana Terranes). As these plates separated, clastic passive-margin basins (Nickol River, Soanesville,

Budjan Creek and Coondamar Basins) formed along the plate margins. With deeper rifting on the northwestern side of the EPT, the sedimentary succession of the Soanesville Basin was intruded by the c. 3.18 Ga Dalton Suite, and these intrusions fed the thick mafic volcanic succession of the Honeyeater Basalt.

During and towards the end of plate separation the 3.20 – 3.16 Ga Mount Billroth Supersuite was intruded along the northern margin of the Kurrana Terrane and on parts of the northwestern margin of the EPT. Diorite, tonalite and granodiorite intrusions of the Mount Billroth Supersuite might have originated through partial melting of the c. 3.2 Ga juvenile mafic crust along the margins of the Regal and Mosquito Creek Basins. The composition of the supersuite is in stark contrast to the monzogranite and syenogranite intrusions of the Cleland Supersuite in the EPT.

A c. 3160 Ma metamorphic event in the northwestern area of the Pilbara Craton coincided with a change from separation of the East Pilbara and Karratha Terranes to their convergence. This convergence caused compression of the relatively thin crust of the Regal Basin, and this resulted in thrusting of part of the Regal Formation across the Karratha Terrane. It also resulted in the formation of a subduction zone within the basin, which developed the magmatic arc of the 3130–3093 Ma Sholl Terrane. The change from plate separation to convergence is inferred to have resulted from collision of the Karratha Terrane with another plate northwest of the Pilbara Craton. Ongoing convergence of the northwestern plate greatly influenced the tectonic and magmatic evolution of the northern Pilbara Craton from c. 3160 to 2900 Ma.

Compression of the northwest Pilbara Craton caused c. 3.07 Ga amalgamation of the Sholl, Karratha and Regal Terranes to form the West Pilbara Superterrane (WPS). Continued compression forced the WPS into contact with the EPT, resulting in the c. 3.07 Ga Prinsep Orogeny, closure of the Regal Basin, and intrusion of the c. 3.07 Ga Elizabeth Hill Supersuite. With closure of the Regal Basin, continuing convergence led to development of a subduction zone along the northwestern margin of the Pilbara Craton. Evidence of this is provided by the 3.02 – 3.01 Ga magmatic arc of the Orpheus Supersuite.

The Gorge Creek Basin, composed of BIF and sandstone, was formed southeast of this arc in a retro-arc foreland basin setting. As subduction of the northwestern plate extended southeast under the Pilbara Craton, igneous intrusions (3.00 – 2.98 Ga Maitland River Supersuite and 2.95 – 2.92 Ga Sisters Supersuite) migrated southeast into the western half of the EPT. The Gorge Creek Basin evolved through a sedimentary transition succession of BIF, chert and conglomerate into the 3.01 – 2.93 Ga Mallina Basin, still in a retro-arc basin setting. Between c. 2.95 and 2.92 Ga, north–south oblique convergence deformed the relatively thin crust of the central Mallina Basin into a belt of transpressional folding and sinistral strike-slip faulting. This tectonic event is referred to as the North Pilbara Orogeny. With closure of the Mallina Basin, ongoing north–south compression across the northern Pilbara Craton caused a transfer of deformation to the relatively thin crust of the Mosquito Creek Basin. The Coondamar and Mosquito Creek Formations were isoclinally folded, and part of the succession was thrust northwards onto the EPT and southwards onto the Kurrana Terrane.

Following the North Pilbara and Mosquito Creek Orogenies, the internal structure of the northern crust of the Pilbara Craton has remained substantially unchanged to the present day. Intrusion of the 2897–2896 Ma Cutinduna Supersuite in the central Kurrana Terrane might have been related to late development of the Chichester Tectonic Zone.

Conclusions

The stratigraphic, structural and geochronological record of the northern Pilbara Craton establishes that a major change in crustal evolution occurred at c. 3.22 Ga. Rifting of the pre-3.22 Ga Paleoproterozoic volcanic plateau evolved into northwest–southeast separation of three microplates (East Pilbara, Kurrana and Karratha Terranes), separated by two rift basins (Regal and Mosquito Creek Basins) that were flooded by juvenile, MORB-like basaltic crust. This marked the end of Paleoproterozoic vertical deformation and crustal recycling in the Pilbara Craton, and commencement of Mesoproterozoic horizontal plate interaction similar to that of Phanerozoic plate tectonic processes. The northwest–southeast plate separation led to clastic sedimentary deposition of passive-margin successions such as the 3.22 – 3.17 Ga Soanesville Group on the northwestern margin of the EPT. By c. 3.18 Ga, continuing extension had led to deeper rifting with intrusion of the ultramafic–mafic Dalton Suite and eruption of the Honeyeater Basalt.

A c. 3.16 Ga metamorphic event (Karratha Event) across the northern Pilbara Craton, coinciding with a change from plate divergence to convergence, is attributed to collision of the Karratha Terrane with an inferred plate to the northwest. Effects of this reversal in plate motion included compression of the Regal Basin resulting in obduction of parts of its mafic crust (Regal Formation) onto the Karratha Terrane and the EPT, and formation of a subduction zone within the Regal Basin. This subduction zone resulted in eruption of the 10 km-thick Whundo Group between 3.13 and 3.11 Ga. At c. 3.07 Ga the northwestern margin of the EPT collided with the WPS resulting in closure of the Regal Basin, the Prinsep Orogeny, and intrusion of the Elizabeth Hill Supersuite.

With collision and amalgamation of the EPT and WPS, plate interaction shifted to the northwestern margin of the Pilbara Craton. Subduction of the inferred northwestern plate is likely to have commenced shortly after 3.07 Ga, although the oldest magmatic arc exposed on the northwest Pilbara coast is that of the c. 3.02 Ga Orpheus Supersuite. Southeast of the Orpheus Supersuite arc, the Gorge Creek Group was deposited in the retro-arc Gorge Creek Basin, which evolved upwards into the Mallina Basin. These basins overlay thick continental crust formed by the amalgamated EPT and WPS. Numerous well-preserved areas of the Gorge Creek Basin establish that it covered most of the northern Pilbara Craton, and that it had a relatively simple and uniform stratigraphy. In particular, the 500–1000 m-thick BIF, chert and shale succession of the c. 3.02 Ga Cleaverville Formation has been mapped across the east Pilbara Craton and into the northwest Pilbara Craton.

Between c. 3025 and c. 2920 Ma, magmatic arcs related to ongoing subduction along the northwestern margin of the craton migrated progressively southeast, and from c. 2.95 Ga onwards the western half of the EPT was intruded by granites of the Sisters Supersuite. Compression and closure of the Mallina Basin, which was marked by the

2.95 to 2.92 Ga North Pilbara Orogeny, resulted in ongoing northwest–southeast compression shifting to the Mosquito Creek Basin in the southeast Pilbara Craton. Convergence of the East Pilbara and Kurrana Terranes resulted in 2.93 – 2.90 Ga closure of the intervening Mosquito Creek Basin marked by the Mosquito Creek Orogeny. Post-orogenic granites of the Split Rock Supersuite were intruded between 2.85 and 2.83 Ga, possibly due to movement of the Pilbara Craton across a hot spot.

Mineralization

Although mineralization in the east Pilbara Craton is extremely varied, no mined deposits other than iron ore and Sn–Ta–Li have proved to be large by international or Australian standards (Barley and Groves, 1984; Groves and Batt, 1984; Groves et al., 1984; Barley et al., 1992; Witt et al., 1998; Huston et al., 2001c, 2017). The proposed explanation with respect to the Paleoarchean EPT is that hydrothermal fluids generated during vertical recycling of continental crust may have had finite metal sources. This contrasts with Phanerozoic-style plate tectonic settings which have the potential for repeated influxes of metal-charged juvenile material, either above subducting slabs or along major strike-slip faults. Even in the Mesoarchean sedimentary basins, which do contain strike-slip faults and thrusts, plate movements appear to have been between microplates, likely reducing the scale and duration of hydrothermal systems.

Abbreviations

ABDP	Archean Biosphere Drilling Project
ACM	Antarctic Creek Member
AGC	Ancient Gneiss Complex
BCSZ	Bamboo Creek Shear Zone
BGB	Barberton Greenstone Belt
CHUR	Chondritic uniform reservoir
CPTZ	Central Pilbara Tectonic Zone
CTZ	Chichester Tectonic Zone
CWFZ	Coongan–Warralong Fault Zone
EPE	Emu Pool Event
EPT	East Pilbara Terrane
EPTRE	East Pilbara Terrane Rifting Event
KLSZ	Klondyke Shear Zone
KSZ	Kurrana Shear Zone
KT	Karratha Terrane
KUT	Kurrana Terrane
LSZ	Limestone Shear Zone
LWSF	Lalla Rookh – Western Shaw Fault
LWSC	Lalla Rookh – Western Shaw Structural Corridor
MB	Mallina Basin
MBCM	Marble Bar Chert Member
MCB	Mosquito Creek Basin
MLSZ	Mallina Shear Zone
MORB	Mid-ocean ridge basalt
MSZ	Maitland Shear Zone
MUSZ	Mulgandinnah Shear Zone
PBIM	Pincunah Banded-Iron Member
PCMP	Pilbara Craton Mapping Project
PF	Pardoo Fault
SRSZ	Split Rock Shear Zone
SSZ	Sholl Shear Zone
TTG	tonalite–trondhjemite–granodiorite
TTSZ	Tabba Tabba Shear Zone
WPS	West Pilbara Superterrane

References

- Abeyasinghe, PB and Fetherston, JM 1997, Barite and fluorite in Western Australia: Geological Survey of Western Australia, Mineral Resources Bulletin 17, 97p.
- Allen, CM, Wiemer, D and Murphy, DT 2016, Improving LA-ICPMS dating techniques: Experiments on zircon from a c. 3.51 Ga dioritic gneiss, East Pilbara Terrane, Western Australia, *in* Session 35, T39, Go Small or Go Home: Microbeam techniques applied to igneous, metamorphic, and sedimentary petrology of Earth and planetary systems: Geological Society of America, Annual Meeting 2016, Denver, Colorado, 26–28 September 2016, Abstracts with Programs 48, no. 7.
- Allee, J, Bernard, S, Le Guillou, C, Beyssac, O, Sugitani, K and Robert, F 2018, Chemical nature of the 3.4 Ga Strelley Pool microfossils: Geochemical Perspectives Letters, v. 7, p. 37–42, doi:10.7185/geochemlet.1817.
- Allwood, AC, Burch, I and Walter, MR 2007a, Stratigraphy and facies of the 3.43 Ga Strelley Pool Chert in the southwestern North Pole dome, Pilbara Craton, Western Australia: Geological Survey of Western Australia, Record 2007/11, 22p.
- Allwood, AC, Grotzinger, JP, Knoll, AH, Burch, IW, Anderson, MS, Coleman, ML and Kanik, I 2009, Controls on development and diversity of Early Archean stromatolites: Proceedings of the National Academy of Sciences, v. 106, p. 9548–9555.
- Allwood, AC, Kamber, BS, Walter, MR, Burch, IW and Kanik, I 2010, Trace elements record depositional history of an early Archean stromatolitic carbonate platform: Chemical Geology, v. 270, p. 148–163.
- Allwood, AC, Walter, MR, Burch, IW and Kamber, BS 2007b, 3.43 billion-year-old stromatolite reef from the Pilbara Craton of Western Australia: Ecosystem-scale insights to early life on Earth: Precambrian Research, v. 158, p. 198–227.
- Allwood, AC, Walter, MR, Kamber, BS, Marshall, CP and Burch, IW 2006, Stromatolite reef from the Early Archean era of Australia: Nature, v. 441, p. 714–717.
- Allwood, AC, Walter, MR, Marshall, C and Van Kranendonk, M 2004a, Habit and habitat of earliest life on Earth: International Journal of Astrobiology, v. 3 (S1), p. 104.
- Allwood, AC, Walter, MR, Marshall, C and Van Kranendonk, MJ 2004b, Life at 3.4 Ga: paleobiology and paleoenvironment of the stromatolitic Strelley Pool Chert, Pilbara Craton, Western Australia, *in* Session 197, T4, Precambrian geology: Geological Society of America, Annual Meeting 2004, Denver, Colorado, 7–10 November 2004, Abstracts with Programs 36, p. 458.
- Altinok, E and Ohmoto, H 2006, Soil formation beneath the Earth's oldest known (3.46 Ga) unconformity?, *in* T105, Paleosols, Proxies, and Paleoenvironments II: Geological Society of America, 2006 Philadelphia Annual Meeting, Philadelphia, Pennsylvania, 22–25 October 2006, Abstracts and Programs 38, p. 533.
- Amelin, Y, Lee, D-C and Halliday, AN 2000, Early-middle Archean crustal evolution deduced from Lu–Hf and U–Pb isotopic studies of single zircon grains: Geochimica et Cosmochimica Acta, v. 62, no. 24, p. 4205–4225.
- Amelin, Y, Lee, D-C, Halliday, AN and Pidgeon, RT 1999, Nature of the Earth's earliest crust from hafnium isotopes in single detrital zircons: Nature, v. 399, p. 252–255, doi:10.1038/20426.
- Anhaeusser, CR 1971a, The Barberton Mountain Land, South Africa – a guide to the understanding of the Archean geology of Western Australia, *in* Symposium on Archean Rocks, Perth, 23–26 May 1970 *edited by* JE Glover: Geological Society of Australia, Perth, Western Australia, Special Publication 3, p. 103–119.
- Anhaeusser, CR 1971b, Cyclic volcanicity and sedimentation in the evolutionary development of Archean greenstone belts of shield areas, *in* Symposium on Archean Rocks, Perth, 23–26 May 1970 *edited by* JE Glover: Geological Society of Australia, Perth, Western Australia, Special Publication 3, p. 57–70.
- Anhaeusser, CR, Mason, R, Viljoen, MJ and Viljoen, RP 1969, A reappraisal of some aspects of Precambrian shield geology: Geological Society of America Bulletin, v. 80, no. 11, p. 2175–2200.
- Anhaeusser, CR, Roering, C, Viljoen, MJ and Viljoen, RP 1968, The Barberton Mountain Land: A model of the elements and evolution of an Archean fold belt: Geological Society of South Africa, Annexure, v. 71, p. 225–254.
- Archibald, NJ and Bettenay, LF 1977, Indirect evidence for tectonic reactivation of a pre-greenstone sialic basement in Western Australia: Earth and Planetary Science Letters, v. 33, p. 370–378.
- Arndt, NT 1999, Why was flood volcanism on submerged continental platforms so common in the Precambrian? Precambrian Research, v. 97, p. 155–164.
- Arndt, N, Bruzack, G and Reischmann, T 2001, The oldest continental and oceanic plateaus: geochemistry of basalts and komatiites of the Pilbara Craton, Australia, *in* Mantle plumes: their identification through time *edited by* R Ernst and K Buchan: Geological Society of America, Special Paper 352, p. 359–387.
- Arndt, NT, Czamanske, GK, Wooden, JL and Fedorenko, VA 1993, Mantle and crustal contributions to continental flood volcanism: Tectonophysics, v. 223, p. 39–52.
- Arndt, NT and Goldstein, SL 1987, Use and abuse of crust-formation ages: Geology, v. 15, p. 893–895.
- Arndt, NT, Kerr, AC and Tarney, J 1997, Dynamic melting in plume heads: formation of Gorgona komatiites and basalts: Earth and Planetary Science Letters, v. 146, p. 289–301.
- Arndt, NT and Leshner, CM 2004, Komatiite: Encyclopedia of Geology, Elsevier, p. 260–268.
- Atlas Iron Limited 2018, Mineral Resources and Ore Reserves at 30 June 2018: Report to Australian Securities Exchange, 29 August 2018, 4p.
- Bagas, L 2003, Stratigraphic revision of the Warrawoona and Gorge Creek Groups in the Kelly greenstone belt, Pilbara Craton, Western Australia, *in* Geological Survey of Western Australia Annual Review 2001–02: Geological Survey of Western Australia, p. 53–60.
- Bagas, L 2005, Geology of the Nullagine 1:100 000 sheet: Geological Survey of Western Australia, 1:100 000 Geological Series Explanatory Notes, 33p.
- Bagas, L, Beukenhorst, O and Hos, K 2004a, Nullagine, WA Sheet 2954: Geological Survey of Western Australia, 1:100 000 Geological Series.
- Bagas, L, Bierlein, FP, Bodorkos, S and Nelson, DR 2008, Tectonic setting, evolution, and orogenic gold potential of the late Mesoproterozoic Mosquito Creek Basin, North Pilbara Craton, Western Australia: Precambrian Research, v. 160, p. 237–244.
- Bagas, L, Farrell, TR and Nelson, DR 2004b, The age and provenance of the Mosquito Creek Formation, *in* Geological Survey of Western Australia Annual Review 2003–04, p. 62–70.
- Bagas, L, Smithies, RH and Champion, DC 2003, Geochemistry of the Corunna Downs Granitoid Complex, East Pilbara Granite-Greenstone Terrane, *in* Geological Survey of Western Australia Annual Review 2001–02: Geological Survey of Western Australia, p. 61–69.
- Bagas, L, Van Kranendonk, MJ and Pawley, MJ 2004c, Geology of the Split Rock 1:100 000 sheet: Geological Survey of Western Australia, 1:100 000 Geological Series Explanatory Notes, 43p.
- Baker, DEL and Collins, WJ 2001, Structural history of the northern East Strelley Belt, Pilbara Craton, Western Australia, *in* Extended Abstracts – 4th International Archean Symposium, Perth, 24–28 September 2001 *edited by* KF Cassidy, J Dunphy and MJ Van Kranendonk: AGSO (Geoscience Australia), Record 2001/37, p. 282–284.
- Baker, DEL, Seccombe, PK and Collins, WJ 2002, Structural history and timing of gold mineralization in the northern East Strelley Belt, Pilbara Craton, Western Australia: Economic Geology, v. 97, p. 775–785.
- Banks, MJ 1981, Progress Report on Temporary Reserves 7437H and 7439H, Shaw River District, Western Australia: Anaconda Australia Inc.: Geological Survey of Western Australia, Statutory mineral exploration report A9832, 163p.
- Barley, ME 1978, Shallow-water sedimentation during deposition of the Archean Warrawoona Group, eastern Pilbara Block, Western Australia, *in* Archean Cherty Metasediments, *edited by* JE Glover and DI Groves: The University of Western Australia Geology Department and Extension Service, Publication 2, p. 22–29.

- Barley, ME 1981, Relations between volcanic rocks in the Warrawoona Group: continuous or cyclic evolution? Geological Society of Australia, Special Publication, v. 7, p. 263–273.
- Barley, ME 1982, Porphyry-style mineralization associated with early Archean calc-alkaline igneous activity, eastern Pilbara, Western Australia: *Economic Geology*, v. 77, p. 1230–1236.
- Barley, ME 1984, Volcanism and hydrothermal alteration, Warrawoona Group, East Pilbara, in *Archaean and Proterozoic basins of the Pilbara, Western Australia: Evolution and mineralization potential* edited by JR Muhling, DI Groves and TS Blake: The University of Western Australia, Geology Department and University Extension, Publication no 9, p. 23–36.
- Barley, ME 1987, The Archaean Whim Creek Belt, an ensialic fault-bounded basin in the Pilbara Block, Australia: *Precambrian Research*, v. 37, no. 3, p. 199–215, doi:10.1016/0301-9268(87)90067-2.
- Barley, ME 1992, A review of Archean volcanic-hosted massive sulfide and sulfate mineralization in Western Australia: *Economic Geology*, v. 87, no. 3, p. 855–872.
- Barley, ME 1993, Volcanic, sedimentary and tectonostratigraphic environments of the ~3.46 Ga Warrawoona Megasequence: A review: *Precambrian Research*, v. 60, no. 1–4, p. 47–67.
- Barley, ME 1997, The Pilbara Craton, in *Greenstone belts* edited by MJ De Wit and L Ashwal: Oxford University Press, Oxford, UK, Oxford Monographs on Geology and Geophysics 35, p. 657–664.
- Barley, M, Bekker, A and Krapež, B 2005, Late Archean to Early Paleoproterozoic global tectonics, environmental change and the rise of atmospheric oxygen: *Earth and Planetary Science Letters*, v. 238, no. 1–2, p. 156–171, doi:10.1016/j.epsl.2005.06.062.
- Barley, ME, Brown, SJA, Krapež, B and Kositsin, N 2008, Physical volcanology and geochemistry of a Late Archean volcanic arc: Kurnalpi and Gindalbie Terranes, Eastern Goldfields Superterrane, Western Australia: *Precambrian Research*, v. 161, no. 1, p. 53–76.
- Barley, ME, Dunlop, JSR, Glover, JE and Groves, D 1979, Sedimentary evidence for an Archean shallow-water volcanic-sedimentary facies, Eastern Pilbara Block, Western Australia: *Earth and Planetary Science Letters*, v. 43, p. 74–84.
- Barley, ME and Groves, DI 1984, Constraints on mineralization of the Warrawoona Group, in *Archaean and Proterozoic basins of the Pilbara, Western Australia: Evolution and mineralization potential* edited by JR Muhling, DI Groves and TS Blake: The University of Western Australia, Geology Department and University Extension, Publication no 9, p. 54–67.
- Barley, ME, Groves, DI and Blake, TS 1992, Archaean metal deposits related to tectonics: Evidence from Western Australia, in *The Archaean: Terrains, processes and metallogeny: Proceedings for the Third International Archaean Symposium, 17–21 September 1990* edited by JE Glover and SE Ho: Geology Department and University Extension, The University of Western Australia, Perth, Western Australia, Publication 22, p. 307–324.
- Barley, ME, Loader, SE and McNaughton, NJ 1998, 3430 to 3417 Ma calc-alkaline volcanism in the McPhee Dome and Kelley Belt, and growth of the eastern Pilbara Craton: *Precambrian Research*, v. 88, p. 3–24.
- Barley, ME and Pickard, AL 1999, An extensive, crustally-derived, 3325 to 3310 Ma silicic volcanoplutonic suite in the eastern Pilbara Craton: Evidence from the Kelly Belt, McPhee Dome and Corunna Downs Batholith: *Precambrian Research*, v. 96, p. 41–62.
- Barley, ME, Sylvester, GC and Groves, DI 1984, Archaean calc-alkaline volcanism in the Pilbara Block, Western Australia: *Precambrian Research*, v. 24, no. 3–4, p. 285–319.
- Baxter, JL 1978, Molybdenum, tungsten, vanadium and chromium in Western Australia: Geological Survey of Western Australia, Mineral Resources Bulletin 11, 140p.
- Bédard, JH, Harris, LB and Thurston, PC 2013, The hunting of the snArc: *Precambrian Research*, v. 229, p. 20–48.
- Beintema, KA 2003, Geodynamic evolution of the west and central Pilbara Craton: A mid-Archaean active continental margin: *Geologica Ultraiectina*, Utrecht University, Utrecht, The Netherlands, PhD thesis (unpublished), 248p.
- Beintema, KA, de Leeuw, GAM, White, SH and Hein, KAA 2001, Tappa Tappa shear: A crustal-scale structure in the Pilbara Craton, WA, in *Extended Abstracts – 4th International Archaean Symposium*, Perth, 24–28 September 2001 edited by KF Cassidy, J Dunphy and MJ Van Kranendonk: AGSO (Geoscience Australia), Record 2001/37, p. 285–287.
- Beintema, KA, Mason, PRD, Nelson, DR, White, SH and Wijbrans, JR 2003, New constraints on the timing of tectonic activity in the Archaean central Pilbara Craton, Western Australia: *Journal of the Virtual Explorer*, v. 13, doi:10.3809/jvirtex.vol.2003.013.
- Bekker, A, Planavsky, NJ, Krapež, B, Rasmussen, B, Hofmann, A, Slack, JF, Rouxel, OJ and Konhauser, KO 2014, Iron formations: Their origins and implications for ancient seawater chemistry, in *Treatise on Geochemistry* edited by KK Turekian: Elsevier, Oxford, UK, p. 561–628.
- Bekker, A, Slack, JF, Planavsky, NJ, Krapež, B, Hofmann, AW, Konhauser, KO and Rouxel, OJ 2010, Iron formation: The sedimentary product of a complex interplay among mantle, tectonic, oceanic, and biospheric processes: *Economic Geology*, v. 105, p. 467–508.
- Belousova, EA, Kostitsyn, YA, Griffin, WL, Begg, GC, O'Reilly, SY and Pearson, NJ 2010, The growth of the continental crust: Constraints from zircon Hf-isotope data: *Lithos*, v. 119, no. 3–4, p. 457–466.
- Bennett, VC, Nutman, AP and McCulloch, MT 1993, Nd isotopic evidence for transient, highly depleted mantle reservoirs in the early history of the Earth: *Earth and Planetary Science Letters*, v. 119, no. 3, p. 299–317, doi:10.1016/0012-821X(93)90140-5.
- Bettenay, LF, Bickle, MJ, Boulter, CA, Groves, DI, Morant, P, Blake, TS and James, BA 1981, Evolution of the Shaw Batholith – An Archaean granitoid-gneiss dome in the eastern Pilbara, Western Australia, in *Archaean Geology: Second International Symposium*, Perth 1980 edited by JE Glover and DI Groves: Geological Society of Australia, Special Publication 7, p. 361–372.
- Bickle, MJ, Bettenay, LF, Barley, ME, Chapman, HJ, Groves, DI, Campbell, IH and de Laeter, JR 1983, A 3500 Ma plutonic and volcanic calc-alkaline province in the Archaean East Pilbara Block: Contributions to Mineralogy and Petrology, v. 84, p. 25–35.
- Bickle, MJ, Bettenay, LF, Boulter, CA, Groves, DI and Morant, P 1980, Horizontal tectonic interaction of an Archaean gneiss belt and greenstones, Pilbara block, Western Australia: *Geology*, v. 8, no. 11, p. 525–529.
- Bickle, MJ, Bettenay, LF, Chapman, HJ, Groves, DI, McNaughton, NJ, Campbell, IH and de Laeter, JR 1989, The age and origin of younger granitic plutons of the Shaw batholith in the Archaean Pilbara Block, Western Australia: Contributions to Mineralogy and Petrology, v. 101, p. 361–376.
- Bickle, MJ, Bettenay, LF, Chapman, HJ, Groves, DI, McNaughton, NJ, Campbell, IH and de Laeter, JR 1993, Origin of the 3500–3300 Ma calc-alkaline rocks in the Pilbara Archaean: isotopic and geochemical constraints from the Shaw Batholith: *Precambrian Research*, v. 60, p. 117–149.
- Bickle, MJ, Morant, P, Bettenay, LF, Boulter, CA, Blake, TS and Groves, DI 1985, Archaean tectonics of the Shaw Batholith, Pilbara Block, Western Australia: structural and metamorphic tests of the batholith concept, in *Evolution of Archaean supracrustal sequences* edited by LD Ayers, PC Thurston, KD Card and W Weber: Geological Association of Canada, Special Paper 28, p. 325–341.
- Binns RA, Gunthorpe RJ and Groves, DI 1976, Metamorphic patterns and development of greenstone belts in the eastern Yilgarn Block, Western Australia, in *The early History of the Earth*, edited by BF Windley: John Wiley and Sons, New York, US, p. 303–313.
- Bjornnes, E and Lindsay, JF 2005, The depositional setting of Earth's earliest sedimentary rocks: *Lunar and Planetary Science*, v. XXXVI, article no. 1821.
- Blake, TS 1984a, The lower Fortescue Group of the northern Pilbara Craton – stratigraphy and paleogeography, in *Archaean and Proterozoic basins of the Pilbara, Western Australia: Evolution and mineralization potential* edited by JR Muhling, DI Groves and TS Blake: The University of Western Australia, Geology Department and University Extension, Publication no 9, p. 123–143.
- Blake, TS 1984b, Evidence for stabilization of the Pilbara Block, Australia: *Nature*, v. 307, p. 721–723.

- Blake, TS 1993, Late Archean crustal extension, sedimentary basin formation, flood basalt volcanism, and continental rifting. The Nullagine and Mount Jope Supersequences, Western Australia: Precambrian Research, v. 60, p. 185–241.
- Blake, TS and Barley, ME 1992, Tectonic evolution of the Late Archean to Early Proterozoic Mount Bruce megasequence set, Western Australia: Tectonics, v. 11, p. 1415–1425.
- Bleeker, W 2003, The late Archean record: A puzzle in ca. 35 pieces: Lithos, v. 71, p. 99–134.
- Blewett, RS 2000, A 'virtual' structural field trip of the North Pilbara: Australian Geological Survey Organisation (Geoscience Australia), Record 2000/45.
- Blewett, RS 2002, Archean tectonic processes: a case for horizontal shortening in the North Pilbara granite–greenstone terrane, Western Australia: Precambrian Research, v. 113, no. 1–2, p. 87–120.
- Blewett, RS and Champion, DC 2005, Geology of the Wodgina 1:100 000 sheet: Geological Survey of Western Australia, 1:100 000 Geological Series Explanatory Notes, 33p.
- Blewett, RS, Champion, DC, Smithies, RH, Van Kranendonk, MJ, Farrell, TR and Thost, D 2001, Wodgina, WA Sheet 2655: Geological Survey of Western Australia, 1:100 000 Geological Series.
- Blewett, RS, Huston, DL, Mernagh, TP and Kamprad, J 2002, The diverse structure of Archean lode gold deposits of the southwest Mosquito Creek Belt, east Pilbara Craton, Western Australia: Economic Geology, v. 97, no. 4, p. 787–800.
- Blewett, RS, Wellman, P, Ratajkoski, M and Huston, DL 2000, Atlas of north Pilbara, geology and geophysics, 1:1.5 million scale: Australian Geological Survey Organisation, Record 2000/4, 36p.
- Blichert-Toft, J and Puchtel, IS 2010, Depleted mantle sources through time: evidence from Lu–Hf and Sm–Nd systematics of Archean komatiites: Earth and Planetary Science Letters, v. 297, p. 598–606.
- Blockley, JG 1975, Pilbara Block, in The geology of Western Australia compiled by Geological Survey of Western Australia: Geological Survey of Western Australia, Memoir 2, p. 81–93.
- Blockley, JG 1980, The tin deposits of Western Australia, with special reference to the associated granites: Geological Survey of Western Australia, Mineral Resources Bulletin 12, 184p.
- Bodorkos, S and Sandiford, M 2006, Thermal and mechanical controls on the evolution of Archean crustal deformation: examples from Western Australia, in Archean Geodynamics and Environments edited by K Benn, J-C Mareschal and KC Condie: American Geophysical Union, Geophysical Monograph 164, p. 131–147, doi:10.1029/164GM10.
- Bontognali, TRR, Sessions, AL, Allwood, AC, Fischer, WW, Grotzinger, JP, Summons, RE and Eiler, JM 2012, Sulfur isotopes of organic matter preserved in 3.45-billion-year-old stromatolites reveal microbial metabolism: Proceedings of the National Academy of Sciences, v. 109, p. 15146–15151.
- Boulter, CA, Bickle, MJ, Gibson, B and Wright, RK 1987, Horizontal tectonics pre-dating upper Gorge Creek group sedimentation Pilbara Block, Western Australia: Precambrian Research, v. 36, no. 3–4, p. 241–258.
- Bouma, AH 1962, Sedimentology of some Flysch deposits: A graphic approach to facies interpretation: Elsevier, Amsterdam, 168p.
- Brasier, MD, Antcliffe, J, Saunders, M and Wacey, D 2015, Changing the picture of Earth's earliest fossils (3.5–1.9 Ga) with new approaches and new discoveries: Proceedings of the National Academy of Sciences, v. 112, p. 4859–4864.
- Brasier, MD, Green, OR, Jephcoat, AP, Klepe, AP, Van Kranendonk, MJ, Lindsay, JF, Steele, A and Grassineau, NV 2002, Questioning the evidence for Earth's oldest fossils: Nature, v. 416, p. 76–81.
- Brasier, MD, Green, OR, Lindsay, JF, McLoughlin, N, Steele, A and Stokes, C 2005, Critical testing of Earth's oldest putative fossil assemblage from the ~3.5 Ga Apex chert, Chinaman Creek, Western Australia: Precambrian Research, v. 140, p. 55–102.
- Brasier, MD, Green, OR, Lindsay, JF, McLoughlin, N, Stoakes, CA, Brasier, AT and Wacey, D 2011, Geology and putative microfossil assemblage of the c. 3460 Ma 'Apex chert', Chinaman Creek, Western Australia – a field and petrographic guide: Geological Survey of Western Australia, Record 2011/7, 60p.
- Brasier, MD, Matthewman, R, McMahon, S, Kilburn, MR and Wacey, D 2013, Pumice from the ~3460 Ma Apex Basalt, Western Australia: A natural laboratory for the early biosphere: Precambrian Research, v. 224, p. 1–10.
- Brauhart, C 1999, Regional alteration systems associated with Archean volcanogenic massive sulphide deposits at Panorama, Pilbara, Western Australia: The University of Western Australia, Perth, Western Australia, PhD thesis (unpublished), 194p.
- Brauhart, C, Groves, DI and Morant, P 1998, Regional alteration systems associated with volcanogenic massive sulphide mineralization at Panorama, Pilbara, Western Australia: Economic Geology, v. 93, p. 292–302.
- Brauhart, CW, Huston, DL and Andrew, AS 2000, Oxygen isotope mapping in the Panorama VMS district, Pilbara Craton, Western Australia: applications to estimating temperatures of alteration and to exploration: Mineralium Deposita, v. 35, p. 727–740.
- Brett, JW 2018, 80 m radiometric merged grids of Western Australia 2018 version 1: Geological Survey of Western Australia, <www.dmp.wa.gov.au/geophysics>.
- Brown, A, Cudahy, T, Walter, MR and Hickman, AH 2011, Hyperspectral alteration mapping of early Archean hydrothermal systems in the North Pole Dome, Pilbara Craton: Geological Survey of Western Australia, Record 2011/15, 28p.
- Brown, AJ, Cudahy, TJ and Walter, MR 2006, Hydrothermal alteration at the Panorama Formation, North Pole Dome, Pilbara Craton, Western Australia: Precambrian Research, v. 151, p. 211–223.
- Bryan, SE and Ernst, RE 2008, Revised definition of large igneous provinces (LIP): Earth-Science Reviews, v. 86, p. 175–202.
- Buick, R and Barnes, KR 1984, Cherts in the Warrawoona Group: Early Archean silicified sediments deposited in shallow-water environments, in Archean and Proterozoic basins of the Pilbara, Western Australia: Evolution and mineralization potential edited by JR Muhling, DI Groves and TS Blake: The University of Western Australia, Geology Department and University Extension, Publication no 9, p. 37–53.
- Buick, R, Brauhart, CW, Morant, P, Thornett, JR, Mani, JG, Archibald, NJ, Doepel, MG, Fletcher, IR, Pickard, AL, Smith, JB, Barley, ME, McNaughton, NJ and Groves, DI 2002, Geochronology and stratigraphic relationships of the Sulphur Springs Group and Strelley Granite: a temporally distinct igneous province in the Archean Pilbara Craton, Australia: Precambrian Research, v. 114, p. 87–120.
- Buick, R and Dunlop, JSR 1990, Evaporitic sediments of early Archean age from the Warrawoona Group, North Pole, Western Australia: Sedimentology, v. 37, no. 2, p. 247–277, doi:10.1111/j.1365-3091.1990.tb00958.xl.
- Buick, R, Dunlop, JSR and Groves, DI 1981, Stromatolite recognition in ancient rocks: An appraisal of irregular laminated structures in an early Archean chert-barite unit from North Pole, Western Australia: Alcheringa, v. 5, p. 161–181.
- Buick, R, Thornett, J, McNaughton, N, Smith, JB, Barley, ME and Savage, MD 1995, Record of emergent continental crust ~3.5 billion years ago in the Pilbara Craton of Australia: Nature, v. 375, p. 574–577.
- Button, A 1976, Transvaal and Hamersley Basins – review of basin development and mineral deposits: Mineral Science Engineering, v. 8, p. 262–293.
- Byerly, GR, Lowe, DR, Wooden, JL and Xie, X 2002, An Archean impact layer from the Pilbara and Kaapvaal cratons: Science, v. 297, p. 1325–1327.
- Cammack, JN, Spicuzza, MJ, Cavosie, AJ, Van Kranendonk, MJ, Hickman, AH, Kozdon, R, Orland, IJ, Kitajima, K and Valley, JW 2018, SIMS microanalysis of the Strelley Pool Formation cherts and the implications for the secular-temporal oxygen-isotope trend of cherts: Precambrian Research, v. 304, p. 125–139.

- Campana, B, Hughes, FE, Burns, WG, Whitcher, IG and Muceniakas, E 1964, Discovery of the Hamersley iron deposits: Australasian Institute of Mining and Metallurgy Proceedings, v. 210, p. 1–30.
- Campbell, IH and Griffiths, RW 1990, Implications of mantle plume structure for the evolution of flood basalts: Earth and Planetary Science Letters, v. 99, p. 79–93.
- Campbell, IH, Griffiths, RW and Hill, RI 1989, Melting in an Archaean mantle plume: heads it's basalts, tails it's komatiites: Nature, v. 339, p. 697–699.
- Carter, JD 1981, Uranium exploration in Western Australia: A history of investigation and a guide to microfilm open-file information: Geological Survey of Western Australia, Record 1981/6, 29p.
- Carter, JD and Gee, RD 1988, Geology and exploration history of uraniferous and auriferous pyritic conglomerates, Western Australia, in Professional papers: Geological Survey of Western Australia, Report 23, p. 17–36.
- Cawood, PA, Hawkesworth, CJ and Dhuime, B 2012, Detrital zircon record and tectonic setting: Geology, v. 40, p. 875–878.
- Cawood, PA, Hawkesworth, CJ and Dhuime, B 2013, The continental record and the generation of continental crust: Journal of the Geological Society, v. 125, no. 1–2, p. 14–32, doi:10.1130/B30722.1.
- Cawood, PA, Hawkesworth, CJ, Pisarevsky, SA, Dhuime, B, Capitanio, FA and Nebel, O 2018, Geological archive of the onset of plate tectonics: Philosophical Transactions of the Royal Society A: Mathematical, Physical and Engineering Sciences, v. 376, article no. 0170405, 30p., doi:10.1098/rsta.2017.0405.
- Champion, DC 2013, Neodymium depleted mantle model age map of Australia: explanatory notes and user guide: Geoscience Australia, Record 2013/44, 209p.
- Champion, DC and Huston, DL 2016, Radiogenic isotopes, ore deposits and metallogenic terranes: Novel approaches based on regional isotopic maps and the mineral systems concept: Ore Geology Reviews, v. 76, p. 229–256, doi:10.1016/j.oregeorev.2015.09.025.
- Champion, DC, and Smithies, RH 2000, The geochemistry of the Yule Granitoid Complex, East Pilbara Granite–Greenstone Terrane; evidence for early felsic crust: Geological Survey of Western Australia, Annual Review 1999–2000, p. 42–48.
- Champion, DC and Smithies, RH 2001, Archaean granites of the Yilgarn and Pilbara cratons, Western Australia, in Extended Abstracts – 4th International Archaean Symposium, Perth, 24–28 September 2001 edited by KF Cassidy, J Dunphy and MJ Van Kranendonk: AGSO (Geoscience Australia), Record 2001/37, p. 134–136.
- Champion, DC and Smithies, RH 2007, Geochemistry of Paleoarchean granites of the East Pilbara Terrane, Pilbara Craton, Western Australia: implications for early Archean crustal growth, in Earth's oldest rocks edited by MJ Van Kranendonk, VC Bennett and RH Smithies: Elsevier BV, Burlington, Massachusetts, USA, Developments in Precambrian Geology 15, p. 369–410.
- Cheney, ES 1996, Sequence stratigraphy and plate tectonic significance of the Transvaal succession of southern Africa and its equivalent in Western Australia: Precambrian Research, v. 79, no. 1–2, p. 3–24.
- Cheney, ES, Roering, C and Stettler, E 1988, Valbara, in Geocongress '88: extended abstracts, Johannesburg, Republic of South Africa: Geological Society of South Africa, p. 85–88.
- Cohen, BA, Swindle, TD and Kring, DA 2000, Support for the lunar cataclysm hypothesis from lunar meteorite impact melt ages: Science, v. 290, p. 1754–1756.
- Collerson, KD and McCulloch, MT 1983, Field and Sr–Nd isotopic constraints on Archaean crust and mantle evolution in the east Pilbara Block, Western Australia, in Australian National University, Research School of Earth Sciences, Annual Report 1982, Canberra, ACT, p. 167–168.
- Collins, WJ 1989, Polydiapirism of the Archean Mount Edgar batholith, Pilbara Block, Western Australia: Precambrian Research, v. 43, no. 1–2, p. 41–62.
- Collins, WJ 1993, Melting of Archaean sialic crust under high H₂O conditions: genesis of 3300 Ma Na-rich granitoids in the Mount Edgar Batholith, Pilbara Block, Western Australia: Precambrian Research, v. 60, p. 151–174.
- Collins, WJ and Van Kranendonk, MJ 1999, Model for the development of kyanite during partial convective overturn of Archaean granite–greenstone terranes: the Pilbara Craton, Australia: Journal of Metamorphic Geology, v. 17, p. 145–156, doi:10.1046/j.1525-1314.1999.00187.x.
- Collins, WJ, Van Kranendonk, MJ and Teyssier, C 1998, Partial convective overturn of Archaean crust in the east Pilbara Craton, Western Australia: driving mechanisms and tectonic implications: Journal of Structural Geology, v. 20, no. 9–10, p. 1405–1424, doi:10.1016/S0191-8141(98)00073-X.
- Compston, W and Kröner, A 1988, Multiple zircon growth within early Archaean tonalite gneiss from the Ancient Gneiss Complex, Swaziland: Earth and Planetary Science Letters, v. 87, p. 13–28.
- Condie, KC 2001, Mantle plumes and their record in Earth history: Cambridge University Press, Cambridge, UK, 306p.
- Condie, KC 2004, Supercontinents and superplume events: Distinguishing signals in the geologic record, v. 146, no. 1–2, p. 319–332.
- Condie, KC 2016, Earth as an evolving planetary system (3rd edition): Academic Press, Waltham, US, 430p.
- Condie, KC, Belousova, EA, Griffin, WL and Sircombe, KN 2009, Granitoid events in space and time: constraints from igneous and detrital zircon age spectra: Gondwana Research, v. 15, p. 228–242.
- Cooper, JA, James, PR and Rutland, RWR 1982, Isotopic dating and structural relationships of granitoids and greenstones in the eastern Pilbara, Western Australia: Precambrian Research, v. 18, p. 199–236.
- Cullers, RL, DiMarco, MJ, Lowe, DR and Stone, J 1993, Geochemistry of a silicified felsic volcanic suite from the early Archean Panorama Formation, Pilbara Block, Western Australia – an evaluation of depositional and post-depositional processes with special emphasis on the rare earth elements: Precambrian Research, v. 60, p. 99–116.
- Cummins, B and Cairns, B 2017, Spinifex Ridge molybdenum–copper deposit, in Australian Ore Deposits edited by GN Phillips: Australasian Institute of Mining and Metallurgy, Monograph 32, p. 343–344.
- Daigneault, R, Mueller, WU and Chown, EH 2004, Abitibi Greenstone Belt plate tectonics: the diachronous history of arc development, accretion, and collision, in The Precambrian Earth: tempos and events edited by PG Eriksson, W Altermann, DR Nelson, WU Mueller and O Catuneanu: Elsevier, Amsterdam, The Netherlands, Developments in Precambrian Geology 12, p. 83–103.
- Dalrymple, GB and Rhyder, G 1993, ⁴⁰Ar/³⁹Ar age spectra of Apollo 15 impact melt rocks by laser step-heating, and their bearing on the history of lunar basin formation: Journal of Geophysical Research: Planets, v. 98, p. 13085–13095, doi:10.1029/93JE01222.
- Davids, C, Wijbrans, JR and White, SH 1997, ⁴⁰Ar/³⁹Ar laserprobe ages of metamorphic hornblendes from the Coongan Belt, Pilbara Western Australia: Precambrian Research, v. 83, no. 4, p. 221–242.
- Davy, R and Lewis, JD 1981, The geochemistry of the Mount Edgar Batholith, Pilbara area, Western Australia, in Archaean Geology: Second International Symposium, Perth 1980 edited by JE Glover and DI Groves: Geological Society of Australia, Special Publication 7, p. 373–383.
- Davy, R and Lewis, JD 1986, The Mount Edgar Batholith, Pilbara area, Western Australia: Geochemistry and petrography: Geological Survey of Western Australia, Report 17, 73p.
- Dawes, PR, Smithies, RH, Centofanti, J and Podmore, DC 1995a, Sunrise Hill unconformity: a newly discovered regional hiatus between Archaean granites and greenstones in the northeastern Pilbara Craton: Australian Journal of Earth Sciences, v. 42, no. 6, p. 635–639.
- Dawes, PR, Smithies, RH, Centofanti, J and Podmore, DC 1995b, Unconformable contact relationships between the Muccan and Warrawagine batholiths and the Archaean Gorge Creek Group in the Yarrrie mine area, northeast Pilbara: Geological Survey of Western Australia, Record 1994/3, 23p.
- De Gregorio, BT, Sharp, TG, Flynn, GJ, Wirick, S and Hervig, RL 2009, Biogenic origin for Earth's oldest putative microfossils: Geology, v. 37, p. 631–634.

- De Grey Mining Limited 2014, Turner River – base metals project update: Australian Securities Exchange (ASX), released 11 April 2012, 27p.
- De Grey Mining Limited 2020, Consolidated Annual Financial Report for the Year Ended 30 June 2020: Report to Australian Securities Exchange (ASX), released 29 October 2020, 76p.
- De Kock, MO, Beukes, NJ and Armstrong, RA 2012, New SHRIMP U–Pb zircon ages from the Hartswater Group, South Africa: implications for correlations of the Neoproterozoic Ventersdorp Supergroup on the Kaapvaal craton and with the Fortescue Group on the Pilbara Craton: *Precambrian Research*, 204–205, p. 66–74.
- De Kock, MO, Evans, DAD and Beukes, NJ 2009, Validating the existence of Vaalbara in the Neoproterozoic: *Precambrian Research*, v. 174, no. 1–2, p. 145–154.
- de Laeter, JR and Blockley, JG 1972, Granite ages within the Pilbara Block, Western Australia: *Journal of the Geological Society of Australia*, v. 19, no. 3, p. 363–370.
- de Vries, ST 2004, Early Archean sedimentary basins: depositional environment and hydrothermal systems – examples from the Barbeton and Coppin Gap greenstone belts: Faculty of Geosciences, Utrecht University, *Gologica Ultraiectina* no. 244, 160p.
- de Vries, ST, Nijman, W and De Boer, PL 2010, Sedimentary geology of the Palaeoproterozoic Buck Ridge (South Africa) and Kittys Gap (Western Australia) volcano-sedimentary complexes: *Precambrian Research*, v. 183, p. 749–769.
- de Vries, ST, Nijman, W, Wijbrans, JR and Nelson, DR 2006, Stratigraphic continuity and early deformation of the central part of the Coppin Gap Greenstone Belt, Pilbara, Western Australia: *Precambrian Research*, v. 147, p. 1–27.
- De Wit, MJ 1991, Archean greenstone belt tectonism and basin development: some insights from the Barberton and Pietersburg greenstone belts, Kaapvaal Craton, South Africa: *Journal of African Earth Sciences*, v. 13, p. 45–63.
- De Wit, MJ, de Ronde, CEJ, Tredoux, M, Roering, C, Hart, RJ, Armstrong, RA, Green, RWE, Peberdy, E and Hart, RA 1992, Formation of an Archean continent: *Nature*, v. 357, p. 553–562.
- Del Ventisette, C, Montanari, D, Sani, F and Bonini, M 2006, Basin inversion and reactivation in laboratory experiments: *Journal of Structural Geology*, v. 28, p. 2067–2083.
- Délor, C, Burg, JP and Clarke, G 1991, Relations diapirisme-metamorphisme dans la Province du Pilbara (Australie occidentale): implications pour les régimes thermiques et tectoniques à la Archéen: *Compte Rendu Academie de Sciences Paris*, v. 312, no. 3, p. 257–263.
- DePaolo, DJ 1980, Crustal growth and mantle evolution: inferences from models of element transport and Nd and Sr isotopes: *Geochimica et Cosmochimica Acta*, v. 44, p. 1185–1196.
- DePaolo, DJ 1988, Neodymium isotope geochemistry: an introduction: Springer-Verlag, Berlin, Germany, Minerals and Rocks Series no. 20, 187p.
- DiMarco, MJ 1986, Stratigraphy, sedimentology, and sedimentary petrology of the early Archean Coongan Formation, Warrawoona Group, Eastern Pilbara block, Western Australia: Louisiana State University, Baton Rouge, Louisiana, PhD thesis (unpublished), 323p.
- DiMarco, MJ and Lowe, DR 1989a, Shallow-water volcanoclastic deposition in the Early Archean Panorama Formation, Warrawoona Group, eastern Pilbara Block, Western Australia: *Sedimentary Geology*, v. 64, no. 1–2, p. 43–63.
- DiMarco, MJ and Lowe, DR 1989b, Stratigraphy and sedimentology of an Early Archean felsic volcanic sequence, eastern Pilbara block, Western Australia, with special reference to the Duffer Formation and implications for crustal evolution: *Precambrian Research*, v. 44, p. 147–169.
- Dixon, JM and Summers, JM 1983, Patterns of total and incremental strain in subsiding troughs: experimental centrifugal models of inter-diapir synclines: *Canadian Journal of Earth Sciences*, v. 20, p. 1843–1861.
- Djokic, T, Van Kranendonk, MJ, Campbell, KA, Walter, MR and Ward, CR 2017, Earliest signs of life on land preserved in ca. 3.5 Ga hot spring deposits: *Nature Communications*, v. 8, article no. 15263, 9p., doi:10.1038/ncomms15263.
- Drabon, N, Lowe, DR, Byerly, GR and Harrington, JA 2017, Detrital zircon geochronology of sandstones of the 3.6–3.2 Ga Barberton greenstone belt: no evidence for older continental crust: *Geology*, v. 45, p. 803–806.
- Duda, J-P, Van Kranendonk, MJ, Thiel, V, Ionescu, D, Strauss, H, Schafer, N and Reitner, N 2016, A rare glimpse of Paleoproterozoic life: geobiology of an exceptionally preserved microbial mat facies from the 3.4 Ga Strelley Pool Formation, Western Australia: *PLoS One*, v. 11, no. 1, article no. 0147629, doi:10.1371/journal.pone.0147629.
- Dunlop, JSR 1978, Shallow-water sedimentation at North Pole, Pilbara, Western Australia, in *Archean cherty metasediments: their sedimentology, micropaleontology, biogeochemistry and significance to mineralization edited by JE Glover and DI Groves*: Extension Service, The University of Western Australia, Perth, p. 30–38.
- Dunlop, JSR and Buick, R 1981, Archean epiclastic sediments derived from mafic volcanic rocks, North Pole, Pilbara Block, Western Australia, in *Archean Geology: Second International Symposium, Perth 1980 edited by JE Glover and DI Groves*: Geological Society of Australia, Special Publication 7, p. 225–233.
- Dunlop, JSR, Milne, VA, Groves, DI and Muir, MD 1978, A new microfossil assemblage from the Archean of Western Australia: *Nature*, v. 274, p. 676–678.
- Duuring, P, Teitler, Y, Hagemann, S and Angerer, T 2016, MRIWA Report Project M426: Exploration targeting for BIF-hosted iron deposits in the Pilbara Craton, Western Australia: Geological Survey of Western Australia, Report 163, 263p.
- Duuring, P, Teitler, Y and Hagemann, SG 2017, Banded iron formation-hosted iron ore deposits of the Pilbara Craton, in *Australian Ore Deposits edited by GN Phillips*: Australasian Institute of Mining and Metallurgy, Monograph 32, p. 345–350.
- Eriksson, KA 1981, Archean platform-to-trough sedimentation, East Pilbara Block, Australia, in *Archean Geology: Second International Symposium, Perth 1980 edited by JE Glover and DI Groves*: Geological Society of Australia, Special Publication 7, p. 235–244.
- Eriksson, KA 1982, Geometry and internal characteristics of Archean submarine channel deposits, Pilbara Block, Western Australia: *Journal of Sedimentary Research*, v. 52, no. 2, p. 383–393.
- Eriksson, KA 1983, Siliciclastic hosted iron formations in the early Archean Barberton and Pilbara sequences: *Journal of the Geological Society of Australia*, v. 30, p. 473–482.
- Eriksson, KA, Kidd, WSF and Krapez, B 1988, Basin analysis in regionally metamorphosed and deformed early Archean terrains: examples from southern Africa and Western Australia, in *New perspectives in basin analysis edited by K Kleinspehn and C Paola*: Springer-Verlag, New York, *Frontiers in sedimentary geology*, p. 371–404.
- Eriksson, KA, Krapež, B and Fralick, PW 1994, Sedimentology of Archean greenstone belts: signatures of tectonic evolution: *Earth-Science Reviews*, v. 37, p. 1–88.
- Eriksson, PG, Condie, KC, van der Westhuizen, W, van der Merwe, R, de Bruijn, H, Nelson, DR, Altermann, W, Catuneanu, O, Bumby, AJ and Lindsay, J 2002, Late Archean superplume events: a Kaapvaal-Pilbara perspective: *Journal of Geodynamics*, v. 34, no. 2, p. 207–247.
- Ernst, RE 2007, Mafic–ultramafic large igneous provinces (LIPs): importance of the pre-Mesozoic record: *Episodes*, v. 30, no. 2, p. 108–114.
- Ernst, RE 2014, Large igneous provinces: Cambridge University Press, Cambridge, UK, 653p.
- Ernst, RE, Buchan, KL and Prokoph, A 2004, Large igneous province record through time, in *The Precambrian Earth: tempos and events edited by PG Eriksson, W Altermann, DR Nelson, WU Mueller and O Catuneanu*: Elsevier, Amsterdam, The Netherlands, *Developments in Precambrian Geology* 12, p. 173–180.
- Farrell, TR 2005, Eastern Creek, WA Sheet 3054: Geological Survey of Western Australia, 1:100 000 Geological Series.
- Farrell, TR 2006, Geology of the Eastern Creek 1:100 000 sheet: Geological Survey of Western Australia, 1:100 000 Geological Series Explanatory Notes, 33p.

- Farrell, TR and Smithies, RH 2005, Noreena Downs, WA Sheet 2953: Geological Survey of Western Australia, 1:100 000 Geological Series.
- Ferguson, KM and Ruddock, I 2001, Mineral occurrences and exploration potential of the East Pilbara: Geological Survey of Western Australia, Report 81, 114p.
- Finucane, KJ 1936, The North Pole mining centre, Pilbara Goldfield: Aerial Geological and Geophysical Survey of Northern Australia, Western Australia Report No 2, 5p.
- Fisher, CM and Vervoort, JD 2018, Using the magmatic record to constrain the growth of continental crust – the Eoarchean zircon Hf record of Greenland: *Earth and Planetary Science Letters*, v. 488, p. 79–91.
- Fitton, MJ, Horwitz, RC and Sylvester, G 1975, Stratigraphy of the early Precambrian in the west Pilbara, Western Australia: CSIRO Minerals Research Laboratories, Division of Mineralogy, Report FP 11, 41p.
- Fortescue Metals Group Limited 2020, Annual Report for the Year Ended 30 June 2020: Report to Australian Securities Exchange, released 24 August 2020, 162p.
- Fowers, C, Kepert, D, Absalom, M and Nitschke, N 2013, Discovery, geology and structural setting of the Nyidinghu iron ore deposit, Hamersley Province, Western Australia, in *Conference proceedings edited by Australian Institute of Mining and Metallurgy: Iron Ore Conference 2013*, Perth, Western Australia, 12–14 August 2013, p. 81–90.
- François, C, Philippot, P, Rey, PF and Rubatto, D 2014, Burial and exhumation during Archean sagduction in the east Pilbara granite–greenstone terrane: *Earth and Planetary Science Letters*, v. 396, p. 235–251.
- Frogtech Geoscience 2017, 2017 Canning Basin SEEBASE study and GIS data package: Geological Survey of Western Australia, Report 182, 297p.
- Furnell, R 1982, 1981 Annual Report, Lalla Rookh Temporary Reserve 7437H, Shaw River Temporary Reserves 7438H, George Range Temporary Reserve 7439H, Temporary Reserves for gold and other minerals 8119H – 8152H, Marble Bar District – Western Australia: Anaconda Australia Inc.: Geological Survey of Western Australia, Statutory mineral exploration report A11184, 122p.
- Furnes, H, Banerjee, NR, Staudigel, H, Muehlenbachs, K, McLoughlin, N, De Wit, M and Van Kranendonk, MJ 2007, Comparing petrographic signatures of bioalteration in recent to Mesoproterozoic pillow lavas: tracing subsurface life in oceanic igneous rocks: *Precambrian Research*, v. 158, p. 156–176.
- Furnes, H, De Wit, M and Dilek, Y 2014, Four billion years of ophiolites reveal secular trends in oceanic crust formation: *Geoscience Frontiers*, v. 5, p. 571–603.
- Furnes, H, Dilek, Y and Wit, M de 2015, Precambrian greenstone sequences represent different ophiolite types: *Gondwana Research*, v. 27, no. 2, p. 649–685, doi:10.1016/j.jgr.2013.06.004.
- García Ruiz, JM, Carnerup, A, Christy, AG, Welham, NJ and Hyde, ST 2002, Morphology: an ambiguous indicator of biogenicity: *Astrobiology*, v. 2, p. 353–369.
- Garcia Ruiz, JM, Hyde, ST, Carnerup, AM, Christy, AG, Van Kranendonk, MJ and Welham, NJ 2003, Self-assembled silica-carbonate structures and detection of ancient microfossils: *Science*, v. 302, p. 1194–1197.
- Gardiner, NJ, Hickman, AH, Kirkland, CL, Lu, Y, Johnson, T and Zhao, J-X 2017, Processes of crust formation in the early Earth imaged through Hf isotopes from the East Pilbara Terrane: *Precambrian Research*, v. 297, p. 56–76, doi:10.1016/j.precamres.2017.05.004.
- Gardiner, NJ, Hickman, AH, Kirkland, CL, Lu, Y, Johnson, TE and Wingate, MT 2018, New Hf isotope insights into the Paleoproterozoic magmatic evolution of the Mount Edgar Dome, Pilbara Craton: Implications for early Earth and crust formation processes: Geological Survey of Western Australia, Report 181, 41p.
- Gauger, T, Konhauser, K and Kappler, A 2015, Protection of phototrophic iron(II)-oxidizing bacteria from UV irradiation by biogenic iron(III) minerals: implications for early Archean banded iron formation: *Geology*, v. 43, p. 1067–1170.
- Geolnicht, NM, Groves, IM, Groves, DI, Ho, SE and McNaughton, NJ 1988, A comparison between mesothermal gold deposits of the Yilgarn Block and gold mineralization at Telfer and Miralga Creek, Western Australia – indirect evidence for a non-magmatic origin for greenstone-hosted gold deposits, in *Advances in understanding Precambrian gold deposits*, vol. 2 edited by SE Ho and DI Groves: Geology Department and University Extension, The University of Western Australia, Publication 12, p. 23–40.
- Geological Survey of Western Australia 2017, 1:500 000 tectonic units of Western Australia: Geological Survey of Western Australia, digital data layer, <www.dmirs.wa.gov.au/geoview>.
- Glass, BP and Simonson, BM 2012, Distal impact ejecta layers: spherules and more: *Elements*, v. 8, p. 43–48.
- Glass, BP and Simonson, BM 2013, Distal impact ejecta layers: a record of large impacts in sedimentary deposits: Springer, Berlin, Germany, *Impact Studies by Koeberl, C.*, 716p.
- Glikson, AY 1971, Primitive Archean element distribution patterns: chemical evidence and geotectonic significance: *Earth and Planetary Science Letters*, v. 12, p. 309–320.
- Glikson, AY 1972, Early Precambrian evidence of a primitive ocean crust and island nuclei of sodic granite: *Geological Society of America Bulletin*, v. 83, no. 11, p. 3323–3344.
- Glikson, AY 1978, On the basement of Canadian greenstone belts: *Geoscience Canada*, v. 5, no. 1, p. 3–12.
- Glikson, AY 2001, The astronomical connection of terrestrial evolution: crustal effects of post-3.8 Ga mega-impact clusters and evidence for major 3.2 Ga bombardment of the Earth–Moon system: *Journal of Geodynamics*, v. 32, p. 205–229.
- Glikson, AY 2004, Early Precambrian asteroid impact-triggered tsunamis: excavated seabed debris flows exotic boulders and turbulence features associated with 3.47–2.47 Ga-old asteroid impact fallout units, Pilbara Craton, Western Australia: *Astrobiology*, v. 4, p. 1–32.
- Glikson, AY 2005a, Geochemical and isotopic signatures of Archean to Palaeoproterozoic extraterrestrial impact ejecta/fallout units: *Australian Journal of Earth Sciences*, v. 52, p. 785–798.
- Glikson, AY 2005b, Geochemical signatures of Archean to Early Proterozoic Maria-scale oceanic impact basins: *Geology*, v. 33, p. 125–128, doi:10.1130/G21034.1.
- Glikson, AY 2006, Asteroid impact ejecta units overlain by iron-rich sediments in 3.5–2.4 Ga terrains, Pilbara and Kaapvaal cratons: accidental or cause–effect relationships? *Earth and Planetary Science Letters*, v. 246, p. 149–160.
- Glikson, AY 2007a, Early Archean asteroid impacts on Earth: stratigraphic and isotopic age correlations and possible geodynamic consequences, in *Earth's oldest rocks edited by MJ Van Kranendonk, VC Bennett and RH Smithies*: Elsevier BV, Burlington, Massachusetts, USA, *Developments in Precambrian Geology* 15, p. 1087–1103.
- Glikson, AY 2007b, Siderophile element patterns, PGE nuggets and vapour condensation effects in Ni-rich quench chromite-bearing microkrystite spherules, 3.24 Ga S3 impact unit, Barberton Greenstone Belt, Kaapvaal Craton, South Africa: *Earth and Planetary Science Letters*, v. 253, p. 1–16.
- Glikson, AY 2008, Field evidence of Eros-scale asteroids and impact-forcing of Precambrian geodynamic episodes, Kaapvaal (South Africa) and Pilbara (Western Australia) Cratons: *Earth and Planetary Science Letters*, v. 267, p. 558–570.
- Glikson, AY 2013, The asteroid impact connection of planetary evolution: With special reference to large Precambrian and Australian impacts: Springer, The Netherlands, *SpringerBriefs in Earth Sciences* XII, 149p., doi:10.1007/978-94-007-6328-9.
- Glikson, AY 2014, The Archean: Geological and geochemical windows into the early Earth: Springer, The Netherlands, *SpringerBriefs in Earth Sciences* IX, 238p., doi:10.1007/978-3-319-07908-0.
- Glikson, AY, Allen, C and Vickers, J 2004, Multiple 3.47-Ga-old asteroid impact fallout units, Pilbara Craton, Western Australia: *Earth and Planetary Science Letters*, v. 21, p. 383–396.

- Glikson, AY, Davy, R and Hickman, AH 1986, Geochemical data files of Archean volcanic rocks, Pilbara Block, Western Australia, BMR (Geoscience Australia) Record 1986/014, 136p.
- Glikson, AY, Davy, R, Hickman, AH, Pride, C and Jahn, B 1987, Trace elements geochemistry and petrogenesis of Archean felsin igneous units, Pilbara Block, Western Australia, BMR (Geoscience Australia) Record 1987/030, 63p.
- Glikson, AY, Duck, LJ, Golding, SD, Hofmann, A, Bolhar, R, Webb, RE, Baianco, JCF and Sly, LI 2008, Microbial remains in some earliest Earth rocks: Comparison with a potential modern analogue: *Precambrian Research*, v. 164, p. 187–200, doi:10.1016/j.precamres.2008.05.002.
- Glikson, AY and Hickman, AH 1981a, Geochemical stratigraphy and petrogenesis of Archean basic-ultrabasic volcanic units, eastern Pilbara Block, Western Australia: Geological Society of Australia Special Publications, v. 7, p. 287–300.
- Glikson, AY and Hickman, AH 1981b, Geochemistry of Archean volcanic successions, eastern Pilbara Block, Western Australia, BMR (Geoscience Australia) Record 1981/036, 83p.
- Glikson, AY, Hickman, AH, Evand, NJ, Kirkland, CL, Park, J-W, Rapp, R and Romano, SS 2016, A new ~3.46 Ga asteroid impact ejecta unit at Marble Bar, Pilbara Craton, Western Australia: A petrological, microprobe, and laser ablation ICPMS study: *Precambrian Research*, v. 279, p. 103–122.
- Glikson, AY and Vickers, J 2006, The 3.26 – 3.24 Ga Barberton asteroid impact cluster: Tests of tectonic and magmatic consequences, Pilbara Craton, Western Australia: *Earth and Planetary Science Letters*, v. 241, no. 1–2, p. 11–20.
- Glikson, AY and Vickers, J 2010, Asteroid impact connections of crustal evolution: *Australian Journal of Earth Sciences*, v. 57, p. 79–95.
- Glikson, M, Hickman, AH, Duck, LJ, Golding, SD and Webb, RE 2012, Integration of observational and analytical methodologies to characterize organic matter in early Archean rocks: Distinguishing biological from abiotically synthesized carbonaceous matter structures, in *Earliest Life on Earth: Habitats, environments and methods of detection edited by SD Golding and M Glikson*: Springer Science and Business Media, Amsterdam, The Netherlands, p. 209–238.
- Goodwin, AM 1968, Archean protocontinental growth and early crustal history of the Canadian Shield: International Geological Congress, 23rd, Prague, v. I, p. 69–89.
- Gorman, BE, Pearce, TH and Birkett, TC 1978, On the structure of Archean greenstone belts: *Precambrian Research*, v. 6, p. 23–41.
- Green, MG, Sylvester, PJ and Buick, R 2000, Growth and recycling of early Archean continental crust: Geochemical evidence from the Coonterunah and Warrawoona Groups, Pilbara Craton, Australia: *Tectonophysics*, v. 322, no. 1, p. 69–88.
- Grey, K, Clarke, JDA and Hickman, AH 2012, The proposed Dawn of Life geotourism trail, Marble Bar, Pilbara Craton, Western Australia – geology and evidence for early life: Geological Survey of Western Australia, Record 2012/9, 27p.
- Grey, K, Hickman, AH, Van Kranendonk, MJ and Freeman, MJ 2002, 3.45 billion year-old stromatolites in the Pilbara region of Western Australia: Proposals for site protection and public access: Geological Survey of Western Australia, Record 2002/17, 11p.
- Grey, K, Roberts, FI, Freeman, MJ, Hickman, AH, Van Kranendonk, MJ and Bevan, AWR 2010, Management plan for state geoheritage reserves: Geological Survey of Western Australia, Record 2010/13, 23p.
- Griffin, WL, Belousova, EA, O'Neill, C, O'Reilly, SY, Malkovets, V, Pearson, NJ, Spetsius, S and Wilde, SA 2014, The world turns over: Hadean–Archean crust–mantle evolution: *Lithos*, v. 189, p. 2–15, doi:10.1016/j.lithos.2013.08.018.
- Griffin, WL, Pearson, NJ, Belousova, EA, Jackson, SE, O'Reilly, SY, van Achterbergh, E and Shee, SR 2000, The Hf isotope composition of cratonic mantle: LAM-MC-ICPMS analysis of zircon megacrysts in kimberlites: *Geochimica et Cosmochimica Acta*, v. 64, no. 1, p. 133–147, doi:10.1016/S0016-7037(99)00343-9.
- Gross, GA 1980, A classification of iron formations based on depositional environments: *The Canadian Mineralogist*, v. 18, no. 2, p. 215.
- Groves, DI and Blatt, WD 1984, Spatial and temporal variations of Archean metallogenic associations in terms of evolution of granitoid–greenstone terrains with particular emphasis on the Western Australian Shield, in *Archean geochemistry edited by A Kroner*, GN Hanson and AM Goodwin: Springer-Verlag, Berlin, Germany, p. 73–98.
- Groves, DI, Dunlop, JSR and Buick, R 1981, An early habitat of life: *Scientific American*, v. 245, p. 64–73.
- Groves, DI, Phillips, GN, Ho, SE, Henderson, CA, Clark, ME and Woad, GM 1984, Controls on distribution of Archean hydrothermal gold deposits in Western Australia, in *Proceedings edited by R Foster*: Gold '82: the geology, geochemistry and genesis of gold deposits, Harare, Zimbabwe, 24 May 1982: Geological Society of Zimbabwe, p. 689–712.
- Gruau, G, Jahn, BM, Glikson, AY, Davy, R, Hickman, AH and Chauvel, C 1987, Age of the Archean Talga-Talga subgroup, Pilbara Block, Western Australia, and the early evolution of the mantle: new Sm–Nd isotopic evidence: *Earth and Planetary Science Letters*, v. 85, p. 105–116.
- Guitreau, M, Blichert-Toft, J, Martin, H, Mojzsis, SJ and Albarède, F 2012, Hafnium isotope evidence from Archean granitic rocks for deep-mantle origin of continental crust: *Earth and Planetary Science Letters*, v. 337, p. 211–223.
- Guj, P, McIntosh, D and Stephenson, P 1983, De Grey Gold Project, Mt Grant Prospect EL 45/50, Pilbara Mineral Field, W.A., First Progress Report to August 31, 1983: Technical Report: Carpentaria Exploration Company: Geological Survey of Western Australia, Statutory mineral exploration report A13799, 226p.
- Guj, P, McIntosh, D and Stephenson, P 1984, De Grey Gold Project, Mt Grant Prospect EL 45/50, Pilbara Mineral Field, W.A., Second Progress Report to December 31, 1983: Technical Report: Carpentaria Exploration Company: Geological Survey of Western Australia, Statutory mineral exploration report A13800, 118p.
- Gutzmer J, Banks D, de Kock MQ, McClung CR, Strauss H, Mezger K 2006, The origin and paleoenvironmental significance of stratabound barites from the Mesoarchean Fig Tree Group, Barberton Mountainland, South Africa: SSAGI–V, South America Symposium on Isotope Geology, 24–27 April 2006, Uruguay, Abstract Volume, p. 311–314.
- Hallberg, JA 1974, Whole-rock geochemical orientation trip to the Pilbara: CSIRO Mineral Research Laboratories, Division of Mineralogy, Report FP3.
- Hamilton, PJ, Evensen, NM, O'Nions, RK, Glikson, AY and Hickman, AH 1981, Sm–Nd dating of the North Star basalt, Warrawoona Group, Pilbara Block, Western Australia, in *Archean Geology: Second International Symposium, Perth 1980 edited by JE Glover and DI Groves*: Geological Society of Australia, Special Publication 7, p. 187–192.
- Hamilton, WB 2007, Earth's first two billion years – the era of internally mobile crust, in *4-D framework of continental crust edited by RD Hatcher, MP Carlson, JH McBride and JR Martinez Catalan*: Geological Society of America, Memoir 200, p. 233–296, doi:10.1130/2007.1200(13).
- Hao, J, Sverjensky, DA and Hazen, RM 2017, A model for late Archean chemical weathering and world average river water: *Earth and Planetary Science Letters*, v. 457, p. 191–203.
- Harris, AC, White, NC, McPhie, J, Bull, SW, Line, MA, Skrzeczynski, R, Mernagh, TP and Tosdal, RM 2009, Early Archean hot springs above epithermal veins, North Pole, Western Australia: new insights from fluid inclusions microanalysis: *Economic Geology*, v. 104, no. 6, p. 793–814, doi:10.2113/gsecongeo.104.6.793.
- Harris, PT, MacMillan-Lawler, M and Baker, EK 2014, Geomorphology of the oceans: *Marine Geology*, v. 352, p. 4–24.
- Hassler, SW, Simonson, BM, Sumner, DY and Bodin, L 2011, Paraburdoo spherule layer (Hamersley Basin, Western Australia): distal ejecta from a fourth large impact near the Archean–Proterozoic boundary: *Geology*, v. 39, no. 4, p. 307–310.
- Heinrich, CA 2015, Witwatersrand gold deposits formed by acid rain, anoxic rivers, and Archean life: *Nature Geoscience*, v. 8, p. 206–209.

- Henderson, P 1984, Rare earth element geochemistry: Developments in Geochemistry 2, Elsevier Science Publishing, The Netherlands, 510p.
- Hickman, AH 1973, The North Pole barite deposits, Pilbara Goldfield: Geological Survey of Western Australia, Annual Report 1972, p. 57–60.
- Hickman, AH 1975a, Precambrian structural geology of part of the Pilbara Region, in Annual report for the year 1974: Geological Survey of Western Australia, p. 68–73.
- Hickman, AH 1975b, Explanatory notes on the Nullagine 1:250 000 geological sheet: Geological Survey of Western Australia, Record 1975/5, 50p.
- Hickman, AH 1977a, New and revised definitions of rock units in the Warrawoona Group, Pilbara Block, in Annual report for the year 1976: Geological Survey of Western Australia, p. 53.
- Hickman, AH 1977b, Barite deposits near Cooke Bluff Hill, Port Hedland 1:250 000 sheet: Geological Survey of Western Australia, Record 1976/22, 26p.
- Hickman, AH (compiler) 1978, Nullagine, Western Australia (2nd edition): Geological Survey of Western Australia, 1:250 000 Geological Series Explanatory Notes, 22p.
- Hickman, AH 1980a, Excursion guide – Archaean geology of the Pilbara Block: Second International Archaean Symposium, Perth 1980: Geological Society of Australia, WA Division, Perth, Western Australia, 55p.
- Hickman, AH 1980b, Crustal evolution of the Pilbara Block, in Second International Archaean Symposium, Perth 1980, Extended Abstracts, edited by JE Glover and DI Groves: Geological Society of Australia and IGCP Archaean Geochemistry Project, Perth 1980, p. 78–79.
- Hickman, AH 1980c, Lithological map and stratigraphic interpretation of the Pilbara Block (1:1 000 000 scale), in Geology of the Pilbara Block and its environs by AH Hickman: Geological Survey of Western Australia, Bulletin 127, Plates 1A and 1B.
- Hickman, AH 1980d, Major structural units of the Pilbara Block (inset to Plates 1A, 1B), in Geology of the Pilbara Block and its environs by AH Hickman: Geological Survey of Western Australia, Bulletin 127, 268p.
- Hickman, AH 1980e, Archaean stratigraphic successions in various parts of the Pilbara Block (correlation chart), in Geology of the Pilbara Block and its environs by AH Hickman: Geological Survey of Western Australia, Bulletin 127, Plate 2.
- Hickman, AH 1981, Crustal evolution of the Pilbara Block, in Archaean Geology: Second International Symposium, Perth 1980 edited by JE Glover and DI Groves: Geological Society of Australia, Special Publication 7, p. 57–69.
- Hickman, AH 1983, Geology of the Pilbara Block and its environs: Geological Survey of Western Australia, Bulletin 127, 268p.
- Hickman, AH 1984, Archaean diapirism in the Pilbara Block, Western Australia, in Precambrian tectonics illustrated edited by A Kröner and RE Greiling: Schweizerbart'sche Verlagsbuchhandlung, Stuttgart, Germany, p. 113–127.
- Hickman, AH 1990, Geology of the Pilbara Craton: Granite–greenstone terrain (Pilbara and Hamersley Basin), in Excursion guidebook: Third International Archaean Symposium, Perth 1990 (17–21 September) edited by SE Ho, JE Glover, JS Myers and JR Muhling: The Geology Department and University Extension, The University of Western Australia, Publication 21, p. 2–13.
- Hickman, AH 1997, A revision of the stratigraphy of Archaean greenstone successions in the Roebourne–Whundo area, west Pilbara, in Geological Survey of Western Australia Annual Review 1996–97: Geological Survey of Western Australia, p. 76–81.
- Hickman, AH 1999, New tectono-stratigraphic interpretations of the Pilbara Craton, Western Australia, in GSWA 99 extended abstracts: new geological data for WA explorers: Geological Survey of Western Australia, Record 1999/6, p. 4–6.
- Hickman, AH 2001a, The West Pilbara Granite–Greenstone Terrane and its place in the Pilbara Craton, in Extended Abstracts – 4th International Archaean Symposium, Perth, 24–28 September 2001 edited by KF Cassidy, J Dunphy and MJ Van Kranendonk: AGSO (Geoscience Australia), Record 2001/37, p. 319–321.
- Hickman, AH 2001b, East Pilbara diapirism: New evidence from mapping, in GSWA 2001 extended abstracts: new geological data for WA explorers edited by Geological Survey of Western Australia: Geological Survey of Western Australia, Record 2001/5, p. 23–25.
- Hickman, AH 2001c, Geology of the Dampier 1:100 000 sheet: Geological Survey of Western Australia, 1:100 000 Geological Series Explanatory Notes, 39p.
- Hickman, AH 2002, Geology of the Roebourne 1:100 000 sheet: Geological Survey of Western Australia, 1:100 000 Geological Series Explanatory Notes, 35p.
- Hickman, AH 2004, Two contrasting granite–greenstones terranes in the Pilbara Craton, Australia: Evidence for vertical and horizontal tectonic regimes prior to 2900 Ma: Precambrian Research, v. 131, p. 153–172.
- Hickman, AH 2005, Evidence of early life from international collaborative drilling in the Pilbara Craton: Geological Survey of Western Australia, Annual Review 2004–05, p. 27–32.
- Hickman, AH 2008, Regional review of the 3426–3350 Ma Strelley Pool Formation, Pilbara Craton, Western Australia: Geological Survey of Western Australia, Record 2008/15, 27p.
- Hickman, AH 2010, Marble Bar, WA Sheet SF50-8 (3rd edition): Geological Survey of Western Australia, 1:250 000 Geological Series.
- Hickman, AH 2011, Pilbara Supergroup of the East Pilbara Terrane, Pilbara Craton: Updated lithostratigraphy and comments on the influence of vertical tectonics, in Geological Survey of Western Australia Annual Review 2009–10: Geological Survey of Western Australia, p. 50–59.
- Hickman, AH 2012, Review of the Pilbara Craton and Fortescue Basin, Western Australia: Crustal evolution providing environments for early life: Island Arc, v. 21, p. 1–31.
- Hickman, AH 2013a, North Shaw, WA Sheet 2755 (2nd edition): Geological Survey of Western Australia, 1:100 000 Geological Series.
- Hickman, AH 2013b, Split Rock, WA Sheet 2854 (2nd edition): Geological Survey of Western Australia, 1:100 000 Geological Series.
- Hickman, AH 2013c, Wodgina, WA Sheet 2655 (2nd edition): Geological Survey of Western Australia, 1:100 000 Geological Series.
- Hickman, AH 2016, Northwest Pilbara Craton: A record of 450 million years in the growth of Archean continental crust: Geological Survey of Western Australia, Report 160, 104p.
- Hickman, AH and Bagas, L 1999, Geological evolution of the Palaeoproterozoic Talbot Terrane and adjacent Meso- and Neoproterozoic successions, Paterson Orogen, Western Australia: Geological Survey of Western Australia, Report 71, 91p.
- Hickman, AH, Chin, RJ and Gibson, DL 1983, Yarrie, WA.: Geological Survey of Western Australia, 1: 250 000 Geological Series Explanatory Notes, 40p.
- Hickman, AH and Gibson, DL (compilers) 1982, Port Hedland – Bedout Island, Western Australia (2nd edition): Geological Survey of Western Australia, 1:250 000 Geological Series Explanatory Notes, 28p.
- Hickman, AH and Harrison, PH 1986, A review of the occurrence and potential for Precambrian conglomerate-hosted gold mineralization within Western Australia, in Geocongress '86: extended abstracts, Johannesburg, Republic of South Africa, 7–11 July: Geological Society of South Africa, p. 301–319.
- Hickman, AH, Huston, DL, Van Kranendonk, MJ and Smithies, RH 2006a, Geology and mineralization of the west Pilbara – a field guide: Geological Survey of Western Australia, Record 2006/17, 50p.
- Hickman, AH and Kojan, CJ 2003, Geology of the Pindri Hills 1:100 000 sheet: Geological Survey of Western Australia, 1:100 000 Geological Series Explanatory Notes, 36p.
- Hickman, AH and Lipple, SL 1975, Explanatory notes on the Marble Bar 1:250 000 geological sheet, Western Australia: Geological Survey of Western Australia, Record 1974/20, 90p.
- Hickman, AH and Lipple, SL 1978a, Marble Bar, WA Sheet SF50-8 (2nd edition): Geological Survey of Western Australia, 1:250 000 Geological Series.
- Hickman, AH and Lipple, SL (compilers) 1978b, Marble Bar, Western Australia (2nd edition): Geological Survey of Western Australia, 1:250 000 Geological Series Explanatory Notes, 24p.
- Hickman, AH and Smithies, RH 2001, Roebourne, Western Australia (2nd edition): Geological Survey of Western Australia, 1:250 000 Geological Series Explanatory Notes, 52p.

- Hickman, AH, Smithies, RH and Huston, DL 2000, Archean geology of the west Pilbara granite-greenstone terrane and the Mallina Basin, Western Australia – a field guide: Geological Survey of Western Australia, Record 2000/9, 61p.
- Hickman, AH, Smithies, RH, Pike, G, Farrell, TR and Beintema, KA 2001, Evolution of the West Pilbara granite-greenstone terrane and Mallina Basin, Western Australia – a field guide: Geological Survey of Western Australia, Record 2001/16, 65p.
- Hickman, AH, Smithies, RH and Strong, CA 2006, Interpreted bedrock geology of the northwestern Pilbara Craton (1:250 000): Geological Survey of Western Australia, Report 92 (Plate 1).
- Hickman, AH, Smithies, RH and Tyler, IM 2010, Evolution of active plate margins: West Pilbara Superterrane, De Grey Superbasin, and the Fortescue and Hamersley Basins – a field guide: Geological Survey of Western Australia, Record 2010/3, 74p.
- Hickman, AH and Strong, CA 1998, Structures in the Cape Preston area, northwest Pilbara Craton – new evidence for a convergent margin, *in* Geological Survey of Western Australia Annual Review 1997–98: Geological Survey of Western Australia, p. 77–84.
- Hickman, AH and Strong, CA 2001, Dampier – Barrow Island, WA Sheet SF50-2 and part of Sheet SF 50-1 (2nd edition): Geological Survey of Western Australia, 1:250 000 Geological Series.
- Hickman, AH and Strong, CA 2003, Dampier – Barrow Island, Western Australia: Geological Survey of Western Australia, 1:250 000 Geological Series Explanatory Notes, 75p.
- Hickman, AH and Van Kranendonk, MJ 2004, Diapiric processes in the formation of Archean continental crust, east Pilbara granite-greenstone terrane, Australia, *in* The Precambrian Earth: tempos and events *edited by* PG Eriksson, W Altermann, DR Nelson, WU Mueller and O Catuneanu: Elsevier, Amsterdam, The Netherlands, Developments in Precambrian Geology 12, p. 54–75.
- Hickman, AH and Van Kranendonk, MJ 2008a, Archean crustal evolution and mineralization of the northern Pilbara Craton – a field guide: Geological Survey of Western Australia, Record 2008/13, 79p.
- Hickman, AH and Van Kranendonk, MJ 2008b, Marble Bar, WA Sheet 2855: Geological Survey of Western Australia, 1:100 000 Geological Series.
- Hickman, AH and Van Kranendonk, MJ 2012, Early earth evolution: evidence from the 3.5 – 1.8 Ga geological history of the Pilbara region of Western Australia: Episodes, v. 35, no. 1, p. 283–297, doi:10.18814/epiugs/2012/v35i1/028.
- Hickman, AH, Van Kranendonk, MJ and Grey, K 2011, State Geoheritage Reserve R50149 (Trendall Reserve), North Pole, Pilbara Craton, Western Australia – geology and evidence for early Archean life: Geological Survey of Western Australia, Record 2011/10, 32p.
- Hoashi, M, Bevacqua, DC, Otake, T, Watanabe, Y, Hickman AH, Utsunomiya, S and Ohmoto, H 2009, Primary hematite formation in an oxygenated sea 3.46 billion years ago: Nature Geosciences, v. 2, p. 301–306.
- Hofmann, AW 1997, Mantle geochemistry: the message from oceanic volcanism: Nature, v. 385, p. 219–229.
- Hofmann, HJ, Grey, K, Hickman, AH and Thorpe, R 1999, Origin of 3.45 Ga coniform stromatolites in the Warrawoona Group, Western Australia: Geological Society of America Bulletin, v. 111, p. 1256–1262.
- Holland, HD 2002, Volcanic gases, black smokers and the Great Oxidation Event: Geochimica et Cosmochimica Acta, v. 66, no. 21, p. 3811–3826.
- Horwitz, RC 1979, The Whim Creek Group, a discussion: Royal Society of Western Australia Journal, v. 61, p. 67–72.
- Horwitz, RC 1990, Palaeogeographic and tectonic evolution of the Pilbara Craton, Northwestern Australia: Precambrian Research, v. 48, p. 327–340.
- Hunter, DR 1957, The geology, petrology and classification of the Swaziland granites and gneisses: Transactions of the Geological Society of South Africa, v. 60, p. 85–120.
- Huston, DL, Blewett, RS and Champion, DC 2012, Australia through time: a summary of its tectonic and metallogenic evolution: Episodes, v. 35, no. 1, p. 23–43.
- Huston, DL, Blewett, RS, Mernagh, TP, Sun, S-S and Kamprad, J 2001a, Gold deposits of the Pilbara Craton: Australian Geological Survey Organisation (Geoscience Australia), Record 2001/10, 86p.
- Huston, DL, Blewett, RS and Sun, S-S 2001b, Metallogeneses and tectonic evolution of the North Pilbara Craton, Western Australia, *in* Extended Abstracts – 4th International Archean Symposium, Perth, 24–28 September 2001 *edited by* KF Cassidy, J Dunphy and MJ Van Kranendonk: AGSO (Geoscience Australia), Record 2001/37, p. 435–437.
- Huston, DL, Blewett, RS, Sweetapple, M, Brauhart, C, Cornelius, H and Collins, PLF 2001c, Metallogeneses of the North Pilbara granite-greenstones, Western Australia – a field guide: Geological Survey of Western Australia, Record 2001/11, 87p.
- Huston, DL, Brauhart, CW, Dreier, SL, Davidson, GJ and Groves, DI 2001d, Metal leaching and inorganic sulphate reduction in volcanic-hosted massive sulphide mineral systems: evidence from the paleo-Archean Panorama district, Western Australia: Geology, v. 29, p. 687–690.
- Huston, DL, Morant, P, Cummins, B, Baker, D and Mernaugh, TP 2007, Paleoproterozoic mineral deposits of the Pilbara Craton: genesis, tectonic environment and comparison with younger deposits, *in* Earth's oldest rocks *edited by* MJ Van Kranendonk, VC Bennett and RH Smithies: Elsevier BV, Burlington, Massachusetts, USA, Developments in Precambrian Geology 15, p. 217–230.
- Huston, DL, Sun, S-S, Blewett, R, Hickman, AH, Van Kranendonk, MJ, Phillips, D, Baker, D and Brauhart, C 2002, The timing of mineralization in the Archean North Pilbara Terrain, Western Australia: Economic Geology, v. 97, p. 733–755.
- Huston, DL, Wyche, NL, Hickman, AH and Norman, M 2017, Pilbara Craton geology and metallogeny, *in* Australian Ore Deposits *edited by* GN Phillips: Australasian Institute of Mining and Metallurgy, Monograph 32, p. 325–330.
- Iizuka, T, Yamaguchi, T, Itano, K, Hibiya, Y and Suzuki, K 2017, What Hf isotopes in zircon tell us about crust-mantle evolution: Lithos, 274–275, p. 304–327, doi:10.1016/j.lithos.2017.01.006.
- Ingram, PAJ 1977, A summary of the geology of a portion of the Pilbara Goldfield, Western Australia, *in* The Archean: Search for the beginning *edited by* GJH McCall: Dowden, Hutchinson and Ross, Stroudsburg, Pennsylvania, US, p. 208–216.
- Isozaki, Y, Kabashima, T, Ueno, Y, Kitajima, K, Maruyama, S, Kato, Y, and Terabayashi, M, 1997, Early Archean mid-ocean ridge rocks and early life in the Pilbara Craton, W. Australia: Eos, v. 78, p. 399.
- Isozaki, Y, Maruyama, S and Kimura, G 1991, Middle Archean (3.3 Ga) Cleaverville accretionary complex in northwestern Pilbara Block, Western Australia: Eos, v. 72, p. 542.
- Jahn, B, Glikson, AY, Peucat, JJ and Hickman, AH 1981, REE geochemistry and isotopic data of Archean silicic volcanics and granitoids from the Pilbara Block, Western Australia: implications for the early crustal evolution: Geochimica et Cosmochimica Acta, v. 45, no. 9, p. 1633–1652.
- Johnson, IM, Watanabe, Y, Stewart, B and Ohmoto, H 2009, Earth's oldest (~3.4 Ga) lateritic paleosol in the Pilbara Craton, Western Australia, *in* Challenges to Our Volatile Planet: Goldschmidt 2009, Davos, Switzerland, 21–26 June 2009, Abstracts, A601.
- Johnson, IM, Watanabe, Y, Yamaguchi, K, Hamasaki, H and Ohmoto, H 2008, Discovery of the oldest (~3.4 Ga) lateritic paleosols in the Pilbara Craton, Western Australia, *in* Abstracts and Programs: Geological Society of America, Joint Annual Meeting, Houston, Texas, 29 September – 10 October 2008, p. 143.
- Johnson, SP, Cutten, HN, Tyler, IM, Korsch, RJ, Thorne, AM, Blay, OA, Kennett, BLN, Blewett, RS, Joly, A, Dentith, MC, Aitken, ARA, Goodwin, JA, Salmon, M, Reading, A, Boren, G, Ross, J, Costelloe, RD and Fomin, T 2011, Preliminary interpretation of deep seismic reflection lines 10GA-CP2 and 10GA-CP3: Crustal architecture of the Gascoyne Province, and Edmund and Collier Basins, *in* Capricorn Orogen seismic and magnetotelluric (MT) workshop 2011: extended abstracts *edited by* SP Johnson, A Thorne and IM Tyler: Geological Survey of Western Australia, Record 2011/25, p. 49–60.

- Johnson, SP, Sheppard, S, Rasmussen, B, Wingate, MTD, Kirkland, CL, Muhling, JR, Fletcher, IR and Belousova, E 2010, The Glenburgh Orogeny as a record of Paleoproterozoic continent–continent collision: Geological Survey of Western Australia, Record 2010/5, 54p.
- Johnson, SP, Thorne, AM, Tyler, IM, Korsch, RJ, Kennett, BLN, Cutten, HN, Goodwin, J, Blay, OA, Blewett, RS, Joly, A, Dentith, MC, Aitken, ARA, Holzschuh, J, Salmon, M, Reading, A, Heinson, G, Boren, G, Ross, J, Costelloe, RD and Fomin, T 2013, Crustal architecture of the Capricorn Orogen, Western Australia and associated metallogeny: *Australian Journal of Earth Sciences*, v. 60, no. 6–7, p. 681–705, doi:10.1080/08120099.2013.826735.
- Johnson, TE, Brown, M, Gardiner, NJ, Kirkland, CL and Smithies, RH 2017, Earth's first stable continents did not form by subduction: *Nature*, v. 543, no. 7644, p. 239–242.
- Jones, CB 1990, Coppin Gap copper–molybdenum deposit: Australasian Institute of Mining and Metallurgy, Monograph, v. 14, p. 141–144.
- Jones, FH 1938, Aerial, geological and geophysical survey of Northern Australia: The Warrawoona area, Pilbara Gold-field, Western Australia: Government Printer, Canberra, ACT, Report 20, 10p. + 3 plates.
- Jones-Zimmerlin, S, Simonson, BM, Kreiss-Tomkins, D and Garson, D 2006, Using impact spherule layers to correlate sedimentary successions: A case study of the Neoproterozoic Jeerinah layer (Western Australia): *South African Journal of Geology*, v. 109, no. 12, p. 245–261.
- Kabashima, T, Isozaki, Y, Hirata, T, Maruyama, S, Kiminami, K and Nishimura, Y 2003, U–Pb zircon ages by laser ablation ICP-MS techniques from the Archean felsic intrusive and volcanic rocks in the North Pole Area, Western Australia: *Journal of Geography*, v. 112, p. 1–17.
- Kambhu, D and Simonson, BM 2013, Spatial variation in spherule sizes in distal ejecta layers close to the Archean–Proterozoic boundary (Abstract no. 1427), in *Proceedings: 44th Lunar and Planetary Science Conference*, Texas, Houston, USA, 18–22 March 2013, 2p.
- Kato, Y and Nakamura, K 2003, Origin and global tectonic significance of Early Archean cherts from the Marble Bar greenstone belt, Pilbara Craton, Western Australia: *Precambrian Research*, v. 125, p. 191–243.
- Kato, Y, Suzuki, K, Nakamura, K, Hickman, AH, Nedachi, M, Kusakabe, M, Bevacqua, DC and Ohmoto, H 2009, Hematite formation by oxygenated groundwater more than 2.76 billion years ago: *Earth and Planetary Science Letters*, v. 278, p. 40–49.
- Kemp, AIS, Hawkesworth, CJ, Collins, WJ, Gray, CM, Blevin, PL and EIMF 2009, Isotopic evidence for rapid continental growth in an extensional accretionary orogen: the Tasmanides, eastern Australia: *Earth and Planetary Science Letters*, v. 284, no. 3–4, p. 455–466.
- Kemp, AIS, Hickman, AH and Kirkland, CL 2015b, Early evolution of the Pilbara Craton, Western Australia, from hafnium isotopes in detrital and xenocrystic zircons: Geological Survey of Western Australia, Report 151, 26p.
- Kemp, AIS, Hickman, AH, Kirkland, CL and Vervoort, JD 2015a, Hf isotopes in detrital and xenocrystic zircons of the Pilbara Craton provide no evidence for Hadean continents: *Precambrian Research*, v. 261, p. 112–126.
- Kemp, AIS, Vervoort, JD, Bjorkman, KE and Iaccheri, LM 2017, Hafnium isotope characteristics of Palaeoproterozoic zircon OG1/OGC from the Owens Gully Diorite, Pilbara Craton, Western Australia: *Geostandards and Geoanalytical Research*. doi:10.1111/ggr.12182.
- Kemp, AIS, Vervoort, JD, Hickman, AH, Smithies, RH, Wyche, S, Wingate, MTD and Kirkland, CL 2014, Growing ancient Australia: hafnium and neodymium isotope constraints from the Yilgarn and Pilbara cratons, in *Dynamic planet – Precambrian geochronology (Abstracts): Australian Earth Sciences Convention 2014*, Newcastle, NSW, Australia, 7–10 July 2014, p. 205–206.
- Kemp, AIS, Vervoort, JD, Smithies, RH, Hickman, AH and Van Kranendonk, MJ 2011, Recoupling the Nd–Hf isotope record of the early Earth? Evidence from the Pilbara Craton, Western Australia (Abstract V44B-04), in *Abstracts: American Geophysical Union Fall meeting 2011*, San Francisco, California, 5–9 December 2011, 1p.
- Kimura, G, Maruyama, S and Isozaki, Y 1991, Early Archean accretionary complex in the eastern Pilbara craton, Western Australia – detailed field occurrence in the Marble Bar area: *Eos*, v. 72, p. 542.
- Kinny, PD 2000, U–Pb dating of rare-metal (Sn–Ta–Li) mineralized pegmatites in Western Australia by SIMS analysis of tin and tantalum-bearing ore minerals, in *Abstracts and Proceedings: Beyond 2000, New Frontiers in Isotope Geoscience*, Lorne, Victoria, p. 113–116.
- Kirkland, CL, Johnson, SP, Smithies, RH, Hollis, JA, Wingate, MTD, Tyler, IM, Hickman, AH, Cliff, JB, Belousova, EA, Murphy, RC and Tessalina, S 2013, The crustal evolution of the Rudall Province from an isotopic perspective: Geological Survey of Western Australia, Report 122, 30p.
- Kisters, AFM, Belcher, RW, Poujol, M and Dziggel, A 2010, Continental growth and convergence-related arc plutonism in the Mesoarchean: evidence from the Barberton granitoid-greenstone terrain, South Africa: *Precambrian Research*, v. 178, p. 15–26.
- Kitajima, K, Hirata, T, Maruyama, S, Yamanashi, T, Sano, Y and Liou, JG 2008, U–Pb zircon geochronology using LA-ICP-MS in the North Pole Dome, Pilbara Craton, Western Australia: a new tectonic growth model for the Archean chert/greenstone succession, v. 80, p. 1–14.
- Kitajima, K, Maruyama, S, Utsunomiya, S and Liou, JG 2001, Seafloor hydrothermal alteration at an Archean mid-ocean ridge: *Journal of Metamorphic Geology*, v. 19, p. 583–599.
- Kitajima, K, Ushikubo, T, Kita, NT, Maruyama, S and Valley, JW 2012, Relative retention of trace element and oxygen isotope ratios in zircon from Archean rhyolite, Panorama Formation, North Pole Dome, Pilbara Craton, Western Australia: *Chemical Geology*, v. 332–333, p. 102–115.
- Kiyokawa, S 1993, Stratigraphy and structural evolution of a Middle Archean greenstone belt, northwestern Pilbara Craton, Australia: University of Tokyo, PhD thesis (unpublished).
- Kiyokawa, S, Aihara, Y, Takehara, M and Horie, K 2019, Timing and development of sedimentation of the Cleaverville Formation and a post-accretion pull-apart system in the Cleaverville area, coastal Pilbara Terrane, Pilbara, Western Australia: *Island Arc*, v. 28, no. 6, article no. e12324, 23p., doi:10.1111/iar.12324.
- Kiyokawa, S, Ito, T, Ikehara, M, Yamaguchi, KE, Koge, S and Sakamoto, R 2012, Lateral variations in the lithology and organic chemistry of a black shale sequence on the Mesoarchean seafloor affected by hydrothermal processes: the Dixon Island Formation of the coastal Pilbara Terrane, Western Australia: *Island Arc*, v. 21, no. 2, p. 118–147.
- Kiyokawa, S and Taira, A 1998, The Cleaverville Group in the west Pilbara coastal granite–greenstone terrane of Western Australia: an example of a mid-Archaean immature oceanic island-arc succession: *Precambrian Research*, v. 88, p. 102–142.
- Kiyokawa, S, Taira, A, Byrne, T, Bowring, S and Sano, Y 2002, Structural evolution of the middle Archean coastal Pilbara terrane, Western Australia: *Tectonics*, v. 21, no. 1044, p. 1–24, doi:10.1029/2001TC001296.
- Kloppenborg, A 2003, Structural evolution of the Marble Bar Domain, Pilbara granite–greenstone terrain, Australia: the role of Archaean mid-crustal detachments: *Geologica Ultraeetina*, no. 237: Utrecht University, Utrecht, the Netherlands, PhD thesis (unpublished), 256p.
- Kloppenborg, A, White, SH and Zegers, TE 2001, Structural evolution of the Warrawoona Greenstone Belt and adjoining granitoid complexes, Pilbara Craton, Australia: Implications for Archaean tectonic processes: *Precambrian Research*, v. 112, no. 1–2, p. 107–147.
- Kojima, S, Hanamuro, T, Hayashi, K, Haruna, M and Ohmoto, H 1998, Sulphide minerals in early Archean chemical sedimentary rocks of the eastern Pilbara district, Western Australia: *Mineralogy and Petrology*, v. 64, p. 219–235.
- Komiya, T and Maruyama, S 2007, A very hydrous mantle under the western Pacific region: implications for formation of marginal basins and style of Archean plate tectonics: *Gondwana Research*, v. 11, no. 1–2, p. 132–147.
- Komiya, T, Maruyama, S, Hirata, T and Yurimoto, H 2002, Petrology and geochemistry of MORB and OIB in the mid-Archaean North Pole Region, Pilbara Craton, Western Australia: implications for the composition and temperature of the upper mantle at 3.5 Ga, v. 44, p. 988–1016.
- Konhauser, KO, Planavsky, NJ, Hardisty, DS, Robbins, LJ, Warchola, TJ, Haugaard, R, Lalonde, SV, Partin, CA, Oonk, P, Tsikos, H, Lyons, TW, Bekker, A and Johnson, CM 2017, Iron formations: a global record of Neoproterozoic to Palaeoproterozoic environmental history: *Earth-Science Reviews*, v. 172, p. 140–177, doi:10.1016/j.earscirev.2017.06.012.

- Korsch, RJ, Johnson, SP, Tyler, IM, Thorne, AM, Blewett, RS, Cutten, HN, Joly, A, Dentith, MC, Aitken, ARA, Goodwin, JA and Kennett, BLN 2011, Geodynamic implications of the Capricorn deep seismic survey: from the Pilbara Craton to the Yilgarn Craton, in *Capricorn Orogen seismic and magnetotelluric (MT) workshop 2011: extended abstracts* edited by SP Johnson, A Thorne and IM Tyler: Geological Survey of Western Australia, Record 2011/25, p. 107–114.
- Krapež, B 1984, Sedimentation in a small, fault-bounded basin: The Lalla Rookh sandstone, east Pilbara Block, in *Archean and Proterozoic basins of the Pilbara, Western Australia: Evolution and mineralization potential* edited by JR Muhling, DI Groves and TS Blake: University of Western Australia, Geology Department and University Extension, Publication no. 9, p. 89–110.
- Krapež, B 1993, Sequence stratigraphy of the Archean supracrustal belts of the Pilbara Block, Western Australia: *Precambrian Research*, v. 60, p. 1–45.
- Krapež, B and Barley, ME 1987, Archean strike-slip faulting and related ensialic basins: evidence from the Pilbara Block, Australia, v. 124, no. 6, p. 555–567, doi:10.1017/S0016756800017386.
- Krapež, B, Blake, TS and Barley, ME 1990, Origin and reactivation of lineaments in the Pilbara Craton, Western Australia, in *Extended abstracts volume* edited by JE Glover and SE Ho: Third International Archean Symposium, 17–21 September 1990: Geoconferences (W.A.) Inc, Perth, Western Australia, p. 23–24.
- Krapež, B and Eisenlohr, B 1998, Tectonic settings of Archean (3325–2775 Ma) crustal–supracrustal belts in the West Pilbara Block: *Precambrian Research*, v. 88, p. 173–205.
- Krapež, B and Furnell, RG 1987, Sedimentology, origin and gold potential of the Late Archean Lalla Rookh Basin, East Pilbara Block, Western Australia, in *Uranium deposits in quartz-pebble conglomerates*: International Atomic Energy Agency, Vienna, Austria, p. 427–459.
- Krapež, B and Groves, DI 1984, Gold mineralization potential of Archean clastic sequences in the east Pilbara Block, in *Archean and Proterozoic basins of the Pilbara, Western Australia: Evolution and mineralization potential* edited by JR Muhling, DI Groves and TS Blake: The University of Western Australia, Geology Department and University Extension, Publication no 9, p. 111–122.
- Kriewaldt, M 1964, The Fortescue Group of the Roebourne Region, north-west division, in *Annual report for the year 1963*: Geological Survey of Western Australia, p. 30–34.
- Kröner, A, Anhaeusser, CR, Hoffmann, J., Wong, J, Geng, E, Hegner, E, Xie, H, Yang, J and Liu, D 2016, Chronology of the oldest supracrustal sequences in the Palaeoarchean Barberton Greenstone Belt, South Africa and Swaziland.: *Precambrian Research*, v. 279, p. 123–143.
- Kröner, A, Compston, W and Williams, IS 1989, Growth of early Archean crust in the Ancient Gneiss Complex of Swaziland as revealed by single zircon dating: *Tectonophysics*, v. 161, p. 271–298.
- Kröner, A, Hoffmann, JE, Xie, H, Monker, C, Hegner, E, Wan, Y, Hofmann, A, Liu, D and Yang, J 2014, Generation of early Archean grey gneisses through melting of older crust in the eastern Kaapvaal craton, southern Africa: *Precambrian Research*, v. 255, no. 3, p. 823–846, doi:10.1016/j.precamres.2014.07.017.
- Kröner, A and Tegtmeier, A 1994, Gneiss–greenstone relationships in the Ancient Gneiss Complex of southwestern Swaziland, southern Africa, and implications for early crustal evolution: *Precambrian Research*, v. 67, p. 109–139.
- Lambert, IB, Donnelly, TH, Dunlop, JSR and Groves, DI 1978, Stable isotope compositions of early Archean sulphate deposits of probable evaporitic and volcanogenic origins: *Nature*, v. 276, p. 808–811.
- Li, W, Czaja, AD, Van Kranendonk, MJ, Beard, BL, Roden, EE and Johnson, CM 2013, An anoxic, Fe(II)-rich, U-poor ocean 3.46 billion years ago: *Geochimica et Cosmochimica Acta*, v. 120, p. 65–79.
- Lindsay, JF, Brasier, MD, McLoughlin, N, Green, OR, Fogel, M, McNamara, KM, Steele, A and Mertzman, SA 2003, Abiotic Earth – establishing a baseline for earliest Life, data from the Archean of Western Australia, in *Program and technical sessions 2003: Lunar and Planetary Science Conference XXXIV*, Houston, Texas, 17–21 March 2003: Lunar and Planetary Institute, Abstract 1137, 2p.
- Lindsay, JF, Brasier, MD, McLoughlin, N, Green, OR, Fogel, M, Steele, A and Mertzman, SA 2005, The problem of deep carbon – an Archean paradox: *Precambrian Research*, v. 143, p. 1–22.
- Lipple, SL 1975, Definitions of new and revised stratigraphic units of the Eastern Pilbara Region, in *Annual report for the year 1974*: Geological Survey of Western Australia, p. 58–63.
- Lowe, DR 1980, Stromatolites 3,400-Myr old from the Archean of Western Australia: *Nature*, v. 284, p. 441–443.
- Lowe, DR 1983, Restricted shallow-water sedimentation of Early Archean stromatolitic and evaporitic strata of the Strelley Pool Chert, Pilbara Block, Western Australia: *Precambrian Research*, v. 19, p. 239–283.
- Lowe, DR 1999, Petrology and sedimentology of cherts and related silicified sedimentary rocks in the Swaziland Supergroup, in *Geologic evolution of the Barberton Greenstone Belt, South Africa* edited by DR Lowe and GR Byerly: Geological Society of America, Special Papers 329, p. 83–114.
- Lowe, DR and Byerly, GR 1986, Early Archean silicate spherules of probable impact origin: *Geology*, v. 14, p. 83–86.
- Lowe, DR and Byerly, GR 1999, Stratigraphy of the west-central part of the Barberton Greenstone Belt, South Africa, in *Geologic evolution of the Barberton Greenstone Belt, South Africa* edited by DR Lowe and GR Byerly: Geological Society of America, Special Papers 329, p. 1–36.
- Lowe, DR and Byerly, GR 2007, An overview of the geology of the Barberton Greenstone Belt and vicinity: implications for early crustal development, in *Earth's oldest rocks* edited by MJ Van Kranendonk, VC Bennett and RH Smithies: Elsevier BV, Burlington, Massachusetts, USA, *Developments in Precambrian Geology* 15, p. 481–526.
- Lowe, DR and Byerly, GR 2010, Did LHB end not with a bang but a whimper? the geologic evidence, in *Program and technical sessions: 41st Lunar and Planetary Science Conference*, Woodlands, Texas, 1–5 March 2003: Lunar and Planetary Institute, Abstract 2563, 2p.
- Lowe, DR, Byerly, GR, Asario, F and Kyte, FT 1989, Geological and geochemical record of 3400-million-year-old terrestrial meteorite impacts: *Science*, v. 245, p. 959–962.
- Lowe, DR, Byerly, GR and Kyte, FT 2014, Recently discovered 3.42 – 3.23 Ga impact layers, Barberton Belt, South Africa: 3.8 Ga detrital zircons, Archean impact history, and tectonic implications: *Geology*, v. 42, p. 747–750.
- Lowe, DR, Byerly, GR, Kyte, FT, Shukolyukov, A, Asaro, F and Krull, A 2003, Characteristics, origin, and implications of Archean impact-produced spherule beds, 3.47 – 3.22 Ga, in the Barberton Greenstone Belt, South Africa: keys to the role of large impacts on the evolution of the early Earth: *Astrobiology*, v. 3, p. 7–48.
- Lu, Y, Wingate, MTD and Johnson, SP 2018, 216546: biotite metamonzogranite, Great Northern Highway: *Geochronology Record* 1520: Geological Survey of Western Australia, 4p.
- Maidment, DW 2017, Geochronology from the Rudall Province, Western Australia: Implications for the amalgamation of the West and North Australian Cratons: Geological Survey of Western Australia, Report 161, 95p.
- Marshall, AO, Jehlicka, J, Rouzaud, J-N and Marshall, CP 2014, Multiple generations of carbonaceous material deposited in Apex chert by basin-scale pervasive hydrothermal fluid flow: *Gondwana Research*, v. 25, p. 284–289.
- Marshall, CP, Emry, JR and Marshall, AO 2011, Haematite pseudomicrofossils present in 3.5-billion-year-old Apex chert: *Nature Geoscience*, v. 4, p. 240–243.
- Marston, RJ 1979, Copper mineralization in Western Australia: Geological Survey of Western Australia, Mineral Resources Bulletin 13, 210p.
- Martin, DMcB, Clendenin, CW, Krapež, B and McNaughton, NJ 1998a, Tectonic and geochronological constraints on late Archean and Palaeoproterozoic stratigraphic correlation within and between the Kaapvaal and Pilbara Cratons: *Journal of the Geological Society*, v. 155, p. 311–322.
- Martin, DMcB, Li, ZX, Nemchin, AA and Powell, CMcA 1998b, A pre-2.2 Ga age for giant hematite ores of the Hamersley Province, Australia? *Economic Geology*, v. 93, p. 1084–1090.

- Martin, H, Smithies, RH, Rapp, R, Moyen, J-F and Champion, DC 2005, An overview of adakite, tonalite–trondhjemite–granodiorite (TTG), and sanukitoid: relationships and some implications for crustal evolution: *Lithos*, v. 79, p. 1–24, doi:10.1016/j.lithos.2004.04.048.
- McCall, GJH 1971, Some ultrabasic and basic igneous rock occurrences in the Archaean of Western Australia, in *Symposium on Archaean Rocks*, Perth, 23–26 May 1970 edited by JE Glover: Geological Society of Australia, Perth, Western Australia, Special Publication 3, p. 429–442.
- McCulloch, MT 1987, Sm–Nd isotopic constraints on the evolution of Precambrian crust in the Australian continent, in *Proterozoic lithosphere evolution* edited by A Kroener, American Geophysical Union Geodynamics Series 17, p. 111–120.
- McCulloch, MT and Bennett, VC 1993, Evolution of the early Earth: constraints from ^{143}Nd – ^{142}Nd isotope systematics: *Lithos*, v. 30, p. 327–355.
- McCulloch, MT and Wasserburg, GJ 1978, Sm–Nd and Rb–Sr chronology of continental crust formation: *Science*, v. 200, p. 1003–1011.
- Menzies, MA, Klemperer, SL, Ebinger, CJ and Baker, J 2002, Characteristics of volcanic rifted margins, *Geological Society of America Special Paper* 362, 14p.
- Moly Mines Ltd. 2012, Spinifex Ridge Mo–Cu Deposit Western Australia – updated NI 43-101 Technical Report: Report to the Australian Securities Exchange (ASX), released 10 February 2012, 77p.
- Morag, N, Williford, KH, Kitajima, K, Philippot, P, Van Kranendonk, MJ, Lepot, K, Thomazo, C and Valley, JW 2016, Microstructure-specific carbon isotopic signatures of organic matter from ~3.5 Ga cherts of the Pilbara Craton support a biologic origin: *Precambrian Research*, v. 275, p. 429–449.
- Morant, P 1995, The Panorama Zn–Cu volcanogenic massive sulfide deposits, Western Australia: Recent developments in base metal geology and exploration: *Australian Institute of Geoscientists Bulletin*, v. 16, p. 75–84.
- Morant, P 1998, Panorama zinc–copper deposits: *Australasian Institute of Mining and Metallurgy, Monograph*, v. 22, p. 287–292.
- Morris, RC and Horwitz, RC 1983, The origin of the iron formation-rich Hamersley Group of Western Australia – deposition on a platform: *Precambrian Research*, v. 21, no. 3–4, p. 273–297, doi:10.1016/0301-9268(83)90044-X.
- Moyen, J-F, Stevens, G and Kisters, A 2006, Record of mid-Archaean subduction from metamorphism in the Barberton terrain, South Africa: *Nature*, v. 442, p. 559–562, doi:10.1038/nature04972.
- Müller, SG, Krapež, B, Barley, ME and Fletcher, IR 2005, Giant iron-ore deposits of the Hamersley province related to the breakup of Paleoproterozoic Australia: new insights from in situ SHRIMP dating of baddeleyite from mafic intrusions: *Geology*, v. 33, no. 7, p. 577–580.
- Neale, J 1975, Mount Goldsworthy iron ore deposits, W.A., in *Economic geology of Australia and Papua New Guinea-Metals*, edited by CL Knight: Australasian Institute of Mining and Metallurgy, Monograph 5, p. 932–936.
- Nebel, O, Campbell, IH, Sossi, PA and Van Kranendonk, MJ 2014, Hafnium and iron isotopes in early Archaean komatiites record a plume-driven convection cycle in the Hadean Earth: *Earth and Planetary Science Letters*, v. 397, p. 111–120.
- Nebel-Jacobsen, Y, Münker, C, Nebel, O, Gerdes, A, Mezger, K and Nelson, DR 2010, Reworking of Earth's first crust: constraints from Hf isotopes in Archean zircons from Mt Narryer, Australia: *Precambrian Research*, v. 182, no. 3, p. 175–186, doi:10.1016/j.precamres.2010.07.002.
- Nebel-Jacobsen, Y, Nebel, O, Wille, M and Cawood PA 2018, A non-zircon Hf isotope record in Archean black shales from the Pilbara craton confirms changing crustal dynamics ca. 3 Ga ago: *Nature, Scientific Reports*, v. 8, article no. 922, doi:10.1038/s41598-018-19397-9
- Nelson, DR 1996a, 114305: bedded felsic tuff, east of Mount Sholl; *Geochronology Record* 477: Geological Survey of Western Australia, 4p.
- Nelson, DR 1996b, 124755: biotite granodiorite, Sunrise Hill West 4 pit; *Geochronology Record* 439: Geological Survey of Western Australia, 4p.
- Nelson, DR 1997a, 118965: equigranular biotite monzogranite gneiss, old highway – Sherlock River crossing; *Geochronology Record* 457: Geological Survey of Western Australia, 4p.
- Nelson, DR 1997b, 127320: quartz granophyre, Mount Ada; *Geochronology Record* 440: Geological Survey of Western Australia, 4p.
- Nelson, DR 1998a, 127330: volcanoclastic sedimentary rock, Cleaverville; *Geochronology Record* 442: Geological Survey of Western Australia, 4p.
- Nelson, DR 1998b, 136899: volcanogenic sedimentary rock, Wickham; *Geochronology Record* 416: Geological Survey of Western Australia, 4p.
- Nelson, DR 1998c, 141936: welded tuff, Red Hill; *Geochronology Record* 396: Geological Survey of Western Australia, 3p.
- Nelson, DR 1998d, 142661: foliated biotite tonalite, Zebra Hill; *Geochronology Record* 409: Geological Survey of Western Australia, 3p.
- Nelson, DR 1998e, 142828: heterogeneous granodiorite gneiss, Fred Well; *Geochronology Record* 389: Geological Survey of Western Australia, 4p.
- Nelson, DR 1998f, 142830: volcanogenic sedimentary rock, Mount Ada; *Geochronology Record* 390: Geological Survey of Western Australia, 4p.
- Nelson, DR 1998g, 142842: volcanoclastic sedimentary rock, Nunyerry Gap; *Geochronology Record* 379: Geological Survey of Western Australia, 4p.
- Nelson, DR 1998h, 142865: alkali granite, Marble Bar road; *Geochronology Record* 377: Geological Survey of Western Australia, 4p.
- Nelson, DR 1998i, 142878: foliated biotite monzogranite, Hillside Track; *Geochronology Record* 349: Geological Survey of Western Australia, 3p.
- Nelson, DR 1998j, 142884: schlieric biotite syenogranite, Mount Webber; *Geochronology Record* 353: Geological Survey of Western Australia, 4p.
- Nelson, DR 1998k, 143994: quartzite, Kittys Gap; *Geochronology Record* 266: Geological Survey of Western Australia, 4p.
- Nelson, DR 1998l, 143995: quartzite, Friendly Stranger Mine; *Geochronology Record* 267: Geological Survey of Western Australia, 4p.
- Nelson, DR 1998m, 143996: quartzite, Shay Gap; *Geochronology Record* 268: Geological Survey of Western Australia, 4p.
- Nelson, DR 1998n, 144210: rhyodacite, Mount Fisher; *Geochronology Record* 269: Geological Survey of Western Australia, 4p.
- Nelson, DR 1998o, 144256: rhyolite tuff, De Witt Hill; *Geochronology Record* 271: Geological Survey of Western Australia, 4p.
- Nelson, DR 1999a, 142170: foliated biotite monzogranite, Kangan Homestead; *Geochronology Record* 399: Geological Survey of Western Australia, 4p.
- Nelson, DR 1999b, 142176: megacrystic foliated biotite monzogranite, Yandeyarra Homestead; *Geochronology Record* 400: Geological Survey of Western Australia, 4p.
- Nelson, DR 1999c, 142835: tonalitic gneiss, Whundo, *Geochronology Record* 392: Geological Survey of Western Australia, 3p.
- Nelson, DR 1999d, 142867: volcanoclastic sedimentary rock, Cattle Well; *Geochronology Record* 378: Geological Survey of Western Australia, 4p.
- Nelson, DR 1999e, 142870: banded biotite tonalite gneiss, 6 Mile Well; *Geochronology Record* 345: Geological Survey of Western Australia, 4p.
- Nelson, DR 1999f, 148500: lapilli tuff, McPhee Reward mine; *Geochronology Record* 246: Geological Survey of Western Australia, 4p.
- Nelson, DR 1999g, 153188: biotite granodiorite, Wilson Well; *Geochronology Record* 252: Geological Survey of Western Australia, 4p.
- Nelson, DR 2000a, 142936: leucocratic monzogranite, Yandeyarra Pool; *Geochronology Record* 323: Geological Survey of Western Australia, 4p.
- Nelson, DR 2000b, 142937: leucocratic monzogranite, Numbana Pool; *Geochronology Record* 324: Geological Survey of Western Australia, 4p.
- Nelson, DR 2000c, 142938: biotite–hornblende tonalite, Cheearra Hill; *Geochronology Record* 325: Geological Survey of Western Australia, 4p.
- Nelson, DR 2000d, 142942: metasandstone, Croydon Well; *Geochronology Record* 327: Geological Survey of Western Australia, 5p.

- Nelson, DR 2000e, 142945: plagioclase–hornblende–pyroxene andesite porphyry, Jigimining Pool; Geochronology Record 296: Geological Survey of Western Australia, 4p.
- Nelson, DR 2000f, 142946: foliated biotite tonalite, Flat Rocks; Geochronology Record 297: Geological Survey of Western Australia, 4p.
- Nelson, DR 2000g, 142948: tonalite, Flat Rocks; Geochronology Record 298: Geological Survey of Western Australia, 4p.
- Nelson, DR 2000h, 142951: sandstone, Lalla Rookh Well; Geochronology Record 301: Geological Survey of Western Australia, 5p.
- Nelson, DR 2000i, 142952: porphyritic felsic tuff, Tremain Well; Geochronology Record 302: Geological Survey of Western Australia, 4p.
- Nelson, DR 2000j, 142975: crystal-lithic tuff, Glen Herring Radio Tower; Geochronology Record 295: Geological Survey of Western Australia, 4p.
- Nelson, DR 2000k, 142976: porphyritic granophyre, 26 Mile Well; Geochronology Record 280: Geological Survey of Western Australia, 4p.
- Nelson, DR 2000l, 142977: monzogranite, Moolyella tin mine; Geochronology Record 281: Geological Survey of Western Australia, 4p.
- Nelson, DR 2000m, 148498: tuffaceous chert, Eight Mile Bore; Geochronology Record 245: Geological Survey of Western Australia, 4p.
- Nelson, DR 2000n, 148502: porphyritic tuffaceous rhyolite, Gallop Well; Geochronology Record 247: Geological Survey of Western Australia, 4p.
- Nelson, DR 2000o, 142967: biotite monzogranite, Unices Well; Geochronology Record 307: Geological Survey of Western Australia, 4p.
- Nelson, DR 2001a, 160727: biotite granodiorite, Chillerina Well; Geochronology Record 241: Geological Survey of Western Australia, 4p.
- Nelson, DR 2001b, 160745: foliated biotite granodiorite, old Marble Bar Road – Tabba Tabba Creek crossing; Geochronology Record 213: Geological Survey of Western Australia, 4p.
- Nelson, DR 2001c, 168908: crystal–lithic tuff, Copper Hills; Geochronology Record 222: Geological Survey of Western Australia, 4p.
- Nelson, DR 2001d, 168909: vitric tuff, Gilbert Cairn; Geochronology Record 223: Geological Survey of Western Australia, 4p.
- Nelson, DR 2001e, 168915: rhyolite, Warrery Gap; Geochronology Record 212: Geological Survey of Western Australia, 4p.
- Nelson, DR 2002a, 160220: altered rhyolite, Farrel Well; Geochronology Record 237: Geological Survey of Western Australia, 4p.
- Nelson, DR 2002b, 168989: coarse volcanoclastic metasandstone, Cooke Bluff Hill; Geochronology Record 158: Geological Survey of Western Australia, 4p.
- Nelson, DR 2002c, 168990: quartzite, Cooke Bluff Hill; Geochronology Record 159: Geological Survey of Western Australia, 4p.
- Nelson, DR 2002d, 168993: volcanoclastic metasandstone, Bob Bore; Geochronology Record 162: Geological Survey of Western Australia, 4p.
- Nelson, DR 2002e, 168995: tuffaceous rhyolite, Fieldings Gully Well; Geochronology Record 163: Geological Survey of Western Australia, 4p.
- Nelson, DR 2002f, 168996: altered coarse crystal tuff, Farrel Well; Geochronology Record 164: Geological Survey of Western Australia, 4p.
- Nelson, DR 2002g, 168997: quartzite, Farrel Well; Geochronology Record 165: Geological Survey of Western Australia, 4p.
- Nelson, DR 2002h, 169008: quartz–sericite schist, Coongan Belt Well; Geochronology Record 171: Geological Survey of Western Australia, 4p.
- Nelson, DR 2002i, 169014: foliated biotite–hornblende quartz diorite, Mount Gratwick, Geochronology Record 139: Geological Survey of Western Australia, 4p.
- Nelson, DR 2002j, 169016: foliated biotite–quartz diorite, Mount Gratwick, Geochronology Record 140: Geological Survey of Western Australia, 3p.
- Nelson, DR 2004a, 168992: volcanoclastic metasandstone, Bob Bore; Geochronology Record 161: Geological Survey of Western Australia, 5p.
- Nelson, DR 2004b, 168999: quartzite, Pethernurrina Spring; Geochronology Record 59: Geological Survey of Western Australia, 5p.
- Nelson, DR 2004c, 169013: metasandstone, Punduna Pool; Geochronology Record 138: Geological Survey of Western Australia, 5p.
- Nelson, DR 2004d, 169042: biotite granodiorite, Wilina Well; Geochronology Record 40: Geological Survey of Western Australia, 5p.
- Nelson, DR 2004e, 169044: muscovite–biotite monzogranite, Ripon Hills Road – Yandicoogina Creek crossing; Geochronology Record 130: Geological Survey of Western Australia, 4p.
- Nelson, DR 2004f, 169200: coarse lithic–quartz sandstone, Branchies Well; Geochronology Record 94: Geological Survey of Western Australia, 6p.
- Nelson, DR 2004g, 178012: biotite tonalite gneiss, Quartz Hill; Geochronology Record 96: Geological Survey of Western Australia, 4p.
- Nelson, DR 2005a, 178010: lithic–quartz sandstone, Mount Olive; Geochronology Record 549: Geological Survey of Western Australia, 5p.
- Nelson, DR 2005b, 178013: quartz diorite gneiss, Quartz Hill; Geochronology Record 550: Geological Survey of Western Australia, 4p.
- Nelson, DR 2005c, 178014: biotite monzogranite, Quartz Hill; Geochronology Record 551: Geological Survey of Western Australia, 4p.
- Nelson, DR 2005d, 178019: coarse sandstone, Mount Grant; Geochronology Record 552: Geological Survey of Western Australia, 5p.
- Nelson, DR 2005e, 178020: pebble conglomerate, Mount Grant; Geochronology Record 553: Geological Survey of Western Australia, 5p.
- Nelson, DR 2005f, 178031: porphyritic biotite granodiorite, Mulgandoona Hill; Geochronology Record 556: Geological Survey of Western Australia, 4p.
- Nelson, DR 2005g, 178042: altered volcanoclastic sandstone, Table Top Well; Geochronology Record 564: Geological Survey of Western Australia, 4p.
- Nelson, DR 2005h, 178043: lithic–quartz sandstone, Strelley Pool; Geochronology Record 565: Geological Survey of Western Australia, 5p.
- Nelson, DR 2005i, 178045: sandstone, Quininya Well; Geochronology Record 567: Geological Survey of Western Australia, 5p.
- Nelson, DR 2005j, 178230: biotite granodiorite, Limestone Bore; Geochronology Record 574: Geological Survey of Western Australia, 4p.
- Nelson, DR 2005k, 178231: biotite monzogranite, Limestone Bore; Geochronology Record 575: Geological Survey of Western Australia, 4p.
- Nelson, DR 2005l, 178022: biotite granodiorite, Granite Well; Geochronology record 554; Geological Survey of Western Australia, 4p.
- Nelson, DR. 2005m, 178023: foliated biotite tonalite, Florries Well; Geochronology record 555: Geological Survey of Western Australia, 4p.
- Nelson, DR, Bodorkos, S, Love, GJ and Wingate, MTD 2006, 178084: biotite–hornblende monzogranite, Tony Well; Geochronology Record 630: Geological Survey of Western Australia, 4p.
- Nelson, DR, Trendall, AF and Altermann, W 1999, Chronological correlations between the Pilbara and Kaapvaal cratons: *Precambrian Research*, v. 97, no. 3–4, p. 165–189.
- Nelson, DR, Trendall, AF, de Laeter, JR, Grobler, NJ and Fletcher, IR 1992, A comparative study of the geochemical and isotopic systematics of late Archaean flood basalts from the Pilbara and Kaapvaal cratons: *Precambrian Research*, v. 54, p. 231–256.
- Neumayr, P, Ridley, JR, McNaughton, NJ, Kinny, PD, Barley, ME and Groves, DI 1998, Timing of gold mineralization in the Mount York district, Pilgangoora greenstone belt and implications for the tectonic and metamorphic evolution of an area linking the western and eastern Pilbara Craton: *Precambrian Research*, v. 88, p. 249–265.
- Newmont Pty Limited 1979, Annual report on mineral claim numbers 45/8674 to 45/8684 inclusive North Pole area, Pilbara W.A.: Geological Survey of Western Australia, Statutory mineral exploration report, A8544 (unpublished).
- Newmont Pty Limited 1980, Final report on Temporary Reserve 6712H North Pole area, Pilbara Goldfield: Geological Survey of Western Australia, Statutory mineral exploration report, A9093 (unpublished).
- Nijman, W, Clevis, Q and de Vries, ST 2010, The waning stage of a greenstone belt: the Mesoarchean Mosquito Creek Basin of the East Pilbara, Western Australia: *Precambrian Research*, v. 180, p. 251–271.
- Nijman, W, de Bruijne, KCH and Valkering, ME 1998, Growth fault control of Early Archaean cherts, barite mounds and chert–barite veins, North Pole Dome, Eastern Pilbara, Western Australia: *Precambrian Research*, v. 88, p. 25–52.

- Nijman, W, de Bruijne, KCH and Valkering, ME 1999, Growth fault control of Early Archaean cherts, barite mounds and chert-barite veins, North Pole Dome, Eastern Pilbara, Western Australia (Erratum to Precambrian Research, v. 88, p. 25–52): *Precambrian Research*, v. 95, p. 247–274.
- Nijman, W and de Vries, ST 2004, Early Archaean crustal collapse structures and sedimentary basin dynamics, *in* *The Precambrian Earth: tempos and events* edited by PG Eriksson, W Altermann, DR Nelson, WU Mueller and O Catuneanu: Elsevier, Amsterdam, The Netherlands, *Developments in Precambrian Geology* 12, p. 139–154.
- Nijman, W, de Vries, ST and Houtzager, O 2001, Earth's earliest sedimentary basins: the Lower Archaean of the Pilbara and Kaapvaal compared, *in* *Extended Abstracts – 4th International Archaean Symposium*, Perth, 24–28 September 2001 edited by KF Cassidy, J Dunphy and MJ Van Kranendonk: AGSO (Geoscience Australia), Record 2001/37, p. 520–522.
- Nijman, W, Kloppenburg, A and de Vries, ST 2017, Archaean basin margin geology and crustal evolution: an East Pilbara traverse: *Journal of the Geological Society*, v. 174, p. 1090–1112.
- Nisbet, EG and Chinner, GA 1981, Controls on the eruption of mafic and ultramafic lavas: Ruth Well Cu–Ni prospect, western Pilbara: *Economic Geology*, v. 76, no. 6, p. 1729–1735.
- Noffke, N, Christiansen, D, Wacey, D and Hazen, RM 2013, Microbially induced sedimentary structures recording an ancient ecosystem in the ca. 3.48 billion-year-old Dresser Formation, Pilbara, Western Australia: *Astrobiology*, v. 13, no. 12, p. 1103–1124, doi:10.1089/ast.2013.1030.
- Noldart, AJ and Wyatt, JD 1962, The geology of portion of the Pilbara Goldfield, covering the Marble Bar and Nullagine 4 mile map sheets: *Geological Survey of Western Australia, Bulletin* 115, 198p.
- Oehler, DZ, Walsh, MM, Sugitani, K, Liu, M-C and House, CH 2017, Large and robust lenticular microorganisms on the young Earth: *Precambrian Research*, v. 296, p. 112–119.
- Ohmoto, H, Watanabe, Y, Allwood, AC, Birch, IW, Knauth, P, Yamaguchi, KE and Johnson, I 2006, Discovery of probable >3.43 paleolaterites in the Pilbara Craton, Western Australia, *in* *Program and Abstracts* edited by AGU: American Geophysical Union, Fall Meeting 2006, 10–15 December 2006, Abstract V24B-07.
- Ohta, H, Maruyama, S, Takahashi, E, Watanabe, Y and Kato, Y 1996, Field occurrence, geochemistry and petrogenesis of the Archaean Mid-Oceanic Ridge Basalts (AMORBs) of the Cleaverville area, Pilbara Craton, Western Australia: *Lithos*, v. 37, p. 199–221.
- Oliver NSH and Cawood PA 2001, Early tectonic dewatering and brecciation on the overturned sequence at Marble Bar, Pilbara Craton, Western Australia: dome related or not?: *Precambrian Research*, v. 105, p. 1–15.
- Olivier, N, Dromart, G, Collice, N, Flament, N, Rey, P and Sauvestre, R 2012, A deep subaqueous fan depositional model for the Palaeoarchean (3.46 Ga) Marble Bar Cherts, Warrawoona Group, Western Australia: *Geological Magazine*, v. 149, p. 743–749.
- Orberger, B, Rouchon, V, Westall, F, de Vries, ST, Pinti, DL, Wagner, C, Wirth, R and Hashizume, K 2006, Microfacies and origin of some Archean cherts (Pilbara, Australia), *in* *Processes on the early Earth* edited by WU Reimold and RL Gibson: Geological Society of America, Special Paper 405, p. 133–156, doi:10.1130/2006.2405(08).
- Oversby, VM 1976, Isotopic ages and geochemistry of Archaean acid igneous rocks from the Pilbara, Western Australia: *Geochimica et Cosmochimica Acta*, v. 40, p. 817–829.
- Pawley, MJ, Van Kranendonk, MJ and Collins, WJ 2004, Interplay between deformation and magmatism during doming of the Archaean Shaw granitoid complex, Pilbara craton, Western Australia: *Precambrian Research*, v. 131, no. 3, p. 213–230.
- Pearce, J 2008, Geochemical fingerprinting of oceanic basalts with applications to ophiolite classification and the search for Archean oceanic crust: *Lithos*, v. 100, p. 14–48.
- Pease, V, Percival, J, Smithies, RH, Stevens, G and Van Kranendonk, MJ 2008, When did plate tectonics begin? Evidence from the orogenic record, *in* *When did plate tectonics begin on planet Earth?* edited by KC Condie and V Pease: Geological Society of America, Special Paper 440, p. 199–228.
- Perry, EC, Hickman, AH and Barnes, IL 1975, Archaean sedimentary barite, Pilbara Goldfield, Western Australia, *in* *Program with abstracts: Geological Society of America*, p. 1226.
- Peter, JM and Scott, SD 1997, Windy Craggy, Northwestern British Columbia: the world's largest Besshi-type deposit, *in* *Volcanic-hosted massive sulfide deposits: processes and examples in modern and ancient settings* edited by CT Barrie and MD Hannington: Society of Economic Geologists, *Reviews in Economic Geology* 8, p. 261–295.
- Petersson, A, Kemp, AIS, Gray, CM and Whitehouse, MJ 2020, Formation of early Archean granite–greenstone terranes from a globally chondritic mantle: insights from igneous rocks of the Pilbara Craton, Western Australia: *Chemical Geology*, v. 551, p. 1–25, article no. 119757, doi:10.1016/j.chemgeo.2020.119757.
- Petersson, A, Kemp, AIS, Hickman, AH, Van Kranendonk, MJ, Whitehouse, MJ, Martin, L and Gray, CM 2019a, A new 3.59 Ga magmatic suite and a chondritic source to the east Pilbara Craton: *Chemical Geology*, v. 511, p. 51–70, doi:10.1016/j.chemgeo.2019.01.021.
- Petersson, A, Kemp, AIS, Hickman, AH, Whitehouse, MJ, Martin, L and Gray, CM 2019b, Early Earth evolution of the Pilbara Craton, with implication for continental growth (abstract): *Goldschmidt2019, Barcelona*, 18–23 August 2019, article no. 2639, 1p.
- Petersson, A, Kemp, AIS and Whitehouse, MJ 2019c, A Yilgarn seed to the Pilbara Craton (Australia)? Evidence from xenocrystic zircons: *Geology*, v. 47, no. 11, p. 1098–1102, doi:10.1130/G46696.1.
- Philippot, P, Van Zuilen, M, Lepot, K, Thomazo, C, Farquhar, J and Van Kranendonk, MJ 2007, Early Archaean microorganisms preferred elemental sulfur, not sulphate: *Science*, v. 317, p. 1534–1537.
- Phillips, GN and Powell, R 2010, Formation of gold deposits: a metamorphic devolatilization model: *Journal of Metamorphic Geology*, v. 28, p. 689–718.
- Pickard, AL 2003, SHRIMP U–Pb zircon ages for the Palaeoproterozoic Kuruman Iron Formation, Northern Cape Province, South Africa: evidence for simultaneous BIF deposition in the Kaapvaal and Pilbara Cratons: *Precambrian Research*, v. 125, p. 275–315.
- Pickard, AL, Barley, ME and Krapež, B 2004, Deep-marine depositional setting of banded iron formation: sedimentological evidence from interbedded clastic sedimentary rocks in the early Palaeoproterozoic Dales Gorge Member of Western Australia: *Sedimentary Geology*, v. 170, p. 37–62.
- Pidgeon, RT 1978a, 3450-m.y.-old volcanics in the Archaean layered greenstone succession of the Pilbara Block, Western Australia: *Earth and Planetary Science Letters*, v. 37, no. 3, p. 421–428, doi:10.1016/0012-821X(78)90057-2.
- Pidgeon, RT 1978b, Geochronological investigation of granite batholiths of the Archaean granite–greenstone terrain of the Pilbara Block, Western Australia, *in* *Proceedings of the 1978 Archaean geochemistry conference*, University of Toronto, Ontario edited by IEM Smith and JG Williams, p. 360–362.
- Pike, G and Cas, RAF 2002, Stratigraphic evolution of Archaean volcanic rock-dominated rift basins from the Whim Creek Belt, west Pilbara Craton, Western Australia: *Sedimentology*, Special Publication, no. 33, p. 213–234.
- Pike, G, Cas, RAF and Hickman, AH 2006, Archean volcanic and sedimentary rocks of the Whim Creek greenstone belt, Pilbara Craton, Western Australia: *Geological Survey of Western Australia, Report* 101, 104p.
- Pinti, DL, Hashizume, K, Orberger, B, Gallien, J-P, Cloquet, C and Massault, M 2007, Biogenic nitrogen and carbon in Fe–Mn-oxyhydroxides from an Archean chert, Marble Bar, Western Australia: *Geochemistry Geophysics Geosystems*, v. 8, no. 2, doi:10.1029/2006GC001394.
- Pinti, DL, Hashizume, K, Sugihara, A, Massault, M and Philippot, P 2009a, Isotopic fractionation of nitrogen and carbon in Paleoproterozoic cherts from Pilbara craton, Western Australia: origin of ¹⁵N-depleted nitrogen: *Geochimica et Cosmochimica Acta*, v. 73, p. 3818–3848.
- Pinti, DL, Mineau, R and Clement, V 2009b, Hydrothermal alteration and microfossil artefacts of the 3,465-million-year-old Apex chert: *Nature Geoscience*, v. 2, p. 640–643.
- Pirajno, F 2007, Ancient to modern Earth: The role of mantle plumes in the making of continental crust, *in* *Earth's oldest rocks* edited by MJ Van Kranendonk, VC Bennett and RH Smithies: Elsevier BV, Burlington, Massachusetts, USA, *Developments in Precambrian Geology* 15, p. 1037–1064.

- Pirajno, F 2009, Hydrothermal processes and mineral systems: Springer, The Netherlands, 1250p., doi:10.1007/978-1-4020-8613-7.
- Pirajno, F and Van Kranendonk, MJ 2005, Review of hydrothermal processes and systems on Earth and implications for Martian analogues: *Australian Journal of Earth Sciences*, v. 52, no. 3, p. 329–351, doi:10.1080/08120090500134571.
- Poujol, M, Robb, LJ, Anhaeusser, CR and Gericke, B 2003, A review of the geochronological constraints on the evolution of the Kaapvaal Craton, South Africa: *Precambrian Research*, v. 127,
- Ramsay, JG 1967, Folding and fracturing of rocks: McGraw-Hill, New York, USA, Series in Earth and Planetary Sciences 160, 568p., doi:10.1126/science.160.3826.410.
- Rasmussen B 2000, Filamentous microfossils in a 3235-million-year-old volcanogenic massive sulphide deposit: *Nature*, v. 405, p. 676–679.
- Rasmussen, B, Blake, TS and Fletcher, IR 2005, U–Pb zircon age constraints on the Hamersley spherule beds: evidence for a single 2.63 Ga Jeerinah–Carawine impact ejecta layer: *Geology*, v. 33, no. 9, p. 725–728.
- Rasmussen B and Buick R 2000, Oily old ores: Evidence for hydrothermal petroleum generation in an Archean volcanogenic massive sulfide deposit: *Geology*, v. 28, p. 731–734.
- Rasmussen, B, Fletcher, IR and Muhling, JR 2007, In situ U–Pb dating and element mapping of three generations of monazite: unravelling cryptic tectonothermal events in low-grade terranes: *Geochimica et Cosmochimica Acta*, v. 71, no. 3, p. 670–690.
- Rasmussen, B, Krapež, B and Meier, DB 2014a, Replacement origin for hematite in 2.5 Ga banded iron formation: evidence for postdepositional oxidation of iron-bearing minerals: *Geological Society of America Bulletin*, v. 126, no. 3/4, p. 438–446.
- Rasmussen, B, Krapež, B and Muhling, JR 2014b, Hematite replacement of iron-bearing precursor sediments in the 3.46-b.y.-old Marble Bar Chert, Pilbara Craton, Australia: *Geological Society of America Bulletin*, v. 126, p. 1245–1258.
- Rasmussen, B, Muhling, JR, Suvorova, A and Krapež, B 2016, Dust to dust: evidence for the formation of 'primary' hematite dust in banded iron formations via oxidation of iron silicate nanoparticles: *Precambrian Research*, v. 284, p. 49–63.
- Reading, AM, Tkalčić, H, Kennett, BL, Johnson, SP and Sheppard, S 2012, Seismic structure of the crust and uppermost mantle of the Capricorn and Paterson Orogens and adjacent cratons, Western Australia, from passive seismic transects: *Precambrian Research*, v. 196–197, p. 295–308, doi:10.1016/j.precamres.2011.07.001.
- Retallack, GJ 2018, The oldest known paleosol profiles on Earth: 3.46 Ga Panorama Formation, Western Australia: *Palaeogeography, Palaeoclimatology, Palaeoecology*, v. 489, p. 230–248.
- Retallack, GJ, Krinsley, DH, Fischer, R, Razink, JJ and Langworthy, KP 2106, Archean coastal-plain paleosols and life on land: *Gondwana Research*, v. 40, p. 1–20.
- Reynolds, DG, Brook, WA, Marshall, AE and Allchurch, PD 1975, Volcanogenic copper–zinc deposits in the Pilbara and Yilgarn Archean Blocks, in *Economic geology of Australia and Papua New Guinea, 1. Metals* edited by CL Knight: Australasian Institute of Mining and Metallurgy, Monograph 5, p. 185–195.
- Rhyder, G 1991, Accretion and bombardment of the Earth–Moon system: the lunar record: *Lunar and Planetary Science Contributions*, v. 746, p. 42–43.
- Richards, JR, Fletcher, IR and Blockley, JG 1981, Pilbara galenas: Precise isotopic assay of the oldest Australian leads; model ages and growth-curve implications: *Mineralium Deposita*, v. 16, no. 1, p. 7–30.
- Roberts, NMW and Spencer, CJ 2015, The zircon archive of continent formation through time, in *Continent formation through time* edited by NMW Roberts, M Van Kranendonk, S Parman and PD Clift: The Geological Society, London, Special Publications 389, p. 197–225, doi:10.1144/SP389.14.
- Runnegar, B, Dollase, WA, Ketcham, RA, Colbert, M and Carlson, WD 2001, Early Archean sulfates from Western Australia first formed as hydrothermal barites not gypsum evaporites: *Geological Society of America, Annual Meeting*, November 5–8, 2001, Paper No. 166-0.
- Ryan, GR 1965, The geology of the Pilbara Block: *Australasian Institute of Mining and Metallurgy Proceedings*, v. 214, p. 61–94.
- Ryan, GR and Kriewaldt, M 1964, Facies changes in the Archean of the West Pilbara Goldfield, in *Annual report for the year 1963: Geological Survey of Western Australia*, p. 28–30.
- Scherer, E, Münker, C and Mezger, K 2001, Calibration of the lutetium–hafnium clock: *Science*, v. 293, p. 683–687. doi: 10.1126/science.1061372.
- Schopf, JW 1992, Paleobiology of the Archean, in *The Proterozoic biosphere: a multidisciplinary study* edited by JW Schopf and C Klein: Cambridge University Press, New York, p. 25–39.
- Schopf, JW 1993, Microfossils of the early Archean Apex Chert: new evidence of the antiquity of life: *Science*, v. 260, p. 640–646.
- Schopf, JW 2006, Fossil evidence of Archean life: *Philosophical Transactions of the Royal Society B: Biological Sciences*, v. 361, p. 869–885, doi:10.1098/rstb.2006.1834.
- Schopf, JW, Kitajima, K, Spicuzza, MJ, Kudryavtsev, AB and Valley, JW 2018, SIMS analyses of the oldest known assemblage of microfossils document their taxon-correlated carbon isotope compositions: *Proceedings of the National Academy of Sciences*, v. 115, no. 1, p. 53–58, doi:10.1073/pnas.1718063115.
- Schopf, JW and Kudryavtsev, AB 2005, Three-dimensional Raman imagery of Precambrian microscopic organisms: *Geobiology*, v. 3, p. 1–12.
- Schopf, JW, Kudryavtsev, AB, Agresti, DG, Wdowiak, TJ and Czaja, AD 2002a, Laser-Raman imagery of Earth's earliest fossils: *Nature*, v. 416, p. 73–76.
- Schopf, JW, Kudryavtsev, AB, Agresti, DG, Wdowiak, TJ and Czaja, AD 2002b, Images of the Earth's earliest fossils? (discussion and reply): *Nature*, v. 420, p. 476–477.
- Schopf, JW, Kudryavtsev, AB, Czaja, AD and Tripathi, AB 2007, Evidence of Archean life: stromatolites and microfossils: *Precambrian Research*, v. 158, p. 141–155.
- Schopf, JW and Packer, BM 1987, Early Archean (3.3-billion to 3.5-billion-year-old) microfossils from the Warrawoona Group, Australia: *Science*, v. 237, p. 70–73.
- Schopf, JW and Walter, MR 1983, Archean microfossils: New evidence of ancient microbes, in *Earth's earliest biosphere: Its origin and evolution*, edited by JW Schopf: Princeton University Press, Princeton, NJ, p. 214–239.
- Shackleton, RM 1995, Tectonic evolution of greenstone belts, in *Early Precambrian processes* edited by MP Coward and AC Reis: The Geological Society, London, Special Publications 95, p. 53–65.
- Sheppard, S, Krapež, B, Zi, JW, Rasmussen, B and Fletcher, I 2017, SHRIMP U–Pb zircon geochronology establishes that banded iron formations are not chronostratigraphic markers across Archean greenstone belts of the Pilbara Craton: *Precambrian Research*, v. 292, p. 290–304.
- Sheppard, S, Occhipinti, SA and Nelson, DR 2005, Intracontinental reworking in the Capricorn Orogen, Western Australia: The 1680–1620 Ma Mangaroon Orogeny: *Australian Journal of Earth Sciences*, v. 52, p. 443–460.
- Simonson, BM and Hassler, SW 2002, Revisiting an Archean impact layer – Comment: *Science*, v. 298, p. 750.
- Simonson, BM, Sumner, DY, Beukes, NJ, Johnson, S and Gutzmer, J 2009, Correlating multiple Neoproterozoic–Paleoproterozoic impact spherule layers between South Africa and Western Australia: *Precambrian Research*, v. 169, no. 1–4, p. 100–111.
- Smirnov, AV, Evans, ADA, Ernst, RE, Söderlund, U and Li, ZX 2013, Trading partners: tectonic ancestry of southern Africa and western Australia, in *Archean supercratons Vaalbara and Zimgarn: Precambrian Research*, v. 224, p. 11–12.
- Smith, AJB 2015, The life and times of banded iron formations: *Geology*, v. 43, no. 12, p. 1111–1112, doi:10.1130/focus122015.1.
- Smith, JB 2003, The episodic development of intermediate to silicic volcano-plutonic suites in the Archean West Pilbara, Australia: *Chemical Geology*, v. 194, p. 275–295.

- Smith, JB, Barley, ME, Groves, DI, Krapež, B, McNaughton, NJ, Bickle, MJ and Chapman, HJ 1998, The Sholl Shear Zone, West Pilbara; evidence for a domain boundary structure from integrated tectonostratigraphic analysis, SHRIMP U–Pb dating and isotopic and geochemical data of granitoids: *Precambrian Research*, v. 88, p. 143–172.
- Smithies, RH 1997, The Mallina Formation, Constantine Sandstone and Whim Creek Group: a new stratigraphic and tectonic interpretation for part of the western Pilbara Craton, in *Geological Survey of Western Australia Annual Review 1996–97: Geological Survey of Western Australia*, p. 83–88.
- Smithies, RH 1998a, Geology of the Sherlock 1:100 000 sheet: Geological Survey of Western Australia, 1:100 000 Geological Series Explanatory Notes, 29p.
- Smithies, RH 1998b, Geology of the Mount Wohler 1:100 000 sheet: Geological Survey of Western Australia, 1:100 000 Geological Series Explanatory Notes, 19p.
- Smithies, RH 2000, The Archaean tonalite–trondhjemite–granodiorite (TTG) series is not an analogue of Cenozoic adakite: *Earth and Planetary Science Letters*, v. 182, p. 115–125.
- Smithies, RH 2002a, Archaean boninite-like rocks in an intracratonic setting: *Earth and Planetary Science Letters*, v. 197, no. 1–2, p. 19–34.
- Smithies, RH 2002b, De Grey, WA Sheet 2757: Geological Survey of Western Australia, 1:100 000 Geological Series.
- Smithies, RH 2002c, Pardoo, WA Sheet 2857: Geological Survey of Western Australia, 1:100 000 Geological Series.
- Smithies, RH 2003a, Geology of the White Springs 1:100 000 sheet: Geological Survey of Western Australia, 1:100 000 Geological Series Explanatory Notes, 16p.
- Smithies, RH 2003b, Geology of the Hooley 1:100 000 sheet: Geological Survey of Western Australia, 1:100 000 Geological Series Explanatory Notes, 15p.
- Smithies, RH 2004, Geology of the De Grey and Pardoo 1:100 000 sheets: Geological Survey of Western Australia, 1:100 000 Geological Series Explanatory Notes, 23p.
- Smithies, RH and Champion, DC 2000, The Archaean high-Mg diorite suite: links to tonalite–trondhjemite–granodiorite magmatism and implication for early Archaean crustal growth: *Journal of Petrology*, v. 41, no. 12, p. 1653–1671.
- Smithies, RH, Champion, DC and Blewett, RS 2001a, Wallaringa, WA Sheet 2656: Geological Survey of Western Australia, 1:100 000 Geological Series.
- Smithies, RH, Champion, DC and Blewett, RS 2002, Geology of the Wallaringa 1:100 000 sheet: Geological Survey of Western Australia, 1:100 000 Geological Series Explanatory Notes, 27p.
- Smithies, RH, Champion, DC and Cassidy, KF 2003, Formation of Earth's early Archaean continental crust: *Precambrian Research*, v. 127, p. 89–101.
- Smithies, RH, Champion, DC and Sun, S-S 2004, Evidence for early LREE-enriched mantle source regions: diverse magmas from the c. 3.0 Ga Mallina Basin, Pilbara Craton, NW Australia: *Journal of Petrology*, v. 45, no. 8, p. 1515–1537.
- Smithies, RH, Champion, DC, Van Kranendonk, MJ and Hickman, AH 2007a, Geochemistry of volcanic rocks of the northern Pilbara Craton, Western Australia: Geological Survey of Western Australia, Report 104, 47p.
- Smithies, RH, Champion, DC and Van Kranendonk, MJ 2007b, The oldest well-preserved volcanic rocks on Earth: Geochemical clues to the early evolution of the Pilbara Supergroup and implications for the growth of a Paleoproterozoic continent, in *Earth's oldest rocks edited by MJ Van Kranendonk, VC Bennett and RH Smithies*: Elsevier BV, Burlington, Massachusetts, USA, *Developments in Precambrian Geology* 15, p. 339–367.
- Smithies, RH, Champion, DC and Van Kranendonk, MJ 2009, Formation of Paleoproterozoic continental crust through infracrustal melting of enriched basalt: *Earth and Planetary Science Letters*, v. 281, no. 3, p. 298–306.
- Smithies, RH, Champion, DC and Van Kranendonk, MJ 2019, The oldest well-preserved felsic volcanic rocks on Earth: geochemical clues to the early evolution of the Pilbara Supergroup and implications for the growth of a Paleoproterozoic protocontinent, in *Earth's oldest rocks (2nd ed.) edited by MJ Van Kranendonk, VC Bennett and JE Hoffmann*: Elsevier B.V., p. 463–486.
- Smithies, RH, Champion, DC, Van Kranendonk, MJ, Howard, HM and Hickman, AH 2005a, Modern-style subduction processes in the Mesoarchaean: geochemical evidence from the 3.12 Ga Whundo intra-oceanic arc: *Earth and Planetary Science Letters*, v. 231, no. 3–4, p. 221–237.
- Smithies, RH and Farrell, TR 2000a, Satirist, WA Sheet 2555: Geological Survey of Western Australia, 1:100 000 Geological Series.
- Smithies, RH and Farrell, TR 2000b, Geology of the Satirist 1:100 000 sheet: Geological Survey of Western Australia, 1:100 000 Geological Series Explanatory Notes, 42p.
- Smithies, RH, Hickman, AH and Nelson, DR 1999, New constraints on the evolution of the Mallina Basin, and their bearing on relationships between the contrasting eastern and western granite–greenstone terranes of the Archaean Pilbara Craton, Western Australia: *Precambrian Research*, v. 94, p. 11–28.
- Smithies, RH, Ivanic, TJ, Lowrey, JR, Morris, PA, Barnes, SJ, Wyche, S and Lu, Y-J 2018, Two distinct origins for Archaean greenstone belts: *Earth and Planetary Science Letters*, v. 487, p. 106–116.
- Smithies, RH, Nelson, DR and Pike, G 2001b, Development of the Archaean Mallina Basin, Pilbara Craton, northwestern Australia; a study of detrital and xenocrystic zircon ages: *Sedimentary Geology*, 141–142, p. 79–94.
- Smithies, RH, Van Kranendonk, MJ and Champion, DC 2005b, It started with a plume – early Archaean basaltic proto-continental crust: *Earth and Planetary Science Letters*, v. 238, no. 3–4, p. 284–297.
- Smithies, RH, Van Kranendonk, MJ and Champion, DC 2007c, The Mesoarchaean emergence of modern-style subduction, in *Island arcs: past and present edited by S Maruyama and M Santosh*, *Gondwana Research* v. 11, no. 1–2, p. 50–68, doi:10.1016/j.gr.2006.02.001.
- Spaggiari, CV, Wartho, J-A and Wilde, SA 2008, Proterozoic deformation in the northwest of the Archaean Yilgarn Craton, Western Australia: *Precambrian Research*, v. 162, p. 354–384.
- Stein, HJ, Barley, ME, Zimmerman, A and Cummins, B 2007, A 3.3 Ga Mo–Cu porphyry-style deposit at Spinifex Ridge, East Pilbara, Western Australia: Re–Os dating of Paleoproterozoic molybdenite: *Geochimica et Cosmochimica Acta*, v. 71, article no. A970.
- Stern, RA, Bodorkos, S, Kamo, SL, Hickman, AH and Corfu, F 2009, Measurement of SIMS instrumental mass fractionation and Pb isotopes during zircon dating: *Geostandards and Geoanalytical Research*, v. 33, p. 145–168.
- Storey, M 1995, The role of mantle plumes in continental breakup: case histories from Gondwanaland: *Nature*, v. 377, p. 301–308.
- Strik, G, Blake, TS, Zegers, TE, White, SH and Langereis, CG 2003, Palaeomagnetism of flood basalts in the Pilbara Craton, Western Australia: Late Archaean continental drift and the oldest known reversal of the geomagnetic field: *Journal of Geophysical Research*, v. 108, no. B12, article no. 2551, doi:10.1029/2003JB002475.
- Strong, CA, Hickman, AH and Kojan, CJ 2000, Preston, WA Sheet 2156: Geological Survey of Western Australia, 1:100 000 Geological Series.
- Sugahara, H, Sugitani, K, Mimura, K, Yamashita, F and Yamamoto, K 2010, A systematic rare-earth elements and yttrium study of Archaean cherts at the Mount Goldsworthy greenstone belt in the Pilbara Craton: implications for the origin of microfossil-bearing black cherts: *Precambrian Research*, v. 177, p. 73–87.
- Sugitani, K 1992, Geochemical characteristics of Archaean cherts and other sedimentary rocks in the Pilbara Block, Western Australia: evidence for Archaean seawater enriched in hydrothermally derived iron and silica: *Precambrian Research*, v. 57, p. 21–47.
- Sugitani, K, Grey, K, Allwood, A, Nagaoka, T, Mimura, K, Minami, M, Marshall, CP, Van Kranendonk, MJ and Walter, MR 2007, Diverse microstructures from Archaean chert from the Mount Goldsworthy–Mount Grant area, Pilbara Craton, Western Australia: microfossils, dubiofossils, or pseudofossils? *Precambrian Research*, v. 158, p. 228–262.

- Sugitani, K, Grey, K, Nagaoka, T, Mimura, K and Walter, MR 2009a, Taxonomy and biogenicity of spheroidal microfossils (c. 3.0 Ga) from the Mount Goldsworthy–Mount Grant area in the northeastern Pilbara Craton, Western Australia, *in* World summit on ancient microfossils, 27 July – 2 August 2008 *edited by* JW Schopf and DJ Bottjer: IGPP Center for the Study of Evolution and the Origin of Life (CSEOL), University of California, Precambrian Research 173, p. 50–59.
- Sugitani, K, Grey, K, Nagaoka, T and Mimura, K 2009b, Three-dimensional morphological and textural complexity of Archean putative microfossils form the northeastern Pilbara Craton: indications of biogenicity of large (>15 µm) spheroidal and spindle-like structures: *Astrobiology*, v. 9, p. 603–615.
- Sugitani, K, Lepot, K, Mimura, K, Van Kranendonk, MJ, Oehler, D and Walter, MR 2010, Biogenicity of morphologically diverse carbonaceous microstructures from the ca. 3400 Ma Strelley Pool Formation, in the Pilbara Craton, Western Australia: *Astrobiology*, v. 10, p. 899–920.
- Sugitani, K, Mimura, K, Nagaoka, T, Lepot, K and Takeuchi, M 2013, Microfossil assemblage from the 3400 Ma Strelley Pool Formation in the Pilbara Craton, Western Australia: results from a new locality: *Precambrian Research*, v. 226, p. 59–74.
- Sugitani, K, Mimura, K, Suzuki, K, Nagamine, K and Sugisaki, R 2003, Stratigraphy and sedimentary petrology of an Archean volcanic-sedimentary succession at Mt Goldsworthy in the Pilbara Block, Western Australia: implications of evaporite (nahcolite) and barite deposition: *Precambrian Research*, v. 120, no. 1–2, p. 55–79.
- Sugitani, K, Mimura, K, Takeuchi, M, Lepot, K, Ito, S and Javaux, EJ 2015, Early evolution of large micro-organisms with cytological complexity revealed by microanalyses of 3.4 Ga walled microfossils: *Geobiology*, v. 13, p. 507–521.
- Sugitani, K, Yamashita, F, Nagaoka, T, Minami, M, Mimura, K and Suzuki, K 2006, Geochemistry and sedimentary petrology of Archean clastic sedimentary rocks at Mt. Goldsworthy, Pilbara Craton, Western Australia: evidence for the early evolution of continental crust and hydrothermal alteration: *Precambrian Research*, v. 147, p. 124–147.
- Sullivan, CJ 1939, The Hong Kong, Pilbara and Egina mining centres, Pilbara Goldfield: Aerial Geological and Geophysical Survey of Northern Australia, Western Australia Report No 52, 6p.
- Sun, S-S and Hickman, AH 1998, New Nd-isotopic and geochemical data from the west Pilbara – implications for Archean crustal accretion and shear zone development: Australian Geological Survey Organisation, Research Newsletter, no. 28, p. 25–29.
- Sun, S-S and Hickman, AH 1999, Geochemical characteristics of ca 3.0-Ga Cleaverville greenstones and later mafic dykes, west Pilbara: implication for Archean crustal accretion: Australian Geological Survey Organisation, Research Newsletter, no. 31, p. 23–29.
- Sutton, J 1971, Some developments in the crust, *in* Symposium on Archean Rocks, Perth, 23–26 May 1970 *edited by* JE Glover: Geological Society of Australia, Perth, Western Australia, Special Publication 3, p. 1–10.
- Sweetapple, MT 2000, Characteristics of Sn–Ta–Be–Li industrial mineral deposits of the Archean Pilbara Craton, Western Australia: AGSO, Canberra, Record 2000/044, 54p.
- Sweetapple, MT and Collins, PLF 1998, Tantalum–tin mineralized pegmatites at Wodgina and Mt. Cassierite, Pilbara Craton, Western Australia, *in* Geoscience for the new millenium *edited by* Geological Society of Australia: 14th Australian Geological Convention, Townsville, Queensland, 6–10 July 1998, p. 435.
- Sweetapple, MT and Collins, PLF 2002, Genetic framework for the classification and distribution of Archean rare metal pegmatites in the North Pilbara Craton, Western Australia: *Economic Geology*, v. 97, p. 873–895.
- Sweetapple, MT, Collins, PLF and Hickey, RJ 2001, Classification, distribution, and petrogenetic affiliation of the Archean rare metal pegmatites, Pilbara Craton, W.A., *in* Extended Abstracts – 4th International Archean Symposium, Perth, 24–28 September 2001 *edited by* KF Cassidy, J Dunphy and MJ Van Kranendonk: AGSO (Geoscience Australia), Record 2001/37, p. 475–477.
- Sweetapple, MT, Holmes, J, Yong, J, Grigson, MW, Barnes, L and Till, S 2017, Pilgangoora lithium–tantalum pegmatite deposit, *in* Australian Ore Deposits *edited by* GN Phillips: Australasian Institute of Mining and Metallurgy, Monograph 32, 339–342.
- Taylor, T 1985, De Grey Project – Mt Grant E.L. 45/50 Pilbara Mineral Field, W.A. Sedimentological Appraisal of the Amphitheatre Gold Prospect: Technical Report: Carpentaria Exploration Company Pty Ltd: Geological Survey of Western Australia, Statutory mineral exploration report A15836 (unpublished), 21p.
- Terabayashi, M, Masuda, Y and Ozawa, H 2003, Archean ocean floor metamorphism in the North Pole area, Pilbara Craton, Western Australia: *Precambrian Research*, v. 127, p. 167–180.
- Tessalina, SG, Bourdon, B, Van Kranendonk, M, Birck, JL and Philippot, P 2010, Influence of Hadean crust evident in basalts and cherts from the Pilbara Craton: *Nature Geoscience*, v. 3, no. 3, p. 214–217.
- Thébaud, N and Rey, PF 2013, Archean gravity-driven tectonics on hot and flooded continents: controls on long-lived hydrothermal systems away from continental margins: *Precambrian Research*, v. 229, p. 93–104.
- Thom, R, Hickman, AH and Chin RJ 1980, Nullagine, WA Sheet SF51-5 (2nd edition): Geological Survey of Western Australia, 1:250 000 Geological Series.
- Thorne, AM and Trendall, AF 2001, Geology of the Fortescue Group, Pilbara Craton, Western Australia: Geological Survey of Western Australia, Bulletin 144, 249p.
- Thorne, AM, Tyler, IM, Korsch, RJ, Johnson, SP, Brett, JW, Cutten, HN, Blay, OA, Kennett, BLN, Blewett, RS, Joly, A, Dentith, MC, Aitken, ARA, Holzschuh, J, Goodwin, JA, Salmon, M, Reading, A and Boren, G 2011, Preliminary interpretation of deep seismic reflection line 10GA-CP1: crustal architecture of the northern Capricorn Orogen, *in* Capricorn Orogen seismic and magnetotelluric (MT) workshop 2011: extended abstracts *edited by* SP Johnson, A Thorne and IM Tyler: Geological Survey of Western Australia, Record 2011/25, p. 19–26.
- Thorpe, R, Hickman, AH, Davis, D, Morton, JGG and Trendall, AF 1992a, U–Pb zircon geochronology of Archean felsic units in the Marble Bar region, Pilbara Craton, Western Australia: *Precambrian Research*, v. 56, p. 169–189.
- Thorpe, R, Hickman, AH, Davis, DW, Mortensen, JK and Trendall, AF 1992b, Constraints to models for Archean lead evolution from precise U–Pb geochronology from the Marble Bar region, Pilbara Craton, Western Australia, *in* The Archean: Terrains, processes and metallogeny: Proceedings for the Third International Archean Symposium, 17–21 September 1990 *edited by* JE Glover and SE Ho: Geology Department and University Extension, The University of Western Australia, Perth, Western Australia, Publication 22, p. 395–408.
- Thorpe, RI, Hickman, AH, Davis, DW, Mortensen, JK and Trendall, AF 1990, Application of recent zircon U–Pb geochronology in the Marble Bar region, Pilbara Craton, to modelling Archean lead evolution, *in* Extended abstracts volume *edited by* JE Glover and SE Ho: Third International Archean Symposium, 17–21 September 1990: Geoconferences (W.A.) Inc, Perth, Western Australia, p. 11–13.
- Tice, MM and Lowe, DR 2004, Photosynthetic microbial mats in the 3,416-Myr-old ocean: *Nature*, v. 43, p. 549–552.
- Trendall, AF 1968, Three great basins of Precambrian banded iron-formation deposition: a systematic comparison: *Geological Society of America Bulletin*, v. 79, no. 11, p. 1527–1544.
- Trendall, AF 1975, Precambrian – introduction, *in* The geology of Western Australia *compiled by* Geological Survey of Western Australia: Geological Survey of Western Australia, Memoir 2, p. 25–32.
- Trendall, AF 1990a, Pilbara Craton – Introduction, *in* Geology and mineral resources of Western Australia *compiled by* Geological Survey of Western Australia: Geological Survey of Western Australia, Memoir 3, p. 128.
- Trendall, AF 1990b, Pilbara Craton – Hamersley Basin, *in* Geology and mineral resources of Western Australia *compiled by* Geological Survey of Western Australia: Geological Survey of Western Australia, Memoir 3, p. 163–189.

- Trendall, AF 1995, Paradigms for the Pilbara, in *Early Precambrian processes edited by MP Coward and AC Reis: The Geological Society, London, Special Publications* 95, p. 127–142.
- Trendall, AF and Blockley, JG 1970, The iron formations of the Precambrian Hamersley Group, Western Australia, with special reference to the associated crocidolite: Geological Survey of Western Australia, Bulletin 119, 366p.
- Tungsten Mining NL 2018, Big Hill Project, East Pilbara, WA: Australian Securities Exchange (ASX), released 31/10/2018, <www.listcorp.com/asx/tgn/tungsten-mining/news/2018-annual-report-2009244.html>.
- Tyler, IM, Fletcher, IR, de Laeter, JR, Williams, IR and Libby, WG 1992, Isotope and rare earth element evidence for a late Archaean terrane boundary in the southeastern Pilbara Craton, Western Australia: *Precambrian Research*, v. 54, p. 211–229.
- Tyler, IM, Hunter, WM and Williams, IR 1991, Newman, Western Australia: Geological Survey of Western Australia, 1:250 000 Geological Series Explanatory Notes, 36p.
- Tyler, IM and Thorne, AM 1990, The northern margin of the Capricorn Orogen, Western Australia – an example of an early Proterozoic collision zone: *Journal of Structural Geology*, v. 12, p. 685–701.
- Ueno, Y 2007, Stable carbon and sulfur isotope geochemistry of the ca. 3490 Ma Dresser Formation hydrothermal deposit, Pilbara Craton, Western Australia, in *Earth's oldest rocks edited by MJ Van Kranendonk, VC Bennett and RH Smithies: Elsevier BV, Burlington, Massachusetts, USA, Developments in Precambrian Geology* 15, p. 203–236.
- Ueno, Y, Isozaki, Y, Yurimoto, H and Maruyama, S 2001a, Carbon isotopic signatures of individual Archean microfossils(?) from Western Australia: *International Geology Review*, v. 43, no. 3, p. 196–212.
- Ueno, Y, Maruyama, S, Isozaki, Y and Yurimoto, H 2001b, Early Archean (ca. 3.5 Ga) microfossils and ^{13}C -depleted carbonaceous matter in the North Pole area, Western Australia: field occurrence and geochemistry, in *Geochemistry and the origin of life edited by S Nakashima, S Maruyama, A Brack and BF Windley: Universal Academic Press, Inc., Tokyo, Japan*, p. 203–236.
- Ueno, Y, Yamada, K, Yoshida, N, Maruyama, S and Isozaki, Y 2006, Evidence from fluid inclusions for microbial methanogenesis in the early Archaean era: *Nature*, v. 440, p. 516–519.
- van den Boorn, SHJM, van Bergen, MJ, Nijman, W and Vroon, PZ 2007, Dual role of seawater and hydrothermal fluids in early Archean chert formation: evidence from silicon isotopes: *Geology*, v. 35, no. 10, p. 939–942.
- van den Boorn, SHJM, van Bergen, MJ, Vroon, PZ, de Vries, ST and Nijman, W 2010, Silicon isotope and trace element constraints on the origin of ~3.5 Ga cherts: implications for Early Archean marine environments: *Geochimica et Cosmochimica Acta*, v. 74, p. 1077–1103.
- van Haften, WM and White, SH 1998, Evidence for multiphase deformation in the Archean basal Warrawoona Group in the Marble Bar area, East Pilbara, Western Australia: *Precambrian Research*, v. 88, no. 1–4, p. 53–66.
- van Haften, WM and White, SH 2001, Reply to comment on 'Evidence for multiphase deformation in the Archean basal Warrawoona Group in the Marble Bar area, East Pilbara, Western Australia' by MJ Van Kranendonk, AH Hickman and WJ Collins: *Precambrian Research*, v. 105, p. 79–84.
- van Koolwijk, ME, Beintema, KA, White, SH and Wijbrans, JR 2001, Petrogenesis and structures of the basal Warrawoona Group, Marble Bar Belt, Pilbara Craton, WA, in *Extended Abstracts – 4th International Archaean Symposium, Perth, 24–28 September 2001 edited by KF Cassidy, J Dunphy and MJ Van Kranendonk: AGSO (Geoscience Australia), Record* 2001/37, p. 102–103.
- Van Kranendonk, MJ 1997, Results of field mapping, 1994–1996, in the North Shaw and Tambourah 1:100 000 sheet areas, eastern Pilbara Craton, northwestern Australia: Australian Geological Survey Organisation (Geoscience Australia), Record 1997/23, 44p.
- Van Kranendonk, MJ 1998, Litho-tectonic and structural components of the North Shaw 1:100 000 sheet, Archaean Pilbara Craton, in *Geological Survey of Western Australia Annual Review 1997–98: Geological Survey of Western Australia*, p. 63–70.
- Van Kranendonk, MJ 1999a, North Shaw, WA Sheet 2755: Geological Survey of Western Australia, 1:100 000 Geological Series.
- Van Kranendonk, MJ 1999b, Two-stage degassing of the Archaean mantle: evidence from the 3.46 Ga Panorama volcano, Pilbara Craton, Western Australia, in *GSWA 99 extended abstracts: new geological data for WA explorers: Geological Survey of Western Australia, Record* 1999/6, p. 1–3.
- Van Kranendonk, MJ 2000a, Geology of the North Shaw 1:100 000 sheet: Geological Survey of Western Australia, 1:100 000 Geological Series Explanatory Notes, 86p.
- Van Kranendonk, MJ 2000b, Evidence of thick Archaean crust in the East Pilbara, in *GSWA 2000 extended abstracts: geological data for WA explorers in the new millennium: Geological Survey of Western Australia, Record* 2000/8, p. 1–3.
- Van Kranendonk, MJ 2001, Volcanic degassing, hydrothermal circulation and the flourishing of early life on Earth: new evidence from the c. 3.46 Ga Warrawoona Group, Pilbara Craton, Western Australia: *The West Australian Geologist*, no. 402, p. 3.
- Van Kranendonk, MJ 2003, Geology of the Tambourah 1:100 000 sheet: Geological Survey of Western Australia, 1:100 000 Geological Series Explanatory Notes, 57p.
- Van Kranendonk, MJ 2004a, Carlindie, WA Sheet 2756: Geological Survey of Western Australia, 1:100 000 Geological Series.
- Van Kranendonk, MJ 2004b, Geology of the Carlindie 1:100 000 sheet: Geological Survey of Western Australia, 1:100 000 Geological Series Explanatory Notes, 45p.
- Van Kranendonk, MJ 2004c, Coongan, WA Sheet 2856: Geological Survey of Western Australia, 1:100 000 Geological Series.
- Van Kranendonk, MJ 2006, Volcanic degassing, hydrothermal circulation and the flourishing of early life on Earth: a review of the evidence from c. 3490–3240 Ma rocks of the Pilbara Supergroup, Pilbara Craton, Western Australia: *Earth-Science Reviews*, v. 74, p. 197–240.
- Van Kranendonk, MJ 2007, A review of the evidence for putative Paleoproterozoic life in the Pilbara Craton, in *Earth's oldest rocks edited by MJ Van Kranendonk, VC Bennett and RH Smithies: Elsevier BV, Burlington, Massachusetts, USA, Developments in Precambrian Geology* 15, p. 855–896.
- Van Kranendonk, MJ 2008, Structural geology of the central part of the Lalla Rookh – Western Shaw structural corridor, Pilbara Craton, Western Australia: Geological Survey of Western Australia, Report 103, 29p.
- Van Kranendonk, MJ 2010a, Three and a half billion years of life on earth: A transect back into deep time: Geological Survey of Western Australia, Record 2010/21, 93p.
- Van Kranendonk, MJ 2010b, Two types of Archean continental crust: plume and plate tectonics on early Earth: *American Journal of Science*, v. 310, no. 10, p. 1187–1209, doi:10.2475/10.2010.01.
- Van Kranendonk, MJ 2010c, Geology of the Coongan 1:100 000 sheet: Geological Survey of Western Australia, 1:100 000 Geological Series Explanatory Notes, 67p.
- Van Kranendonk, MJ 2011, Cool greenstone drips and the role of partial convective overturn in Barberton greenstone belt evolution: *Journal of African Earth Sciences*, v. 60, no. 5, p. 346–352, doi:10.1016/j.jafrearsci.2011.03.012.
- Van Kranendonk, MJ 2014, Earth's early atmosphere and surface environments: A review, in *Earth's early atmosphere and surface environment edited by GH Shaw: Geological Society of America, Special Paper* 504, p. 105–130, doi:10.1130/2014.2504(12).
- Van Kranendonk, MJ and Collins, WJ 1998, Timing and tectonic significance of Late Archaean, sinistral strike-slip deformation in the Central Pilbara Structural Corridor, Pilbara Craton, Western Australia: *Precambrian Research*, v. 88, no. 1–4, p. 207–232, doi:10.1016/s0301-9268(97)00069-7.

- Van Kranendonk, MJ and Collins, WJ 2001, A review of the evidence for vertical tectonics in the Archean Pilbara Craton, Western Australia, *in* Extended Abstracts – 4th International Archean Symposium, Perth, 24–28 September 2001 *edited by* KF Cassidy, J Dunphy and MJ Van Kranendonk: AGSO (Geoscience Australia), Record 2001/37, p. 365–367.
- Van Kranendonk, MJ, Collins, WJ, Hickman, AH and Pawley, MJ 2004a, Critical tests of vertical vs horizontal tectonic models for the Archean East Pilbara granite–greenstone terrane, Pilbara Craton, Western Australia: *Precambrian Research*, v. 131, no. 3, p. 173–211.
- Van Kranendonk, MJ and Hickman, AH 2000, Archean geology of the North Shaw region, East Pilbara granite–greenstone terrane, Western Australia – a field guide: Geological Survey of Western Australia, Record 2000/5, 64p.
- Van Kranendonk, MJ, Hickman, AH and Collins, WJ 2001b, Comment on ‘Evidence for multiphase deformation in the Archean basal Warrawoona Group in the Marble Bar area, East Pilbara, Western Australia’: *Precambrian Research*, v. 105, p. 73–78.
- Van Kranendonk, MJ, Hickman, AH and Huston, DL 2006b, Geology and mineralization of the east Pilbara – a field guide: Geological Survey of Western Australia, Record 2006/16, 90p.
- Van Kranendonk, MJ, Hickman, AH, Smithies, RH and Champion, DC 2007a, Paleoproterozoic development of a continental nucleus: the East Pilbara Terrane of the Pilbara Craton, Western Australia, *in* Earth’s oldest rocks *edited by* MJ Van Kranendonk, VC Bennett and RH Smithies: Elsevier B.V., Burlington, Massachusetts, USA, *Developments in Precambrian Geology* 15, p. 307–337.
- Van Kranendonk, MJ, Hickman, AH, Smithies, RH, Nelson, DN and Pike, G 2002, Geology and tectonic evolution of the Archean North Pilbara terrain, Pilbara Craton, Western Australia: *Economic Geology*, v. 97, p. 695–732, doi:10.2113/gsecongeo.97.4.695.
- Van Kranendonk, MJ, Hickman, AH, Smithies, RH, Williams, IR, Bagas, L and Farrell, TR 2006a, Revised lithostratigraphy of Archean supracrustal and intrusive rocks in the northern Pilbara Craton, Western Australia: Geological Survey of Western Australia, Record 2006/15, 57p.
- Van Kranendonk, MJ, Hickman, AH, Williams, IR and Nijman, W 2001a, Archean geology of the East Pilbara granite–greenstone terrane, Western Australia – a field guide: Geological Survey of Western Australia, Record 2001/9, 134p.
- Van Kranendonk, MJ and Johnston, J 2009, Discovery trails to early Earth – a traveller’s guide to the east Pilbara of Western Australia: Geological Survey of Western Australia, 168p.
- Van Kranendonk, MJ, Kröner, A, Hoffman, JE, Nagel, T and Anhaeusser, CR 2014, Just another drip: re-analysis of a proposed Mesoarchean suture from the Barberton Mountain Land, South Africa: *Precambrian Research*, v. 254, p. 19–35, doi:10.1016/j.precamres.2014.07.022.
- Van Kranendonk, MJ, McGuinness, SA, Bodorkos, S and Hickman, AH 2012, Carlindie, WA Sheet 2756 (2nd edition): Geological Survey of Western Australia, 1:100 000 Geological Series.
- Van Kranendonk, MJ and Morant, P 1998, Revised Archean stratigraphy of the North Shaw 1:100 000 sheet, Pilbara Craton, in Geological Survey of Western Australia Annual Review 1997–98: Geological Survey of Western Australia, Perth, Western Australia, p. 55–62.
- Van Kranendonk, MJ and Nijman, W 2001, Geology of the North Pole Dome, *in* Archean geology of the East Pilbara Granite–Greenstone Terrane, Western Australia – a field guide *edited by* MJ Van Kranendonk, AH Hickman, IR Williams, and W Nijman: Geological Survey of Western Australia, Record 2001/9, p. 53–72.
- Van Kranendonk, MJ and Pawley, MJ 2002, Tambourah, WA Sheet 2754: Geological Survey of Western Australia, 1:100 000 Geological Series.
- Van Kranendonk, MJ, Philippot, P and Lepot, K 2006c, The Pilbara drilling project: c. 2.72 Ga Tumbiana Formation and c. 3.49 Ga Dresser Formation, Pilbara Craton, Western Australia: Geological Survey of Western Australia, Record 2006/14, 25p.
- Van Kranendonk, MJ, Philippot, P, Lepot, K, Bodorkos, S and Pirajno, F 2008, Geological setting of Earth’s oldest fossils in the c. 3.5 Ga Dresser Formation, Pilbara Craton, Western Australia: *Precambrian Research*, v. 167, p. 93–124.
- Van Kranendonk, MJ and Pirajno, F 2004, Geochemistry of metabasalts and hydrothermal alteration zones associated with c. 3.45 Ga chert and barite deposits: Implications for the geological setting of the Warrawoona Group, Pilbara Craton, Australia: *Geochemistry: Exploration, Environment, Analysis*, v. 4, p. 253–278.
- Van Kranendonk, MJ and Smithies, RH 2006, Port Hedland – Bedout Island, WA Sheet SF 50-4 and Part Sheet SE 50-16 (3rd edition): Geological Survey of Western Australia, 1:250 000 Geological Series.
- Van Kranendonk, MJ, Smithies, RH and Champion, DC 2019, Chapter 19 – Paleoproterozoic development of a continental nucleus: the East Pilbara Terrane of the Pilbara Craton, Western Australia, *in* Earth’s oldest rocks (2nd edition) *edited by* MJ Van Kranendonk, VC Bennett and JE Hoffmann: Elsevier B.V., p. 437–462, doi:10.1016/B978-0-444-63901-1.00019-8.
- Van Kranendonk, MJ, Smithies, RH, Griffin, WL, Huston, DL, Hickman, AH, Champion, DC, Anhaeusser, CR and Pirajno, F 2015, Making it thick: a volcanic plateau origin of Paleoproterozoic continental lithosphere of the Pilbara and Kaapvaal cratons: Geological Society, London, Special Publications, v. 389, p. 89–111, doi:10.1144/SP389.12.
- Van Kranendonk, MJ, Smithies, RH, Hickman, AH, Bagas, L, Williams, IR and Farrell, TR 2004b, Archean supergroups and supersuites in the northern Pilbara Craton: the application of event stratigraphy to 1 Ga of crustal and metallogenic evolution, *in* GSWA 2004 extended abstracts: promoting the prospectivity of Western Australia: Geological Survey of Western Australia, Record 2004/5, p. 5–7.
- Van Kranendonk, MJ, Smithies, RH, Hickman, AH, Bagas, L, Williams, IR, and Farrell, TR 2004c, Event stratigraphy applied to 700 million years of Archean crustal evolution, Pilbara Craton, Western Australia: Geological Survey of Western Australia, Annual Review 2003–04, p. 49–61.
- Van Kranendonk, MJ, Smithies, RH, Hickman, AH and Champion, DC 2007b, Secular tectonic evolution of Archean continental crust: Interplay between horizontal and vertical processes: *Terra Nova*, v. 19, p. 1–38.
- Van Kranendonk, MJ, Smithies, RH, Hickman, AH, Wingate, MTD and Bodorkos, S 2010, Evidence for Mesoarchean (~3.2 Ga) rifting of the Pilbara Craton: the missing link in an early Precambrian Wilson cycle: *Precambrian Research*, v. 177, p. 145–161.
- Van Kranendonk, MJ, Webb, GE and Kamber, BS 2003, Geological and trace element evidence for a marine sedimentary environment of deposition and biogenicity of 3.45 Ga stromatolitic carbonates in the Pilbara Craton, and support for a reducing Archean ocean: *Geobiology*, v. 1, p. 91–108.
- van Schijndel, V, Stevens, G, Zeh, A, Frei, D and Lana, C 2017, Zircon geochronology and Hf isotopes of the Dwalile Supracrustal Suite, Ancient Gneiss Complex, Swaziland: Insights into the diversity of Palaeoproterozoic source rocks, depositional and metamorphic ages: *Precambrian Research*, v. 295, p. 48–66.
- Vearncombe, S, Barley, ME, Groves, DI, McNaughton, NJ, Mikucki, EJ and Vearncombe, JR 1995, 3.26 Ga black smoker-type mineralization in the Strelley Belt, Pilbara Craton, Western Australia: *Journal of the Geological Society, London*, v. 152, p. 587–590.
- Vearncombe, S and Kerrich, R 1999, Geochemistry and geodynamic setting of volcanic and plutonic rocks associated with Early Archean volcanogenic massive sulphide mineralization, Pilbara Craton: *Precambrian Research*, v. 98, p. 243–270.
- Vearncombe, S, Vearncombe, JR and Barley, ME 1998, Fault and stratigraphic controls on volcanogenic massive sulphide deposits in the Strelley belt, Pilbara Craton, Western Australia: *Precambrian Research*, v. 88, no. 1-4, p. 67–82.
- Venturex Resources Limited 2017, An emerging copper–zinc producer with exceptional exploration upside in WA’s Pilbara: Australian Securities Exchange (ASX), released 28/11/2017, 29p.
- Venturex Resources Limited 2020, Financial report for the year ended 30 June 2020: Report to Australian Securities Exchange (ASX), released 25 September 2020, 60p.
- Vervoort, JD 2011, Evolution of the depleted mantle–revisited, *in* Abstracts: American Geophysical Union Fall meeting 2011, San Francisco, California, 5–9 December 2011, abstract ID V43E-06, 2p.

- Vervoort, JD and Blichert-Toft, J 1999, Evolution of the depleted mantle: Hf isotope evidence from juvenile rocks through time: *Geochimica et Cosmochimica Acta*, v. 63, p. 533–556.
- Vervoort, JD and Kemp, AIS 2016, Clarifying the zircon Hf isotope record of crust–mantle evolution: *Chemical Geology*, v. 425, p. 65–75, doi:10.1016/j.chemgeo.2016.01.023.
- Viljoen, RP and Viljoen, MJ 1971, The geological and geochemical evolution of the Onverwacht volcanic group of the Barberton Mountain Land, South Africa, in *Symposium on Archaean Rocks*, Perth, 23–26 May 1970 edited by JE Glover: Geological Society of Australia, Perth, Western Australia, Special Publication 3, p. 133–149.
- Wacey, D, Kilburn M. R., Saunders, M, Cliff, J and Brasier, MD 2011, Microfossils of sulphur-metabolizing cells in 3.4-billion-year-old rocks of Western Australia: *Nature Geoscience*, v. 4, p. 698–702.
- Wacey, D, McLoughlin, N, Stoakes, CA, Kilburn, MR, Green, OR and Brasier, MD 2010, The 3426–3350 Ma Strelley Pool Formation in the East Strelley greenstone belt – a field and petrographic guide: Geological Survey of Western Australia, Record 2010/10, 64p.
- Walker, JCG 1978, Early history of oxygen and ozone in the atmosphere: *Pure and Applied Geophysics*, v. 117, p. 498–512.
- Walter MR 1983, Archaean stromatolites: Evidence of the Earth's earliest benthos, in *Earth's Earliest Biosphere: Its Origin and Evolution*, edited by JW Schopf: Princeton University Press, Princeton, NJ, p. 187–213.
- Walter, MR, Buick, R and Dunlop, JSR 1980, Stromatolites 3,400–3,500 Myr old from the North Pole area, Western Australia: *Nature*, v. 284, p. 443–445.
- Weir, DJ 1989a, Annual Report for 1989 on ELs 45/701 – 45/714 (SHAY 1–14), Yarrie SF51-01, Western Australia: CRA Exploration Pty Limited: Geological Survey of Western Australia, Statutory mineral exploration report A28257 (unpublished), 27p.
- Weir, DJ 1989b, Annual Report for 1989 on C.E.C Joint Venture Area, Cattle Gorge, EL 45/430, Yarrie SF51-01, Western Australia: CRA Exploration Pty Limited: Geological Survey of Western Australia, Statutory mineral exploration report A29365 (unpublished), 94p.
- White, RS and McKenzie, D 1989, Magmatism at rift zones: the generation of volcanic continental margins and flood basalts: *Journal of Geophysical Research*, v. 94, p. 76785–77729.
- White, SH, Zegers, TE, van Haaften, WM, Kloppenburg, A and Wijbrans, JR 1998, Tectonic evolution of the eastern Pilbara, Australia: *Geologie en Mijnbouw*, v. 76, p. 343–347.
- White, WM 2013, *Geochemistry*: Wiley-Blackwell, Chichester, UK, 660p.
- Wiemer, D, Schrank, CE, Murphy, DT and Hickman, AH 2016, Lithostratigraphy and structure of the early Archaean Doolena Gap greenstone belt, East Pilbara Terrane, Western Australia: *Precambrian Research*, v. 282, p. 121–138.
- Wiemer, D, Schrank, CE, Murphy, DT, Wenham, L and Allen, CM 2018, Earth's oldest stable crust in the Pilbara Craton formed by cyclic gravitational overturns: *Nature Geoscience*, v. 11, no. 5, p. 357–361, doi:10.1038/s41561-018-0105-9.
- Wijbrans, JR and McDougall, I 1987, On the metamorphic history of an Archaean granitoid greenstone terrane, East Pilbara, Western Australia, using the $^{40}\text{Ar}/^{39}\text{Ar}$ age spectrum technique: *Earth and Planetary Science Letters*, v. 84, p. 226–242.
- Wilhelmij, HR 1986, Depositional history of the middle Archaean sedimentary sequences in the Pilbara Block, Western Australia – a genetic stratigraphic analysis of the terrigenous rocks of the Pilgangoora syncline: The University of Western Australia, Perth, PhD thesis (unpublished).
- Wilhelmij, HR and Dunlop, JSR 1984, A genetic stratigraphic investigation of the Gorge Creek Group in the Pilgangoora syncline, in *Archaean and Proterozoic basins of the Pilbara*, Western Australia: Evolution and mineralization potential edited by JR Muhling, DI Groves and TS Blake: The University of Western Australia, Geology Department and University Extension, Publication no 9, p. 68–88.
- Wille, M, Nebel, Q, Van Kranendonk, MJ, Schoenberg, R, Kleinhanns, IC and Ellwood, MJ 2013, Mo–Cr isotope evidence for a reducing Archean atmosphere in 3.46–2.76 Ga black shales from the Pilbara, Western Australia: *Chemical Geology*, v. 340, p. 68–76.
- Williams, IR 1968, Yarraloola, Western Australia: Geological Survey of Western Australia, 1:250 000 Geological Series Explanatory Notes, 30p.
- Williams, IR 1989, Balfour Downs, Western Australia (2nd edition): Geological Survey of Western Australia, 1:250 000 Geological Series Explanatory Notes, 38p.
- Williams, IR 1998, Muccan, WA Sheet 2956: Geological Survey of Western Australia, 1:100 000 Geological Series.
- Williams, IR 1999a, Geology of the Muccan 1:100 000 sheet: Geological Survey of Western Australia, 1:100 000 Geological Series Explanatory Notes, 39p.
- Williams, IR 1999b, Cooragoora, WA Sheet 2957: Geological Survey of Western Australia, 1:100 000 Geological Series.
- Williams, IR 2000, Geology of the Cooragoora 1:100 000 sheet: Geological Survey of Western Australia, 1:100 000 Geological Series Explanatory Notes, 23p.
- Williams, IR 2001, Geology of the Warrawagine 1:100 000 sheet: Geological Survey of Western Australia, 1:100 000 Geological Series Explanatory Notes, 33p.
- Williams, IR 2003, Yarrie, Western Australia (3rd edition): Geological Survey of Western Australia, 1:250 000 Geological Series Explanatory Notes, 84p.
- Williams, IR 2007, Geology of the Yilgalong 1:100 000 sheet: Geological Survey of Western Australia, 1:100 000 Geological Series Explanatory Notes, 45p.
- Williams, IR and Bagas, L 2007a, Geology of the Mount Edgar 1:100 000 sheet: Geological Survey of Western Australia, 1:100 000 Geological Series Explanatory Notes, 62p.
- Williams, IR and Bagas, L 2007b, Mount Edgar, WA Sheet 2955 (version 2): Geological Survey of Western Australia, 1:100 000 Geological Series.
- Williams, IR and Hickman, AH 2000, Archaean geology of the Muccan region, East Pilbara granite–greenstone terrane, Western Australia – a field guide: Geological Survey of Western Australia, Record 2000/4, 30p.
- Williams, IR and Hickman, AH 2007, Nullagine, WA Sheet SF 51-16 (3rd edition): Geological Survey of Western Australia, 1:250 000 Geological Series.
- Williams, IR and Trendall, AF 1998, Geology of the Isabella 1:100 000 sheet: Geological Survey of Western Australia, 1:100 000 Geological Series Explanatory Notes, 24p.
- Williams, IR and Tyler, IM 1991, Robertson, Western Australia (2nd edition): Geological Survey of Western Australia, 1:250 000 Geological Series Explanatory Notes, 36p.
- Williams, IS and Collins, WJ 1990, Granite–greenstone terranes in the Pilbara Block, Australia, as coeval volcano–plutonic complexes: evidence from U–Pb zircon dating of the Mount Edgar batholith: *Earth and Planetary Science Letters*, v. 97, p. 41–53, doi:10.1098/rsta.1973.0004.
- Williams, IS, Page, RW, Foster, JJ, Compston, W, Collerson, KD and McCulloch, MT 1983a, Zircon U–Pb ages from the Shaw Batholith, Pilbara Block, determined by ion microprobe: Australian National University, Research School of Earth Sciences, Annual Report for 1982, p. 199–203.
- Williams, IS, Page, RW, Froude, D, Foster, JJ and Compston, W 1983b, Early crustal components in the Western Australian Archaean: zircon U–Pb ages by ion microprobe analysis from the Shaw Batholith and Narryer Metamorphic Belt: Geological Society of Australia, Abstracts Series v. 9, p. 169.
- Winchester, JA and Floyd, PA 1977, Geochemical discrimination of different magma series and their differentiation products using immobile elements: *Chemical Geology*, v. 20, p. 325–343.
- Windley, BF 1973, A discussion on the evolution of the Precambrian crust – crustal development in the Precambrian: *Philosophical Transactions of the Royal Society A: Mathematical, Physical and Engineering Sciences*, v. 273, p. 321–341.
- Windley, BF 1977, *The Evolving Continents*: John Wiley and Sons Ltd, UK, 385p.
- Windley, BF 1995, *The Evolving Continents* (3rd edition): John Wiley and Sons Ltd, U.K., 526p.
- Wingate, MTD 1998, A palaeomagnetic test of the Kaapvaal – Pilbara (Vaalbara) hypothesis at 2.78 Ga: *South African Journal of Geology*, v. 101, p. 257–274.

- Wingate, MTD, Bodorkos, S and Van Kranendonk, MJ 2009a, 178185: gabbro sill, Sulphur Springs; Geochronology Record 804: Geological Survey of Western Australia, 4p.
- Wingate, MTD, Bodorkos, S and Van Kranendonk, MJ 2009b, 180048: felsic metavolcanic rock, Cattle Well; Geochronology Record 807: Geological Survey of Western Australia, 4p.
- Wingate, MTD, Bodorkos, S and Van Kranendonk, MJ 2009c, 180056: granophyre, Eel Creek; Geochronology Record 808: Geological Survey of Western Australia, 4p.
- Wingate, MTD, Bodorkos, S and Van Kranendonk, MJ 2009d, 180057: tonalitic orthogneiss, Big Junction Well; Geochronology Record 809: Geological Survey of Western Australia, 4p.
- Wingate, MTD, Bodorkos, S and Van Kranendonk, MJ 2009e, 180070: volcanoclastic sandstone, drillcore PDP2c, Dresser Mine; Geochronology Record 811: Geological Survey of Western Australia, 4p.
- Wingate, MTD, Bodorkos, S and Van Kranendonk, MJ 2009f, 180095: felsic volcanoclastic metasandstone, Pioneer Mine; Geochronology Record 812: Geological Survey of Western Australia, 5p.
- Wingate, MTD, Bodorkos, S and Van Kranendonk, MJ 2009g, 180098: welded rhyolitic tuff, Hong Kong Mine; Geochronology Record 814: Geological Survey of Western Australia, 4p.
- Wingate, MTD, Kirkland, CL, Bodorkos, S and Hickman, AH 2010, 160258, felsic metavolcanic rock, Orchard Well; Geochronology Record 840: Geological Survey of Western Australia, 4p.
- Wingate, MTD, Kirkland, CL, Bodorkos, S, Van Kranendonk, MJ and Hickman, AH 2012a, 160958: volcanoclastic metasandstone, Trendall Reserve; Geochronology Record 1070: Geological Survey of Western Australia, 6p.
- Wingate, MTD, Kirkland, CL, Hickman, AH and Van Kranendonk, MJ 2012b, 160956: metarhyolite, Black Hill Well; Geochronology Record 1068: Geological Survey of Western Australia, 4p.
- Wingate, MTD, Kirkland, CL, Hickman, AH and Van Kranendonk, MJ 2012c, 160957: felsic volcanoclastic rock, Mount York; Geochronology Record 1069: Geological Survey of Western Australia, 4p.
- Wingate, MTD, Kirkland, CL and Hickman, AH 2015a, 178011: biotite granodiorite, Cookes Creek; Geochronology Record 1226: Geological Survey of Western Australia, 4p.
- Wingate, MTD, Kirkland, CL and Hickman, AH 2015b, 178170: leucogabbro, Little Fortune mine; Geochronology Record 1227: Geological Survey of Western Australia, 4p.
- Wingate, MTD, Lu, Y and Hickman, AH 2016, 178047: porphyritic metamonzogranite, Mulga Well; Geochronology Record 1349: Geological Survey of Western Australia, 4p.
- Wingate, MTD, Lu, Y and Johnson, SP 2017a, 195897: quartzite, Cubana Well; Geochronology Record 1364: Geological Survey of Western Australia, 6p.
- Wingate, MTD, Lu, Y and Johnson, SP 2017b, 203712: quartzite, Cubana Well; Geochronology Record 1576: Geological Survey of Western Australia, 7p.
- Wingate, MTD, Lu, Y, Kirkland, CL and Johnson, SP 2018a, 195898: biotite monzogranite, 4 Mile Bore; Geochronology Record 1486: Geological Survey of Western Australia, 4p.
- Wingate, MTD, Lu, Y, Kirkland, CL and Johnson, SP 2018b, 195899: biotite monzogranite, Great Northern Highway; Geochronology Record 1487: Geological Survey of Western Australia, 4p.
- Wingate, MTD, Lu, Y and Johnson, SP 2019a, 216542: metamonzogranite, Garden Well; Geochronology Record 1560: Geological Survey of Western Australia, 4p.
- Wingate, MTD, Lu, Y and Johnson, SP 2019b, 216545: metatonalite, Mujee Pool; Geochronology Record 1566: Geological Survey of Western Australia, 5p.
- Wingate, MTD, Lu, Y and Johnson, SP 2019c, 216594: metatonalite, Mujee Pool; Geochronology Record 1567: Geological Survey of Western Australia, 4p.
- Wingate, MTD, Lu, Y and Johnson, SP 2019d, 216598: metarhyolite, Cubana Well; Geochronology Record 1568: Geological Survey of Western Australia, 5p.
- Witt, WK, Hickman, AH, Townsend, DB and Preston, WA 1998, Mineral potential of the Archean Pilbara and Yilgarn Cratons, Western Australia: *Journal of Australian Geology and Geophysics*, v. 17, p. 201–221.
- Zegers, TE 1996, Structural, kinematic, and metallogenic evolution of selected domains of the Pilbara granite–greenstone terrain: *Geologica Ultraiectina*, Utrecht University, Utrecht, the Netherlands, PhD thesis (unpublished), 208p.
- Zegers, TE, Barley, ME, Groves, DI, McNaughton, NJ and White, SH 2002, Oldest gold: deformation and hydrothermal alteration in the early Archean shear zone-hosted Bamboo Creek Deposit, Pilbara, Western Australia: *Economic Geology*, v. 97, p. 757–773.
- Zegers, TE, De Wit, MJ, Dann, J and White, SH 1998b, Vaalbara, Earth's oldest assembled continent? A combined structural, geochronological, and palaeomagnetic test: *Terra Nova*, v. 10, p. 250–259.
- Zegers, TE, Keijzer, M de, Passchier, CW and White, SH 1998a, The Mulgandinnah shear zone; an Archean crustal scale strike-slip zone, eastern Pilbara, Western Australia: *Precambrian Research*, v. 88, p. 233–248.
- Zegers, TE, Nelson, DR, Wijbrans, JR and White, SH 2001, SHRIMP U-Pb zircon dating of Archean core complex formation and pancratonic strike-slip deformation in the East Pilbara granite–greenstone terrain: *Tectonics*, v. 20, no. 6, p. 883–908.
- Zegers, TE, White, SH, de Keijzer, M and Dirks, P 1996, Extensional structures during deposition of the 3460 Ma Warrawoona Group in the eastern Pilbara Craton, Western Australia: *Precambrian Research*, v. 80, no. 1, p. 89–105.
- Zegers, TE, Wijbrans, JR and White, SH 1999, $^{40}\text{Ar}/^{39}\text{Ar}$ age constraints on tectonothermal events in the Shaw area of the eastern Pilbara granite–greenstone terrain (Western Australia): 700 Ma of Archean tectonic evolution: *Tectonophysics*, v. 311, p. 45–81.
- Zeh, A, Jaguin, J, Poujal, M, Boulvais, P, Block, S and Paquette, J-L 2013, Juvenile crust formation in the northeast Kaapvaal Craton at 2.97 Ga – Implications for Archean terrane accretion, and the source of the Pietersburg gold: *Precambrian Research*, v. 233, p. 20–43.
- Zeh, A, Stern, RA and Gerdes, A 2014, The oldest zircons of Africa – their U–Pb–Hf–O isotope and trace element systematics, and implications for Hadean–Archean crust–mantle evolution: *Precambrian Research*, v. 241, p. 203–230.
- Zhao, G, Cawood, PA, Wilde, SA and Sun, M 2002, Review of global 2.1–1.8 Ga orogens: implications for a pre-Rodinia supercontinent: *Earth-Science Reviews*, v. 59, no. 1–4, p. 125–162.
- Zhao, G, Sun, M, Wilde, SA and Li, S 2004, A Paleo-Mesoproterozoic supercontinent: assembly, growth and breakup: *Earth-Science Reviews*, v. 67, no. 1–2, p. 91–123.

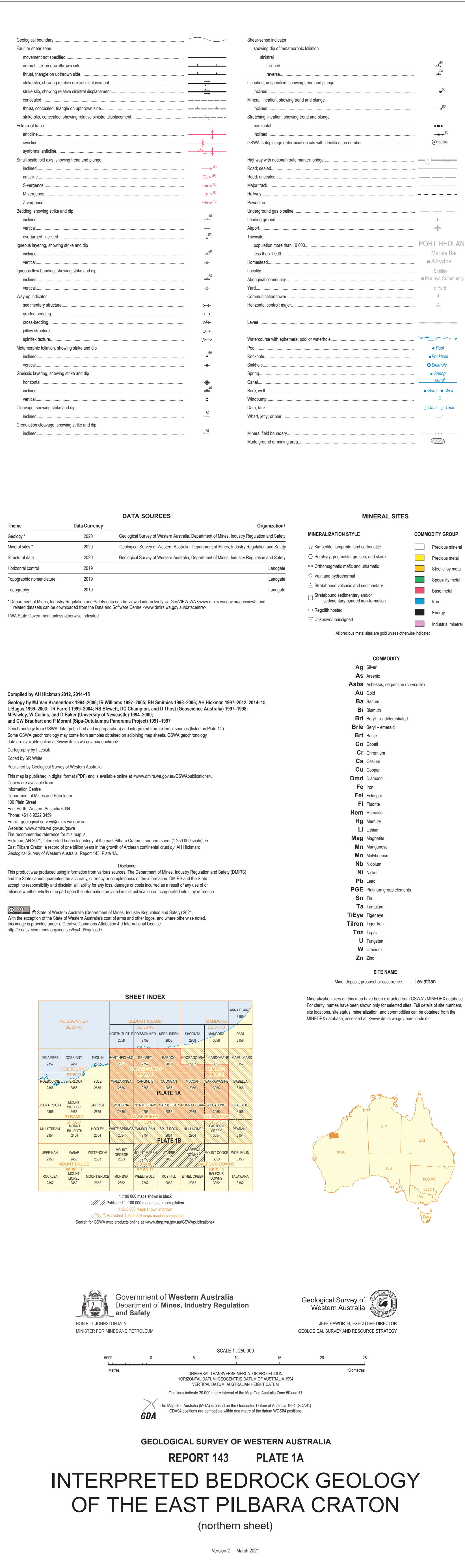
The east Pilbara Craton provides the most complete geological record of Paleoarchean crustal evolution that is available in any of Earth's Archean cratons. Extensive geochemical, geochronological and isotopic evidence indicates that its greenstone succession, the 15 km-thick Pilbara Supergroup, evolved during a series of plume-related magmatic events over 300 Ma, forming a large continental volcanic plateau overlying Eoarchean to early Paleoarchean sialic crust, also formed over almost 300 Ma. The continental plateau setting precludes once-popular tectonic models in which early Archean greenstones were interpreted to be remnants of ancient oceanic crust. Those models were largely based on the belief that Phanerozoic-style plate tectonic processes also operated

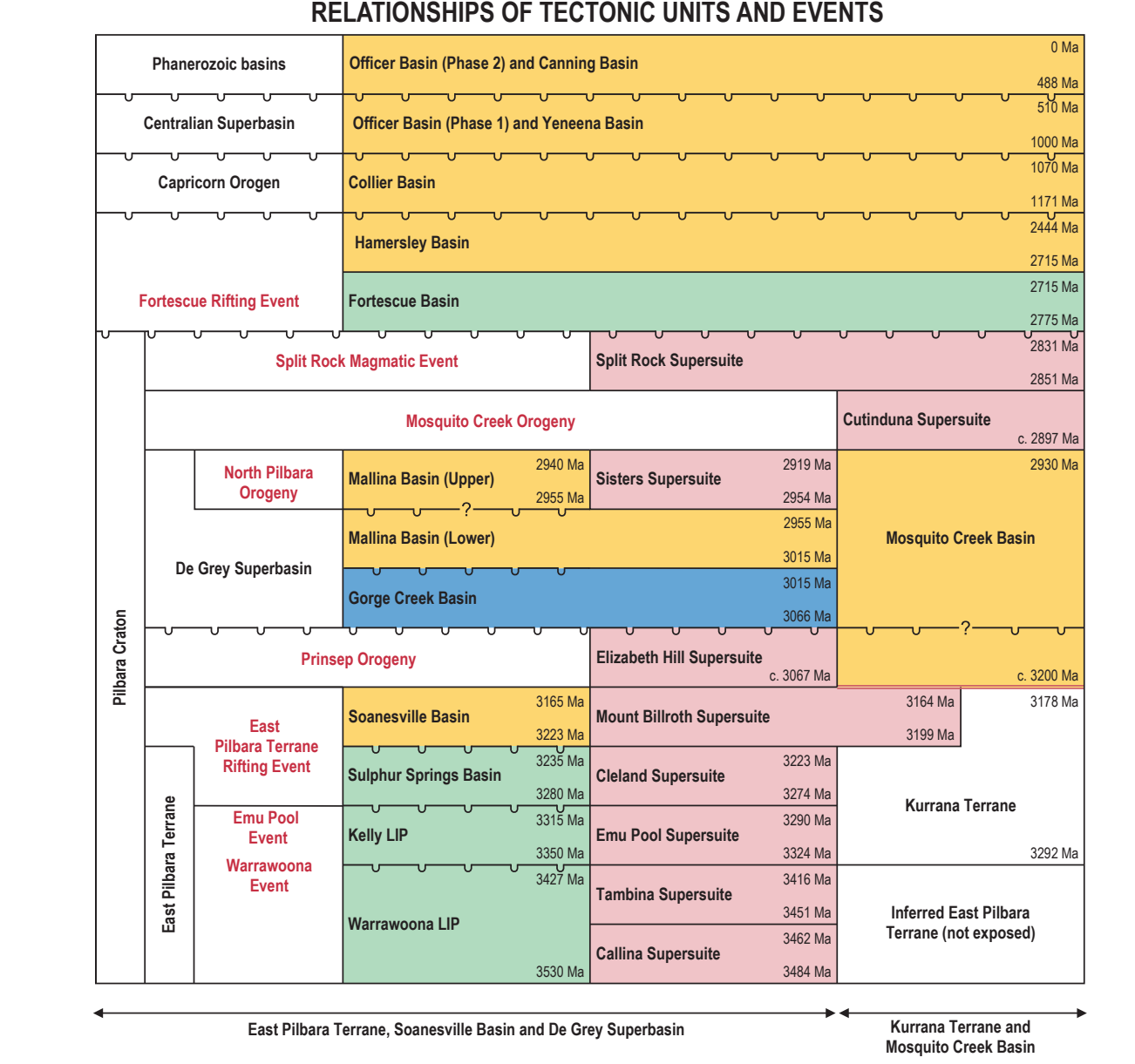
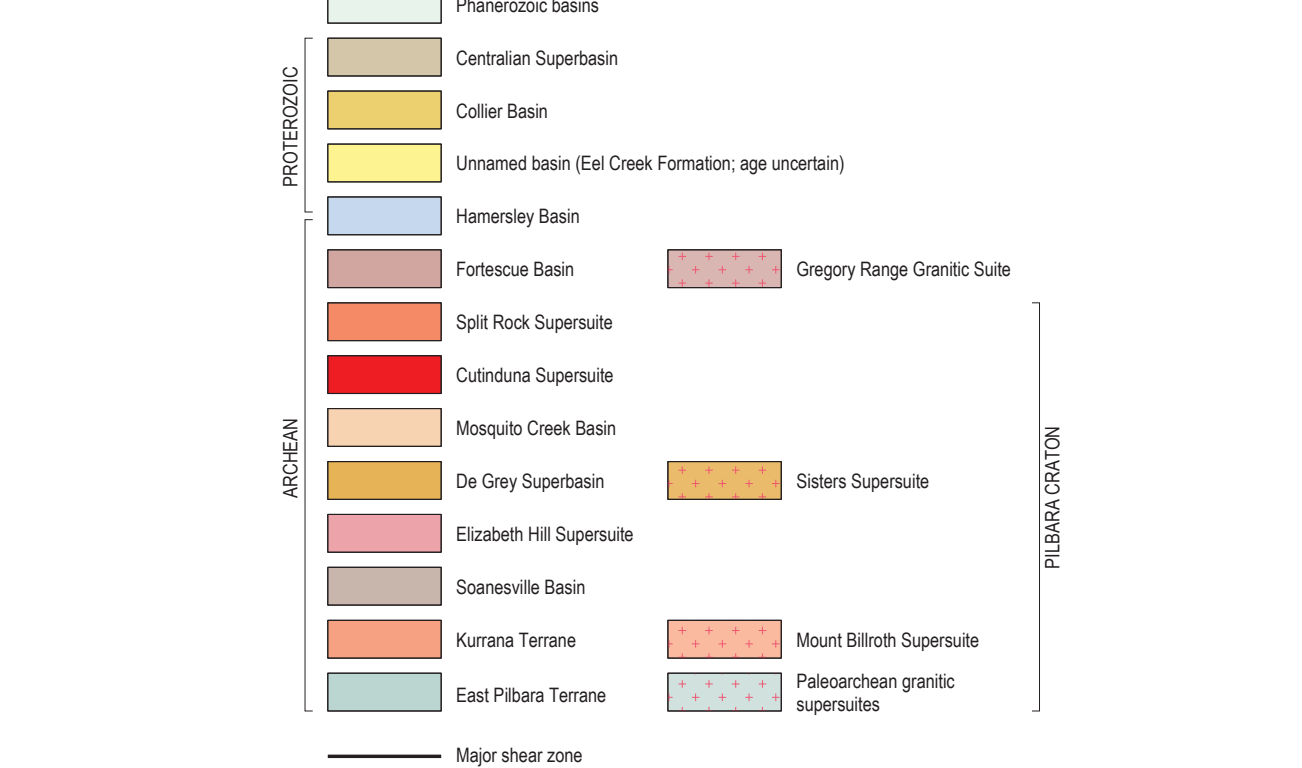
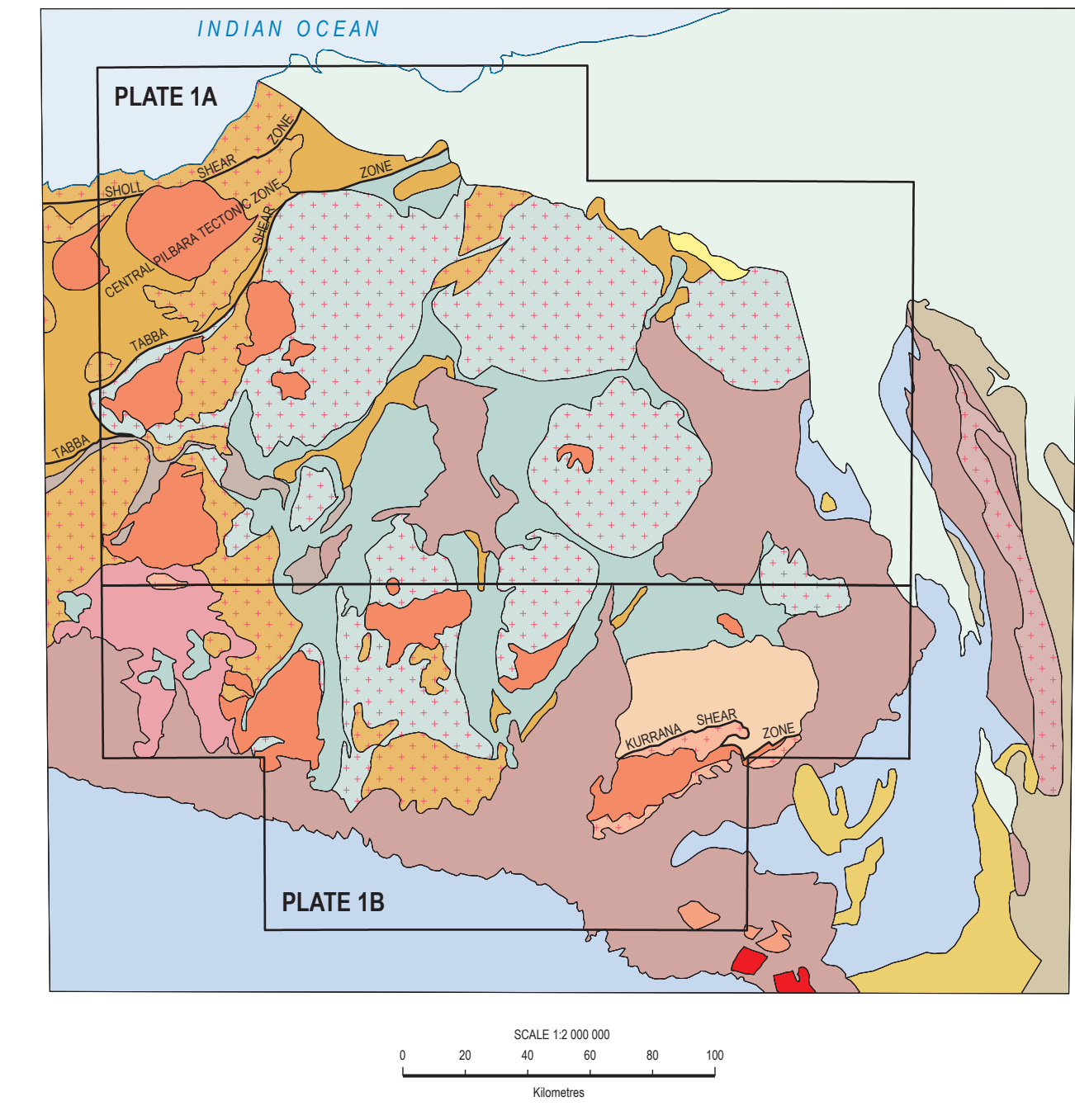
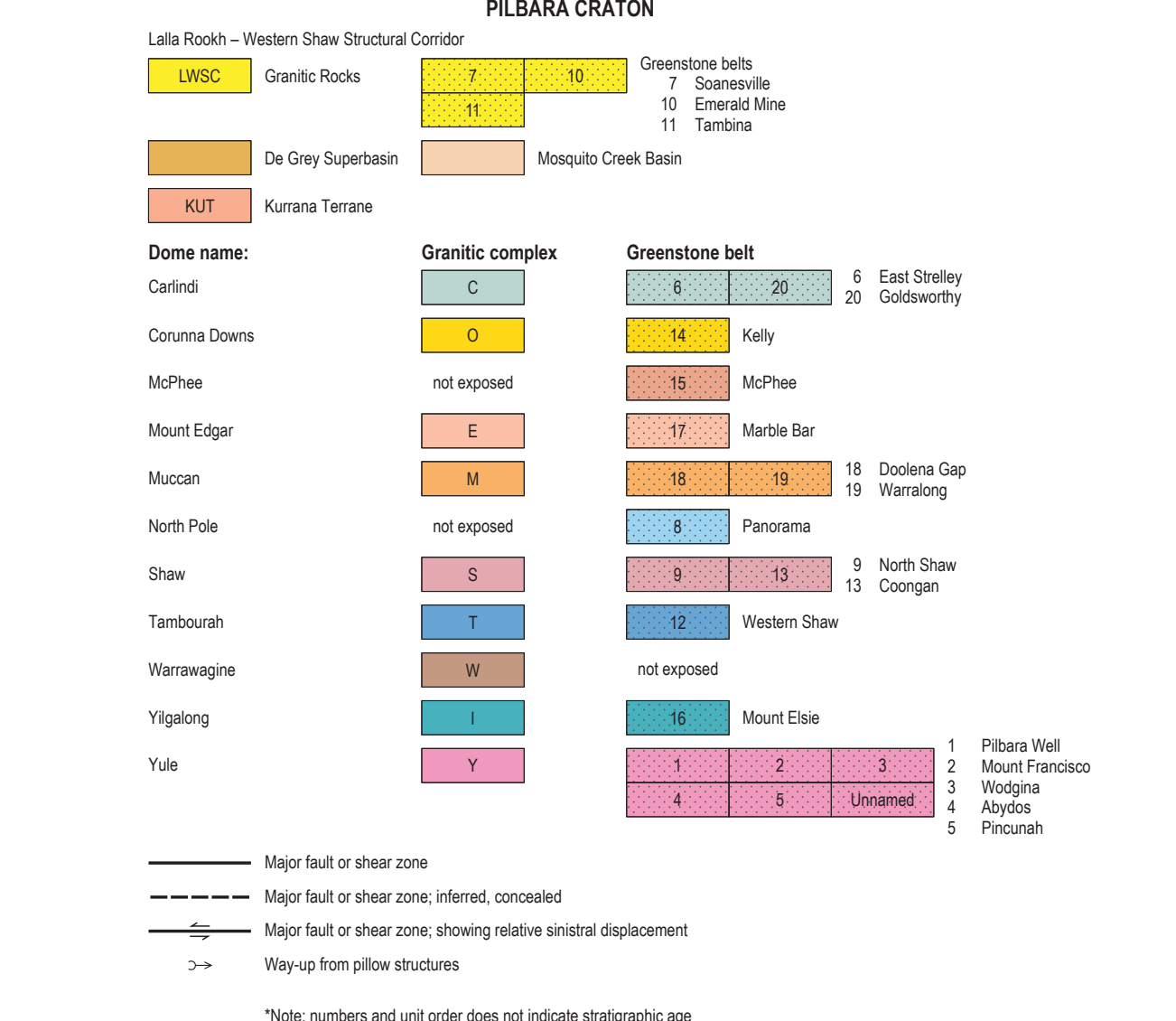
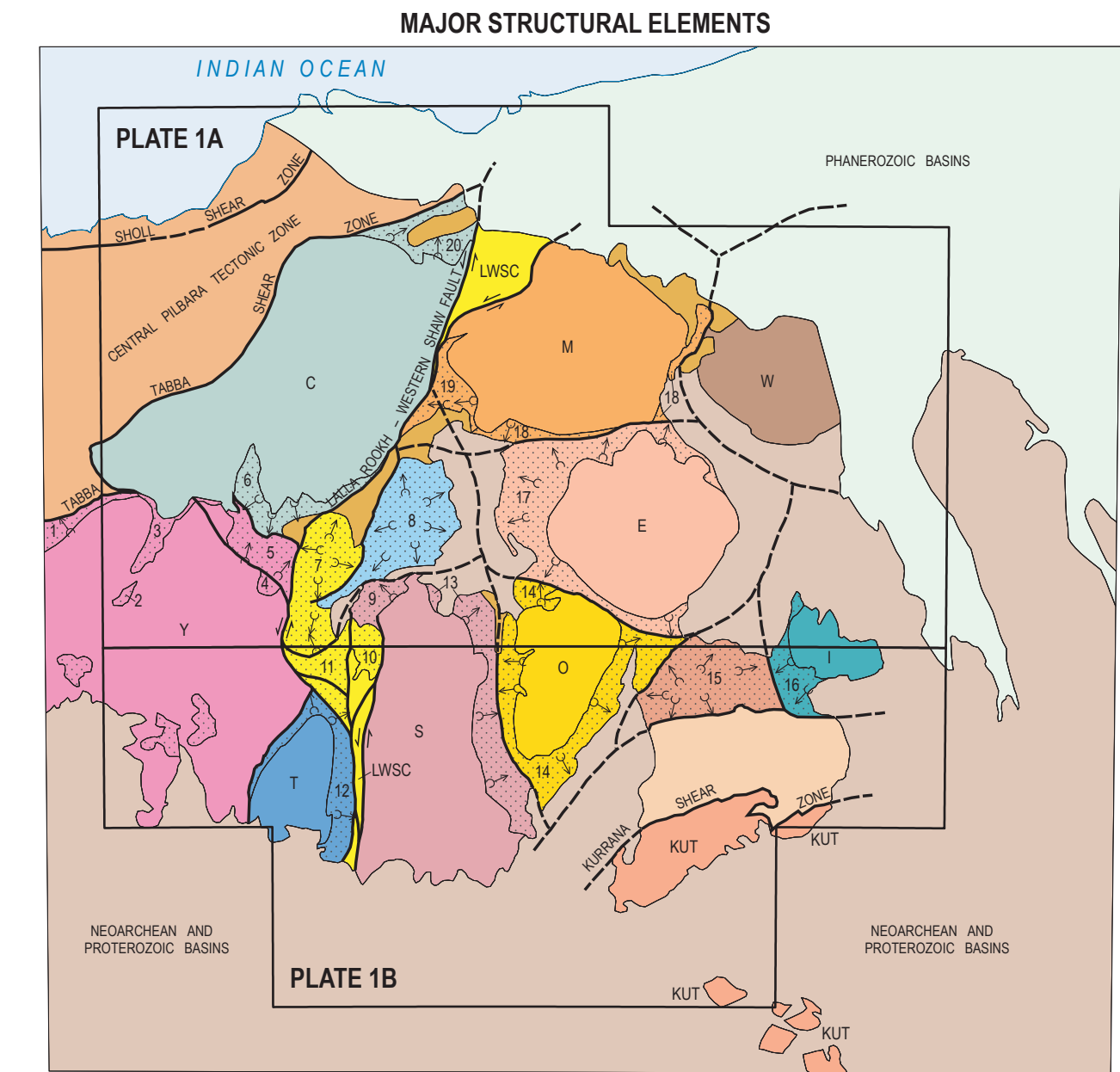


throughout the Archean. However, detailed investigations in the east Pilbara Craton have revealed that crustal evolution was by vertical tectonic processes, and there is no sustainable evidence for plate-tectonic process until 3.22 Ga. At that time, the Paleoarchean continental volcanic plateau broke up and separated into three microplates. Plate separation and subsequent interaction over another 300 Ma led to Mesarchean plate tectonic processes including subduction, obduction, plate collision and orogeny. This Report reviews the stratigraphy, structure, geochemistry, geochronology, crustal evolution and mineralization of the east Pilbara Craton.

Further details of geoscience products are available from:

Information Centre
Department of Mines, Industry Regulation and Safety
100 Plain Street
EAST PERTH WA 6004
Phone: (08) 9222 3459 Email: publications@dmirs.wa.gov.au
www.dmirs.wa.gov.au/GSWApublications



[illegible]